ACTA PHYSICA

ACADEMIAE SCIENTIARUM HUNGARICAE

TOMUS XXIII FASCICULUS 1

AKADÉMIAI KIADÓ, BUDAPEST
1967

ACTA PHYSICA

A MAGYAR TUDOMÁNYOS AKADÉMIA FIZIKAI KÖZLEMÉNYEI

SZERKESZTŐSÉG ÉS KIADÓHIVATAL: BUDAPEST V., ALKOTMÁNY UTCA 21.

Az *Acta Physica* német, angol, francia és orosz nyelven közöl értekezéseket a fizika tárgyköréből.

Az *Acta Physica* változó terjedelmű füzetekben jelenik meg: több füzet alkot egy kötetet.

A közlésre szánt kéziratok a következő címre küldendők:

Acta Physica, Budapest 502, P. O. B. 24.

Ugyanerre a címre küldendő minden szerkesztőségi és kiadóhivatali levelezés.

Az *Acta Physica* előfizetési ára kötetenként belföldre 120 forint, külföldre 165 forint. Megrendelhető a belföld számára az Akadémiai Kiadónál (Budapest V., Alkotmány utca 21. Bankszámla 05-915-111-46), a külföld számára pedig a „Kultúra" Könyv- és Hírlap Külkereskedelmi Vállalatnál (Budapest I., Fő u. 32. Bankszámla 43-790-057-181 sz.), vagy annak külföldi képviseleteinél és bizományosainál.

Die *Acta Physica* veröffentlichen Abhandlungen aus dem Bereich der Physik in deutscher, englischer, französischer und russischer Sprache.

Die *Acta Physica* erscheinen in Heften wechselnden Umfanges. Mehrere Hefte bilden einen Band.

Die zur Veröffentlichung bestimmten Manuskripte sind an folgende Adresse zu richten:

Acta Physica, Budapest 502, P. O. B. 24.

An die gleiche Anschrift ist auch jede für die Redaktion und den Verlag bestimmte Korrespondenz zu senden.

Abonnementspreis pro Band: 165 Forint. Bestellbar bei dem Buch- und Zeitungs-Aussenhandels-Unternehmen »Kultúra« (Budapest I., Fő u. 32. Bankkonto Nr. 43-790-057-181) oder bei seinen Auslandsvertretungen und Kommissionären.

ACTA PHYSICA

ACADEMIAE SCIENTIARUM HUNGARICAE

TOMUS XXIII

AKADÉMIAI KIADÓ, BUDAPEST
1967

ACTA PHYSICA

Tomus XXIII

INDEX

J. Bitó: On the Role of Auxiliary Electrodes in A. C. Discharges. — *Я. Бито:* О роли вспомогательных электродов, применяемых в разрядах переменного тока 1

K. L. Nagy: Spontaneous Symmetry Breaking and Constant Gauge Transformations. — *К. Л. Надь:* Спонтанное нарушение симметрии и постоянные калибровочного преобразования 17

M. Pósch and *E. Krén:* Magnetic Ground State Spin Configurations in Face-Centred Cubic and Cu_3Au-Type Crystals. — *М. Пош* и *Е. Крен:* Магнитное основное состояние спин-конфигурации в лобоцентральных кубических кристаллах и в кристаллах типа Cu_3Au 29

J. Nyiri and *A. Sebestyén:* Algebraic Methods in the Theory of Special Unitary Groups II. Special Quasispin and Multiplet Structure. — *Ю. Нири* и *А. Шебештен*: Алгебраические методы в теории специальных унитарных групп. II. Квазиспин и структура мультиплетов 37

L. Jánossy: The Lorentz Principle and the General Theory of Relativity Part IV. — — *Л. Яноши:* Принцип Лоренца и общая теория относительности. Часть IV. 53

N. A. Eissa, Z. Meligy, A. H. El Farrash and *S. Girgis:* Relative Intensity and Conversion Coefficients of the Transitions in the Decay $Zr^{95}—Nb^{95}—Mo^{95}$. — *Н. А. Исса, З. Мелиги, А. Х. Эл Фарраш* и *С. Гиргис:* Относительная интенсивность и коэффициенты преобразования переходов в распаде $Zr^{95}—Nb^{95}—Mo^{95}$ 67

I. Hevesi: Determination of Optical Constants and Thickness of Anisotropic Crystal Plates From Transmission Measurements. — *И. Хевеши:* Определение оптических констант и толщины анизотропных кристаллических пластинок по измерению пропускания 75

J. Csikai and *G. Pető:* Influence of Direct Inelastic Scattering on $(n, 2n)$ Cross Sections. — — *Й. Чикаи* и *Г. Петэ:* Влияние прямого неупругого рассеяния на поперечное сечение $(n, 2n)$ 87

Th. Neugebauer: Über die Niveaudichte der Atomkerne. — *Т. Найгебаер:* Плотность энергетических уровней атомных ядер 95

F. Kelemen: Eine Wärmeimpulsmethode zur Bestimmung der Temperaturleitzahl an kurzen Proben 111

J. Bitó: On the Thermal Effects of Auxiliary Electrodes on Hg—A Discharges..... 117

I. Angeli and *I. Hunyadi:* Measurement of Average Total Cross-Section Fluctuation for Al at 14 MeV Neutron Energy 123

A. L. Mehra: Hubble's Expansion in Vectors Formed by $\triangle$-tensors 125

Zs. Náray: J. H. Sanders, The Velocity of Light (Recensio) 131

Zs. Csoma: R. A. R. Tricker, Early Electrodynamics (Recensio) 131

P. Szépfalusy: J. R. Schrieffer, Theory of Superconductivity (Recensio) 133

J. I. Horváth: A. B. Arons, Development of Concepts of Physics (Recensio)..... 133

J. I. Horváth: Alfredo Baños, jr., Dipole Radiation in the Presence of a Conducting Half-Space (Recensio)..... 134

P. Surányi: G. Barton, Introduction to Dispersion Techniques in Field Theory (Recensio) 134

A. Szalay and *A. Kovách:* Fission Product Precipitation from the Atmosphere in Debrecen, Hungary, between 1963 and 1965. — *А. Салаи* и *А. Ковач:* Осаждение продуктов деления из атмосферы в г. Дебрецен, Венгрия, в 1963—1965 гг. 137

G. Knapecz: General Relativistic Theory of Lagrangian Functions I. — *Г. Кнапец:* Общее релятивистская теория лагранжианов. I. 145

Л. Пал: Влияние флуктуации внутреннего магнитного поля на эффект Мэссбауэра. *L. Pál:* The Effect of the Fluctuation of the Internal Magnetic Field on the Mössbauer Pattern. 161

I. Abonyi: The Crocco—Vázsonyi Equation in Relativistic Hydrodynamics of Ideal Fluids. — *И. Абони:* Уравнение Крокко—Важони в релятивистской гидродинамике идеальной жидкости 185

M. Z. v. Krzywoblocki: Gravitational Waves. — *М. З. Кржывоблоцки:* Гравитационные волны 193

G. Knapecz: Symmetry Theory of the Equations of Motion I. — *Г. Кнапец:* Теория уравнений движения на основе симметрии пространства. I. 203

M. L. Császár und *E. Koczkás:* Das Elektronenbandenspektrum des CsD-Moleküls im sichtbaren Spektralgebiet. — *М. Л. Часар* и *Э. Коцкаш:* Спектр электронной связи молекулы CsD в видимой области 211

M. Huszár: Non-relativistic Approximation of the Dirac Current. — *М. Гусар:* Нерелятивистическое приближение тока Дирака 225

A. Székely: Die Fluoreszenz von 4,4'-bis-Triazinilaminostilben-2,2'-Disulfonsäurederivaten 237

I. Abonyi: Sur la solution de l'équation de Boltzmann relativiste sans collisions en présence de certains champs extérieurs 247

P. Gombás: Wolfgang Pauli: Collected Scientific Papers (Recensio) 251

L. F. Landovitz: Quadratic Interaction in Quantum Field Theory. — *Л. Ф. Ландовиц:* Квадратичное взаимодействие в квантовой теории поля 253

N. A. Eissa and *Gy. Máté:* Problematics on the Application of Delayed Coincidence Devices. — *Н. А. Эисса* и *Дь. Матей:* Проблематики применения запаздывающего совпадения 259

Z. Meligy and *N. A. Eissa:* Systematics of Some Properties of the Odd Mass Nuclei in the Region Near the Mass Number 190. — *З. Мелиги* и *Н. А. Эйсса:* Систематичность некоторых свойств нечетных ядер в области, близкий к массовому числу 190 277

Gy. Büti: On the Exchange Energy in an SCF Method Using Nonorthogonal Basis Functions. — *Дь. Быти:* Об обменной энергии в методе самосогласованного поля, использующем неортогональные басисные функции 287

L. Jánossy and P. Király: The Lorentz Principle and the General Theory of Relativity, Part. V. — *Л. Яноши и П. Кирай:* Принцип Лоренца и общая теория относительности. Часть V. 291

J. Ravatin and *G. Mesnard:* Etude de formalisme pour méthodes de perturbations. 311

M. Süveges: Higher Dimensional Spaces and Symmetries Arising on Gravitational Fields 315

J. Ladik: A Semiempirical Method for the Calculation of the Excited States of Molecules 317

T. Geszti: I. E. Farquhar, Ergodic Theory in Statistical Mechanics (Recensio) 321

L. Detre: The Structure and Evolution of Galaxies (Recensio) 321

L. Detre: R. J. Mackin—M. Neugebauer, The Solar Wind (Recensio) 322

P. Szépfalusy: D. Pines-Ph. Nozières, Theory of Quantum Liquids (Recensio) 322

P. Gombás: M. A. Preston, Physics of the Nucleus (Recensio) 323

O. S. Beryland—R. I. Gavrilova—A. P. Prudnikov, Tables of Integral Error Functions and Hermite Polynomials (Recensio) 324

J. M. Ziman, Principles of the Theory of Solids (Recensio) 324

H. S. Green—C. A. Hurst, Order Disorder Phenomena (Recensio) 324

P. B. Jones: The Optical Model (Recensio) 324

J. Balázs: Mukul R. Kundu, Solar Radio Astronomy. (Recensio) 325

E. A. Saad, N. A. Eissa, I. Bartchouk, O. H. El-Mofty and *A. F. El-Bidewy:* Thermal Neutron Flux Distribution and Flux Trap Effect in the Active Core of the UA-RR-I Reactor. — *Е. А. Сад, Н. А. Эйсса, И. Барчук, О. Г. Эл-Мофти* и *А. Ф. Эл-Байдеи:* Распределение потока тепловых нейтронов и эффект ловушки потока в активной зоне реактора UA—RR—I. 327

J. Bakos and *J. Szigeti:* Measurement of the Lifetime of Atomic Excited Levels by Time Analyser. — *Й. Бакош* и *Я. Сигети:* Определение времени жизни атомных возбужденных уровней временным анализатором 341

Á. Tóth: Determination of the Counting Efficiency in Cases of Radiation Measurement of the Widespread Solid Alpha Sources. — *А. Тот:* Определение эффективности счёта случая неточеных твёрдых α-излучающих источников 349

G. Pataki and *F. Beleznay:* On the Effect of a High Magnetic Field on Recombination Through Centres. — *Г. Патаки* и *Ф. Белезнаи:* О влиянии сильных полей на рекомбинацию, происходящую через рекомбинационные центры 363

L. Csillag, M. Jánossy and *K. Kántor:* Experimental Investigation of the Spatial Coherence of a He—Ne Laser. — *Л. Чиллаг, М. Яноши* и *К. Кантор:* Экспериментальное исследование пространственной когерентности лазера He—Ne 373

Э. Ватаи: Использование метода ($\beta^+ \gamma^\pm$) совпадений при исследовании позитронного распада ядер. — *E. Vatai:* On the Use of the ($\beta^+ \gamma^\pm$) Coincidence Method in Investigations on Positron-Emitting Nuclides. 381

B. Pődör: Effect of Dislocations on Galvanomagnetic Properties of *n*-Type Ge. — *Б. Пэдэр:* Влияние дислокаций на плотность и подвижность носителей тока германа *n*-типа 393

Gy. Máthé: Investigation of the Signal Shape Given by $n - p$ and $p - n$ Type Semiconductor Detectors with Pulse Shape Discrimination. — *Дь. Матэ:* Исследование формы сигнала полупроводниковых детекторов $n—p$ и $p—n$ дискриминатором импульсных форм 407

I. Hevesi: On the Optical Properties of Vanadium Pentoxide Single Crystals. — *И. Хевеши:* Оптические свойства монокристаллов пятиокиси ванадия 415

A. Jucys, I. I. Glembockys and *R. Gáspár:* Investigations with Modified Universal Potential Fields. — *А. Юцис, И. И. Глембоцкис* и *Р. Гашпар:* Исследования модифицированными универсальными потенциальными полями 425

P. Gombás und *O. Kunvári:* Zur Prüfung der Pseudopotentialmethode am Wasserstoffatom. — *П. Гомбаш* и *О. Кунвари:* Об испытании метода псевдопотенциалов в случае атома водорода 443

S. S. Rathi and *M. K. Machwe:* Effect of Concentration on Fluorescence Spectrum of Eosin 449

K. Ladányi: Relativistic Trion Model for Hadrons 453

P. Gombás: R. Hofstadter—L. J. Schiff, Nucleon Structure. (Recensio) 457

A. A. Sokolov, Elementary Particles (Recensio) 457

R. Brout—P. Carruthers, Lectures on the Many-Electron Problem (Recensio) 457

P. Roman, Advanced Quantum Theory (Recensio) 458

H. Muirhead, The Physics of Elementary Particles (Recensio) 458

A. A. Sokolov—J. M. Loskutow—I. M. Ternow, Quantenmechanik (Recensio) 458

A. S. Davydov, Quantum Mechanics (Recensio) 459

T. A. Littlefield—N. Thorley, Atomic and Nuclear Physics (Recensio) 459

W. A. Harrison, Pseudopotentials in the Theory of Metals (Recensio) 459

Acta Physica Academiae Scientiarum Hungaricae, Tomus 23 (1), pp. 1—15 (1967)

ON THE ROLE OF AUXILIARY ELECTRODES IN A.C. DISCHARGES*

By

J. Bitó

INDUSTRIAL RESEARCH INSTITUTE FOR ELECTRONICS, BUDAPEST

(Presented by G. Szigeti — Received 19. X. 1965)

Only the phenomena taking place near the discharge-heated, oxide-coated electrode of low-pressure mercury-argon arcs are treated by the author for the case when two auxiliary electrodes of the same surface area, arranged parallel to each other protrude into the space around the electrode. The radial movement of the auxiliary electrodes and examination of the influence thereof on the space surrounding the electrode is facilitated by a discharge tube of special design made especially for this purpose. The current consumption of the auxiliary electrodes in their various positions is determined and the total currents as well as the variations of the tube voltage are measured. Starting from the results thus obtained, the influence of the auxiliary electrodes used in a.c. discharges on the space around the electrode is discussed. Using time distribution through the previously employed a.c. probe measurements, the instantaneous value of cathode fall and the mean value obtained from the cathode fall and anode fall relative to one half period are determined as functions of the position of the auxiliary electrodes. The results and functions obtained are compared with the relationships derived from the tests carried out hitherto with d.c. discharges.

1. Introduction

While the phenomena in the positive column of various gas and vapour discharges can be characterized with more or less accuracy through the sufficiently exact determination of the relevant micro and macro parameters, the description of the spaces surrounding the electrode gives rise to some difficulties strongly restricting the accuracy of the results of the measurements. To characterize the plasma of the positive column, there are several approximating methods available which are relatively quick and provide also for the general plasma diagnosis. However, the description of the spaces around the electrodes, and the "transition spaces" between the regions of the positive column and the electrodes involves several problems caused by the character and size of the spaces themselves. At the same time, these spaces are of primary importance as to the maintenance and design of the discharge but many, relatively unclear phenomena are encountered due to the difficulties in testing (above all the problem of measurement free of perturbations which could affect the discharge). One of these problems is the influence of the auxiliary electrodes made of conductive material and protruding into the proximity

* Lecture delivered at the 3rd Czechoslovak Conference on Electronics and Vacuum Physics. Sept. 1965.

of the electrodes on the discharge region. Though previous papers [1, 2] contained interesting statements, emphasizing the considerable influence of the auxiliary electrodes in some cases, detailed experimental, or theoretical results have not been published up to now.

HINMAN and FOX [1] pointed out that auxiliary electrodes conveniently arranged near the electrode may decrease the voltage fall across the region ahead of the electrode — and thus also the power loss taking place across the electrode — and this effect would be proportional to the auxiliary electrode surface area within a certain range. But this paper [1] contains no answer as to whether the phenomena occurring in the proximity of the electrode are subject to more significant influence of the auxiliary electrode at the cathode side or anode side of the a.c. discharge. This statement has not been supported by more detailed data obtained either theoretically or experimentally. The author participated earlier in experiments [2] carried out to classify the influence of the auxiliary electrodes on the cathode fall in the case of a.c. discharge. By means of these investigations [2] it could be shown that in the cathode half cycle the auxiliary electrode has a considerable effect because it reduces the cathode fall. In the same paper [2] the function of the auxiliary electrodes in d.c. discharges has also been treated.

The purpose of the present paper is to report the results of further investigations, determining the current consumption of the auxiliary electrodes of given size, arranged symmetrically to the main electrode, movable in radial direction, of equal surface area, shape and material, their influence in the case of the d.c. discharge both at the cathode and the anode sides, the variations on the tube voltage caused by the above influence and finally, the main deviations of the a.c. discharges which would take place in the cathode half-cycle relative to the examined electrode, likewise due to the above phenomena.

2. Experimental conditions, measuring methods

The design of the special tube used in the measurements is shown in Fig. 1. Glass-wall discharge tube T has an inner diameter of 36 mm and an interelectrode distance of 1090 mm. At both ends of the tube, there are two tungsten double spirals of the same design coated with the electron emitting material S to form the electrodes together with the corresponding current inlets I. Near the first electrode two radially movable auxiliary electrodes are built in. These plate-like auxiliary electrodes are made of nickel, with a thickness of 0,1 mm and with 7 and 12 mm sides. They are built symmetrically in the direction of the spiral axis. They are displaced by an electromagnet through the iron cores fastened to them. Any turning is prevented by an iron shoulder matching into the guide groove formed in the glass. Having been

adjusted to the required position, the magnet was removed from the space of discharge. Complete introduction into the discharge region was also prevented by a reduced glass sector along the guide slot. The auxiliary electrodes could be adjusted arbitrarily to the radial distance from the spiral between 2 and 17 mm. This adjustment was checked by a reading device with mm divisions designed especially for this purpose.

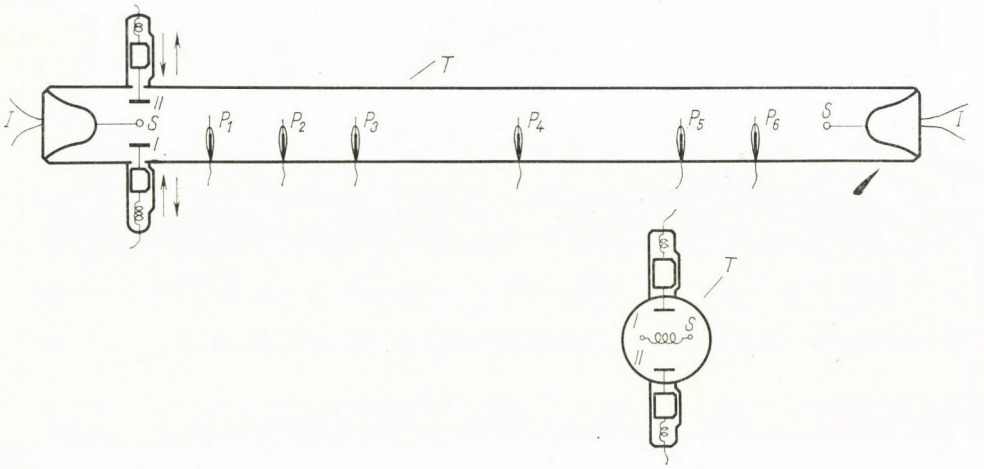

Fig. 1. Scheme of the discharge tube used for the experiments. T — glass wall of the tube S — double spiral forming the electrode, I — current inlets of the electrode, — I and II — two movable auxiliary electrodes, P_1 — P_6 — cylindrical probes

In addition six probes were placed into the discharge tube, the active parts of which were made of nickel, and had a length of 2 mm and a diameter of 0,2 mm. The cylindrical probes were arranged in the discharge region in the manner that the discharge tube axis would divide the 2 mm current pic-up part of the probes into two halves. Besides, the arrangement of the probes was determined according to the considerations: on one hand, they had to protrude into the positive column to be taken for homogeneous in that case, and on the other, their arrangement had to enable the entire discharge region to be characterized as accurately as possible in the range between the cathode fall and the anode fall.

The measurements were carried out at mercury-argon discharge in quiet atmospheric conditions, at $25 \pm 1°$ C air temperature. Accordingly, the lowest wall temperature of the discharge tube amounted to about $40 \pm 1°$ C in the middle of the glass wall, which resulted in a mercury vapour pressure of about $6 \pm 0{,}5 \cdot 10^{-3}$ mmHg. The pressure of the argon gas in the tube was 3 mmHg. The glass parts which served for the displacement of the auxiliary electrodes — in order to decrease the undesirable oscillations of the vapour pressure — have been maintained constantly at the temperature of 50° C.

The circuit diagram used in the operation of the tube is shown in Fig. 2. Discharge tube T was fed by source SPS of stabilized voltage supplied in each case by an 50 c/s a.c., or a d.c. voltage source and accordingly limiting resistance Z had an inductive or pure ohmic character. Both the a.c. and d.c. measurements were carried out at a discharge current of 430 mA. Auxiliary electrodes I and II could be interconnected with any arbitrary terminals of the spirals of switches K_{I} and K_{II}, respectively. Before the beginning of each measurement the discharge tube was operated under the test conditions specified for

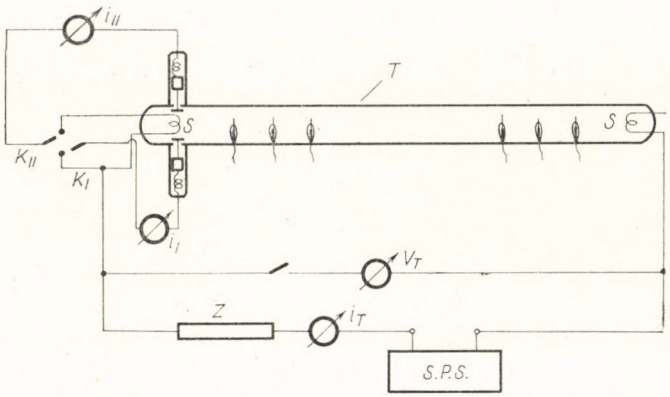

Fig. 2. Scheme of the electrical circuit: Ammeters i_{I} and i_{II} measure the current of the relevant auxiliary electrodes; i_T — the discharge current, V_T — the tube voltage, Z — restrictive impedance, K_{I}, K_{II} — three-position switch, SPS — stabilized voltage source

a duration of 20 minutes with the results that the parameters intended for measurement could stabilize to the necessary extent.

Both for the d.c. and a.c. probe measurements, the measuring method developed by the author [4] on the basis of the WAYMOUTH pulse technique [3] was applied. The benefits of this probe measurement method were primarily apparent for the a.c. measurements in view of the suitable time resolution. The accuracy of the procedure was $\pm 0{,}2$ V.

3. Test results

The auxiliary electrodes moving in the discharge region consume different currents depending upon their position relative to the spiral taken for the main electrode. The relevant experiments carried out by the author were published in another paper [5]. In the present case, only the manipulations near one electrode of the a.c. discharge will be shown, the essential results being plotted in Fig. 3. The horizontal axis of Fig. 3 indicates distance d of

the electrodes considered from the spiral axis whereas the vertical axis shows the current consumed by the auxiliary electrodes in mA. Of the marks of the parameters near the curves, I and II distinguishes the two auxiliary electrodes and index s indicates the state when the auxiliary electrode is connected to that spiral end near which the arc is located.

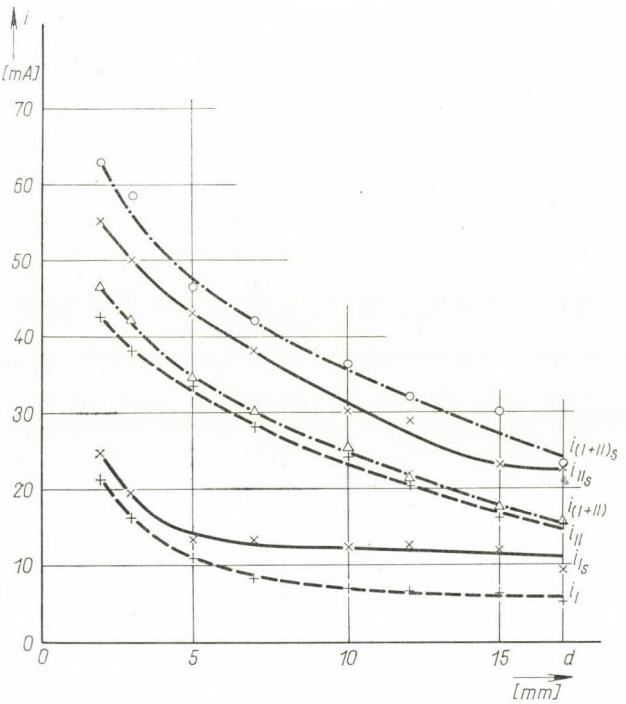

Fig. 3. Current plotted for 430 mA discharge current produced by auxiliary electrodes at various distances from the spiral in a.c. discharge. i_I, i_{II} — the current consumed by auxiliary electrodes I and II; i_{I+II} — the sum of the above currents. s gives the position of the auxiliary electrode connected to the spiral terminal closer to the arc spot whereas the characteristics not marked characterize the connection of the auxiliary electrodes attached to the other spiral end. The horizontal axis contains the distance of the individual auxiliary electrodes from the spiral end

As both of the auxiliary electrodes are of same surface area, shape and material, one could expect that in a position equal in relation to the spiral, also their surface current density would be equal. But as it is evident from a comparison of curves i_I and i_{II} in Fig. 3, even the same parameters do not result in equal current density at the surfaces of the auxiliary electrodes; in the given case, the auxiliary electrode marked II always consumes a current intensity higher than I. As shown by an optical experiment, the position of the discharge arc spot is in our case of asymmetrical arrangement to the spiral axis, consequently it is located much closer to the auxiliary electrode II than

to I. As the arc spot has been displaced along the spiral axis during the subsequent investigations, its position became symmetrical and then asymmetrical again, but in the opposite sense, i.e. in that case with the spot being closer to auxiliary electrode I. In the course of the spot movement, value i_{I} equals i_{II} in the symmetry condition and moving further, up to the extreme asymmetrical position, it was already i_{I} which took a higher current consumption than i_{II} in the corresponding position. In addition to the above, Fig. 3 makes also evident that, with the given auxiliary electrode connected electrically to the point of the spiral used for main electrode at which the arc spot is located, the current consumption of the auxiliary electrode is higher than in the case when its potential is equal to the potential of the other spiral end. This is because a considerable voltage difference exists between the two spiral ends, namely in the cathode half cycle the ions are falling mainly into the cathode spot and this represents the conductive part of lowest potential. The auxiliary electrode connected to this part will take the same potential. The other spiral end has a higher potential and thus also the auxiliary electrode connected to it will be more positive than the auxiliary electrode connected to the spiral end where the cathode spot is to be found. The consequence is that the latter auxiliary electrode absorbs less positive ions from the discharge. Taken this condition for outgoing basis, one can deduce some very interesting conclusions. Namely, it is easy to state that the current difference of the two auxiliary electrodes connected to both of the spiral ends is proportional to the potential difference of the two spiral ends and this in turn is in good approximation proportional to the average temperature of the spiral. This gives a further possibility to determine the average spiral temperature.

During the investigations measurements were undertaken in a connection scheme in which both of the auxiliary electrodes were connected at the same time to the same spiral end. The curves obtained from such measurements are given by curves $i_{(\mathrm{I}+\mathrm{II})}$ and $i_{(\mathrm{I}+\mathrm{II})s}$ in Fig. 3 to which index s in the latter notation indicates connection to the spiral end near the arc spot. From the current consumption of the auxiliary electrodes and from the total current value, it is evident that

$$i_{\mathrm{I}} + i_{\mathrm{II}} > i_{(\mathrm{I}+\mathrm{II})} \tag{1}$$

and

$$i_{\mathrm{I}_s} + i_{\mathrm{II}_s} > i_{(\mathrm{I}+\mathrm{II})_s} \, . \tag{2}$$

From the above considerations it will be evident even in the case of arbitrary spiral surface area F and auxiliary surface area relationships f_1, f_2 — which in turn, determine the current consumption — that inequalities (1) and (2) are correct, namely these are satisfied when inequality

$$\frac{f_1}{f_1 + F} + \frac{f_2}{f_2 + F} > \frac{f_1 + f_2}{(f_1 + f_2) + F} \tag{3}$$

is true. But this latter condition can be proved even with theoretical considerations taking into account that each of f_1, f_2 and F is a positive real number differing from 0. Namely

$$\frac{f_1+f_2}{F+(f_1+f_2)} = \frac{f_1}{F+(f_1+f_2)} + \frac{f_2}{F+(f_1+f_2)} \tag{4}$$

and because of

$$\frac{f_1}{F+(f_1+f_2)} < \frac{f_1}{F+f_1} \tag{5}$$

and

$$\frac{f_2}{F+(f_1+f_2)} < \frac{f_2}{F+f_2} \tag{6}$$

we have

$$\frac{f_1+f_2}{F+(f_1+f_2)} < \frac{f_1}{F+f_1} + \frac{f_2}{F+f_2} . \tag{7}$$

The role of the auxiliary electrodes both in the case of the cathode and the anode regions is most conveniently investigated through the current measurements indicated above, through the probe measurements and through the temperature measurements at the electrode surfaces.

The influence taken for d.c. mercury-argon arcs at 430 mA discharge current is shown in Fig. 4 for the cathode region. The auxiliary electrodes moving in the cathode region have a certain influence on the tube voltage, mainly, however, on the cathode fall and through it on the tube voltage. In Fig. 4, the interrupted vertical axis indicates the voltage values in V. The curve marked V_T shows the changes in the tube voltage whereas curve V_{T_s} gives the case in which the two auxiliary electrodes are connected to both of the terminals of the cathode spiral. It is to be seen that in the latter case the tube voltage is lower by approx. 0,5—1 V. As neither the gradient of the positive column (here not shown) nor the anode fall V_A have considerable changes, it can be supposed that the tube voltage has diminished due to the influence exerted by the auxiliary electrodes on the cathode region because of the fact that the auxiliary electrodes are connected to the same potential which the cathode spiral has at both of its ends. From Fig. 4 is to be seen that such an influence in the cathode region causes no variation in the anode region and moreover — as shown by the measurements — neither the gradient of the positive column is changed by it. The active presence of the auxiliary electrode in the cathode region would, under such conditions, somewhat reduce the cathode fall and through it the tube voltage, too. Marking a gives the voltage conditions produced by the auxiliary electrode connected

electrically to the spiral and the marking in brackets indicates the measuring points pertaining to the corresponding curves. If there is no index *a* at the characteristic in question, this means that the auxiliary electrode is moving in the cathode region but is not connected to the spiral and has a negative "wall potential" and through it only the wall charging current is flowing. The same notations apply to the subsequent diagrams.

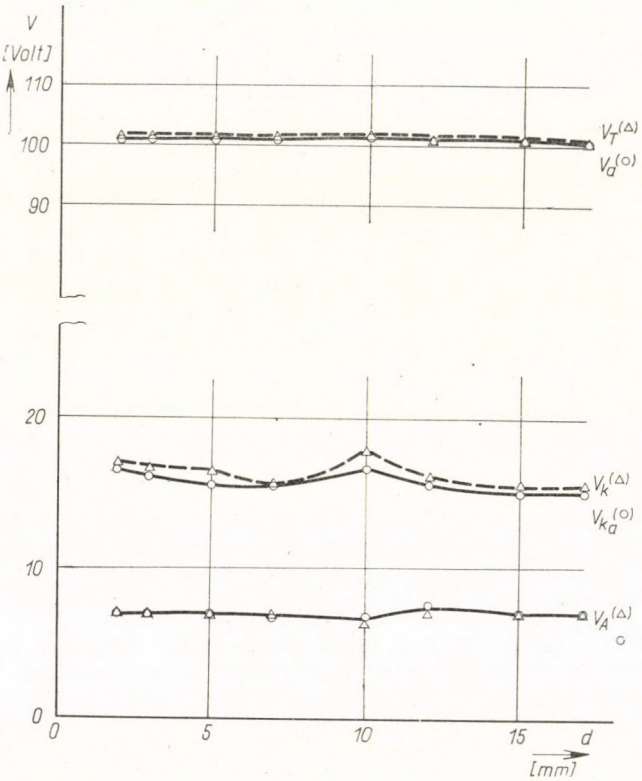

Fig. 4. Influence of auxiliary electrodes, moving radially at the cathode side of the discharge, on tube voltage V_T, cathode fall V_K and anode fall V_A. Marks in brackets are measured points; index *a* indicates the auxiliary electrode wiring connected electrically to the spiral

The experiments to determine the anode side influence of the auxiliary electrodes with the above conditions were also carried out under d.c.discharge conditions. The results are shown in Fig. 5. Strikingly, the anode side shows a more sensitive reaction to the influence than the cathode side, which is also apparent from the auxiliary electrode current characteristics [4]. Apart from the larger difference due to 5 mm distance between spiral and auxiliary electrodes, it can be stated with good approximation that also the tube voltage follows the changes in the anode fall and similarly, the auxiliary electrodes,

which have the potentials of the spiral terminals participating actively in the discharge, may in some cases reduce the tube voltage through the anode fall. From the results of Fig. 4 it is evident here too, that the influence through auxiliary electrodes at one end of the discharge tube causes no change in the regions of the other tube end. The cathode fall curves V_K V_{Ka} and V_{Ka} of Fig. 5 are nearly coincident, their shape is not considerably affected by the influence

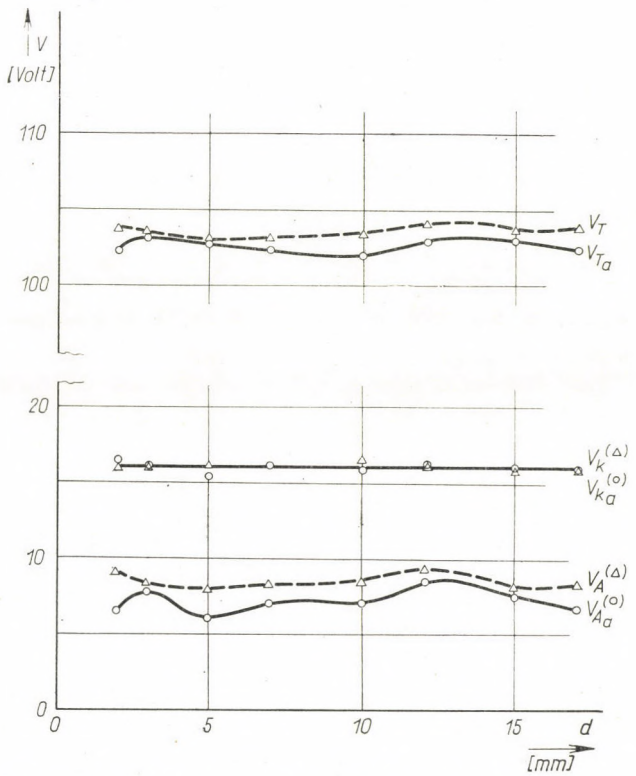

Fig. 5. Influence of auxiliary electrodes, moving radially at the anode side, on tube voltage V_T, cathode fall V_K and anode fall V_A

at the anode side in either case. The determination of the cathode and anode falls was effected in both cases by probe measurement [4].

The same probe measuring method [4] has given the possibility of more detailed a.c. investigations. The determination of the parameters which can be measured by probe measurement, was carried out in every 10° phase shift within a selected haf cycle i.e. in 18 instants. In this case, the calculation of the cathode and anode falls was made with the use of the instantaneous values of the plasma potentials measured at the points of the probes protruding into the discharge through linear extrapolation and thus, from this the time

dependence thereof and the shape of the cathode and anode falls within a half cycle could be obtained. Starting from the characteristic plotted from the mean integral value of this curve related to the half cycle and published earlier [2], the behaviour of the electrode under consideration could be estimated in the given period. To indicate the cathode fall, also required descriptions of the instantaneous values of the tube voltage and of the changes in length

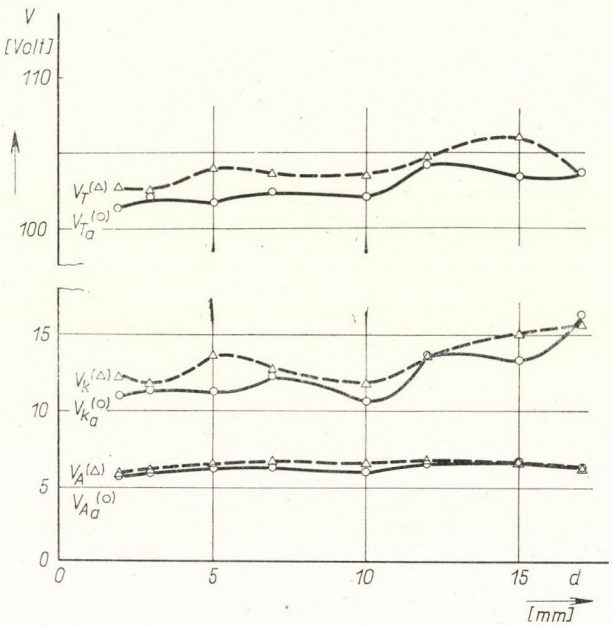

Fig. 6. Influence of auxiliary electrodes, moving in the region of one main electrode of a.c. discharge, on the tube voltage, V_T, cathode fall V_K and anode fall V_A in the cathode half cycle of the relevant main electrode

of the cathode fall range. The instantaneous values of the tube voltage could be taken oscilloscopically whereas the time dependence of the cathode fall related to a half cycle could be plotted by means of a phase-shifter controlled stroboscope [6]. The description of the relevant partial results and the time dependence of the cathode dark space will not be described in the present paper as they have been published elsewhere [6].

Thus, Fig. 6 shows the cathode fall and anode fall average values obtained in the way described above and related to the half cycle together with the average values calculated in a similar way from the instantaneous values of the tube voltage. It is worthwhile to mention that the latter value differs from the tube voltage values to be measured by means of a V-meter, only in the additive constant. The shape of both the characteristics V_T plotted with the methods above, are similar.

The values of the tube voltage — in conformity with literature data — are subject to the application of the auxiliary electrode even in this case. It can be observed that even the simple motion of the auxiliary electrode not connected to the spiral ends sensitively influences the tube voltage. If only this figure (Fig. 6) were taken into consideration, the idea might arise that the tube voltage fluctuation apparent from Fig. 6 is only due to the scattering of the measured data and perhaps both characteristics may be represented by a straight line with positive tangent. This means that the closer the auxiliary electrode is to the cathode, — regarding that subsequently the experiments are restricted only to the cathode half cycle and this shall not be especially mentioned later on — the lower will be the tube voltage. This linearization, however, should be avoided, on the one hand because it would involve neglections considerably higher than the measuring accuracy and, on the other, situations contradictory to the variations of the cathode fall and the temperature of the cathode spot could arise. The minimum of the tube voltage occurs in both cases when using auxiliary electrodes arranged close to the cathode spiral with the auxiliary electrode at 2—3 mm from the spiral axis. Among the d.c. cases shown previously comparison should be drawn with the tube voltage shape plotted for the cathode-side auxiliary electrode as shown in Fig. 4. Apparently the cathode-side influence of the auxiliary electrodes will be much more considerable for the a.c. than it was for the d.c. measurements and at the same time, also the shape of the characteristics will be more intricate.

In comparing the anode fall characteristics — as shown in Figs. 4 and 6 — some agreement can be found. The introduction of the auxiliary electrodes at the cathode side has no significant influence on the voltage fall of the anode region, not even in a.c. discharge just as in the d.c. case. The shape of the d.c. and a.c. discharges is like in the d.c. case. The shape of the d.c. and a.c. discharge characteristics shown before — Figs. 3, 4, 5, 6 — gives relationships which have not been published up to now and their knowledge may lead to further useful discussions. However, the most interesting of these characteristics is the dependence of the cathode fall of the electrode acting as cathode in the half cycle of a.c. discharge on the position of auxiliary electrodes. The shape of characteristics V_K shown in Fig. 6 is similar to the shape of the tube voltage characteristics which can be more or less expected when knowing the anode fall characteristics and the potential gradient curve of the positive column which changes relatively little in spite of the intervention.

The cathode fall characteristics plotted for a.c. discharge (see Fig. 6) essentially differ from the corresponding characteristics of Fig. 4. Namely, in the case of d.c. discharge, the curve of the auxiliary electrodes of wall potential and moving in radial direction, is similar to the cathode fall cha-

racteristic obtained for auxiliary electrodes connected to the cathode terminals. For a.c. discharge, the shape of the two characteristics is opposite to each other. While for d.c. discharge the maximum of the cathode fall characteristics lies at an auxiliary electrode distance of 10 mm at each side, here a definite minimum takes place at the same distance.

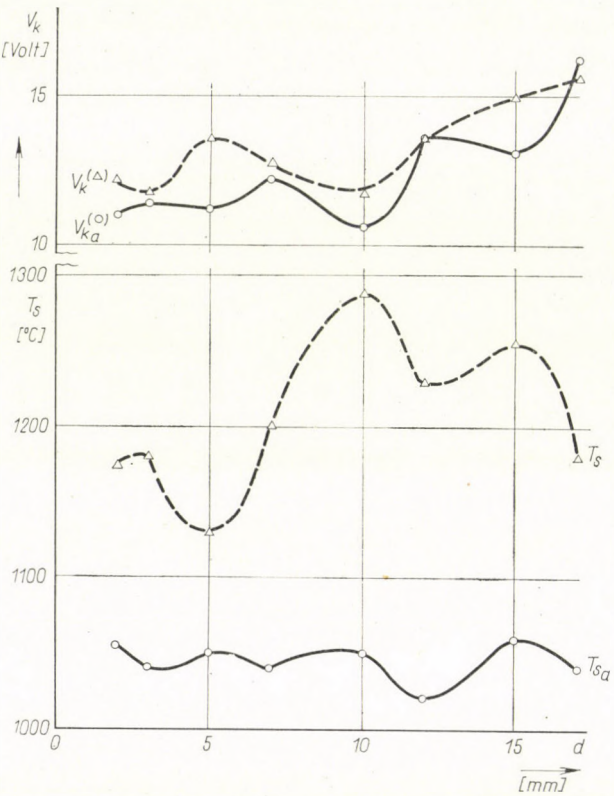

Fig. 7. Influence of auxiliary electrode, moving in the region of one main electrode of a.c. discharge, on cathode fall V_K and cathode spot temperature T_S of the relevant main electrode in the cathode half cycle of the same main electrode

In order to give a more detailed analysis of the cathode fall characteristics under the cathode fall characteristics taken from Fig. 6, Fig. 7 shows the temperature in °C of the relevant cathode spot measured by means of an optical pyrometer. Comparison of the corresponding characteristics shows that any approximation of the tube voltage characteristics through a straight line would be wrong as then the same would have been necessary for the cathode fall characteristic to which the development of the spot temperatures was contradictory. As the temperature of the cathode spot could not be measured with the same time resolution as the cathode fall, it is assumed that

the measured spot temperatures would change at least proportionally to the changes in the real cathode spot temperature not only in respect of the possible measuring inaccuracy but also in spite of the temperature variations taking place in each half cycle due to the variations of the cathode and anode half cycles (taking a half cycle duration of 0,01 sec into account). The correctness of the latter assumption has been proved by subsequent experiments.

Where the cathode fall characteristic has its minimum, the cathode spot temperature curve has its maximum for both of the characteristics pairs shown in Fig. 7 and vice versa. It is supposed that the variation of the cathode spot temperature is a primary phenomenon and as its consequence, the cathode fall changes in the same proportion in a manner that the cathode region can supply the electron quantity necessary for the discharge in each position of the auxiliary electrode. It is very interesting to observe that the auxiliary electrode connected electrically to the spiral and thus having cathode potential, reduces to a considerable extent the cathode spot temperature even without any metal contact in the discharge region — merely through the electrical connection; thus, in that case the heat conduction between the metal conductive parts could not participate in the process.

The spot temperature characteristics has three maxima. Their positions are in all probability related to the shape and size of the discharge space around the cathode, and to the features of the space charge range formed near the cathode spot at the side of the cathode. Of course, the auxiliary electrode protruding into these spaces influences also their shape and dimensions [6]. Approximately, it can be stated that at the entry from the immediate proximity of the discharge wall into the cathode discharge region, and at the protruding point into the immediate proximity of the cathode, the cathode spot temperature probably varies more considerably. This ought to be apparent also from the power consumption of the auxiliary electrodes, it is interesting, however, that it cannot be seen in Fig. 3.

To describe the changes taking place in the cathode fall and the cathode spot temperature certain approximate electronoptical considerations are required. Two models may be constructed. In the first the parallel auxiliary electrodes have approximately the same amount of wall potential which is lower than the cathode potential. Then, the auxiliary electrodes behave like focusing lenses for the electrons and accelerate the ions towards the cathode.

In the second model each of the two auxiliary electrodes have the potential of one end of the cathode. Between them, an approximately plane-symmetrical electrical field occurs, which, however, is distorted not only by boundary surface phenomena but also by the presence of the cathode spot and the cathode spiral. The field strength thus produced is determined by the cathode fall (taken along the spiral axis) and the distance of the auxiliary electrodes.

Both of the above electronoptical models are difficult to handle not only due to the variety of the charge carriers and neutral atoms but also to the badly perturbed potential conditions. On the basis of the above model, however, it can be imagined that closer conclusions can be made regarding this influence on the cathode space. As a first step, the idea can be adopted that the approach of the auxiliary electrodes to the spiral may result in acceleration and deviation with optimum conditions the ultimate result of which may be that the cathode spot temperature and through it the cathode fall change to such extent.

4. Conclusions

On the basis of the experiments carried out so far it is apparent that under the discharge conditions described in this paper both in d.c. and a.c. mercury-argon arcs the tube voltage, and the cathode fall for cathode-side influence or the anode fall for d.c. anode-side influence depend on the presence and position of the auxiliary electrodes to various extents. During the course of the experiments carried out here these have an electrical influence on the discharge region, as could be observed in the case of a.c. discharge when they electrically cooled the cathode spot. For a.c. discharge, a close relationship could be established between the temperature of the cathode spot and the cathode fall and this could probably be interpreted in more detail on the basis of approximate electronoptical considerations.

5. Acknowledgement

The author wishes to thank Mr. G. LAKATOS for raising the problem and Mr. E. VÁRBIRÓ for carrying out the special glass work.

REFERENCES

1. D. D. HINMAN and R. S. FOX, Ill. Eng., **56,** 3, 222, 1961.
2. G. LAKATOS and J. BITÓ, Proc. Symp. Electron and Vacuum Physics, Balatonvöldvár, Hungary, p. 305, 1962.
3. J. F. WAYMOUTH, J. Appl. Phys., **30,** 9, 1404, 1959.
4. J. BITÓ and I. SZEMZŐ, Magyar Fizikai Folyóirat, **12,** 2, 121, 1964.
5. J. BITÓ, Acta Phys. Hung., **20,** 383, 1966.
6. J. BITÓ, Z. für Physik, **21,** 367, 1966.

О РОЛИ ВСПОМОГАТЕЛЬНЫХ ЭЛЕКТРОДОВ, ПРИМЕНЯЕМЫХ В РАЗРЯДАХ ПЕРЕМЕННОГО ТОКА

Я. БИТО

Р е з ю м е

Автором исследуется протекающие явления в разряде ртутных паров-аргона низкого давления при электродах, нагреваемых только разрядом и обладающих нанесенным слоем окиси, в том случае, когда в близлежащее к электроду пространство вводятся два параллельных вспомогательных электрода равной поверхности. Радиальное движение вспомогательных электродов и наблюдение их воздействия на смежные с электродами области осуществляется изготовленной для этой цели специальной разрядной трубкой. Автором определяются токи на вспомогательных электродах в различных их положениях, измеряются суммарные токи, а также изменения напряжения горения. На основе полученных результатов дискутируется влияние вспомогательных электродов, применяемых в разрядах переменного тока, на смежное с электродами поле. Разработанным раньше измерительным методом зонд переменного тока, применяя разложение по времени, определяется мгновенное значение катодного падения, далее зависимость среднего значения катодного и анодного падений в полупериоде от расположения вспомогательных электродов. Полученные результаты сравниваются с данными опытов по разрядам постоянного тока.

Acta Physica Academiae Scientiarum Hungaricae, Tomus 23 (1), pp. 17—27 (1967)

SPONTANEOUS SYMMETRY BREAKING AND CONSTANT GAUGE TRANSFORMATIONS

By

K. L. NAGY

INSTITUTE FOR THEORETICAL PHYSICS, ROLAND EÖTVÖS UNIVERSITY, BUDAPEST

(Presented by K. F. Novobátzky. — Received 10. III. 1966)

Symmetry breaking solutions of several model theories are investigated with the result that constant gauge transformations of the fields describing zero mass Goldstone particles are responsible for the formal possibility of the spontaneous symmetry breaking.

1. We wish to deal here with a certain type of spontaneous symmetry breaking solutions of several model theories described by some field equations

$$D\,\Phi_i = F_i\,[\Phi]$$

and equal time commutation relations possibly originating from a Lagrangian. F denotes some functional and D a differential operator. Under the solution of the problem we mean to find a representation of the field Φ as an operator distribution over the Fock space of the free incoming or outgoing fields. Furthermore we require that the proper Lorentz group should be represented by unitary operators. Under these circumstances — which can be formulated more precisely [1] — the solution of the field equations will be represented by a Volterra expansion of the normal products of the free incoming (outgoing) fields

$$\varphi_i = \varkappa_i + c_{ij}\,\varphi_j + F_1^{(i)}\,[:\varphi\,(x)\,\varphi\,(y):] + F_2^{(i)}\,[:\varphi\,(x)\,\varphi\,(y)\,\varphi\,(z):] + \cdots \qquad (1)$$

here $\varkappa_i$, c_{ij} are c-numbers independent of x, :: denotes a normal product. φ_i-s are free fields with

$$(\Box - m_i^2)\,\varphi_i = 0,\ [\varphi_i\,(x),\ \varphi_j\,(y)] = -\,i\delta_{ij}\,\triangle\,(x-y;\,m_i)\ \text{for bosons,}$$

and

$$(\gamma_\mu\,\partial_\mu + M_j)\,\varphi_j = 0,\ \{\varphi_j\,(x),\ \bar{\varphi}_k\,(y)\} = i\,\delta_{jk}\,S\,(x-y;\,M_j)\ \text{for fermions.}$$

When the proper Lorentz group is represented it follows

$$<0\,|\,\Phi_i\,|\,0> = \text{for fermions, -vectors, -tensors, etc.}$$

$$<0\,|\,\Phi_i\,|\,0> = \text{constant } c \text{ number} = \varkappa_i \text{ for scalar, (pseudoscalar) bosons.}$$

When we require that also the space reflection should be represented, we have $\varkappa = 0$ for pseudoscalar, $\varkappa =$ constant, not necessarily zero, for scalar bosons. $|\,0\rangle$ denotes the vacuum state of the representing Fock space $\varphi_i^{(+)}\,|\,0\rangle = 0$, for all i $\langle 0\,|\,0\rangle = 1$.

Turning from classical to quantum theory, the right hand side functionals in the field equations are in general not well defined. Since the definition of them as normal products in the fields φ_i introduces a non-local theory and especially a non-unitary S-matrix [1], we keep them as they stand, e.g. $g\,\Phi^2(x) = gT(\Phi^2(x))$ and not $:\Phi^2(x):$, meaning that when in solving the field equations we meet with the term $F[\Phi]$, tadpole diagrams often and necessarily appear.

From the point of view of the symmetry properties of the theories the following nomenclature is used: If we find that the field equations (and the commutation relations) are invariant under the substitution

$$\Phi_i \to \Phi'_i = F\,[\Phi]$$

we speak of algebraic or substitutional invariance. When the field equations and the equal time commutation relations are derived from a Lagrangian, from quite general theorems (e.g. for continuous transformations from Noether's theorem) it follows that this transformation is performed by a time-independent form U which is a functional of Φ

$$U\,\Phi_i\,U^{-1} = \Phi'_i\,.$$

We speak of a spontaneous symmetry breaking if U is not represented by a time-independent unitary operator on the Fock space of the free fields φ_i. For quantum field theories, where the number of degrees of freedom of the system is infinite, this possibility is allowed. We know, and we shall see later that from $\varkappa \neq 0$ the spontaneous symmetry breaking follows. The transformation $\Phi = \Phi'$ induces a transformation $\varphi \to \varphi'$ on φ through the solution of the field equations (1). This transformation need not have the same form as that for Φ. This was called formerly the spontaneous breakdown of the form of the symmetry [2] or in a much more suggestive way by UMEZAWA [3] as the dynamical rearrangement of the symmetry.

In solving the field equations the simplest, NAMBU's or UMEZAWA's, approximation [4] is used, where we neglect the higher order terms $F_1^{(i)}, F_2^{(i)}, \ldots$ and then we take $\langle 0\,|\,0\rangle$ and $\langle 0|$ one particle $\rangle$ matrix elements. This corresponds to tadpole diagrams + pole approximation.

The aim of this paper is to emphasise by means of simple or even rather well known models the meaning of the Goldstone theorem and the importance of the constant gauge transformation associated with the fields corresponding to zero mass particles [3, 5].

2. As a first model we consider the system of two real spin zero bosons coupled bilinearly described by the field equations and commutation relations

$$\begin{aligned}(\Box - \mu^2)\Phi_1 &= g\,\Phi_2\,,\\ (\Box - \mu^2)\Phi_2 &= g\,\Phi_1\,,\\ [\Phi_i(x),\ \Phi_j(x')]_{t=t'} &= \delta(x - x')\,\delta_{ij}\,.\end{aligned} \tag{2}$$

This model was already studied [6] with another method. Here for finding the solution we suppose

$$\begin{aligned}\Phi_1 &= \varkappa_1 + c_{11}\varphi_1 + c_{12}\varphi_2\,,\\ \Phi_2 &= \varkappa_2 + c_{21}\varphi_1 + c_{22}\varphi_2\,,\end{aligned} \tag{3}$$

where $\varkappa$, c are real c-numbers independent of x, φ_1 and φ_2 two free fields with the masses m_1 and m_2 satisfying usual free field commutation relations. These fields are supposed to describe the real particles. Owing to the simplicity of the model, higher order terms in (3) do not occur. Substituting (3) into (1), taking into account what we have required on $\varkappa$ and φ, we get from the field equations

$$\begin{aligned}\mu^2\varkappa_1 + g\varkappa_2 &= 0\,,\\ g\varkappa_1 + \mu^2\varkappa_2 &= 0\,,\end{aligned} \tag{4}$$

$$c_{11}^2 = c_{21}^2\,, \qquad c_{22}^2 = c_{12}^2\,, \tag{5}$$

whereas the masses have to be given by

$$m_1^2 = \mu^2 + g\frac{c_{21}}{c_{11}}\,, \qquad m_2^2 = \mu^2 + g\frac{c_{12}}{c_{22}}\,,$$

and from the commutation relations we have

$$c_{11}^2 + c_{12}^2 = c_{21}^2 + c_{22}^2 = 1\,, \quad c_{11}c_{21} + c_{12}c_{22} = 0\,. \tag{6}$$

The necessary condition for a nontrivial solution for $\varkappa$ is

$$\mu^4 - g^2 = 0\,, \quad \text{i.e.} \quad \mu^2 = \pm g\,. \tag{7}$$

If

$$\mu^2 = g\,, \quad \varkappa_1 = -\varkappa_2 = \varkappa\,, \tag{8,a}$$

$$\mu_2 = -g\,, \quad \varkappa_1 = \varkappa_2 = \varkappa\,, \tag{8,b}$$

$\varkappa$ is arbitrary. The symmetry properties of the model for $\varkappa = 0$ were studied elsewhere [2], here the case $\varkappa \neq 0$, when one usually speaks about the spontaneous breakdown of the symmetry, will be studied. We mention that whether

spontaneous symmetry breaking is possible or not depends on the special structure and on the specific dynamics of the theory. Analyzing equations (5)—(8) we find for $\varkappa \neq 0$:

(i) one of the real masses is zero (Goldstone theorem), the other mass $m^2 = 2\mu^2$,

(ii) on the right hand side of (3) the zero mass field appears for the case of (8a) with opposite, for the case of (8b) with the same sign. Thus with $m_1^2 = 0$, $m_2^2 = 2\mu^2$ i.e. with

$$\Box \varphi_1 = 0\,, \quad (\Box - 2\mu^2)\,\varphi_2 = 0$$

for $m^2 = g$

$$\Phi_1 = \varkappa + \frac{1}{\sqrt{2}}(\varphi_1 + \varphi_2)\,,$$

$$\Phi_2 = -\varkappa - \frac{1}{\sqrt{2}}(\varphi_1 - \varphi_2)\,, \tag{9}$$

for $m^2 = -g$

$$\Phi_1 = \varkappa + \frac{1}{\sqrt{2}}(\varphi_1 - \varphi_2)\,,$$

$$\Phi_2 = \varkappa + \frac{1}{\sqrt{2}}(\varphi_1 + \varphi_2) \tag{10}$$

are solutions. Thus the problem is completely solved; e.g. the original Lagrangian

$$L(\Phi_1, \Phi_2) = -\frac{1}{2}\left[(\partial_\mu \Phi_1)^2 + \mu^2 \Phi_1^2 + (\partial\mu\, \Phi_2)^2 + \mu^2 \Phi_2^2\right] - g\,\Phi_1\,\Phi_2$$

expressed by φ-s is

$$L(\varphi_1, \varphi_2) = -\frac{1}{2}\left[(\partial_\mu \varphi_1)^2 + (\partial_\mu \varphi_2)^2 + 2\mu^2 \varphi_2^2\right].$$

Of course the asymptotic condition does not follow in the usual form since

$$<0\,|\,\Phi(x)\,|\,0> \neq 0\,.$$

(1) or (11) is invariant under the transformations

$$\begin{aligned} &(\mathrm{C}) \quad \Phi_1 \to \Phi_2\,, \qquad \Phi_2 \to \Phi_1\,, \\ &(-\mathrm{C}) \quad \Phi_1 \to -\Phi_2\,, \quad \Phi_2 \to -\Phi_1\,. \end{aligned}$$

("Charge conjugation"). These transformations give for real particle fields in case (9)

$$\begin{aligned} &(\mathrm{C}) \quad \varphi_1 \to -\varphi_1 - 2\sqrt{2}\,\varkappa\,, \quad \varphi_2 \to \varphi_2\,, \\ &(-\mathrm{C}) \quad \varphi_1 \to \varphi_1\,, \qquad\qquad\quad \varphi_2 \to -\varphi_2\,. \end{aligned}$$

and in case (10)

$$(C) \quad \varphi_1 \to \varphi_1, \qquad \varphi_2 \to -\varphi_2,$$

$$(-C) \quad \varphi_1 \to -\varphi_1 - 2\sqrt{2}\,\varkappa, \quad \varphi_2 \to \varphi_2.$$

We see that these transformations possess quite different forms in terms of bare or real fields. The same happens also with the symmetry transformation

$$(P) \; \Phi_1 \to -\Phi_1, \quad \Phi_2 \to -\Phi_2,$$

where in both cases

$$(P) \; \varphi_1 \to -\varphi_1 - 2\sqrt{2}\,\varkappa, \quad \varphi_2 \to -\varphi_2.$$

We observe, that in all of these transformations the Goldstone particle undergoes besides the existing and well defined ordinary transformations $\varphi_1 \to \pm\varphi_1$ also a constant gauge transformation. This was already found in other models to the discussion of which we come back later.

Now we proceed to treat the simplest one-field non trivial example

$$(\Box - \mu^2)\,\Phi = g\,\Phi^2 \tag{11}$$

although such a model is not expected to have a lowest energy state. In the approximation specified before

$$\Phi = \varkappa + \varphi, \quad (\Box - m^2)\,\varphi = 0,$$

one gets

$$-\mu^2\varkappa + (m^2 - \mu^2)\,\varphi = g\,(\varkappa^2 + \varphi^2 + 2\varkappa\varphi) = g\,(\varkappa^2 + :\varphi^2: + \frac{1}{2}\Delta_F(0, m) + 2\varkappa\varphi),$$

from which, taking matrix elements

$$-\mu^2\varkappa = g\,\varkappa^2 + \frac{g}{2}\Delta_F(0, m),$$

$$m^2 = \mu^2 + 2g\varkappa$$

follows. We see that $\varkappa = 0$ is not a solution and

$$\varkappa = \frac{-\mu^2 \pm \sqrt{\mu^4 - 2g\,\Delta_F(0, m)}}{2g},$$

and

$$m^2 = \pm\sqrt{\mu^4 - 2g\,\Delta_F(0, m)}.$$

To obtain a physical result one must have

$$0 \leq \mu^4 - 2g\,\Delta_F(0, m) < \infty$$

and only the + sign is allowed. $m = 0$ is not at all necessary. $\varkappa \neq 0$ is compensated usually by an additional renormalization constant [1], thus treating the equation

$$(\Box - \mu^2)\,\Phi = g\,\Phi^2 + c$$

instead of (11). If we take, however, (11) at a face value $\varkappa \neq 0$ follows in any order of g. This implies as a consequence that a large class of transformations of Φ induces a constant gauge transformation on φ. Among them, however, we cannot find here any symmetry transformations.

The main consequences of the above model also follow for the scalar coupling of fermions

$$(\gamma_\mu \partial_\mu + K)\,\Psi = g\,\Phi\,\Psi\,,$$
$$(\Box - \mu^2)\,\Phi = g\,\overline{\Psi}\,\Psi\,.$$

With

$$\Phi = \varkappa + \varphi\,, \quad \Psi = \Psi_0$$
$$(\Box - m^2)\,\varphi = 0\,, \quad (\gamma_\mu \partial_\mu + M)\,\Psi_0 = 0\,,$$

one gets

$$\varkappa = -\frac{2g}{\mu^2}\,M\,\Delta_F(0, M)\,,$$

$$M = K + \frac{2g^2}{\mu^2}\,M\,\Delta_F(0, M)\,,$$

$$m^2 = \mu^2\,.$$

We mention that this approximation for

$$\overline{\Psi}\,\Psi \to \overline{\Psi}\,\Omega\,\Psi$$

with Ω containing odd numbers of γ-s gives $\varkappa = 0$, $M = K$; thus e.g. with $\Omega = \gamma_5$, Φ pseudoscalar, the parity cannot be spontaneously violated by $\varkappa \neq 0$ unless $K = 0$.

The results of this approximation for the first Goldstone model

$$(\Box - \mu^2)\,\Phi = g\,\Phi^3\,,$$
$$\Phi = \varkappa + \varphi\,, \quad (\Box - m^2)\,\varphi = 0\,,$$

are widely known [5, 7, 8]:

$$\varkappa\left[g\,\varkappa^2 + \mu^2 + g\,\frac{3}{2}\,\Delta_F(0, m)\right] = 0\,,$$

$$m^2 = \mu^2 + 3g\left[\varkappa^2 + \frac{1}{2}\,\Delta_F(0, m)\right],$$

with the consequence that $\varkappa \neq 0$ does not imply $m^2 = 0$. The symmetry transformation

$$\Phi \to -\Phi$$

gives for φ

$$\varphi \to -\varphi - 2\varkappa$$

which is again a constant gauge transformation but now for a non-zero mass particle. The same consequences follow also for the second Goldstone model

$$(\Box - \mu^2)\,\Phi_i = g\,[\Phi_1^2 + \Phi_2^2]\,\Phi_i\,, \qquad \mathrm{i} = 1{,}2\,.$$

Requiring [5]

$$\begin{aligned} \Phi_1 &= \varkappa + \varphi_1\,, \quad (\Box - m_1^2)\,\varphi_1 = 0\,, \\ \Phi_2 &= \varphi_2\,, \quad (\Box - m_2^2)\,\varphi_2 = 0 \end{aligned} \tag{12}$$

implies

$$\varkappa\left[g\,\varkappa^2 + \mu^2 + g\,\frac{3}{2}\,\Delta_F(0, m_1) + g\,\frac{1}{2}\,\Delta_F(0, m_2)\right] = 0\,,$$

$$m_1^2 = \mu^2 + 2g\,\varkappa^2 + g\left[\varkappa^2 + \frac{3}{2}\,\Delta_F(0,\ m_1) + \frac{1}{2}\,\Delta_F(0,\ m_2)\right],$$

$$m_2^2 = \mu^2 + g\left[\varkappa^2 + \frac{3}{2}\,\Delta_F(0, m_2) + \frac{1}{2}\,\Delta_F(0, m_1)\right],$$

with the result that from $\varkappa \neq 0$ does not follow $m_i = 0$. The symmetry transformations

$$\Phi_1 \to -\Phi_1\,; \quad \Phi_1 \to \Phi_2\,, \quad \Phi_2 \to \Phi_1$$

e.t.c. again induce a constant gauge transformation

$$\varphi_1 \to -\varphi_1 - 2\varkappa\,; \quad \varphi_1 \to \varphi_2 - \varkappa\,, \quad \varphi_2 \to \varphi_1 + \varkappa$$

while the continuous symmetry transformation

$$\Phi \to e^{\,i\Theta\tau}\Phi\,, \quad \Phi = \begin{pmatrix}\Phi_1\\ \Phi_2\end{pmatrix}, \quad \tau = \begin{pmatrix}0 & -i\\ i & 0\end{pmatrix}$$

corresponding to the conserved current

$$j_\mu = -\,i\,\alpha\,\frac{\partial\Phi}{\partial x_\mu}\,\tau\,\Phi = \alpha\,[\Phi_1\,\partial_\mu\Phi_2 - \Phi_2\,\partial_\mu\Phi_1]\,, \qquad \partial_\mu j_\mu = 0\,,$$

expressed by φ is

$$\varphi \to e^{i\Phi\tau}\,\varphi + (e^{i\Phi\tau} - 1)\,\varkappa\,, \quad \varphi = \begin{pmatrix}\varphi_1\\ \varphi_2\end{pmatrix}, \quad \varkappa = \begin{pmatrix}\varkappa\\ 0\end{pmatrix}.$$

Because of the lack of a Goldstone particle, and a mass splitting, in this approximation j_μ is not conserved. Indeed

$$\partial_\mu j_\mu = a\left[\varkappa m_2^2 \varphi_2 + (m_2^2 - m_1^2)\varphi_1 \varphi_2)\right]. \tag{13}$$

$\varkappa = 0$, of course, gives a conserved current since then also $m_1^2 = m_2^2$. These results are not consequences of the asymmetric assumption (12), which can be required without loss of generality owing to the apparent $R(2)$ symmetry.

The above approximation method seems to be more suitable in case of the pair interaction theory

$$(\Box - \mu^2)\Phi = 2g\,\overline{\Psi}\Psi\Phi\,,$$

$$(\gamma_\mu \partial_\mu + K)\Psi = -g\,\Phi^2\Psi\,.$$

Supposing here

$$\Phi = \varkappa + \varphi\,, \quad (\Box - m^2)\varphi = 0\,,$$

$$\Psi = \Psi_0\,, \quad (\gamma_\mu \partial_\mu + M)\Psi_0 = 0$$

one gets

$$\varkappa\left(\mu^2 - 4g\,M\,\Delta_F(0, M)\right) = 0\,,$$

$$m^2 = \mu^2 - 4g\,M\,\Delta_F(0, M)\,,$$

$$M = K - g\left(\varkappa^2 + \frac{1}{2}\Delta_F(0, m)\right),$$

which for $\varkappa \neq 0$ gives $m^2 = 0$, thus a Goldstone boson appears. The symmetry transformation

$$\Phi \to -\Phi$$

induces

$$\varphi \to -\varphi - 2\varkappa\,.$$

3. Having analysed these models we find two types of transformations. Since after solving the problem they are applied to free fields, one can write them down explicitely. In the first group one finds well-known transformations like

$$\varphi \to \varphi' = \pm\varphi\,, \quad \varphi_{1,2} \to \varphi' = \pm\varphi_{2,1}\,, \quad \varphi \to \varphi' = e^{i\Theta\tau}\varphi,$$

etc. In the case of $\varkappa \neq 0$ they appear together with a constant field translation (second group). Thus the operator performing the whole transformation

$$U\,\varphi\,U^{-1} = \varphi'$$

consists of two parts

$$U = V\,U\,.$$

U performing the translation, V the more familiar remaining transformation. Let us start with U, which is the necessary consequence of $\varkappa \neq 0$. The solution of the free-field equation can be written as

$$\varphi(x) = \frac{1}{(2\pi)^{3/2}} \int \frac{1}{\sqrt{2\, k_0(k)}} \left(a(k)\, e^{ikx} + a^*(k)\, e^{-ikx}\right) dk\,,$$

$$k_0(k) = \sqrt{k^2 + m^2} \tag{14}$$

On the algebra of the creation and annihilation operators characterized by the usual commutation relations the transformation

$$U\, a(k)\, U^+ = a(k) + f(k)\,,$$
$$U\, a^*(k)\, U^* = a^*(k) + f^*(k)\,,$$

where $f(k)$ is a c-number function is performed by the formally unitary form

$$U = e^B, \quad B = \int \left(f^*(k)\, a(k) - f(k)\, a^*(k)\right) dk\,. \tag{15}$$

U is a unitary operator over the Fock space of φ then and only then if

$$\int |f(k)|^2\, dk < \infty\,. \tag{16}$$

$\varphi \to \varphi + \varkappa$ requires

$$f(k) = (2\pi)^{3/2} \sqrt{2k_0(k)}\; e^{ik_0(k)x_0} \frac{c}{2}\, \delta(k)\,.$$

If $m^2 \neq 0$, U possesses a well-defined form, but since f is not square integrable, it is not a unitary operator over the Fock space. Thus of course e.g. $U\,|\,0> \neq |\,0>$. Moreover in this case U is *time-dependent*. Thus at the same time when $\varkappa \neq 0$ does not imply $m^2 = 0$, that is when the Goldstone theorem is not valid, U no longer has the privilege to be associated with any conserved quantity.

From this point of view Gondstone's theorem must be necessarily valid, making first U time-independent. But if so, i.e. if $m^2 = 0$, U — and as a matter of fact (14) — formally (that is already algebra) is not well defined, and cannot be defined in a simple way. For example turning instead of (14) to finite volume and exempting the zero mode does not help much. One can visualise things here by some kind of limiting process; this may be e.g. $m^2 \to 0$. An other possibility which was worked out from an other point of view in more detail is to fix $m^2 = 0$, but to allow to change $\varkappa$ slightly on x. More accurately, we keep $f(k)$ concentrated around zero in such a way that

$$\int |f(k)|^2\, dk = \infty\,,$$

but

$$\int |k| |f(k)|^2 dk < \infty .$$

Then the following happens [9]: U is a well-defined time-independent unitary form on the algebra but because of (16), it is not defined as unitary operator over the Fock space of the $a(k)$-s; $U \mid 0> \neq \mid 0>$. On the Fock space, of course, the Lorentz group is represented possessing a normalised vacuum state $\mid 0>$. The algebra of the $a(k)$-s, φ and *also* the translation group is represented on the Fock space of the operators, $b(k) = a(k) + f(k)$, $b(k) \mid 0>_b = 0$, ${}_b<0 \mid 0>_b = 1$ but here $P_0 = H$ does not have any normalised eigenstate. Furthermore, for physically observable quasilocal operators these two representations are equivalent. Formally

$$\mid 0>_b = U \mid 0> ,$$

thus U can be regarded as an operator connecting two physically equivalent representation spaces. Physically the situation is extremely simple from the beginning. $U \mid 0>$ corresponds to a state, where an infinite number of zero mass zero momentum particles are swarming around, which from every practical point of view cannot be distinguished from the empty vacuum, but this state is not contained in the Fock space.

At the end the fact remains, that if $\varkappa \neq 0$, $U \mid 0> \neq \mid 0>$ therefore the usual nomenclature as "spontaneous symmetry breaking" is justified.

In the above examples the other constituents of the transformations are much more familiar. V has to be also time-independent. Thus e.g. V cannot perform an exchange of two fields φ_i with different masses.

From the point of view of our examples in the first exactly soluble model everything is fulfilled. In the second Goldstone model the approximation (12) destroyed completely the symmetry. Here

(i) because of the lack of the Goldstone boson U becomes time-dependent,

(ii) since $m_1^2 \neq m_2^2$, V performing

$$V \varphi V^* = e^{i\Theta\tau} \varphi ,$$

$$V = e^{iF\Theta}, \quad F = i \int \dot{\varphi} \tau \varphi \, dx ,$$

becomes time-dependent [cf. (13)] non-existing operator over the Fock space.

In the most general case $\varkappa \neq 0$, the transformation $\Phi \to \Phi'$ produces a change $\varkappa \to \varkappa' =$ another c number. This can hardly be produced otherwise than by a constant gauge transformation of the φ fields. Thus the role of the Goldstone particle is to produce a time-independent unitary form which is not represented on the Fock space.

REFERENCES

1. J. G. Taylor, Nuovo Cimento, Suppl. I. **1,** 857, 1963.
2. K. L. Nagy, T. Nagy and G. Pócsik, Acta Phys. Hung., **19,** 91, 1965.
3. H. Umezawa and L. Leplace, R. N. Sen and H. Umezawa, Naples preprints, 1965.
4. S. Kamefuchi and H. Umezawa, Nuovo Cimento, **31,** 429, 1964.
5. H. Umezawa, Nuovo Cimento, **38,** 1416, 1965.
6. W. S. Hellman and P. Roman, Boston Univ. preprint, 1965.
7. G. Marx, Phys. Rev., **140B,** 1683, 1965.
8. G. Kuti and G. Marx, Acta Phys. Hung., **19,** 67, 1965.
9. H. J. Borchers, R. Haag and B. Schroer, Nuovo Cimento, **29,** 148, 1963.

СПОНТАННОЕ НАРУШЕНИЕ СИММЕТРИИ И ПОСТОЯННЫЕ КАЛИБРОВОЧНОГО ПРЕОБРАЗОВАНИЯ

К. Л. НАДЬ

Р е з ю м е

Исследуются решения нескольких модельных теорий, нарушающие симметрию с результатом, согласно которому постоянные калибровочного преобразования полей описывающих частиц Голдстона нулевой массы, ответственны за формальную возможность спонтанного нарушения симметрии.

Acta Physica Academiae Scientiarum Hungaricae, Tomus 23 (1), pp. 29—35 (1967)

MAGNETIC GROUND STATE SPIN CONFIGURATIONS IN FACE-CENTRED CUBIC AND Cu_3Au-TYPE CRYSTALS

By

M. PÓSCH and E. KRÉN

CENTRAL RESEARCH INSTITUTE FOR PHYSICS, BUDAPEST

(Presented by L. Pál — Received 31. III. 1966)

Assuming various interaction pairs, the generalized LUTTINGER—TISZA method (GLTM) is used to determine the ground state spin configurations in face-centred cubic and Cu_3Au-type lattices. The configurations assigned as obtained in terms of magnetic interactions include, with a few exceptions, every magnetic structure observed in the above types of crystal lattices and permit for systems with various ground state spin configurations to establish unambiguously the predominant interactions and to estimate their sign as well as their relative magnitudes. Finally some experimental observations are discussed in the light of the results obtained by the GLT method.

The growing number of magnetic structures observed in experiments has stimulated the theoretical formulation of the problem. The possible magnetic structures can be evaluated either from the LANDAU—LIFSHITZ theory of second order phase transformations, minimizing the free energy set up from symmetry considerations or with the use of a phenomenological Hamiltonian formulated from actual magnetic interactions [1].

Using the LUTTINGER—TISZA method generalized by LYONS and KAPLAN [2], it is possible to minimize the HEISENBERG exchange energy

$$E_{ex} = -\sum_{f,g} I_{fg} \hat{S}_f \hat{S}_g .$$

Except for some cases the possible ground state spin configurations can be obtained as functions of magnetic interactions from the minimized energy in terms of their Fourier components at $T = 0$ °K. The magnetic moment of the ν-th atom in the n-th cell is

$$S_{n\nu} = \sum_k S_k \, e^{ikR n\nu}.$$

For given crystal structures the spin configurations can be specified by the wave vectors $k = (k_x, k_y, k_z)$ and by the directions S_k (k is given in units of $\frac{\pi}{a}$, where a is the lattice parameter).

The GLTM was used for the evaluation of magnetic structures in face-centred cubic and Cu_3Au-type crystal lattices by considering interaction pairs

formed from interactions between first, second and third neighbours, symbolized by J_1, J_2 and J_3, respectively. $J < 0$ is taken to be ferromagnetic, $J > 0$ antiferromagnetic interaction. The following cases were investigated:

1) Face-centred cubic lattice with J_1, J_2 interaction;
2) Cu_3Au-type lattice
   a) J_2, J_3 interaction, with $S = 0$;
   b) J_1, J_2 interaction, with $S < 1$ (where S is the absolute value of the ratio of moments of face-centre to corner lattice sites).

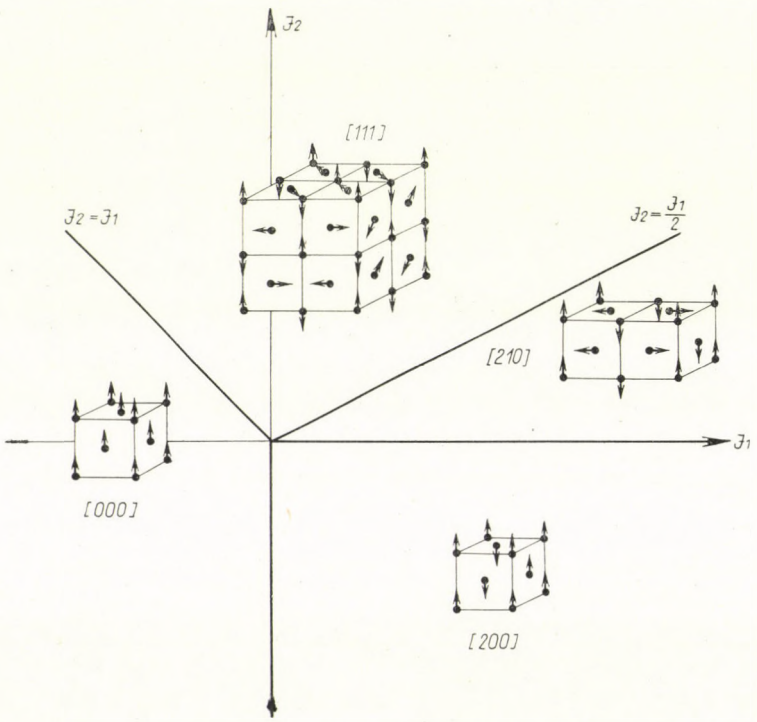

Fig. 1. Ground state spin configurations in face-centred cubic lattice with J_1 and J_2 interactions. The angles between magnetic moments and crystallographic axes and the angles between non-parallel magnetic moments are arbitrary

The ground state spin configurations assigned in terms of magnetic interactions to face-centred cubic and Cu_3Au-type lattices are seen in Figs 1, 2 and 3, respectively. Fig. 2 illustrates at the same time the structures in primitive magnetic lattice with first and second neighbour interactions. For the face-centred cubic lattice it would be easy to obtain the results also for the combinations J_1, J_3, but J_3 interaction does not seem likely for physical reasons.

The structures obtained can be characterized as follows.

In both the face-centred cubic and the Cu_3Au-type lattices the [000] structure is collinear ferromagnetic. The [000]* structure is collinear ferrimagnetic (the asterisk* indicates that the directions S_k in the face-centres are opposite to those in the [000] structure).

The configurations [100], [110] and [200] are characterized by antiparallel coupling of the ferromagnetic planes (100), (110) and (200).

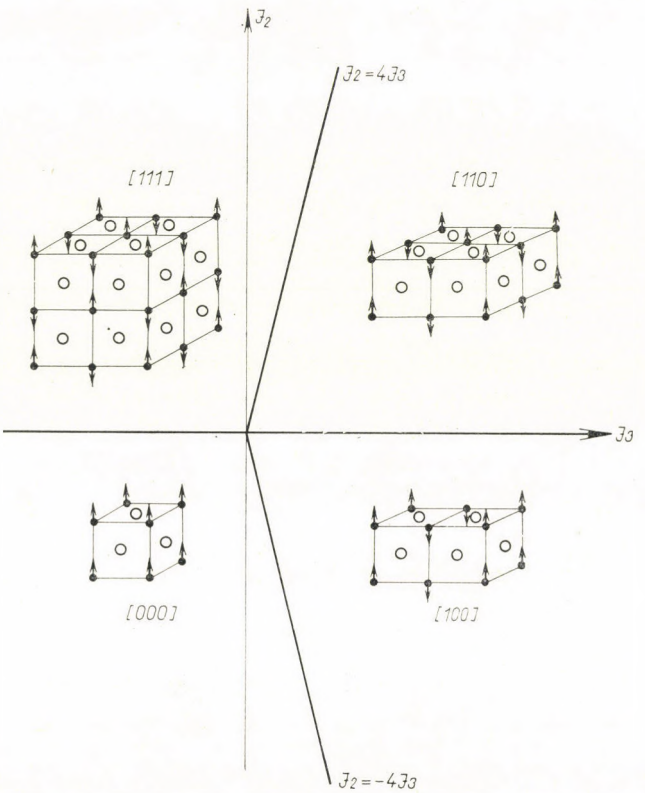

Fig. 2. Ground state spin configurations in Cu_3Au type lattice with J_2 and J_3 interactions, $S = 0$. The angles between magnetic moments and crystallographic axes are arbitrary

For the [111] configuration in Cu_3Au-type lattice the second neighbours (first neighbours in the primitive lattice) are oriented in antiparallel directions. In face-centred lattices the configuration [111] is composed of four [111] sublattices oriented independently of one another, the structure is generally non-collinear.

The structure [210] is a combination of four sublattices, three of them being of [100], while one of [001] type, collinearly coupled per pair and the two pairs may have any relative orientations.

In the configuration [[000] + [111]] and [[000]* + [111]], a [111] structure is added normal to one of the sublattices (at the corner) of the [000] and the [000]* structures, respectively.

In the vacant area shown in Fig. 3 the GLT method did not yield and result.

The angles between the directions of the crystallographic axes and the magnetic moments and in many cases even the relative positions of the sub-

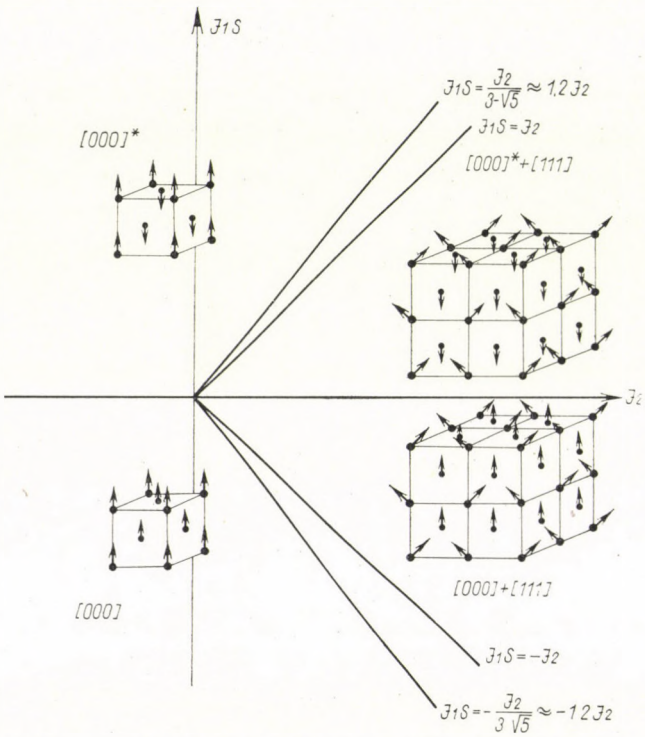

Fig. 3. Ground state spin configurations in Cu_3Au type lattice with J_1 and J_2 interactions, $S < 1$. The angles between magnetic moments and crystallographic axes are arbitrary

lattices cannot be determined from the minimized HEISENBERG energy, these could be evaluated by taking account of the anisotropic energy too.

For interactions at the boundaries the two different configurations as well as the complex structures obtainable from them have the same exchange energies. The structure which is actually realized is again determined by the neglected second order energy terms. Since at the boundaries the interactions are balanced, weak and long range interactions as well as other perturbations may also assert themselves and produce modified and unstable versions of the above structures.

The calculations were performed for $T = 0°K$. Since it has been shown by SMART [3] that for a single species of magnetic atom the structures obtained in the molecular field approximation from both the minimized free and the minimized magnetic energies are identical, if the magnetic interactions are assumed to be constant, Figs. 1, 2 and 3 hold up to the Curie point. It follows that the results can be compared with experimental data obtained at $T > 0$ in the cases where no phase transformation occurs below the temperature T.

The results summarized in Figs. 1, 2 and 3 enable one to select unambiguously the dominant interactions and to estimate their sign and magnitude

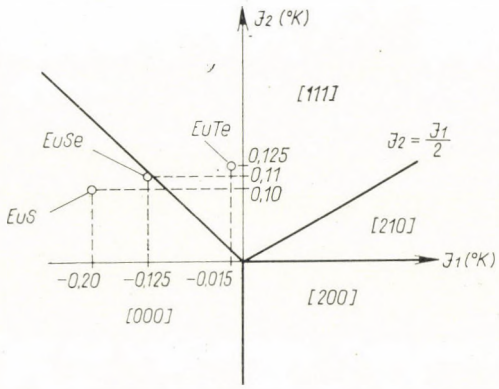

Fig. 4. Variation of magnetic interactions in Eu compounds

in systems where the ground state spin configuration (the magnetic structure measured at low temperatures) is observed to vary with the chemical composition. In the following some experiments will be considered in this light.

The EuO, EuS, EuSe, EuTe series (NaCl-type crystal, face-centred cubic magnetic lattice) was investigated by MCGUIRE et al. [4]. EuO and EuS are ferromagnetic, EuTe [111] antiferromagnetic, while EuSe is a modified [111] structure which transforms in external magnetic field first to the combination of [111] and [000] structures, then to pure [000] [5]. In Fig. 1 the transition observed in the magnetic structure is well apparent and shows that this series can be described by predominantly J_1, J_2 interactions while the interactions in EuSe seem to lie on the boundary between the [000] and [111] configurations. It can be seen from the Figure that by going from EuS towards EuTe (increasing the lattice parameter) the ratio J_2/J_1 increases. The values of J_1 and J_2 calculated from the experimental data [4] in molecular field approximation have been plotted in Fig. 4. The picture is seen to be in agreement with the predictions.

A similar transition in magnetic structure is observable in the NaCl-type compounds of rare earth metals with nitrogen group elements. The nitrides

are ferromagnetic (somewhat modulated) the phosphides are either combinations of [000] and [111] structures (HoP, DyP), or pure [111] type (ErP, TbP), while the antimonides are of [111] structure [6]. The structures of phosphides are unstable and transform in external magnetic field to ferromagnetic. These compounds too can be described by J_1, J_2 interactions. In phosphides and, to a smaller extent, in nitrides the interactions are assumed to be close to the boundary. The complex (canted) structures of HoP and DyP are stabilized by dipolar forces [7].

The change in magnetic structure, observed also in the group of MnS_2, $MnSe_2$, $MnTe_2$ (FeS_2-type) compounds [8], can be interpreted in a similar way from J_1 and J_2 interactions by making use of Fig. 1. MnS_2 is of [210], $MnTe_2$ of [200], while $MnSe_2$ of an intermediate structure of the [210] kind, not illustrated in the Figure.

The variation of the exchange interactions in the above examples may be attributed to a change in lattice parameter.

The effect of anisotropy energy which has not been taken into account in present calculations, is well manifested by the FeO, NiO, MnS, MnSe, CoO group of NaCl-type compounds. Their magnetic structures are of the [111] type, but with different orientations of magnetic moments relative to the crystallographic axes [8], moreover, contrary to the other compounds of the series, CoO is non-collinear, the four sublattices lying at oblique angles to one another [9].

The configurations in Figs 1, 2 and 3 include thus all structures observed in face-centred cubic and Cu_3Au-type lattices to our knowledge, with the only exception of CrN [10] which has NaCl-type crystal and collinear magnetic structure consisting of four [110] sublattices. This type of structure can be well interpreted for face-centered cubic lattice from J_2 and J_3 interactions, but the assumption of J_3 interaction does not seem to be reasonable.

In spite of the known limitations of the HEISENBERG model the above calculations prove to be useful if qualitative inferences are to be drawn from experimental data.

REFERENCES

1. E. F. BERTAUT, Magnetism, Vol. III. Edited by B. T. RADÓ and H. SUHL, Academic Press New York, London 1963.
2. D. H. LYONS and T. A. KAPLAN, Phys. Rev., **120,** 1580, 1960.
3. J. S. SMART, Phys. Rev., **90,** 55, 1953.
4. T. R. MCGUIRE and M. W. SHAFER, J. Appl. Phys., **35,** 984, 1964.
5. S. J. PICKART and H. A. ALPERIN, Bull. Am. Phys. Soc,. **10,** 32, 1965.
6. H. R. CHILD, M. K. WILKINSON, J. W. CABLE, W. C. KOEHLER and E. O. WOLLAN, Phys. Rev., **131,** 922, 1963.
7. G. T. TRAMMEL, Phys. Rev., 131, 932, 1963.
8. G. E. BACON, Neutron Diffraction, 2nd Edition, Clarendon Press, Oxford, 1962.
9. B. VAN LAAR, Phys. Rev., **138,** A 584, 1965.
10. L. M. CORLISS, N. ELLIOTT and J. M. HASTINGS, Phys. Rev., 117, 929, 1960.

МАГНИТНОЕ ОСНОВНОЕ СОСТОЯНИЕ СПИН-КОНФИГУРАЦИИ В ГРАНЕЦЕНТРИРОВАННЫХ КУБИЧЕСКИХ КРИСТАЛЛАХ И В КРИСТАЛЛАХ ТИПА Cu_3Au

М. ПОШ и Е. КРЕН

Р е з ю м е

Предполагая разные взаимодействующие пары, для определения спин-конфигураций основного состояния в гранецентрированных кубических решетках и в решетках типа Cu_3Au используется обобшенный метод Луттингера—Тисы (ОМЛТ). Конфигурации, полученные на основе магнитных взаимодействий, содержат с некоторыми исключениями все магнитные структуры, обнаруженные в кристаллических решетках упомянутых выше типов и разрешат для систем с разными спин-конфигурациями основного состояния определять однозначно преобладающие взаимодействия и судить как об их знаке, так и об их относительной величине. Наконец, используются несколько экспериментальных наблюдений в свете результатов ОМЛТ.

Acta Physica Academiae Scientiarum Hungaricae, Tomus 23, (1), pp. 37—51 (1967)

ALGEBRAIC METHODS IN THE THEORY OF SPECIAL UNITARY GROUPS

II. QUASISPIN AND MULTIPLET STRUCTURE

By

A. SEBESTYÉN and J. NYIRI

CENTRAL RESEARCH INSTITUTE FOR PHYSICS, BUDAPEST

(Presented by L. Jánossy. — Received 31. III. 1966)

In this paper a simple method revealing the multiplet structure of irreducible representations of SU(3) is discussed.

In the preceding paper [1] we calculated the generator matrix elements of SU(3). Using the same algebraic techniques, we now turn to the multiplet structure of the irreducible representation (I. R.) of SU(3). However, before doing so, we introduce some general notions which shall be used in this and the following papers. These general remarks will be made in Section 1, while in Section 2 we shall deal with the multiplet structure of weights in an I. R. of SU(3). We shall derive formulae for dimensions, number of weights and excess.

1.

It is well known that the generators of any compact semisimple Lie algebra may be arranged in such a manner, that they fulfill the following commutation rules:

$$[H_i, H_k] = 0, \qquad i, k = 1, \cdots, l,$$

$$[\vec{H}, E_\alpha] = \vec{r}(\alpha) E_\alpha, \qquad \vec{H} = (H_1, \cdots, H_l),$$

$$[E_\alpha, E_{-\alpha}] = \vec{r}(\alpha)\vec{H}, \quad \vec{r}(\alpha) = (r_1(\alpha), \cdots, r_l(\alpha)), \quad \vec{r}(-\alpha) = -\vec{r}(\alpha) \quad E_\alpha^+ = E_{-\alpha}$$

$$[E_\alpha, E_\beta] = N_{\alpha\beta}^{\gamma} E_\gamma. \tag{1}$$

All the related notions (rank, root vectors e.t.c.) and properties of structure constants can be found in e.g. [2]. In the case of SU(3) the relations between this basis and the generators introduced in [1] are the following

$$H_1 = \frac{1}{\sqrt{3}} I_z, \quad E_1 = \frac{1}{\sqrt{6}} I_+, \quad E_{-1} = \frac{1}{\sqrt{6}} I_-,$$

$$H_2 = \frac{1}{2} Y, \quad E_2 = \frac{1}{\sqrt{6}} F_+, \quad E_{-2} = \frac{1}{\sqrt{6}} G_-,$$

$$E_3 = \frac{1}{\sqrt{6}} F_-, \quad E_{-3} = -\frac{1}{\sqrt{6}} G_+, \tag{2}$$

$$\vec{r}(1) = \left(\frac{1}{\sqrt{3}}, 0\right),$$

$$\vec{r}(2) = \left(\frac{1}{2\sqrt{3}}, \frac{1}{2}\right), \qquad \vec{r}^2(\alpha) = \frac{1}{3}.$$

$$\vec{r}(3) = \left(-\frac{1}{2\sqrt{3}}, \frac{1}{2}\right).$$

We introduce now the notion of quasispin. We define the operators

$$S_{\pm}(\alpha) = \sqrt{\frac{2}{(\vec{r}(\alpha)\vec{r}(\alpha))}}\, E_{\pm\alpha},$$

$$S_z(\alpha) = \frac{(\vec{r}(\alpha)\vec{H})}{(\vec{r}(\alpha)\vec{r}(\alpha))}.$$

As it is easily seen from relations (1), these quantities satisfy

$$[S_+(\alpha), S_-(\alpha)] = 2\, S_z(\alpha),$$

$$[S_z(\alpha), S_{\pm}(\alpha)] = \pm\, S_{\pm}(\alpha)$$

which are the well known rules of the SU(2) algebra. We call $S_{\pm}(\alpha)$ and $S_z(\alpha)$ the generators of the α-th quasispin of the Lie algebra. In [1], for the case of SU(3), we have introduced a labelling system $| T, M, Y >$ of an I. R. Now we see that for a fixed value of Y we have achieved actually the arrangement of states according to the first quasispin (so-called I-spin) multiplets of SU(3) as

$$S_{\pm}(1) = \sqrt{\frac{2}{(\vec{r}(1)\vec{r}(1))}}\, E_{\pm 1} = I_{\pm},$$

$$S_z(1) = \frac{(\vec{r}(1)\vec{H})}{(\vec{r}(1)\vec{r}(1))} = \sqrt{3}\, H_1 = I_z,$$

where we have used relations (2).

Naturally, it is possible to arrange the states of an I. R. of SU(3) according to its second or third quasispin multiplet, which are called V- and U-spin, respectively. That would correspond to different choices of SU(2) subgroups of SU(3) in BIEDENHARN's labelling theorem. (See [3] and Section 1 of [1].) The different quasispin representations are related to each other by the Weyl reflections; this problem will be discussed in detail in the next paper.

2.

In this section we consider the multiplet structure of an I. R. of SU(3) specified by λ and μ, denoted by $D(\lambda, \mu)$ in the following. We make use of the generators of [1], for which we find

$$[I_z, I_\pm] = \pm I_\pm\,, \qquad [I_+, I_-] = 2\,I_z\,, \tag{3}$$

$$[I_+, F_-] = F_+\,, \qquad [I_z, F_\pm] = \pm\frac{1}{2}F_\pm\,, \tag{4}$$

$$[I_+, G_-] = G_+\,, \qquad [I_z, G_\pm] = \pm\frac{1}{2}G_\pm\,, \tag{5}$$

$$[Y, F_\pm] = F_\pm\,, \qquad [Y, G_\pm] = -G_\pm\,, \tag{6}$$

$$[F_\pm, G_\pm] = \mp I_\pm\,, \qquad [F_\pm, G_\mp] = I_z \pm \frac{3}{2}Y\,. \tag{7}$$

All the other commutators are zero.

$$Y\,|\,T, M, Y> = Y\,|\,T, M, Y>\,, \tag{8}$$

$$\begin{aligned} I^2\,|\,T, M, Y> &= T(T+1)\,|\,T, M, Y>\,,\\ I_z\,|\,T, M, Y> &= M\,|\,T, M, Y>\,,\\ I_\pm\,|\,T, M, Y> &= \sqrt{(T \mp M)(T \pm M + 1)}\,|\,T, M, Y>\,, \end{aligned} \tag{9}$$

$$\left.\begin{aligned} &F_\pm\,|\,T, M, Y> =\\ &= \sqrt{\frac{T \pm M + 1}{2T+1}}\,\alpha(TY)\left|\,T + \frac{1}{2}, M \pm \frac{1}{2}, Y + 1\right\rangle \mp\\ &\mp \sqrt{\frac{T \mp M}{2T+1}}\,\beta(TY)\cdot\left|\,T - \frac{1}{2}, M \pm \frac{1}{2}, Y + 1\right\rangle,\\ &G_\pm\,|\,T, M, Y> =\\ &= \mp\sqrt{\frac{T \mp M}{2T}}\,\alpha\left(T - \frac{1}{2}Y - 1\right)\left|\,T - \frac{1}{2}, M \pm \frac{1}{2}, Y - 1\right\rangle -\\ &- \sqrt{\frac{T \pm M + 1}{2T+2}}\,\beta\left(T + \frac{1}{2}Y - 1\right)\left|\,T + \frac{1}{2}, M \pm \frac{1}{2}, Y - 1\right\rangle, \end{aligned}\right\} \tag{10}$$

$$\alpha(TY) =$$
$$= \left[\frac{\left(\frac{\lambda-\mu}{3}+T+\frac{Y}{2}+1\right)\left(\frac{2\lambda+\mu}{3}-T-\frac{Y}{2}\right)\left(\frac{\lambda+2\mu}{3}+T+\frac{Y}{2}+2\right)}{2T+2}\right]^{1/2},$$

$$\beta(TY) =$$
$$= \left[\frac{\left(\frac{2\lambda+\mu}{3}+T-\frac{Y}{2}+1\right)\left(\frac{\mu-\lambda}{3}+T-\frac{Y}{2}\right)\left(\frac{\lambda+2\mu}{3}-T+\frac{Y}{2}+1\right)}{2T}\right]^{1/2}. \tag{11}$$

First we make a few general remarks. We call a pair (M, Y) occurring in an I. R. a weight. We emphasise that this definition differs slightly from that used in the general canonical scheme of Lie algebras.

We say, that (M_1, Y_1) is higher than (M_2, Y_2), if

a) $M_1 > M_2$ or

b) if $M_1 = M_2$ then $Y_1 > Y_2$.

Let us suppose that a generator Z has the following property for a state $|T, M, Y>$

$$Z|T, M, Y> = \varrho\,|T, M, Y>,$$

where ϱ is a number and it may be zero.

Then the expression

$$A_1 A_2 \cdots A_i Z A_{i+1} \cdots A_n |T, M, Y>,$$

where A_j are arbitrary generators, and can be reduced in the following way:

$$A_1 A_2 \cdots A_i Z A_{i+1} \cdots A_n |T, M, Y> =$$
$$= \sum_{r=i+1}^{n} A_1 A_2 \cdots A_{r-1} [Z, A_r] A_{r+1} \cdots A_n |T, M, Y> +$$
$$+ A_1 A_2 \cdots A_n Z |T, M, Y> =$$
$$= \sum_{r=i+1}^{n} A_1 A_2 \cdots A_{r-1} [Z, A_r] A_{r+1} \cdots A_n |T, M, Y> +$$
$$+ \varrho A_1 \cdots A_n |T, M, Y>.$$

Obviously, the number of generators is less by one than in the initial expression. If in a term of the sum Z is still present this reduction can be repeated. We may conclude that the effect of any operator Z of a product of generators

on the state $|T, M, Y>$ is equivalent to the effect of a sum of products of generators containing no Z.

Now we try to obtain the values Y occurring in $D(\lambda, \mu)$. We have shown [1] that there is a state

$$\left| \frac{\lambda}{2}, \frac{\lambda}{2}, \frac{\lambda + 2\mu}{3} \right\rangle$$

corresponding to the largest value of Y in $D(\lambda, \mu)$

$$Y_{max} = \frac{\lambda + 2\mu}{3}$$

for which

$$F_+ \left| \frac{\lambda}{2}, \frac{\lambda}{2}, \frac{\lambda + 2\mu}{3} \right\rangle = F_- \left| \frac{\lambda}{2}, \frac{\lambda}{2}, \frac{\lambda + 2\mu}{3} \right\rangle =$$

$$= I_+ \left| \frac{\lambda}{2}, \frac{\lambda}{2}, \frac{\lambda + 2\mu}{3} \right\rangle = 0 ,$$

$$I_z \left| \frac{\lambda}{2}, \frac{\lambda}{2}, \frac{\lambda + 2\mu}{3} \right\rangle = \frac{\lambda}{2} \left| \frac{\lambda}{2}, \frac{\lambda}{2}, \frac{\lambda + 2\mu}{3} \right\rangle ,$$

$$Y \left| \frac{\lambda}{2}, \frac{\lambda}{2}, \frac{\lambda + 2\mu}{3} \right\rangle = \frac{\lambda + 2\mu}{3} \left| \frac{\lambda}{2}, \frac{\lambda}{2}, \frac{\lambda + 2\mu}{3} \right\rangle .$$

Because of irreducibility any state $|T, M, Y>$ may be obtained in the form of linear combinations of states

$$I_-^{\varrho} G_-^{\sigma} G_+^{\tau} \left| \frac{\lambda}{2}, \frac{\lambda}{2}, \frac{\lambda + 2\mu}{3} \right\rangle . \tag{12}$$

We note here that F_+, F_-, I_+, I_z and Y are not included as they fulfill the conditions of our general theorem. One might argue that the place of I_- relative to G_+ is relevant, but it is always possible to make adequate commutations and get the form (12).

Now the value Y of (12) is $\frac{\lambda + 2\mu}{3} - \sigma - \tau$, as the generators $G_\pm$ lower Y by one [see (6)], and I_- commutes with Y. This way in searching for the possible values of Y it is enough to consider the states

$$G_-^{\sigma} G_+^{\tau} \left| \frac{\lambda}{2}, \frac{\lambda}{2}, \frac{\lambda + 2\mu}{3} \right\rangle .$$

Our aim is now to determine those values of σ and τ for which

$$G_-^{\sigma} G_+^{\tau} \left| \frac{\lambda}{2}, \frac{\lambda}{2}, \frac{\lambda + 2\mu}{3} \right\rangle = 0 .$$

For this end we shall calculate the square of the norm $f(\sigma, \tau)$ of this state

$$f(\sigma,\tau) = (-1)^{\tau}\left\langle \frac{\lambda}{2}, \frac{\lambda}{2}, \frac{\lambda+2\mu}{3} \middle| F_-^{\tau} F_+^{\sigma} G_-^{\sigma} G_+^{\tau} \middle| \frac{\lambda}{2}, \frac{\lambda}{2}, \frac{\lambda+2\mu}{3} \right\rangle =$$

$$=(-1)^{\tau}\left\langle \frac{\lambda}{2}, \frac{\lambda}{2}, \frac{\lambda+2\mu}{3} \middle| F_-^{\tau} F_+^{\sigma-1}\left(\sum_{r=0}^{\sigma-1} G_-^{r}\left(I_z + \frac{3}{2}Y\right) G_-^{\sigma-r-1}\right) G_+^{\tau} \middle| \frac{\lambda}{2}, \frac{\lambda}{2}, \frac{\lambda+2\mu}{3} \right\rangle =$$

$$=(-1)^{\tau}\left\langle \frac{\lambda}{2}, \frac{\lambda}{2}, \frac{\lambda+2\mu}{3} \middle| F_-^{\tau} F_+^{\sigma-1} G_-^{\sigma-1} G_+^{\tau} \middle| \frac{\lambda}{2}, \frac{\lambda}{2}, \frac{\lambda+2\mu}{3} \right\rangle \sum_{r=0}^{\sigma-1} (\lambda+\mu-2\sigma-\tau+2r+2) =$$

$$= f(\sigma-1,\tau)\,\sigma\,(\lambda+\mu-\sigma-\tau+1),$$

where we made use of relations (7) and

$$(G_{\pm})^{+} = \mp F_{\mp},$$

$$I_z G_-^{\alpha} G_+^{\beta} \mid T, M, Y> = \left(M + \frac{\beta-\alpha}{2}\right) G_-^{\alpha} G_+^{\beta} \mid T, M, Y>,$$

$$Y G_-^{\alpha} G_+^{\beta} \mid T, M, Y> = (Y-\alpha-\beta)\, G_-^{\alpha} G_+^{\beta} \mid T, M, Y>,$$

[the last two being the consequences of (5), (6)]. Thus we have a recursion relation for $f(\sigma, \tau)$ in σ which may be solved giving

$$f(\sigma,\tau) = f(0,\tau)\,\sigma!\,\frac{(\lambda+\mu-\tau)!}{(\lambda+\mu-(\sigma+\tau))!}.$$

In the last equation $f(0, \tau)$ is the square of the norm of the state

$$G_+^{\tau}\left| \frac{\lambda}{2}, \frac{\lambda}{2}, \frac{\lambda+2\mu}{3} \right\rangle.$$

This quantity can be obtained by making use of a similar recursion procedure

$$f(0,\tau) = \tau!\,\frac{\mu!}{(\mu-\tau)!}.$$

Finally

$$f(\sigma,\tau) = \sigma!\,\tau!\,\frac{\mu!\,(\lambda+\mu-\tau)!}{(\mu-\tau)!\,(\lambda+\mu-(\sigma+\tau))!}.$$

From this we can see that for $\tau > \mu$ and $\tau + \sigma > \lambda + \mu$ we have $f(\sigma, \tau) = 0$, that is,

$$G_-^\sigma G_+^\tau \left| \frac{\lambda}{2}, \frac{\lambda}{2}, \frac{\lambda + 2\mu}{3} \right\rangle = 0 .$$

Thus the smallest value of Y corresponding to $D(\lambda, \mu)$ is

$$Y_{\min} = \frac{\lambda + 2\mu}{3} - (\lambda + \mu) = - \frac{2\lambda + \mu}{3} .$$

We see that for the values of Y occurring in $D(\lambda, \mu)$ the following statements are valid.

a) They differ from each other by integer values.

b) $Y_{\max} = \dfrac{\lambda + 2\mu}{3} \geqslant Y \geqslant - \dfrac{2\lambda + \mu}{3} = Y_{\min}$;

c) The number of possible values of Y is $N_Y = Y_{\max} - Y_{\min} + 1 = \lambda + \mu + 1$.

Making use of these results we construct the state with the largest value of T and M equal to T for a value of $Y = Y_{\max} - \tau$, where τ is integer; the operator leading to this state from $\left| \dfrac{\lambda}{2}, \dfrac{\lambda}{2}, \dfrac{\lambda + 2\mu}{3} \right\rangle$ must not contain I_- and G_- as these lower the value of M. Thus the operator in question is G_+^τ, and

$$(-1)^\tau \sqrt{f(0, \tau)} \left| T, T, \frac{\lambda + 2\mu}{3} - \tau \right\rangle = G_+^\tau \left| \frac{\lambda}{2}, \frac{\lambda}{2}, \frac{\lambda + 2\mu}{3} \right\rangle , \qquad (13)$$

where

$$T = \frac{\lambda + \tau}{2}$$

is a consequence of the fact that whenever G_+ acts on a state $| T, T, Y \rangle$, then $G_+ | T, T, Y \rangle$ has a definite value $T' = T + \dfrac{1}{2}$ as it might be seen from (10).

This procedure can be continued up to $\tau = \mu$.

$$G_+^\mu \left| \frac{\lambda}{2}, \frac{\lambda}{2}, \frac{\lambda + 2\mu}{3} \right\rangle = \mu! \left| \frac{\lambda + \mu}{2}, \frac{\lambda + \mu}{2}, \frac{\lambda - \mu}{3} \right\rangle ;$$

the state on the right hand side has the properties

$$F_+ \left| \frac{\lambda + \mu}{2}, \frac{\lambda + \mu}{2}, \frac{\lambda - \mu}{3} \right\rangle = G_+ \left| \frac{\lambda + \mu}{2}, \frac{\lambda + \mu}{2}, \frac{\lambda - \mu}{3} \right\rangle =$$

$$= I_+ \left| \frac{\lambda + \mu}{2}, \frac{\lambda + \mu}{2}, \frac{\lambda - \mu}{3} \right\rangle = 0 \qquad (14)$$

what can be verified e.g. by the inspection of the explicit forms (9), (10) and (11). As F_+, G_+, I_+ all raise the value of M by one, the weight $\left(\frac{\lambda+\mu}{2}, \frac{\lambda-\mu}{3}\right)$ of the state $\left|\frac{\lambda+\mu}{2}, \frac{\lambda+\mu}{2}, \frac{\lambda-\mu}{3}\right\rangle$ is the highest weight of $D(\lambda, \mu)$. A further lowering of the value of Y can be carried out by the application of G_-, giving succesively

$$G_-^\sigma \left|\frac{\lambda+\mu}{2}, \frac{\lambda+\mu}{2}, \frac{\lambda-\mu}{3}\right\rangle = \sqrt{\sigma! \frac{\lambda!}{(\lambda-\sigma)!}} \left| T, T, \frac{\lambda-\mu}{3} - \sigma \right\rangle, \quad (15)$$

where the normalization factor can be calculated by means of recursion and we have

$$T = \frac{\lambda+\mu}{2} - \frac{\sigma}{2}$$

and

$$I_+ G_-^\sigma \left|\frac{\lambda+\mu}{2}, \frac{\lambda+\mu}{2}, \frac{\lambda-\mu}{3}\right\rangle = \sigma G_-^{\sigma-1} G_+ \left|\frac{\lambda+\mu}{2}, \frac{\lambda+\mu}{2}, \frac{\lambda-\mu}{3}\right\rangle = 0$$

as G_- lowers the value of M by one half. The largest possible value of σ is $\sigma = \lambda$ and

$$G_-^\lambda \left|\frac{\lambda+\mu}{2}, \frac{\lambda+\mu}{2}, \frac{\lambda-\mu}{3}\right\rangle = \lambda \left|\frac{\mu}{2}, \frac{\mu}{2}, -\frac{2\lambda+\mu}{3}\right\rangle,$$

thus we have reached $Y_{\min}$.

We have constructed now the possible maximal T values T_Y for a fixed $Y = Y_{\max} - n$ (n integer). The successive action of I_- on these states will lead to any M occurring in $D(\lambda, \mu)$.

We give now a graphical representation of the possible weights (M, Y) in a coordinate system with axes M, Y. The so-called weight diagram will be represented by a lattice, having $\lambda + \mu + 1$ rows corresponding to the possible values Y, and each row is displaced symmetrically to the Y axis, with the highest $M = T_Y$ and the lowest $M = -T_Y$. In Figure 1 we have worked out the representation $\lambda = 7$, $\mu = 4$ with the highest row $Y_{\max} = \frac{\lambda+2\mu}{3} = 5$, and the lowest row $Y_{\min} = -\frac{2\lambda+\mu}{3} = -6$. The T_Y is increasing from $\frac{\lambda}{2} = \frac{7}{2}$ to $\frac{\lambda+\mu}{2} = \frac{11}{2}$. The point A is the highest weight of $D(7, 4)$, that is $\left(\frac{\lambda+\mu}{2}, \frac{\lambda-\mu}{3}\right) = \left(\frac{11}{2}, 1\right)$ in our case. The states (13) are displaced along the line AB while the states (15) can be found along AC.

Taking into consideration the selection rules:

$$\Delta M = \pm\frac{1}{2}, \quad \Delta Y = 1 \text{ for } F_{\pm}; \Delta M = \pm\frac{1}{2}, \quad \Delta Y = 1 \text{ for } G_{\pm};$$

$\Delta M = \pm 1$, $\Delta Y = 0$ for $I_{\pm}$, the effect of these generators can be represented by steps correponding to six different directions as it is indicated by arrows.

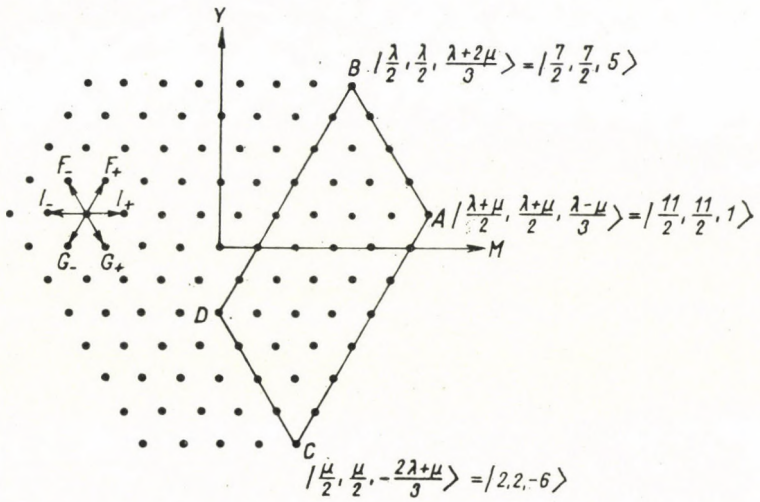

Fig. 1

It is possible now to determine the number of weights in $D(\lambda, \mu)$. The number of admissible values of M in a row Y, $M = 2\,T_Y + 1$ for the states (13) up to $\tau = \mu - 1$ is

$$\sum_{r=0}^{\mu-1}(2T_y + 1) = \sum_{r=0}^{\mu-1} 2\,\frac{\lambda + r}{2} + 1 = \frac{\mu}{2}(2\lambda + \mu + 1);$$

for the states (15) up to $\sigma = \lambda$

$$\sum_{r=0}^{\lambda}(2T_y + 1) = \sum_{r=0}^{\lambda} 2\,\frac{\lambda + \mu - r}{2} + 1 = \frac{\lambda + 1}{2}(\lambda + 2\mu + 2).$$

Thus the total number of weights is:

$$N_W = \frac{\mu}{2}(2\lambda + \mu + 1) + \frac{\lambda + \mu}{2}(\lambda + 2\mu + 2) =$$

$$= \frac{1}{2}(4\lambda\mu + \lambda^2 + \mu^2 + 3\mu + 3\lambda + 2).$$

In our case this is equal to 106.

However, the number of states generally exceeds the number of weights of $D(\lambda, \mu)$. This can be seen as follows. Let us consider a state $|T, T, Y>$ i.e. $I_+ \,|\, T, T, Y> = 0$. For the state $G_+ \,|\, T, T, Y>$ we have

$$G_+ \,|\, T, T, Y > \sim \left| T + \frac{1}{2}, T + \frac{1}{2}, Y - 1 \right\rangle$$

($\sim$ means: equal to, apart from a normalization factor). This is true because of the relations

$$I_z G_+ \,|\, T, T, Y > = \left(T + \frac{1}{2}\right) G_+ \,|\, T, T, Y > ,$$

$$Y\, G_+ \,|\, T, T, Y > = (Y - 1)\, G_+ \,|\, T, T, Y >$$

and $I_+ G_+ \,|\, T, T, Y> = 0$.

So for $I_- G_+ \,|\, T, T, Y>$ we have

$$I_- G_+ \,|\, T, T, Y > \sim \left| T + \frac{1}{2}, T - \frac{1}{2}, Y - 1 \right\rangle .$$

Now the state $\left(G_- - \dfrac{1}{2T+1} I_- G_+\right) |\, T, T, Y >$ has also the same weight as $I_- G_+ \,|\, T, T, Y>$:

$$I_z \left(G_- - \frac{1}{2T+1} I_- G_+\right) |\, T, T, Y > =$$

$$= \left(T - \frac{1}{2}\right) \left(G_- - \frac{1}{2T+1} I_- G_+\right) |\, T, T, Y > ,$$

$$Y \left(G_- - \frac{1}{2T+1} I_- G_+\right) |\, T, T, Y > =$$

$$= (Y - 1) \left(G_- - \frac{1}{2T+1} I_- G_+\right) |\, T, T, Y > .$$

However, the application of I_+ gives zero:

$$I_+ \left(G_- - \frac{1}{2T+1} I_- G_+\right) |\, T, T, Y > = \left(G_+ - \frac{2}{2T+1} I_z G_+\right) |\, T, T, Y > =$$

$$= \left(G_+ - \frac{2T+1}{2T+1} G_+\right) |\, T, T, Y > = 0 .$$

That means

$$\left(G_- - \frac{1}{2T+1} I_- G_+\right) |\, T, T, Y > \sim \left| T - \frac{1}{2}, T - \frac{1}{2}, Y - 1 \right\rangle .$$

So the states $I_-G_+ \mid T, T, Y>$ and $\left(G_- - \frac{1}{2T+1} I_-G_+\right) \mid T, T, Y>$ have the same weight but they are orthogonal to each other. The weight $\left(T - \frac{1}{2}, Y - 1\right)$ is at least a double weight, i.e. there are at least two orthogonal states with the same weight $\left(T - \frac{1}{2}, Y - 1\right)$. In this definition of multiple weights it would be enough to say 'linearly independent' instead of the attribute 'orthogonal'. It is just the operator $\left(G_- - \frac{1}{2T+1} I_-G_+\right)$ that will reveal the complete structure of multiple weights in $D(\lambda, \mu)$. Indeed, applying this operator to the state $\left|\frac{\lambda}{2}, \frac{\lambda}{2}, \frac{\lambda + 2\mu}{3}\right\rangle$ with $T = \frac{\lambda}{2}$, we have

$$\left(G_- - \frac{1}{\lambda+1} I_-G_+\right)\left|\frac{\lambda}{2}, \frac{\lambda}{2}, \frac{\lambda+2\mu}{3}\right\rangle \sim \left|\frac{\lambda-1}{2}, \frac{\lambda-1}{2}, \frac{\lambda+2\mu}{3} - 1\right\rangle.$$

The repeated application of $\left(G_- - \frac{1}{2T+1} I_-G_+\right)$ now with $T = \frac{\lambda-1}{2}$ will give

$$\left(G_- - \frac{1}{\lambda} I_-G_+\right)\left(G_- - \frac{1}{\lambda-1} I_-G_+\right)\left|\frac{\lambda}{2}, \frac{\lambda}{2}, \frac{\lambda+2\mu}{3}\right\rangle \sim$$

$$\sim \left|\frac{\lambda-2}{2}, \frac{\lambda-2}{2}, \frac{\lambda+2\mu}{3} - 2\right\rangle$$

and generally

$$\left[\prod_{r=1}^{\sigma}\left(G_- - \frac{1}{\lambda+2-r} I_-G_+\right)\right]\left|\frac{\lambda}{2}, \frac{\lambda}{2}, \frac{\lambda+2\mu}{3}\right\rangle \sim$$

$$\sim \left|\frac{\lambda-\sigma}{2}, \frac{\lambda-\sigma}{2}, \frac{\lambda+2\mu}{3} - \sigma\right\rangle. \tag{16}$$

All the weights $\left(\frac{\lambda-\sigma}{2}, \frac{\lambda+2\mu}{3} - \sigma\right)$ of the states on the right hand side of the last relation are situated along a straight line on the weight diagram which has the equation

$$Y = 2M - \frac{2}{3}(\lambda - \mu). \tag{17}$$

The maximal value of σ in (16) can be easily obtained by calculating the norm of the state on the left hand side by means of a recursion procedure.

$$\left|\left|\left[\prod_{r=1}^{\sigma}\left(G_- - \frac{1}{\lambda+2-r} I_- G_+\right)\right]\left|\frac{\lambda}{2}, \frac{\lambda}{2}, \frac{\lambda+2\mu}{3}\right\rangle\right|\right| =$$

$$= \left[\frac{\lambda!\,\sigma!\,(\lambda+\mu+1)!\,(\lambda-\sigma+1)!}{(\lambda-\sigma)!\,(\lambda+\mu-\sigma+1)!\,(\lambda+1)!}\right]^{1/2}.$$

Here the right hand side vanishes unless $\sigma \leqslant \lambda$. For $\sigma = \lambda$ we see from (16) that

$$\left[\prod_{r=1}^{\lambda}\left(G_- - \frac{1}{\lambda+2-r} I_- G_+\right)\right]\left|\frac{\lambda}{2}, \frac{\lambda}{2}, \frac{\lambda+2\mu}{3}\right\rangle \sim \left|0, 0, \frac{2}{3}(\mu-\lambda)\right\rangle,$$

which shows that the weight $\left|0, \frac{2}{3}(\mu-\lambda)\right|$ always appears in $D(\lambda, \mu)$ with $T = 0$. In Fig. 1 point D has this weight [in our case it is $(0, -2)$], and the line corresponding to (17) is the one which connects B and D. The fact that a value $T = 0$ always occurs in $D(\lambda, \mu)$, will be widely utilized in the next paper in the determination of phases of the Weyl reflections.

Now, starting from any state on the right hand side of (16), a sequence of states might be built up in the form

$$G_+^{\tau}\left|\frac{\lambda-\sigma}{2}, \frac{\lambda-\sigma}{2}, \frac{\lambda+2\mu}{3}-\sigma\right\rangle \qquad \tau = 1,2,\ldots$$

which have, as it was already shown, a definite value of T, i.e.

$$G_+^{\tau}\left|\frac{\lambda-\sigma}{2}, \frac{\lambda-\sigma}{2}, \frac{\lambda+2\mu}{3}-\sigma\right\rangle \sim$$
$$\sim \left|\frac{\lambda-\sigma+\tau}{2}, \frac{\lambda-\sigma+\tau}{2}, \frac{\lambda+2\mu}{3}-\sigma-\tau\right\rangle. \tag{18}$$

The maximal value of τ might be obtained by calculating the norm of the left hand side of (18).

$$\left|\left| G_+^{\tau}\left|\frac{\lambda-\sigma}{2}, \frac{\lambda-\sigma}{2}, \frac{\lambda+2\mu}{3}-\sigma\right\rangle\right|\right| =$$

$$= \left[\frac{(\lambda-\sigma+1)}{(\lambda+\tau-\sigma+1)} \frac{(\lambda+\tau+1)!\,\tau!\,\mu!\,(\lambda-\sigma)!}{(\lambda+1)!\,(\mu-\tau)!\,(\lambda-\sigma+\tau)!}\right]^{1/2}.$$

The last quantity vanishes unless $\tau \leq \mu$. The weights

$$\left(\frac{\lambda - \sigma + \tau}{2}, \frac{\lambda + 2\mu}{3} - (\sigma + \tau)\right)$$

lie all along the parallel lines

$$Y = -2M + \frac{2}{3}(2\lambda + \mu) - 2\sigma, \qquad 0 \leqslant \sigma \leqslant \lambda. \tag{19}$$

In Fig. 1 the line connecting points D and C is the one from set (19) which corresponds to $\sigma = \lambda$. For $\sigma = 0$ we get the line connecting B and A. It can be seen easily also that AC is parallel to BD. Thus the weights

$$\left(\frac{\lambda}{2}, \frac{\lambda + 2\mu}{3}\right), \left(0, \frac{2}{3}(\mu - \lambda)\right), \left(\frac{\mu}{2}, -\frac{2\lambda + \mu}{3}\right) \text{ and } \left(\frac{\lambda + \mu}{2}, \frac{\lambda - \mu}{3}\right)$$

(in our case B, D, C and A) define a parallelogram on the weight diagram, which has the following property: for any weight (M, Y) lying inside or on the boundary of it there exists such a state $|T, T, Y>$ that $T = M$. So this state is the state with the highest eigenvalue of I_z of an I-spin multiplet. All the states of this multiplet can be constructed by the successive application of I_-.

For a fixed value of Y the weight (M, Y) with $M = T_Y$ is a simple weight, as the state $|T_Y, T_Y, Y>$ is one of the states of either (13) or (15). These are the states on the right hand side boundary of our parallelogram. (AB or AC in Fig. 1.) Making one step to the left in the same row, the weight $(T_Y - 1, Y)$ is obviously a double weight as

$$I_- | T_Y, T_Y, Y > \sim | T_Y, T_Y - 1, Y >$$

and, as it is a weight of our parallelogram, there is also a $T = T_Y - 1$, i.e. a state $|T_Y - 1, T_Y - 1, Y>$. Making further steps to the left, the multiplicity is always increasing by one. After we have reached the left hand side boundary of the parallelogram (BD or DC), the multiplicity remains constant, as far as we reach the weight (M, Y), where M has the smallest possible non-negative value in that row. Achieving this procedure for every row, the multiplet structure of the right half of the weight diagram can be constructed. The left hand side multiplicities are obtained by reflection of the right hand side multiplicities with respect to the Y axis, as every I-spin multiplet is displaced symmetrically to the Y axis.

In Fig. 2 we show the weight diagram together with the multiplet structure of $D(7,4)$, the so-called state diagram. Now we proceed to determine the number of states (the dimension) N_S of $D(\lambda, \mu)$. Fig. 2 shows that a complete state diagram can be obtained by overlapping hexagonals, the greatest of which has sides containing points $\lambda + 1$ and $\mu + 1$ and the smallest of which is an equilateral triangle having a side of $|\lambda - \mu| + 1$ points. The number

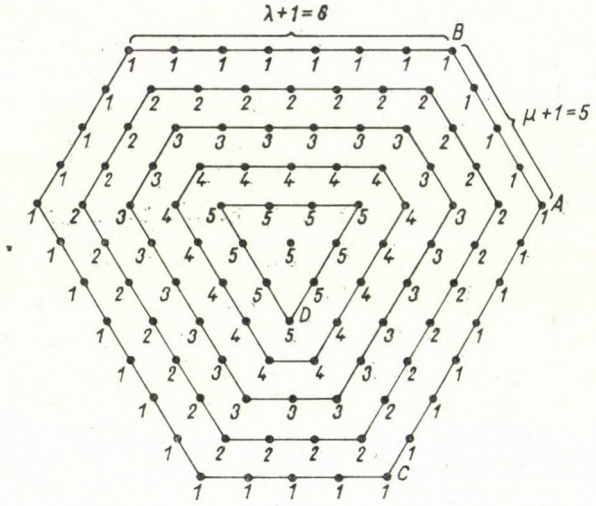

Fig. 2

of points of each hexagonal can be calculated and the sum of these numbers gives

$$N_S = \frac{(\lambda + 1)(\mu + 1)(\lambda + \mu + 2)}{2}.$$

N_S exceeds N_W:

$$\varepsilon = N_S - N_W = \frac{\lambda\mu(\lambda + \mu)}{2}.$$

ε vanishes if $\lambda = 0$ or $\mu = 0$, meaning that in $D(0, \mu)$ and $D(\lambda, 0)$ every weight is a simple weight. The weight diagrams of these I. R.-s have a triangular shape.

Thus the multiplet structure of $D(\lambda, \mu)$ is completely clarified. State diagrams like that of $D(7.4)$ in Fig. 2 are frequently used in graphical representation of Kronecker products of I. R.-s and in the application of the theory of Weyl characters. These problems will also be discussed later.

REFERENCES

1. J. Nyiri and A. Sebestyén, Acta Phys. Hung., **21**, 243, 1966.
2. R. E. Behrends, J. Dreitlein, C. Fronsdal and B. W. Lee, Rev. Mod. Phys., **34**, 1, 1962.
3. L. C. Biedenharn and G. E. Baird, Journ. Math. Phys., **4**, 1449, 1963.

АЛГЕБРАИЧЕСКИЕ МЕТОДЫ В ТЕОРИИ СПЕЦИАЛЬНЫХ УНИТАРНЫХ ГРУПП II

Квазиспин и структура мультиплетов

А. ШЕБЕШТЕН и Ю. НИРИ

Р е з ю м е

В данной работе с помощью простого метода определяется структура мультиплетов неприводимых представлений группы SU(3).

Acta Physica Academiae Scientiarum Hungaricae, Tomus 23 (1), pp. 53—65 (1967)

THE LORENTZ PRINCIPLE AND THE GENERAL THEORY OF RELATIVITY IV

By

L. JÁNOSSY

CENTRAL RESEARCH INSTITUTE OF PHYSICS, BUDAPEST

(Received 3. V. 1966)

It is shown that the Lorentz transformation as defined in Parts I—III is ambiguous regarding terms of higher order. The ambiguity cannot be eliminated mathematically; it is shown that this ambiguity reflects upon the fact, that the behaviour of an extended physical system in a gravitational field is affected by its inner structure.

§ 1. In the preceding Parts I, II and III [1] we have shown that the formalism of the general theory of relativity can be derived from the generalized Lorentz principle. The Lorentz principle can be formulated considering some physical system $\mathfrak{Q}$; we can construct a new system

$$\mathfrak{Q}^* = \mathscr{L}_\mathfrak{q}(\mathfrak{Q}), \tag{1}$$

corresponding to $\mathfrak{Q}$ where $\mathscr{L}_\mathfrak{q}$ denotes a Lorentz transformation characterized by parameters $\mathfrak{q}$.

The Lorentz principle can be stated postulating that provided $\mathfrak{Q}$ is a real physical system, then $\mathfrak{Q}^*$ is a possible system (obeying the same laws as $\mathfrak{Q}$), — further it can be added that as the result of an adiabatic interference a system $\mathfrak{Q}$ changes into Lorentz deformed states $\mathfrak{Q}^*$.

The problem we dealt with in particular in Part II of this series was to give a definition of the Lorentz transformation in regions where noticeable gravitational fields are present.

So as to be able to define the Lorentz transformation generalized for such regions, it is necessary to consider representations of the systems $\mathfrak{Q}$. We suppose, that $\mathfrak{Q}$ consists of a number of points $\mathfrak{P}_1, \mathfrak{P}_2, \ldots, \mathfrak{P}_N$ the four coordinates of which can be written $\mathfrak{x}_1, \mathfrak{x}_2, \ldots, \mathfrak{x}_N$, and in a representation K we have

$$K(\mathfrak{x}_\nu) = \mathbf{x}_\nu, \tag{2}$$

where

$$\mathbf{x}_\nu = \mathbf{r}_\nu, \; t_\nu \qquad \nu = 1, 2, \ldots, N.$$

More precisely the orbit of a point $\mathfrak{P}_N$ can be given in a parametric representation in the form

$$\mathbf{x}_\nu = \mathbf{r}_\nu(p), \; t_\nu(p), \tag{3}$$

where $dt_\nu(p)/dp > 0$ and thus varying the parameter p equ. (3) describes in a parametric representation the motion of the points $\mathfrak{P}_\nu$ in the representation K.

§ 2. It is convenient to single out a fourpoint $\mathfrak{x}$ in the centre of the region inside which Ω is contained. Introducing distances from the centre of the region, we may also write in place of (3)

$$\left.\begin{aligned} &\mathbf{x}_\nu = \mathbf{x} + \xi_\nu \qquad\qquad \mathbf{x} = \mathbf{r}, t \\ &\xi_\nu = \rho_\nu(p), \quad \tau_\nu(p)\,. \end{aligned}\right\} \quad (4)$$

and

A coordinate transformation leading from the representation K into another representation K' can be obtained with the help of four-functions in the form

$$\mathbf{x}' + \xi' = \mathbf{f}(\mathbf{x} + \xi)\,. \quad (5)$$

We shall also write

$$\mathbf{x}' = \mathbf{f}(\mathbf{x}) = \mathbf{x} + \mu\,, \quad (6)$$

and also

$$\left.\begin{aligned} &\mathbf{f}(\mathbf{x} + \xi) - \mathbf{f}(\mathbf{x}) = \varphi(\xi)\,, \\ &\xi' = \varphi(\xi)\,. \end{aligned}\right\} \quad (7)$$

and

The Lorentz transformations must themselves have the form of coordinate transformations as otherwise relation (1) could not be formulated independently of the particular representation.

So as to obtain those coordinate transformations which can be regarded to represent Lorentz transformations, we consider the representation of $\mathfrak{g}$ the propagation tensor. Suppose thus

$$K(\mathfrak{g}) = \mathbf{g}(\mathbf{x} + \xi)\,.$$

The propagation of light obeys thus the following differential equation

$$\frac{d\,\xi(p)}{dp}\,\mathbf{g}(\mathbf{x} + \xi)\,\frac{d\,\xi(p)}{dp} = 0\,, \quad (8)$$

where the four-coordinates $\xi(p) = \rho(p)$, $\tau(p)$ describe the orbit of a beam of light in the vicinity of $\mathbf{x}$.

We note that (8) provides only a necessary conditions for orbits of light — indeed, (8) provides one equation for the four components of $\xi(p)$ thus (8) does not determine the orbits of beams of light — not even, if initial conditions are added to (8).

Subjecting (8) to a transformation of coordinates, we obtain for the representation of (8) relative to a system K'

$$\frac{d\,\xi'(p)}{dp}\,\mathbf{g}'(\mathbf{x}'+\xi')\,\frac{d\,\xi'(p)}{dp}=0\,, \tag{9}$$

where we have

$$\mathbf{g}'(\mathbf{x}'+\xi')=\widetilde{\mathbf{S}}^{-1}(\xi)\,\mathbf{g}(\mathbf{x}+\xi)\,\mathbf{S}^{-1}(\xi) \tag{10}$$

and $\mathbf{S}(\xi)$ is a matrix with elements

$$S_{\nu\mu}(\xi)=\frac{\partial\varphi_\nu(\xi)}{\partial\xi_\mu}\,, \qquad \nu,\mu=1,2,3,4\,. \tag{11}$$

§ 3. One might (in accord with Part II) try to define as a Lorentz transformation such coordinate transformations which leave the representation of $\mathfrak{g}$ unchanged. Thus we might postulate that the representations K and K' are connected by a Lorentz transformation if we find that $K(\mathfrak{g})=K'(\mathfrak{g})$ or more explicitly written

$$\mathbf{g}'(\mathbf{x}'+\xi')=\mathbf{g}(\mathbf{x}+\xi)\,, \tag{12}$$

where the transformed quantities are to be taken in accord with (5), (6), (7) and (10). We might require thus

$$\widetilde{\mathbf{M}}^{-1}(\xi)\,\mathbf{g}(\mathbf{x}+\xi)\,\mathbf{M}^{-1}(\xi)=\mathbf{g}(\mathbf{x}'+\xi')\,, \tag{13}$$

where

$$M_{\nu\mu}(\xi)=\frac{\partial\lambda_\nu(\xi)}{\partial\xi_\mu}\,, \qquad \nu,\mu=1,2,3,4 \tag{14}$$

and

$$\xi'=\boldsymbol{\lambda}(\xi)\,, \qquad \mathbf{x}'=\mathbf{x}+\mu \tag{15}$$

for a Lorentz transformation.

The above definition of the Lorentz transformation is, however, too narrow. Indeed, in general for given $\mathbf{g}(\mathbf{x}+\xi)$ relations (13), (14) and (15) cannot be satisfied simultaneously. Relations (13) give *ten* equations which the *four* components of $\boldsymbol{\lambda}(\xi)$ have to obey, thus (13) provides in general an overdetermined system.

In the particular case, however, when

$$\mathbf{g}(\mathbf{x}+\xi)=\text{ constant }=\mathbf{g}_0\,, \tag{16}$$

elation (13) is satisfied by constant matrices $\mathbf{M}(\underline{\xi}) = \mathbf{M}_0$ such that

$$\widetilde{\mathbf{M}}_0 \mathbf{g}_0 \mathbf{M}_0 = \mathbf{g}_0 . \tag{17}$$

Thus in this particular case we are led to the original definition of the Lorentz transformation. Further, if light is propagated homogeneously in the vicinity of $\underline{x}$ but K gives a curvilinear representation, then there exists always a transformation $\varphi(\underline{\xi})$ with matrices $\mathbf{S}(\xi)$ such that

$$\widetilde{\mathbf{S}}^{-1}(\xi)\, \mathbf{g}(\mathbf{x} + \xi)\, \mathbf{S}^{-1}(\xi) = \mathbf{g}_0 , \tag{18}$$

and applying the same transformation to a point $\mathbf{x}' + \xi'$ we have also

$$\widetilde{\mathbf{S}}^{-1}(\xi')\, \mathbf{g}(\mathbf{x}' + \xi')\, \mathbf{S}^{-1}(\xi') = \mathbf{g}_0 . \tag{19}$$

Thus with the help of (17), (18) and (19) we find that the matrices

$$\mathbf{M}(\xi) = \mathbf{S}^{-1}(\xi')\, \mathbf{M}_0\, \mathbf{S}(\xi)$$

satisfy (13). Thus in the case where light is propagated homogeneously, relation (13) defines the ordinary Lorentz transformations in a form independent of the representation.

§ 4. In a region where a noticeable gravitational field acts, no transformation of the type (18) exists and therefore it is impossible to require that a Lorentz transformation should satisfy (13) in the whole of the vicinity of a point $\underline{x}$. A weaker postulate, i.e.

$$\widetilde{\mathbf{M}}(\xi)\, \mathbf{g}(x' + \xi')\, \mathbf{M}(\xi) = \mathbf{g}(\mathbf{x} + \xi) \qquad \text{for } \xi = 0 , \tag{20}$$

can, however, always be satisfied. The latter relation corresponds to the definition we had in mind, when writing Part II. Definition (20) can be made more precise by requiring, that apart from (20) also its first derivative in the point $\xi = 0$ should give a correct relation. Thus we may add to the condition (20) the further conditions

$$\frac{\partial}{\partial \xi}\left(\widetilde{\mathbf{M}}(\xi)\, \mathbf{g}(\mathbf{x}' + \xi')\, \mathbf{M}(\xi) - \mathbf{g}(\mathbf{x} + \xi)\right) = 0 \qquad \text{for } \xi = 0 . \tag{21}$$

Relations (21) can always be fulfilled. So as to obtain explicit expressions, we develop the transformation functions $\lambda(\underline{\xi})$ into powers of ξ. We write

$$\xi' = \lambda(\xi) = \mathbf{M}\xi + \frac{1}{2}\mathbf{B}^{(2)}\xi^2 + \frac{1}{6}\mathbf{B}^{(3)}\xi^3 + \ldots . \tag{22}$$

and also

$$\mathbf{M}(\xi) = \frac{\partial \lambda(\xi)}{\partial \xi} = \mathbf{M} + \mathbf{B}^{(2)}\xi + \frac{1}{2}\mathbf{B}^{(3)}\xi^2 + \ldots * . \tag{23}$$

From (20) it follows that

$$\widetilde{\mathbf{M}}\,\mathbf{g}'\,\mathbf{M} = \mathbf{g}\,, \tag{24}$$

therefore $\mathbf{M}$ is a constant matrix depending only on $\mathbf{x}$ the coordinate of the centre of the region, and $\mathbf{x}' = \mathbf{x} + \mu$ the transformed measure of $\mathfrak{x}$, the centre coordinate of the region considered.

Relation (24) defines a six parameter group for the matrices $\mathbf{M}$, the latter was considered in some detail in Part I. Using the notation (22), (23) we obtain from (21)

$$\widetilde{\mathbf{B}}^{(2)}\,\mathbf{g}'\,\mathbf{M} + \widetilde{\mathbf{M}}\,\mathbf{g}'\,\mathbf{B}^{(2)} + \widetilde{\mathbf{M}}\,\frac{\partial \mathbf{g}'}{\partial \xi'} = \frac{\partial \mathbf{g}}{\partial \xi}\,. \tag{25}$$

In (25) we have written $\widetilde{\mathbf{B}}^{(2)}$ for the three-dimensional matrix with elements

$$\widetilde{B}^{(2)}_{\varkappa\lambda\nu} = B^{(2)}_{\nu\varkappa\lambda}\,.$$

Further we wrote

$$\mathbf{g}' = \mathbf{g}(\mathbf{x}'), \quad \mathbf{g} = \mathbf{g}(\mathbf{x}) \text{ and } \frac{\partial \mathbf{g}}{\partial \xi} = \left(\frac{\partial \mathbf{g}(\mathbf{x}+\xi)}{\partial \xi}\right)_{\xi=0}.$$

Finally we have made use of the relation

$$\left(\frac{\partial \mathbf{g}(\mathbf{x}'+\xi')}{\partial \xi'}\,\mathbf{M}(\xi)\right)_{\xi=0} = \left(\frac{\partial \mathbf{g}(\mathbf{x}+\xi)}{\partial \xi}\right)_{\xi=0}$$

which relation can be written short as

$$\frac{\partial \mathbf{g}'}{\partial \xi'}\,\mathbf{M} = \frac{\partial \mathbf{g}}{\partial \xi}\,.$$

* When we are dealing with matrices of various dimensions, we shall take the product always as the sum over the last suffix of the matrix to the left with the first suffix of the matrix to the right, e.g. if $\mathbf{B}^{(2)}$ is a three-dimensional matrix with elements $B^{(2)}_{\nu\varkappa\lambda}$

$$(\mathbf{B}^{(2)}\,\xi)_{\nu\varkappa} = \sum_{\lambda} B^{(2)}_{\nu\varkappa\lambda}\,\xi_\lambda\,,$$

or $\mathbf{B}^{(2)}\,\xi^2 = (\mathbf{B}^{(2)}\,\xi)\,\xi$ to be a vector with elements $(\mathbf{B}^{(2)}\,\xi^2)_\nu = \Sigma\, B^{2}_{\nu\varkappa\lambda}\xi_\varkappa\xi_\lambda$. Similarly if we take e.g. $\mathbf{B}^{(3)}$ to be a four-dimensional matrix with elements $B^{(3)}_{\nu\varkappa\lambda\sigma}$ and

$$(\mathbf{B}^{(3)}\,\xi^2)_{\nu\varkappa} = \sum_{\lambda\sigma} B^{(3)}_{\nu\varkappa\lambda\sigma}\,\xi_\lambda\,\xi_\sigma\,, \qquad (\mathbf{B}^{(3)}\,\xi^3)_\nu = \sum_{\varkappa\lambda\sigma} B^{(3)}_{\nu\varkappa\lambda\sigma}\,\xi_\varkappa\,\xi_\lambda\,\xi_\sigma\,.$$

From (25) it follows that

$$\mathbf{B}^{(2)} = \mathbf{g}'^{-1}\left(\tilde{\mathbf{M}}^{-1} \frac{\partial \mathbf{g}}{\partial \xi} - \frac{\partial \mathbf{g}'}{\partial \xi} + \mathbf{A} \right),$$

where $\mathbf{A}$ is a three-dimensional matrix which is antisymmetric in the second and third suffix, i.e.

$$A_{\nu\varkappa\lambda} = - A_{\nu\lambda\varkappa}.$$

We may write in place of the above relation

$$\mathbf{B}^{(2)} = \mathbf{M}\,\mathbf{g}^{-1}\left(\frac{\partial \mathbf{g}}{\partial \xi} - \frac{\partial \mathbf{g}'}{\partial \xi'} + \mathbf{A}' \right),$$

where $\mathbf{A}'$ has symmetry properties similar to those of $\mathbf{A}$. Taking the symmetry properties of both $\mathbf{A}'$ and $\mathbf{B}^{(2)}$ we can determine $\mathbf{A}'$ uniquely, we thus find

$$\mathbf{B}^{(2)} = \mathbf{M}\,\mathbf{g}^{-1}(\mathscr{C} - \mathscr{C}')$$

where $\mathscr{C}$ has components

$$\mathscr{C}_{\nu\mu\varkappa} = \frac{\partial g_{\nu\mu}}{\partial \xi_\varkappa} + \frac{\partial g_{\nu\varkappa}}{\partial \xi_\mu} - \frac{\partial g_{\mu\varkappa}}{\partial \xi_\nu}.$$

The components of $\mathscr{C}'$ are obtained from those of $\mathscr{C}$ by replacing the derivatives $\dfrac{\partial \mathbf{g}}{\partial \xi}$ by $\dfrac{\partial \mathbf{g}'}{\partial \xi'}$.

§ 5. The transformations (22), (23) cannot be further restricted in a simple manner. Indeed, we cannot require, e.g. in addition to (20) and (21) that

$$\left.\begin{aligned} \frac{\partial^k}{\partial \xi^k}\left(\tilde{\mathbf{M}}(\xi)\,\mathbf{g}(\mathbf{x}' + \xi')\,\mathbf{M}(\xi) - \mathbf{g}(\mathbf{x} + \xi)\right) = 0 \\ \text{for } k = 2, 3, 4, \ldots, \xi = 0 \end{aligned}\right\} \quad (26)$$

because in general relations (26) give an overdetermined set of equations. In particular for $k = 2$ (26) gives one hundred conditions for the eighty independent components of $\mathbf{B}^{(3)}$ and therefore relations (26) in general cannot be satisfied for $k = 2$. For $k > 2$ the relations give an even more strongly overdetermined set.

It follows from (26), as we have shown e.g. in Part III, that from the fact that (26) is overdetermined for $k = 2$ it follows that there exist twenty expressions built up of the components of $\mathbf{g}$ and its first and second derivatives, such that these expressions do not change their values at $\xi = 0$, if we

carry out a coordinate transformation satisfying (20) and (21). The latter twenty quantities can be represented by the twenty independent components of the Riemann—Christoffel tensor.

It follows therefore that we cannot restrict the definition of the Lorentz transformation by requiring that it should not change the values of the second derivatives of $\mathbf{g}$, i.e. we cannot require, that Lorentz transformations should satisfy (26) for $k = 2$. The weaker requirement that a Lorentz transformation should not change the components of the Riemann—Christoffel tensor at $\xi = 0$ is automatically fulfilled, if transformations satisfying (20) and (21) are considered and therefore the latter requirement does not restrict the coefficients $\mathbf{B}^{(3)}$ in any way. It seems that no simple condition can be found which would restrict the coefficients $\mathbf{B}^{(3)}$ and those of the still higher order terms.

We see thus that the transformation function $\lambda(\xi)$ determining Lorentz transformation can only be fixed up to terms of second order in ξ, the higher order terms remain ambiguous. The ambiguity contained in the definition of the Lorentz transformation appears at first sight as a deficiency of our considerations. However, examining the problem further, we find, that the latter ambiguity has its deep physical significance.

§ 6. The significance of the ambiguity of the transformation functions $\lambda(\xi)$ becomes apparent, if we consider the Lorentz transformations not as coordinate transformations, but as deformation operators, which define to a physical system $\mathfrak{Q}$ a deformed system $\mathfrak{Q}^*$.

The contents of (1) can be made more precise supposing that $\mathfrak{Q}$ consists of a number of points $\mathfrak{P}_1, \mathfrak{P}_2, \ldots$ represented by coordinates relative to a system K as

$$K(\mathfrak{P}_k) = \mathbf{x} + \xi_k \qquad k = 1, 2, \ldots .$$

The deformed system $\mathfrak{Q}^*$ consists of points $\mathfrak{P}_1^*, \mathfrak{P}_2^*, \ldots$ represented relative to K by coordinates

$$K(\mathfrak{P}_k^*) = \mathbf{x}^* + \xi_k^*, \qquad k = 1, 2, \ldots$$

where

$$\mathbf{x}^* = \mathbf{x} + \mu, \qquad \xi_k^* = \lambda(\xi_k), \tag{27}$$

and $\lambda(\xi)$ is a transformation function satisfying (20) and (21).

The function $\lambda(\xi)$ depends on six parameters, i.e. the (constant) independent components of $\mathbf{M}$ and the transformation depends also on the four components of μ. Thus the transformation depends on ten parameters, like the Lorentz transformation in the homogeneous case. Apart from this, the transformation depends on the higher order terms of $\lambda(\xi)$, i.e. on the coefficients $\mathbf{B}^{(3)}, \mathbf{B}^{(4)}, \ldots$.

If we consider a given object $\mathfrak{Q}$ shift it by an amount μ turn it round and accelerate it to amounts described by the six independent components

of **M**, then we expect that the resulting deformation is uniquely determined, However, the deformation which results in this way can only be expected to be uniquely determined by **M** and μ for one *given* system $\mathfrak{Q}$, and it is to be expected that having different systems $\mathfrak{Q}$, $\overline{\mathfrak{Q}}$, $\overline{\overline{\mathfrak{Q}}}$, . . . they will suffer somewhat different deformations when subjected to the same shift μ, **M**.

§ 7. The fact that systems $\mathfrak{Q}$, $\overline{\mathfrak{Q}}$, . . . etc. subjected to one and the same shift μ, **M** react differently, can be seen easily. Consider e.g. a stellar body placed into an inhomogeneous gravitational field. The field will try to accelerate the elements of the system differently and the system can only be kept together by inside forces which compensate the inhomogeneous part of the gravitational action. The equilibrium configuration which results, depends on both the variation of gravitational field and the nature of the inner forces, which establish the equilibrium.

If we consider two different systems $\mathfrak{Q}$ and $\overline{\mathfrak{Q}}$ in a homogeneous region, then no stresses compensating the gravitational action are to be expected. If we move in an adiabatic manner, both $\mathfrak{Q}$ and $\overline{\mathfrak{Q}}$ into an inhomogeneous region, then they will deform. Part of the deformations are the Lorentz deformations which deformations are common to all physical systems in the case of adiabatic shift, and these deformations are uniquely determined by the parameters of **M** and μ. Apart from this, both systems will suffer deformations producing inner stresses which stresses in their turn compensate the inhomogeneous part of the gravitational action in the new surroundings. The latter stresses and deformations depend on the mechanical and other inner properties of the systems $\mathfrak{Q}$ and $\overline{\mathfrak{Q}}$, therefore the deformations suffered by $\mathfrak{Q}$ and those by $\overline{\mathfrak{Q}}$ will differ from each other. Roughly speaking a softer body will deform more strongly than a harder one if both are brought into the same inhomogeneous gravitational field.

Returning to the problem of the Lorentz transformation, we conclude: Even if we were to succeed in defining uniquely some functions $\lambda(\mathbf{M}, \mu; \xi)$ which we were to regard as to determine the Lorentz transformations as functions of the ten usual parameters **M** and μ, we could not expect these functions to describe the real Lorentz deformations of arbitrary physical systems. Indeed, as we have seen by the example of the two stellar bodies, physical systems react on shifts **M**, μ differently in accord with their inner structure.

It seems reasonable to suppose that while a given system $\mathfrak{Q}$ deforms, say, according to (27) with transformation functions $\lambda(\xi)$ depending on **M** and μ, another system $\overline{\mathfrak{Q}}$ deforms according to

$$\left.\begin{aligned} \mathbf{x}^* &= \mathbf{x} + \mu\,, \\ \xi_k^* &= \bar{\lambda}(\bar{\xi}_k)\,, \end{aligned}\right\} \tag{28}$$

where the $\bar{\lambda}$ are functions differing from the λ. It seems thus, that the transformations (27) or (28) can be restricted to such an extent only, that the respective transformation functions λ resp. $\bar{\lambda}$ obey (20) and (21), but they may differ as regards to higher order terms. The latter terms depend on the inner structure of the systems Ω or $\bar{\Omega}$ which is being subjected to deformation.

The ambiguity of the definition leaves thus room for the different behaviour of physical systems of different inner structure; if an unambiguous mathematical definition of the transformation was given, then the latter transformation would apply only to some kind of "ideal" matter and thus it would be void of interest, as we are in practice only interested as how *real* matter of a specified kind behaves, when moved about. From the empirical fact, that different type of matter reacts differently on being moved about, it follows that no general law for the exact behaviour of "matter as such" can be given.

§ 8. It seems, however, that the fact that we can determine at least the lower order terms of the transformation functions $\lambda(\xi)$ implies, that all types of matter have certain common features which are reflected by the lower terms of the transformation functions. These common features of various types of physical systems can be further elucidated as follows.

In a homogeneous region any closed physical system, if accelerated adiabatically, suffers the same length contraction — no matter what the particular inner properties of the system are. Thus the length contraction is a general feature to all physical systems.

However, it is necessary to note, that even when regarding the length contraction of a system we cannot quite forget about its inner properties. Indeed, the contraction takes place independent of the inner structure of the system — however, whether or not a given rate of acceleration can be regarded as adiabatic, depends on the particular properties of the system.

Considering for the sake of example the relativistic slowing down of a system instead of the length contraction, — we know that an atom can be accelerated during a very short period of time, so as to move with a velocity comparable that of light and the inner period of the atom thus accelerated will slow down adiabatically, as can be seen e.g. from the observation of the perpendicular Doppler effect. A real watch accelerated at a similar rate would obviously go to pieces and would not show the slowing down which is shown by simple atoms.

If a physical system is subjected to an adiabatic shift in an inhomogeneous region, then it will suffer the Lorentz deformations which it were to suffer in a homogeneous region — apart from that it adjusts itself adiabatically to the change of gravitational surrounding. The latter adjustment consists of certain deformations and the change of inner rhythms. This latter effect appears e.g. as the gravitational red shift of spectral lines. These deformations

and changes can be derived from the lower order terms of the transformation functions, thus these effects are fully determined by the parameters $\mathbf{M}$ and μ.

Apart from the changes described above which are common to closed systems moved about adiabatically, we expect further deformations which depend on the reaction of the system to the inhomogeneity of the gravitational field.

The inhomogeneity of the field is connected largely with the second derivatives $\partial^2 \mathbf{g}/\partial \xi^2$ of $\mathbf{g}$ and therefore the amount of adjustment of a closed physical system to the stress caused by the gravitational fields is of the order of these derivatives. We can thus suppose that roughly speaking the $\mathbf{B}^{(3)}$ describing the behaviour of a particular system are of the order of the second derivatives of $\mathbf{g}$ — the exact values depending on the particular physical properties of the system.

§ 9. The above statement must be made a little more precise. We note that if we consider the systems Ω, $\overline{\Omega}$ placed in a homogeneous region, their Lorentz deformations can be given in an unambiguous way, if we consider the representations in a curvilinear representation K, then because of the peculiar form of representation the second and higher derivatives of $\mathbf{g}$ are not zero.

Thus to obtain a formulation which gives the physical facts correctly, we must distinguish clearly between curvilinear coordinates and the real inhomogeneity of propagation of light.

No problem arises as long as we are concerned with the first derivatives of $\mathbf{g}$ only. Regarding the second derivatives, we may look for a representation in which the second derivatives are "as small as possible". This means, they may be supposed to be of the order of the components of the Riemann—Christoffel tensor. We may therefore suppose, that the inner forces which contribute to a deformation, are of the same order as the change of inhomogeneity of the gravitational field in the course of the displacement and therefore we may suppose that in a representation K, where the second derivatives of $\mathbf{g}$ are of the same order of magnitude as the components of the Riemann—Christoffel tensor, in this representation the coefficients $\mathbf{B}^{(3)}$ are of the order of the change of the components of the Riemann—Christoffel tensor, which occur during the shift $\mu, \mathbf{M}$ in the region occupied by the system Ω.

The latter assumption permits just sufficient margin for the play of the inner forces without determining them precisely. In particular in a homogeneous region, where the components of the Riemann—Christoffel tensor are all zero, the above condition requires that in the representation where $\mathbf{g} =$ constant we should have also $\mathbf{B}^{(3)} = 0$ as it must be expected. Physically this means that in a region where gravitation produces no inner stress there appear no inner forces to keep up the equilibrium with gravitational forces and therefore the deformations produced by adiabatic shifts can be determined uniquely.

In reality there exist no absolutely homogeneous regions therefore the components of the Riemann—Christoffel tensor are never exactly equal to zero. We may, however, regard for practical purposes a region to be homogeneous, if the second and higher order terms are too small to be noticeable. Under such circumstances the laws for homogeneous regions are practically valid.

§ 10. The gravitational field in the vicinity of a point ξ is characterized only to a first approximation by the second derivatives of $\mathbf{g}$. There exist also invariants composed of the third and higher derivatives of $\mathbf{g}$. With the help of these higher invariants it is possible to restrict the orders of magnitudes of the coefficients $\mathbf{B}^{(4)}, \mathbf{B}^{(5)}, \ldots$ etc. — the above remark seems, however, important only in principle, but it has no practical consequences, as the effects connected with the third or higher derivatives of $\mathbf{g}$ seem to be negligibly small under practical circumstances.

Summarizing we see thus, that the ambiguity of the definition of the Lorentz transformation which remains if we accept the definition given by (20) and (21) can be reasonably restricted when we suppose, that in a suitable representation the coefficients of the higher order terms of the transformation function are of the same order of magnitude as the corresponding invariants of the gravitational field. This margin cannot be narrowed down further — even if some mathematical method could be found to reduce the remaining ambiguity — as the margin thus obtained for the transformations is necessary to account for the different behaviour of systems of various inner structures.

Finally, it may be added that for the treatment of many practical problems the ambiguous higher order terms can be neglected. Indeed, we are usually dealing with closed systems of such small dimensions inside which the gravitational field can be taken to be homogeneous. As an evident example we mention the determination of the orbits of planets; these orbits can be obtained with great precision from the Lorentz transformation in its ambiguous form as this was shown e.g. in Part III.

We note, however, that considering the motion of planets in finer detail, we expect that the orbits are affected to a small extent by the higher order terms. Indeed, if a planet is not taken as a "point", but if we consider its inner structure then the gravitational force acting upon the system as a whole is slightly affected by deformations of the planetary body.

Roughly speaking the orbit of the planet is affected by the tides the body of the planet suffers in the inhomogeneous field of the central body. The deviations from the orbit obtained for a mass point caused by the tides inside the planet are very small, but they must be expected to depend strongly on the inner structure of the planets. Indeed, the gravitational force acting on the whole of the planet can be written

$$\mathbf{F} = -\operatorname{grad} \int \Phi(\mathbf{r})\, \sigma(\mathbf{r})\, d^3\mathbf{r}\,, \tag{29}$$

where $\Phi(\mathbf{r})$ is the gravitational potential and $\sigma(\mathbf{r})$ gives the distribution of the density of the planet. Denote the coordinate of the centre of gravity of the planet by

$$\mathbf{R} = \int \mathbf{r}\, \sigma(\mathbf{r})\, d^3\mathbf{r}/m\,, \tag{30}$$

where m is the mass of the planet. We may thus write neglecting higher order terms

$$\Phi(\mathbf{R}+\rho) = \Phi(\mathbf{R}) + \rho \text{ grad } \Phi(\mathbf{R}) + \frac{1}{2}\rho \frac{\partial^2 \Phi(\mathbf{R})}{\partial \mathbf{R}^2}\rho + \dots$$

and thus

$$\mathbf{F} = \mathbf{F}_0 + \mathbf{F}_2 + \dots,$$

where

$$\mathbf{F}_2 = -\frac{1}{2}\int \rho \frac{\partial^2 \Phi(\mathbf{R})}{\partial \mathbf{R}^2}\rho\, \sigma(\mathbf{R}+\rho)\, d^3\rho\,.$$

(The contribution $\mathbf{F}_1$ proportional to the first derivatives of Φ, i.e.

$$\mathbf{F}_1 = -\text{ grad } \Phi \int \varrho\, \sigma(\mathbf{R}+\rho)\, d^3\rho = 0$$

vanishes as can be seen from (30).)

The mass distribution $\sigma(\mathbf{R}+\rho)$ in the inside of the planet adjusts itself adiabatically to the gravitational field in the vicinity of $\mathbf{R}$ and thus the component $\mathbf{F}_2$ of the force acting on the centre of gravity is affected by the form of the equilibrium configuration which comes about at various points of the orbit. The latter configuration depends partly on the gravitational field but also on the mechanical properties of the planet.

While the planet moves the adjustment changes slowly with the change of gravitational field and thus affects the orbit to some extent. We expect therefore, that there is a certain deviation between the orbit of the centre of gravity of the planet and that of the orbit of a mass point situated at the centre of gravity. The deviation between the latter two orbits depends on the particular mechanical structure of the planet.

As was shown in Part II, the orbit of a planet can be obtained by means of a continuous succession of Lorentz deformations. The ambiguity of the function $\lambda(\xi)$ defining the Lorentz transformation leaves just room for the various planetary orbits obtained for planets with different inner structures. Even if in practice the tidal effect thus described is very small it is important to note that with the help of the generalized Lorentz transformation the orbit of a sufficiently small planet can be determined precisely, while the deviations which are expected to occur as soon as the size of the planet cannot anymore be neglected altogether, can be described by adjusting the ambiguous higher order terms of $\lambda(\xi)$ properly. The latter terms have to be chosen so as to describe appropriately the actual mechanical properties of the planet to be considered.

REFERENCES

1. L. JÁNOSSY, Acta Phys. Hung. **21**, 1, 17, 329, 1966.

ПРИНЦИП ЛОРЕНЦА И ОБЩАЯ ТЕОРИЯ ОТНОСИТЕЛЬНОСТИ

Часть IV

Л. ЯНОЩИ

Р е з ю м е

Показано, что преобразование Лоренца, определённое в частях I—III, неоднозначно для членов высшего порядка. Эту неоднозначность нельзя устранить математически; показано, что она отражает тот факт, что внутренняя структура протяжённой физической системы влияет на поведение самой системы в гравитационном поле.

Acta Physica Academiae Scientiarum Hungaricae, Tomus 23 (1), pp. 67—73 (1967)

RELATIVE INTENSITY AND CONVERSION COEFFICIENTS OF THE TRANSITIONS IN THE DECAY $Zr^{59}—Nb^{95}—Mo^{95}$

By

N. A. EISSA

FACULTY OF ENGINEERING, AL AZHAR UNIVERSITY, CAIRO, UAR

Z. MELIGY

FACULTY OF SCIENCE, EIN SHAMS UNIVERSITY, CAIRO, UAR

and

A. H. EL FARRASH and S. GIRGIS

UAR ATOMIC ENERGY ESTABLISHMENT, CAIRO, UAR

(Presented by A. Szalay. — Received 19. V. 1966)

The external and internal conversion spectra in the decay of $Zr^{95}—Nb^{95}$ were measured in a double focusing beta spectrometer. Applying the correction for the anisotropic distribution of the photoelectrons ejected from a uranium convertor it was possible to determine accurately the relative gamma ray intensities of the 237, 726 and 757 keV transitions in Nb^{95}, and the 762 and 765 keV transitions in Mo^{95}. Applying the internal-external conversion method, the absolute k-conversion coefficients were determined for the above transitions. The 237 keV transition was found to be M_4 transition and the 726 keV transition is M_1 transition, while the other ones are M_1 or E_2 transitions. The spin of the level at 726 keV in Nb^{95} has value of $\frac{7^+}{2}$.

1. Introduction

A long lived radioactivity in zirconium was produced as a fission product from uranium and was first obtained in 1940 by A. GOSSE and F. FOOTH [1]. SAGANE et al. [2] found that the half life of the activity was 63 days and associated it with the isotope of mass 93. Subsequent investigations have shown that the activity is more likely in Zr^{95} which decays to the radioactive daughter product Nb^{95}. In 1953 CORK et al. [3] used a semicircular magnetic spectrometer for the study of the beta and gamma radiations and the half life of the decay. They found that Zr^{95} emits three beta rays of energies 910, 405 and 360 keV with half life of 65,2 days, each followed by a gamma transition leading to radioactive Nb^{95}. The gamma energies determined by CORK were 235, 725 and 758 keV. The Nb^{95} decays by 165 keV endpoint energy beta transition into Mo^{95} with accompanying gamma energies of 753 and 768 keV. MITTELMAN [4] studied the Zr^{95} spectra with a double focusing beta ray

spectrometer and also measured the coincidences between beta and gamma rays in cascade to the ground state of Nb^{95}. He found that the decay of Zr^{95} proceeds by three beta-gamma cascades, two of the beta transitions of 360 and 396 keV are allowed and proceed to 755 and 722 keV levels and, the third beta transition of 885 keV to the 235 keV level. From the K-conversion coefficient and the shell model, the 722 and 755 keV levels are both assigned even parity and a spin of $\frac{5}{2}$ or $\frac{7}{2}$. In a succession of investigations [5—11] many measurements have been carried out on the beta and gamma transitions in the decay processes with rather wide divergence in the expressed values as shown in Table 1.

In the present investigation it was decided to study the external and internal conversion spectra by a high resolution double focusing spectrometer to determine the relative gamma ray intensities and the absolute conversion coefficients. These methods were not applied before the present work in the study of the decay of $Zr^{95}—Nb^{95}—Mo^{95}$.

2. Apparatus and source preparation

Iron-yoke double focusing spectrometer of 22,5 cm radius, type ПББ-2, was used in the present measurements. The spectrometer was operated at a 0,5% resolution during the present study. The detector was an end window G. M. counter filled with 90% argon and 10% ethyl alcohol with 1,8 mgm/cm^2 mica window.

The source material used in all the measurements consisted of a $Zr^{95}—Nb^{95}$ oxalate mixture of high radiochemical purity which was obtained from Amersham Radiochemical Centre. About eight millicurie source for internal conversion spectrum study was prepared by the liquid deposition method with insulin used to define a rectangular source area of 3×30 mm^2 and to promote uniform spreading of the activity. The source was covered with a thin zapon film. The external conversion source was of about 40 millicurie activity which was introduced into a prespex cylinder of 1 mm wall thickness. It was inserted into another copper cylinder of 1 mm thickness to absorb the beta rays. A 1,7 mgm/cm^2 uranium convertor of the same dimensions as those used in case of the internal conversion source was fastened on the source holder.

The method of external conversion [12] was used to determine the relative gamma ray intensities which can be applied now with good accuracy (2%) in even complex decay schemes. Relative gamma ray intensities are calculated from the following equation when rectangular source and convertor are used,

$$I = \frac{(A_{ex})_j}{T_j \cdot f_j \cdot c \cdot d}, \tag{1}$$

where $(A_{ex})_j$ is the intensity of the external photoelectric conversion line from the j-shell of the convertor. This intensity was obtained by calculating the area under the shaped peak profile extended to five half widths then dividing by the corresponding H_ϱ value. T_j is the photoelectric cross-section for the j-shell of the convertor. The K-photoelectric cross-section T_k was obtained from the recent calculations of HULTBERG, NAGAL and OLSSON [13]. c is the spectrometer transmission which was kept constant during all these measurements. d is the convertor thickness. f_j is the correction factor which corrects for the anisotropical distribution of the photoelectrons from the j-shell of the convertor. These f factors were computed according to the present experimental geometry, on the basis of theoretical photoelectric angular functions on the Swedish computer Besk,* for uranium convertor at different energies and taking into account the absorption in the copper cylinder used for beta absorption. The K-conversion coefficient α_k for the gamma transitions was calculated by the internal-external conversion (IEC) method [12, 14], where α_k is given by:

$$\alpha_K = \frac{(N_{in})_K}{(N_{ex})_K} = \frac{(A_{in})_K}{(A_{ex})_K} \cdot {}^{T}K \cdot {}^{f}K \cdot b \cdot d \cdot k, \tag{2}$$

where $(A_{in})_K$ and $(A_{ex})_K$ are the areas of the internal and external K-conversion lines for a given transition. k is the relative strength of the internal and external conversion sources, d is the convertor thickness, b is a dimension factor and T_K and F_K are defined in case (1).

3. Results and discussion

The K-external photoelectric and internal conversion lines of the 237, 726, 756, 762 and 765 keV transitions were measured three times each. The transition energies were accurately determined by making a mixed source of Cs^{137}—Zr^{95} on aluminium foil.

A typical measurement of the internal and external conversion spectra are shown in Figs. 1 and 2. The dimensions of the circles in the Figures are of the order of the standard deviation in the counting rates. The shapes of partially unresolved lines were constructed on the basis of resolution and line shapes of other standard lines.

It was not necessary to correct for decay the data shown in Figs. 1 and 2 since the time for the measurement of any series of lines was short in comparison with the half life. However, the area of each of the lines was decay corrected to the same time. The decay corrected areas of each gamma ray

* Curtesy to Dr. S. HULTBERG for doing these calculations.

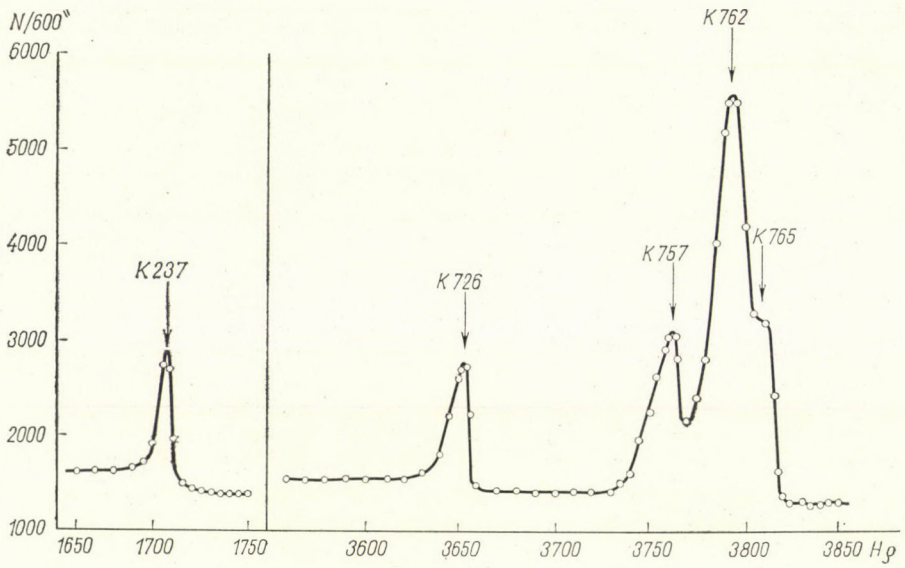

Fig. 1. K — internal conversion lines from a Zr^{95}—Nb^{95} source

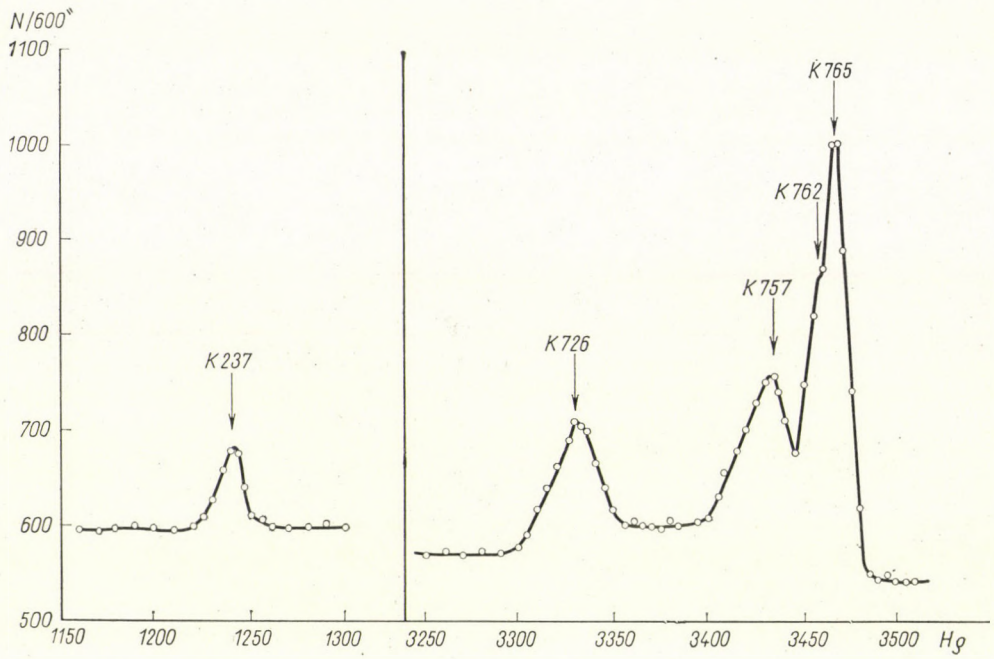

Fig. 2. K — external conversion lines from a Zr^{95}—Nb^{95} source, using 1,7 mgm/cm² uranium convertor

Table 1

Reference	Transition energy	$10^3\ \alpha_K$	Multipolarity
11	726	1,3	E_2 or M_1
4	722	1,38	E_2 or M_1
9	721	2,4	
6	722	1,6	E_2 or M_1
11	760	1,8	E_2 or M_1
4	754	1,14	E_2 or M_1
3	235	$K/LM = 4{,}5$	M^4
15	232	$K/LM = 3{,}5$	M^4
15	236	$K/L = 3{,}7$	M^4
3	753	—	
3	768	$K/LM = 7{,}6$	E_2 or M_1
5	770	2,05	—
11	770	$K/LM = 7{,}4$	E_2 or, M
15	775	$K/LM = 6{,}6$	E_2 or M_1

were averaged to obtain the values of A_{in} and A_{ex} given in Table 2. The errors assigned to A_{in} and A_{ex} were estimated from the possible limiting curves which may be drawn through the data.

The absolute conversion coefficient was calculated according to equation (2). But as it was not easy to determine the relative strength K of the internal and external sources, so the following procedure was used which is a slight modification of the internal-external conversion method. The same original activity was used for preparing the external and internal conversion sources. Then the k-external and k-internal conversion lines for the 237 keV transition were measured and the relative conversion coefficient was determined from the K/L ratio. This transition is very well known as a pure M_4 transition[15]. The obtained value of $\alpha_{K_{237}}$ was substituted in equation (2) in the following form:

$$\alpha K_{237} = B \frac{(A_{\text{in}})_{K\ 237}}{(A_{\text{ex}})_{K\ 237}} \cdot (T \cdot f)_{K\ 237}\,, \tag{3}$$

where B is a constant depending on the geometry of the spectrometer, the convertor thickness and the relative intensity of the two sources. All these factors were kept constant during all the measurements. After knowing the value of B from equation (3) the value of α_K for the other transitions was calculated.

The results of these measurements are shown in Table 2, together with the data used in the calculations. The 726 keV transition depopulating the

Table 2

Transition occurring in	Transition energy keV	Relative $\frac{(A_{ex})_K}{C}$	T_K	f_K	Relative gamma intensity	Internal K-conversion line intensity	Theoretical values of α_K according to sliv and Band $\times 10^5$		Experimental value of $\alpha_K \times 10^3$	Multipolarity
							3 (M_4) 2,4×10 (M_4)			
							M_1	M_2		
Nb^{95}	237,23 ± 0,41	350 ± 17	240	0,3980	8,56 ± 0,52	52 ± 3,5			2,2 ± 0,18	M_4
	726,38 ± 1,30	453 ± 22	16,4	0,6688	96,6 ± 5,8	405 ± 34	1,42	1,52	1,28 ± 0,13	M_1
	757,1 ± 1,30	428 ± 62	14,7	0,6825	100 ± 17	400 ± 69	1,40	1,43	1,42 ± 0,26	M_1 or E_2
Mo^{95}	762,5 ± 2,0	78 ± 15	14,5	0,6840	7,7 ± 1,7	44 ± 4,5	1,33	1,34	1,32 ± 0,30	M_1 or E_2
	765,6 ± 1,8	1000 ± 25	14,4	0,6843	1000 ± 270	400 ± 55	1,32	1,33	1,26 ± 0,25	M_1 or E_2

726 keV level in Nb^{95} is most probably an M_1 transition which leads to the conclusion that this level has spin $7/2^+$. The multipolarities of the transitions given in Table 1 were determined form the relative conversion coefficients. So, it was not possible to differentiate between M_1 or E_2. The transition multipolarities in the present work were determined on the basis of the absolute conversion coefficient determination applying the (IEC) method in which the uncertainties in the distribution of photoelectrons ejected by the gamma rays were avoided and the accuracy in the determined values reaches 5% in some cases.

It is a pleasure to express our gratitude to Professor M. A. El Nadi, Head of the Nuclear Physics Department UAR Atomic Energy Establishment, for his encouraging interest in this work.

REFERENCES

1. A. Gosse and F. Footh, Phys. Rev., **57,** 664, 1940.
2. R. Sagene, S. Kojima, G. Miyamotos and M. Korwa, Phys. Rev., **57,** 1179, 1940.
3. T. M. Cork, T. M. Le Blanc, O. W. Martin, W. H. Nester and M. K. Brice, Phys. Rev., **90,** 579, 1953.
4. P. S. Mittelman, Phys. Rev., **94,** 99, 1954.
5. E. F. Stucken, Z. O. Friel and A. H. Weber, Phys. Rev., **93,** 1053, 1954.
6. R. C. Rohr and R. D. Birkhoff, Phys. Rev., **98,** 1266, 1955.
7. Bernard L. Cohen, Phys. Rev., **126,** 1358, 1962.
8. L. G. Mann, S. D. Bloom and R. T. Nagle, Nucl. Phys., **30,** 636, 1962.
9. H. Slatis and L. Zappa, Arkiv fysik, **6,** 81, 1953.
10. N. I. Zaiko, O. F. Nemets and A. M. Yasnogorski, Izv. Akad. Nauk. SSSR. Ser. Fiz., **28,** 1160, 1964.
11. G. M. Drabkin, V. I. Orlov and L. I. Rusinov, Izvest. Akad. Nauk. SSSR, Ser. Fiz., **19,** 324, 1955.
12. S. Hultberg, Arkiv Fysik, **15,** 307, 1959.
13. S. Hultberg, B. Nagal and P. Olsson, Arkiv Fysik, **20,** 27, 1961.
14. F. Frey, H. Hamilton and S. Hultberg, Arkiv Fysik, **211,** 383, 162.
15. Nuclear Data Sheets, National Academy of Sciences-National Research Council, Washington.

ОТНОСИТЕЛЬНАЯ ИНТЕНСИВНОСТЬ И КОЭФФИЦИЕНТЫ ПРЕОБРАЗОВАНИЯ ПЕРЕХОДОВ В РАСПАДЕ Zr^{95}—Nb^{95}—Mo^{95}

Н. А. ИССА, З. МЕЛИГИ, А. Х. ЭЛ ФАРРАШ и С. ГИРГИС

Резюме

Бэта-спектрометром двойной фокусировки измерялись спектры внешней и внутренней конверсий в распаде Zr^{95}—Nb^{95}. Используя коррекцию к анизотропному распределению фотоэлектронов, выступающих из уранового конвертера, имеется возможность для определения точного значения относительной интенсивности гамма-лучей переходов 237, 726 и 757 Кэв в Nb^{95} и переходов 762, 765 Кэв в Mo^{95}. При помощи метода внутренне-внешней конверсии для упомянутых переходов определяется абсолютное значение коэффициента конверсии к. Оказывается, что переход 237 Кэв является переходом M_4, переход 726 Кэв — переходом M_1, в то время как другие переходы относятся или к переходам типа M_1, или к переходам E_2. Спин уровня при 726 Кэв в Nb^{95} имел значение $\frac{7^+}{2}$.

Acta Physica Academiae Scientiarum Hungaricae, Tomus 23 (1), pp. 75—85 (1967)

DETERMINATION OF OPTICAL CONSTANTS AND THICKNESS OF ANISOTROPIC CRYSTAL PLATES FROM TRANSMISSION MEASUREMENTS

By

I. HEVESI

INSTITUTE OF EXPERIMENTAL PHYSICS, JÓZSEF ATTILA UNIVERSITY, SZEGED

(Presented by A. Budó. — Received 7. VI. 1966)

A method for determining optical constants and thickness of thin, homogeneous weakly absorbing anisotropic crystal plates is presented. Calculations for orthorhombic crystals are based on extreme values of transmission curves measured with linearly polarized light vibrating parallel to the crystallographic axes and incident at right angles to the crystal surface. The method can be applied to crystals of insulators and semiconductors and has been tested with plane parallel single crystal plates of V_2O_5. The method proved to work well and to give valuable information on the anisotropic optical behaviour of the crystals in adequate spectral ranges.

Introduction

The measurement of optical transmission on layers of insulators and semiconductors enables one to determine several important optical characteristics and semiconductor parameters. A great variety of methods of evaluation can be found in the literature, owing to the different simplifying suppositions and approximations used. A relatively simple method, applicable to the determination of the optical constants and thickness of thin layers (from 0,5 to 10μ thick) of isotropic insulators and semiconductors, has been given by LIASHENKO and MILOSLAVSKI [1]. Their approximate calculations are based on interference maxima and minima of transmission curves. The method can be used in spectral ranges for which $n \gg k$ (i.e. absorption is weak).

It seemed desirable to extend the methods given in [1] to the case of thin, weakly absorbing anisotropic crystal plates. This was the object of our investigations reported in the present paper. The measurements were made on vanadium pentoxide because of its properties, which seemed favourable for our purpose.

V_2O_5, crystallizing in the orthorhombic system [2], gives birefringent, optically inactive biaxial crystals. It is comparatively easy to obtain crystals of lamellar structure by slow cooling of the melt. From these, plane parallel crystal plates of various thickness and (010) orientation can be split off. These crystal plates of a few microns thickness can be very well used to study the interference observed in transmission measurements in the visible spectral range.

Electric anisotropy of V_2O_5 has been studied by several authors [3—6], but publications on its anisotropic optical behaviour can hardly be found in the literature [7]. In earlier studies of optical transmission, anisotropy has not been taken into account [3—4]. This led to results which were not satisfactorily reproducible and to divergences between the shape of curves obtained with different samples. In the course of our researches described in the present paper it proved possible to obtain informations on the anisotropic optical behaviour of V_2O_5 in the visible spectral range by taking into consideration the optical orientation of the V_2O_5 crystal plates and applying the method described in [1] to orthorhombic crystals.

1. Method of investigation

As is well-known, light of arbitrary polarization incident on an anisotropic crystal plate will be split up in the crystal into two rays of definite polarization (referred to as "1" and "2"). If the plane of vibration of a polarized light ray incident at right angles on a plane parallel crystal plate of thickness d is chosen in a way that only one of both refracted plane waves ("1" or "2" respectively) is produced, the transmissions T_1 and T_2 of the plate for both cases will be given by the relation (see in [8])

$$T_s = \left| \frac{4\bar{n}_s \cdot e^{-\frac{2\pi i}{\lambda}\bar{n}_s d}}{(\bar{n}_s + 1)^2 - (\bar{n}_s - 1)^2 \cdot e^{-\frac{4\pi i}{\lambda} n_s d}} \right|^2 \quad (s = 1, 2). \tag{1}$$

$\bar{n}_s$ is a complex refractive index defined by

$$\bar{n}_s = n_s - ik_s \qquad (s = 1, 2), \tag{2}$$

where n_s means the respective refractive index and k_s the extinction coefficient. In setting up eq. (1) the plate was supposed to be in contact with air or vacuum on both faces.

The conditions of validity of eq. (1) are fulfilled for example if the direction of vibration of a linearly polarized light ray incident at right angles on an orthorhombic crystal coincides with one of the three crystallographic axes. We shall refer to the case when the direction of vibration of the linearly polarized light is parallel to the c or a axis of the V_2O_5 crystal plate of (010) orientation as position 1 and 2 of the crystal, respectively.

LIASHENKO and MILOSLAVSKI calculated the optical constants of isotropic, homogeneous, weakly absorbing layers from transmission maxima and

minima by successive approximation. In the present paper relatively simple formulas for the optical constants are given, which immediately yield sufficiently exact results under the given conditions.

In semiconductor and insulator crystals, besides the range of fundamental absorption, there generally exist spectral ranges for which the condition $n_s \gg k_s$ is fulfilled. In the case $n_1 \gg k_1$ eq. (1) can be brought into the simpler form

$$T_1 = \frac{16\, n_1^2 \eta_1}{(n_1+1)^4 + (n_1-1)^4 \eta_1^2 - 2\,(n_1^2-1)^2 \eta_1 \cos\dfrac{4\pi}{\lambda} n_1 d}, \tag{3}$$

where

$$\eta_1 = e^{-\frac{4\pi}{\lambda} k_1 d}. \tag{4}$$

Provided that besides $n_1 \gg k_1$, valid in the spectral range under investigation, another condition is fulfilled, namely that n_1 and k_1 vary only slightly with λ, the dependence of T_1 on wavelength will be governed by the cosinus factor in the denominator of eq. (3) and T_1 will reach its extreme values when

$$\frac{4\pi}{\lambda} n_1 d = m\pi \qquad (m = \text{an integer}). \tag{5}$$

Thus we obtain for the maxima and minima of transmission

$$T_{1\max} = \frac{16\, n_1^2 \eta_1}{[(n_1+1)^2 - (n_1-1)^2 \eta_1]^2} \tag{6}$$

and

$$T_{1\min} = \frac{16\, n_1^2 \eta_1}{[(n_1+1)^2 + (n_1-1)^2 \eta_1]^2}, \tag{7}$$

respectively. For n_1 and η_1 the following physically consistent solutions are obtained from eqs. (6) and (7):

$$n_1 = \frac{A_1 + B_1}{A_1 - B_1}, \quad \eta_1 = \left[\frac{A_1}{a_1 + b_1}\right]^2, \tag{8a—b}$$

where

$$a_1 = \sqrt{T_{1\max}}, \qquad b_1 = \sqrt{T_{1\min}},$$

$$A_1 = \sqrt{(a_1 b_1)^2} + \sqrt{a_1^2 - b_1^2 + (a_1 b_1)^2}, \qquad B_1 = \sqrt{a_1^2 - b_1^2}.$$

Under these conditions n_1 and η_1 can be calculated from eq. (8a—b) in the ranges of wavelength determined by a maximum $T_{1\max}$ and the subsequent

minimum $T_{1\min}$ (or inversely) of the transmission curve $T_1(\lambda)$ if these extreme values are known. The knowledge of the curve $n_1(\lambda)$ and of the wavelengths belonging to the extreme values enables us to calculate the thickness d of the plate with eq. (5). On the other hand, knowing $\eta_1(\lambda)$ and d, the curve $k_1(\lambda)$ can be constructed [see eq. (4)]. Analogous results for n_2 and η_2 can be obtained from $T_2(\lambda)$ if the condition $n_2 \gg k_2$ is fulfilled.

It is to be noted that only the optical constants n_1, n_2, k_1 and k_2 can be determined with V_2O_5 single crystal plates of (010) orientation. To obtain the refractive index n_3 and the extinction coefficient k_3 in a similar way, transmission measurements should be made on single crystal plates of (100) or (001) orientation. However, the preparation of plates of such orientations with surfaces of sufficient dimensions presents practically unsurmountable difficulties.

2. Experimental equipment and preparation of samples

The autocollimating plane grating monochromator of a single beam spectrophotometer Type Optica Milano CF4 was used for measurements of transmission. Measurements were made at every mμ in the spectral range under examination (0,48 to 0,85 μ) with a constant slit aperture of 0,18 mm corresponding to a band width of 0,27 mμ. A tungsten filament lamp fed from a stabilized electronic power supply unit served as light-source. Secondary spectra of the grating were eliminated by a red filter in the range of $\lambda > 600$ mμ. The detecting instrument was an end window photomultiplier Type EMI 9558A, fed from an anode battery, with a connected Zeiss "Skalen-Galvanometer" having a sensibility of $4 \cdot 10^{-10}$ Amp. per scale division. To polarize the light beam a Hilger polaroid filter was inserted between the exit slit of the monochromator and the sample.

V_2O_5 powder of analytical reagent grade supplied by the Chinoin-works was used as starting material. By heating over the melting point in a platinum crucible and by slow cooling, crystal plates of lamellar structure and of relatively great dimensions (6 to 10 cm^2, 1 to 2 mm thick) could be grown. It was easy to split off crystal plates of various thickness (0,1 to 0,3 mm) in the (010) plane from the grown crystal. However, the transmission of these plates was low and they did not show the interference structure necessary to test the method.

A comparatively simple method allowed to reduce the thickness of the plates by about two orders of magnitude and to prepare samples 1 to 2 μ thick and even thinner. The method is based on the fact that plates of various thickness (from 0,1 mm to 0,5 μ) can be split off from the crystal with the aid of a substance strongly sticking to its lustrous surface (e.g. paraffine half congealed on a glass slab). Those parts of these crystal plates which were not

in contact with the sticking material can be well used as samples. These plane parallel plates (1 to 3 μ thick) determined by two natural cleavage planes [(010) planes] of the crystal, are considerably transparent in the greatest part of the visible spectral range and display sufficient homogeneity.

The samples were fixed on a sample holder which had a circular aperture of 2 to 6 mm diameter and was inserted between the polaroid filter and the photomultiplier. A sliding support enabled the sample to be removed from the pathway of light. The sample holder could be rotated round an axis perpendicular to the plane of the crystal plate and adjusted with the aid of a scale. Before measuring the transmission, the extinction positions (positions 1 and 2) of the crystal were found between crossed positions of the polaroid filter and a nicol inserted in the place of the photomultiplier, then the nicol was removed. Positions different from both extinction positions, that is directions of vibration of the polarized light at angles to the crystal axes, could be adjusted with the aid of the scale. Besides the extinction positions, measurements were made for every 10° of the angle α between the c axis and the direction of vibration of linearly polarized light incident at right angles to the surface of the crystal plate.

Extinction angle, optic orientation and sign of the crystals were determined with the aid of a polarizing microscope Type Panphot. It could be stated on the basis of the interference figures that the V_2O_5 crystal plates used for transmission measurements were sections perpendicular to the acute bisectrix.

3. Results

The transmission curves T_1, T_2 and T_{45}, obtained with a thin sample in the positions $\alpha = 0$ (direction of vibration of the light coincident with the c axis), $\alpha = 90°$ (direction of vibration of the light coincident with the a axis), and $\alpha = 45°$ respectively are plotted with solid lines in Figs. 1a, 1b and 1c. Optical constants n_1, n_2, k_1, k_2 and thickness d of the plate were determined on the basis of the curves T_1 and T_2. The conditions of applicability of the method employed were well fulfilled between 560 and 800 mμ, that is in the greater part of the spectral range examined. Alternating extreme values follow each other at relatively small intervals (8 to 18 mμ) and therefore the extinction coefficients and refractive indices can be considered as constant in the respective ranges of wavelength. The half intensity of the bands of interference varies between 7 and 20 mμ, i.e. it is far above the spectral half-width of the apparatus.

Similar or higher values of η can be expected from eq. (6) owing to the transmission maxima of $\sim$0,9 to 0,96. According to eqs. (6) and (7) it can be inferred from the high transmission values (η near to unit) that η will be

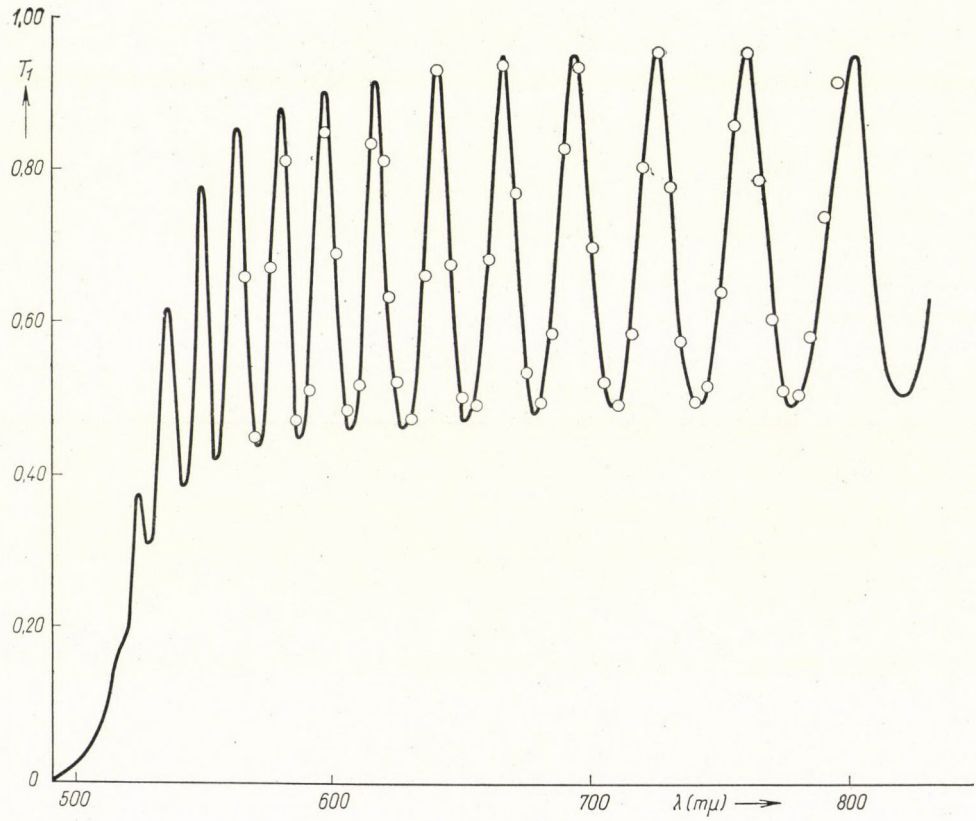

Fig. 1a. Transmission of a thin crystal plate in position 1. Values measured for every mμ wavelength represented by a solid line, those calculated with Eq. 3 for every 5th mμ marked by small circles

chiefly determined by T_{max} and n by T_{min}. Accordingly the curves $n(\lambda)$ have been constructed by coordinating the mean values of two refractive indices, calculated with eq. (8a) from a T_{min} and the two neighbouring T_{max}, to the mean of the wavelengths corresponding to the two T_{max}'s. These mean values of $n(\lambda)$ are marked by circles on the curves n_1 and n_2 in Fig. 3. The rather considerable differences between n_1 and n_2 were to be expected in consequence of the relatively great differences between the minima of the curves T_1 and T_2, respectively. The curves for $\eta(\lambda)$ were calculated similarly with eq. (8b) using two T_{min}'s neighbouring a T_{min}. The thickness of the plate calculated with eq. (5) from the refractive indices and wavelengths belonging to different extreme values of the transmission curves T_1 and T_2 gave only slight deviations, the mean being $d = 2{,}86\ \mu$. The curves $k_1(\lambda)$ and $k_2(\lambda)$ in Fig. 3 were constructed in the way described in Section 1. It can be seen that the character of these curves corresponds to the T_{max} values shown in Figs. 1a and 1b, in accordance with what has been said above.

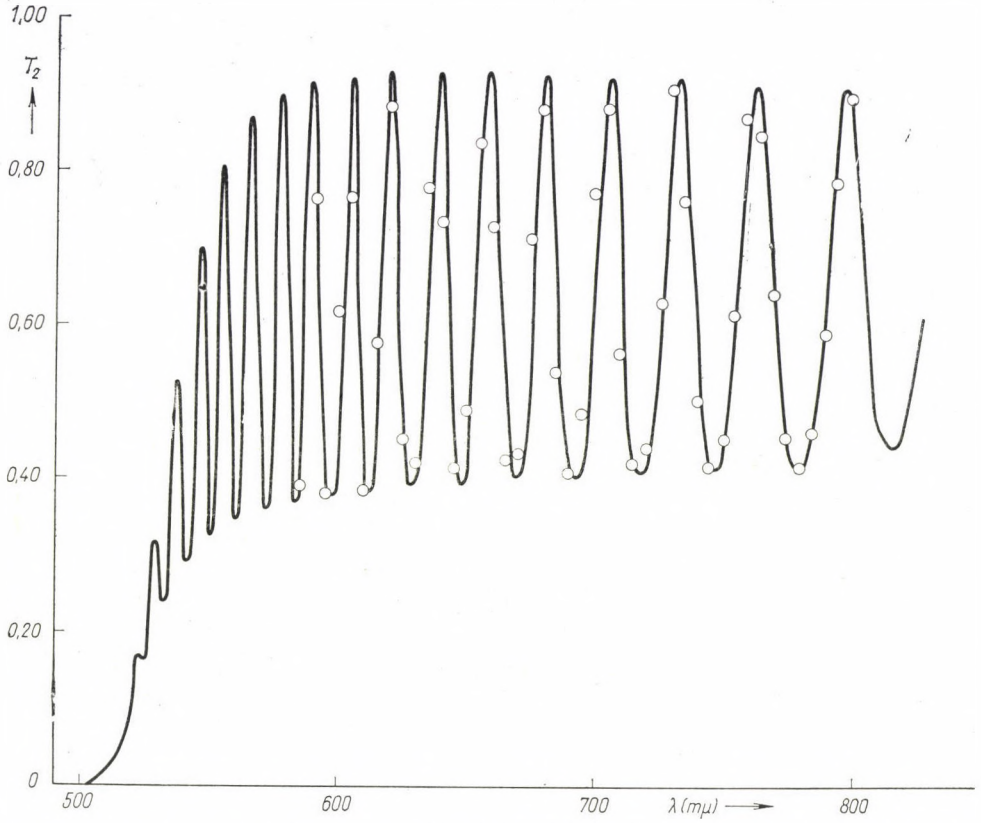

Fig. 1b. Transmission of a thin crystal plate in position 2. Values measured for every mμ wavelength represented by a solid line, calculated values for every 5th mμ marked by small circles

Figs. 2a and 2b show the changes in transmission of a crystal plate of $d = 35\ \mu$ in position 1 and 2, respectively (the thickness was measured with a mechanical method). At greater wavelengths, interference causes random fluctuations of about 4 to 10% between the transmission minima and maxima (see points of measurements marked with small circles between the dotted lines in Figs. 2a and 2b). These fluctuations decrease with increasing thickness of the plates, and for $d >$ about 0,14 mm continuous curves are obtained.

Transmission $T_1(\lambda)$ has been calculated by substituting $n_1(\lambda)$, $k_1(\lambda)$ and the thickness $d = 2{,}86\mu$ obtained into eq. (3). The results for every fifth μ are shown in Fig. 1a. The $T_2(\lambda)$ values shown in Fig. 1b were calculated in a similar way. The good accordance between the results of measurements and calculations, in particular for the extreme values, proves the efficiency of the method. If the direction of vibration of the polarized light is at an angle α to the c axis, the relation $T_\alpha = T_1 \cos^2\alpha + T_2 \sin^2\alpha$ will hold for the transmission [8]. A very good agreement has been obtained between the trans-

missions measured with different angles α and the values calculated with the above relation for T_α from measured values of T_1 and T_2. The values calculated for $\alpha = 45°$ $\left(\text{i.e. } T_{45°} = \dfrac{T_1 + T_2}{2}\right)$ are shown by small circles in Fig. 1c.

It can be seen from the shape of the curves $n_1(\lambda)$ and $n_2(\lambda)$ that, besides the normal dispersion of the refractive indices, also the dispersion of the bire-

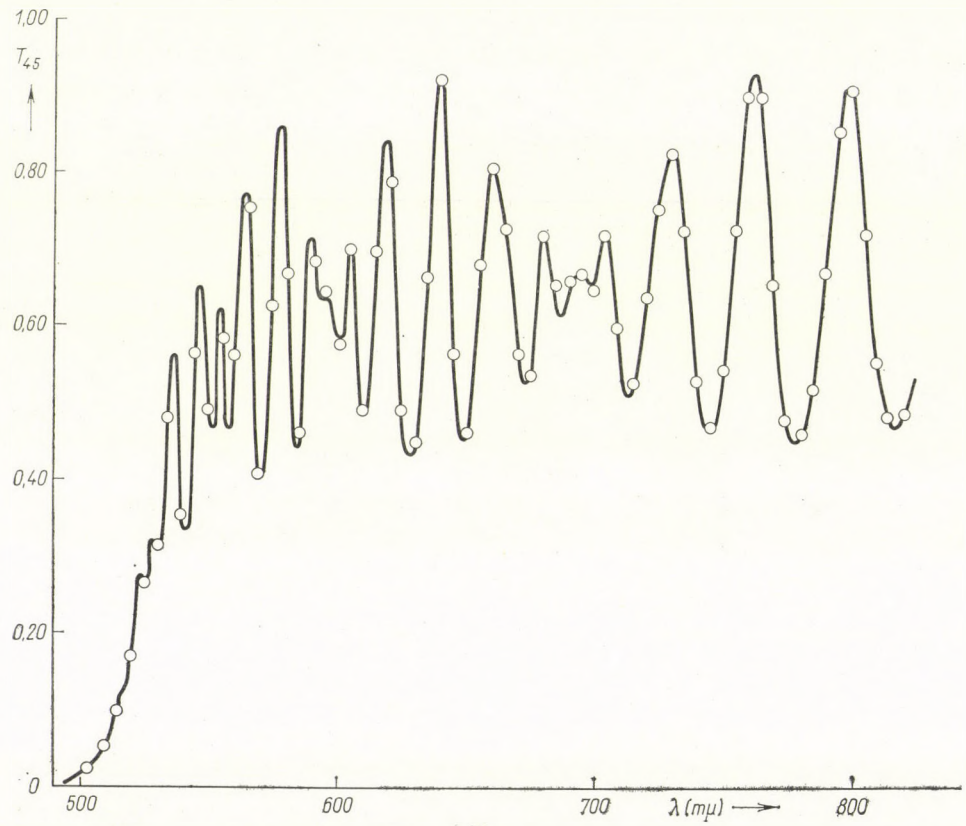

Fig. 1c. Transmission of a thin crystal plate in the position $\alpha = 45°$. Values measured for every mμ wavelength represented by a solid line, values of $\dfrac{T_1 + T_2}{2}$ calculated for every 5th mμ marked by small circles

fringence appears. According to [7] the principal refractive indices of V_2O_5 for $\lambda = 589$ mμ are $N_m = 2{,}53$, $N_g = 2{,}84$ and $N_p = 1{,}986$. For the same wavelength our values obtained for n_1 (corresponding to N_m) and n_2 (corresponding to N_g) were $n_1 = 2{,}53$ and $n_2 = 2{,}88$, respectively.

The curves $k_1(\lambda)$ and $k_2(\lambda)$ show the anisotropic absorption of the V_2O_5 crystal. Anisotropy of a similar character can be inferred from the shape of

the transmission curves for thick samples (Figs. 2a and 2b). The values of the absorption coefficients $K_1(\lambda)$ and $K_2(\lambda)$ calculated from Eq. 4 varied between $0{,}85 \cdot 10^2$ cm^{-1} and $3{,}9 \cdot 10^2$ cm^{-1}. These values agree in order of magnitude with those given by ARSENEVA and KURCHATOV [3], who did not take into account the anisotropy of absorption and determined some kind of mean absorption.

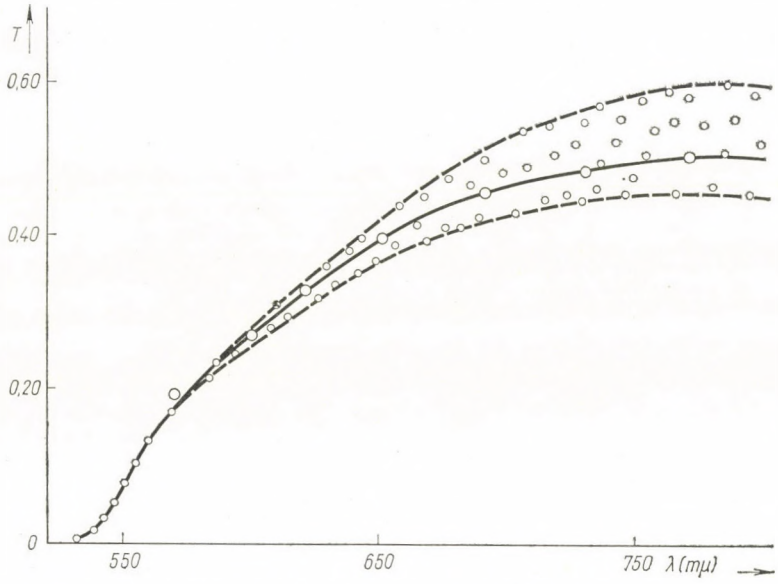

Fig. 2a. Transmission of a sample of $d = 35\ \mu$. Values measured in position 1 marked by small circles, values calculated with the optical constants of thin crystal plates ($d = 2{,}76\ \mu$) marked by larger circles

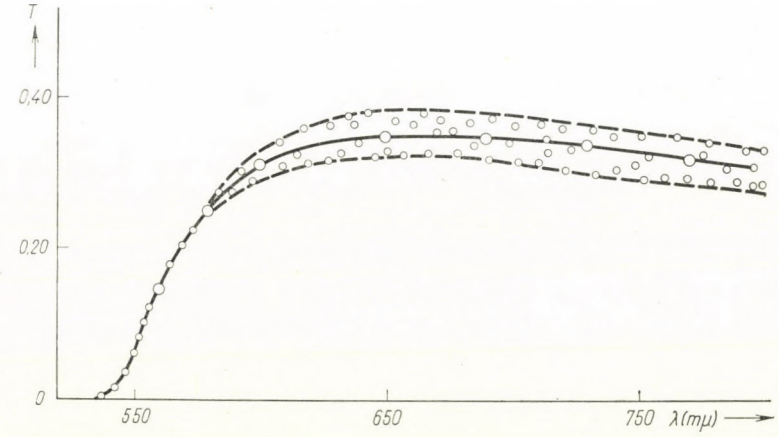

Fig. 2b. Transmission of a sample of $d = 35\ \mu$. Values measured in position 2 marked by small circles, values calculated with the optical constants of thin crystal plates ($d = 2{,}76\ \mu$) marked by larger circles

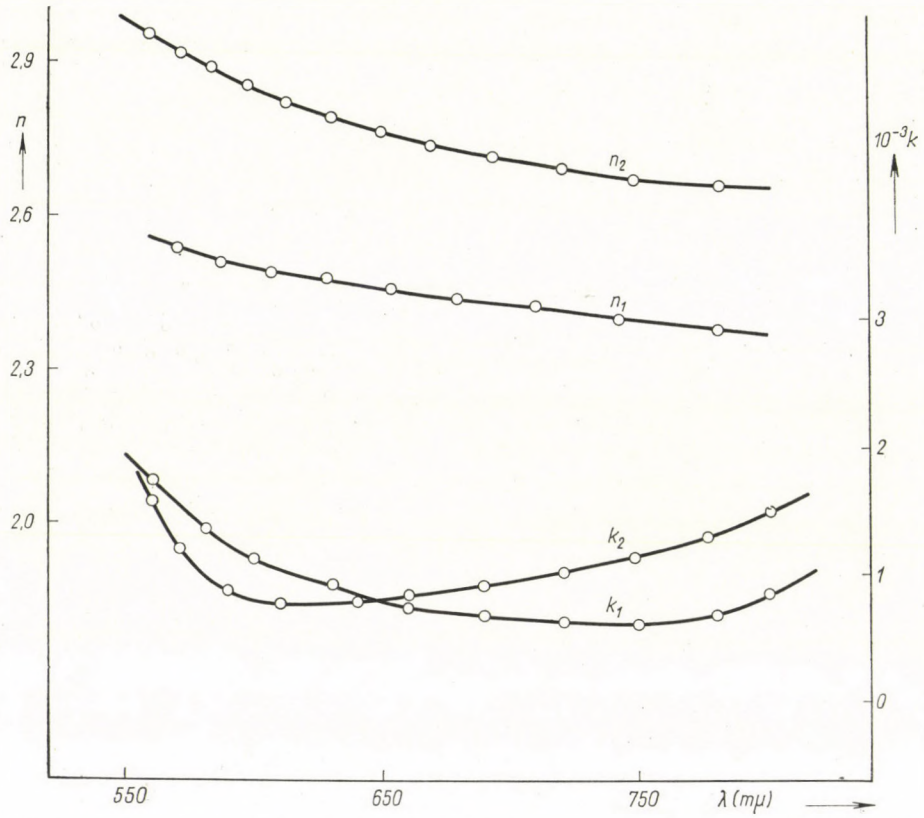

Fig. 3. Optical constants n_1, n_2, k_1, k_2 calculated from transmission curves (T_1, T_2) of thin crystal plates

A good agreement with the measured values has been obtained by calculating the transmission of samples of some 10^{-2} mm thickness with the absorption coefficients and refractive indices determined from the transmission curves of thin samples (see e.g. the calculated values for a sample of $d = 35\ \mu$ plotted as a solid line in Figs. 2a and 2b). In the case of plates of several 10^{-1} mm thickness divergences between calculated and measured values are observed. These divergences can be attributed to inhomogeneities which become more perceptible in plates of such thickness.

It is evident from measurements and the transmission curves shown in the Figures that the fundamental region of absorption of V_2O_5 lies in the visible spectral range. Further, it can be seen from the curves that the position of the fundamental absorption edge seems to be dependent on the direction of vibration of the linearly polarized light. This phenomenon has been observed in other anisotropic crystals too [9]. These problems, which are connected with the determination of the band gap will be dealt with in a further paper.

Acknowledgements

The author is indebted to Professor ZALÁN BODÓ, Research Institute for Technical Physics of the Hungarian Academy of Sciences, Budapest, for calling his attention to the problem and for valuable advices during the work. He has also to express his thanks to Professor Á. BUDÓ, Director of the Institute of Experimental Physics of the A. József University, Szeged, for his interest in the work and for kindly allowing to make the optical measurements in this Institute.

The crystals have been prepared by the author at the Institute of Experimental Physics of the Technical University, Budapest.

REFERENCES

1. С. П. Ляшенко и В. К. Милославский, Опт. и спектр., **1,** 151, 1964.
2. H. G. BACHMANN, F. R. AHMED and W. H. BARNES, Z. Kristallogr., **115,** 110, 1961.
3. А. Н. Арсеньева и Б. В. Курчатов, ЖЭТФ., **4,** 576, 1934.
4. J. BOROS, Zeitschr. f. Phys., **126,** 721, 1949.
5. И. Б. Патрина и В. А. Йоффе, ФТТ., **6,** 3227, 1964.
6. T. KAWAGUCHI, Kagaku, **23,** 534, 1953.
7. М. П. Глазырин и А. А. Фотиев, Кристаллография, **9,** 506, 1964.
8. А. М. Гончаренко и Ф. И. Федоров, Опт. и спектр., **14,** 94, 1963.
9. G. DRESSELHAUS, Phys. Rev., **105,** 135, 1957.

ОПРЕДЕЛЕНИЕ ОПТИЧЕСКИХ КОНСТАНТ И ТОЛЩИНЫ АНИЗОТРОПНЫХ КРИСТАЛЛИЧЕСКИХ ПЛАСТИНОК ПО ИЗМЕРЕНИЮ ПРОПУСКАНИЯ

И. ХЕВЕШИ

Р е з ю м е

Излагается метод для определения оптических констант и толщины тонких, однородных, слабо поглощающих анизотропных кристаллических пластинок. Разработка проводилась с помощью крайних значений кривых пропусканий. Метод проверен в случае монокристалла пятиокиси ванадия. Установлено, что этот метод хорошо оправдывается на практике и в определенной спектральной области дает полезные сведения о поведении оптической анизотропии кристаллов.

Acta Physica Academiae Scientiarum Hungaricae, Tomus 23 (1), pp. 87—94 (1967)

INFLUENCE OF DIRECT INELASTIC SCATTERING ON $(n, 2n)$ CROSS SECTIONS

By

J. CSIKAI

INSTITUTE OF NUCLEAR RESEARCH OF THE HUNGARIAN ACADEMY OF SCIENCES, DEBRECEN

and

G. PETŐ

INSTITUTE FOR EXPERIMENTAL PHYSICS, DEBRECEN

(Presented by A. Szalay. — Received 8. VI. 1966)

The $(n, 2n)$ cross sections were measured for the nuclei N^{14}, F^{19}, Ca^{48}, Sc^{45}, Mn^{55}, Ni^{58}, Cu^{65}, Zn^{64}, Zn^{66}, Se^{82}, Rb^{85}, Rb^{87}, Y^{89}, Zr^{90}, Mo^{92}, Sn^{112}, Sm^{144} at an excess energy 3 MeV above threshold. In addition, the $(n, 2n)$ cross sections for the nuclei Zn^{64}, Zn^{70}, Ga^{69}, Ga^{71}, As^{75}, Mo^{100}, Pb^{204} as well as the cross section of the process Pb^{204} (n, n') Pb^{204m} were determined at 14,7 MeV bombarding neutron energy. At 3 MeV excess energy a strong $N - Z$ dependence has been found in the $(n, 2n)$ cross sections, valid for a broad region of neutron numbers which can be accounted for by the influence of direct inelastic scattering leading to low lying levels of the target nucleus. An empirical formula is given for calculating $(n, 2n)$ cross sections.

Introduction

Various trends have been observed in $(n, 2n)$ cross sections vs. N, Z or A for neutrons of about 14 MeV [5—8]. Near the threshold the $(n, 2n)$ cross section depends strongly on the difference between bombarding and threshold energy, so the trends are predominantly determined by the Q-values (Fig. 1). It seems interesting to examine the behaviour of $(n, 2n)$ cross sections by normalising the excitation functions to each other, that is by taking constant bombarding-threshold energy difference.

Experimental procedures and results

The total $(n, 2n)$ reaction cross sections were measured with the activation method, choosing an excess energy of 3 MeV above the threshold. The neutrons were produced by the 300 keV neutron generator of ATOMKI, in D + T reaction. The samples were placed at different angles from the direction of the bombarding deuteron beam for varying the neutron energy (Fig. 2). The activities of the irradiated samples were measured by a NaI(Tl) scintillation gamma-spectrometer connected with a 100 and 128 channel amplitude analyser, respectively, or by a mica end window GM counter. The following

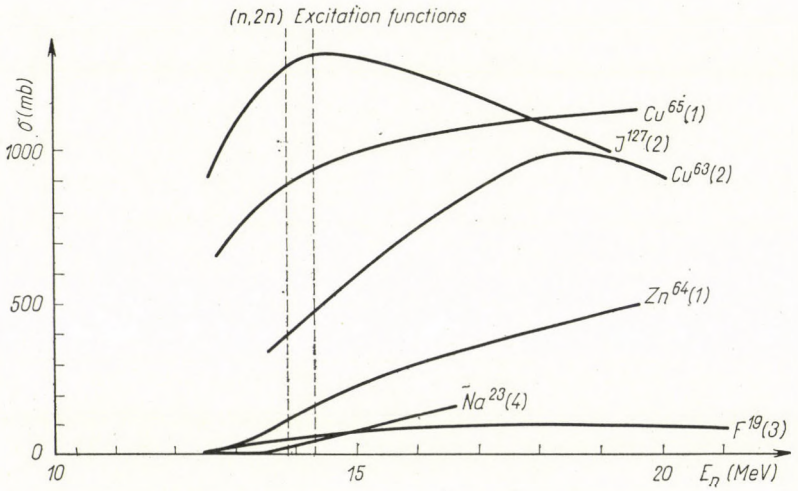

Fig. 1. Excitation functions of $(n, 2n)$ reactions

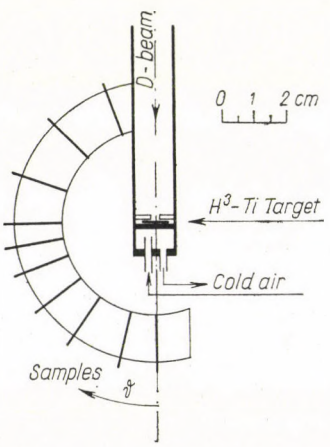

Fig. 2. Geometrical arrangement for irradiation

standard sources were used for calibration: $Sr^{90} + Y^{90}$, C^{14}, Co^{60}, Cs^{137}, Pb^{210}, Tl^{204} in the case of the GM counter, Hg^{203}, Mn^{54}, Cs^{137}, Y^{88} (IAEA Vienna) in the case of the scintillation spectrometer. The relative energy efficiency of the gamma spectrometer was determined by using isotopes of known decay scheme. The neutron flux was monitored continuously by a $B^{10}F_3$ long-counter and a plastic scintillator during the irradiation. The reactions $Al^{27}(n, \alpha)$, $Al^{27}(n, p)$, $Cu^{63}(n, 2n)$ and $Cu^{65}(n, 2n)$ were used as monitor reactions. The data for the decay schemes have been taken from Nuclear Data Sheets. The results obtained at 3 MeV excess energy are summarized in Table 1.

Table 1

Cross sections measured at an excess energy of 3 MeV

Target	Reaction	E_{thr} (MeV) (25)	$\sigma_{n,2n} \pm 15\%$ (mb) at E_{exc}=3 MeV	Monitor reaction	Method
Enriched					
$Ca^{48}CO_3$	$Ca^{48}(n, 2n)\ Ca^{47}$	10,28	860	$Al^{27}(n, \alpha)$; 117 mb $E_n = 14{,}1$ MeV	β
$RbNO_3$	$Rb^{85}(n, 2n)\ Rb^{84}$	10,65	830	,,	β
$RbNO_3$	$Rb^{87}(n, 2n)\ Rb^{86}$	10,03	1290	,,	β
Y_2O_3	$Y^{89}(n, 2n)\ Y^{88}$	11,99	1010	,,	γ : 899 keV
Se	$Se^{82}(n, 2n)\ Se^{81}$	9,29	1490*	,,	β
Sc	$Sc^{45}(n, 2n)\ Sc^{44}$	11,57	320	$Cu^{65}(n, 2n)$: 940 mb at $E_n = 14{,}1$ MeV	γ : 511 and 270 keV
MnO_2	$Mn^{55}(n, 2n)\ Mn^{54}$	10,41	750	,,	γ : 835 keV
Cu	$Cu^{65}(n, 2n)\ Cu^{64}$	10,06	810	,,	γ : 511 keV
Zn	$Zn^{66}(n, 2n)\ Zn^{65}$	11,21	550	,,	γ : 1114 keV
Zr	$Zr^{90}(n, 2n)\ Zr^{89}$	12,07	800	,,	γ : 511 and 915 keV
Sr	$Sr^{86}(n, 2n)\ Sr^{85}$	11,59	570	,,	γ : 514 keV
Ni	$Ni^{58}(n, 2n)\ Ni^{57}$	12,40	45	$Cu^{63}(n, 2n)$: 488 mb at $E_n = 14{,}1$ MeV	γ : 511
Cu	$Cu^{63}(n, 2n)\ Cu^{62}$	11,01	495	,,	γ : 511 keV
Zn	$Zn^{64}(n, 2n)\ Zn^{63}$	12,04	288	,,	γ : 511 keV
Mo	$Mo^{92}(n, 2n)\ Mo^{91}$	13,27	280*	,,	γ : 511 keV
Sm	$Sm^{144}(n, 2n)\ Sm^{143}$	10,75	1600	,,	γ : 511 keV
$C_6H_{12}N_4$	$N^{14}(n, 2n)\ N^{13}$	11,31	8,2	,,	γ : 511 keV
CF_2	$F^{19}(n, 2n)\ F^{18}$	10,99	63	,,	γ : 511 keV
Sn	$Sn^{112}(n, 2n)\ Sn^{111}$	11,19	1530	,,	γ : 511 keV

* Extrapolated to 3 MeV.

In addition, the $(n, 2n)$ cross sections at a neutron energy of 14,7 MeV were determined for some nuclei for which no previous data are available (Zn^{70}, Pb^{204}) or the existing data are not unambiguous. The experimental arrangements were identical with those described above except for the irradiation geometry. The results obtained are indicated in Table 2.

Table 2

Cross sections measured at a neutron energy of 14,7 MeV

Target	Reaction	$\sigma_{n\,2n}$ (mb) $E_n = 14{,}7 \pm 0{,}3$ MeV	Monitor reaction $E_n = 14{,}7 \pm 0{,}3$ MeV	Method
Enriched $Zn^{70}O$	$Zn^{70}(n, 2n)\,Zn^{69}$	1307 ± 130	$Al^{27}(n, \alpha)$: 117 mb	β
Enriched $Zn^{70}O$	$Zn^{64}(n, 2n)\,Zn^{63}$	225 ± 25	,,	β
Mo	$Mo^{100}(n, 2n)\,Mo^{99}$	1762 ± 200	,,	β
Ga_2O_3	$Ga^{69}(n, 2n)\,Ga^{68}$	1088 ± 100	$Al^{27}(n, p)$: 73 mb	β
Ga_2O_3	$Ga^{71}(n, 2n)\,Ga^{70}$	961 ± 100	,,	β
As_2O_3	$As^{75}(n, 2n)\,As^{74}$	1092 ± 120	$Cu^{65}(n, 2n)$: 970 mb	γ : 511 + 596 keV
Pb	$Pb^{204}(n, 2n)\,Pb^{203}$	1575 ± 160	,,	γ : 279 keV
Pb	$Pb^{204}(n, n')\,Pb^{204m}$	$76{,}5 \pm 8$	,,	γ : 899 + 912 keV

Discussion

In accordance with the previous results [9] the cross section values measured at 3 MeV excess energy were found to differ from each other markedly even if the neutron numbers are identical. Plotting these values against $N-Z$ at given N, the data lie on a straight line (Fig. 3, dots), independently

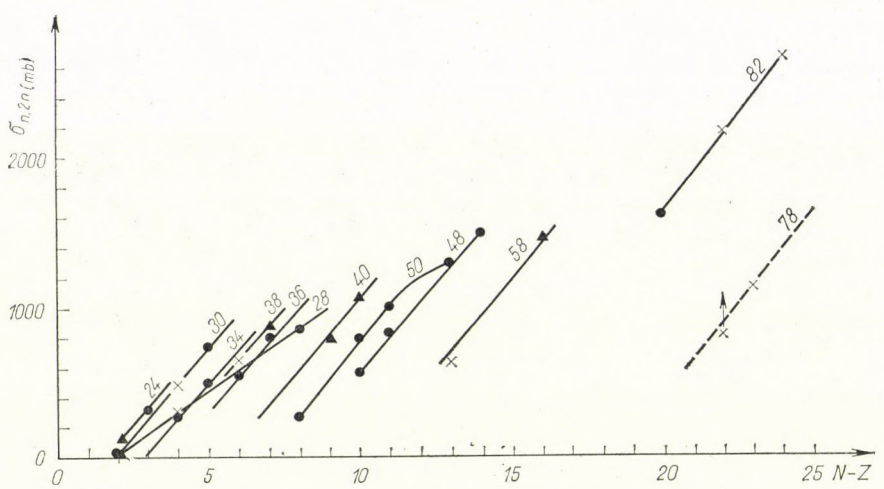

Fig. 3. The cross section for the $(n, 2n)$ reaction as a function of $N-Z$ with N as a parameter. Dots: values measured at $E_n = E_{thr} + 3$ MeV; triangles: values measured at $E_n = 14{,}7$ MeV and reduced to $E_n - E_{\mathrm{thr}} = 3$ MeV; crosses: values from references [2], [10—15], reduced to $E_n - E_{\mathrm{thr}} = 3$ MeV

of Z being even or odd. The straight lines belonging to different N are parallel to each other in a good approximation, except for $N = 28$. For studying this trend it is more favourable to fix N rather than Z because this permits to extend the investigation to more nuclei.

In order to extend the investigation to a broader region, the data of Table 2 measured in the region $E_{\text{thr}}(n, 2n) < E_n < E_{\text{thr}}(n, 3n)$ as well as some data given by others (Ti^{46}, Fe^{54} [10], Ge^{70} [11], Fe^{56} [12], Rh^{103} [13], Nd^{142} [14], Ba^{134m}, Ce^{140} [15] and Cs^{133} [2]) have been reduced to 3 MeV excess energy by using the "WEISSKOPF estimate" [17]:

$$\sigma_{n,2n} = \sigma_{n,M}\left[1 - \left(1 + \frac{E_{\text{exc}}}{T}\right) e^{-\frac{E_{\text{exc}}}{T}}\right],$$

where $\sigma_{n,M}$ is the neutron emission cross section, E_{exc} is the excess energy above the threshold, T is the temperature of the intermediate residual nucleus. The nuclear temperature has been calculated by means of the formula $T = \sqrt{\frac{E_n}{0{,}115\,A}}$ [16]. As it has been found [10], the above formula describes the form of the $(n, 2n)$ excitation functions well. Plotting these cross sections too (Fig. 3, triangles and crosses) it is seen that the $N - Z$ dependence of $\sigma_{n,2n}$ is identical in a broad region of neutron numbers.

On this basis a single formula can be given for calculating $(n, 2n)$ cross sections:

$$\sigma(Z \pm \Delta Z, N) = [\sigma(Z, N) \mp m(E_{\text{exc}})\,\Delta Z].$$

For $E_{\text{exc}} = 3$ MeV one finds $m(E_{\text{exc}}) = 231$ mb. If the value of $\sigma_{n,2n}$ is known for a definite N and Z, this formula allows to calculate $\sigma_{n,2n}$ for other Z values at the same N. The empirical formula gives good cross section values in the interval $30 \leq N \leq 120$ investigated. The empirical formula given can be applied also to other energies by using the "WEISSKOPF estimate" for taking into account the energy dependence.

As it can be seen from the data of Table 1, the $\sigma_{n,2n}$ values differ greatly even for the same target neutron number (e.g. the nuclei Ni^{58}, Fe^{56}, Mn^{55} belonging to $N = 30$ have the cross section values 45 mb, 500 mb and 750 mb, respectively), so no significant shell effect can be recognised vs. the target neutron or mass number.

The Q values of the $(n, 2n)$ reactions for $N - Z = \text{const.}$ show a shell effect vs. neutron number [18]. According to the WEISSKOPF relation this shell effect must appear in the cross sections too. Choosing a constant excess energy, the shell effect caused by the neutron binding energy can be eliminated. This allows to investigate the other trends that may appear in $(n, 2n)$ cross section, under clearer conditions.

The $N-Z$ dependence of $\sigma_{n,2n}$ must be attributed to the quantity $\sigma_{n,M}$: The trend appearing in the same manner in a broad region of neutron numbers cannot be accounted for by concurrent charged particle reactions supposed formerly [7], since the trend is independent of whether the cross sections of charged particle reactions are high or low as compared with $\sigma_{n,2n}$. The $N-Z$ dependence cannot be explained by (n, γ) reactions either because of the negligibly small cross sections. Differences in the relative excess energy

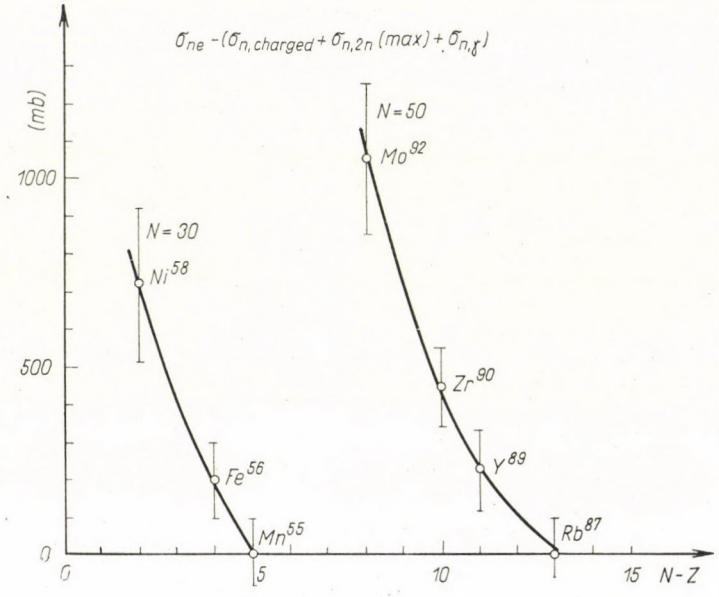

Fig. 4

(arising because of the differences in Q even at the same excess energy) may influence the $(n, 2n)$ cross section. However, the pairs of nuclei Zn^{70}, Ga^{71} as well as Y^{89}, Zr^{90} exhibit the same $N-Z$ dependence which was observed for other nuclei, although their Q values are identical.

The nonelastic cross section $\sigma_{ne} = \sigma_{n,M} + \sigma_{n,\text{charged}} + \sigma_{n,\gamma}$ is a smooth function of the mass number [26]. For heavy nuclei $\sigma_{ne} \approx \sigma_{n,M}$. Since $\sigma_{n,M} = \sigma_{n,n'} + \sigma_{n,2n}$, on the basis of the statistical model $\sigma_{n,2n}$ has a maximum value, where $\sigma_{n,2n}(\text{max}) = \sigma_{n,M}$. This means that one can neglect the cross section of nonelastic scattering leading to low-lying levels of the target nucleus [under the binding energy (B_n) of the last neutron] as well as the γ-de-excitation from the levels above B_n.

According to the experimental data, the difference $\sigma_{ne} - (\sigma_{n,2n}(\text{max}) + \sigma_{n,\text{charged}} + \sigma_{n,\gamma})$ depends on $N-Z$ and for a given N it tends to zero with increasing $N-Z$ (see e.g. Fig. 4). The values σ_{ne}; $\sigma_{n,\text{charged}}$; $\sigma_{n,\gamma}$ and

$\sigma_{n,2n}$(max) are known experimentally (e.g. for $N = 50$), so the deviation can be caused by the (n, n') process, i.e. $\sigma_{n,2n}(\max) \neq \sigma_{n,M}$. Supposing that γ-deexcitation from the levels above B_n is negligible as compared with neutron emission (which can be expected in the energy region where $\sigma_{n,2n}$ is near its maximum value [19]), the cross sections for (n, n') processes leading to levels under B_n must depend on $N-Z$ and have to be considerably greater than expected on the basis of the statistical model. This supposition is supported by experimental data on inelastic scattering. E.g. $\sigma_{n,n'}$ belonging to the first 2^+ state of Fe^{56} (20) and Th^{232} (21) has a considerably large value even at a bombarding neutron energy of about 15 MeV. According to our measurements, at $E_n = 14{,}7$ MeV the cross section ratio for $Pb^{204}(n, 2n)\,Pb^{203}$ and $Pb^{204}(n, n')\,Pb^{204m}$ is 21, while the ratio predicted by the statistical model is greater than 300. According to the measurements of STELSON et al. [22] as well as PEARLSTEIN and WINHOLD [23], the excitation of low lying collective levels is considerable also at a neutron energy of $E_n > 10$ MeV and does not vary strongly with increasing neutron energy. The peaks corresponding to these levels appear significant in the spectrum of scattered neutrons in a broad region of mass number. The cross sections for inelastic scattering which lead to the excitation of collective levels have been successfully interpreted by the PEREY—BUCK optical potential containing $N-Z$ dependence [24].

According to the above considerations, the $N-Z$ dependence of the $(n, 2n)$ cross sections can probably be accounted for by the influence of direct inelastic scattering.

We are indebted to Professor A. SZALAY for his interest in the present work and for the excellent working conditions he provided. The authors thank L. BUNKÓCZI for his assistance in operating the neutron generator.

REFERENCES

1. H. LISKIEN and A. PAULSEN, Nukleonik, **7**, 117, 1965.
2. M. BORMANN, S. CIERJACKS, R. LANGKAN and H. NEUERT, Z. Phys., **166**, 477, 1962.
3. J. PICARD and C. WILLIAMSON, Nucl. Phys., **63**, 673, 1965.
4. H. LISKIEN and A. PAULSEN, Nucl. Phys., **63**, 393, 1965.
5. M. BORMANN, Nucl. Phys., **65**, 257, 1965.
6. F. MANERO, Int. Conf. on the Study of Nucl. Structure with Neutrons, Antwerpen c. 120, 1965.
7. D. W. BARR, C. I. BROWNE and J. S. GILMORE, Phys. Rev., **123**, 859, 1961.
8. P. STROHAL, N. CINDRO and B. EMAN, Nucl. Phys., **30**, 49, 1962.
9. J. CSIKAI and G. PETŐ, Physics Letters, **20**, 52, 1966.
10. J. CSIKAI, Int. Conf. on the Study of Nucl. Structure with Neutrons, Antwerpen c. 102, 1965.
11. R. J. PRESTWOOD and B. P. BAYHURST, Phys. Rev., **121**, 1438, 1961 and J. Inorg. Nucl. Chem., **23**, 173, 1961.
12. V. J. ASHBY, H. C. CATRON, L. L. NEWKIRK and C. J. TAYLOR, Phys. Rev., **111**, 616, 1958.
13. H. A. TEWES, A. A. CARETTO, A. E. MILLER and D. R. NETHAWAY, UC 34—WASH. 1028, 1960.
14. L. A. RAYBURN, Phys. Rev., **122**, 168, 1961.
15. R. G. WILLE and R. W. FINK, Phys. Rev., **118**, 242, 1960.
16. T. ERICSON, Advances Phys., **9**, 425, 1960.

17. J. M. Blatt and V. F. Weisskopf, Theoretical Nuclear Physics, John Wiley and Sons, New York 1952.
18. P. E. Nemirovszkij, Szovremennüje modeli atomnovo jadra. Atomizdat, Moszkva, p. 60, 1960.
19. H. Büttner, A. Linder and H. Meldner, Nucl. Phys., **63,** 615, 1965.
20. J. T. Prud'homme et al. BNL. 400 Second Edition. Volumen II. of II. 26-0-10.
21. B. Baldoni and V. Benzi, Int. Conf. on the Study of Nuclear Structure with Neutrons, Antwerpen c. 145, 1965.
22. P. H. Stelson, R. L. Robinson, H. J. Kim, J. Rapaport and G. R. Satchler, Nucl. Phys., **68,** 97, 1965.
23. S. Pearlstein and E. J. Winhold, J. Nucl. Energy, A/B. **19,** 497, 1965.
24. F. Perey, Nuclear Structure Study with neutrons, North-Holland Publishing Company. Amsterdam, p. 418, 1966.
25. R. J. Howerton et al. UCRL—14 000, 1964.
26. N. N. Flerov and V. M. Talyzin, J. Nuclear Energy, **4,** 529, 1957; V. I. Strizhak, J. Nucl. Energy, **5,** 853, 1957; Mac Gregor et al. Phys. Rev., **108,** 726, 1957; Phys. Rev., **130,** 1471, 1963.

ВЛИЯНИЕ ПРЯМОГО НЕУПРУГОГО РАССЕЯНИЯ НА СЕЧЕНИЕ (n, $2n$)

Й. ЧИКАИ и Г. ПЕТЭ

Р е з ю м е

Измерялись сечения для реакции (n, $2n$) для ядер N^{14}, F^{19}, Ca^{48}, Sc^{45} Mn^{55}, Ni^{58}, Cu^{65}, Zn^{64}, Zn^{66}, Se^{82}, Rb^{85}, Rb^{87}, Y^{89}, Zr^{90}, Mo^{92}, Sn^{112}, Sm^{144} с излишком энергии в 3 Мэв над порогом. Наряду с этим, сечения реакции (n, $2n$) определялись как для ядер Zn^{64}, Zn^{70}, Ga^{69}, Ga^{71}, As^{75}, Mo^{100}, Pb^{204}, так и для процесса $Pb^{204}(n, n')\,Pb^{204m}$ энергии 14,7 Мэв бомбардирующих нейтронов. При излишней энергии 3 Мэв в сечении реакции (n, $2n$) наблюдалась сильная $N-Z$ зависимость, действительная для широкого интервала числа нейтронов, о котором можно судить по влиянию прямого неупругого рассеяния, ведущего к низко лежащим уровням ядер мишени. Дается эмпирическая формула для вычисления поперечных сечений реакции (n, $2n$).

Acta Physica Academiae Scientiarum Hungaricae, Tomus 23 (1), pp. 95—110 (1967)

ÜBER DIE NIVEAUDICHTE DER ATOMKERNE

Von

TH. NEUGEBAUER

INSTITUT FÜR THEORETISCHE PHYSIK DER ROLAND EÖTVÖS-UNIVERSITÄT, BUDAPEST

(Vorgelegt von K. F. Novobátzky. — Eingegangen: 14. VI. 1966)

Nach einer kurzen Diskussion der Frage, weshalb wir das elementare zwischen zwei Nukleonen wirkende Kraftgesetz noch immer nicht kennen und wofür hauptsächlich der Mangel an angeregten Niveaus der leichtesten Kerne verantworlich gemacht wird, folgt die zuerst rein klassische Besprechung des Problems, dass in welchen Gebieten bei den in der Kernphysik hauptsächlich in Rede kommenden Potentialansätzen die Energie negativ sein kann. Weiter wird dann zuerst mit Hilfe der Bohrschen Theorie berechnet, ob es in diesen Gebieten auch Quantenzustände geben kann. Im nächsten Paragraphen werden dann diese Resultate vom Standpunkte der Quantenmechanik aus betrachtet. Im letzten Teil wird endlich gezeigt, dass wenn es sich um die Wechselwirkung von vielen Nukleonen handelt, die Gebiete in denen die Energie negativ ist, sehr wesentlich vergrössert werden, die Quantenbedingungen sich dagegen nur viel weniger ändern. Die Ursache dieses Umstandes ist kurz, dass sich die potentiellen Energien als Skalare, die Kräfte dagegen als Vektoren addieren. Dieser Tatbestand erklärt ganz ungezwungen das Auftreten von verwickelten Termschemata bei schweren Kernen, also von solchen Erscheinungen, die schon teilweise zu denen in der Elektronenhülle auftretenden analog sind.

Einleitung

Man kann es nicht leugnen, dass sich die Theorie der Atomkerne, trotz sehr vielen Bemühungen, noch immer in dem bedauernswerten Zustande befindet, dass wir die elementare zwischen zwei Nukleonen auftretende Wechselwirkung — wenn wir die auch im allgemeinsten Sinne des Wortes verstehen — noch garnicht kennen. Bezüglich der Ursache weshalb theoretische Untersuchungen hier keinen Erfolg gehabt haben, sei hier nur folgendes erwähnt: In der Physik der Elektronenhülle ist selbstverständlich das einfachste Problem das des Wasserstoffatoms, der analoge einfachste Fall in der Kerntheorie wäre das Deuteron. Vom Wasserstoffatom waren jedoch schon vor der Entdeckung der eigentlichen Quantentheorie dutzende von Spektrallinien bekannt, das Deuteron besitzt dagegen gar keine angeregten Energieniveaus, sondern nur einen Triplett-Grundzustand und einen — jedoch nur mehr virtuellen — angeregten Singulettzustand. Wenn wir also auch den letzteren noch als genau bekannt betrachten, so sind auch das nur zwei Daten und da man weiter zur Erklärung der Bindung des Deuterons ein Potential annehmen muss, dass sich wenigstens in grösseren Entfernungen sehr schnell ändert, so muss solch ein Potentialansatz doch wenigstens zwei

Konstanten enthalten und wenn dieser Ausdruck nur nicht ganz ungeschickt gewählt ist, so ist die Bedigung des Auftretens der erwähnten zwei Niveaus mathematish immer erfüllbar. Es ist zwar wahr, dass das Deuteron ausserdem auch noch ein elektrisches Quadrupolmoment besitzt. Zur Erklärung von dem muss man jedoch unbedingt annehmen, dass die zwischen den zwei Nukleonen wirkende Kraft nicht ganz zentral ist und dazu muss im Potentialansatz doch noch wenigstens eine weitere Konstante eingeführt werden, welche dann wieder so wählbar ist, dass das erwähnte Quadrupolmoment richtig herauskommt. Das magnetische Dipolmoment des Deuterons weicht dagegen nur so wenig von der algebraischen Summe der Momente des Protons und des Neutrons ab, dass man daraus keine wertvolle Schlüsse bezüglich unseres Problems ziehen kann.

Die nächstfolgenden einfachsten Kerne wären das Triton und das ^{3}He. Doch sind die schon Dreikörperprobleme. Es ist schon wahr, dass diesem Problem die Quantenmechanik nicht so machtlos gegenübersteht, wie die klassische Theorie — das beweisen z. B. die aus der RITZschen Methode ausgehenden Berechunngen von HYLLERAAS, welche beim He die experimentelle Genauigkeit erreichen — doch wären umgekehrt solche Berechnungen kaum dazu geeignet aus ihnen zwangsläufige Schlüsse auf das auftretende Kraftgesetz zu ziehen. Angeregte Niveaus besitzen diese Kerne ebenfalls nicht.

Gegen unsere bisherigen Betrachtungen könnte man einwenden, dass wenn auch das Deuteron keine angeregten Zustände besitzt, an denen man einen angenommenen Potentialansatz ausprobieren könnte, man doch an Nukleonen Streuversuche vollführen kann und je grössere Energien man dabei anwendet, desto mehr erfährt man darüber, wie sich das Potential bei kleinen Entfernungen verhält. Das ist zweifellos richtig, doch muss man hier den folgenden Umstand beachten: Die Streukurve ist selbstverständlich eine kontinuierliche Funktion und aus der zieht man dann Schlüsse auf eine weitere ebenfalls kontinuierliche Funktion, nämlich auf den Potentialansatz. Es ist jedoch eine bekannte mathematische Erfahrung, dass analytisch sehr verschieden aussehende Funktionen — wenigstens in einem gewissen Bereich — praktisch ganz den selben Funktionengang beschreiben können. Im vorliegenden Fall ist es deshalb garnicht sicher, ob man ein tatsächliches Naturgesetz oder nur eine geschickte Interpolationsformel gefunden hat. In der Physik der Elektronenhülle waren die Verhältnisse diametral entgegengesetzt. Die Balmerformel, die nicht eine kontinuierliche Funktion sondern ein Punktspektrum darstellt, hätte ganz unmöglich bloss eine geschickte Interpolationsformel sein können, sondern es war gleich nach ihrer Entdeckung klar, dass sie ein damals noch unbekanntes jedoch wirkliches Naturgesetz enthalten muss.

1.

Zuerst wollen wir rein klassisch die Frage besprechen, dass wo — bei der Annahme von verschiedenen Kraftgesetzen — überhaupt negative Energiewerte auftreten können, weil ja das die erste Bedingung dafür ist, dass es nach der Quantenmechanik in solchen Gebieten stabile Niveaus geben soll. Betrachten wir zuerst zu diesem Zwecke den einfachsten Fall in dem die auftrende Kraft zu einer negativen Potenz der Entfernung proportional ist, setzen wir also

$$K = -\frac{A}{r^n} \tag{1}$$

und nehmen ausserdem an, dass es sich um Kreisbahnen handelt. Aus der Gleichheit der zentripetalen und zentrifugalen Kraft folgt dann in den gewohnten Bezeichnungen

$$\frac{A}{r^n} = \frac{mv^2}{r} . \tag{2}$$

Weiter besteht die Energiegleichnung

$$E = -\frac{1}{n-1}\frac{A}{r^{n-1}} + \frac{1}{2}mv^2 ; \tag{3}$$

und durch Elimination von v aus (2) und (3) folgt

$$E = -\frac{1}{n-1}\frac{A}{r^{n-1}} + \frac{1}{2}\frac{A}{r^{n-1}} = \left(\frac{1}{2} - \frac{1}{n-1}\right)\frac{A}{r^{n-1}} . \tag{4}$$

$n = 2$ ist selbstverständlich der Bohrsche Fall des Wasserstoffatoms. Bei $n = 3$ ist E bei allen Werten von r gleich Null und wenn $n > 3$ ist, so wird E positiv, man müsste also Energie zuführen, damit das Teilchen auf einem tieferen Niveau verweilen kann. Solche Potentialansätze würden also zu einer Art Katastrophe führen; das umkreisende Teilchen müsste in das Kraftzentrum hineinfallen und dabei würde eine unendlich grosse Energie frei werden. Im fall $n = 2$ würde zwar beim Hineinfallen des Teilchens in das Kraftzentrum ebenfalls eine unendliche Energie auftreten, bei diesem Kraftgesetz kann jedoch das umkreisende Teilchen dauernd auf einer stabilen Bahn (tiefste Quantenbahn) verweilen.

Den ganz speziellen Fall $n = 1$ müssen wir noch gesondert betrachten. Dann haben wir nämlich für die potentielle Energie;

$$V = A\int_{\infty}^{r_0}\frac{1}{r}dr = A\ \log\ r/r_0^{\infty} = -\infty , \tag{5}$$

also für jeden Wert von r_0

$$E = -\infty . \tag{6}$$

Stabile Niveaus kann es also bei der Gültigkeit des Kraftansatzes (1) nur dann geben, wenn $3>n>1$ ist. Das Auftreten von gebrochenen Potenzen in (1), das ja nach den vorangehenden Gedankengang zwischen diesen Grenzen möglich wäre, ist jedoch aus dimensionalen Gründen recht unwahrscheinlich, weil es sich ja dann um ein Naturgesetz handeln müsste, in dem auch die Dimension der Konstante A eine gebrochene Potenz der Länge enthalten müsste. Es bleibt also allein der Wert $n = 2$ als vernünftige Lösung übrig und tatsächlich ist (wenigstens im Euclidischen Raum) nur dieses Kraftgesetz verwirklicht, wie ja das das elektrische, das magnetische und das Gravitationsfeld zeigen. Multipolkräfte die scheinbar eine Ausnahme von dieser Regel bilden würden, kann man ja immer auf Singulettpolkräfte zurückführen, weil ja Multipole bloss eine mathematische Abstraktion sind. Ideale Multipole gibt es in der Natur nicht. Bei elektrischen Kräften ist diese Behauptung unmittelbar evident, aber auch im magnetischen Falle sieht man es gleich, dass trotz dem, dass die Feldintensität jetzt durch einen axialen Vektor beschrieben wird, man z. B. das Feld einer Stromschleife zwar durch eine Doppelschicht beschreiben kann, man kann jedoch diese flächenhaft verteilte Dipolschicht nicht in ein punktförmiges (also mathematisches) Dipol von endlichem Dipolment zusammenziehen. Im Zusammenhang mit dieser Frage ist es noch interessant zu erwähnen, dass nach den neuen HOFSTADTERSCHEN und WILSONSCHEN Messungen, sogar auch das magnetische Moment der Nukleonen in einem endlichen Volumen verteilt ist. Die VAN DER WAALSSCHE Energie ist ausserdem auch nur ein gewisser zeitlicher Mittelwert von den von Dipolkräften verursachten Energieänderungen. Ausser diesen erwähnten Umständen besteht ja selbstverständlich auch die elementare Regel, dass wenn sich irgend eine Wirkung, die nicht verlorengehen kann, gleichmässig im Raume verteilt, deren Dichte proportional zu $1/r^2$ abnehmen muss.

Zur Ergänzung der hier gesagten führen wir noch die kinetische Energie $T = \frac{1}{2} mv^2$ ein, dann haben wir

$$E = \left(\frac{1}{2} - \frac{1}{n-1}\right) 2T. \tag{7}$$

Also folgt im Bohrschen Falle ($n = 2$)

$$E = -T; \tag{8}$$

ist dagegen $n = 3$, so haben wir dauernd

$$E = 0, \tag{9}$$

und bei dem Auftreten eines logarithmischen Potentials ($n = 1$)

$$E = 2\left(\frac{1}{2} - \infty\right) T = -\infty . \tag{10}$$

2.

Nach diesen elementaren Betrachtungen wollen wir jetzt sehen, wie die analogen Verhältnisse bei den halbempirischen, zur Beschreibung der Kernkräfte (also der sogenannten starken Wechselwirkung) eingeführten Potentialansätzen sein werden. Besonders vier Funktionen haben bei der Beschreibung dieser Wechselwirkung eine gewisse Bedeutung erlangt, das einfache Kastenpotential, das YUKAWA-Potential, das GAUSS-Potential und das Exponentialpotential. Zuerst wollen wir das wahrscheinlich wichtigste von denen, dem man ja auch eine gewisse theoretische Begründung geben kann, das YUKAWA-Potential, betrachten. Aus dem folgt für die potentielle Energie

$$V = -\frac{A}{r} e^{-br} . \tag{11}$$

Aus der Gleichheit der zentrifugalen und der zentripetalen Kraft erhalten wir wieder

$$m\frac{v^2}{r} = \frac{A}{r}\left(\frac{1}{r} + b\right) e^{-br} \tag{12}$$

und für die ganze Energie

$$E = -\frac{A}{r} e^{-br} + \frac{1}{2} mv^2 = \frac{A}{2}\left(b - \frac{1}{r}\right) e^{-br} . \tag{13}$$

Es können also nur dort stabile Niveaus vorhanden sein, wo $1/r > b$ ist, also bei kleinem r. Führen wir wieder explizit die kinetische Energie $T = \frac{1}{2} mv^2$ ein, so folgt

$$E = -\frac{br - 1}{1 + br} T . \tag{14}$$

Ist r so klein, dass auch noch $br \ll 1$ ist, so geht (14) in

$$E = -T \tag{15}$$

über, also in unser Resultat (8). Auf die Besprechung der beim YUKAWA-Potential auftretenden weiteren Verhältnissen kommen wir im nächsten Paragraphen noch zurück.

Im Falle des GAUSS-Potentials haben wir

$$V = -Ae^{-br^2}, \tag{16}$$

und aus der Gleichheit der Kräfte bei Kreisbahnen folgt wieder

$$\frac{mv^2}{r} = 2Ab\, r\, e^{-br^2}. \tag{17}$$

Aus (16) und (17) erhalten wir also für die ganze Energie

$$E = V + \frac{1}{2} mv^2 = A\,(br^2 - 1)\, e^{-br^2}. \tag{18}$$

Stabile Niveaus kann es also nur dort geben, wo $1/r^2 > b$ ist, d. h. wieder bei kleine r.

Bei der Benützung eines einfachen Exponentialpotentials haben wir

$$V = -Ae^{-br} \tag{19}$$

und weiter wieder bei Kreisbahnen

$$\frac{mv^2}{r} = Abe^{-br} \tag{20}$$

und

$$E = -Ae^{-br} + \frac{1}{2} mv^2 = A\left(\frac{1}{2} br - 1\right) e^{-br}. \tag{21}$$

Stabile Niveaus können also nur dort auftreten, wo $r < 2/b$ ist.

In den beiden zuletzt betrachteten Fällen wollen wir jetzt wieder die kinetische Energie explizit einführen. Bei einem GAUSSschen Potential folgt dann aus (17),

$$T = \frac{1}{2} mv^2 = Ab\, r^2\, e^{-br^2} \tag{22}$$

und weiter aus (18)

$$E = \frac{br^2 - 1}{br^2}\, T. \tag{23}$$

Wird wieder r sehr klein, so nähert sich nach (22) und (23) E dem konstanten Wert

$$E = -A \tag{24}$$

und T zu

$$T = 0. \tag{25}$$

Bei der Benützung des einfachen Exponentialpotentials vom Typ (19) folgt dagegen, wenn wir wieder die kinetische Energie T explizit einführen

$$T = \frac{1}{2} mv^2 = \frac{1}{2} Ab\, r\, e^{-br} \tag{26}$$

und aus (21)

$$E = \left(1 - \frac{2}{br}\right) T. \tag{27}$$

Für sehr kleine r erhält man also auch jetzt

$$T = 0 \text{ und } E = -A. \tag{28}$$

Im Falle eines einfachen Kastenpotentials hätten wir

$$V(r) = \begin{cases} -V_0 & \text{für } r < b \\ 0 & \text{für } r > b. \end{cases} \tag{29}$$

Tatsächlich kann man oft die wirklich auftretenden Verhältnisse mit Hilfe von solch einem Potential phenomenologisch ganz richtig beschreiben, als wirkliches Naturgesetz wäre jedoch solch ein Potentialansatz (wenn man nur nicht eine diskontinuierliche Raumstruktur annehmen würde) höchst unwahrscheinlich. Negative Energiewerte kann es nach (29) selbstverständlich überall geben, wo $r < b$ ist, und für die kinetische Energie kann man klassisch keinen fixen Wert angeben, sie muss nur kleiner als V_0 sein.

Selbstverständlich könnte man sich noch sehr viele Potentialtypen ausdenken, die mit abnehmendem r sehr schnell (numerisch) grösser werden[1]. Dieser Bedingung würde z. B. sogar auch die potentielle Energie

$$V = -Ae^{+\frac{b}{r}} \tag{30}$$

genügen. Dann hätten wir

$$m\frac{v^2}{r} = \frac{Ab}{r^2} e^{+\frac{b}{r}} \tag{31}$$

und

$$E = A\left(\frac{1}{2}\frac{b}{r} - 1\right) e^{+\frac{b}{r}} \tag{32}$$

oder

$$E = \left(1 - \frac{2r}{b}\right) T. \tag{33}$$

Stabile Niveaus gibt es in diesem Falle also nur im Gebiet, in dem $\frac{2r}{b} > 1$ ist, ein für die Kernphysik ganz absurdes Resultat.

3.

Wegen der grossen Wichtigkeit des YUKAWA-Potentials kommen wir jetzt nocheinmal auf diese Frage zurück. Bekanntlich kann man für diese Wechselwirkung eine Art theoretische Herleitung geben. Betrachten wir nämlich die (skalare) KLEIN—GORDONsche Wellengleichung für ein Teilchen, das die Masse μ besitzt, und setzen wir (ganz willkürlich) die zweite Ableitung nach der Zeit in dieser Gleichung gleich Null, so erhalten wir

$$\Delta \Psi - \frac{4\pi^2 \mu^2 c^2}{h^2} \Psi = 0 . \tag{34}$$

Als Lösung dieser Differentialgleichung folgt bekanntlich wie man leicht nachrechnet,

$$\Psi = \pm \frac{g^2}{r} e^{-2\pi \frac{\mu c}{h} r} , \tag{35}$$

wobei g^2 eine Integrationskonstante ist. (35) ist, abgesehen von den benützten anderen Bezeichnungen, die von uns in (11) eingeführte potentielle Energie

$$V = -\frac{A}{r} e^{-br} . \tag{36}$$

Berücksichtigen wir noch, dass die Kernkräfte eine ungefähre Reichweite von dem klassischen Elektronenradius (e^2/mc^2) haben, also $1/b$ von dieser Grössenordnung sein muss, so folgt dass μ ungefähr die Grösse einer Mesonenmasse hat. Deshalb nimmt man an, dass das Kernfeld hauptsächlich π-Mesonen verursachen. Jedenfalls kann diese Übereinstimmung auch nur ein blosser Zufall sein, für unsere Betrachtungen ist jedoch der Umstand sehr wichtig, dass da auf der rechten Seite von (36) der exponentielle Faktor eine dimensionslose Grösse ist, A notwendigerweise die Dimension von dem Quadrat einer elektrischen Ladung besitzen muss. Weiter ist es interessant zu bemerken, dass eben die Kernkräfte (also die sogennannte starke Wechselwirkung) nur mit nicht ganz zwei Grössenordungen die elektromagnetische Wechselwirkung übertrifft. Dagegen ist die schwache Wechselwirkung von der elektromagnetischen und diese wieder von der Gravitationswechselwirkung um sehr viel mehr Grössenordnungen verschieden.

Führen wir jetzt in (36) statt A die Grösse $\sqrt{A} = a$ ein, welche also die Dimension einer elektrischen Ladung besitzt, so können wir statt der potentiellen Energie V das Potential

$$\varphi = \frac{a}{r} e^{-br} \tag{37}$$

einführen. φ genügt selbstverständlich ebenfalls unserer Differentialgleichung (34), die wir jetzt in der Form

$$\Delta \varphi - b^2 \varphi = 0 \tag{38}$$

schreiben können.

(38) hat jedoch vollständing die Form einer POISSONschen Differentialgleichung

$$\Delta \varphi + 4\pi \varrho = 0 . \tag{39}$$

Durch Vergleich von (38) und (39) folgt also

$$4\pi \varrho = - b^2 \varphi \tag{40}$$

und daraus

$$\varrho = - \frac{b^2}{4\pi} \varphi . \tag{41}$$

Setzen wir hier noch (37) ein, so folgt weiter

$$\varrho = - \frac{b^2}{4\pi} \frac{a}{r} e^{-br} . \tag{42}$$

Diese verschmierte «Ladungsdichte» umgibt also das im Mittelpunkte sich befindende Kraftzentrum von der «Ladung» a und schwächt dessen Feld von einem coulombartigen auf das YUKAWAsche ab. Ist diese Behauptung tatsächlich richtig, muss die Ladungsdichte (42) das YUKAWAsche Potential reproduzieren. In einer Entfernung r_0 vom Zentrum müssen wir also nach der Potentialtheorie das Potential

$$\varphi(r_0) = \frac{a}{r_0} + 4\pi \frac{1}{r_0} \int_0^{r_0} \varrho \, r^2 \, dr + 4\pi \int_{r_0}^{\infty} \varrho \, r \, dr \tag{43}$$

beobachten.

Tatsächlich folgt, wenn wir ϱ aus (42) in (43) einsetzen,

$$\varphi(r_0) = \frac{a}{r_0} e^{-br_0} , \tag{44}$$

und damit ist unsere Behauptung bewiesen.

Ergänzend wollen wir noch die ganze um das Zentrum herum verschmierte «Ladung» berechnen. Wir haben

$$Q = 4\pi \int_0^\infty \varrho \, r^2 \, dr \,, \tag{45}$$

und setzen wir hier wieder ϱ aus (42) ein, so folgt nach elementaren Rechnungen

$$Q = -a \,. \tag{46}$$

Im Unendlichen neutralisiert also diese verschmierte Ladung die zentrale vollständig, praktisch jedoch schon in einer Entfernung, die gross im Verhältnis zur Reichweite der Kernkräfte ist.

Im Zusammenhang mit dieser Frage ist es interessant zu erwähnen, dass nach den HOFSTADTERschen und WILSONschen Untersuchungen [2] die Nukleonen keine DIRACschen Teilchen sind, also sicher nicht als punktförmig betrachtet werden können, sondern eine räumliche Struktur besitzen, deren Ausdehnung von der selben Grössenordnung wie die Reichweite der Kernkräfte ist.

Wir sehen also, dass das YUKAWA-Potential auch in dieser Hinsicht eine ganz ausgezeichnete Rolle spielt. Unsere Potentialansätze (16) oder (19) würden z. B. eine so einfache und plausible physikalische Interpretation gar nicht zulassen.

4.

Alle unsere bisherigen Betrachtungen waren rein klassisch. Wir wollen jetzt sehen, was an unseren Resultaten abzuändern ist, wenn wir zuerst die BOHRsche Quantentheorie einführen. Im Falle unseres Kraftansatzes (1), also

$$K = -\frac{A}{r^n} \tag{47}$$

sind (bei der Annahme von Kreisbahnen) die BOHRschen Quantenbedingungen

$$2\pi \, m \, r \, v = kh \tag{48}$$

bei jedem Wert von n erfüllbar. Doch erhält man stabile Bahnen, wie wir das schon im § 1 besprochen haben, nur, wenn die Ungleichung $3 > n > 1$ besteht, und auch von diesen Werten von n wird wahrscheinlich nur das Gesetz mit $n = 2$ eine naturwissenschaftliche Realität besitzen.

Im Falle eines YUKAWA-Potentials ist die Quantelung bei Kreisbahnen ebenfalls möglich. Aus der Gleichsetzung der zentrifugalen und der zentripetalen Kraft folgt

$$m\frac{v^2}{r} = \frac{A}{r}\left(\frac{1}{r} + b\right)e^{-br}. \tag{49}$$

Für die Energie haben wir also

$$E = V + T = -\frac{A}{r}e^{-br} + \frac{1}{2}mv^2 = Ae^{-br}\left(-\frac{1}{2r} + \frac{b}{2}\right). \tag{50}$$

Weiter erhalten wir aus der Quantenbedingung (48)

$$m^2 r^2 v^2 = \left(\frac{kh}{2\pi}\right)^2 \tag{51}$$

und aus (49)

$$m^2 r^2 v^2 = m r^2 A\left(\frac{1}{r} + b\right)e^{-br}. \tag{52}$$

Die Gleichsetzung von (51) und (52) gibt den Zusammenhang

$$k^2 h^2 = 4\pi^2 m r^2 A\left(\frac{1}{r} + b\right)e^{-br}. \tag{53}$$

Durch Elimination von Ae^{-br} folgt weiter aus (50) und (53) nach elementaren Rechnungen

$$E = \frac{k^2 h^2}{8\pi^2 m r^2}\left(1 - \frac{2}{1 + br}\right), \tag{54}$$

also dasselbe Resultat, das schon von RAWLS und SCHULTZ [3] hergeleitet wurde. Setzen wir in (54) $b = 0$, so erhalten wir die Resultate der BOHRschen Theorie.

In (54) ist es nicht gelungen, r zu eliminieren, das bedeutet jedoch nicht, dass diese Grösse noch frei wählbar wäre, weil deren Wert ist schon durch (48) und (49) eindeutig festgelegt.

Im Falle eines GAUSS-Potentials können wir wieder unter Annahme von Kreisbahnen analog verfahren. Nach (16) schreiben wir die dabei auftretende potentielle Energie in der Form

$$V = -Ae^{-br^2}. \tag{55}$$

Analog zu (49) folgt dann weiter

$$\frac{m\,v^2}{r} = 2Ab\,r\,e^{-br^2}\,. \tag{56}$$

Für die Energie erhalten wir jetzt

$$E = V + \frac{1}{2}\,m\,v^2 = (br^2 - 1)\,Ae^{-br^2}\,. \tag{57}$$

Berechnen wir wieder $m^2r^2v^2$ einerseits aus (48) und andererseits aus (56) und setzen diese Ausdrücke einander gleich, so folgt analog zu (53)

$$k^2\,h^2 = 8\pi^2\,b\,m\,r^4\,Ae^{-br^2}\,. \tag{58}$$

Aus (57) und (58) erhalten wir durch Elimination von Ae^{-br^2}

$$E = \frac{k^2\,h^2}{8\pi^2\,m\,r^2}\left(1 - \frac{1}{br^2}\right). \tag{59}$$

Bei einem einfachen Exponentialpotential haben wir nach (19)

$$V = -\,Ae^{-br} \tag{60}$$

und analog zu (49)

$$\frac{mv^2}{r} = Abe^{-br}, \tag{61}$$

und weiter ähnlich zu (53)

$$k^2\,h^2 = 4\pi^2\,m\,r^3\,b\,Ae^{-br}\,. \tag{62}$$

Für die Energie folgt

$$E = V + \frac{1}{2}\,mv^2 = \left(\frac{1}{2}\,br - 1\right)Ae^{-br}, \tag{63}$$

und, wenn wir Ae^{-br} wieder aus (62) und (63) eliminieren,

$$E = \frac{k^2\,h^2}{8\pi^2\,m\,r^2}\left(1 - \frac{2}{br}\right). \tag{64}$$

Die Berücksichtigung von Ellipsenbahnen wäre in den hier besprochenen Fällen mit sehr grossen mathematischen Schwierigkeiten verbunden, da ja dieses Problem auch schon in dem BOHRschen Fall nicht ganz einfach ist. Man

könnte es jedoch kaum erwarten, dass aus solchen Berechnungen etwas qualitative wesentlich anderes herauskommen würde als die hier erhaltenen Resultate.

Es sei nur noch bemerkt, dass bei kleine Werte von r im Falle eines YUKAWA-Potentials die kinetische Energie T nach (15) in die aus der BOHRschen Theorie folgende übergeht, bei der Benützung eines GAUSSSCHEN oder eines einfach exponentiellen Potentials geht dagegen T in diesem Falle nach (25) und (28) zu Null. Da jedoch dann notwendigerweise auch die Geschwindigkeit v zu Null gehen muss, so werden die Quantenbedingungen unerfüllbar. Dieser Umstand beweist auch die grosse Überlegenheit des YUKAWA-Potentials.

5.

Jetzt wollen wir noch die Frage besprechen, das was die Anwendung der Quantenmechanik zu unseren bisherigen Resultaten hinzusetzen kann. Erstens kann man alle unsere in den vorigen Paragraphen erhaltenen Ergebnisse mit Hilfe der WENTZEL—BRILLOUIN—KRAMERSschen Approximationsmethode oder mit Hilfe von einer weiteren Vervollkommnung derselben angenähert in die Quantenmechanik übertragen. Zur exakten Lösung der bereits besprochenen Probleme nach der Wellenmechanik muss man jedoch für jeden einzelnen Fall eine andere mathematische Lösungsmethode ausarbeiten, und erhält deshalb garnicht solch eine einfache Übersicht über die auftretenden Verhältnisse, wie nach der BOHRschen Theorie.

In einigen einfachen Fällen kann man jedoch die Wellengleichung, die entsteht, wenn wir für die potentielle Energie einen Ausdruck von denen, die wir in unserem §2 besprochen haben, einsetzen, im kugelsymmetrisch angenommenen Grundzustande tatsächlich lösen. So erhält man für den Fall des einfachen Kastenpotentials innerhalb dieses »Kastens« als Lösung eine einfache Sinusfunktion und ausserhalb eine Exponentialfunktion selbstverständlich mit negativen Exponenten. Bei der Benützung eines einfachen Exponentialpotentials von der Form (19) kann man dagegen die entstehende Wellengleichung mit Hilfe von BESSEL-Funktionen positiver Ordnung lösen.

Das Problem des zu $1/r^2$ proportionalen Potentials haben zuerst MOTT und MASSEY [4] quantemechanisch betrachtet. Nach ihnen hat sich AADNA ORE [5] mit diesem Problem beschäftigt, und weiter dann CASE [6]. Unter Berücksichtigung seiner Resultate hat dann AADNA ORE seine eigenen etwas korrigiert. Nach CASE, der ausser der SCHRÖDINGERschen Theorie auch die DIRACsche angewandt hat, können bei einem zu $1/r^2$ proportionalen Potential nur dann Energieniveaus auftreten, wenn man in die Wellenfunktion eine Phasenkonstante B einführt, die also für kleine x in der Form

$$u = C x^{1/2} \cos (\lambda' \log \text{nat } x + B) \tag{65}$$

schreibt. Anschaulich entspricht das der Annahme, dass die Gültigkeit der Potentialfunktion bei einem kleinen Wert von $r (r = \varepsilon)$ aufhört. Der Wert von B hängt dann unmittelbar mit diesem ε zusammen. Sonst gibt es in diesem Fall nach dem genannten Verfasser keine Niveaus, und das ist dasselbe Resultat, das wir in unserem § 1 für den Kraftansatz

$$K = -\frac{A}{r^3} \tag{66}$$

auf elementarem Wege hergeleitet haben. CASE erhielt nach seiner Methode, wenn er auch die erwähnte Phasenkonstante einführte, ein punktartiges Energiespektrum von minus Unendlich bis Null, wo ein Verdichtungspunkt auftritt und über dem ein positives Kontinuum. Ein interessantes Ergebnis dieser Berechnungen war noch, dass sich mehr Eigenfunktionen als die zur Bildung einer kompletten orthogonalen Funktionenreihe genügenden (also eine überkomplette Reihe) ergeben haben.

Mit dem so wichtigen Problem der Lösung der SCHRÖDINGERgleichung, wenn man für die potentielle Energie das YUKAWA-Potential (11) benützt hat sich in letzterer Zeit HARRIS [7] beschäftigt. Er benützte perturbations- und variationstechnische Methoden zur angenäherten Lösung dieses Problems.

6.

In den vorangehenden Abschnitten haben wir es gesehen, dass bei den in der Kernphysik in erster Linie in Frage kommenden Potentialansätzen es nur sehr wenig stabile Energieniveaus geben kann. Die Ursache von diesem Tatbestand ist erstens, dass die Gesamtenergie nur in verhältnismässig beschränkten Bereichen negativ ist, und dazu kommt noch, dass dort selbstverständlich auch die Quantenbedingungen erfüllt sein müssen. Tatsächlich besitzen ausser dem Deuteron auch die bekannten Dreikörperprobleme der Kernphysik (das Triton und das ^{3}He) keine angeregten Zustände. Bezüglich der Existenz von angeregten Niveaus des ^{4}He verweisen wir auf die neue kritische Besprechung dieser Frage von ARGAN, MANTOVANI, MARAZZINI, PIAZZOLI und SCANNICCHIO [8]. Die weiteren Kerne besitzen schon angeregte Zustände, jedoch noch relative wenige. Die Daten für die Kerne von $A = 5$ bis $A = 10$ sind in dem zusammenfassenden Bericht von LAURITSEN und AJZENBERG—SELOVE [9] zu finden. Noch weitere Kerne besitzen schon mehr angeregte Zustände; diesbezüglich erwähnen wir die schon ältere Arbeit von ENDT und VAN DER LEUN [10] für die Systemnummern von 11 bis 20. Andererseits haben Kerne, welche aus vielen Nukleonen aufgebaut sind, sehr viele Energieniveaus und meistens ziemlich verwickelte Termschemata. Über diese Frage liegen in der Fachliteratur sehr zahlreiche Veröffentlichungen vor.

Auf Grund unserer bisherigen Betrachtungen bezüglich der Kernkräfte, wollen wir jetzt sehen, wie dieser scheinbare Widerspruch zustande kommt. Nehmen wir z. B. für die Anordnung der Nukleonen in einem schweren Kern eine kubisch dichteste Kugelpackung an, so besitzt jedes Teilchen 12 unmittelbare Nachbarn. So krass wird zwar die Sache bei angeregten Zuständen auch schon deshalb nicht sein, weil erstens solche Teilchen ja grösstenteils auf der Oberfläche des Kernes verweilen werden und zweitens weil ja Kernkräfte teilweise einen Austauschcharakter besitzen, doch wird die Zahl der unmittelbaren Nachbarn wesentlich grösser als eins bleiben.

Kräfte addieren sich jedoch als Vektoren, die Potentiale dagegen als skalare Grössen. Sind also tatsächlich mehrere unmittelbare Nachbarn vorhanden und bezeichnen wir deren Zahl mit N, kann zwar in unseren Gleichungen (2), (12), (17), und (20) bzw. (49), (56) und (61), welche die Gleichheit der zentripetalen und der zentrifugalen Kräfte ausdrücken und die wir zusammenfassend in der Form

$$V' = \frac{mv^2}{r} \tag{67}$$

schreiben können, die zentrifugale Kraft grösser werden. Berücksichtigen wir diesen Umstand mit Hilfe eines Faktors f, so haben wir statt (67)

$$\sum_{l=1}^{N} V'_l = f\frac{mv^2}{r}, \tag{68}$$

doch wird f immer wesentlich kleiner bleiben als N. Aus (68) folgt, dass wir jetzt für die kinetische Energie angenähert

$$T = f\frac{1}{2}mv^2 \tag{69}$$

schreiben müssen. Die hier auftretenden potentiellen Energien multiplizieren sich dagegen einfach mit N. Statt unsere Gleichungen (3), (13), (18) und (21) bzw. (50), (57) und (63) haben wir also

$$E = NV + f\frac{1}{2}mv^2. \tag{70}$$

Da wie wir das jedoch schon besprochen haben f wesentlich kleiner als N sein muss, so werden jetzt die Gebiete, in denen die Energie E negativ ist, bedeutend grösser werden. Die Quantenbedingungen ändern sich dagegen bei weitem nicht so wesentlich, weil ja $\sqrt{f} \cdot v$ viel weniger von v verschieden sein wird. Es können also schon deshalb viel mehr stabile Niveaus auftreten, und dazu

kommt noch, dass auch viel mehr Teilchen vorhanden sind. Alles das erklärt ganz ungezwungen die Tatsache, dass aus wenig Nukleonen aufgebaute Kerne keine angeregten Zustände besitzen, schwere Kerne dagegen sehr viele angeregte Niveaus und deshalb meistens ein verwickeltes Termschema haben.

LITERATUR

1. J. L. Gammel und R. M. Thaler, Phys. Rev., **107,** 1337, 1957; P. S. Signell und R. E. Marshak, Phys. Rev., **109,** 1229, 1958; J. H. Naqvi, Nuclear Phys., **36,** 578, 1962; K. A. Bruckner und J. L. Gammel, Phys. Rev. **109,** 1023, 1958; T. Hamada und I. D. Johnston, Nuclear Phys. **34,** 382, 1962; K. A. Brueckner und K. S. Masterson Jr., Phys. Rev., **128,** 2267, 1962; P. Signell und N. R. Yoder, Phys. Rev., **132,** 1707, 1963 u. **134 B,** 100, 1964. Vgl. auch R. Wilson, The Nucleon-Nucleon Interaction. J. Wiley and Sons, New York, London 1963.
2. Vgl. z. B. H. Schopper, Physik. Blätter **7,** 316, 1961.
3. J. M. Rawls und M. Schultz, Amer. J. Phys. **33,** 444, 1965.
4. N. F. Mott und H. S. W. Massey, The Theory of Atomic Collisions. 1. Aufl. Oxford. Clarendon Press, 1949. S. 30.
5. Aadna Ore, Nature **167,** 402 u. 728, 1951.
6. K. M. Case, Phys. Rev., **80,** 797, 1950.
7. G. M. Harris, Phys. Rev., **125,** 1131, 1962.
8. P. E. Argan, G. C. Mantovani, P. Marazzini, A. Piazzoli und D. Scannicchio, Nuovo Cimento Suppl., **3,** 245, 1965.
9. T. Lauritsen und F. Ajzenberg-Selove, Nuclear Phys., **78,** 1, 1966.
10. P. M. Endt und C. van der Leun, Nuclear Phys., **34,** 1, 1962.

ПЛОТНОСТЬ ЭНЕРГЕТИЧЕСКИХ УРОВНЕЙ АТОМНЫХ ЯДЕР

Т. НАЙГЕБАЕР

Резюме

В вводной части работы рассматривается вопрос, в чем заключается, на самом деле, причина того, что до сих пор мы не знаем элементарного закона сил, действующих между двумя нуклонами. Это мы считаем обусловленным полным отсутствием возбужденных уровней в самых простых атомных ядрах. После этого, исходя из чисто классических соображений, рассматривается, что в случае наиболее часто встречающихся в ядерной физике потенциальных функций в каких областях наблюдается отрицательная энергия; далее на основе теории Бора исследуется возможность появления квантовых состояний в данной области. В следующем параграфе данные вопросы рассматриваются на основе квантовой механики. Наконец, в последней части работы показывается, что в случае взаимодействия многих нуклонов области, обладающие отрицательной энергией, становятся намного большими (сильно расширяются), а квантовые условия изменяются во много меньшей мере. Данное обстоятельство обусловливается складыванием потенциальных энергий как скалярных, а сил — как векторных величин. Данное обстоятельство без всяких усилий объясняет появление очень сложных систем термов в тяжелых атомных ядрах, то есть такого экспериментального факта, который частично подобен наблюдаемому в физике электронных оболочек.

Acta Physica Academiae Scientiarum Hungaricae, Tomus 23 (1), pp. 111—115 (1967)

COMMUNICATIONES BREVES

EINE WÄRMEIMPULSMETHODE ZUR BESTIMMUNG DER TEMPERATURLEITZAHL AN KURZEN PROBEN

Von

F. KELEMEN

LEHRSTUHL FÜR MECHANIK UND WÄRMELEHRE AN DER BABES–BOLYAI-UNIVERSITÄT, CLUJ, RUMÄNIEN

(Eingegangen: 17. II. 1966)

Einleitung. Durch Messung der Temperaturleitzahl (a) ist es möglich, eine schnelle Bestimmung der Wärmeleitzahl (k) vorzunehmen, wenn die Dichte (ϱ) und spezifische Wärme (c) des Körpers bekannt sind ($k = \varrho\, ca$).

In jüngster Zeit wurden für die Bestimmung der Temperaturleitzahl besonders die Wärmewellen-Methoden entwickelt: 1) die sogenannten Angström-Methoden, bei denen die Dämpfung der Amplitude bzw. die Verschiebung der Phase der sinusoidalen Temperaturwellen längs der Probe oder in Abhängigkeit von der Frequenz gemessen wird [1]—[3]; 2) die Wärmeimpulsmethoden, bei denen eine Temperaturwelle an der Vorderseite des Probekörpers hervorgerufen und in einem Punkt der Probe die zeitliche Veränderung der Temperatur bestimmt wird [4]—[7].

Es wurde schon früher darauf hingewiesen [7], dass nach den Wärmeimpulsmethoden reelle Werte für die Temperaturleitzahl nur dann gewonnen werden können, wenn ähnlich wie bei den Angström-Methoden auch hier der Einfluss des Wärmeübergangs beseitigt wird. Dies kann praktisch erreicht werden, a) wenn bei dem als unendlich lang angenommenen Probekörper die Temperaturveränderung in zwei verschiedenen Punkten registriert wird [7, 8], b) wenn eine so kurze Probe verwendet wird, dass in der zur Registrierung der Temperaturveränderung nötigen Zeit der Einfluss des Wärmeübergangs vernachlässigt werden kann [5, 6]. In diesem Falle müssen jedoch Wärmeimpulse von 10^{-3} sec Dauer hervorgerufen und Temperaturveränderung von 10^{-1} bis 10^{-2} sec registriert werden. Natürlich beansprucht dieses Verfahren eine dem erwähnten Zwecke entsprechende moderne Apparatur. Ausserdem ergibt sich in diesem Falle eine beträchtliche systematische Fehlerquelle durch die Verspätung der Temperaturveränderung, wenn der Kontakt zwischen Probekörper und Schweisstelle des Thermoelementes nicht vollkommen ist.

In vorliegender Arbeit wird eine Variante der Wärmeimpulsmethode beschrieben, die es gestattet, die Temperaturleitzahl durch Registrieren einer

einzigen Temperatur-Zeit-Kurve, bei Verwendung eines einfachen Messinstrumentes, zu bestimmen. Diese Methode kann bei der Untersuchung der Temperaturabhängigkeit der Temperaturleitzahl an festen Körpern jeder Art (Metalle, Halbleiter, Isolatoren), angewandt werden. Die Probekörper können je nach der Temperaturleitzahl der zu untersuchenden Proben relativ kurz (cca. 0,3 bis 3 cm lang) sein.

Das Prinzip der Methode. Es sei angenommen, dass sich der Probekörper, der die Länge l und den Querschnitt S hat, an der hinteren Oberfläche S_2 in Kontakt mit einem unendlichen Medium M befindet und dass an der vorderen Oberfläche S_1 eine dünne Schicht von der Dicke $\xi \ll l$ plötzlich erwärmt wird, indem dem Körper ein Wärmeimpuls zugeführt wird (Abb. 1). Aus der Lösung

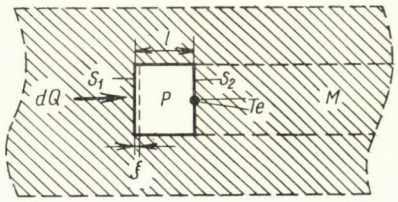

Abb. 1

der Differentialgleichung der Wärmeleitung, die auch den Wärmeübergang durch die seitliche Oberfläche des Probekörpers berücksichtigt, ergibt sich [8], dass die Temperaturleitzahl durch den Ausdruck

$$a = \frac{l^2}{2t_m(1 + 2bt_m)} \tag{1}$$

bestimmt wird. Dabei stellt t_m die Zeit dar, in der die Temperatur an der Oberfläche S_2 nach Erzeugung des Wärmeimpulses ihren Höchstwert erreicht. (Die Temperaturveränderung wird mit Hilfe des Thermoelementes *Te* gemessen.) Der Koeffizient b charakterisiert den Wärmeübergang durch die seitliche Oberfläche des Probekörpers. Er errechnet sich zu

$$b = h\frac{p}{\varrho c S}. \tag{2}$$

wo h die Wärmeübergangszahl, S den Querschnitt, p den Umfang dieses Querschnittes, ϱ die Dichte und c die spezifische Wärme bezeichnet.

Aus der in Funktion der Zeit an der hinteren Oberfläche S_2 registrierten Temperaturveränderung kann die Zeit t_m leicht bestimmt werden (Abb. 2),

doch lässt sie sich mit guter Annäherung auch aus dem Ausdruck

$$t_m = t_2 \frac{\log_n N}{N-1} \tag{3}$$

berechnen, in dem $N = t_2/t_1$ ist, während t_1 und t_2 die Zeitdauern bedeuten, die einem bestimmten Temperaturwert auf der Temperatur-Zeit-Kurve entsprechen (s. Abb. 2). Dieser Ausdruck stellt eine um so bessere Annäherung dar, je kleiner die Differenz zwischen t_1 und t_2 ist.

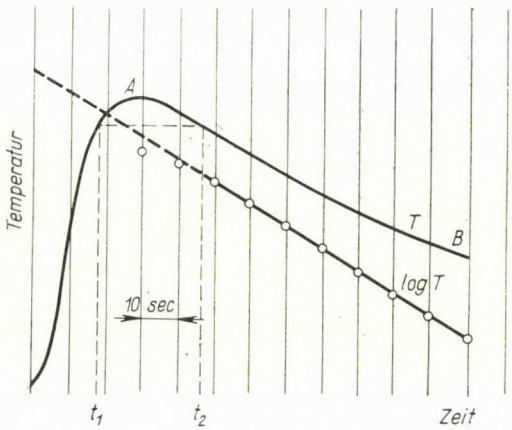

Abb. 2

Ist der Probekörper nicht nur an der hinteren, sondern auch an der seitlichen und vorderen Oberfläche durch Medium M begrenzt, dann kennzeichnet der AB-Teil der Temperatur-Zeit-Kurve die Abkühlung des Körpers in diesem Medium. In diesem Falle erhält man aus dem NEWTONschen Abkühlungsgesetz unter Berücksichtigung von Gl. (2)

$$b = \frac{pl}{S_0} \frac{\log_n {}^{T_1/T_2}}{t_2 - t_1}, \tag{4}$$

worin S_0 die Gesamtoberfläche der Probe und $(t_2 - t_1)$ das auf dem AB-Teil der Temperatur-Zeit-Kurve eingezeichnete Zeitintervall bedeutet, in dessen Verlauf die Temperatur von T_1 auf T_2 fällt. Der Ausdruck $\log T_1/T_2$ ergibt eine geradlinige zeitabhängige Veränderung (s. Abb. 2). Bestimmt man aus Gl. (4) den Koeffizienten b und misst man das t_m, hat man die Möglichkeit aus der Gl. (1) die Temperaturleitzahl zu berechnen.

Versuchsapparatur und Versuchsergebnisse. Um die Gültigkeit des mit Gl. (4) kombinierten Ausdruckes (1) experimentell zu überprüfen, wurden Messungen mit Probekörpern aus rostfreiem Stahl und Steinsalz durchgeführt.

Das Schema der Versuchsapparatur ist in Abb. 3 dargestellt. Ihr Hauptteil bilden zwei keramische Blöcke *A* und *B*, zwischen die der Probekörper in einem zylinderförmigen Hohlraum gelegt wird. Die Länge des Hohlraumes kann vergrössert werden, indem zwischen *A* und *B* ein Ring *D* von entspre-

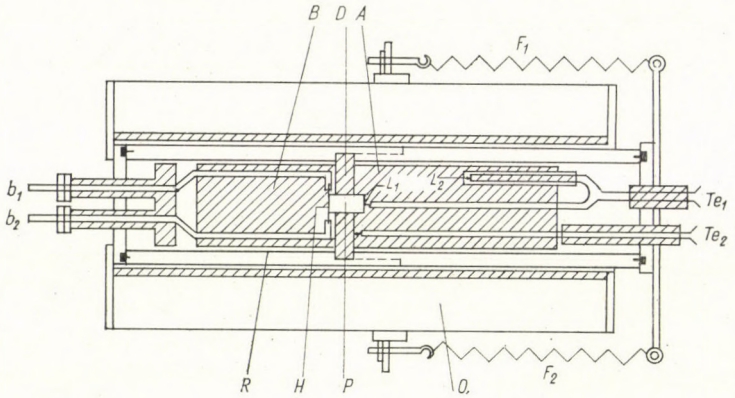

Abb. 3

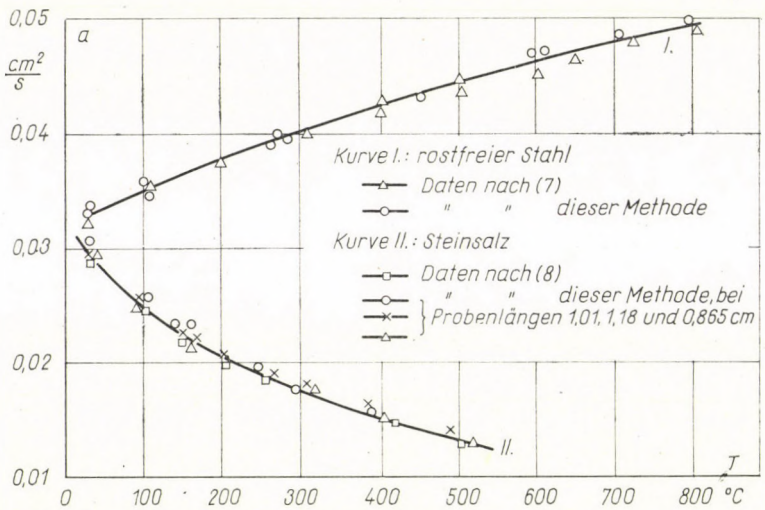

Abb. 4

chender Länge eingeführt wird, der aus dem gleichen keramischen Material gefertigt ist wie die Blöcke *A* und *B*. Der Wärmeimpuls an der vorderen Oberfläche der Probe wird mit Hilfe eines 0,1 mm dicken Nickelinplättchens H erzeugt, wenn dieses cca. 0,5 sec lang von Strom durchflossen wird. Die Temperaturänderung an der hinteren Probeoberfläche wird mit ein Eisen-

Konstantan-Thermoelement Te_1 gemessen, an das ein Silberplättchen von 0,2 mm Dicke angeschweisst ist. Den guten Kontakt zwischen Heizelement und Probe bzw. zwischen Probe und Silberplättchen sichert eine dünne Schicht Silberpaste. Die Temperaturänderung wird mit einem »Multiflex«-Galvanometer mit geringem Innenwiderstand registriert.

Den Zusammenhang zwischen den gemessenen Temperaturleitzahlwerten und der Temperatur veranschaulicht die Abb. 4.

In dieser Abbildung sind auch die Versuchsergebnisse dargestellt, die nach den in [7] bzw. [8] beschriebenen Methoden ermittelt wurden. Die Differenzen zwischen den nach diesen und nach den angeführten Methoden bestimmten Werten überschreiten die Grenzen der experimentellen Fehler nicht. Ebenso stimmen die von uns gemessenen Werte mit jenen anderer Autoren an rostfreiem Stahl [6] und Steinsalz [9] überein.

Ausser an diesen Stoffen wurden Messungen auch an einigen Halbleitern (HgSe, HgTe, ZnTe) unternommen. An diesen Stoffen wurden die Messungen auch unter anderen experimentellen Bedingungen wiederholt: das die Proben umgebende Medium war Luft, und der Wärmeimpuls wurde durch (0,5 bis 1,0 sec lange) Bestrahlung der vorderen Probeoberfläche mit einem Lichtstrahl erzeugt. Es wurde eine gute Übereinstimmung zwischen den Temperaturleitzahlwerten beider experimenteller Verfahren gefunden.

Bei kurzen Proben, bei denen die Dauer des Wärmeimpulses t_i gegenüber der Zeit t_m nicht vernachlässigt werden kann, bei denen also die Bedingung $\xi \ll l$ nicht erfüllt ist, erhält man nach der Gl. (1) für die Temperaturleitzahl kleinere Werte als die reellen. Die Versuche zeigen, dass der Einfluss der Wärmeimpulsdauer vernachlässigt werden kann, wenn $t_i/t_m \leq 0{,}1$.

LITERATUR

1. F. X. Eder, Moderne Messmethoden der Physik, Teil 2. S. 333 VEB Deutscher Verlag der Wissenschaften, Berlin 1956.
2. A. D. Stuckes, Brit. J. Appl. Phys., **12,** 675, 1961.
3. J. Gatecel und G. Weill, J. Phys. Radium, **23,** 95A, 1962. P. Leroux-Hugon, und G. Weill, J. Phys. Radium, **23,** 215A, 1962.
4. E. L. Woisard, J. Appl. Phys., **32,** 40, 1961.
5. W. J. Parker, R. J. Jenkins, C. P. Butler und G. L. Arbott, J. Appl. Phys., **32,** 1679, 1961. R L. Rudkin, R. J. Jenkins und W. J. Parker, Rev. Sci. Instr. **33,** nr. 1, 1962.
6. H. W. Deen und W. D. Wood, Rev. Sci. Instrum., **33,** 1107, 1962.
7. F. Kelemen, Z. angew. Phys., **17,** 562, 1964.
8. F. Kelemen, F. Bota und A. Néda, Studii Cerc. Fiz., **16,** 809, 1964.
9. Gmelins Handbuch der anorg. Chemie, Na (21), 8. Aufl. Berlin 1928, S. 319.

Acta Physica Academiae Scientiarum Hungaricae, Tomus 23 (1), pp. 117—121 (1967)

ON THE THERMAL EFFECTS OF AUXILIARY ELECTRODES ON Hg—A DISCHARGES

By

J. Bitó

INDUSTRIAL RESEARCH INSTITUTE FOR TELECOMMUNICATION TECHNIQUE, BUDAPEST

(Received 20. II. 1966)

As is known [1, 2] auxiliary electrodes arranged in the space of discharge electrodes may appreciably affect the discharge processes taking place in their environment, and also the electrode phenomena.

The author of this paper determined the effect of movable auxiliary electrodes located at one of the discharge electrodes on the temperature of the electrode for d.c. and 50 c/s a.c. discharges, at an ambient temperature of 25 $\pm$ 1 degrees centigrade, and at a current of 430 mA. The inner diameter of the glass-walled tube used for the experiment was 36 millimetres, and the electrodes were spaced 1090 millimetres apart. The tube was filled with about 50 milligrams of mercury and argon of a pressure of 3 millimetres of mercury. The auxiliary electrodes were 0,1 millimetre thick, 7 by 12-millimetre nickel plates arranged parallel to one another and to the axis of the electron emission material, coated W double spirals forming the electrodes. The nickel plates could be actuated in a radial direction by means of an electromagnet. Their distance from the spiral axis was adjustable between 2 and 17 millimetres, independently of one another. An optical pyrometer was used to determine the electrode temperature, and to calculate the plate and cathode drops a probe measurement method [3] was employed. Allowance was made for adequate stabilization, and measurements and calculations were made under stationary discharge and environmental conditions.

Fig. 1 shows the results of intervention on the cathode side of the d.c. discharge, i.e. the variation of the cathode drop owing to the change of position of the auxiliary electrodes with respect to it. The cathode spiral was at point $d = 0$. At the same place the dependence of the cathode spot temperature T_s on the distance of the auxiliary electrodes is shown. During the tests there was no metallic contact between the auxiliary electrodes and the spiral in the discharge space. In the first case (V_K, T_s), the auxiliary electrodes had a wall potential only, in the second set of tests, however, the electrodes were connected to both ends of the spiral outside the discharge tube, so that the electrodes had the different potentials of the corresponding spiral ends. Whereas the spot temperatures measured in this case were scattered within the measuring

inaccuracy for auxiliary electrodes with spiral potentials the values obtained at cathode drop values were smaller. The highest value of the cathode drop was 2 volts, i.e. an average of one volt. The cathode spot temperature was influenced neither by the auxiliary electrodes with wall potential, nor by those

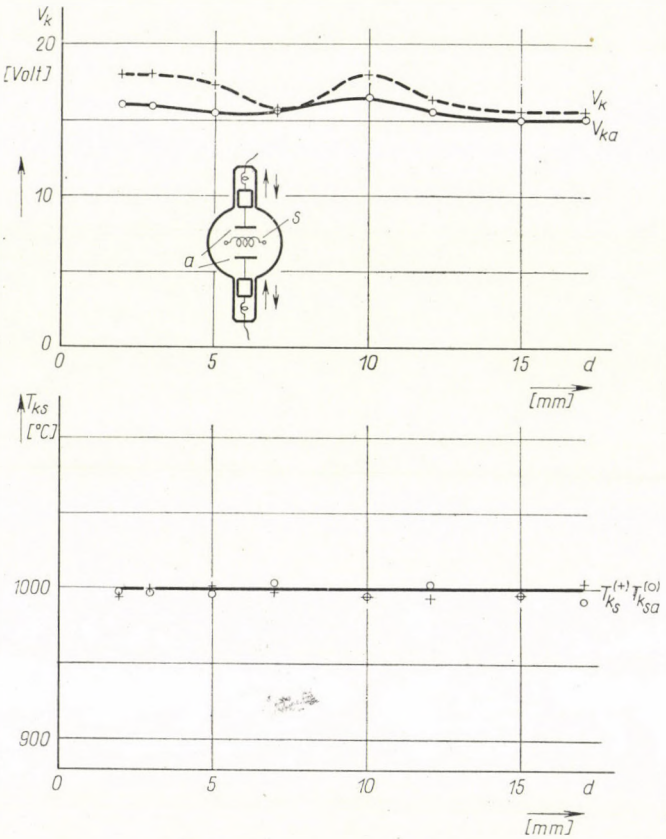

Fig. 1. Influence of the auxiliary electrodes moving in the d.c. cathode space of the Hg—A discharge on cathode drop V_K and cathode spot temperature T_{Ks}, when the auxiliary electrodes have wall potential, and for cases V_{Ka}, T_{Ka}, when the auxiliary electrodes have spiral-end potentials. The distances marked on the X-axis denote the distance of each auxiliary electrode from the spiral axis. The section of the test tube shown represents the arrangement of the spiral S and of the radially movable auxiliary electrodes *a*

having spiral end potentials, so that the value of the temperature could be considered constant. When the same intervention took place on the anode side of d.c. discharge, the anode drop and anode spot temperature values shown in Fig. 2 were obtained. The auxiliary electrodes with wall potentials did not affect the temperature of the anode spot ($T_{A,s}$), and except for a single curve section in the neighbourhood of the 12-millimetre auxiliary electrode

distance, the anode drop also remained constant. However, the anode drop value V_A obtained at 12 millimetres could not be accepted as a measuring error, the accuracy of the probe measuring method being within $\pm 0{,}2$ volts. From a comparison of Figs. 1 and 2 it was evident that for otherwise uniform

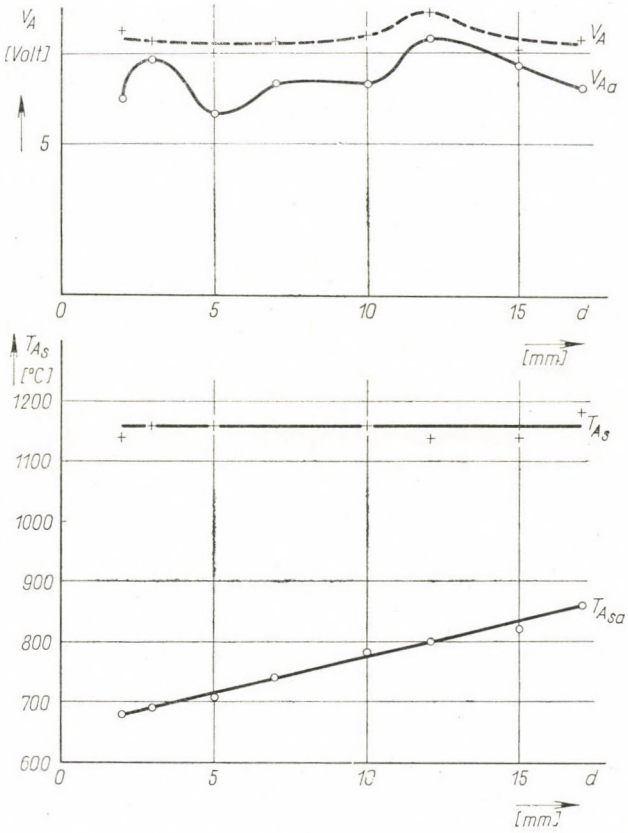

Fig. 2. Influence of the auxiliary electrodes moving in the anode space of the d.c. Hg—A discharge on the anode drops V_A, V_A, and the anode spot temperatures, T_{AS}, T_{Asa}

test conditions the temperature of the anode spot exceeded that of the cathode spot by about 160 degrees centigrade, No sooner had the auxiliary electrodes moving in the plate space reached a potential corresponding to the two ends of the spiral forming the anode than, owing to the extra-discharge metallic connection, the temperature of the anode spot dropped by 300 to 400 degrees centigrade. This phenomenon was not observed with cathode interference, although there, too, the auxiliary electrodes consumed current [4]. However, this current was appreciably smaller than that of the auxiliary electrodes moving in the anode space. It was interesting to note the linear drop of the

anode spot temperature $T_{A_{sa}}$ shown in Fig. 2 in response to the approach of the spot to the anode. This could be explained in all certainty by a strong rise of the electron current absorbed by the auxiliary electrodes meanwhile. However, this rise was in an interesting way in excess of linear [4]. Apparently there was no correlation between the trend of the corresponding curve V_V

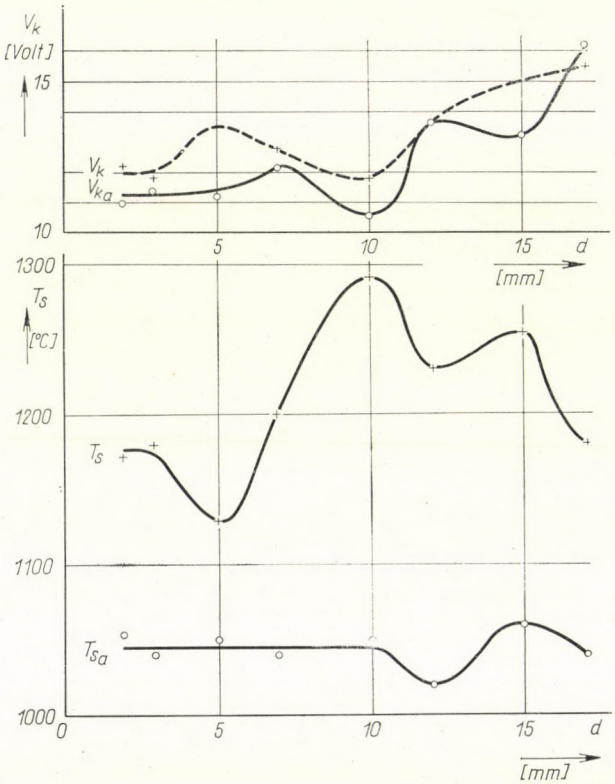

Fig. 3. Influence of the auxiliary electrodes moving in the space of the electrode in the cathodic half-cycle of the a.c. Hg—A discharge on the cathode drops V_k, V_{Ka}, and the cathode-spot temperatures T_S, T_{sa}

and the earlier parameters. In any event, in the curves in Fig. 2 representing two anode drops in that for the auxiliary electrodes connected to the spiral, the anode drops were smaller. Under such conditions the auxiliary electrode was able to reduce the anode drop by one or two volts.

The results of the measurements made for a 50 c/s a.c. discharge at 430 mA are shown in Fig. 3. The electric parameters were determined by time definition, in the half-cycle when the preferred electrode, i.e. the one where the interference by means of auxiliary electrodes took place, performed cathodic functions. Accordingly the cathode drop values V_K and V_{K_a} were, with the notation

introduced earlier, average values referred to a half-cycle [2, 3]. On determining the spot temperatures T_s and T_{sy}, associated with V_k and V_{K_a} respectively, the two half-cycles were not separated, on the assumption that the spot temperatures measured in this manner were at least proportional to the cathode spot temperatures resulting at intervals of a half-cycle. In this instance the influence of the auxiliary electrode was appreciably greater than on the cathode side of the d.c. discharge shown in Fig. 1. The auxiliary electrodes having one potential of the corresponding spiral ends reduces the cathode spot temperature by more than 150 degrees centigrade, and the consequences of this reduction manifested itself also in the trend of the average values of the cathode drop. This trend of the cathode drop was related to the spot temperature: in general lower spot temperatures entailed a cathode drop of higher degree, and vice versa, higher spot temperatures were followed by a smaller cathode drop [2]. This was found valid for both sets of curves shown in the diagrams. For a detailed analysis of the trend of the curves recourse has to be taken to electron-optical models, when the start should be made from a potential system having an accelerating, decelerating or deflecting effect on the ions, as the case may be.

From the curves it will then become obvious that in a d.c. discharge of this type the temperature of the anode spot is in all cases higher than that of the cathode spot, while the temperature of the cathode spot is not affected by the auxiliary electrodes to the same extent as is that of the anode spot. At the same time in the cathodic half-cycle of a 50 c/s a.c. discharge both the position and the potential of the auxiliary electrodes will have a strong effect on the spot temperature, and in this case, the cathode drop will also vary in conformity with the variations of the spot temperature. Since, during the measurements, there was no metallic contact in the discharge space between auxiliary electrodes and cathode, or in the d.c. case, between auxiliary electrodes and anode, the electrodes modified the anode and cathode drops and the spot temperatures exclusively as a result of their space charge and superficial current density effects, in conformity with their position with respect to the spiral as main electrodes, and not as a result of their thermal conductivity.

REFERENCES

1. D. D. HINMAN and R. S. FOX, Ill. Eng., **56**, 3, 222, 1961.
2. J. BITÓ, Lecture given at the Third Czechoslovak Conference on Electronics and Vacuum Physics, Prague, 1965.
3. J. BITÓ and I. SZEMZŐ, Magyar Fizikai Folyóirat, **12**, 2, 121, 1964.
4. J. BITÓ, Acta Phys. Hung. (in the press).

Acta Physica Academiae Scientiarum Hungaricae, Tomus 23 (1), pp. 123—124 (1967)

MEASUREMENT OF AVERAGE TOTAL CROSS-SECTION FLUCTUATION FOR Al AT 14 MeV NEUTRON ENERGY

By

I. ANGELI and I. HUNYADI

INSTITUTE OF NUCLEAR RESEARCH OF THE HUNGARIAN ACADEMY OF SCIENCES, DEBRECEN

(Received 12. V. 1966)

In the experimental investigation of cross section fluctuations one of the most critical requirements is the energy resolution. As TSUKADA has pointed out [1], in many cases the half-width of the correlation function obtained experimentally cannot be uniquely identified with the average $\langle \Gamma \rangle$ linewidth, as a result of poor energy resolution. In the same paper he suggested the "self-indication" method for determining the squared average of total cross-section fluctuations, and — provided that the shape — elastic cross section is known — so also for determining the $\langle \Gamma \rangle / D$-ratio. The essence of the method is as follows: A neutron beam of intensity I_0 is attenuated to I_1 and I_2 by samples of length N and 2 N, respectively. If the neutron beam were strictly mono-energetic, then the equation

$$a \equiv \frac{I_1^2}{I_0 I_2} = 1$$

would hold, because of the exponential intensity-attenuation. Should the incident neutron beam not be mono-energetic, the intensity as a function of sample length will not be exactly exponential, therefore $\alpha \neq 1$.

The squared average of total cross-section fluctuation is

$$\langle \Delta \sigma_T^2 \rangle \approx \frac{1}{N^2} \frac{1-\alpha}{2\alpha - 1} \equiv \frac{1}{N^2} \varepsilon$$

Accordingly, on the basis of the equation

$$\frac{\langle \Delta \sigma_c^2 \rangle}{\langle \sigma_c \rangle^2} = \frac{\langle \Delta \sigma_T^2 \rangle}{(\langle \sigma_T \rangle - \langle \sigma_{SE} \rangle)^2} = \left(\frac{1}{\pi} + \frac{4}{3\pi^2} \right) \Big/ \frac{\langle \Gamma \rangle}{D}$$

$\langle \Gamma \rangle / D$ can be obtained.

The method described above has been employed for investigating Al target material at about 14 MeV neutron energy.

The experimental arrangement was described in an earlier paper [2]. The energy inhomogeneity of the neutron beam, i.e. the averaging interval, was about 160—200 keV. The pulses from the neutron detector were fed into a 100-channel pulse-height analyser, and for evaluation the so-called "bias-window" method [3] was used in order to eliminate amplification changes. Background and in-scattering corrections were taken into account. Obviously ε changes as N^2, therefore it is worth using the longest possible samples. The use of very long samples, on the other hand, is limited by poor counting statistics. The samples examined were of 5, 10 and 20 cm length and 4 cm diameter.

The result

$$\varepsilon = 0{,}003\ (\pm\ 0{,}003)$$

was obtained, which gives

$$\langle \Delta\, \sigma_T^2 \rangle = (0{,}17\ \text{barn})^2.$$

By using the data concerning σ_T and σ_{SE} [4, 5] we have: $\langle \Gamma \rangle / D = 13{,}2$; and as a lower limit (corresponding to $\varepsilon = 0{,}003 + 0{,}003$),

$$(\langle \Gamma \rangle / D) \geq 6{,}6$$

was obtained.

Thanks are due to Mr. L. Bunkóczi for his help during the operation of the neutron generator.

REFERENCES

1. K. Tsukada and Tsong Jen Lee, Phys. Letters, **11,** 141, 1964.
2. I. Angeli and I. Hunyadi, ATOMKI Közl., **7,** 95, 1965.
3. A. Bratenahl, J. M. Peterson and J. P. Stoering, Phys. Rev., **110,** 927, 1958.
4. R. J. Hoverton, Tabulated Neutron Cross-Sections 0,001—14,5 MeV, Contract No. W-7405-eng.-48. Univ. of Calif. Radiation Laboratory, 1958.
5. M. D. Goldberg, V. M. May and J. R. Stehn, Angular Distributions in Neutron Induced Reactions, BNL-400, 2nd Ed., Sigma Center Brookhaven National Laboratory, 1962.

Acta Physica Academiae Scientiarum Hungaricae, Tomus 23 (1), pp. 125—129 (1967)

HUBBLE'S EXPANSION IN VECTORS FORMED BY Δ-TENSORS

By

A. L. MEHRA

DEPARTMENT OF MATHEMATICS, UNIVERSITY OF JODHPUR, JODHPUR, INDIA

(Received 12. V. 1966)

It is found that the time components of the vectors formed by Δ-tensors, correspond to HUBBLE's expansion.

1. Introduction

The Christoffel three-index symbols

$$\{\alpha\,\beta,\lambda\} = \frac{1}{2}\left(\frac{\partial g_{\alpha\lambda}}{\partial x^{\beta}} + \frac{\partial g_{\beta\lambda}}{\partial x^{\alpha}} - \frac{\partial g_{\alpha\beta}}{\partial x^{\lambda}}\right) \tag{1.1}$$

and

$$\left\{\begin{matrix}\lambda\\ \alpha\beta\end{matrix}\right\} = g^{\lambda\delta}\{\alpha\,\beta,\delta\} \tag{1.2}$$

for the metric of general relativity

$$ds^2 = g_{\mu\nu}\,dx^{\mu}\,dx^{\nu} \tag{1.3}$$

are not tensors. If the Christoffel three-index symbols

$$[\alpha\,\beta,\lambda] = \frac{1}{2}\left(\frac{\partial \gamma_{\alpha\lambda}}{\partial x^{\beta}} + \frac{\partial \gamma_{\beta\lambda}}{\partial x^{\alpha}} - \frac{\partial \gamma_{\alpha\beta}}{\partial x^{\lambda}}\right) \tag{1.4}$$

and

$$\Gamma^{\lambda}_{\alpha\beta} = \gamma^{\lambda\delta}\,[\alpha\,\beta,\delta] \tag{1.5}$$

correspond to another metric

$$ds^2 = \gamma_{\mu\nu}\,dx^{\mu}\,dx^{\nu}, \tag{1.6}$$

then one can easily prove that

$$\left\{\begin{matrix}\lambda\\ \alpha\beta\end{matrix}\right\} - \Gamma^{\lambda}_{\alpha\beta} = \Delta^{\lambda}_{\alpha\beta} \tag{1.7}$$

is a tensor. The Δ-tensors have been used by NARLIKAR and SINGH [1] to

explain the appearance of gravitational force of the Newtonian theory in the general theory of relativity. They have also evaluated some vectors and scalar invariants formed by Δ-tensors for some static metrics. They found that the three space components of the vectors correspond to Newtonian force whereas the fourth (time) component of each of the vectors does not have Newtonian analogues.

In the present paper the vectors are evaluated for some non-static cosmological models. It is found that their time components correspond to HUBBLE's expansion. The important vectors for the present study are [1]

$$R_\alpha = \Delta^\mu_{\mu\alpha} = \frac{K, \alpha}{K} \tag{1.8}$$

and

$$S_i = \Delta^\mu_{\alpha\beta} g^{\alpha\beta} g_{\mu i} = g^{\alpha\beta} g_{\alpha i, \beta} - \frac{K,_i}{K}, \tag{1.9}$$

where $K = \sqrt{\frac{g}{\gamma}}$.

2. Values of R_α and S_i in important cosmological models

(a) *Space-time conformally flat*

If we take line-element [2]

$$ds^2 = [w(t)]^2 (-dx^2 - dy^2 - dz^2 + dt^2) \tag{2.1}$$

with the corresponding metric for flat substratum

$$d\sigma^2 = -(dx^2 + dy^2 dz^2) + dt^2, \tag{2.2}$$

we find that

$$\begin{aligned} g_{\mu\nu} &= \text{diag } [-w^2, -w^2, -w^2, w^2], \\ g^{\mu\nu} &= \text{diag } [-w^{-2}, -w^{-2}, -w^{-2}, w^{-2}], \\ \gamma_{\mu\nu} &= \text{diag } [-1, -1, -1, 1], \\ K &= w^4, \end{aligned} \tag{2.3}$$

$$R_\alpha = \left[0, 0, 0, \frac{4}{w}\left(\frac{\partial w}{\partial t}\right)\right],$$

$$S_i = \left[0, 0, 0, -\frac{2}{w}\left(\frac{\partial w}{\partial t}\right)\right].$$

The HUBBLE's expansion is given by [2]

$$\sigma' = \frac{1}{w}\left(\frac{\partial w}{\partial t}\right). \tag{2.4}$$

The time components R_4 and S_4, therefore, correspond to HUBBLE's expansion. The other components R_1, R_2, R_3 and S_1, S_2, S_3 are null vectors.

(b) *Spatially isotropic Universe*

Let us take the metric [3]

$$ds^2 = -\frac{R^2}{(1+\alpha r^2)^2}(dx^2 + dy^2 + dz^2) + dt^2, \tag{2.5}$$

where R is a function of time alone and α is a constant. Its corresponding flat metric is given by (2.2). Then

$$\begin{aligned} g_{\mu\nu} &= \text{diag}\left[-\frac{R^2}{(1+\alpha r^2)^2}, -\frac{R^2}{(1+\alpha r^2)^2}, -\frac{R^2}{(1+\alpha r^2)^2}, 1\right], \\ g^{\mu\nu} &= \text{diag}\left[-\frac{(1+\alpha r^2)^2}{R^2}, -\frac{(1+\alpha r^2)^2}{R^2}, -\frac{(1+\alpha r^2)^2}{R^2}, 1\right], \end{aligned} \tag{2.6}$$

$$\gamma_{\mu\nu} = \text{diag}\ [-1, -1, -1, 1],$$

$$K = \frac{R^3}{(1+\alpha r^2)^3},$$

$$R_\alpha = \left[\frac{-6\alpha x}{1+\alpha r^2}, \frac{-6\alpha y}{1+\alpha r^2}, \frac{-6\alpha z}{1+\alpha r^2}, \frac{3}{R}\left(\frac{\partial R}{\partial t}\right)\right],$$

$$S_i = \left[\frac{2\alpha x}{1+\alpha r^2}, \frac{2\alpha y}{1+\alpha r^2}, \frac{2\alpha z}{1+\alpha r^2}, \frac{-3}{R}\left(\frac{\partial R}{\partial t}\right)\right].$$

The components R_1, R_2, R_3 and S_1, S_2, S_3 are proportional to the corresponding components of the force vector and the time components R_4 and S_4 correspond to HUBBLE's expansion $\frac{1}{R}\left(\frac{\partial R}{\partial t}\right)$.

3. Gravitational force in terms of R_1 and S_1

(a) *Spatially isotropic Universe*

Let us consider the metric

$$ds^2 = -\frac{R^2}{(1+\alpha r^2)^2}[dr^2 + r^2 d\theta^2 + r^2 \sin^2\theta d\varphi^2] + dt^2 \tag{3.1}$$

with the corresponding flat metric as

$$d\sigma^2 = -[dr^2 + r^2 d\theta^2 + r^2 \sin^2\theta d\varphi^2] + dt^2 . \tag{3.2}$$

In this case we have

$$\begin{aligned} g_{\mu\nu} &= \text{diag}\left[-\frac{R^2}{(1+\alpha\gamma^2)^2}, -\frac{R^2}{(1+\alpha\gamma^2)^2} - \frac{R^2}{(1+\alpha\gamma^2)^2}, 1\right], \\ g^{\mu\nu} &= \text{diag}\left[-\frac{(1+\alpha\gamma^2)^2}{R^2}, -\frac{(1+\alpha\gamma^2)^2}{R^2}, -\frac{(1+\alpha\gamma^2)^2}{R^2}, 1\right], \\ \gamma_{\mu\nu} &= \text{diag}\ [-1, -r^2, -r^2 \sin^2\theta, 1], \end{aligned} \tag{3.3}$$

$$K = \frac{R^3}{(1+\alpha r^2)^3},$$

$$R_\alpha = \left[\frac{-6\alpha r}{1+\alpha r^2}, 0, 0, \frac{3}{R}\left(\frac{\partial R}{\partial t}\right)\right],$$

$$S_i = \left[\frac{2\alpha r}{1+\alpha r^2}, 0, 0, -\frac{3}{R}\left(\frac{\partial R}{\partial t}\right)\right].$$

The components R_1 and S_1 correspond to the gravitational force and R_4 and S_4 correspond to HUBBLE's expansion.

(b) *The well known Robertson—Walker line element*

$$ds^2 = -[R(t)]^2\left[\frac{dr^2}{1+Kr^2} + r^2 d\theta^2 + r^2 \sin^2\theta d\Phi^2\right] + dt^2 \tag{3.4}$$

with the corresponding flat space metric (3.2) gives

$$\begin{aligned} g_{\mu\nu} &= \text{diag}\left[-\frac{R^2}{1-Kr^2}, -R^2 r^2, -R^2 r^2 \sin^2\theta, 1\right], \\ g^{\mu\nu} &= \text{diag}\left[-\frac{1-Kr^2}{R^2}, -\frac{1}{R^2 r^2}, -\frac{1}{R^2 r^2 \sin^2\theta}, 1\right], \\ \gamma_{\mu\nu} &= \text{diag}\ [-1, -r^2, -r^2 \sin^2\theta, 1], \end{aligned} \tag{3.5}$$

$$K = \frac{R^3}{(1 - K\gamma^2)^{\frac{1}{2}}},$$

$$R_\alpha = \left[\frac{Kr}{1 - Kr^2}, 0, 0, \frac{3}{R}\left(\frac{\partial R}{\partial t}\right), \right.$$

$$S_i = \left[\frac{K\gamma}{1 - Kr^2}, 0, 0, -\frac{3}{R}\left(\frac{\partial R}{\partial t}\right) \right].$$

Again, the components R_1 and S_1 correspond to the gravitational force and R_4 and S_4 correspond to HUBBLE's expansion.

4. Conclusion

Thus we may conclude that the three components $(\varkappa^1, \varkappa^2, \varkappa^3)$ of the gravitational field force are along the space axes and the fourth component $(\varkappa^4)$ corresponds to HUBBLE's expansion.

Acknowledgements

My thanks are due to Professor R. S. KUSHWAHA and Dr. P. K. BHATIA for their kind interest in this paper.

REFERENCES

1. V. V. NARLIKAR and K. P. SINGH, Proc. Ind. Acad. Sc., **17**, 311, 1951.
2. J. L. SYNGE, Relativity: the general theory, Interscience, New York, p. 322, 1960.
3. J. WEBER, General relativity and gravitational waves, Interscience, New York, 1961.

RECENSIONES

J. H. SANDERS: **The Velocity of Light**

Pergamon Press (Oxford—London—Edinburgh—New York—Paris—Frankfurt) 1965

In the past few decades there has been an enormous increase in the number of phenomena discovered, and theories elaborated in physics. This rapid evolution confronts lecturers with the difficulty of summarizing the main results in a given field of physics and of giving suitable information about the methods applied in related research work within the limited period of a course.

Collections of reprints of papers dealing with the most important developments in physics may contribute largely in overcoming this difficulty. Thanks are due to the Pergamon Press for satisfying these educational demands by publishing a new series of volumes entitled "Selected Readings in Physics".

One of that series is the book by J. H. SANDERS to be reviewed here. In Part 1 of this book, after a short introduction describing the basic methods for measuring the velocity of light, the author discusses the most appropriate measurements. This introductory part ends with a short list of the relevant literature.

Part 2 contains reprints of the papers on the three most important measurements of the velocity of light, those of MICHELSON, PEACE and PEARSON, of ESSEN and GORDON-SMITH, and, finally, of BERGSTRAND.

As about two-thirds of the book is made up of the papers on the three basic measurements, it is only their selection and the remaining third part which can be an object of our comments.

In Part 1 the problem of measuring the velocity of light is discussed. No mention is made, however, either of the fact that GALILEI first proposed a method of measuring the velocity of light, or of the particularly remarkable measurement of RÖMER (the only direct method, in which the velocity of propagation of a light signal passing through a distance of known length in only one direction, was measured).

If editorial requirements limit the size of the volumes of the series, thus determining the number of reprints included in SANDERS book, then the selection of the reproduced papers is justified. Attention must be drawn, however, to the fact that there are some important methods of measuring the velocity of light, — most of them closely related to the experimental verification of the principles of relativity — which it would be useful to publish in a similar volume.

In conclusion it should be emphasized that the book achieves its basic aim in its present form.

ZS. NÁRAY

R. A. R. TRICKER: **Early Electrodynamics**

Pergamon Press (Oxford—London—Edinburgh—New York—Paris—Frankfurt) 1965.

This book deals with the origin and initial position of electrodynamics. Many details make uselful and enjoyable reading not only for the physicist but also for the layman. The rest is supported by mathematical formulae at university level. Part 1 consists of four chapters and comprises 110 pages. Part 2 gives the original papers of OERSTED, BIOT and SAVART, AMPÈRE and finally of GRASSMANN in an English translation extending to 101 pages.

Chapter I of Part 1 is entitled "The Stage". The preliminaries and circumstances of the development of electrodynamics are described here. The writer expounds the role of FRANKLIN,

PRIESTLEY, COULOMB, VOLTA and DAVY in the science of electricity and magnetism before 1820, including the work of POISSON in the third decade of the nineteenth century. At that time the fields of electrostatics and magnetism were looked upon as entirely distinct from the other. They presented many similarities, but no connecting link had been found. In 1820 the announcement of OERSTED's discovery led to the rapid development of the electrodynamics of steady currents.

Chapter II embracing 10 pages has the title "Dramatic Personae". OERSTED is the first, of whom we learn that from 1797 he was a university professor at Copenhagen and though a man of genius he was an unhappy experimenter. After his great discovery he said that he has tumbled over it by accident. But according to LAGRANGE: "such accidents only happen to people who deserve them". BIOT was a professor at the College de France. As for his activity, he produced a number of mathematical works, but it is as an experimentalist on which his claims to fame rest. FELIX SAVART collaborated with BIOT in experiments on the magnetic field of electric currents.

ANDRÉ MARIE AMPÈRE is the principal actor in the early development of electrodynamics. As we can read by the age of 50 he was a member of most of the learned societies in Europe. In spite of his scientific success, in his private life he presents a truly tragic figure. In addition to his contributions to mathematics and physics he also wrote philosophical works. His last major work was on the classification of the sciences, in which he was able to employ his great breadth of knowledge.

Chapter III, "Commentary", is the longest. Its sections correspond to those into which the extracts from the papers are grouped in Part 2 of this volume.

A) The work of OERSTED was the door for the opening of which the scientific world had been waiting. B. BIOT and SAVART in the same year announced the results of their experiments by which they determined forces. Though BIOT and SAVART were extremely fine experimenters, they were less successful in the theoretical interpretation of their results, and laid themselves open to the criticism of AMPÈRE.

C) The early work of AMPÈRE and his theory of magnetism comprises the following line of reasoning. OERSTED's experiments demonstrate that a magnet is orientated by an electric current. It is also orientated by the Earth. If the Earth is a great magnet by virtue of currents which circulate in it, could not such currents also explain the properties of ordinary magnets. At this stage AMPÈRE is obviously thinking of macroscopic currents rather than the molecular currents which he later proposed. AMPÈRE proceeded to try to imitate the behaviour of magnets by means of electric currents flowing in helical coils of wire.

D) AMPÈRE's philosophy of science is readable from the papers published at the Academie Royale des Sciences. Though in this he set out to follow NEWTON the line which he actually followed is rather in advance of that which NEWTON himself set out explicity in the Principia. The attitude of NEWTON is one of severe empiricism. AMPÈRE writes as though he accepted NEWTON's position completely. In the theory of gravitation NEWTON was already provided with a knowledge of a range of phenomena. AMPÈRE had to discover the laws as well as provide the theory. Mathematics and physics were not separated in the mind of AMPÈRE. He looked upon his mathematical investigations as applying to the world of experience.

E) The design of AMPÈRE's basic experiments is recorded in his paper. The writer of this book performs one of the four experiments on the lines described in the Mémoire.

F) AMPÈRE's theory of the action of current elements was the result of his experiments. We can read the formula of AMPÈRE for the force between two current elements and we find examples of its use. This is followed by the verification of the identity of the formulae of AMPÈRE and BIOT-SAVART when integrated of a complete circuit. After this the writer provides a simple deduction of the BIOT-SAVART formula from the experimental results of AMPÈRE and describes AMPÈRE's theory of the equivalent magnetic shell, from which the well-known "work rule" arises. Then we use AMPÈRE's law in differential form to establish a vector potential. The representation of the magnetic field of an electric current by means of lines of force and the magnetic induction as a now-divergent vector is discussed here. This section of the book concludes with a reference to the question of units and dimensions.

G) AMPÈRE's quantitative theory of magnetism remains the last section of the chapter. AMPÈRE looks on magnets as assemblies of particles, all orientating in the same direction round which electric currents circulate. AMPÈRE shows that his law of action of current elements accounts satisfactorily for the forces experienced by a magnet. The effects of currents in the interior of substances uniformly magnetized cancel each other out. When the magnetization is not uniform, there will be a current density through the material. As an example of the application of the idea of Ampèrean currents the writer considers the magnetic circuit.

Chapter IV is entitled "The Critics". AMPÈRE's interpretation of the interaction of two electric circuits as being the sum of the interactions in pairs of the constituent current

elements has since been criticized by some physicists. We become acquinted with the criticism of MAXWELL, GRASSMANN, HEAVISIDE, WHITTAKKER and finally that of BUILDER and ROSSER. Though an isolated element of a steady current is a contradiction in terms; nevertheless, as MAXWELL said, it is perfectly legitimate for purposes of mathematical calculation.

ZS. CSOMA

J. R. SCHRIEFFER: **Theory of Superconductivity**

Benjamin Inc., New York, 1964, pp. 282

The author is one of the originators of the fundamental BCS theory of superconductivity which followed ONNES' discovery of this phenomenon more than 50 years later and which has proved to be highly successful in explaining the basic phenomena observed in the superconducting state. The book is an outgrowth of the series of lectures given by him at the University of Pennsylvania in 1962. It comprises the fundamental aspects of the theory of superconductivity as well as a number of formal techniques developed for dealing with the superconducting state. The aim set by the author is not primarily to present a broad survey of the whole field of superconductivity, but rather to present material which can "serve as a background for reading the literature in which detailed applications of the microscopic theory are made to specific problems". The book contains a basic text, indispensable to those concerned with the theoretical aspects of superconductivity.

Chapter 1 contains a survey of the most important experimental facts about superconductors and the phenomenological theories conceived to explain them. Chapter 2 gives an account of the pairing theory of superconductivity of BARDEEN, COOPER and SCHRIEFFER and Chapter 3 is devoted to various applications of the pairing theory: the calculation of the acoustic attenuation rate, nuclear spin relaxation rate, electromagnetic absorption and electron tunnelling. In Chapter 4 the coupled electron-phonon system is treated with the aim of obtaining a more complete understanding of superconductivity. An introduction to field theoretic methods in the manybody problem forms the subject of Chapter 5. The GREEN's function technique is treated in detail. In Chapter 6 the elementary excitations in normal metals are discussed in the framework of the random phase approximation. The field-theoretic methods developed in previous Chapters (Chapter 4—Chapter 6) are applied to superconductivity in Chapter 7 in order to provide a more realistic description of the superconducting properties of real metals. The strong role played by retardation and damping effects and the consequent breakdown of the quasiparticle picture in the case of strong coupling superconductors is emphasized. In the final Chapter the electromagnetic properties of superconductors are discussed. It is shown how the MEISSNER effect follows from microscopic considerations and a discussion of the problem of gauge invariance in the theory is given. The collective excitations of the system are treated as well. In the Appendix a summary of second quantization can be found.

The treatment of the book is systematic, clear and concise. The reader is led from the elements of the subject to the frontiers of present-day research activity in careful stages. The book published by Benjamin Inc. will certainly become one of the most widely-used textbooks in the field of superconductivity.

P. SZÉPFALUSY

A. B. ARONS: **Development of Concepts of Physics from the Rationalization of Mechanics to the First Theory of Atomic Structure**

(Addison-Wesley, Reading, Massachusetts, USA, 1965; XX + 972 pages, $. 11.25)

Intended for introductory courses, this excellent text-book presents general physics from the 17th-century rationalization of mechanics to the first theory of atomic structure. It emphasizes the historical and philosophical aspects of scientific thought. The principal emphasis is, of course, on the subject matter of physics itself, but attention is paid to the origin and significance of physical concepts; to the way in which conceptual insights produce unification of our view of apparently unrelated phenomena; to the impact of science on intellectual history and the way in which growing actual and theoretical scientific knowledge

has altered man's view of himself and of the Universe; to aspects of sociology as reflected in the motivation and behaviour of scientists. In order to arouse the student's interest considerable pains have been taken to motivate each conceptual development and to show how various elements of knowledge were acquired: how we know what we think we know; why we accept a given conceptual or theoretical aspect; what is the role of idealizations and approximations.

The main problem of modern physics teaching, to select the topics for a general introductory course, is solved by the author by the familiar method of having a one-year course for non-science majors including prospective teachers in mind, but the text can be used to supplement a two-year course for students of science and engineering. The book is mathematically self-contained, analytical geometry and calculus being developed to just the extent necessary to deal correctly with problems involving continuous changes.

J. I. HORVÁTH

ALFREDO BAÑOS, JR.: **Dipole Radiation in the Presence of a Conducting Half-Space**

International Series of Monographs in Electromagnetic Waves, Vol. 9;
Pergamon Press Ltd., Oxford, 1966; (VII + 245 pages, 20 figures; 70 s)

Since SOMMERFELD's memoir published in 1909, the problem of electromagnetic radiation from an elementary HERTZian dipole in the presence of a dissipative half-space based on different methods of the classical boundary value problem has been developed by several distinguished scientists. The underlying basis of the author's treatment is the application of the double saddle-point method of integration coupled, when necessary, with the technique for the subtraction of a first order pole from the vicinity of a saddle point.

The book starts with Fourier integral representation in Cartesian co-ordinates in configuration space as well as in transform space, and shows that the author's formulation contains all known formulations in either or both configuration and transform space. The two-media boundary value problem is reduced to the evaluation of two axially symmetric foundamental integrals, by which the electromagnetic field can be computed for all relevant cases of dipole radiation: whether the elementary HERTZian dipole be electric or magnetic, vertical or horizontal in respect of the plane interface separating the dielectric above (air) from the homogeneous and isotropic conducting medium below (earth, sea water); whether it is located in the air above or embedded in the conductive medium, and finally, whether the point of observation lies in the medium containing the source dipole or in the opposite one. The next stage presents asymptotic expansions which are valid generally quite for points of observation close to the interface, as well as useful approximations valid in the near, intermediate and far zones, respectively. The last chapter is devoted to the computation of the field of dipoles embedded in the conducting media with special reference to the low frequency case for which the present results are ideally suited.

This monograph represents the synthesis and development of the author's researches of the last ten years insofar as the SOMMERFELD problem is concerned and from several references, to earlier and modern references it can be checked that the suggested general results contain all known formulae as special cases.

J. I. HORVÁTH

G. BARTON: **Introduction to Dispersion Techniques in Field Theory**

W. A. Benjamin. Inc. 1965. New-York, Amsterdam

In the last decade dispersion techniques have become one of the most important tools of field theory. They are applied in all branches of physics where the method of quantized fields is used, e.g. elementary particle physics, nuclear physics, solid state physics etc. Several textbooks deal with the problem of proof of dispersion relations or with their application to scattering processes, but very few books systematically deal with the problem of three point or vertex functions. The analytical behaviour of vertex functions plays a very important role in electromagnetic and weak interaction theories, where the form factors appearing alone determine the S-matrix element.

This book by G. BARTON is a very clear and elegant description of all the phenomena connected with the analytical properties of form factors. The content of the book is based on lectures given to graduate students at the University of Sussex. The main value of these lecture notes is that they provide a practical guide to people making dynamical calculations. Throughout the book illuminating examples are employed to classify and elucidate the text. A prior knowledge of the elements of field theory is required for reading the book.

The lecture notes contain some introductory chapters on the elements of S-matrix theory. States and fields are introduced axiomatically, and complications connected with spin and charge are treated in detail. The LEHMANN—SYMANZIK—ZIMMERMANN reduction formula is proved, unitarity and crossing symmetry of the S-matrix are discussed. The methods of dispersion theory are represented in the simple example of two point function. These chapters are followed by the most essential parts of the book dealing with form factors. The behaviour of scalar and vector form factors under LORENTZ transformations (involving reflections) is discussed. The analytic properties of form factors are treated systematically (involving questions of spectral representations, asymptotic behaviour, etc.). The author pays much attention to the connection of form factors and scattering amplitudes. The OMNÉS integral equation for the form factor is solved in the two-particle approximation. As the solutions of the OMNÉS equation depend on scattering phase shifts, several approximations for the determination of partial wave amplitudes are presented. In this connection the possible types of singularities of partial wave amplitudes (including anomalous threshold) are analyzed. The end of the book contains some applications such as the electromagnetic structure of nucleons and partial conservation of the axial vector current.

The book is published as the first volume of a series: Lecture Notes and Supplements in Physics. There is no doubt that this book has achieved its purpose, to provide graduate students with a survey of the current literature. We eagerly await subsequent volumes of this series after this successful first one.

P. SURÁNYI

Reviews of the Hungarian Academy of Sciences are obtainable at the following addresses:

ALBANIA

Ndermarja Shtetnore e Botimeve
Tirana

AUSTRALIA

A. Keesing
Box 4886, GPO
Sydney

AUSTRIA

Globus Buchvertrieb
Salzgries 16
Wien I.

BELGIUM

Office International de Librairie
30, Avenue Marnix
Bruxelles 5
Du Monde Entier
5, Place St. Jean
Bruxelles

BULGARIA

Raznoiznos
1 Tzar Assen
Sofia

CANADA

Pannonia Books
2 Spadina Road
Toronto 4, Ont.

CHINA

Waiwen Shudian
Peking
P. O. B. 88.

CZECHOSLOVAKIA

Artia
Ve Smeckách 30
Praha 2
Postova Novinova Sluzba
Dovoz tisku
Vinohradska 46
Praha 2
Madarská Kultura
Václavské nám. 2.
Praha I
Postova Novinova Sluzba
Dovoz tlace
Leningradska 14
Bratislava

DENMARK

Ejnar Munksgaard
Nörregade 6
Copenhagen

FINLAND

Akateeminen Kirjakauppa
Keskuskatu 2
Helsinki

FRANCE

Office International de Documentation et Librairie
48, rue Gay Lussac
Paris 5

GERMAN DEMOCRATIC REPUBLIC

Deutscher Buch-Export und Import
Leninstraße 16.
Leipzig 701
Zeitungsvertriebsamt
Clara Zetkin Straße 62.
Berlin N. W.

GERMAN FEDERAL REPUBLIC

Kunst und Wissen
Erich Bieber
Postfach 46
7 Stuttgart S.

GREAT BRITAIN

Collet's Holdings Ltd.
Dennington Estate
London Rd.
Wellingborough. Northamps.
Robert Maxwell and Co. Ltd.
Waynflete Bldg. The Plain
Oxford

HOLLAND

Swetz and Zeitlinger
Keizersgracht 471—487
Amsterdam C.
Martinus Nijhof
Lange Voorhout 9
The Hague

INDIA

Current Technical Literature Co. Private Ltd.
India House OPP.

GPO Post Box 1374
Bombay I.

ITALY

Santo Vanasia
Via M. Macchi 71
Milano
Libreria Commissionaria Sansoni
Via La Marmora 45
Firenze

JAPAN

Nauka Ltd.
92. Ikebukur O-Higashi 1-chome
Toshima-ku
Tokyo
Maruzen and Co. Ltd.
P. O. Box 605
Tokyo-Central
Far Eastern Booksellers
Kanda P. O. Box 72
Tokyo

KOREA

Chulpanmul
Phenjan

NORWAY

Johan Grundt Tanum
Karl Johansgatan 43
Oslo

POLAND

RUCH
ul. Wilcza 46.
Warszawa

ROUMANIA

Cartimex
Str. Aristide Briand 14—18.
Bucuresti

SOVIET UNION

Mezhdunarodnaja Kniga
Moscow G—200

SWEDEN

Almquist and Wiksell
Gamla Brogatan 26
Stockholm

USA

Stechert Hafner Inc.
31 East 10th Street
New York, N. Y. 1003
Walter J. Johnson
111 Fifth Avenue
New York, N. Y. 1003

VIETNAM

Xunhasaba
19, Tran Quoc Toan
Hanoi

YUGOSLAVIA

Forum
Vojvode Misica broj 1.
Novi Sad
Jugoslovenska Knjiga
Terazije 27.
Beograd

Printed in Hungary

A kiadásért felel az Akadémiai Kiadó igazgatója — Műszaki szerkesztő: Farkas Sándor

A kézirat nyomdába érkezett: 1966. XII. 28. — Terjedelem: 12 (A/5) ív, 32 ábra

66.63270 Akadémiai Nyomda, Budapest — Felelős vezető: Bernát György

The *Acta Physica* publish papers on physics, in English, German, French and Russian.
The *Acta Physica* appear in parts of varying size, making up volumes.
Manuscripts should be addressed to:

Acta Physica, Budapest 502, P. O. B. 24.

Correspondence with the editors and publishers should be sent to the same address.
The rate of subscription to the *Acta Physica* is 165 forints a volume. Orders may be placed with "Kultúra" Foreign Trade Company for Books and Newspapers (Budapest I., Fő u. 32. Account No. 43-790-057-181) or with representatives abroad.

Les *Acta Physica* paraissent en français, allemand, anglais et russe et publient de travaux du domaine de la physique.
Les *Acta Physica* sont publiés sous forme de fascicules qui seront réunis en volumes.
On est prié d'envoyer les manuscrits destinés à la rédaction à l'adresse suivante:

Acta Physica, Budapest 502, P. O. B. 24.

Toute correspondance doit être envoyée à cette même adresse.
Le prix de l'abonnement est de 165 forints par volume.
On peut s'abonner à l'Entreprise du Commerce Extérieur de Livres et Journaux «Kultúra» (Budapest I., Fő u. 32. — Compte-courant No. 43-790-057-181) ou à l'étranger chez tous les représentants ou dépositaires.

«*Acta Physica*» публикуют трактаты из области физических наук на русском, немецком, английском и французском языках.
«*Acta Physica*» выходят отдельными выпусками разного объема. Несколько выпусков составляют один том.
Предназначенные для публикации рукописи следует направлять по адресу:

Acta Physica, Budapest 502, P. O. B. 24.

По этому же адресу направлять всякую корреспонденцию для редакции и администрации.
Подписная цена «*Acta Physica*» — 165 форинтов за том. Заказы принимает предприятие по внешней торговле книг и газет «*Kultúra*» (Budapest I., Fő u. 32. Текущий счет: № 43-790-057-181) или его заграничные представительства и уполномоченные.

INDEX

J. Bitó: On the Role of Auxiliary Electrodes in A. C. Discharges. — *Я. Бито:* О роли вспомогательных электродов, применяемых в разрядах переменного тока 1
K. L. Nagy: Spontaneous SymmetryBreaking and Constant Gauge Transformations. — *К. Л. Надь:* Спонтанное нарушение симметрии и постоянные калибровочного преобразования 17
M. Pósch and *E. Krén:* Magnetic Ground State Spin Configurations in Face-Centred Cubic and Cu_3Au-Type Crystals. —*М. Пош* и *Е. Крен:* Магнитное основное состояние спин-конфигурации в лобоцентральных кубических кристаллах и в кристаллах типа Cu_3Au 29
A. Sebestyén and *J. Nyiri:* Algebraic Methods in the Theory of Special Unitary Groups II. Quasispin and Multiplet Structure. — *Ю. Нири* и *А. Шебештен:* Алгебраические методы в теории специальных унитарных групп. II. Квазиспин и структура мультиплетов 37
L. Jánossy: The Lorentz Principle and the General Theory of Relativity Part IV. — — *Л. Яноши:* Принцип Лоренца и общая теория относительности. Часть IV. 53
N. A. Eissa, Z. Meligy, A. H. El Farrash and *S. Girgis:* Relative Intensity and Conversion Coefficients of the Transitions in the Decay Zr^{95}—Nb^{95}—Mo^{95}. — *Н. А. Исса, З. Мелиги, А. Х. Эл Фарраш* и *С. Гиргис:* Относительная интенсивность и коэффициенты преобразования переходов в распаде Zr^{95}—Nb^{95}—Mo^{95} 67
I. Hevesi: Determination of Optical Constants and Thickness of Anisotropic Crystal Plates From Transmission Measurements. — *И. Хевеши:* Определение оптических констант и толщины анизотропных кристаллических пластинок по измерению пропускания 75
J. Csikai and *G. Pető:* Influence of Direct Inelastic Scattering on $(n, 2n)$ Cross Sections. — — *Й. Чикаи* и *Г. Петэ:* Влияние прямого неупругого рассеяния на сечение $(n,2n)$ 87
Th. Neugebauer: Über die Niveaudichte der Atomkerne. — *Т. Найгебаер:* Плотность энергетических уровней атомных ядер 95

COMMUNICATIONES BREVES

F. Kelemen: Eine Wärmeimpulsmethode zur Bestimmung der Temperaturleitzahl an kurzen Proben 111
J. Bitó: On the Thermal Effects of Auxiliary Electrodes on Hg—A Discharges 117
I. Angeli and *I. Hunyadi:* Measurement of Average Total Cross-Section Fluctuation for Al at 14 MeV Neutron Energy 123
A. L. Mehra: Hubble's Expansion in Vectors Formed by $\triangle$-tensors 125

RECENSIONES

Zs. Náray: J. H. Sanders, The Velocity of Light 131
Zs. Csoma: R. A. R. Tricker, Early Electrodynamics 131
P. Szépfalusy: J. R. Schrieffer, Theory of Superconductivity 133
J. I. Horváth: A. B. Arons, Development of Concepts of Physics 133
J. I. Horváth: Alfredo Baños, jr., Dipole Radiation in the Presence of a Conducting Half-Space 134
P. Surányi: G. Barton, Introduction to Dispersion Techniques in Field Theory 134

Acta Phys. Hung. Tom. XXIII. Fasc. 1. Budapest, V. 28. 1967 Index: 26.022

ACTA PHYSICA

ACADEMIAE SCIENTIARUM HUNGARICAE

TOMUS XXIII FASCICULUS 2

AKADÉMIAI KIADÓ, BUDAPEST
1967

ACTA PHYS. HUNG.

ACTA PHYSICA

A MAGYAR TUDOMÁNYOS AKADÉMIA FIZIKAI KÖZLEMÉNYEI

SZERKESZTŐSÉG ÉS KIADÓHIVATAL: BUDAPEST V., ALKOTMÁNY UTCA 21.

Az *Acta Physica* német, angol, francia és orosz nyelven közöl értekezéseket a fizika tárgyköréből.

Az *Acta Physica* változó terjedelmű füzetekben jelenik meg: több füzet alkot egy kötetet.

A közlésre szánt kéziratok a következő címre küldendők:

Acta Physica, Budapest 502, P. O. B. 24.

Ugyanerre a címre küldendő minden szerkesztőségi és kiadóhivatali levelezés.

Az *Acta Physica* előfizetési ára kötetenként belföldre 120 forint, külföldre 165 forint. Megrendelhető a belföld számára az Akadémiai Kiadónál (Budapest V., Alkotmány utca 21. Bankszámla 05-915-111-46), a külföld számára pedig a „Kultúra" Könyv- és Hírlap Külkereskedelmi Vállalatnál (Budapest I., Fő u. 32. Bankszámla 43-790-057-181 sz.), vagy annak külföldi képviseleteinél és bizományosainál.

Die *Acta Physica* veröffentlichen Abhandlungen aus dem Bereich der Physik in deutscher, englischer, französischer und russischer Sprache.

Die *Acta Physica* erscheinen in Heften wechselnden Umfanges. Mehrere Hefte bilden einen Band.

Die zur Veröffentlichung bestimmten Manuskripte sind an folgende Adresse zu richten:

Acta Physica, Budapest 502, P. O. B. 24.

An die gleiche Anschrift ist auch jede für die Redaktion und den Verlag bestimmte Korrespondenz zu senden.

Abonnementspreis pro Band: 165 Forint. Bestellbar bei dem Buch- und Zeitungs-Aussenhandels-Unternehmen »Kultúra« (Budapest I., Fő u. 32. Bankkonto Nr. 43-790-057-181) oder bei seinen Auslandsvertretungen und Kommissionären.

Acta Physica Academiae Scientiarum Hungaricae, Tomus 23 (2), pp. 137—144 (1967)

FISSION PRODUCT PRECIPITATION FROM THE ATMOSPHERE IN DEBRECEN, HUNGARY, BETWEEN 1963 AND 1965

By

A. SZALAY and A. KOVÁCH

INSTITUTE OF NUCLEAR RESEARCH OF THE HUNGARIAN ACADEMY OF SCIENCES, (ATOMKI), DEBRECEN

(Received 22. III. 1966)

In the period investigated, most of the radioactive fallout originated from nuclear tests carried out in 1962, though the presence of fission products of previous origin could also be demonstrated. Since the cessation of atmospheric nuclear tests the activity of rainwater decreased again in 1965 to a low level similar to that obtained in 1961, the average decontamination half period being the same as determined in our earlier works.

Fission products from the nuclear test on the 16th October 1964 could be detected in the Debrecen rainwater by the significant increase of specific activity on the 25th October and on the 18th November 1964, the detectability on the 25th October being caused by tropospheric transport. The effect of the second test carried out on the 14th May 1965 could not be detected.

Introduction

Measurements carried out to determine the fission product content of atmospheric precipitation was begun at this Institute in 1952 [1] [2] and was followed by the regular and uninterrupted observation of total fission product beta activity of precipitation during the following years [3, 4, 5, 6, 7].

The techniques of collecting, handling and measuring the samples have remained essentially unchanged since 1952, except for a minor modification in 1954. For a description of the techniques employed the reader is referred to our earlier works [4]. The procedure followed enabled us to recover the whole radioactive content of atmospheric precipitation without substantial losses in the course of collection and preparation. Fission products from rainwater are collected to about 100%; the dry fallout deposited with dust and representing only a small part (less than about 10%) of the total fallout activity [8, 9] is recovered with an estimated efficiency of about 75%.

Results of measurements

Fig. 1 shows the results of our measurements carried out in the years 1963 to 1965. As in our previous works [4, 6, 7] the actual activity measurements made with a circular collection surface of 40 cm diameter have been reduced to the surface of a standard meteorological ombrometer, i. e. to a

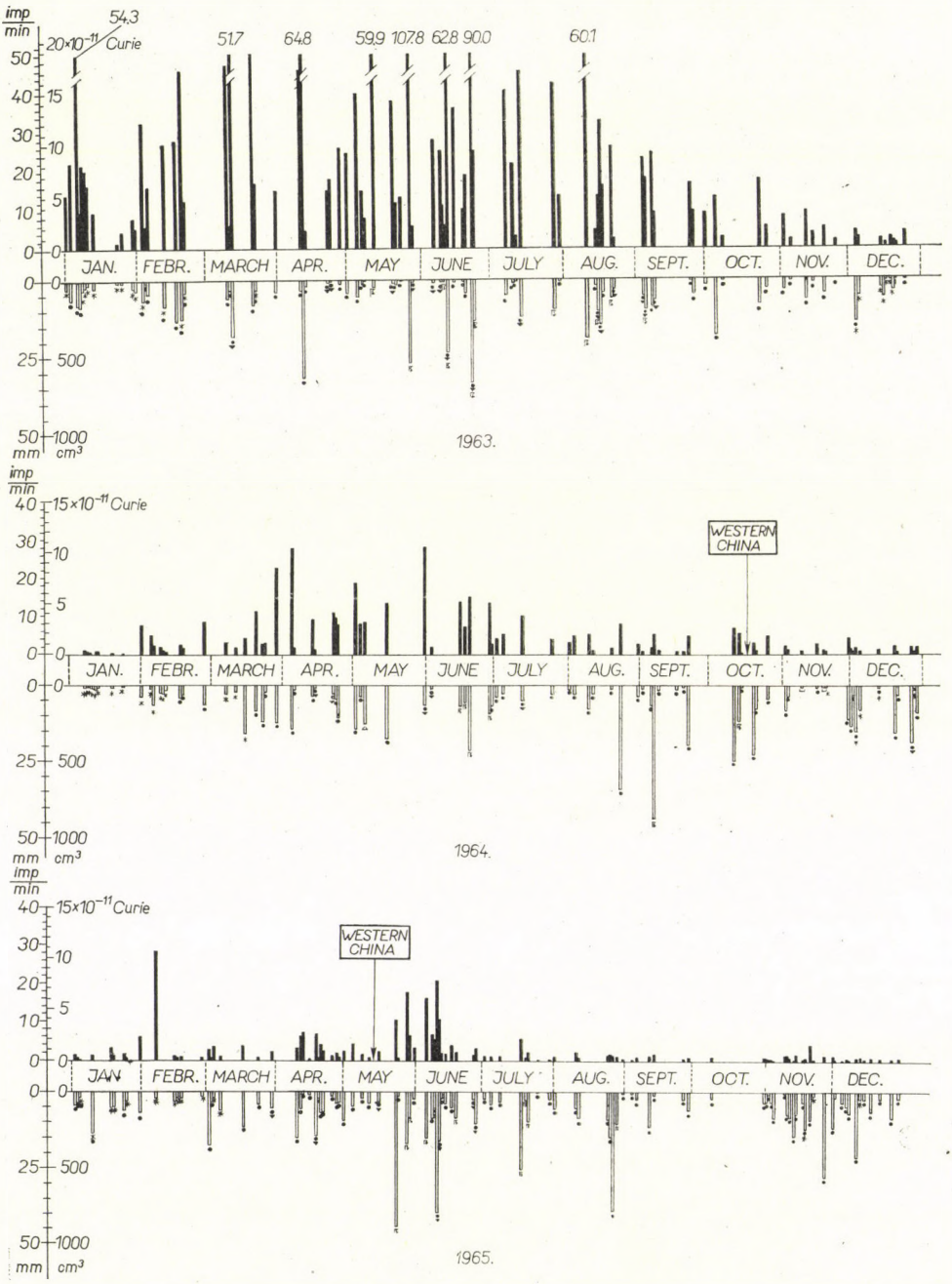

Fig. 1. Fission product precipitation from the atmosphere in Debrecen, Hungary, between 1963 and 1965. Ordinate upwards, right: activity in 10^{-11} Curie units, corrected for the geometry of the counting equipment. Ordinate upwards, left: activity observed in cpm reduced to 1/50 m² ombrometer surface. Very large activities are not shown linearly but by numbers indicating cpm values. Ordinate downwards, right: one day's rainfall expressed as water volume collected by an exposed area of 1/50 m². Ordinate downwards, left: one day's rainfall in mm. Abscissa: calendar time

collection surface of 1/50 m². Fig. 1 illustrates not only the total measured beta activity plotted on the ordinate in cpm and in 10^{-11} Curie units but the quantity of daily precipitation, downwards on the ordinate in mm rainfall and total collected water volume. Apart from the considerable amount of radioactive fallout in the first half of 1963 the results indicate a rather marked decrease of activity from 1963 on, with an average decontamination half period similar to that determined earlier [6]. The effect of increased exchange between the stratosphere and troposphere during springtime results in a marked "spring peak" in total fallout during each year, the peak in 1963 being less prominent because of the presence and decay of shortlived fission products.

The monthly total amounts of fission products are given in Table 1 in mC/km² units, determined by summarizing the activites of all samples in the given month, without applying a correction to radioactive decay.

The monthly average specific activity of atmospheric precipitation is given in Table 2 in 10^{-12} C/ml units, calculated on the basis of the uncorrected total monthly activity and the total quantity of precipitation during the month. Since the precipitation water samples collected by us also contain the dry fallout of previous days without precipitation, the specific activity values are probably somewhat higher (by an estimated value of about 10%) than the actual ones.

As can be seen from Table 2, a rather large increase in specific activity was observed in February, 1965. This comparatively high value, however, is due to a single sample only, collected on the 7th February, representing about

Table 1

Monthly total quantities of fission products measured in the precipitation fallen over Debrecen

Month	1963	1964	1965
	mC/km²	mC/km²	mC/km²
January	35,2	0,62	2,52
February	31,5	5,69	5,87
March	35,2	9,16	2,73
April	32,8	12,99	6,49
May	72,8	14,79	9,18
June	59,1	10,23	13,69
July	31,3	4,40	2,37
August	29,2	5,15	1,82
September	18,8	2,69	0,79
October	8,9	3,96	0,21
November	5,4	2,33	2,28
December	3,0	1,96	1,16

Table 2

Variation of the average specific activity of precipitation in Debrecen between 1963 and 1965

Month	1963	1964	1965
	pico C/ml	pico C/ml	pico C/ml
January	0,66	0,106	0,050
February	0,51	0,179	0,445
March	0,80	0,167	0,056
April	0,82	0,350	0,107
May	1,57	0,280	0,104
June	0,72	0,205	0,115
July	1,05	0,337	0,047
August	0,48	0,097	0,020
September	0,49	0,036	0,033
October	0,26	0,055	0,038
November	0,27	0,089	0,027
December	0,07	0,022	0,016

90% of the total activity measured during this month, though the quantity of precipitation corresponded only to 14,5% of the total amount of precipitation in February. This sample, during the measurement of its subsequent decay, showed a remarkable self-activation till the middle of February. This self-activation can be semiquantitatively explained by the presence of ^{95}Zr and ^{147}Nd together with their decay products in near fission yield proportions, originating from the nuclear test carried out in October 1964, since the activity of the mixture of these nuclides in fission yield proportions reaches a maximum in about three months after the explosion. A slight enrichment of ^{147}Nd with respect to ^{95}Zr can shift the activity maximum, as observed in this case. We should like to emphasize, however, that this explanation is only an assumption since no radiochemical tests have been carried out on the given sample.

Detection in Debrecen of the nuclear test of 16th October 1964

In earlier years the measurement of the decay of total fission product activities enabled us to determine the date of the nuclear test supplying the fission products with remarkable accuracy [5]. After 1958, however, the integral measurement of total activity decay was no longer suitable for this purpose.

The cessation of nuclear tests between 1958 and 1961 led to the conclusion that the decontamination of the stratosphere is much quicker than was anticipated [6]. Though in the years 1961 and 1962 a rather large amount of

fission products (equivalent to a total yield of about 230 MT) was injected into the stratosphere, from the end of 1962 on, the fallout activity again strongly decreased, and as can be seen from Table 1, at the end of 1964 the total monthly activity decreased to a value of only 2,5—3 mC/km². It could be expected that even a low-yield nuclear test carried out far from Europe might be detected under such circumstances. Under similar background conditions the French nuclear test carried out in the Sahara could be detected in Central Europe in 1960 [11], though fallout from these tests could not be traced in Debrecen.

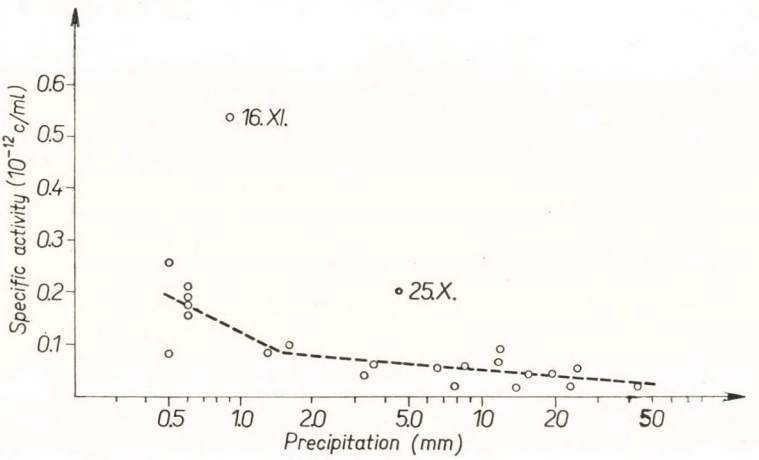

Fig. 2. The specific activity of atmospheric precipitation as a function of daily rainfall quantity from the 1st September till the 30th November 1964

The first atmospheric nuclear test of the Chinese People's Republic was carried out on the 16th October 1963 in the western desert area of China. Assuming a stratospheric transport in an easterly direction for fallout particles, the appearance of activity originating from this test was not to be expected in Central Europe earlier than the middle of November.

No increase in total beta ray activity was detected in Debrecen after the announced explosion date as shown in Fig. 1. However, the presence of fresh fission products could be proved from the specific activity of rainwater [8].

In a previous work SZALAY and BERÉNYI [4] discussed the correlation between specific activity and quantity of rainfall. Later experience in a period free from nuclear tests showed that the correlation between the specific activity and the logarithm of rainfall quantity is even more pronounced [7].

As one can see from Fig. 2, a rather close correlation between specific activity and the logarithm of rainfall existed in the autumn of 1964. The measured points in the diagram of Fig. 2 can be interpolated with a hyper-

bolic curve, or with the sum of two logarithmic functions. (The form of the interpolation function is not discussed here as it has no bearing on our results.)

It could be stated from Fig. 2 that the deviation of the measured points from the interpolation curve for the 25th October as well as for the 16th November can be regarded as significant, demonstrating that these samples might contain some radioactivity in excess of their expected values, in spite of the fact that this is not reflected in the absolute values of radioactivity given in Fig. 1. Although the total beta activities of these samples were rather low, about 300 and 170 dpm, respectively, the decay of their activity has been followed over a longer period. Using the WAY—WIGNER formula [5] it could be stated that the overwhelming part of the activity of the sample from the 16th November 1964 originated from the nuclear test carried out on the 16th October, while the sample from the 25th October contains about 30% of fresh fission products [8]. The appearance of fission products from the nuclear test on the 16th October 1964 as early as the 25th October is confirmed by other authors too [12, 13].

It is undoubtedly surprising that fission products from a nuclear test carried out in the inner part of Asia could be detected in Central Europe 9 days after the explosion. This short interval renders it probable that the radioactivity reached the Carpathian Basin by westbound tropospheric transport, since our earlier results have shown that the radioactive fallout of nuclear tests carried out in the Northern American continent reaches Debrecen with a delay of 8—10 days, while nuclear debris from Soviet tests could be detected only after about 4 weeks [5]. Thus, assuming a stratospheric transport in W—E direction, the increase in radioactivity was to be expected later, about the middle of November 1964.

The meteorogical situation at the end of October 1964, however, supports our assumption of tropospheric transport. Until the 24th October Atlantic air masses were dominant in Central Europe, but from the 24th October on, the anticyclonal situation formed over the European part of the U.S.S.R. became effective, too. On the 24th October a Mediterranean front intruded into the Carpathian Basin from a near southerly direction, but it became stagnating and dissolved during the same day, after influencing the meteorological situation in Western Hungary only. In the evening of the 25th October a cold front penetrated the Carpathian Basin in an E—W direction, causing moderate precipitation, from which our sample originates. The tropospheric wind direction during the day was constantly E—W.

This all means that during the meteorological changes causing the precipitation on the evening of the 25th October, air masses of an easterly origin reached the Carpathian Basin. Taking into consideration that at the end of October a situation corresponding to the continental monsoon was already present in Western Asia, it is quite probable that fission products from the

nuclear test carried out in the western desert of the Chinese People's Republic could have reached the air masses in the environment of the Caspian Sea by direct transport. The effect of the centrifugal monsoon is also supported by some press information, according to which the fission products could be traced in India shortly after the explosion.

The further path of tropospheric fallout in Central and Western Europe was also well traceable. An activity exceeding the total amount of fallout deposited during three months was observed on the 25th October in Bratislava [14] (possible presence of a hot particle?) while in the Bavarian Alps the first rise in activity was observed on the 26th October [12]. In Denmark, the first indication of new fission products was found in an air filter exposed between the 23—26th October; filters sampled on the 28th and 30th October gave an activity about 10 to 1000 times higher [13].

The appearance of fission products from the Chinkiang nuclear test in the precipitation of the 16th November 1964 is clearly due to stratospheric transport, the arrival time being in good accordance with the assumed stratospheric transport delay, as already stated. In the middle of November, Atlantic air masses intruded into the Carpathian Basin; jet stream conditions were normal.

All this strikingly shows that stratospheric transport is the main process by which fission products are distributed on a world-wide scale, but under appropriate meteorological conditions the possibility of direct tropospheric transport in an E—W direction cannot be excluded, even at a considerable distance from the nuclear test site.

A second nuclear test was carried out in the same area on the 14th May, 1965, but our efforts to detect fission products from this explosion in Debrecen rainwater have been unsuccessful.

REFERENCES

1. A. Szalay and D. Berényi sen., Acta Phys. Acad. Sci. Hung., **5**, 1. 1955.
2. A. Szalay and D. Berényi sen., MTA III. Oszt. Közl., **5**, 89, 1955.
3. A. Szalay and D. Berényi sen., MTA III. Oszt. Közl., **9**, 175, 1959.
4. A. Szalay and D. Berényi sen., Proc. 2nd Geneva Conf., P/1953, Vol. 18, p. 570.
5. A. Kovách and A. Szalay, ATOMKI Közlemények, **2**, 229, 1960.
6. A. Szalay and A. Kovách, Acta Phys. Acad. Sci. Hung., **13**, 281, 1961.
7. A. Szalay and A. Kovách, Acta Phys. Acad. Sci. Hung., **16**, 321, 1964.
8. A. Kovách, ATOMKI Közlemények, **7**, 57, 1965.
9. W. Anderson et al., Nature, **186**, 925, 1960.
10. N. G. Stewart et al., Report AERE HP/R 1701, 1955.
11. W. Santholzer, Atomnaya Energija, **12**, 432, 1962.
12. R. Reiter, Naturwiss., **52**, 128, 1965.
13. J. J. Led and L. Kristensen, Nature, **205**, 1307, 1965.
14. W. Santholzer, Private communication.

ОСАЖДЕНИЕ ПРОДУКТОВ ДЕЛЕНИЯ ИЗ АТМОСФЕРЫ В Г. ДЕБРЕЦЕН, ВЕНГРИЯ, В 1963—1965 ГГ.

А. САЛАИ и А. КОВАЧ

Р е з ю м е

В исследованном промежутке времени основная часть радиоактивного осадка происходила из атомных взрывов произведенных в 1962 г., хотя можно показать и наличие продуктов деления более раннего происхождения. Со времени прекращения атмосферных атомных испытаний радиоактивность выпадения уменьшалось и в 1965 г. и достигла низкого значения замеченного в 1961 г. Период полудеконтаминации был подобен к определенному нами в опубликованных раньше работах.

Продукты деления атомного взрыва в 16 октября 1964 г. можно было наблюдать в дожде в Дебрецене по резкому возрастанию удельной радиоактивности в 25 октября и 18 ноября 1964 г. Появление продуктов деления в 25 октября было обусловлено тропосферным транспортом.

Влияние второго испитания произведенного в 14. мая 1965 г. не было замечено.

Acta Physica Academiae Scientiarum Hungaricae, Tomus 23 (2), pp. 145—160 (1967)

GENERAL RELATIVISTIC THEORY OF LAGRANGIAN FUNCTIONS

PART I.

SCALAR AND VECTOR FIELDS IN THE SPACE X_1

By

G. KNAPECZ

PHYSICAL INSTITUTE OF THE UNIVERSITY OF TECHNICAL SCIENCES, BUDAPEST

(Presented by A. Kónya — Received 26. IV. 1966)

A deductive method is given for the derivation of general relativistic Lagrangian functions (densities). The method consists of the solution of a functional equation which is equivalent to the Lie equation. Some exact solutions of this equation are given. Whenever a Lagrangian density of the supposed type does not exist, the mathematical proof of the non-existence is given.

1. Introduction

1.1. Symmetries play an important role in nature, and therefore the symmetry groups (pseudogroups, gruppoids, . . .) play an important role in the description of physical phenomena and in the construction of physical theories.

The oldest known exact symmetry [1] is that of coordinate symmetry, usually called the principle of general relativity. According to this principle the mathematical description of nature should be invariant under *any* $\left(\det \frac{\partial \bar{x}^k}{\partial x^l} \neq 0\right)$ coordinate transformation. This is the guiding principle of the general relativity theory, and is applied in this work too.

1.2. Many different physical systems can be described by field variables. For example, the electromagnetic field may be described by an antisymmetric cotensor field $B_{ik}(x)$, the gravitational field by a symmetric cotensor field $g_{ik}(x)$, etc.

The equations of motion of the fields $\Phi_A(x)$ are mostly the Euler equations of a Lagrangian function (density) $L = f(\Phi_A, \Phi_{A,k}, \ldots)$. Physical systems of this kind throughout this work will be called "Lagrangian models", or simply "models".

The properties and the behaviour of the Lagrangian models are concentrated in their Lagrangian function L. Therefore the Lagrangian function of the model is its basic characteristic.

This paper deals with the derivation of the general relativistic Lagrangian densities.

1.3. Recently, EDELEN [2] has examined the equation obeyed by the

Lagrangian functions of a kind of Lagrangian systems, called by him "variant fields" and "field spaces", if only the principle of general relativity is postulated.

In the present paper a similar problem is discussed. We set up a new, general relativistic fundamental functional equation, which should be satisfied by the Lagrangian functions, and we solve this equation in a series of cases. If the functional equation of a hypothetical model has no solutions at all, we give the mathematical proof of the non-existence of such Lagrangians.

In the first part of the paper there is a short account of the geometric objects, and the deduction of the fundamental equation. The second part contains the derivation of Lagrangian functions of models which are embedded in a one dimensional space X_1 (the time). The two-dimensional and the four-dimensional cases will be treated in two subsequent papers.

1.4. If one compares the present status of the theory of elementary particles and that of the theory of general relativity, one finds some unpleasant "anticoincidency" among them. On the one hand, we have a lot of elementary particles, but no general relativistic theory of them. On the other hand we have a satisfactory general relativistic theory of gravitation, but the gravitons are not found experimentally.

Now the following questions arise:

(i) are the elementary particles, or the elementary fields belonging to them explicable by a general relativistic theory?

(ii) Does a general relativistic theory of elementary fields exist at all, i.e., can it be constructed within the frames of the general relativity theory?

(iii) What are the possibilities of the general relativistic theories?

Although the general relativity theory is fifty years old, it seems that these questions are so far unanswered. Therefore, it seems that a general relativistic study of the derivation of the Lagrangian functions is not only of a mathematical, but also of a physical interest. The examination of the question, what restrictions follow from the only principle of general relativity, may be only useful.

I. The fundamentals

2. The geometric objects

According to the mathematical formulation of the principle of general relativity the physical phenomena should be described, and the physical theories should be formulated by geometric objects. As alredy mentioned, geometric objects are, for example, the covectors $A_k(x)$, the cotensors $B_{ik}(x)$ or $g_{ik}(x)$, the connections $\Gamma^i_{kl}(x)$, the scalars $s(x)$, the ordinary densities $d(x)$, etc.

According to WUNDHEILER's definition [3] (in physical terminology) the geometric objects are those entities which have the following properties:

(i) The components $\Phi_A(x)$ $(A = 1, 2, \ldots, M)$ of the object Φ are functions of the coordinates x^k of space-time.

(ii) In the case of an *arbitrary* coordinate transformation

$$\bar{x}^k = f^k(x^l), \quad \det \frac{\partial \bar{x}^k}{\partial x^l} \neq 0, \quad k, l = 0, 1, 2, 3, \tag{1}$$

the components of the object should be transformed according to a rule

$$\Phi_A(\bar{x}_P) = \Psi_A[\Phi_B(x_P), T_{\bar{k}\bar{l}}], \qquad A, B = 1, 2, \ldots, M \tag{2A}$$

where $T_{\bar{k}\bar{l}}$ denotes a set of variables which depend on the coordinate transformation, i.e.,

$$T_{\bar{k}\bar{l}} \equiv \left(\bar{x}^k, \frac{\partial \bar{x}^k}{\partial x^l}, \frac{\partial^2 \bar{x}^k}{\partial x^l \partial x^m}, \ldots\right). \tag{2B}$$

(iii) The functions Ψ_A obey the transitivity condition.

The transitivity condition and other details on the geometric objects may be found in [3] and [4]. Since in the present paper only the well known scalar and covector fields and their Lagrangians are studied, it is sufficient if we mention briefly the following:

According to GOLAB [3—4] geometric objects may be characterized by three numbers: (m, n, s). (i) m denotes the number of the components of the object. In the case of a covariant vector of four dimensional spacetime m equals 4. In the case of a scalar m equals 1. (ii) n denotes the dimensionality of the space in question. In the case of the preceding objects n equals 4. (iii) s is the "class" of the object. If $T_{\bar{k}\bar{l}}$ consists of $\partial \bar{x}^k / \partial x^l$ only, then s equals 1. If $\partial^2 \bar{x}^k / \partial x^l \partial x^m$ also occurs in the transformation formula (2), then s equals 2.

For example, the scalars are of the type (1, 4, —). The first derivatives of the scalars and the covectors are of the type (4, 4, 1).

Mathematicians have found a lot of geometric objects [3—4]. In the course of this series of papers we will give a survey of them, but for the purposes of the present paper it is sufficient if we say a few words about the densities of weight 1.

Two kinds of densities of weight one exist: (i) the ordinary densities of weight one, and (ii) the Weyl densities of weight one. Both objects are of the type (1, n, 1). Both may serve as Lagrangian densities, depending on how the volume element is defined.

Definition 1. An ordinary density $d_0(x)$ of weight one is an object of the type (1, n, 1), which in the case of the coordinate transformation (1) is transformed as follows

$$\bar{d}_0(\bar{x}_P) = \left(\det \frac{\partial x^k}{\partial \bar{x}^l}\right) \cdot d_0(x_P). \tag{3. Ord}$$

Definition 2. A Weyl density $d_W(x)$ of weight one is an object, which under (1) is transformed as follows

$$\bar{d}_W(\bar{x}_P) = \left|\det \frac{\partial x^k}{\partial \bar{x}^l}\right| \cdot d_W(x_P). \tag{3. Weyl}$$

3. The physical fields

Every "specific" geometric object [3—4] is a field in the physical sense of the word.

It is known from the special relativistic theory of fields, that there is some correspondence between fields and elementary particles. To elementary particles of different kinds correspond fields of different kinds, which belong to some representations of the Poincaré group (of Lorentz group). Similarly, the geometric objects belong to the gruppoid of the general coordinate transformations [3—4]. They play the same role in the case of the general relativistic description of the world as the objects of the representations of the Poincaré group (the pseudoscalars, the spinors, the vectors, . . .) in the case of the special relativistic description of physical phenomena.

If one wishes to construct general relativistic field theories, one should solve the question as to what Lagrangians may be constructed from a given set of geometric objects $\Phi_A(x)$ and their derivatives up to some order.

As will be seen, the answer to this question is in the majority of cases a negative one: no Lagrangians can be constructed from some hypothetically given set of geometric objects. Fortunately, however, there are cases when the answer is an affirmative one. The fundamental equation in the case of some hypothetical combinations of fields does have solutions. The search for these solutions is the aim of the present work.

4. The fundamental equation

4.1. (i) If the behaviour of a *system* of fields $\Phi_A(x)$ is concentrated into a Lagrangian L, then according to physical experience L should be a function of the $\Phi_A(x)$ and of their derivatives up to some order.

(ii) According to the principle of general relativity the Lagrangian should be a geometric object.

Therefore, in the theory of Lagrangian functions it is necessary to require:

Postulate 1. The Lagrangian should be a concomitant [3—4] of the set of fields $\Phi_A(x)$ and of their derivatives $\partial\Phi_A/\partial x^k$, . . . $\partial^n\Phi_A/\partial x^k \ldots \partial x^s$ $(n > 0)$, i.e.

$$L = l\left[\Phi_A(x), \frac{\partial\Phi_A(x)}{\partial x^k}, \ldots\right]. \tag{4}$$

4.2. Not every concomitant of the kind (4) is a Lagrangian. If, according to physical experience, we require that the action A of the system of fields

$$A \int\int\int\int L\, dV \tag{5}$$

should be an invariant with respect to (1), then we must set up

Postulate 2. The Lagrangians should have the transformation rule

$$\bar{L} = \varepsilon \cdot \left(\det \frac{\partial \bar{x}^k}{\partial x^l}\right)^{-1} \cdot L, \qquad (6, L)$$

where $\bar{L}$ is the transformed Lagrangian, which belongs to the new coordinate system, and

$$\varepsilon = \begin{Bmatrix} 1 \\ \text{sign } (\det \ \partial \bar{x}/\partial x) \end{Bmatrix} \qquad (6, \varepsilon)$$

depending on how dV is defined. If dV is defined as an ordinary density of weight -1, then the Lagrangian should be an ordinary density of weight one. Then $\varepsilon = 1$. If the volume element is defined as a Weyl density of weight -1, then the Lagrangian should be a Weyl density of weight one. This question will have significance in the case of the gauge symmetries only. Therefore, we do not go into further details here.

4.3. From the two postulates it follows that

$$l\left[\bar{\Phi}_{\bar{A}}(\bar{x}_P), \bar{\Phi}_{\bar{A},\bar{k}}(\bar{x}_P), \ldots\right] = \varepsilon \cdot \left(\det \frac{\partial x^l}{\partial \bar{x}^k}\right) \cdot l\left[\Phi_A(x_P), \Phi_{A,k}(x_P), \ldots\right]. \qquad (7)$$

Inserting (2) into (7) we get the necessary condition for l to be a Lagrangian. This condition will be called the

Fundamental equation:

$$l\left[\Psi_A\left[\Phi_B(x_p), T_{\bar{k}l}\right], \ldots\right] = \varepsilon \cdot \left(\det \frac{\partial x^l}{\partial \bar{x}^k}\right) \cdot l\left[\Phi_A(x_p), \Phi_{A,k}(x), \ldots\right], \qquad (8)$$

where Ψ_A and $\bar{x}^k = f^k(x^l)$ are given, l is the unknown function, and the subscript P in $\bar{x}_P$ and x_P denotes that $\bar{x}_P$ abd x_P are the coordinates of the *same* instant-point P in the old and new coordinate systems, respectively.

The solution of equation (8) is the necessary task.

4.4. Every solution l of (8) is a density and a concomitant of the fields. But not all density-concomitants are Lagrangians. There are densities whose Euler equations vanish identically. These solutions should be disregarded. Therefore we set up the

Supplementary condition: Only those solutions of (8) are Lagrangians whose Euler equations do not vanish identically.

Every solution of the fundamental equation which also satisfies the supplementary condition is a mathematically possible general relativistic model of a system of interacting fields. Whether it has a physical meaning, too, is another question.

5. The mathematical problem

The mathematical solution of (8) is a difficult problem in the case of fields which have a complicated transformation rule. Therefore, in the search for the solutions of (8) we shall proceed step by step, from simple systems to more and more complicated ones, from the one dimensional time X_1 to the four dimensional spacetime X_4.

In the case of the space X_1 there are no mathematical difficulties, and the method of the direct derivation of general relativistic Lagrangian functions appears clearly. As will be seen, this method is more simple than that of LIE [5], YANG-MILLS [6] and UTIYAMA-KIBBLE [7], and EDELEN [2].

II. Fields in the time X_1

6. Preliminaries

In this part of the paper the "fields" $\Phi(\tau)$ depending on a single variable, on time τ, are discussed. The time is assumed to be a space X_1 [3—4]. The fields in question are, for example, the cartesian coordinates $x(\tau)$, $y(\tau)$, $z(\tau)$ of a moving mass-point, the angular coordinate $\varphi(\tau)$ of a rotating body, etc.

Definition 3. The points of the X_1 will be called "instants".

Definition 4. The general relativistic time coordinate τ of X_1, which has in general no metric properties, and therefore is only a parameter (or label) of the instant, will be called "paratime" (from *para*meter and *time*).

Definition 5. If a geometric object is a function of several geometric objects it is usually called a concomitant, or simply a comitant of them. If the concomitant is a scalar, it is usually called invariant. If the comitant is an ordinary density of weight one, it will be called "ordinary densitant" (from *densit*y and comi*tant*).

Definition 6. Those comitants which are Weyl densities of weight one, will be called "Weyl densitants".

The last objects, however, will be treated in the later publication only.

7. Single vector field in X_1

Definition 7. The object $v(\tau)$ which, in the case of an arbitrary coordinate transformation

$$\bar{\tau} = f(\tau), \qquad a \overset{\text{def}}{=} -\frac{d\bar{\tau}}{d\tau} = \det \frac{d\bar{\tau}}{d\tau} \neq 0, \tag{9}$$

is transformed by the formula

$$\bar{v}(\bar{\tau}_P) = a^{-1} v(\tau_P), \tag{10}$$

will be called a "covector". In the mathematical literature it is called an ordinary density of weight one.

The transformation formula (10) may be written

$$\bar{v} = \beta_1 v, \tag{11}$$

where

$$\beta_1 \overset{\text{def}}{=} \alpha_1^{-1} = d\tau/d\bar{\tau}\,. \tag{12}$$

Theorem 1. The general densitant of a covector field $v(\tau)$ is

$$l[v(\tau)] = k \cdot v(\tau)\,, \tag{13}$$

where k is a scalar constant. (Proof. The fundamental equation (8) reads as follows in this case:

$$l[\bar{v}(\bar{\tau}_P)] = \beta_1 l[v(\tau_P)]\,. \tag{14}$$

Taking into account (11) eq. (14) becomes

$$l[\beta_1 v] = \beta_1 l[v] \tag{15}$$

which is an identity in β and v. Among the general coordinate transformations there are some for which at the given instant P

$$\alpha(\tau_P) = v(\tau_P)\,. \tag{16}$$

Under these restrictions (15) reduces to

$$l(1) = v^{-1} l(v)\,, \tag{17}$$

i.e.

$$l[v(\tau)] = v(\tau) \cdot l(1) = k \cdot v(\tau)\,, \tag{18}$$

where k is an arbitrary scalar constant. Since no further restrictions on l may be given, (18) is (as called in the mathematical literature) the general solution of (15).

We mention that the degenerate solutions of (8) will always be disregarded.

Thus the theorem is proved).

Theorem 2. The general densitant of a covector v and its first derivative v_τ is

$$l[v(\tau), v_\tau(\tau)] = k \cdot v(\tau)\,, \tag{19}$$

where k is an arbitrary scalar constant. (Proof. With the notations

$$a \overset{\text{def}}{=} v_\tau \overset{\text{def}}{=} \frac{d\,v(\tau)}{d\,\tau} \tag{20}$$

and

$$\beta_2 \overset{\text{def}}{=} \frac{d^2\,\tau}{d\,\bar{\tau}^2} \tag{21}$$

and taking into account the transformation formula of $a\ (\tau)$

$$\bar{a}\,(\bar{\tau}_P) = \beta_1^2\,a\,(\tau_P) + \beta_2\,v\,(\tau_P) \tag{22}$$

the fundamental equation (8) reads

$$l\,(v\,\beta_1,\, a\,\beta_1^2 + v\,\beta_2) = \beta_1\,l\,(v, a)\,. \tag{23}$$

Among the general coordinate transformations (9) there are some for which at the instant P the following relations are valid

$$v\,\beta_1 = 1,\ \text{i. e.,}\ \beta_1 = v^{-1} \tag{24}$$

and

$$a\,\beta_1^2 + v\,\beta_2 = 0,\ \text{i. e.,}\ \beta_2 = -\,a\,v^{-3}\,. \tag{25}$$

At this point P eq. (23) reads

$$l\,(1{,}0) = v^{-1}\,l\,(v, a) \tag{26}$$

Therefore, the general solution of (23) is

$$l\left[v\,(\tau)\,,\ \frac{d\,v\,(\tau)}{d\,\tau}\right] = v \cdot l\,[1.0] = k \cdot v\,(\tau) \tag{27}$$

QED).

Theorem 3. No Lagrangian of the form

$$L = l\,(v, v_\tau) \tag{28}$$

exists. (Proof. (19) does not contain v_τ).

Theorem 4. The general densitant of $v\ (\tau)$, v_τ and $v_{\tau\tau}$ is

$$l\,(v, v_\tau, v_{\tau\tau}) = k\,v\,, \tag{29}$$

where k is an arbitrary scalar constant. (Proof. The transformation formula of v is (11), that of v_τ is (23), and that of $v_{\tau\tau}$ is

$$\bar{v}_{\bar{\tau}\bar{\tau}} = \beta_1^3 v_{\tau\tau} + 3\beta_1 \beta_2 v_\tau + \beta_3 v, \tag{30}$$

where

$$\beta_3 \overset{\text{def}}{=} \frac{d^3 \tau}{d \bar{\tau}^3}. \tag{31}$$

The fundamental equation reads

$$l(v \beta_1, v_\tau \beta_1^2 + v \beta_2, v_{\tau\tau} \beta_1^3 + 3\beta_1 \beta_2 v_\tau + v \beta_3) = \beta_1 l(v, v_\tau, v_{\tau\tau}). \tag{32}$$

At a given instant P we may take

$$v \beta_1 = 1, \tag{33}$$

$$v_\tau \beta_1^2 + v \beta_2 = 0 \tag{34}$$

and

$$v_{\tau\tau} \beta_1^3 + 3 v_\tau \beta_1 \beta_2 + v \beta_3 = 0. \tag{35}$$

Then

$$l(1, 0, 0) = v^{-1} l(v, v_\tau, v_{\tau\tau}) \tag{36}$$

and thus the theorem is proved).

Theorem 5. No Lagrangian of the form

$$L = l[v(\tau), v_\tau(\tau), v_{\tau\tau}(\tau)] \tag{37}$$

exists. (Proof. (29) does not contain v_τ and $v_{\tau\tau}$).

There is a strong probability that no Lagrangian of the form

$$L = l\left[v(\tau), \frac{d v}{d \tau}, \ldots, \frac{d^u v}{d \tau^u}\right] \tag{38}$$

exists.

8. Single scalar field in X_1

Theorem 6. No densitant of a scalar field $s(\tau)$ exists. (Proof. Let us suppose that l exists. Then in the case of a transformation (9) one gets

$$[\bar{s}(\bar{\tau}_P)] = \beta_1 l[s(\tau_P)]. \tag{39}$$

Since $s(\tau)$ is a scalar, i.e.,

$$\bar{s}(\bar{\tau}_P) = s(\tau_P), \tag{40}$$

(39) may be written as follows

$$l = \beta_1 l. \tag{41}$$

Since this must be true for arbitrary values of β_1, l should be identically zero

$$l[s(\tau)] \equiv 0 . \tag{42}$$

The theorem is now proved).

Theorem 7. The general densitant of a scalar $s(\tau)$ and of its derivative $s_\tau(\tau)$ is

$$l[s, s_\tau] = s_\tau F(s) \tag{44}$$

where F is an invariant. (Proof. The fundamental equation (8) now reads

$$l\left[\bar{s}, \frac{d\bar{s}}{d\bar{\tau}}\right] = \beta_1 l\left[s, \frac{ds}{d\tau}\right], \tag{45}$$

i.e.

$$l(s, s_\tau \beta_1) = \beta_1 l(s, s_\tau) . \tag{46}$$

At a given instant P, one may take

$$\beta_1 s_\tau = 1 \tag{47}$$

and, therefore,

$$l\left[s(\tau), \frac{ds(\tau)}{d\tau}\right] = \frac{ds}{d\tau} l(s, 1) = \frac{ds(\tau)}{d\tau} F(s(\tau)) . \tag{48}$$

QED).

Theorem 8. No Lagrangian of the form

$$L = l[s(\tau), s_\tau(\tau)] \tag{49}$$

exists. (Proof. The densitant in question is (48)

$$L = s_\tau F(s) . \tag{48}$$

Its Euler equation identically vanishes:

$$\frac{\partial L}{\partial s} - \left(\frac{\partial L}{\partial s_\tau}\right)_\tau \equiv s_\tau \frac{dF}{ds} - \frac{dF}{d\tau} \equiv 0 . \tag{50}$$

Thus, the theorem is proved).

Theorem 9. The general densitant of a scalar $s(\tau)$ and of its first two derivatives is of the form

$$l[s, s_\tau, s_{\tau\tau}] = s_\tau F(s) , \tag{51}$$

where F is an invariant. (Proof. As for theorem 3).

Theorem 10. No Lagrangian of the form

$$L = l(s, s_\tau, s_{\tau\tau}) \tag{52}$$

exists. (Proof. The Euler equation of (51) vanishes identically.)

It is highly probable that no Lagrangian of the form

$$L = l\left[s(\tau), \frac{d\,s}{d\,\tau}, \ldots, \frac{d^u\,s}{d\,\tau^u}\right] \tag{53}$$

exists.

9. Two covector fields in X_1

This section also yields positive results.

Theorem 11. The general densitant of two covector fields $v(\tau)$ and $w(\tau)$ is

$$l[v(\tau), w(\tau)] = v(\tau) \cdot F\left[\frac{w(\tau)}{v(\tau)}\right], \tag{54}$$

where F is an arbitrary invariant. (Proof. Eq. (8) now reads

$$l(v\,\beta_1, w\,\beta_1) = \beta_1 \cdot l(v, w), \tag{55}$$

Assuming that

$$v\,\beta_1 = 1, \text{ i.e., } \beta_1 = v^{-1}$$

we get

$$l(v, w) = v\,l\left(1, \frac{w}{v}\right) = v \cdot F\left(\frac{w}{v}\right). \tag{56}$$

QED).

Theorem 12. The general densitant of the vector fields $v(\tau)$ and $w(\tau)$, and their first derivatives is of the form

$$l[v, w, v_\tau, w_\tau] = v\,F\left[\frac{w}{v}, \frac{w_\tau\,v - w\,v_\tau}{v^3}\right], \tag{57}$$

where F is an arbitrary invariant function. (Proof. Introducing the notation

$$a = v_\tau, \qquad b = w_\tau \tag{58}$$

eq. (8) reads

$$l(\beta_1\,v, \beta_1\,w, \beta_1^2\,a + \beta_2\,v, \beta_1^2\,b + \beta_2\,w) = \beta_1\,l(v, w, a, b). \tag{59}$$

Assuming that

$$\beta_1 v = 1 \tag{60}$$

and

$$\beta_1^2 a + \beta_2 v = 0 \tag{61}$$

we get

$$\beta_1 = v^{-1} \tag{62}$$

and

$$\beta_2 = - a v^{-3} . \tag{63}$$

Inserting (60)—(63) into (59) we get

$$l\left(1, \frac{w}{v}, 0, \frac{b}{v^2} - \frac{a w}{v^3}\right) = v^{-1} l(v, w, a, b), \tag{64}$$

i.e.

$$l(v, w, a, b) = v F\left(\frac{w}{v}, \frac{b}{v^2} - \frac{aw}{v^3}\right) \tag{65}$$

QED.)

Theorem 13. The general Lagrangian of two covector fields and their first derivatives is

$$L = v F\left(\frac{w}{v}, \frac{v w_\tau - w v_\tau}{v^3}\right). \tag{66}$$

(Proof. The densitant is (66). Its Euler equation does not vanish identically.)

10. Two scalar fields in X_1

Theorem 14. The general Lagrangian of two scalar fields $s(\tau)$ and $r(\tau)$ and of their first derivatives is of the form

$$L = s_\tau F\left(s, r, \frac{r_\tau}{s_\tau}\right), \tag{67}$$

where F is an arbitrary invariant function of its invariant (or scalar) arguments. (Proof. The fundamental eq. in this case is

$$l(s, r, \beta_1 s_\tau, \beta_1 r_\tau) = \beta_1 l(s, r, s_\tau, r_\tau) . \tag{68}$$

As in the case of theorem 11 we get for the densitant

$$l(s, r, s_\tau, r_\tau) = s_\tau l\left(s, r, 1, \frac{r_\tau}{s_\tau}\right) = s_\tau F\left(s, r, \frac{r_\tau}{s_\tau}\right). \tag{69}$$

The Euler equations of this densitant do not vanish identically. Thus (68) is a Lagrangian.)

In the next section we shall give some examples and the interpretation of models of the type (67).

Theorem 15. The general Lagrangian of two scalar fields and of their first two derivatives is of the form

$$L = l(s, r, s_\tau, r_\tau, s_{\tau\tau}, r_{\tau\tau}) = s_\tau F\left(s, r, \frac{r_\tau}{s_\tau}, \frac{r_{\tau\tau} s_\tau - r_\tau s_{\tau\tau}}{s_\tau^3}\right). \tag{70}$$

(Proof. As for theorem 12.)

We give without proof the following

Theorem 16. The general Lagrangian of two scalar fields and their first three derivatives is of the form

$$L = s_\tau F\left(s, r, \frac{r_\tau}{s^1}, \frac{r_{\tau\tau} s_\tau - r_\tau s_{\tau\tau}}{s_\tau^3}, \frac{r_{\tau\tau\tau} s_\tau - r_\tau s_{\tau\tau\tau}}{s_\tau^4} - 3\,\frac{s_{\tau\tau}(r_{\tau\tau} s_\tau - r_\tau s_{\tau\tau})}{s_\tau^5}\right), \tag{71}$$

where $s(\tau)$ and $r(\tau)$ are the fields.

11. Examples

Example 1. Let us consider a moving mass-point in the Euclidean plane. The cartesian coordinates of the point, $x(\tau)$ and $y(\tau)$, are geometric objects with respect to the general relativistic paratime transformations

$$\bar{\tau} = f(\tau), \quad \frac{d\bar{\tau}}{d\tau} \neq 0. \tag{9}$$

Both x and y are scalars with respect to (9), because

$$\bar{x}(\bar{\tau}_p) = x(\tau_p) \text{ and } \bar{y}(\bar{\tau}_p) = y(\tau_p). \tag{72}$$

Lagrangians of the type $l(x, y, x_\tau, y_\tau)$ are

$$L = x_\tau F\left(x, y, \frac{y_\tau}{x_\tau}\right), \tag{67}$$

where F is an arbitrary invariant function.

So much for the theory.

With regard to physical experience we take the Lagrangian (67) to be

$$L = m\, x_\tau \cdot (1 + y_\tau^2/x_\tau^2)^{\frac{1}{2}}, \tag{73}$$

i.e.

$$L = m \cdot (x_\tau^2 + y_\tau^2)^{\frac{1}{2}}, \tag{74}$$

where m is a scalar constant (the mass) of the moving point. The Euler equations are

$$\frac{d}{d\tau}\left\{\frac{dx/d\tau}{(x_\tau^2 + y_\tau^2)^{\frac{1}{2}}}\right\} = 0 \tag{75}$$

and

$$\frac{d}{d\tau}\left\{\frac{dy/d\tau}{(x_\tau^2 + y_\tau^2)^{\frac{1}{2}}}\right\} = 0\,. \tag{76}$$

From (75) and (75) one can construct several invariant expressions. One of them is

$$\frac{dy}{dx} = \text{const}\,. \tag{77}$$

This equation shows the character of the solutions of general relativistic equations and that of the general relativity theory itself.

(i) Since τ is a label only, the Euler equations (76) and (75) need not be solved because the solutions $x(\tau)$ and $y(\tau)$ contain very little information. The physical information is concentrated (contained) in the *relations* between the fields $x(\tau)$ and $y(\tau)$. If, in the case of two field variables and one paravariable, one finds one invariant relation between the fields which is based on the Euler equations, then one has found the true solution of the problem. Equation (77) is of this kind. It is a true result.

(ii) In this example the two fields $x(\tau)$ and $y(\tau)$ are the described physical phenomena. As seen from (77) the result of the general relativistic equations of motion should be a *comparison* between the physical phenomena.

The general relativity theory is not designed to compare, or to express the physical phenomena (here x and y) with the almost empty paraquantities (here τ) because they are labels only. The paraquantities have a secondary, intermediary role only.

Now we are able to explain physically why no Lagrangians of the form

$$L = l\left(x(\tau), \frac{dx}{d\tau}, \frac{d^2x}{d\tau^2}, \ldots, \frac{d^u x}{d\tau^u}\right)$$

exist. A Lagrangian of this type, i.e. a single field cannot be used for comparisons, and, therefore, it cannot explain anything. One single physical phenomenon within the frames of the general relativity theory is equivalent to nothing.

(iii) The equation (77) is a kinematic result. This is also a characteristic of the general relativity theory.

Example 2. Let us consider the same moving mass-point and a rotating body, which is considered as a physical clock, and which is characterized by its azimuth $\varphi(\tau)$. All fields, $x(\tau)$, $y(\tau)$ and $\varphi(\tau)$ are scalars with respect to (9).

Let us take the concrete Lagrangian of type (67) in the form

$$L = \varphi_\tau \cdot \left[k + \left(\frac{x_\tau}{\varphi_\tau} \right)^2 + \left(\frac{y_\tau}{\varphi_\tau} \right)^2 \right]^{\frac{1}{2}}, \tag{78}$$

where k is a scalar. The Eulerian equations are

$$\frac{d}{d\tau} \left\{ \frac{x_\tau}{(k\varphi_\tau^2 + x_\tau^2 + y_\tau^2)^{\frac{1}{2}}} \right\} = 0, \tag{79}$$

$$\frac{d}{d\tau} \left\{ \frac{y_\tau}{(k\varphi_\tau^2 + x_\tau^2 + y_\tau^2)^{\frac{1}{2}}} \right\} = 0, \tag{80}$$

and

$$\frac{d}{d\tau} \left\{ \frac{\Phi_\tau}{(k\varphi_\tau^2 + x_\tau^2 + y_\tau^2)^{\frac{1}{2}}} \right\} = 0. \tag{81}$$

An invariant consequence is

$$\frac{dx}{d\varphi} = c_1 \text{ and } \frac{dy}{d\varphi} = c_2. \tag{82}$$

This means that the *metric* velocity of the moving mass-point is an invariant and a constant of the motion.

From (82) we again see that in the general relativity theory the invariants are those expressions (quantities) which contain the results obtained by the comparison of the physical phenomena and also those obtained by physical measurements.

It seems that in the general relativistic theory of fields at least one of the fields (or perhaps one of the components of a certain field) is always *that physical object* with which all other objects should be compared, to which all the other objects should be related, and by which all the other objects should be measured [8].

REFERENCES

1. H. Van Dam and E. P. Wigner, Phys. Rev., **138**, B1576, 1965.
2. D. G. B. Edelen, J. Math. and Mech., **13**, 201, 1964 and J. Math. and Mech., **14**, 15, 1965.
3. M. Kucharzewski and M. Kuczma, Basic concepts of the theory of geometric objects, Rozprawy matematyczne vol. XLIII, 1964. Warszawa.
4. J. Aczél and S. Golab, Funktionalgleichungen der Theorie der geometrischen Objekte, 1960, Panstwowe Wyd. Naukowe, Warsawa; J. A. Schouten, Ricci-Calculus, 1954, Springer, Berlin—Göttingen—Heidelberg.

5. E. Noether, Nachrichten Ak. Wiss. Göttingen, **1918,** pag. 235.
6. C. N. Yang and R. L. Mills, Phys. Rev., **96,** 191, 1954;
S. L. Glashow and M. Gell-Mann, Ann. of Phys., **15,** 437, 1961;
A. Salam and J. C. Ward, N. Cim., **11,** 568, 1959;
J. Schwinger, Phys. Rev., **125,** 1043, 1962.
7. R. Utiyama, Phys. Rev., **101,** 1597, 1956;
T. W. B. Kibble, J. of Math. Phys., **2,** 212, 1961.
8. A. Komar, Phys. Rev., **113,** 934, 1959;
A. Uhlmann, Z. Univ. Jena, 1959/60;
J. Synge, Relativity (general theory), 1960, North-Holland, Amsterdam;
F. Pirani, Théories relativistes de la gravitation, 1962, CNRS, Paris;
H. Hönl und H. Dehnen, Z. Phys., **191,** 313, 1966.

ОБЩЕЕ РЕЛЯТИВИТСКАЯ ТЕОРИЯ ЛАГРАНЖИАНОВ

Часть I.

Векторные и скалярные поля в пространстве X.,

Г. КНАПЕЦ

Р е з ю м е

Дается метод для вывода обще релятивистских лагранжианов на основе решения одного функционального уравнения, которое является эквивалентным уравнению Ли (S. Lie). Выведены некоторые решения этого уравнения. Если лагранжиан предполагаемого типа не существует, дается математическое доказательство не-существования.

Acta Physica Academiae Scientiarum Hungaricae, Tomus 23 (2), pp. 161—183 (1967)

ВЛИЯНИЕ ФЛУКТУАЦИИ ВНУТРЕННЕГО МАГНИТНОГО ПОЛЯ НА ЭФФЕКТ МЕССБАУЭРА

Л. ПАЛ

ЦЕНТРАЛЬНЫЙ ИНСТИТУТ ФИЗИЧЕСКИХ ИССЛЕДОВАНИЙ
ВЕНГЕРСКОЙ АКАДЕМИИ НАУК, БУДАПЕШТ

(Поступило 5. V. 1966)

Рассматривается влияние флуктуации направления внутреннего поля на форму линий эффекта Мессбауэра. Доказывается, что с ростом «частоты» флуктуации линии сверхтонкого расщепления расширяются, смещаются и наконец сливаются в одну центральную линию, которая — при дальнейшем росте «частоты» флуктуации — постепенно сужается. Сливание происходит тогда, когда «частота» флуктуации ω_R больше ларморовской частоты ω_L для сливающей пары линий. В момент сливания формы центральной линии заметно отличается от лоренцовской. Наличие внешнего магнитного поля приводит к изменению положения и ширины линий, а также процесса разрушения их сверхтонкой структуры.

В настоящей работе излагается простая вероятностная теория флуктуации внутреннего поля и показывается влияние этой флуктуации на форму линий эффекта Мессбауэра.

Как известно, при наличии внутреннего магнитного поля происходит земановское расщепление ядерных уровней. Если это поле флуктуирует между значениями $+H$ и $-H$, то в зависимости от «частоты» флуктуации меняется спектральная характеристика эффекта Мессбауэра. При случае, когда ларморовская частота ω_L больше характерной «частоты» флуктуации ω_R, земановское расщепление сохраняется. Разрушение расщепления происходит, если «частота» флуктуации больше ларморовской.

Наличие квадрупольного расщепления в основном не меняет картины, только при достаточно больших «частотах» флуктуации внутреннего магнитного поля наблюдается асимметрия в квадрупольном расщеплении. Это естественно, так как вырожденный квадрупольный уровень $\pm 3/2$ расщепляется больше, чем уровень $\pm 1/2$. Поскольку ларморовская частота для переходов $\pm 3/2 \rightarrow \pm 1/2$ больше, чем для переходов $\pm 1/2 \rightarrow \pm 1/2$, $\mp 1/2$, то вполне возможно, что при некоторой «частоте» флуктуации расщепление переходов $\pm 1/2 \rightarrow \pm 1/2$, $\mp 1/2$ уже разрушается, но в то же время этого не происходит в случае переходов $\pm 3/2 \rightarrow \pm 1/2$.

Как видно, влияние флуктуации внутреннего магнитного поля приводит к весьма наглядным эффектам, теоретическое описание которых на первый взгляд не представляет никакой трудности. Несмотря на это, имеется лишь несколько теоретических работ, рассматривающих этот вопрос, хотя в теории ядерного магнитного резонанса аналогичные задачи уже давно известны и решены [1].

После обнаружения сверхтонкой структуры линий Мессбауэра в случае некоторых парамагнитных окислов редкоземельных элементов [2] Афанасьев и Каган [3] развили квантовую теорию, учитывающую спин-решеточную релаксацию магнитного момента электронной оболочки и объяснили главные черты экспериментальных фактов. Ван дер Воуд и Дэккер [4] показали, что сосуществование центральной и сверхтонких линий в грубых чертах может быть объяснено на основе стохастической модели магнитной релаксации Андерсона [1]. Вегенер [5], исходя из простого квантово-механического расчета, вывел приближенные формулы для расширения и сдвига линий эффекта Мессбауэра при наличии флуктуирующего внутреннего поля, но им не был исследован процесс разрушения сверхтонкой структуры. Блуме [6] указал на то, что асимметрия квадрупольного расщепления может быть рассчитана, используя метод Андерсона для магнитной релаксации. Бредфорд и Маршал [7] исследовали влияние релаксации спинового момента электронов на спектр Мессбауэра в случае быстрой релаксации и показали, что расширение линий поглощения обратно пропорционально времени релаксации.

Растущий интерес к явлениям, связанным с флуктуациями внутреннего магнитного поля, объясняется тем, что характерная «частота» флуктуации и, особенно, ее температурная чувствительность дают ценную информацию о движении магнитного момента вблизи точки фазового превращения.

В разделе II данной работы излагается общая теория флуктуации внутреннего поля на основе вероятностной модели и показывается ее влияние на спектральную плотность излучения мессбауэрского ядра. В разделе III рассмотрен самый простой случай, а, именно, релаксация атомного спина $S = 1/2$; в разделе IV показана роль внешнего магнитного поля. Наконец, в разделе V приводятся результаты и анализируется характер сдвига и расширения линий. Дополнительно, в Приложении I изложены отдельные детали вероятностной теории движения квазисвободного магнитного момента, а в Приложении II представлены некоторые соображения по флуктуации внутреннего поля в случае $S > 1/2$.

II. Постановка задачи

Ради простоты и конкретности рассмотрим мессбауэрское излучение ядра Fe^{57}, схема уровней которого хорошо известна и только для наглядности изображена на рис. 1. При переходе из возбужденного состояния $|m'I'>$ в основное $|mI>$ излучается один гамма-квант, векторный потенциал которого может быть написан в следующем виде:

$$A(t, m'I' \to mI, \Theta) = A_0(m'I' \to mI, \Theta) f_0(t) \exp\left[i\delta(m', m)\int_0^t H(t')\,dt'\right], \quad (1)$$

где

$$f_0(t) = \exp\left\{i[\omega_0 + \delta(m', m)H_0]t - \tfrac{1}{2}\Gamma(m')t\right\}. \quad (1')$$

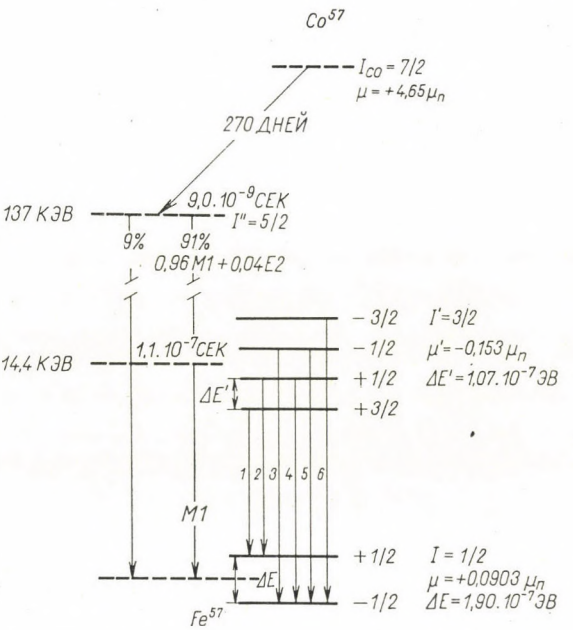

Рис. 1. Схема уровней ядра Fe^{57}

$|A_0(m'I \to mI\Theta)|^2$ определяет интенсивность излучения в направлении, образующем угол Θ с направлением внешнего магнитного поля; $\Gamma(m')$ — ширина уровня m' и $\omega_0 = \dfrac{E' - E}{\hbar}$, а фактор $\delta(m', m)$ имеет вид:

$$\delta(m, m') = -\frac{\mu_n}{\hbar}(m'g' + mg), \quad (2)$$

где g' и g гиромагнитные коэффициенты возбужденного и основного состояний. Через $H(t)$ обозначено флуктуирующее магнитное поле, а через H_0 постоянное внешнее магнитное поле, действующее на ядро. Спектральная плотность излучения может быть определена из корреляционной функции

$$< A(t) A^*(0) > = \sum_{m,m'} w_{m'} < A(t, m'I' \to mI, \Theta) A^*(0, m'I' \to mI, \Theta) >, \quad (3)$$

где $w_{m'}$, статистический вес состояния m'. Спектральная плотность имеет вид:

$$I(\omega) = \frac{1}{\pi} Re\, S(\omega), \tag{4}$$

где

$$S(\omega) = \int_0^\infty e^{-i\omega t} < A(t)\, A^*(0) > dt. \tag{5}$$

Собственно говоря, задача полностью может быть сведена к вычислению выражения

$$f(t) = < \exp\, [i\delta \int_0^t H(t')\, dt'] >, \tag{6}$$

так как

$$< A(t, m'\, I' \to m\, I, \Theta)\, A^*(0, m'\, I' \to m\, I, \Theta) > =$$
$$= |A_0(m'\, I' \to m\, I, \Theta)|^2 f_0(t) f(t). \tag{7}$$

В дальнейшем опускаем индексы m' и m, характеризующие переход, и постараемся найти метод для вычисления среднего значения (6).

Предположим, что флуктуация магнитного поля, действующего на ядро, связана с флуктуациями магнитного момента электронной оболочки. Рассмотрим случай, когда магнитный момент атома обусловлен чистым спиновым магнетизмом. Если некомпенсированный спин электронной оболочки принимает значение S, то во многих случаях законно предположить, что

$$H(t) = H_{\max} \frac{S_z(t)}{S}, \tag{8}$$

где $S_z(t)$ проекция спина на направление внешнего поля в момент времени t, а $H_{\max}$ — максимальное внутреннее поле, действующее на ядро. Имеются всего $2S + 1$ разных проекций, каждая из которых характеризует состояние магнитного момента электронной оболочки. В состоянии k проекция S_z имеет значение $S + 1 - k$. Обозначим через $u(k', k)\Delta t + 0(\Delta t)$ вероятность того, что S_z в течение времени Δt переходит из состояния k' в состояние k. Предполагая, что могут быть разрешены переходы только в соседние состояния, $u(k', k)$ отлична от нуля, если $|k' - k| = 1$. Состояние магнитного момента характеризуется случайной величиной $\nu(t)$, которая может принимать целочисленные значения $1, 2, \ldots, 2S + 1$. Легко показать, что матрица $\overline{\overline{u}}$ определяет динамическое поведение магнитного момента и, рассматривая движение S_z как марковский процесс, можем получить всю необходимую информацию о флуктуациях S_z. В «Приложении I» изложена основная идея вероятностной теории движения S_z.

Для того, чтобы вычислить функцию

$$f(t) = \exp\, [i\delta \int_0^t H(t')\, dt'] >,$$

потребуется функция распределения случайной величины

$$\zeta(t) = \frac{\delta H_{\max}}{S} \int_0^t S_z(t')\, dt' , \tag{9}$$

которая по своему характеру является фазой, испытывающей случайные изломы.

Пусть

$$P\{x \leq \zeta(t) \leq x + dx \mid \nu(0) = k\} = p_k(t, x)\, dx \tag{10}$$

вероятность того, что случайная величина $\zeta(t)$ в момент времени $t > 0$ принимает значение, лежащее в интервале $(x, x + dx)$, при условии, что в момент $t = 0$ проекция спина находилась в состоянии k. Уравнение для $p_k(t, x)$ легко выводится, если учесть, что между двумя соседними переходами фаза линейно растет со временем. Например, в состоянии k до следующего перехода фаза имеет вид:

$$x = \delta H_{\max} \frac{S + 1 - k}{S} t = \omega_L \frac{S + 1 - k}{S} t = x_k(t) . \tag{11}$$

Так как вероятность того, что в интервале времени $(0, t)$ состояние k сохраняется, выражается через $e^{-u_k t}$, где

$$u_k = u(k \to k - 1) + u(k \to k + 1) ,$$

то

$$\begin{aligned} p_k(t, x) &= e^{-u_k t}\, \delta(x - x_k t) + \\ &+ \int_0^t e^{-u_k t'} [u(k \to k - 1)\, p_{k-1}(t - t', x - x_k t') + \\ &+ u(k \to k + 1)\, p_{k+1}(t - t', x - x_k t')]\, dt' \\ &(k = 1, 2, \ldots, 2S + 1) . \end{aligned} \tag{12}$$

Следует заметить, что

$$u_1 = u(1 \to 2) , \qquad u_{2S+1} = u(2S + 1 \to 2S) , \tag{13}$$

так как

$$u(1 \to 0) = u(2S + 1 \to 2S + 2) = 0 . \tag{14}$$

Зная плотность распределения $p_k(t, x)$, интересующую нас функцию $f(t)$ можем вычислить.

$$f(t) = \sum_{k=1}^{2S+1} Q_k f_k(t) = \sum_{k=1}^{2S+1} Q_k \int_{-\infty}^{+\infty} e^{ix} p_k(t, x)\, dx , \tag{15}$$

где Q_k вероятность того, что в произвольно выбранный момент времени проекция спина находится в состоянии k. Определение Q_k приводится в «Приложении I».

После этого остается только проведение элементарных операций, а именно вычисление интеграла

$$G_{m'm}(\omega) = \frac{1}{\pi} Re \int_0^\infty e^{-i\omega t} f_0^{(m',m)}(t) f^{(m',m)}(t)\, dt \tag{16}$$

и составление ряда

$$I(\omega) = \sum w_{m'} |A_0(m'\, I' \to m\, I, \Theta)|^2 G_{m'm}(\omega). \tag{17}$$

Таким образом, в рамках модели, выбранной нами, задача полностью сформулирована. Следует заметить, что рассмотрение флуктуации внутреннего поля на основе уравнения (12) является приближением аналогичным кинетическому уравнению, которое может быть получено — при определенных условиях — из точного уравнения для статистического оператора.

III. Флуктуация внутреннего поля в случае $S = 1/2$

В качестве иллюстрации основных эффектов рассмотрим случай, соответствующий флуктуациям магнитного момента электронной оболочки со спином $S = \frac{1}{2}$. Некоторые проблемы общего случая со спином $S > \frac{1}{2}$ обсуждаются в «Приложении II». Исходя из уравнения (12) и учитывая усреднение (15) для функций $f_k(t)$ $(k = 1,2)$, можем написать следующие уравнения:

$$\begin{aligned} f_1(t) &= \exp\,[-(u_1 - i\,\omega_L)\,t] + u_1 \int_0^t \exp\,[-(u_1 - i\,\omega_L)\,t']\, f_2(t - t')\, dt', \\ f_2(t) &= \exp\,[-(u_2 + i\,\omega_L)\,t] + u_2 \int_0^t \exp\,[-(u_2 + i\,\omega_L)\,t']\, f_1(t - t')\, dt'. \end{aligned} \tag{18}$$

Эти уравнения легко решаются и можно сразу же написать, что

$$\bar{\mathbf{f}}(t) = \bar{\bar{\Omega}}\, \bar{\mathbf{g}}(t),$$

где

$$\bar{\mathbf{f}}(t) = \begin{bmatrix} f_1(t) \\ f_2(t) \end{bmatrix} \quad \text{и} \quad \bar{\mathbf{g}}(t) = \begin{bmatrix} e^{z_1 t} \\ e^{z_2 t} \end{bmatrix}. \tag{19}$$

Элементы матрицы $\bar{\bar{\Omega}}$ определяются следующими выражениями:

$$\Omega_{11} = \frac{z_1 + u + i\,\omega_L}{z_1 - z_2}, \quad \Omega_{12} = \frac{z_2 + u + i\,\omega_L}{z_2 - z_1}$$

$$\Omega_{21} = \frac{z_1 + u - i\,\omega_L}{z_1 - z_2}, \quad \Omega_{22} = \frac{z_2 + u - i\,\omega_L}{z_2 - z_1}. \tag{19''}$$

z_1 и z_2 являются корнями характеристического уравнения

$$z^2 + u\,z + \omega_L^2 - i\,\omega_L\,u\,M = 0\,,$$

где

$$u = u_1 + u_2 \quad \text{и} \quad M = \frac{u_2 - u_1}{u}\,. \tag{20'}$$

Величину M можно рассматривать как относительную намагниченность. На самом деле, при наличии внешнего и некоторого эффективного поля, учитывающего взаимодействие между магнитными моментами атомов, для отношения u_2/u_1 можем написать следующее выражение:

$$u_2/u_1 = \exp\,[g\,\mu_B\,(H_0 + H_e)/k\,T] \tag{21}$$

из которого следует, что

$$M = th\,\frac{g\,\mu_B\,(H_0 + H_e)}{2k\,T}\,.$$

Флуктуация магнитного момента электронной оболочки характеризуется временем релаксации

$$\tau_R = (u/2)^{-1} = \omega_R^{-1}\,. \tag{22}$$

Рассмотрим вначале самый простой случай: свободную релаксацию магнитного момента. При этом $u_1 = u_2$ и так $M = 0$. Корни уравнения (20) могут быть написаны в следующей форме:

$$z_{1,2} = \begin{cases} -\omega_L\,\Delta \pm i\,\omega_L\sqrt{|1 - \Delta^2|}\,, & \text{если} \quad \Delta \leq 1 \\ -\omega_L\,\Delta \mp \omega_L\sqrt{|1 - \Delta^2|}\,, & \text{если} \quad \Delta > 1 \end{cases}, \tag{23}$$

где для удобства была введена безразмерная величина

$$\Delta = \frac{u}{2\omega_L} = \frac{\omega_R}{\omega_L}\,. \tag{24}$$

Как и можно было ожидать, к естественной ширине $1/2\ \Gamma$ добавляется релаксационная ширина

$$1/2\,\Gamma_R = \omega_R \tag{25}$$

и вместо одной линии с частотой ω_0 появляются две линии с частотами

$$\omega_{1,2} = \omega_0 \pm \omega_L \sqrt{|1 - \Delta^2|} \tag{26}$$

в том случае, если $\Delta < 1$, т. е. если релаксационная частота ω_R меньше ларморовской ω_L. Расщепление разрушается, если $\omega_R = \omega_L$. При $\Delta > 1$ появляются две ширины релаксации:

$$1/2\,\Gamma_R^{\pm} = \omega_L(\Delta \pm \sqrt{|1 - \Delta^2|}, \tag{27}$$

одна из которых понижается до нулевого значения, с ростом релаксационной частоты ω_R, а другая увеличивается и, таким образом, восстанавливается чисто лоренцовская форма основной линии. Это явление хорошо известно из теории ядерного магнитного резонанса, как сужение резонансных линий, возникающее вследствие флуктуации.

До сих пор нами был рассмотрен только один переход между состояниями $|m'I'>$ и $|mI>$. При наличии не очень флуктуирующего внутреннего магнитного поля в случае ядра Fe^{57} имеются шесть переходов, симметрично расположенных вокруг основного перехода с частотой ω_0. Для простоты вводим следующие обозначения:

$$|3/2\ 3/2> \to |1/2\ 1/2> \to \omega_1;\ |1/2\ 3/2> \to |-1/2\ 1/2> \to \omega_4$$
$$|1/2\ 3/2> \to |1/2\ 1/2> \to \omega_2;\ |-1/2\ 3/2> \to |-1/2\ 1/2> \to \omega_5$$
$$|-1/2\ 3/2> \to |1/2\ 1/2> \to \omega_3;\ |-3/2\ 3/2> \to |-1/2\ 1/2> \to \omega_6$$

и

$$\Delta\omega_j = \omega_j - \omega_0\,.$$

Напомним еще, что

$$\Delta\omega_6 = -\Delta\omega_1\,,\quad \Delta\omega_5 = -\Delta\omega_2\,,\quad \Delta\omega_4 = -\Delta\omega_3$$

и

$$|\Delta\omega_1| = \omega_L(1) > |\Delta\omega_2| = \omega_L(2) > |\Delta\omega_3| = \omega_L(3)\,.$$

Если внутреннее поле флуктуирует, то линия $\Delta\omega_4$ смещается на $\widetilde{\Delta\omega}_4$ и создается ее зеркальная пара на месте линии $-\widetilde{\Delta\omega}_3$, одновременно линия $-\Delta\omega_3$ смещается на $-\widetilde{\Delta\omega}_3$ и создается ее пара на месте $\widetilde{\Delta\omega}_4$. Аналогичная ситуация возникает и для других симметрично расположенных линий $\Delta\omega_5$; $-\Delta\omega_2$ и $\Delta\omega_6$; $-\Delta\omega_1$. Если для характерной «частоты» флуктуации выполняется условие

$$\omega_R(3) = \omega_L(3)\,,$$

то разрушается расщепление внутренней пары линий и появляется центральная линия с частотой ω_0. В этом случае наблюдается сосуществование центральной («парамагнитной») и сверхтонких линий. При «частотах» флуктуации $\omega_R^{(2)} = \omega_L(2)$ и $\omega_R^{(1)} = \omega_L(1)$ сливаются сначала линии $\widetilde{\Delta\omega}_5$ и $-\widetilde{\Delta\omega}_2$, а потом $\widetilde{\Delta\omega}_6$ и $-\widetilde{\Delta\omega}_1$. Это означает, что при «частотах» флуктуации $\omega_R > \omega_L(1)$ имеется всего одна центральная линия с «частотой» ω_0, форма которой согласно формуле (27) определяется двумя характерными ширинами.

Наконец определим спектральную плотность излучения. На основе (15), (16), (19) и (23) можем написать, что

$$G_j(\omega) = \frac{1}{2\pi}\left\{\frac{1/2\,\Gamma(1+\lambda) - g_j(\lambda)\,[\omega-\omega_0-\widetilde{\omega}_L(\lambda,j)]}{[1/2\,\Gamma(1+\lambda)]^2+[\omega-\omega_0-\widetilde{\omega}_L(\lambda,j)]^2} + \right.$$
$$\left. + \frac{1/2\,\Gamma(1+\lambda) + g_j(\lambda)\,[\omega-\omega_0+\widetilde{\omega}_L(\lambda,j)]}{[1/2\,\Gamma(1+\lambda)]^2+[\omega+\omega_0+\widetilde{\omega}_L(\lambda,j)]^2}\right\}, \tag{28}$$

если $$\lambda \leq 2\omega_L(j)/\Gamma = \lambda_j,$$

и

$$G_j(\omega) = \frac{1}{2\pi}\,\frac{[1-g_j(\lambda)]\,[1/2\,\Gamma(1+\lambda)+\widetilde{\omega}_L(\lambda,j)]}{[1/2\,\Gamma(1+\lambda)+\widetilde{\omega}_L(\lambda,j)]^2+(\omega-\omega_0)^2} +$$
$$+ \frac{[1+g_j(\lambda)]\,[1/2\,\Gamma(1+\lambda)-\widetilde{\omega}_L(\lambda,j)]}{[1/2\,\Gamma(1+\lambda)-\widetilde{\omega}_L(\lambda,j)]^2+(\omega-\omega_0)^2}, \tag{29}$$

если $$\lambda > 2\omega_L(j)/\Gamma = \lambda_j.$$

В формулах (28) и (29) введены следующие обозначения:

$$\lambda = u/\Gamma \tag{30}$$

и

$$\widetilde{\omega}_L(\lambda,j) = \omega_L(j)\sqrt{|1-(\lambda/\lambda_j)^2|}; \quad g_j(\lambda) = \frac{\lambda/\lambda_j}{\sqrt{|1-(\lambda/\lambda_j)^2|}}. \tag{31}$$

Легко убедиться в том, что

$$\lim_{\lambda\to\infty} G_j(\omega) = \frac{1}{\pi}\,\frac{\Gamma/2}{(\Gamma/2)^2+(\omega-\omega_0)^2}$$

и

$$\lim_{\lambda\to\lambda_j} G_j(\omega) = \frac{1}{\pi}\,\frac{\Gamma/2}{[\Gamma/2+\omega_L(j)]^2+(\omega-\omega_0)^2} +$$

$$+\frac{1}{\pi}\frac{2\omega_L(j)\,[\Gamma/2+\omega_L(j)]^2}{\{[\Gamma/2+\omega_L(j)]^2+(\omega-\omega_0)^2\}^2}\,.$$

Для практических целей целесообразно использовать нормированную спектральную плотность и ввести следующие обозначения:

$$\omega-\omega_0=v\frac{\omega_0}{c}\,,\qquad \omega_L(j)=v_j\frac{\omega_0}{c}\,,\qquad \Gamma=\gamma\frac{\omega_0}{c}$$

$$\tilde{v}_j(\lambda)=v_j\sqrt{|1-(\lambda/\lambda_j)^2|}\,. \tag{32}$$

В этом случае вместо $\mathrm{I}(\omega)$ можем написать, что

$$G(v)=\sum_j W_j G_j(v)\,, \tag{33}$$

где

$$G_j(v)=\frac{1}{2\pi}\left\{\frac{1/2\,\gamma(1+\lambda)-g_j(v-\tilde{v}_j)}{[1/2\,\gamma(1+\gamma)]^2+(v-\tilde{v}_j)^2}+\frac{1/2\,\gamma(1+\lambda)+g_j(v+\tilde{v}_j)}{[1/2\,\gamma(1+\lambda)]^2+(v+\tilde{v}_j)^2}\right\}, \tag{34}$$

если

$$\lambda\leq 2v_j/\lambda=\lambda_j$$

и

$$G_j(v)=\frac{1}{2\pi}\left\{\frac{(1-g_j)\,[1/2\,\gamma(1+\lambda)+\tilde{v}_j]}{[1/2\,\gamma(1+\lambda)+\tilde{v}_j]^2+v^2}+\frac{(1-g_j)\,[1/2\,\gamma(1+\lambda)-\tilde{v}_j]}{[1/2\,\gamma(1+\lambda)-\tilde{v}_j]^2+v^2]}\right\}. \tag{35}$$

если

$$\lambda>2v_j/\gamma=\lambda_j\,.$$

Прежде чем обсудить полученные результаты, рассмотрим влияние внешнего магнитного поля на флуктуации.

IV. Влияние внешнего магнитного поля на флуктуации внутреннего поля в случае $S=1/2$

Внешнее магнитное поле приводит к возникновению некоторого магнитного упорядочения и поэтому $M\neq 0$. В этом случае корни уравнения (20) имеют следующий вид:

$$z^{\pm}=-1/2\,\tilde{\Gamma}_R^{\mp}\pm i\,\tilde{\omega}_L\,, \tag{36}$$

где

$$1/2\tilde{\Gamma}_R^{\pm}=\omega_L(\Delta\pm\tilde{\Delta})\,,\quad \tilde{\omega}_L=\omega_L R(\Delta,M)\,,\quad \Delta=M\,\Delta/R(\Delta,M) \tag{37}$$

и

$$R(\Delta, M) = \frac{1}{\sqrt{2}} \left\{ \sqrt{(\Delta^2 - 1)^2 + 4\Delta^2 M^2} - (\Delta^2 - 1) \right\}^{\frac{1}{2}}. \tag{38}$$

Видно, что при удвоении линий появляются две ширины релаксации; одна для «правой», другая для «левой» линии, но асимметрии не наблюдается, так как зеркальная пара рассматриваемой линии удваивается аналогично. Если «частота» флуктуации внутреннего поля совпадает с ларморовской частотой, т. е. $\Delta = 1$, тогда

$$1/2\tilde{\Gamma}_R^{\pm} = \omega_L (1 \pm \sqrt{M}) \text{и } \tilde{\omega}_L = \omega_L \sqrt{M}.$$

Для полноты напишем еще j-тый компонент спектральной плотности при тех же условиях как и в случае $M = 0$, только учитываем, что $Q_1 = 1/2\,(1+M)$ и $Q_2 = 1/2\,(1 - M)$. После элементарного расчета получаем, что

$$G_j(v) = \frac{1}{2\pi} \left\{ \frac{1/2\,\gamma_j^-\,(1 + K_j) - L_j\,(v - \tilde{v}_j^+)}{[1/2\,\gamma_j^-]^2 + (v - \tilde{v}_j^+)^2} + \right.$$
$$\left. + \frac{1/2\,\gamma_j^+\,(1 - K_j) + L_j\,(v + \tilde{v}_j^-)}{[1/2\,\gamma_j^+]^2 + (v + \tilde{v}_j^-)^2} \right\}, \tag{39}$$

где

$$\gamma_j^{\pm} = \gamma\,[1 + \lambda(1 \pm \tilde{M}_j)] \tag{40}$$

и

$$K_j = \tilde{M}_j \frac{(1/2\,\gamma\,\lambda)^2 + \tilde{v}_j^2}{(1/2\,\gamma\,\lambda\,\tilde{M}_j)^2 + v_j^2}, \quad L_j = \frac{1/2\,\gamma\,\lambda\,\tilde{v}_j\,(1 - \tilde{M}_j^2)}{(1/2\,\gamma\,\lambda\,\tilde{M}_j)^2 + v_j^2}. \tag{41}$$

В этих формулах были использованы следующие обозначения:

$$\tilde{v}_j^{\pm} = \tilde{v}_j^{\pm}\, v_{j0} \tag{42}$$

$$\tilde{v}_j = v_j\, R\left(\frac{\lambda}{\lambda_j}, M\right), \quad v_{j0} = \delta_j H_0 \frac{c}{\omega_0}, \quad \tilde{M}_j = M/R\left(\frac{\lambda}{\lambda_j}, M\right).$$

Так как

$$\lim_{M \to 0} R\left(\frac{\lambda}{\lambda_j}, M\right) = \begin{cases} \sqrt{1 - (\lambda/\lambda_j)^2}, & \text{если} \quad \lambda \leq \lambda_j \\ 0, & \text{если} \quad \lambda > \lambda_j \end{cases}$$

и далее

$$\lim_{M\to 0} \widetilde{M}_j = \begin{cases} 0 & , \quad \text{если} \quad \lambda \leq \lambda_j \, , \\ \sqrt{1-(\lambda_j/\lambda)^2} & , \quad \text{если} \quad \lambda < \lambda_j \end{cases}$$

то нетрудно показать, что в случае $M = 0$, выражение (39) сводится к формулам (34) и (35).

V. Обсуждение и выводы

Несмотря на то, что все наши предыдущие рассуждения носят полуклассический характер, полученные результаты могут быть применены в большинстве случаев, так как случайное возмущение переходов $|\, m' I' > \to |\, mI >$ осуществляется стационарными флуктуациями «окружения» рассматриваемого ядра. Можно показать, что при не очень жестких условиях эти флуктуации могут быть приписаны марковскому процессу. Полезно отметить, что полуклассический метод, используемый нами, имеет одно явное преимущество по сравнению с точными методами: он приводит к полному решению задачи в рамках выбранной модели, что нельзя сказать о точных методах.

Сначала мы рассмотрим некоторые выводы в случае отсутствия внешнего магнитного поля.

Если направление внутреннего поля распределяется изотропно относительно волнового вектора гамма-кванта, то

$$w_1 = w_6 = \frac{1}{4}, \qquad w_2 = w_5 = \frac{1}{6}, \qquad w_3 = w_4 = \frac{1}{12}.$$

Для этого случая на рис. 2 приведены характерные кривые нормированной спектральной плотности $G(v)$ при разных значениях параметра λ. В численных расчетах были использованы следующие значения для постоянных:

$$1/2\,\gamma = 4{,}74 \cdot 10^{-2} \text{ сек}^{-1}; \quad \lambda_1 = \lambda_6 = 224{,}0\,, \quad \lambda_2 = \lambda_5 = 127{,}2 \quad \lambda_3 = \lambda_4 = 36{,}4\,.$$

Как видно, уже при «частотах» флуктуации, близких к ларморовской частоте $\omega_L(3)$ (т. е. при значениях λ, близких к значению λ_3), все линии сильно расширяются. После сливания двух внутренних линий остальные линии так размываются, что их ступенчатое сливание едва ли можно наблюдать экспериментально.

Следует заметить, что на основе измерений Нэгла, Фрауенфельдера и других [8] можно считать, что в чистых ферромагнитных металлах (например в Fe, Ni и Co) при температуре Кюри происходит внезапное исчезнове-

ние сверхтонкой структуры. Однако, в некоторых неметаллических магнитных соединениях [9], [10] вблизи температуры магнитного превращения было обнаружено четкое сосуществование центральной (парамагнитной) и сверхтонких линий, что свидетельствует о возможности постепенного разрушения сверхтонкой структуры. В качестве иллюстрации на рис. 3 представлены кривые спектров излучения Мессбауэра из работы [9] для

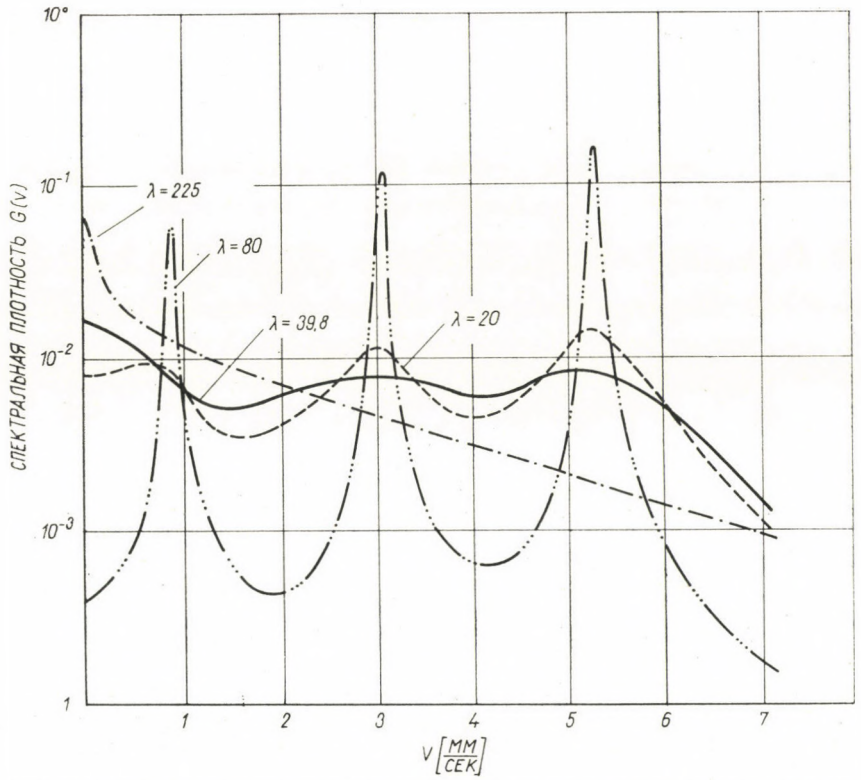

Рис. 2. Спектральная плотность излучения при разных значениях параметра λ, характеризующего «частоты» релаксации магнитного момента

соединения $LiFeO_2$, имеющего упорядоченную тетрагональную структуру. Вблизи точки Нееля ($T_N \sim 300$ °К) помимо четырех боковых линий появляется центральная линия. Кривая, изображенная на рис. 3, по своей формуле совпадает с теоретической кривой (рис. 2. $\lambda \sim 40$), рассчитанной по форме (33). Отсутствие экспериментальных данных о постепенном разрушении сверхтонкой структуры в случае чистых магнитных металлов, вероятно, связано с весьма узким температурным интервалом, в котором «частота» флуктуации магнитного момента может принимать значения, близкие ларморовской частоте. Для успешного изучения сверхтонкого расщепления в

чистых металлах вблизи точки Кюри одним из важнейших условий является значительное увеличение точности измерения, стабильности и гомогенности температуры исследуемого материала.

Хоуард и другие [11] недавно показали, что примесные ядра Fe^{57} в никеле вблизи точки Кюри ($T = T_c - 0{,}7$ °K) находятся в релаксирующем поле, при котором обнаруживается постепенный характер исчезновения

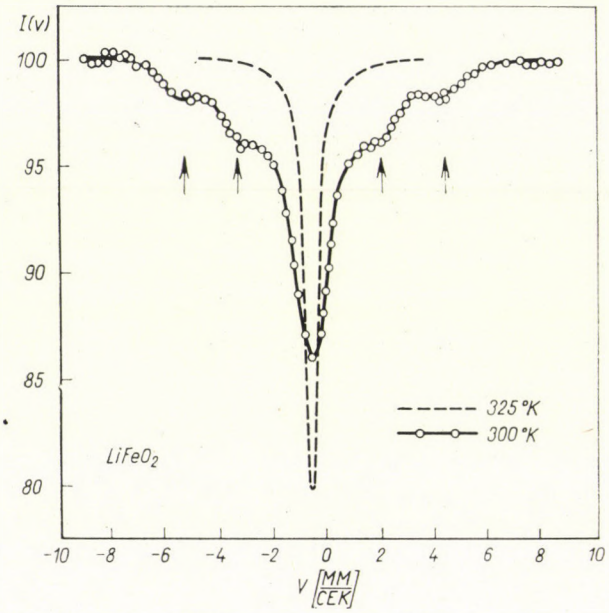

Рис. 3. Спектр Мессбауэра ядер Fe^{57} в соединении $LiFeO_2$ с упорядоченной тетрагональной структурой при температурах вблизи точки Нееля

сверхтонкой структуры. Однако, следует заметить, что наличие примесных атомов в никеле может оказать сильное влияние на тонкие особенности магнитного превращения, поэтому данные Хоаурда надо рассматривать с некоторой осторожностью.

В сплаве Fe_3Al при температуре выше температуры упорядочения, но немного ниже точки Кюри также было обнаружено сосуществование центральной и сверхтонких линий (рис. 4). Однако, в этом случае надо учесть, что вокруг атомов Fe число атомов Al флуктуирует, что, по всей вероятности, приводит к пространственной дисперсии «частоты» релаксации. Эта дисперсия, несомненно, способствует появлению частот, вызывающих сосуществование центральной и боковых линий в спектре Мессбауэра. Вообще, постепенное исчезновение сверхтонкой структуры (через состояние, показывающее сосуществование центральной и боковых линий) часто связано с наличием разных неоднородностей (микрофлуктуация в составе, дефекты) в кристалле [13].

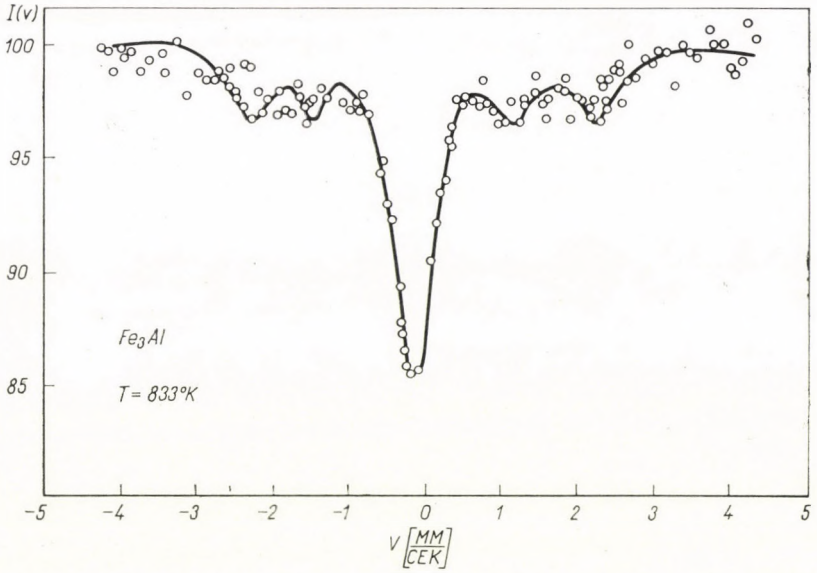

Рис. 4. Спектр Мессбауэра ядер Fe^{57} в сплаве Fe_3Al при температуре $T = 833$ °К

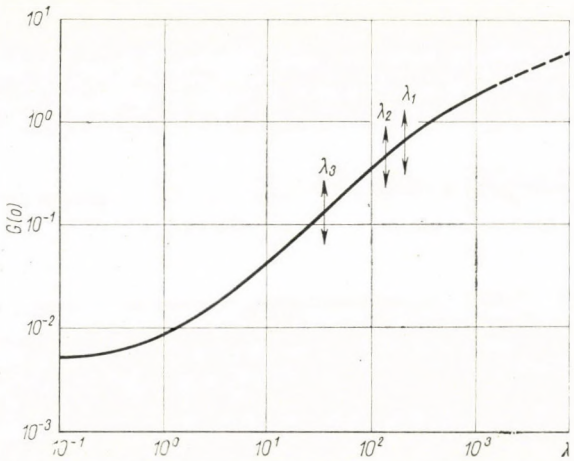

Рис. 5. Зависимость спектральной плотности $G(v)$ при $v = 0$ от параметра релаксации λ

На рис. 5 изображена интенсивность излучения при $v = 0$ в зависимости от параметра λ, характеризующего частоту релаксации. Видно, что увеличение интенсивности $G(0)$ начинается уже при значениях $\lambda \ll \lambda_3$. Это свидетельствует о чувствительности $G(0)$ к частоте релаксации.

Рассмотрим еще механизм сужения линии при больших частотах релаксации магнитного момента. Как уже упоминалось раньше в связи с формулой (27) ширина $1/2\,\gamma^+ = 1/2\,\gamma\,(1 + \lambda) + \tilde{\nu}_j$ растет линейно с ростом λ, если $\lambda \gg \lambda_j$, а ширина

$$1/2\,\gamma_j^- = 1/2\,\gamma\,(1+\lambda) - \tilde{v}_j = 1/2\,\gamma + v_j\left[\lambda/\lambda_j - \sqrt{(\lambda/\lambda_j)^2 - 1}\,\right]$$

в то же время стремится к естественной ширине $1/2\gamma$ по закону

$$1/2\,\gamma_j^- \sim 1/2\,\gamma + v_j^2/\gamma\,\lambda\,.$$
$$(\lambda \gg \lambda_j)$$

Этот результат по своему физическому содержанию совпадает с результатом Бредфорда и Маршала [7]. Однако, следует заметить, что — несмотря на простоту нашей модели — наши формулы (34) и (35) являются более общими, чем формулы Бредфорда и Маршала, и могут быть применены при любых значениях частоты релаксации, чего нельзя сказать о формулах Бредфорда и Маршала, применимость которых ограничена только для больших частот релаксации.

Из выражения (35) при $\lambda \gg \lambda_j$; находим, что

$$G_j(v) \sim -\frac{1}{\pi}\,\frac{1/2\,\gamma + v_j^2/\gamma\,\lambda}{(1/2\,\gamma + v_j^2/\gamma\,\lambda)^2 + v^2}\,. \tag{43}$$

Примесные атомы железа в немагнитных кристаллах могут рассматриваться как квази-свободно релаксирующие магнитные моменты и можно ожидать, что при достаточно низких температурах эта релаксация влияет на ширину линий излучения. Изучая изменение ширины линии в зависимости от температуры, можем получить ценную информацию о механизме релаксации изолированного магнитного момента.

Наконец рассмотрим влияние внешнего магнитного поля на мессбауэрское излучение при условиях флуктуации внутреннего поля. Предположим, что относительная намагниченность $M \ll 1$ и, прежде всего, определим сдвиг линий, возникающий вследствие магнитного порядка. Легко находим, что

$$\tilde{v}_j = v_j \begin{cases} \sqrt{1-(\lambda/\lambda_j)^2}\;\left\{1 + \left[\frac{\lambda/\lambda_j}{1-(\lambda/\lambda_j)^2}\right]^2 M^2 + \ldots,\right\}, & \text{если} \quad \lambda \ll \lambda_j \\ \frac{\lambda/\lambda_j}{(\lambda/\lambda_j)^2 - 1}\,M + \ldots, & \text{если} \quad \lambda \gg \lambda_j \end{cases}. \tag{44}$$

Видно, что положение линий всегда зависит от магнитного порядка вопреки утверждению Дэккера [4], который утверждает, что в случае $\lambda \ll \lambda_j$ такая зависимость не существует. Естественно, при малых значениях M экспериментальное обнаружение квадратичного члена является трудной задачей. Ширины линий также изменяются:

$$\frac{\gamma_j^{\pm}-\gamma}{\lambda\gamma}\sim\begin{cases}1\pm\dfrac{1}{\sqrt{1-(\lambda/\lambda_j)^2}}(M+\ldots), & \text{если } \lambda\ll\lambda_j\\ 1\pm\sqrt{1-(\lambda_j/\lambda)^2}\left\{1+\left[\dfrac{\lambda/\lambda_j}{(\lambda/\lambda_j)^2-1}\right]^2M^2+\ldots\right\}, & \text{если } \lambda\gg\lambda_j\end{cases}. \quad (45)$$

Формулы (44) и (45) не применимы, если $\lambda=\lambda_j$. В этом случае — как на это уже указывалось —

$$\tilde{v}_j=v_j\sqrt{M} \qquad \text{и} \qquad \gamma_j^{\pm}=\gamma+2v_j(1\pm\sqrt{M}). \quad (46)$$

Наконец, напишем также соответствующие выражения для вероятностей w_j. Вследствие выделенного направления, возникающего при наличии внешнего магнитного поля (с которым совпадает направление $\overline{M}$), нарушается изотропное распределение внутреннего поля и поэтому

$$w_1=w_6=\frac{1}{4}\left(1-\frac{1}{3}M\right)+\frac{1}{6}M\cos^2\Theta;$$

$$w_2=w_5=\frac{1}{6}(1-M)+\frac{1}{3}M\sin^2\Theta,$$

$$w_3=w_4=\frac{1}{12}\left(1-\frac{1}{3}M\right)+\frac{1}{18}M\cos^2\Theta. \quad (47)$$

При малых значениях M слабо выражается зависимость интенсивности отдельных линий от угла Θ между направлением внешнего магнитного поля и волновым вектором гамма-излучения.

Приложение I

Вероятностная теория флуктуации квазисвободного магнитного момента

Рассмотрим релаксацию почти изолированного магнитного момента как марковский процесс с конечным числом состояний. Предположим, что имеется некоторое выделенное направление (например, направление внешнего магнитного поля), относительно которого магнитный момент может принимать $2S+1$ разных положений. Положение магнитного момента описывается случайной величиной $\nu(t)$, которая в любой момент времени принимает одно из следующих целочисленных значений: $1,2,\ldots,2S+1$. Если $\nu(t)=k$, то можно сказать, что рассматриваемая система находится в состоянии k. Вероятность перехода за единицу времени из состояния k' в состояние k обозначим через $u(k'\to k)$.

Пусть

$$p\{\nu(t) = k \mid \nu(0) = i\} = Q(t, k \mid i) \tag{1}$$

вероятность того, что система находится в состоянии k в момент времени $t > 0$ при условии, что в момент времени $t = 0$ она находилась в состоянии i. Без особых объяснений ясно, что $Q(t, k \mid i)$ удовлетворяет уравнениям:

$$\frac{dQ(t, k \mid i)}{dt} = -u_i Q(t, k \mid i) + u(i \to i-1) Q(t, k \mid i-1) + u(i \to i+1) Q(t, k \mid i+1) \tag{2}$$

и

$$\frac{dQ(t, k \mid i)}{dt} = -u_k Q(t, k \mid i) + u(k-1 \to k) Q(t, k-1 \mid i) + u(k+1 \to k) Q(t, k+1 \mid i), \tag{3}$$

где

$$u_k = u(k \to k-1) + u(k \to k+1). \tag{4}$$

Уравнение (2) может быть написано в интегральной форме, т. е.

$$Q(t, k \mid i) = e^{-u_i t} \delta_{ik} + \int_0^t e^{-u_i t'} \{u(i \to i-1) Q(t-t', k \mid i-1) + u(i \to i+1) Q(t-t', k \mid i+1)\} dt'. \tag{2'}$$

В случае кратковременной релаксации удобнее пользоваться уравнениями (2) и (2'), а для определения асимптотического поведения $Q(t, k \mid i)$ при больших t целесообразнее использовать уравнение (3). Легко доказать, что

$$\lim_{t \to \infty} Q(t, k \mid i) = Q_k \tag{5}$$

и так

$$-u_k Q_k + u(k-1 \to k) Q_{k-1} + u(k+1 \to k) Q_{k+1} = 0 \tag{6}$$

Решение этого рекуррентного уравнения имеет следующий вид:

$$Q_k = Z_k / \sum_{l=1}^{2S+1} Z_l, \tag{7}$$

где

$$Z_k = \frac{u(1 \to 2) u(2 \to 3) \ldots u(k-1 \to k)}{u(2 \to 1) u(3 \to 2) \ldots u(k \to k-1)} \tag{8}$$

и

$$Z_1 = 1.$$

Отношение

$$Q_k/Q_{k-1} = u\,(k-1 \to k)/u\,(k \to k-1)$$

можно выразить через числа заполнения N_k и N_{k-1}, так как

$$Q_k/Q_{k-1} = N_k/N_{k-1} = e^{-\beta(E_k - E_{k-1})}\,,$$

где

$$\beta = (k\,T)^{-1}\,. \tag{9}$$

Интересно отметить, что в случае приближения молекулярного поля

$$E_k = E_0 - g\,\mu_B\,(S+1-k)\,(H_0 + H_e) \tag{10}$$

и таким образом

$$u\,(k-1 \to k)/u\,(k \to k-1) = e^{-\beta g \mu_B \widetilde{H}} = r\,,$$

где

$$\widetilde{H} = H_0 + H_e\,. \tag{11}$$

Независимость отношения $u(k-1 \to k)/u(k \to k-1)$ от индекса k приводит к тому, что для Q_k можно написать простую формулу:

$$Q_k = \frac{r^{k-1}}{1 + r + \ldots + r^{2S}}, \tag{12}$$

с помощью которой — используя метод производящей функции — легко показать, что относительная намагниченность

$$M = \sum_{k=1}^{2S+1} \frac{S+1-k}{S}\,Q_k = \langle \mu \rangle$$

имеет тот же самый вид, как и в элементарной теории молекулярного поля, т. е.

$$M = \frac{2S+1}{2S}\,cth\,\frac{2S+1}{2S}\,\chi - \frac{1}{2S}\,cth\,\frac{1}{2S}\,\chi\,,$$

где

$$\chi = \beta\,g\,\mu_B\,S\,\widetilde{H}\,.$$

Наконец, покажем метод нахождения стационарной корреляционной функции, характеризующей магнитную релаксацию. По определению, корреляционная функция

$$K\,(t) = \langle \mu\,(t)\,\mu\,(0) \rangle - \langle \mu \rangle^2\,, \tag{13}$$

к вычислению которой потребуется функция распределения

$$P\{\nu(t) = k, \quad \nu(0) = i\} = Q(t, k, i).$$

Если система находится в стационарном состоянии, то

$$Q(t, k, i) = Q_i\, Q(t, k \mid i) \tag{14}$$

и

$$\langle \mu(t)\, \mu(0) \rangle = \sum_{i=1}^{2S+1} \sum_{k=1}^{2S+1} \frac{S+1-i}{S} \frac{S+1-k}{S} Q_i\, Q(t, k \mid i). \tag{15}$$

В качестве иллюстрации напишем $K(t)$ в случае $S = 1/2$. На основе (15) после элементарного расчета получаем, что

где
$$K(t) = (1 - M^2)\, e^{-ut},$$
$$u = u(1 \to 2) + u(2 \to 1). \tag{16}$$

Не представляет трудности получить $K(t)$ и для $S > 1/2$.

Приложение II

Флуктуация внутреннего поля в случае $S > 1/2$

Аналогично уравнениям (18) в случае $S > 1/2$ получаем следующую систему уравнений:

$$f_k(t) = \exp\,[-(u_k - ix_k)\, t] +$$
$$+ \int_0^t \exp\,[-(u_k - ix_k)\, t'] \{u(k \to k-1)\, f_{k-1}(t - t') +$$
$$+ u(k \to k+1)\, f_{k+1}(t - t')\}\, dt', \qquad (k = 1, 2, \ldots, 2S+1), \tag{1}$$

где

$$x_k = -x_{2S+2-k}. \tag{2}$$

Общее решение системы уравнений (1) формально может быть написано в виде:

$$f_k(t) = \sum_{l=1}^{2S+1} \Omega_{kl}\, e^{z_l t}, \tag{3}$$

где z_l $(l = 1,2,\ldots, 2S+1)$ являются корнями характеристического уравнения:

$$\begin{vmatrix} D_1\,, & -u_{12}\,, & 0\,, & \dots & & \\ -u_{21}\,, & D_2\,, & -u_{23}\,, & \dots & & \\ & \dots & \dots & & \dots & \\ & & \dots\,, & 0\,, & -u_{2S+1,2\,S}\,, & D_{2S+1} \end{vmatrix} = 0\,, \qquad (3')$$

где

$$D_k = z + u_k - ix_k\,. \qquad (3'')$$

Отметим, что

$$\sum_{l=1}^{2S+1} \Omega_{kl} = 1 \qquad (k = 1, 2, \dots, 2S+1)\,. \qquad (4)$$

В общем случае

$$z_l = -1/2\,\tilde{\Gamma}_R^{(l)} + i\tilde{\omega}_l$$

и поэтому спектральная плотность $G_j(\omega)$ может быть выражена следующим образом:

$$G_j(\omega) = \frac{1}{\pi} \sum_{k=1}^{2S+1} Q_k \sum_{l=1}^{2S+1} Re\, \frac{\Omega_{kl}(j)}{1/2\,[\Gamma + \tilde{\Gamma}_R^{(l)}(j)] + i\,[\omega - \omega_0 - \omega_{0j} - \tilde{\omega}_l(j)]}\,, \qquad (5)$$

где индекс j характеризует один из шести разрешенных переходов $|\,m'\,I'> \rightarrow |\,m\,I>$ и $\omega_{j0} = \delta_j H_0$. Если все $\tilde{\omega}_l(j)$ отличны от нуля, то появляется спектр, состоящий из $6S + 3$ или $6S + 1$ линий в зависимости от того, что S полуцелое или целое число. При обычных экспериментальных условиях, к сожалению, вряд ли можно надеяться на то, что эти линии разрешаются. Следует заметить, что это размножение линий ожидается в том случае, если флуктуация внутреннего магнитного поля осуществляется в виде скачкообразных переходов между дискретными состояниями.

Если внешнее поле $H_0 = 0$ и релаксация магнитного момента свободна, то $u(k \rightarrow k-1) = u(k \rightarrow k+1) = 1/2\,u$. В этом случае характеристическое уравнение имеет более простой вид, а именно

$$\begin{vmatrix} c_1\,, & -1\,, & 0\,, \dots & & \\ -1\,, & c_2\,, & -1\,, \dots & & \\ & \dots & \dots & \dots & \\ & & \dots\,, & 0\,, -1\,, & c_{2S+1}\,, \end{vmatrix} = 0\,, \qquad (6)$$

где

$$c_k = \frac{2}{u}\,(z - ix_k) + 2 - \varepsilon_k$$

и

$$\varepsilon_k = \begin{cases} 1, & \text{если } k = 1,2S+1 \\ 0, & \text{в других случаях.} \end{cases}$$

При достаточно большом значении «частоты» релаксации все корни будут вещественными, что означает полное разрушение сверхтонкого расщепления. Обозначим через u_c критическое значение «частоты» релаксации и напишем, что

$$1/2\, u_c = \Delta_s\, \omega_L\,,$$

где

$$\Delta_S = \begin{cases} 1{,}00, & \text{если } S = 1/2\,, \\ 1{,}54, & \text{если } S = 1\,, \\ 3{,}62, & \text{если } S = 3/2\,. \end{cases}$$

Вероятно, что с ростом S значение Δ_s растет довольно быстро, но, к сожалению, зависимость Δ_s от S пока не известна.

ЛИТЕРАТУРА

1. P. W. Anderson, J. Phys. Soc. Japan, **9,** 316, 1954.
2. В. В. Скляревский, Б. Н. Самойлов и Е. П. Степанов, ЖЭТФ, **40,** 1874, 1961. V. V. Sklyraevsky, K. P. Aleshin, V. D. Gorobchenco, I. I. Likashevich, B. N. Samoilov and E. P. Stepanov, Phys. Letters, **6,** 157, 1963.
3. А. М. Афанасьев и Ю. Каган, ЖЭТФ, **45,** 1660, 1963.
4. F. van der Woude and A. J. Dekker, Phys. Stat. Sol., **9,** 775, 1965.
5. H. Wegener, Zft. für Phys., **186,** 498, 1965.
6. M. Blume, Phys. Rev. Letters, **14,** 96, 1965.
7. E. Bradford and W. Marshall, Proc. Phys. Soc., **87,** 731, 1966.
8. D. E. Nagle, H. Frauenfelder, R. D. Taylor, D. R. F. Cochran and B. T. Matthias, Phys. Rev. Letters, **5,** 364, 1960.
   R. S. Preston, S. S. Hanna and J. Heberle, Phys. Rev., **128,** 2207, 1962.
9. D. E. Cox, G. Shirane, P. A. Flinn, S. L. Ruby and W. J. Takei, Phys. Rev., **132,** 1547, 1963.
10. F. van der Woude and A. J. Dekker, Phys. Stat. Sol., **13,** 181, 1966.
11. D. G. Howard, B. D. Dunlap and J. G. Dash, Phys. Rev. Letters, **15,** 628, 1965.
12. L. Cser, I. Dézsi, L. Keszthelyi, J. Ostanevich and L. Pál, Phys. Letters, **19,** 99,1965.
13. Y. Nakamura, M. Shiga and N. J. Shikazono, Phys. Soc. Japan, **19,** 1177, 1964.
    C. W. Kocher, Phys. Letters, **14,** 287, 1965.

EFFECT OF FLUCTUATIONS OF THE INTERNAL MAGNETIC FIELD ON MÖSSBAUER SPECTRA

L. PÁL

Summary

The effect of directional fluctuations of the internal magnetic field on the shape of Mössbauer spectra has been investigated. It has been found that for increasing frequency of fluctuations first the lines of hyperfine splitting broaden, then shift and finally merge into a central line narrowing gradually as the frequency continues to increase. The disappearance of the splitting takes place when the frequency ω_R of the fluctuations exceeds the Larmor frequency ω_L of the lines involved. At the instant of coalescence the central line exhibits a substantial deviation from the Lorentzian shape. The position and width of each line as well as the mechanism of coalescence are appreciably affected by an external magnetic field.

Acta Physica Academiae Scientiarum Hungaricae, Tomus 23 (2), pp. 185—191 (1967)

THE CROCCO—VÁZSONYI EQUATION IN RELATIVISTIC HYDRODYNAMICS OF IDEAL FLUIDS

By

I. ABONYI

INSTITUTE FOR THEORETICAL PHYSICS, ROLAND EÖTVÖS UNIVERSITY, BUDAPEST

(Presented by K. F. Novobátzky — Received 12. V. 1966.)

The relativistic CROCCO—VÁZSONYI equation is based on, and derived from the energy-momentum tensor of an ideal fluid given by TAUB. The contribution of a possible external field is taken into account. Three of the four components of the CROCCO—VÁZSONYI equation are the corresponding classical ones with corrections of the order c^{-2}. The fourth component equation provides the equation of continuity for the specific entropy.

Introduction

The problems of relativistic hydrodynamics have been dealt with in quite a number of reports and books (see e. g. LICHNEROWICZ [1], TAUB [2]). It seems to us, however, that in spite of the numerous contributions some questions of the relativity theory of fluid motion have remained unclarified or even untouched. The problem of vorticity has also been investigated but almost exclusively for the case of an ideal fluid on which no external fields different from the electromagnetic one act (e. g. [1], [3], [4]). The relativistic circulation theorem has been formulated by CHAU-CHIN WEI [5], [6], for a fluid moving in an external electromagnetic field.

From a theoretical point of view the free flow of a relativistic fluid — in the sense of there being no external fields acting on it — seems to be the unique area of relativistic hydrodynamics where the meaning of the physical quantities can be seen unambiguously. The reason for this statement can be clarified when we remember the line of thought followed in relativistic hydrodynamics.

The basic theorem that serves as a starting point is that the energy-momentum-tensor of the whole system, (fluid plus fields acting on it) is divergence-free:*

$$\partial_k T'_{ik} = 0 \,. \tag{1}$$

This theorem, as is well known, incorporates the general conservation laws of energy and momentum (and also that of angular momentum, too) for the whole system. If there is no external field, $T'_{ik} = T_{ik}$ will refer only to the fluid.

* Latin indices run from 1 to 4, summation convention being understood. ∂_k stands for $\frac{\partial}{\partial x_k}$.

When, however, it is necessary to speak of an external field, e. g. in the case of the flow of a charged fluid in an electromagnetic field, one is confronted with the difficulty of the splitting up of the energy-momentum-tensor of the system (fluid + field) into two parts, namely, one belonging only to the fluid and the other belonging only to the field, and one would have to do this in an objective and invariant manner. This is a very difficult task since a fluid capable of interaction with a field is naturally some kind of source of that field and, therefore, the field should be split into two parts. This problem seems to be unsolved as yet, and as a matter of fact leads outside the framework of phenomenological hydrodynamics, since it involves the microstructure of the fluid and the precise knowledge of what is going on in a macroscopic system composed of a very large number of mutually interacting elementary constituents.

In spite of this fundamental problem the clarification of some situations would require the use of the concept "fluid interacting with an external field". It is natural that one disregards some features of the internal constitution of the fluid and one has to try to draw the limits of this fluid model.

Here we are concerned with some basic statements of relativistic vortex flows in the presence of external fields.

The fundamental equations of relativistic hydrodynamics in ideal media

An ideal fluid will be considered which is described by the energy-momentum tensor

$$T_{ik} = \mu^0 \left(1 + \frac{\varepsilon^0}{c^2} + \frac{p}{c^2 \mu^0}\right) u_i u_k + \delta_{ik} p ,$$

where μ^0 is the particle density, (number of particles in unit proper volume) and ε^0 is the specific internal energy. In the proper frame of reference, this tensor reduces to a diagonal stress tensor and the rest energy density of the fluid in the proper frame is given by

$$- T_{44} = \mu^0 \left(1 + \frac{\varepsilon^0}{c^2}\right) c^2, \tag{3}$$

The use of μ^0 as a particle density is advantageous since the equation of continuity

$$\partial_k (\mu^0 u_k) = 0 \tag{4}$$

expresses only that the total number of particles does not change, which will be provided for.

The splitting of T_{44} in the form (3) is clarified by the observation (see e.g. ECKART [7], HARRIS [8], TAUB [2]) that the thermodynamic relations hold in the form.

$$d\varepsilon^0 + p\,d\left(\frac{1}{\mu^0}\right) = \Theta\, d\,s, \tag{5}$$

where Θ is the absolute temperature and the enthalpy is

$$w = \varepsilon^0 + \frac{p}{\mu^0}. \tag{6}$$

We remark that μ^0, ε^0, s, w and p are invariant with respect to Lorentz transformations.

The external field will be described by the energy-momentum tensor E_{ik} which will be specialized later on.

The conservation laws (1) now take the form

$$\mu^0 u_k \partial_k \left[\left(1 + \frac{\varepsilon^0}{c^2} + \frac{p}{c^2\mu^0}\right) u_i\right] + \partial_i p = -\partial_k E_{ik}, \tag{7}$$

where use has been made of (4). This is the Euler equation in relativistic hydrodynamics. Apart from the continuity equation, the requirement

$$u_k u_k = -c^2 \tag{8}$$

gives a further equation to be satisfied in order to ensure the interpretation of u_k as a four vector velocity.

Equations (4) (7) and (8) constitute the fundamental system of hydrodynamic equations. They are six for seven unknowns so that one needs either an equation of state or the relations governing the heat flow, and so one cuts the chain of equations at a later stage.

The Crocco—Vázsonyi equation

The form of the Euler equation (7) suggests the introduction of the quantity

$$\Omega_{ik} = \partial_k \left[\left(1 + \frac{\varepsilon^0}{c^2} + \frac{p}{c^2\mu^2}\right) u_i\right] - \partial_i \left[\left(1 + \frac{\varepsilon^0}{c^2} + \frac{p}{\mu^0 c^2}\right) u_k\right]. \tag{9}$$

If we use (9) in (7), we see that

$$\Omega_{ik} = \partial_k \left[\left(1 + \frac{w}{c^2}\right) u_i\right] - \partial_i \left[\left(1 + \frac{w}{c^2}\right) u_k\right]. \tag{10}$$

In other words Ω_{ik} is the generalization of the vorticity vector of ordinary hydrodynamics, which can be inferred if we take the limit of $c \to \infty$.

The Euler equations expressed in terms of Ω_{ik} have the form

$$u_k \Omega_{ik} = -\frac{1}{\mu^0} \partial_i p - u_k \partial_i \left[\left(1 + \frac{\varepsilon^0}{c^2} + \frac{p}{c^2 \mu^0} \right) u_k \right] - \frac{1}{\mu^0} \partial_k E_{ik} .$$

Here we write

$$u_k \partial_i \left[\left(1 + \frac{\varepsilon^0}{c^2} + \frac{p}{c^2 \mu^0} \right) u_k \right] = - c^2 \partial_i \left(1 + \frac{\varepsilon^0}{c^2} + \frac{p}{c^2 \mu^0} \right)$$

as a consequence of (8). Then by means of (5) we obtain

$$u_k \Omega_{ik} = \Theta \partial_i s - \frac{1}{\mu^\circ} \partial_k E_{ik} . \tag{11}$$

This equation may be considered as the relativistic CROCCO—VÁZSONYI equation, generalized so as to include the contribution of the external field.

First we show that equation (11), when projected to the world line of the fluid element, provides the equation of continuity of entropy density:

$$u_i u_k \Omega_{ik} = \Theta u_i \partial_i s - \frac{1}{u^0} u_i \partial_k E_{ik} .$$

Since $\Omega_{ik} = -\Omega_{ki}$, we have

$$\Theta u_i \partial_i s = \frac{1}{\mu^0} u_i \partial_k E_{ik} . \tag{12}$$

In the case of the free flow of the fluid ($E_{ik} \equiv 0$) we obtain

$$u_i \partial_i s = 0 \tag{13}$$

stating that there is no energy dissipation along the world line of the fluid element. The same inference can also be drawn when $E_{ik} \neq 0$ is such that

$$u_i \partial_k E_{ik} = 0 \tag{14}$$

is satisfied. But when condition (14) is not valid, the entropy will change according to (12). Remembering that $\partial_k E_{ik} = f_i$ is the force density four vector and using (5) we have

$$\frac{d \varepsilon^0}{d \tau} + p \frac{d}{d \tau} \left(\frac{1}{\mu^0} \right) = \frac{1}{\mu^0} u_i f_i . \tag{15}$$

In other words the extra dissipation enters just because of the peculiar feature of the external force: $u_i f_i \neq 0$. The rôle and consequences of fields of this type have been investigated by MARX [9], and MARX and SZAMOSI [10]. In general, the pressure contributes to the internal energy change, but there is a clear situation, namely that of the incompressible fluid ($\partial_r u_r = 0$), where the internal energy changes directly because of $u_i f_i \neq 0$, since in this case $\frac{d}{d\tau}\left(\frac{1}{\mu^0}\right) = 0$.

Now we take the normal component of equation (11) to the direction u_i by using the projection tensor

$$\Pi_{ik} = \delta_{ik} + \frac{1}{c^2} u_i u_k \tag{16}$$

and we show that there are only three equations obtained

$$\Pi_{ik}\left(u_r \Omega_{ir} - \Theta \partial_i s + \frac{1}{\mu^0} \partial_r E_{ir}\right) = u_r \Omega_{kr} - \Theta \partial_k s + \frac{1}{\mu^0} \partial_r E_{kr}$$

reduces to the CROCCO—VÁZSONYI equations in the classical limit.

Inserting (10) into (11) we obtain

$$\partial_i w + \left(1 + \frac{w}{c^2}\right) u_k (\partial_k u_i - \partial_i u_k) + \frac{1}{c^2} u_i u_k \partial_k w = \Theta \partial_i s + \frac{1}{\mu^0} f; \tag{17}$$

as another form of CROCCO—VÁZSONYI-equation. For $i = 1, 2, 3$ these equations will be written using the notation

$$u_i = \left\{\vec{v}, u_4\right\}, \quad f_i = \left\{\vec{f}, f_4\right\}, \quad \partial_i = \left\{\vec{\nabla}, \partial_4 = \frac{\partial}{i\, c\, \partial t}\right\}$$

and a relation

$$u_4 \vec{\nabla} u_4 = -\frac{1}{2} \vec{\nabla} (\vec{v})^2$$

which is a consequence of (8). After these substitutions we take the limit c tends to infinity. In this limit the quantity $\vec{v}$ evidently reduces to the ordinary velocity vector of classical hydrodynamics, while μ^0 approaches the classical density of mass ϱ. Finally we obtain

$$\frac{\partial \vec{v}}{\partial t} + \nabla\left(w + \frac{1}{2}\vec{v}^2\right) - \vec{v} \times (\vec{\nabla} \times \vec{v}) = \Theta \vec{\nabla} s + \frac{1}{\varrho} \vec{f}. \tag{18}$$

This equation, with vanishing $\vec{f}$ is known in the literature as the CROCCO—VÁZSONYI equation. (see e. g. LIEPMANN—ROSHKO [11].)

Application to the case of a charged fluid moving in an external electromagnetic field

Let us now consider the case of the external electromagnetic field, then

$$E_{ik} = \frac{1}{4\pi} F_{ie} F_{ke} - \frac{1}{16\pi} \delta_{ik} F_{rs} F_{rs}, \tag{19}$$

where F_{ik} is the electromagnetic tensor governed by Maxwell's equations:

$$\partial_i F_{ke} + \partial_k F_{ei} + \partial_e F_{ik} = 0, \tag{20}$$

$$\partial_i F_{ir} = \frac{4\pi}{c} j_i, \tag{21}$$

where

$$j_i = e \mu^0 u_i. \tag{22}$$

The force density is given by

$$f_i = \frac{e}{c} \mu^0 u_k F_{ik} = \frac{e}{c} \mu^0 u_k (\partial_k A_i - \partial_i A_k),$$

where A_i is the vector potential.

Now the substitution into the form (11) of the CROCCO—VÁZSONYI equation

$$u_k \left\{ \partial_k \left[\left(1 + \frac{w}{c^2} \right) u_i \right] - \partial_i \left[\left(1 + \frac{w}{c^2} \right) u_k \right] \right\} = \Theta \partial_i s - \frac{e}{c} u_k (\partial_k A_i - \partial_i A_k)$$

suggests the regrouping of the terms:

$$u_k \left\{ \partial_k \left[\left(1 + \frac{w}{c^2} \right) u_i + \frac{e}{c} A_i \right] - \partial_i \left[\left(1 + \frac{w}{c^2} \right) u_k + \frac{e}{c} A_k \right] \right\} = \Theta \partial_i s. \tag{23}$$

This equation states that the quantity

$$G_{ik} = \Omega_{ik} + \frac{e}{c} F_{ik}$$

plays an important rôle in the flow of a charged fluid, since all the vorticity theorems obtainable from the CROCCO—VÁZSONYI equation will be valid for G_{ik}; the hydrodynamic vorticity will be coupled to the electromagnetic field strengths.

It should be mentioned that equation (23) is analogous to that obtained by CHAU-CHIN WEI [5]. The form obtained by CHAU-CHIN WEI differs by using another interpretation of the thermodynamic quantities involved and the relation between equation (23) and the CROCCO—VÁZSONYI equation is not observed.

REFERENCES

1. A. LICHNEROWICZ, Théories relativistes de la gravitation et de l'électromagnétisme, Masson, Paris, 1956 p. 71—108.
2. A. H. TAUB, Phys. Rev., **74,** 328, 1948.
3. Y. FOURÉS-BRUHAT, Bull. Soc. Math. France, **86,** 155, 1958.
4. A. H. TAUB. Arch. Rat. Mech. Anal., **3,** 312, 1959.
5. CHAU-CHIN WEI, Phys. Rev., **113,** 1414, 1959.
6. CHAU-CHIN WEI, Phys. Fluids, **3,** 323, 1960.
7. C. ECKART, Phys. Rev., **58,** 919, 1940.
8. E. G. HARRIS, Phys. Rev., **108,** 1357, 1957.
9. G. MARX, Acta Phys. Hung., **6,** 353, 1957.
10. G. SZAMOSI and G. MARX, Ann. Physik (6), **15,** 182, 1955.
11. H. W. LIEPMANN and A. ROSHKO, Elements of Gasdynamics (Chapman & Hall Ltd, London, 1957) Chap. 7. 9.

УРАВНЕНИЕ КРОККО—ВАЖОНИ В РЕЛЯТИВИСТСКОЙ ГИДРОДИНАМИКЕ ИДЕАЛЬНОЙ ЖИДКОСТИ

И. АБОНИ

Р е з ю м е

На основе тензора энергии-импульса идеальной жидкости, данного Таубом, выведено релятивистское уравнение Крокко—Важони. Учитывается добавка возможного внешнего поля. Три компонента уравнения представляют собой уравнения Крокко—Важони, а четвертый — уравнение непрерывности для удельной энтропии.

Acta Physica Academiae Scientiarum Hungaricae, Tomus 23 (2), pp. 193—202 (1967)

GRAVITATIONAL WAVES

By

M. Z. v. KRZYWOBLOCKI

MICHIGAN STATE UNIVERSITY, EAST LANSING, MICHIGAN 48824, USA*

(Presented by A. Kónya — Received 21. VI. 1966)

In the first chapter the author discusses briefly some characteristic features of the gravitational waves and in the second the present technique of the calculation of the velocity of the propagation of the gravitational waves by means of the small perturbation technique. In the third chapter the author calculates a counter-example which shows that the perturbation technique gives the calculated velocity of the gravitational waves different from the velocity of the propagation of light which seems to imply that the technique in question may not be strong enough to furnish the correct answer.

1. Remarks on gravitational waves

EINSTEIN (see [12], p. 218) based his approach to the problem of gravitational waves upon his general theory of relativity. He concluded "that every change in the distribution of matter produces a gravitational effect which is propagated in space with the velocity of light. Oscillating masses produce gravitational waves. Nowhere in the nature accessible to us do mass-oscillations of sufficient power occur to allow the resulting gravitational waves to be observed." Regarding the general conclusions derived by EINSTEIN, one must keep deeply in his mind that EINSTEIN based his derivation of both theories of relativity fundamentally upon the concept of the velocity of light in vacuum as the maximum possible velocity attainable by any matterfull or matterless medium.

RICE ([8], p. 293) writes that "the field of a single gravitating centre is a static field from the point of view of an observer in the same frame of reference as the centre. The field of a number of centres, such as a planetary system, will alter with time. This is, of course, also true in Newtonian theory. But whereas in the latter case the conception of an absolute space and an absolute time is vital to the theory (for the potential at an assigned point and an assigned instant is calculated from the *simultaneous* positions of the gravitating bodies and so gravitation is regarded as an influence which is propagated at an infinite speed), it cannot be so in any law of gravitation consistent with the

* Space Seminar. Presented before the 1965 Summer Meeting of the American Physical Society, University of Hawaii, Honolulu, Hawaii, 2—4, September 1965. The work was supported by the Research Department, Michigan State University, under the Chairmanship of Mr. J. W. HOFFMAN, which is gratefully acknowledged.

relativity principle." Again RICE ([8] p. 296) concludes that "gravitational changes should be propagated with the speed of light, but it must be very definitely borne in mind that this conclusion is valid under two very restrictive limitations introduced above, viz., that we are considering the matter from the point of view of a specially chosen frame of reference, and we are neglecting squares, etc., of $h_{\mu\nu}$ (where $g_{\mu\nu} = \delta_{\mu\nu} + h_{\mu\nu}$, $\delta_{\mu\nu} = 0$ if $\mu \neq \nu$, $\delta_{\mu\nu} = -1$ if $\mu = \nu = 1, 2, 3$, $\delta_{\mu\nu} = 1$ if $\mu = \nu = 4$)."

PAULI ([7], p. 173) repeats the statement that the gravitational effects are propagated with the velocity of light, just as electromagnetic disturbances. FOCK ([5], p. 175) writes that "briefly, one can* (!) say that gravitation is propagated with the speed of light."

EDDINGTON in 1923 ([3], pp. 94, 147) assumes that the gravitation is propagated with the speed of light. But in his excellent mathematical representation of the theory of relativity, he expressed the opinion that "... the deviations of the gravitational potentials are propagated as waves with the velocity of light. But it must be remembered that this representation of the propagation, though always permissible, is not unique." In replacing a system of equations by another one, as EDDINGTON did, there is introduced a restriction — as he concludes — which amounts to choosing a special coordinate system. "Other solutions are possible, corresponding to other coordinate systems. The potentials $g_{\mu\nu}$ pertain not only to the gravitational influence which has objective reality, but also to the coordinate system which we select arbitrarily. We can "propagate" coordinate changes with the *speed of thought*, and these may be mixed up at will with the more dilatory propagation discussed above. There does not seem to be any way of distinguishing a physical and a conventional part in the changes of the $g_{\mu\nu}$."** The statement that in the relativity theory gravitational waves are propagated with the speed of light has, I believe, been based entirely on the foregoing investigation; but it will be seen that it is only true in a very conventional sense. If coordinates are chosen so as to satisfy a certain condition which has no very clear geometrical importance, the speed is that of light; if the coordinates are slightly different the speed is altogether different from that of light. The result stands or falls by the choice of coordinates and, as far as can be judged, the coordinates here used were purposely introduced in order to obtain the simplification which results from representing the propagation as occuring with the speed of light. The argument thus follows a vicious circle." EDDINGTON continues: "... must we then conclude that the speed of propagation of gravitation is necessarily a conventional conception without absolute meaning? I think not. The speed of gravitation is quite definite; only the problem of determining it does not seem to have yet been tackled correctly."

* The exclamation sign was put down by the author of the present paper.
** These remarks can be found also in RICE's book (cited above), p. 299.

SYNGE ([10], p. 228) states that in ordinary parlance, we may say that gravitational shock waves travel with the speed of light. But, he continues, such statement must be taken cum grano salis. As a relativist, familiar with the idea that no casual effect can travel faster than light, SYGNE admits (p. 343) that we would "guess that the change in the gravitational field of a moving body travels out into the space with the speed of light. And we would call this moving disturbance a gravitational wave. Thus, on a very general basis, we must regard physical existence of gravitational waves as self-evident. Confusion enters, however, through the fact that the word wave implies repetition and sometimes does not. When we seek a general understanding of gravitational waves due to a phenomenon on a scale of a vast astronomical catastrophe, it is well to recognize that we are not concerned with the solution of well formulated mathematical problems, but rather with classes of fields satisfying certain conditions. In default of exact solutions, we may fall back on approximations. Here we must be cautious. Mathematically, we have no assurance that any suitable solution exist; but, physically, we do. We set up some definite system of approximation, we cut off the approximation at some step and claim that we have a good approximation to some exact solution, which (physically, but not mathematically) we have reason to believe exists. But such a claim is too vague to argue about, one way or the other, since no linear approximation is likely to satisfy the physical test."

2. Calculation of the velocity of the propagation of the gravitational waves

We cite below the results obtained by EINSTEIN in 1916 (see [4]). Let us begin with EINSTEIN's equation in the general relativity:

$$G_\mu^\nu - \frac{1}{2} g_\mu^\nu G = -8\pi T_\mu^\nu . \tag{2.1}$$

In the limiting case of very weak fields we set:

$$g_{\mu\nu} = \delta_{\mu\nu} + h_{\mu\nu} , \tag{2.2}$$

where $\delta_{\mu\nu}$ represents Galilean values, and $h_{\mu\nu}$ is a small quantity of the first order whose squares are neglected. After inserting Eq. (2.2) into Eq. (2.1), performing various operations, correct to the first order, one gets the equation of wave-motion

$$\Box \left(h_\mu^\alpha - \frac{1}{2} \delta_\mu^\alpha h \right) = 2 \left(G_\mu^\alpha - \frac{1}{2} g_\mu^\alpha G \right) = -16\pi T_\mu^\alpha , \tag{2.3}$$

$$\Box = \frac{\partial^2}{\partial t^2} - \frac{\partial^2}{\partial x^2} - \frac{\partial^2}{\partial y^2} - \frac{\partial^2}{\partial z^2} , \tag{2.4}$$

t having dimension of x by means of a multiplication by the velocity of light. The well-known solution of Eq. (2.3) is:

$$h_\mu^\varkappa - \frac{1}{2}\delta_\mu^\varkappa h = (4\pi)^{-1}\int(-16\pi T_\mu^\varkappa)'(r')^{-1}\,dV'\,. \tag{2.5}$$

Some further simplifications reduce Eq. (2.3) to:

$$\Box h_{\mu\nu} = 2G_{\mu\nu}\,, \tag{2.6}$$

which in empty space has zero on the right hand side. This shows that the deviations of the gravitational potentials are propagated as waves with unit velocity, i.e., the velocity of light.

3. Velocity of the propagation of the gravitational waves (Counter-Examples)

Assume a four dimensional space-time, x^i, $i = 1$ to 4, with x^i, $i = 1, 2, 3$, having dimensions of length, $x^4 = ct$, with c denoting the velocity of light. We write EINSTEIN's field equation of the general relativity in the form:

$$R^{\mu\nu} - \frac{1}{2}g^{\mu\nu}R = -\varkappa_1 T^{\mu\nu}\,, \tag{3.1}$$

(FOCK, [5] pp. 194, 198), where:

$$\varkappa_1 = 8\pi K c^{-2}\,, \tag{3.2}$$

K being the gravitational constant. We assume DINGLE's [1] metric:

$$(ds)^2 = -A(dx^1)^2 - B(dx^2)^2 - C(dx^3)^2 + D(dx^4)^2\,, \tag{3.3}$$

where A, B, C, D, can be any functions of the coordinates, all four of them being regarded as essentially positive quantities so that x^1, x^2, x^3 are space like coordinates and x^4 time-like. The Christoffel symbols corresponding to the line element (3.3) have been computed by DINGLE [1], are cited by TOLMAN ([11], p. 253), etc. We introduce some simplifications:

$$A = 1 + A_1(x^2, x^3, x^4)\,; \qquad B = 1 + B_1 = \text{ const.}\,; \tag{3.4}$$

$$C = 1 + C_1 = \text{ const.}\,; \qquad D = 1 + D_1(x^2, x^3, x^4)\,, \tag{3.5}$$

where A_1, B_1, C_1, D_1 are small quantities of the first order. The energy-momentum tensor, whose components contain only terms of the first order, with higher order terms neglected, and with $(AD)^{-1} \simeq 1$, $(AC^2)^{-1} \simeq 1$, etc., has the form (in which the subscripts in $A_1 D_1$ are omitted and $\partial^2 A/\partial(x^2)^2 \equiv A_{,22}$, etc.):

$$T^{\nu}_{\mu} = -(8\pi K)^{-1} c^2 \times$$

$$\times \begin{Bmatrix} \frac{1}{2}(D_{'22} + D_{'33}) & 0 & 0 & 0 \\ 0 & \frac{1}{2}(A_{'33} - A_{'44} + D_{'33}) & \frac{1}{2}(A_{'23} + D_{'23}) & \frac{1}{2} A_{'24} \\ 0 & -\frac{1}{2}(A_{'23} + D_{'23}) & \frac{1}{2}(A_{'22} - A_{'44} + D_{'22}) & \frac{1}{2} A_{'34} \\ 0 & -\frac{1}{2} A_{'24} & -\frac{1}{2} A_{'34} & \frac{1}{2}(A_{'22} + A_{'33}) \end{Bmatrix}. \quad (3.6)$$

Our next assumption is:

$$A = \alpha(x^2, x^4) + \beta(x^3, x^4) + \gamma(x^2, x^3); \; D = m^2 A, \; m^2 = \text{const.} \quad (3.7)$$

This leads to:

$$T^{\nu}_{\mu} = -(8\pi K)^{-1} c^2 \times$$

$$\times \begin{Bmatrix} \frac{1}{2} m^2(\alpha_{'22} + \beta_{'33} + \gamma_{'22} + \gamma_{'33}) & 0 & 0 & 0 \\ 0 & \frac{1}{2}[(1+m^2)\beta_{'33} - \beta_{'44} - \alpha_{'44} + (1+m^2)\gamma_{'33}] & -\frac{1}{2}(1+m^2)\gamma_{'23} & -\frac{1}{2}\alpha_{'24} \\ 0 & -\frac{1}{2}(1+m^2)\gamma_{'23} & -\frac{1}{2}[(1+m^2)\alpha_{'22} - \alpha_{'44} - \beta_{'44} + (1+m^2)\gamma_{'22}] & -\frac{1}{2}\beta_{'34} \\ 0 & -\frac{1}{2}\alpha_{'24} & -\frac{1}{2}\beta_{'34} & \frac{1}{2}(\alpha_{'22} + \beta_{'33} + \gamma_{'22} + \gamma_{'33}) \end{Bmatrix}. \quad (3.8)$$

From FOCK ([5], pp. 103 to 105), PAULI ([7], p. 133), SYNGE ([10], p. 303), TOLMAN ([11], p. 217) we get:

$$T^{\mu\nu} = \mu u^{\mu} u^{\nu} - p c^{-2} g^{\mu\nu}, \quad \mu = \varrho + P c^{-2}, \quad P = \varrho \int \varrho^{-1} d p, \tag{3.9}$$

where the standard notation is used, and $u = dx^i/ds$. The question, what kind of tensor the symbol $T^{\mu\nu}$ in our case of the small perturbation procedure should represent, is actually an open one. We may quote PAULI ([7], p. 172) that EINSTEIN ([4], p. 688) (see above) has indicated a method by which the G-field for masses moving with arbitrary velocities can be determined approximately, provided the masses are sufficiently small. For in this case, the g_{ik}'s differ only slightly from their normal values so that the squares of these deviations can be neglected. Also, only the linear part of the differential equation (3.1) of the gravitational field need be retained, so that they can be integrated very easily. With $T^{\nu}_{\mu} = g_{\alpha\mu} T^{\alpha\nu}$ one gets to the first order approximation (with the magnitude A_1 neglected with respect to unity):

$$T^{\nu}_{\mu} = \begin{bmatrix} -[\mu (u^1)^2 + p c^2] & -\mu u^1 u^2 & -\mu u^1 u^3 & -\mu u^1 n^4 \\ -\mu u^2 u^1 & -[\mu (u^2)^2 + p c^{-2}] & -\mu u^2 u^3 & -\mu u^2 u^4 \\ -\mu u^3 u^1 & -\mu u^3 u^2 & -[\mu (u^3)^2 + p c^{-2}] & -\mu u^3 u^4 \\ \mu u^4 u^1 & \mu u^2 u^4 & \mu u^3 u^4 & \mu (u^4)^2 - p c^{-2} \end{bmatrix}. \tag{3.10}$$

It may be of a little importance to attempt to consider the order of magnitude of the components of the tensor (3.10), since anyhow in the final stage we operate in a completely empty space.

Comparing tensors (3.8) and (3.10) we obtain a system of equations:

$$p c^{-2} = c^2 m^2 (16\pi K)^{-1} (\alpha'_{22} + \beta'_{33} + \gamma'_{22} + \gamma'_{33}); \quad u^1 = 0; \tag{3.11}$$

$$\mu (u^2)^2 = c^2 (16\pi K)^{-1} [-(m^2 \alpha'_{22} + \alpha'_{44}) + \beta'_{33} - \beta'_{44} - m^2 \gamma'_{22} + \gamma'_{33}]; \tag{3.12}$$

$$\mu (u^3)^2 = c^2 (16\pi K)^{-1} [\alpha'_{22} - \alpha'_{44} - (m^2 \beta'_{33} + \beta'_{44}) + \gamma'_{22} - m^2 \gamma'_{33}]; \tag{3.}$$

$$\mu (u^4)^2 = c^2 (16\pi K)^{-1} (m^2 - 1)(\alpha'_{22} + \beta'_{33} + \gamma'_{22} + \gamma'_{44}). \tag{3.14}$$

We discount the possibility $m^2 = 1$. Next we get from Eqs. (3.8) to (3.14):

$$(T^3_2)^2 = [-(m^2 \alpha'_{22} + \alpha'_{44}) + \beta'_{33} - \beta'_{44} - m^2 \gamma'_{22} + \gamma'_{33}] \cdot [\alpha'_{22} - \alpha'_{44} - (m^2 \beta'_{33} + \beta'_{44}) + \gamma'_{22} - m^2 \gamma'_{33}] = (1 + m^2)^2 (\gamma'_{23})^2; \tag{3.15}$$

$$(T^4_2)^2 = [-(m^2 \alpha'_{22} + \alpha'_{44}) + \beta'_{33} - \beta'_{44} - m^2 \gamma'_{22} + \gamma'_{33}] (m^2 - 1) \cdot (\alpha'_{22} + \beta'_{33} + \gamma'_{22} + \gamma'_{44}) = (\alpha'_{24})^2; \tag{3.16}$$

$$(T^4_3)^2 = [\alpha'_{22} - \alpha'_{44} - (m^2 \beta'_{33} + \beta'_{44}) + \gamma'_{22} - m^3 \gamma'_{33}] \cdot (\alpha'_{22} + \beta'_{33} + \gamma'_{22} + \gamma'_{44}) = (\beta'_{34})^2. \tag{3.17}$$

Eqs. (3.15) to (3.17) give three relations for three unknown functions α, β, γ. The condition $u^1 = 0$ implies $dx^1 = 0$, $x^1 =$ constant, and reduces the metric (3.3) to three terms only. Let us divide Eq. (3.3) by $(ds)^2$, thus obtaining to the first order of approximation:

$$1 + (u^2)^2 + (u^3)^2 - (u^4)^2 = 0 \text{ or } \mu\,[(u^4)^2 - (u^2)^2 - (u^3)^2] = \mu\,. \tag{3.18}$$

Using Eqs. (3.12) to (3.14) in Eq. (3.18) yields:

$$\mu = c^2\,(8\pi K)^{-1}\,[(m^2 - 1)\,(\alpha_{,22} + \beta_{,33} + \gamma_{,22} + \gamma_{,33}) + (\alpha_{,44} + \beta_{,44})]\,. \tag{3.19}$$

Addition of the tensor components, T_2^2, T_3^3, Eq. (3.8), furnishes

$$\nabla^2 A - 2\,[(1 + m^2)\,c^2]^{-1}\,A_{,tt} = -\,16\pi K\,[(1 + m^2)\,c^2]^{-1}\,(T_2^2 + T_3^3)\,, \tag{3.20}$$

$$\nabla^2 D - 2\,[(1 + m^2)\,c^2]^{-1}\,D_{,tt} = -\,16\pi K\,m^2\,[(1 + m^2)\,c^2]^{-1}\,(T_2^2 + T_3^3)\,, \tag{3.21}$$

$$\nabla^2 A = \alpha_{,22} + \beta_{,33} + \gamma_{,22} + \gamma_{,33}\,, \tag{3.22}$$

$$A_{,tt} = \alpha_{,tt} + \beta_{,tt}\,. \tag{3.23}$$

This implies that in an empty space a gravitational wave propagates with a velocity G, $G^2 = \frac{1}{2}(1+m^2)\,c^2$, where m is any arbitrary number (positive, say) different from one. Briefly, one obtains infinitely many velocities of the propagation of the gravitational waves in an empty space, which seems to be a very odd result. One can easily verify that using T_j^j, $j = 1$ to 4, one gets:

$$\nabla^2 A - [(1 + m^2)\,c^2]^{-1}\,A_{,tt} = -\,8\pi K\,[(1 + m^2)\,c^2]^{-1}\left(\frac{1}{2}\,T_1^1 + T_2^2 + T_3^3 + \frac{1}{2}\,T_4^4\right). \tag{3.24}$$

Attention is called to the following aspects of the calculations performed above: we have seven equations from Eqs. (3.8) and (3.10). We have seven unknown variables: α, β, γ, u^2, u^3, p, ϱ. This obviously implies that the pressure—density relation is uniquely defined by the system itself. Hence, it may not be necessarily an isentropic fluid relation. Obviously, the whole approach is based upon a possibility of obtaining a solution of the system of nonlinear equations (3.15) to (3.17).

We may propose more examples of this character. Consider the metric:

$$(d\,s)^2 = -\,(1 + A)\,(d\,x^1)^2 - (1 + B)\,(d\,x^2)^2 - (1 + C)\,(d\,x^3)^2 + (1 + D)\,(d\,x^4)^2\,, \tag{3.25}$$

where A, B, C, D, are essentially positive functions of x^i $(i = 1, 2, 3, 4)$ and are small of the first order in comparison with unity. Neglecting the terms of higher orders, the tensor T_μ^ν takes the form:

$$T_{\mu}^{\nu} = -c^2 (16\pi K)^{-1} \times$$

$$\times \begin{Bmatrix} \left[\begin{matrix}(B_{'33}-B_{'44})+(C_{'22}-C_{'44})\\ +(D_{'22}+D_{'33})\end{matrix}\right] & -(C_{'12}+D_{'12}) & -(B_{'13}+D_{'13}) & -(B_{'14}+C_{'14}) \\ -(C_{'12}+D_{'12}) & \left[\begin{matrix}(A_{'22}-A_{'44})+(C_{'11}-C_{'44})\\ +(D_{'11}+D_{'33})\end{matrix}\right] & -(A_{'23}+D_{'23}) & -(A_{'21}+B_{'24}) \\ -(B_{'13}+D_{'13}) & -(A_{'23}+D_{'23}) & \left[\begin{matrix}(A_{'22}-A_{'44})+(B_{'11}-B_{'44})\\ +(D_{'11}+D_{'22})\end{matrix}\right] & -(A_{'34}+B_{'34}) \\ (B_{'14}+C_{'11}) & (A_{'24}+C_{'24}) & (A_{'34}+B_{34}) & \left[\begin{matrix}(A_{'22}+A_{'33})+(B_{'11}+B_{'33})\\ +(C_{'11}+C_{'22})\end{matrix}\right] \end{Bmatrix} \cdot \quad (3.26)$$

We put: $A = B = C = m^{-2}D$, then:

$$T_{\mu}^{\nu} = -c^2 (16\pi K)^{-1} \times$$

$$\times \begin{Bmatrix} \left[\begin{matrix}(1+m^2)(A_{'22}+A_{'33})-\\ -2A_{'44}-(1+m^2)A_{'12}\end{matrix}\right] & -(1+m^2)A_{'12} & -(1+m^2)A_{'13} & 2A_{'14} \\ -(1+m^2)A_{'12} & \left[\begin{matrix}(1+m^2)(A_{'11}+A_{'33})-\\ -2A_{'44}-(1+m^2)A_{'23}\end{matrix}\right] & -(1+m^2)A_{'23} & 2A_{'24} \\ -(1+m^2)A_{'13} & -(1+m^2)A_{'23} & \left[\begin{matrix}(1+m^2)(A_{'11}+A_{'22})-\\ -2A_{'44}\end{matrix}\right] & 2A_{'34} \\ -2A_{'14} & -2A_{'24} & -2A_{'34} & 2(A_{11}+A_{'22}+A_{'33}) \end{Bmatrix} \cdot \quad (3.27)$$

Let us use a representation:

$$A = \alpha(x^1 . x^4) + \beta(x^2, x^4) + \gamma(x^3, x^4) + \sigma(x^1, x^2) + \lambda(x^2, x^3) + \omega(x^1, x^3) . \quad (3.28)$$

We obtain from Eqs. (3.10) and (3.27) a system of ten equations in eleven unknown dependent variables: α, β, γ, σ, λ, ω, u^1, u^2, u^3, ϱ, p. This implies that the (p, ϱ) —relation can be chosen arbitrarily. An addition of the diagonal elements in the form (3.26) furnishes:

$$\nabla^2 A - 3\left[2(1 + m^2)c^2\right]^{-1} A_{,tt} = -4\pi K c^{-2} \sum_{j=1}^{4} T_j^j , \quad (3.29)$$

which shows that the propagation of the gravitational waves in an empty space is equal to $[2(1 + m^2)/3]^{1/2}c$, i.e., it can take any value. The calculated counter-examples show clearly that the small perturbation technique does not furnish any definite results at all. Practically, both velocities may be equal but the small perturbation is too weak to guarantee this result.

PAULI ([7], p. 143) stated that the special theory of relativity can only be correct in the absence of gravitational fields, because of the dependence of the light velocity on the gravitational potential. Once the gravitational potential is introduced as a physical quantity, the physical laws have to be considered as relations between the other physical quantities and the gravitational potential. But, in another place (p. 182) PAULI says that in perfectly empty space, no G- field exists at all. The propagation of light would then be impossible. FOCK ([5] p. 168 in the lst edition, p. 184 in the 2nd edition) begins with the equation of wave front propagation $c^{-2}(\omega_{,t})^2 = (\text{grad}\ \omega)^2$, which shows that light is propagated in straight lines. But light possesses energy and by the law of proportionality of mass and energy all energy is indissolubly connected with mass. Therefore, light must possess mass. On the other hand, by the law of universal gravitation, any mass located in a gravitational field must experience the action of that field and in general its motion will not be rectilinear. Hence it follows that in a gravitational field the law of wave front propagation must have a form somewhat different from the one given above. But the equation of wave front propagation is a basic characteristic of the properties of space and time. Hence FOCK concludes that the presence of the gravitational field must affect the properties of space and time. As it is known, FOCK ([5,] p. 169) derives a metric form which takes into account the aspects mentioned above.

Concerning the speed of propagation of gravitation Fock begins his discussion of EINSTEIN's gravitation equations with the derivation of the first order equation for their characteristics. He concludes that the system of equations of gravitation has the same characteristics (which represent the propagation of the wave front of a gravitational wave) as D'ALEMBERT's equation

$\Box\Psi = 0$ (the generalized wave equation). This leads to the equation indentical to that one for the front of a light wave in an empty space. The reasoning of FOCK seems to be stronger than the above small perturbation technique in Section 2, which is open to counter-examples constructed in Section 3.

REFERENCES

1. H. DINGLE, Proceed. Nat. Acad. Sci. U. S. A., **19**, 559, 1933a.
2. A. S. EDDINGTON, Space Time and Gravitation. Cambridge, University Press, 1923.
3. A. S. EDDINGTON, The Mathematical Theory of Relativity. Cambridge, University Press, 1924.
4. A. EINSTEIN, Sitzber. Preuss. Akad. Wiss. 1916, p. 688; 1918, p. 154.
5. V. FOCK, The Theory of Space, Time and Gravitation. (Translated from the Russian by N. Kemmer). Pergamon Press, 1959. Second Revised Edition, 1964.
6. W. C. MICHELS and A. L. PATTERSON, Phys. Rev., **60**, 589, 1941.
7. W. PAULI, Theory of Relativity. Pergamon Press, London—New York—Paris, 1958.
8. J. RICE, Relativity. Longmans, Green and Co., London, 1923.
9. N. ROSEN, American Journal of Physics, **20**, 161, 1952.
10. J. L. SYNGE, Relativity: The General Theory. North-Holland Publishing Company, Amsterdam, 1960.
11. R. C. TOLMAN, Relativity, Thermodynamics and Cosmology. Oxford, At the Clarendon Press, 1934.
12. H. WEYL, Space—Time—Matter. Methuen and Co. Ltd., London, 1922.

ГРАВИТАЦИОННЫЕ ВОЛНЫ

М. З. КРЗЫВОБЛОЦКИ

Резюме

В первой главе автором кратко дискутируются некоторые характерные свойства гравитационных волн, во второй главе описывается современная техника определения скорости распространения гравитационных волн с помощью техники небольшого возмущения. В третьей главе автор решает численную задачу, показывающую, что техника возмущения результирует для скорости гравитационной волны отличное и от скорости распространения света значение. Это говорит о том, что применение данной техники не может считаться достаточно строгим для получения точного ответа.

Acta Physica Academiae Scientiarum Hungaricae, Tomus 23 (2), pp. 203—210 (1967)

SYMMETRY THEORY OF THE EQUATIONS OF MOTION

PART I.

SYSTEM OF POINT PARTICLES IN THE E_2 SPACE

By

G. KNAPECZ

PHYSICAL INSTITUTE OF THE UNIVERSITY OF TECHNICAL SCIENCES, BUDAPEST

(Presented by A. Kónya — Received 3. VIII. 1966)

By solving a system of functional equations ([11] and [12]) it is shown that the validity of the Euclidean invariance (symmetry) group ([3] and [4]) restricts the form of the force functions of the dynamical law ([1] and [2]) of a system of point particles embedded in the Euclidean space E_2 to the form given by the expressions [32]—[35].

1. Introduction

The symmetry (invariance) principles are fundamental laws of nature [1]. They do not directly determine the states, or histories of physical systems, but they do specify the form of the dynamic and other laws of nature.

The present paper deals with the question as to what equations of motion of classical point particles are allowed by the known Euclidean symmetry of the space. More precisely the problem is as follows.

2. The physical problem

Let there be N point particles imbedded in the two dimensional Euclidean space E_2 [2]. According to HOUTAPPEL, VAN DAM and WIGNER [1] the states of this system are given by the initial data $x_i(t)$, $y_i(t)$, $\dot{x}_i(t)$ and $\dot{y}(t)$, where $\dot{x} \equiv \frac{dx}{dt}$ and $i = 1, 2, \ldots, N$, and the history (the motion) of system is determined by the following equations of motion

$$\ddot{x}_i = F_i\,(x_k, y_k, \dot{x}_k, \dot{y}_k \,|\, k = 1, 2, \ldots, N) \tag{1}$$

and

$$\ddot{y}_i = G_i\,(x_k, y_k, \dot{x}_k, \dot{y}_k \,|\, k = 1, 2, \ldots, N)\,, \tag{2}$$

where $i = 1,2,\ldots N$, and the force functions F_k and G_k have $4N$ arguments.

It is a known fact that the equations of motion (1,2) should be covariant under the three parameter Euclidean group, whose elements are

$$x_i' = a + x_i \cos \alpha + y_i \sin \alpha\,, \tag{3}$$

$$y_i' = b - x_i \sin \alpha + y_i \cos \alpha, \tag{4}$$

where a, b and α are arbitrary constants.

Now the question arises: what functional forms of F_i and G_i are allowed by this covariance (i. e. symmetry) requirement? The purpose of this paper is a discussion of this problem and its mathematical solution. The solution is given by equations (32)—(35).

The content of the present paper (i e. the problem stated above together with its subsequent solution) may be considered as the continuation or as the generalization both of Chapter 3.1d. of the paper [1], and of Chapter II. of the paper by CURRIE [3].

3. The mathematical formulation of the problem

3.1 *The mathematical problem*

The accelerations and forces under the group (3,4) should be transformed as follows

$$\ddot{x}_k' = \ddot{x}_k \cos \alpha + \ddot{y}_k \sin \alpha \tag{5}$$

and

$$\ddot{y}_k' = -\ddot{x}_k \sin \alpha + \ddot{y}_k \cos \alpha, \tag{6}$$

i. e.

$$F_k' = F_k \cos \alpha + G_k \sin \alpha \tag{7}$$

and

$$G_k' = -F_k \sin \alpha + G_k \cos \alpha. \tag{8}$$

Since the force functions should preserve their functional form under the group (3,4), F' and G' should have the form

$$F_k' = F_k(x_l', y_l', \dot{x}_l', \dot{y}_l' \mid l = 1, 2, \ldots, N) \tag{9}$$

and

$$G_k' = G_k(x_l', y_l', \dot{x}_l', \dot{y}_l' \mid l = 1, 2, \ldots, N). \tag{10}$$

On the basis of (3,4) and (9,10) the mathematical problem is as follows: we have to find the vector concomitants of the coordinates $x_k(t)$, $y_k(t)$ and of the velocity vectors $\dot{x}_k(t)$, $\dot{y}_k(t)$.

3.2 *The basic functional equation*

The vector concomitants in question obey a functional equation which may be derived from (7) and (8) if we take into account (9) and (10). This equation reads as follows

$$F_k(a + x_l \cos\alpha + y_l \sin\alpha,\ b - x_l \sin\alpha + y_l \cos\alpha,\ \dot{x}_l \cos\alpha + \dot{y}_l \sin\alpha,\ -$$
$$- \dot{x}_l \sin\alpha + \dot{y}_l \cos\alpha \,|\, l = 1, 2, \ldots, N) =$$
$$= F_k(x_l, y_l, \dot{x}_l, \dot{y}_l \,|\, l = 1, \ldots, N) \cos\alpha +$$
$$+ G_k(x_l, y_l, \dot{x}_l, \dot{y}_l \,|\, l = 1, 2, \ldots, N) \sin\alpha \qquad (11)$$

and

$$G_k(a + x_l \cos\alpha + y_l \sin\alpha,\ b - x_l \sin\alpha + y_l \cos\alpha,\ \dot{x}_l \cos\alpha + \dot{y}_l \sin\alpha,\ -$$
$$- \dot{x}_l \sin\alpha + \dot{y}_l \cos\alpha \,|\, l = 1, 2, \ldots, N) =$$
$$= - F_k(x_l, y_l, \dot{x}_l, \dot{y}_l \,|\, l = 1, 2, \ldots, N) \sin\alpha +$$
$$+ G_k(x_l, y_l, \dot{x}_l, \dot{y}_l \,|\, l = 1, \ldots, N) \cos\alpha . \qquad (12)$$

This system of functional equations, where the unknown functions are F_k and G_k, must *identically hold* for arbitrary values of a, b, α, x_l, y_l, $\dot{x}_l$ and $\dot{y}_l$, $l = 1, 2, \ldots, N$. It is now necessary to solve equations (11, 12).

This will be acomplished by the methods of the theory of functional equations [4] in the next Chapter.

4. The mathematical solution of the problem

4.1 *The first step*

Let us, for a moment, suppose that $\alpha = 0$. In this case equations (11) and (12) reduce to the following system of functional equations

$$F_k(a + x_l,\ b + y_l,\ \dot{x}_l, \dot{y}_l \,|\, l = 1, \ldots, N) = F_k(x_l, y_l, \dot{x}_l, \dot{y}_l, \,|\, l = 1, \ldots, N) \qquad (13)$$

and

$$G_k(a + x_i,\ b + y_l,\ \dot{x}_l, \dot{y}_l \,|\, l = 1, 2, \ldots, N) = G_k(x_l, y_l, \dot{x}_l, \dot{y}_l \,|\, l = 1, 2, \ldots, N). \qquad (14)$$

These equations must hold for arbitrary a, b, x_l, y_l, $\dot{x}_l$ and $\dot{y}_l$, $l = 1, 2, \ldots N$.

If the equations (13) and (14) are valid for arbitrary values of a and b, then they are valid also in the special case when

$$a + x_k = 0 \qquad (15)$$

and

$$b + y_k = 0 , \qquad (16)$$

where x_k and y_k are exactly the coordinates of that particle whose force functions F_k and G_k we are going to determine. From (15) and (16) it follows that

$$a = - x_k \qquad (17)$$

and

$$b = - y_k . \qquad (18)$$

Inserting (17) and (18) into (13) and (14) one gets

$$F_k(x_l, y_l, \dot{x}_l, \dot{y}_l \,|\, l = 1, 2, \ldots, N) =$$
$$= f_k(x_l - x_k, y_l - y_k, \dot{x}_m, \dot{y}_m \,|\, l = 1, 2, \ldots, k-1, k+1, \ldots N;$$
$$m = 1, 2, \ldots, N) \tag{19}$$

and

$$G_k(x_l, y_l, \dot{x}_l, \dot{y}_l \,|\, l = 1, 2, \ldots, N) =$$
$$= g_k(x_l - x_k, y_l - y_k, \dot{x}_m, \dot{y}_m \,|\, l = 1, 2, \ldots, k-1, k+1, \ldots, N;$$
$$m = 1, 2, \ldots, N), \tag{20}$$

where f_k and g_k are arbitrary functions of their $4N-2$ arguments. The system (19) and (20) is the general solution of (13) and (14).

4.2 *The second step*

Inserting (19) and (20) into (11) and (12), and introducing the abbreviations

$$x_{lk} \equiv x_l - x_k \tag{21}$$

and

$$y_{lk} \equiv y_l - y_k, \tag{22}$$

we obtain the following system of functional equations

$$f_k(x_{lk} \cos \alpha + y_{lk} \sin \alpha, -x_{lk} \sin \alpha + y_{lk} \cos \alpha, \dot{x}_m \cos \alpha + \dot{y}_m \sin \alpha,$$
$$- \dot{x}_m \sin \alpha + \dot{y}_m \cos \alpha) =$$
$$= f_k(x_{lk}, y_{lk}, \dot{x}_m, \dot{y}_m) \cos \alpha + g_k(x_{lk}, y_{lk}, \dot{x}_m, \dot{y}_m) \sin \alpha \tag{23}$$

and

$$g_k(x_{lk} \cos \alpha + y_{lk} \sin \alpha, -x_{lk} \sin \alpha + y_{lk} \cos \alpha, \dot{x}_m \cos \alpha + \dot{y}_m \sin \alpha,$$
$$- x_m \sin \alpha + \dot{y}_m \cos \alpha) =$$
$$= - f_k(x_{lk}, y_{lk}, \dot{x}_m, \dot{y}_m) \sin \alpha + g_k(x_{lk}, y_{lk}, \dot{x}_m, \dot{y}_m) \cos \alpha, \tag{24}$$

where $m = 1, 2, \ldots, N$, and $l = 1, 2, \ldots, k-1, k+1, \ldots N$.

Since the system (23) and (24) must hold for arbitrary α, x_l, y_l, $\dot{x}_m$ and $\dot{y}_m$, it holds, of course, in the special case when

$$- \dot{x}_k \sin \alpha + \dot{y}_k \cos \alpha = 0, \tag{25}$$

i. e.

$$\operatorname{tg} \alpha = \dot{y}_k / \dot{x}_k, \quad \sin \alpha = \dot{y}_k / \dot{r}_k, \quad \text{and} \quad \cos \alpha = \dot{x}_k / \dot{r}_k, \tag{26}$$

where

$$\dot{r}_k \equiv (\dot{x}_k^2 + \dot{y}_k^2)^{\frac{1}{2}}. \tag{27}$$

Inserting (26) into (23) and (24) we get a system of algebraic equations

$$\varphi_k\left(x_{lk}\frac{\dot{x}_k}{\dot{r}_k}+y_{lk}\frac{\dot{y}_k}{\dot{r}_k},-x_{lk}\frac{\dot{y}_k}{\dot{r}_k}+y_{lk}\frac{\dot{x}_k}{\dot{r}_k},\dot{x}_l\frac{\dot{x}_k}{\dot{r}_k}+\dot{y}_l\frac{\dot{y}_k}{\dot{r}_k},\right.$$

$$\left.,-\dot{x}_l\frac{\dot{y}_k}{\dot{r}_k}+\dot{y}_l\frac{\dot{x}_k}{\dot{r}_k},\dot{r}_k\,\middle|\,l=1,2,\ldots,k-1,k+1,\ldots,N\right)=$$

$$=f_k(x_{lk},y_{lk},\dot{x}_m,\dot{y}_m\,|\,l=1,\ldots,k-1,k+1,\ldots,N\,;\,m=1,\ldots,N)\cdot\frac{\dot{x}_k}{\dot{r}_k}+$$

$$+g_k(x_{lk},y_{lk}.\dot{x}_m,\dot{y}_m\,|\,l=1,\ldots,k-1,k+1,N;m=1,\ldots,N)\cdot\frac{\dot{y}_k}{\dot{r}_k}\qquad(28)$$

and

$$\gamma_k\left(x_{lk}\frac{\dot{x}_k}{\dot{r}_k}+y_{lk}\frac{\dot{y}_k}{\dot{r}_k},-x_{lk}\frac{\dot{y}_k}{\dot{r}_k}+y_{lk}\frac{\dot{x}_k}{\dot{r}_k},\dot{x}_l\frac{\dot{x}_k}{\dot{r}_k}+\dot{y}_l\frac{\dot{y}_k}{\dot{r}_k},\right.$$

$$\left.,-\dot{x}_l\frac{\dot{y}_k}{\dot{r}_k}+\dot{y}_l\frac{\dot{x}_k}{\dot{r}_k},\dot{r}_k\,\middle|\,l=1,2,\ldots,k-1,k+1,\ldots,N\right)=$$

$$=-f_k(x_{lk},y_{lk},\dot{x}_m,\dot{y}_m,\,|\,l=1,\ldots,k-1,k+1,\ldots,N\,;\;m=1,\ldots,N)\cdot\frac{\dot{y}_k}{\dot{r}_k}+$$

$$+g_k(x_{lk},y_{lk},\dot{x}_m,\dot{y}_m\,|\,l=1,\ldots,k-1,k+1,\ldots,N;m=1,\ldots,N)\cdot\frac{\dot{x}_k}{\dot{r}_k},\qquad(29)$$

where φ_k and γ_k are arbitrary functions of their $4N-3$ arguments, and f_k and g_k are the unknown force functions.

The functions f_k and g_k may be evaluated from (28) and (29). We get

$$f_k=\frac{\dot{x}_k\varphi_k-\dot{y}_k\gamma}{\dot{r}_k}\qquad(30)$$

and

$$g_k=\frac{\dot{y}_k\varphi_k+\dot{x}_k\gamma_k}{\dot{r}_k}\,.\qquad(31)$$

Taking into consideration that both φ_k and γ_k are explicit functions of $\dot{r}_k$, the denominators of (30) and (31) can be amalgamated into φ_k and γ_k. Consequently the mathematical solution of the problem stated in Chapter 2 of this paper reads as follows

$$F_k(x_l,y_l,\dot{x}_l,\dot{y}_l)=\dot{x}_k A_k-\dot{y}_k B_k\qquad(32)$$

and

$$G_k(x_l,y_l,\dot{x}_l,\dot{y}_l)=\dot{y}_k A_k+\dot{x}_k B_k\,,\qquad(33)$$

where A_k and B_k are arbitrary functions of their $4N-3$ invariant arguments.

$$A_k = A_k(\dot{r}_k, x_{lk}\dot{x}_k + y_{lk}\dot{y}_k, -x_{lk}\dot{y}_k + y_{lk}\dot{x}_k, \dot{x}_l\dot{x}_k + \dot{y}_l\dot{y}_k, , -\dot{x}_l\dot{y}_k + \dot{y}_l\dot{x}_k \mid l = 1, 2, \ldots, k-1, k+1, \ldots, N) \tag{34}$$

and

$$B_k = B_k(\dot{r}_k, x_{lk}\dot{x}_k + y_{lk}\dot{y}_k, -x_{lk}\dot{y}_k + y_{lk}\dot{x}_k, \dot{x}_l\dot{x}_k + \dot{y}_l\dot{y}_k, , -\dot{x}_l\dot{y}_k + \dot{y}_l\dot{x}_k \mid l = 1, 2, \ldots, k-1, k+1, \ldots, N). \tag{35}$$

5. The physical content of the solution (32)—(35)

5.1 *The basic forces in* E_2

First of all, let us remark that in spite of the fact that from the physical point of view the functions (F_i, G_i) are not force functions but acceleration functions, we will call them force functions in what follows, and in this sense we shall speak about forces.

The arguments of (32)—(35) are the invariants

$$I_1 = \dot{r}_k = (\dot{x}_k^2 + \dot{y}_k^2)^{\frac{1}{2}}, \tag{36}$$

$$I_2 = \dot{x}_l\dot{x}_k + \dot{y}_l\dot{y}_k, \tag{37}$$

$$I_3 = \dot{x}_k\dot{y}_l - \dot{x}_l\dot{y}_k, \tag{38}$$

$$I_4 = (x_l - x_k)\dot{x}_k + (y_l - y_k)\dot{y}_k \tag{39}$$

and

$$I_5 = (y_l - y_k)\dot{x}_k - (x_l - x_k)\dot{y}_k. \tag{40}$$

These invariants are the *basic force expressions* in the two dimensional Euclidean space E_2. They are all *velocity-dependent.*

Apparently the well known distance-dependent forces

$$I_6 = (x_l - x_k)^2 + (y_l - y_k)^2 = r_{lk}^2 \tag{41}$$

are not contained among them. But this is not true, because I_6 may be expressed in terms of I_4, I_5 and I_1 as follows

$$I_6 = \frac{I_4^2 + I_5^2}{I_1^2}, \tag{42}$$

i. e.

$$(x_l - x_k)^2 + (y_l - y_k)^2 = \frac{[(x_l - x_k)\dot{x}_k + (y_l - y_k)\dot{y}_k]^2 + [(y_l - y_k)\dot{x}_k - (x_l - x_k)\dot{y}_k]^2}{\dot{x}_k^2 + \dot{y}_k^2}. \tag{43}$$

Relations (42) and (43) allow the interpretation that the distance-dependent forces (41) are not „elementary" forces, but „composed" ones and they have a velocity-dependent dynamism.

5.2 *The transformation character of A_k and B_k*

The force functions F_k and G_k are the components of the vector (F_k, G_k). On the basis of (32) and (33) they may be represented in matrix form as follows:

$$\begin{pmatrix} F_k \\ G_k \end{pmatrix} = A_k \begin{pmatrix} \dot{x}_k \\ \dot{y}_k \end{pmatrix} + \begin{pmatrix} 0 & -B_k \\ B_k & 0 \end{pmatrix} \begin{pmatrix} \dot{x}_k \\ \dot{y}_k \end{pmatrix}. \tag{44}$$

It is seen from (44) that, in accordance with (34), A_k is an invariant.

On the basis of (35) B_k should also be an invariant. In view of the fact that the single component of an antisymmetric tensor (in E_2) is invariant under the group (3, 4), the equation (44) does not conflict with the expression (35). Thus B_k is also an invariant.

Since, on the one hand, both functions A_k and B_k are invariants and, on the other, $\dot{x}_k$ and $\dot{y}_k$ are components of vectors, all F_k and G_k are components of vectors.

5.3 *The "magnetic" forces*

Finally, we remark that the second term in (44), i. e.

$$\begin{pmatrix} F_k \\ G_k \end{pmatrix} = \begin{pmatrix} 0 & -B_k \\ B_k & 0 \end{pmatrix} \begin{pmatrix} \dot{x}_k \\ \dot{y}_k \end{pmatrix} \tag{45}$$

is of magnetic (Lorentz) type.

6. Conclusion

It is seen from (44), (34) and (35) that the validity of a symmetry law *in fact restricts the form* of the dynamic laws of physical systems.

REFERENCES AND NOTES

1. R. M. F. Houtappel, H. van Dam and E. P. Wigner, Rev. Mod. Phys., **37,** 595, 1965.
2. The more realistic (and more complicated) case of three dimensional space will be dealt with in another publication.
3. D. G. Currie, Phys. Rev., **142,** 817, 1966.
4. J. Aczél, Vorlesungen über Funktionalgleichungen, VEB, Berlin, 1961;
M. Ghermanescu, Ecuatii functionale, Ed. Acad. Rep. Popul. Roman, Bucuresti, 1960; and
M. Kuczma, A survey of the theory of functional equations, Publ. Elektroteh. Fak., **130,** Beograd, 1964.

ТЕОРИЯ УРАВНЕНИЙ ДВИЖЕНИЯ НА ОСНОВЕ СИММЕТРИИ ПРОСТРАНСТВА

Часть I

Система точечных частиц в пространстве E_2

Г. КНАПЕЦ

Р е з ю м е

Решением системы функциональных уравнений [(11) и (12)] доказывается, что в силу эвклидовой симметрии пространства E_2 [(3) и (4)] форма силовых функций [(32) — (35)] динамического закона [(1) и (2)] системы точечных частиц является определенной, то есть не может быть произвольной.

Acta Physica Academiae Scientiarum Hungaricae, Tomus 23 (2), pp. 211—223 (1967)

DAS ELEKTRONENBANDENSPEKTRUM DES CsD-MOLEKÜLS IM SICHTBAREN SPEKTRALGEBIET

Von

M. L. CSÁSZÁR

ZENTRALFORSCHUNGSINSTITUT FÜR PHYSIK, BUDAPEST

und

E. KOCZKÁS

ATOMPHYSIKALISCHER LEHRSTUHL DER TECHNISCHEN UNIVERSITÄT, BUDAPEST

(Vorgelegt von I. Kovács. — Eingegangen: 5. VII. 1966)

Das Spektrum des CsD-Moleküls wurde zwischen 4500 Å und 6250 Å aufgenommen und die Rotationsanalyse von 17 Banden durchgeführt. Auf Grund dieser Analyse wurden mit Hilfe des Isotopie-Effektes die von ALMY und RASSWEILER für den angeregten Zustand des CsH-Moleküls angegebenen v' Quantenzahlen um drei Einheiten korrigiert.

Das Elektronenbandenspektrum des CsH-Moleküls wurde von ALMY und RASSWEILER im Jahre 1938 in Absorption aufgenommen [1]. Im Spektralbereich zwischen 4500 Å und 6250 Å erschien das Viellinienspektrum von 31 kantenlosen Banden. Die Analyse bewies, dass das aufgenommene Bandensystem dem Übergang $^1\Sigma \leftarrow {}^1\Sigma$ entspricht. In den Konstanten des oberen Zustandes zeigte sich dieselbe Anomalie wie bei den anderen Alkalihydriden. Die genauere Bestimmung der Konstanten aber erschwert der Umstand, dass die Vibrations-Analyse selbst von ALMY und RASSWEILER als unsicher beurteilt wurde. Es schien daher interessant das Spektrum des CsD-Moleküls zu untersuchen.

Experimentelles

Mit Hilfe des bei Absorptionsaufnamen der Alkalihydride allgemein (auch von ALMY und RASSWEILER) benützten Eisenrohres konnte ein reines CsD-Spektrum nicht photographiert werden. Um ein hydridfreies CsD-Spektrum aufnehmen zu können, haben wir ein Verfahren mit einem geschlossenen Absorptionsrohr aus ziemlich alkalibeständigem Supremaxglas entwickelt. [2] An seinen Enden hatte dieses Rohr keine Quarzfenster, wir begnügten uns mit Supremaxglasfenstern, da doch das CsD-Spektrum in das sichtbare Spektralgebiet fällt. Das Rohr war 110 cm lang mit 1,5 cm lichter Weite, in der Mitte mit einem kurzen Seitenrohr versehen. (siehe Abb. 1). Dieses Seitenrohr diente zur Einführung des Cs-Metalls und des D_2-Gases. Das Cs-Metall wurde aus Caesiumazid durch thermische Dissoziation und durch nachfolgende Vakuum-destillation in das Rohr eingeführt. [3] Danach wurde das D_2-Gas elektrolytisch aus schwerem Wasser (mit 99,9% D_2O) hergestellt und durch eine Pd-Kapillare ebenfalls in das Rohr geführt. Beim gewünschten D_2-Druck wurde das Seitenrohr zugeschmolzen.

Zur Herstellung des CsD-s musste das Gemisch auf 600 °C erhitzt werden. Die Heizung erfolgte mit isolierten Kanthaldrähten. Der größte Teil des Caesiums sammelte sich im Seitenrohr, das bei den Aufnahmen nach unten zu lag. Es wurde von den anderen Teilen getrennt geheizt, um in das Hauptrohr mehr oder weniger Cs-Dampf hineinlassen zu können.

Der Cs-Gehalt betrug etwa 4 g. Am Anfang des Ausheizens, von etwa 370 °C an, machten die dunkelgrünen Cs-Dämpfe eine Aufnahme noch unmöglich. Die CsD-Banden, die wir hauptsächlich im grünen Wellenlängenbereich mit dem Handspektroskop wahrnehmen konnten, erschienen erst

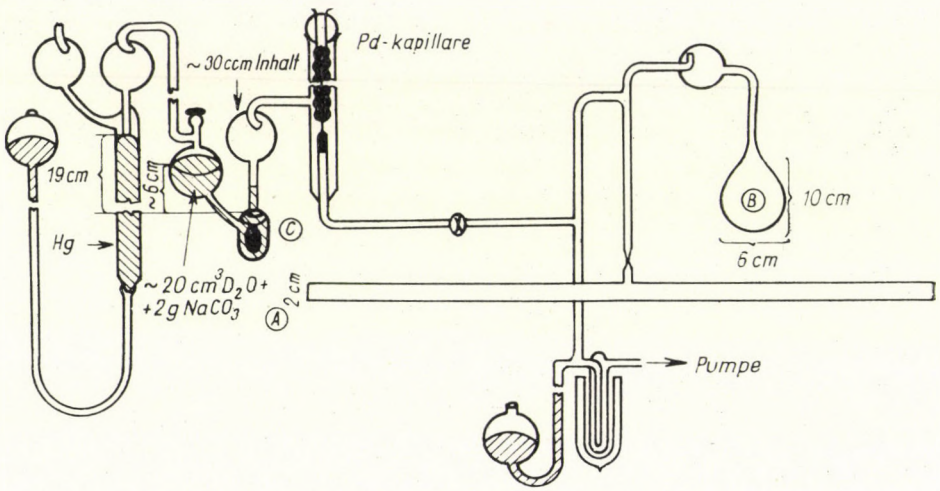

Abb. 1

nach einigen Stunden bei 550° C±20 °C. Als kontinuierliche Lichtquelle diente eine Xenon-Hochdrucklampe von 300 W. Zu den Aufnahmen benützten wir einen Konkavgitterspektrographen mit 1,3 Å/mm reziproker Dispersion. Die Expositionszeiten schwankten zwischen 2 und 4 Stunden.

Im allgemeinen beobachteten wir dass die jeweilige Aufnahme einen Wellenbereich umfaßt, an dessen Grenzen die Spektrallinien rechts und links diffuse und schwächer werden, um dann ganz zu verschwinden. Die Banden des Cs_2-Moleküls verursachten keine Störungen.

Analyse

Auf unseren Aufnahmen konnten ca. 600 Linien (ungefähr 95% sämtlicher von uns beobachteten Linien) gemessen werden. Die Messgenauigkeit beträgt im Durchschnitt etwa 0,03 Å, jedoch nur 0,1 Å bei den diffuseren und

schwächeren Linien. Es ist uns gelungen, diese Linien auf Grund einer Rotationsanalyse in Banden einzureihen. Insgesamt fanden wir 12 Bande mit $v'' = 0$ und 5 Bande mit $v'' = 1$ unterem Zustand.

Wie zu erwarten war, zeigte das CsD-Spektrum die gleiche Struktur wie die Alkalihydride (LiH, NaH, KH, RbH, CsH) und die bisher bekannten Alkalideuteride (LiD, NaD, KD): $^1\Sigma - ^1\Sigma$ Übergang, ziemlich offene, schwer zu erkennende Bandenstruktur. Infolge des Isotopieeffektes, der eine Verdichtung der Linien bewirkt, sind jedoch einzelne Banden leichter wahrnehmbar als beim CsH-Spektrum.

Die Vibrationsanalyse konnten wir jedoch erst nach Beendigung der Rotationsanalyse vornehmen. In mehreren Banden war ein Teil der einzelnen Zweige gut erkennbar, so 10 bis 15 Linien. Es war möglich, die $\Delta\nu_{\text{rot}}$ des CsD-Moleküls, d. h. die Wellenzahlen-Differenzen der aufeinander folgenden Linien mit den CsH-Rotationskonstanten aus der Arbeit von ALMY und RASSWEILER und mit der ϱ-Zahl aus der Formel

$$\varrho^2 = \left(\frac{1}{M_D} + \frac{1}{M_{Cs}}\right) \Big/ \left(\frac{1}{M_H} + \frac{1}{M_{Cs}}\right)$$

rechnerisch zu bestimmen.

Die aus den so ermittelten und aus den im Spektrum gefundenen Linien gebildeten $\Delta\nu_{\text{rot}}$ -Differenzen zeigen eine gute Übereinstimmung. Als Beispiel diene die Tabelle I, in der die Wellenzahlendifferenzen der (12,0) Bande zusammengefasst sind. Auf Grund dieser Übereinstimmung war die J-Numerierung eindeutig gegeben. Mit Hilfe von $\Delta\nu_{\text{rot}}$ liessen sich auch die weniger charakteristischen Zweige erkennen. Es ist uns gelungen, die 600 beobachteten Linien in 17 Bande einzureihen. Indes ist die Änderung der B'_v Konstante mit v' so klein, dass die auf die verschiedenen Vibrationsniveaus bezogenen $\Delta\nu_{\text{rot}}$-Werte innerhalb der Messfehler übereinstimmen und somit keine Grundlage für die Numerierung der v' abgeben können.

Die Intensität der Linien steigt innerhalb der einzelnen Banden mit wachsender Quantenzahl, d. h. bis zu etwa $J = 4$ sind die Linien noch schwach, von da ab bis etwa $J = 24-30$ sind sie von guter Intensität. Die Tabelle II enthält die Wellenzahlen der Bandenlinien.

Die Richtigkeit der Rotationsanalyse wurde mit den Kombinationsdifferenzen für die gleichen unteren Zustände kontrolliert.

Die Rotationskonstanten B_v und D_v berechneten wir nach der aus der Literatur bekannten graphischen Methode [4] (Tabelle III.)

Die Rotationsanalyse hat bewiesen, dass 12 bzw. 5 der Banden den gleichen unteren Zustand haben. Da es sich um eine Absorptionsaufnahme handelt, sind diese Zustände offenbar $v'' = 0$ und $v'' = 1$. Da weiterhin die Rotationskonstanten der Schwingungsniveaus im angeregten (oberen) Zustand

einander sehr ähnliche Werte haben, lässt sich auf Grund der Kombinationsdifferenzen nicht eindeutig bestimmen, welchen Banden mit dem unteren Zustand $v'' = 1$ bzw. $v'' = 0$ der gleiche obere Zustand zugehört. Zur Feststellung der Numerierung war die Schwingungsanalyse erforderlich. Die genauen Werte der einzelnen Bandenkanten bestimmten wir nach der bekannten graphischen Methode. Sie gestattet es die Schwingungsdifferenzen $\Delta G'$ rechnerisch zu ermitteln.

Auf Grund der Schwingungsdifferenzen $\Delta G'$ konnte es nun leicht entschieden werden, welche Bande mit verschiedenem unteren Zustand denselben oberen Zustand besitzen.

In der Annahme, dass die Analyse von ALMY und RASSWEILER richtig ist, bestimmten wir mit ihren Schwingungskonstanten und mit der Zahl ϱ auf Grund der Gleichung [4]

$$\nu = \nu_0 + \left[\varrho\,\omega'_e\left(v' + \frac{1}{2}\right) - \varrho^2\,\omega'_e\,x'_e\left(v' + \frac{1}{2}\right)^2 + \ldots\right] -$$

$$- \left[\varrho\,\omega''_e\left(v'' + \frac{1}{2}\right) - \varrho^2\,\omega''_e\,x''_e\left(v'' + \frac{1}{2}\right)^2\right]$$

die Werte der zu erwartenden Bandenkanten des CsD-Moleküls und wählten v' so, dass der Unterschied zwischen den gefundenen und den berechneten Bandenkanten möglichst klein sei. Doch auch im günstigsten Falle ergab sich eine Abweichung des berechneten Wertes vom gemessenen um etwa 30 cm^{-1}. Offensichtlich muss die Numerierung ALMYs und RASSWEILERS geändert werden.

Die richtige Numerierung suchten wir durch den Vergleich der $\Delta G'$-Werte im angeregten Zustand des CsH-Moleküls mit jenem des CsD-Moleküls zu ermitteln.

In Betracht zu ziehen ist die Tatsache, dass im Sinne der Theorie des Isotopie-Effektes

$$\Delta G'_{\mathrm{CsD}}(v+1) = \varrho\,\Delta G'_{\mathrm{CsH}}(\varrho\,[v+1])$$

ist, dass also die $\Delta G'_{\mathrm{CsD}}$-Werte im angeregten Zustand des CsD-Moleküls aus den analogen $\Delta G'_{\mathrm{CsH}}$-Werten des CsH-Moleküls und mit Hilfe der Zahl ϱ berechnet werden können [5] [6].

Natürlich ist das nur dann richtig, wenn man mit der entsprechenden v'-Numerierung arbeitet. Die auf CsD bezogenen $\Delta G'_{\mathrm{CsD}}$-Werte berechneten wir zuerst auf Grund dieser Gleichung und der Numerierung von ALMY und RASSWEILER, dann auch so, dass wir die v' Werte im Vergleich zu dieser Numerierung um 1, 2, 3, 4, 5. Einheiten höher wählten.

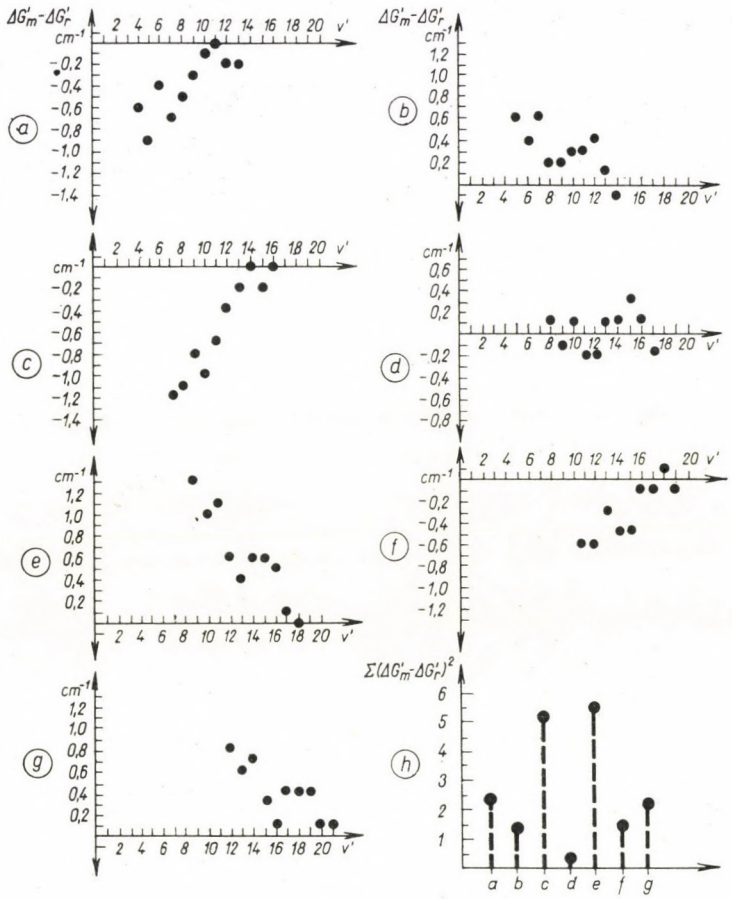

Abb. 2

Die Differenzen der gemessenen Werte $\Delta G'_m$ und der mit den CsH Konstanten berechneten Werte $\Delta G'_r$ des CsD-Moleküls im Falle, wenn:
a) die Berechnung auf Grund von ALMY und RASSWEILERS v' Numerierung ausgeführt wird;
b) v' im Vergleich zur Numerierung von ALMY und RASSWEILERS um 1; c) um 2; d) um 3;
e) um 4; f) um 5; g) um 6 vergrössert ist.
h) Die Werte von $\Sigma (\Delta G'_m - \Delta G'_r)^2$ in den oberen spezifizierten Fällen.

An der Abbildung 2 lässt sich gut erkennen, dass sich zwischen den gemessenen und berechnten $\Delta G'_{CsD}$-Werten die beste Übereinstimmung zeigt, wenn man die v'-Numerierung von ALMY und RASSWEILER bei den CsH-Banden um 3 Einheiten erhöht. Damit wird auch die Vibrationsnumerierung der Banden des CsD-Moleküls bestimmt.

Die Tabelle IV enthält die Bandenkanten des CsD-Moleküls mit der richtigen v'-Numerierung.

Auf die Bestimmung der Vibrationskonstanten und die Untersuchung des Isotopieeffektes werden wir in einer späteren Arbeit kommen.

Zum Schluss sprechen wir Herrn Prof. I. KOVÁCS unseren aufrichtigen Dank aus. Herrn Prof. T. MÁTRAI danken wir verbindlichst für die Anregung zu dieser Arbeit und für sein wohlwollendes Interesse. Wir danken ferner Herrn K. RÓZSA für die Herstellung des Caesiums und für seine Mitarbeit bei den Aufnahmen.

Tabelle I

Gemessene und berechnete Rotationstermdifferenzen der (12,0) Bande des CsD-Moleküls

J	*R*-Zweig			*P*-Zweig		
	$\Delta^* \nu_{rot}$ (gemessen)	$\Delta \nu_{rot}$ (berechnet)	$\Delta^* \nu_{rot} - \Delta \nu_{rot}$	$\Delta^* \nu_{rot}$ (gemessen)	$\Delta \nu_{rot}$ (berechnet)	$\Delta^* \nu_{rot} - \Delta \nu_{rot}$
1						
2	1,5	1,9	−0,4	3,9	4,3	−0,4
3	3,9	3,4	+0,5	5,3	5,7	−0,4
4	5,0	5,0	0	7,8	7,3	+0,5
5	6,6	6,5	+0,1	8,5	8,9	−0,4
6	7,9	8,0	−0,1	10,6	10,4	+0,2
7	9,7	9,6	+0,1	12,1	11,9	+0,2
8	11,0	11,1	−0,1	13,3	13,5	−0,2
9	12,7	12,7	0	15,0	15,0	0
10	14,1	14,0	+0,1	16,5	16,5	0
11	15,9	15,6	+0,3	18,0	17,8	+0,2
12	17,2	17,2	0	19,5	19,4	+0,1
13	18,7	18,7	0	21,1	21,0	0
14	20,4	20,2	+0,2	22,6	22,5	+0,1
15	21,8	21,8	0	24,0	23,9	+0,1
16	23,3	23,1	+0,2	25,5	25,4	+0,1
17	24,9	24,8	+0,1	27,2	27,0	+0,2
18	26,4	26,2	+0,2	28,6	28,5	+0,1
19	28,1	27,9	+0,2	30,2	29,9	+0,3
20	29,5	29,5	0	31,7	31,5	+0,2

Tabelle II

Wellenzahlen der Bandenlinien

J	Die Bande (8,0)		Die Bande (9,0)		Die Bande (10,0)	
	P-Zweig	*R*-Zweig	*P*-Zweig	*R*-Zweig	*P*-Zweig	*R*-Zweig
0		18761,6				
1	18755,3	760,1	18920,6	18924,1	19088,5	
2	751,0	757,3	916,0	922,1	083,7	19089,6
3	745,8	753,5	910,6	919,3	070,5	086,3
4	738,0		903,5	913,8	075,0	081,1
5	729,3	741,9	894,4	907,3	062,1	074,7
6	718,6	733,9	883,7	899,0	051,6	066,7
7	706,8	724,2	871,9	889,7	039,8	057,2
8	693,6	713,5	858,7	878,2	026,4	046,2
9	678,9	700,2	843,3	865,5	011,6	033,6
10	661,9	686,0	826,7	851,2	18995,0	019,4
11	643,6	670,4	808,8	835,4	977,0	003,8
12	623,2	652,9	789,0	818,1	957,5	18986,5
13	603,1	634,1	768,2	799,3	936,8	967,7
14	580,4	613,7	745,8	778,9	913,8	947,4
15	555,9	591,6	721,6	757,3	889,7	925,6
16	530,5	568,4	695,9	733,9	864,2	902,4
17	503,1	543,1	668,8	709,0	836,8	877,3
18	474,2	516,3	640,1	682,5	808,1	850,6
19		488,3	610,3	653,8	778,0	822,6
20	412,5	458,5	578,4	624,8	746,8	793,0
21		427,7	544,8	593,9	713,5	762,4
22			510,4	561,5	678,2	729,3
23	307,9		474,2	527,3	642,5	695,8
24			437,1		604,6	660,3
25					565,6	623,2
26					525,2	586,1
27					483,3	544,8
28					440,7	
29						

Tabelle II (Fortsetzung)

J	Die Bande (11,0)		Die Bande (12,0)		Die Bande (13,0)	
	P-Zweig	*R*-Zweig	*P*-Zweig	*R*-Zweig	*P*-Zweig	*R*-Zweig
0						19610,2
1		19261,9	19431,0	19435,0	19605,8	609,2
2	19254,7	260,5	427,1	433,1		607,3
3	248,8	256,8	421,8	429,6	595,7	603,9
4	241,6	252,2	414,0	424,6	588,0	598,8
5	232,8	245,3	405,5	418,0	579,4	592,2
6	222,4	237,6	394,9	410,1	569,2	584,4
7	210,6	228,0	382,8	400,4	557,1	574,7
8	197,0	217,1	369,5	389,4	543,8	563,6
9	182,1	204,3	354,5	376,7	528,8	551,0
10	165,6	190,0	338,0	362,6	512,3	536,7
11	147,5	174,3	320,0	346,7	494,1	520,9
12	128,0	157,1	300,5	329,5	474,6	503,6
13	106,8	138,2	279,4	310,8	453,5	484,9
14	084,2	117,9	256,8	290,4	431,0	464,3
15	060,0	096,1	232,8	268,6	406,8	442,6
16	034,7	072,4	207,3	245,3	381,1	419,2
17	007,6	047,7	180,1	220,4	354,2	394,3
18	18978,9	021,3	151,5	194,0	325,4	367,8
19	948,9	18993,5	121,3	165,6	295,3	339,8
20	917,3	964,1	089,6	136,4	263,6	310,3
21	883,9	933,1	056,2	105,4	230,6	279,4
22	849,1	900,6	021,8	072,4	195,8	246,9
23	813,1	866,7	18985,7	038,9	159,6	212,9
24	775,7	830,7	948,2	003,3	122,0	177,2
22	736,6	793,9	909,1		082,9	140,0
26	695,9	755,3	868,3		042,1	101,7
27	653,8	715,5			000,2	061,3
28	610,3	673,8			18956,7	019,8
29	565,6	630,9			911,8	18977,0
30	519,0	586,1			865,5	932,6
31	471,1	540,4			817,0	886,0
32	421,1				768,2	
33					717,0	

Tabelle II (Fortsetzung)

J	Die Bande (14,0)		Die Bande (15,0)		Die Bande (16,0)	
	P-Zweig	*R*-Zweig	*P*-Zweig	*R*-Zweig	*P*-Zweig	*R*-Zweig
0						
1		19785,0		19962,2		
2	19777,2	783,0		960,0		20138,1
3	770,8	779,6	19948,0			134,2
4	763,9	774,4	940,6	951,3	20118,7	129,3
5	755,2	768,2	932,0	944,8	109,7	122,5
6	744,9	760,1	921,6	936,8	099,4	114,3
7	732,9	750,3	909,9	927,1	087,4	104,6
8	719,4	739,1	896,4	916,0	073,7	093,6
9	704,4	726,4	881,2	903,2	058,7	080,7
10	687,9	712,2	864,5	888,9	041,8	066,5
11	669,8	696,4	846,7	873,1	024,0	050,3
12	650,3	679,2	826,7	855,7	004,2	033,1
13	629,1	660,4	805,8	836,7	19983,1	014,0
14	606,5	639,9	783,0	816,3	960,0	19993,7
15	582,3	618,1	758,7	794,4	936,0	971,4
16	556,5	594,5	732,9	770,8	910,3	948,0
17	529,4	569,6	705,7	745,8	883,0	922,7
18	500,7	543,0	677,1	719,4	854,2	896,4
19	470,5	515,0	646,8	691,1	823,8	868,1
20	438,7	485,4	615,1	661,6	791,9	838,2
21	405,5	454,4	581,6	630,4	758,7	807,1
22	370,9	421,8	546,9	597,6	723,6	774,3
23	334,8	387,7	510,6	563,6	687,1	740,0
24	297,0	352,2	472,9	527,9	649,5	704,4
25	257,8	314,9	433,7	490,7	610,2	666,9
26	217,1	276,4	392,9	452,0	569,2	628,1
27	175,1	236,2	350,7	411,7	526,7	587,4
28	131,4	194,7	306,9	370,1	483,2	545,9
29	086,3	151,5	261,9	326,9	437,8	502,6
30	039,8	106,8	215,2	282,1	391,1	457,8
31	18991,8	060,7	167,0	236,2	342,9	411,7
32	942,4	013,1	117,5	188,3	293,3	363,8
33	891,3	18964,3		139,2	242,1	314,5
34	838,6	913,8				

Tabelle II (Fortsetzung)

J	Die Bande (17,0)		Die Bande (18,0)		Die Bande (19,0)	
	P-Zweig	*R*-Zweig	*P*-Zweig	*R*-Zweig	*P*-Zweig	*R*-Zweig
0						
1		20316,5				
2						
3	20303,4	312,1				
4		307,4				
5	287,9	301,0				
6	277,8	292,7	20456,0			
7	265,9	282,9	444,1	20461,6		
8	251,3	271,3	430,8	450,0		
9	237,0	258,8	416,6	437,3		
10	220,4	244,4		422,8		
11	202,2	228,6	380,5	406,7		
12	182,5	210,9	360,4	389,0		
13	161,1	192,1	339,0	370,1		
14	138,1	171,3	316,5	349,4		
15	113,7	149,1		327,2		
16	087,9	125,7	265,9	303,4	20444,2	
17	060,6	100,3	238,6	277,8	416,6	20456,0
18	031,4	073,7	209,7	251,3	387,4	428,8
19	001,2	045,1	179,1		357,1	400,3
20	19969,3	015,5	146,9	192,9	324,6	370,2
21	936,0	984,3	113,7	161,1	291,0	339,0
22	900,8	951,3	078,4	128,3	255,9	305,6
23	864,5	916,8	041,8	093,6	218,9	271,3
24	826,7	881,2	003,7	057,6	180,9	
25	786,9	843,5	19963,9	020,3	141,0	197,2
26	745,8	804,8	922,7	19981,3	099,4	157,6
27	703,4	764,1	881,2	940,6	056,9	116,8
28	659,4	722,0	835,9	898,3	012,5	
29	614,2	678,8	790,4	854,2		
30	567,1	633,8	743,6	809,9		
31	518,9	587,4	695,1			
32	469,2	539,4	645,5	714,8		
33	418,0	490,1	593,7	665,3		
34	365,1		540,6	615,1		

Tabelle II (Fortsetzung)

J	Die Bande (8,1)		Die Bande (9,1)		Die Bande (10,1)	
	P-Zweig	*R*-Zweig	*P*-Zweig	*R*-Zweig	*P*-Zweig	*R*-Zweig
0						
1					18466,7	18471,9
2				18302,9	463,6	470,0
3			18290,4	298,3	458,5	466,7
4			284,1	294,1	451,4	461,8
5			274,6	287,7		455,6
6		18114,8	264,7	279,8	432,6	447,9
7	18087,7	105,2	253,1	270,5	421,0	438,4
8	074,6	094,5	239,8	259,7	408,0	427,7
9	060,1	081,8	225,3	247,5	393,1	415,3
10	044,6	068,3	209,3	233,6	377,4	401,7
11	026,2	052,9	191,6	218,4	359,9	386,4
12	007,4	036,1	172,5	201,7	340,8	369,9
13	17986,3	018,0	152,1	183,2	320,2	351,5
14	964,4	17997,8	130,0	163,5	298,3	331,9
15	941,1	976,7	106,8	142,3	274,6	310,5
16	916,2	954,0	081,8	119,6	249,8	287,7
17		929,7	055,3	095,5	223,7	263,6
18			027,3	069,7	195,6	238,1
19			17997,8	042,5	166,2	211,0
20			967,1	013,9	135,5	182,1
21			934,8	17983,7	103,4	152,1
22			901,1	951,8	069,7	120,7
23				918,8	034,4	087,7
24				884,2	17997,8	052,9
25					959,6	017,0
26					920,1	17979,5
27						941,1
28						901,1

Tabelle II (Fortsetzung)

J	Die Bande (11,1)		Die Bande (12,1)	
	P-Zweig	*R*-Zweig	*P*-Zweig	*R*-Zweig
0				
1	18638,9			18815,1
2	634,1	18640,1	18805,3	812,3
3	628,6	637,3	801,4	808,8
4	621,4	632,3	793,9	804,7
5	613,7	626,2	785,6	798,6
6	603,1	618,3	775,4	790,8
7	591,6	609,2	764,2	781,2
8	578,3	598,3	751,1	770,5
9	563,9	586,1	736,6	758,7
10	547,8	572,3		745,0
11	530,5	557,0	702,7	729,3
12	511,2	540,4	683,5	712,8
13	490,7	522,0	663,3	694,7
14	468,7	502,4	641,4	675,0
15	445,2	481,3	617,9	653,8
16	420,4	458,5	592,9	630,9
17	394,1	434,4	566,5	606,9
18	366,2	408,6	538,6	581,2
19	336,6	381,5	509,3	554,0
20	306,1	352,9	478,6	525,2
21	273,9	322,8	446,3	495,3
22	239,8	291,3	412,5	463,6
23	205,0	258,2	377,4	430,7
24	168,4	223,7	340,8	396,1
25	130,0	187,9	302,9	359,9
26	091,2	150,4	263,6	322,8
27	050,1	111,6	222,4	283,1
28	007,4	071,3	180,3	243,6
29	17964,4	029,1	135,5	
30	918,8	17986,3	091,2	158,6
31		943,3	044,0	113,6
32			17997,8	068,3

Tabelle III

Rotationskonstanten des CsD-Moleküls

v'	B'_v
8	0,58
9	0,58
10	0,58
11	0,58
12	0,58
13	0,58
14	0,59
15	0,58
16	0,58
17	0,58
v''	B''
0	1,35
1	1,33

Tabelle IV

Bandenkanten und Schwingungsdifferenzen des CsD-Moleküls

v'	$v''=0$	$v''=1$	$\Delta G'$
8	18758,1		
9	18923,3	18304,0	165,2
10	19091,0	18472,0	167,9
11	19261,6	18642,5	170,6
12	19434,1	18815,0	172,5
13	19608,3		174,2
14	19784,1		175,8
15	19961,1		177,0
16	20139,0		177,9
17	20317,2		178,2
18	20495,6		178,4
19			
$\Delta G''$	619,1		

LITERATUR

1. ALMY und RASSWEILER, Phys. Rev., **53,** 890, 1938.
2. L. CSÁSZÁR, E. KOCZKÁS, T. MÁTRAI, KFKI Közlemények, **12,** 135, 1964.
3. L. CSÁSZÁR und K. RÓZSA, KFKI Közlemények. **12,** 175, 1964.
4. G. HERZBERG, Molecular Spectra and Molecular Structure, Van Nostrand, New York, 1953.
5. R. S. MULLIKEN, Phys. Rev., **25,** 119, 1925.
6. E. OLSSON, Zs. f. Phys. **93,** 206, 1935.

СПЕКТР ЭЛЕКТРОННОЙ СВЯЗИ МОЛЕКУЛЫ CsD В ВИДИМОЙ ОБЛАСТИ

М. Л. ЧАСАР и Э. КОЦКАШ

Р е з ю м е

Дается спектр молекулы CsD в интервале 4500 Å и 6250 Å, проводится ротационный анализ для 17 связей.

Acta Physica Academiae Scientiarum Hungaricae, Tomus 23 (2), pp. 225—236(1967)

NON-RELATIVISTIC APPROXIMATION OF THE DIRAC CURRENT

By

M. HUSZÁR

CENTRAL RESEARCH INSTITUTE FOR PHYSICS, BUDAPEST

(Presented by L. Jánossy. — Received 23. VIII. 1966)

By making use of the FOLDY-WOUTHUYSEN transformation the non-relativistic charge and current density is derived from the Dirac equation up to the second order in p/mc. The terms obtained in addition to non-relativistic Pauli charge and current density are interpreted as follows. The moving magnetic dipole corresponds to an electric one interacting with the electric field like a polarization charge $\varrho_\pi = -\operatorname{div} \pi$. The current corresponding to this polarization charge appears in the usual form $\frac{\partial \pi}{\partial t}$. The Thomas precession gives the contributions $\varrho_T = \frac{1}{2} \operatorname{div} \pi$ and $\mathbf{j}_T = -\frac{1}{2} \frac{\partial \pi}{\partial t}$ to the charge and current density, respectively, and, thus, only half of the polarization charge and current is effective. An $\mathbf{E} \times \sigma$ type term arises in the current since the mechanical and canonical momenta are not now simply related through $m\gamma \mathbf{v} = \boldsymbol{p} - \frac{e}{c} \mathbf{A}$. An additional Darwin type term arises in the charge density which cannot be interpreted classically.

Introduction

The familiar method for the transition to nonrealtivistic approximation of the Dirac equation is as follows [1]:

We separate the equation for the four-component spinor $\Psi = (\varphi_1\ \varphi_2\ \chi_1\ \chi_2)$ into two simultaneous equations for the two-component spinors $(\varphi_1\ \varphi_2)$ and $(\chi_1\ \chi_2)$. Then by expanding φ and χ in powers of p/mc up to a certain order the component χ can be successively eliminated. Thus, in the first step we obtain the Pauli equation. In the following step we also get a Schrödinger type equation which, however, cannot be interpreted as a wave equation since it contains a non-Hermitean Hamiltonian and consequently the norm of the wave function implied is not conserved. This difficulty can be removed by introducing a new wave function $\varphi' = A\varphi$ instead of φ and a new Hamiltonian $H' = AHA^{-1}$ where A is a nonunitary operator which can be found from the requirement that H' should be Hermitean. The FOLDY—WOUTHUYSEN method, on the other hand, uses unitary transformations only so it seems to be a more direct and elegant method for the transition to non-realtivistic approximation [2].

The following conventions and notations will be used. For the Dirac matrices γ^μ $(\mu = 0, 1, 2, 3)$ we adopt the representation where γ^0 is diagonal

and Hermitean and $\gamma^1 \gamma^2, \gamma^3$ are anti-Hermitean. The explicit form of γ^μ is given in [3]. We define also three matrices

$$\Sigma^k = \begin{pmatrix} \sigma^k & 0 \\ 0 & \sigma^k \end{pmatrix} (k = 1, 2, 3),$$

where σ^k are the Pauli matrices. The three dimensional vectors $\boldsymbol{\gamma}^k$, Σ^k, σ^k will be denoted by $\boldsymbol{\gamma}$, Σ and σ, respectively. For the gauge invariant momentum $\mathbf{p} - \frac{e}{c}\mathbf{A} = \frac{\hbar}{i}\nabla - \frac{e}{c}\mathbf{A}$ we write $\mathbf{P}$.

Let φ_1 and φ_2 be two arbitrary spinors and a an operator. Then, operators $\vec{a}$, $\overleftarrow{a}$ and $\ddot{a}$ are defined by

$$\varphi_1^+ \vec{a} \varphi_2 = \varphi_1^+ a \varphi_2, \quad \varphi_1^+ \overleftarrow{a} \varphi_2 = (a \varphi_1)^+ \varphi_2, \quad \ddot{a} = \frac{1}{2}(\vec{a} + \overleftarrow{a}).$$

Derivation of the non-relativistic current

Let us consider operators acting upon the four-component spinors. Following FOLDY we call the operators of type

$$O = \begin{pmatrix} 0 & A \\ B & 0 \end{pmatrix}, \quad E = \begin{pmatrix} A & 0 \\ 0 & B \end{pmatrix}$$

odd and even, respectively, in the given representation of the γ matrices. Here A and B are arbitrary 2×2 matrices. An odd operator mixes the two upper and lower components of Dirac spinors, while an even one does not. Thus, e. g. γ^k is an odd operator while Σ^k kis an even one.

We start from the Dirac equation

$$i\hbar \frac{\partial \Psi}{\partial t} = (c \gamma^0 \boldsymbol{\gamma} \mathbf{P} + \gamma^0 m c^2 + e \Phi) \Psi \equiv H \Psi \tag{1}$$

and introduce the transform of Ψ as

$$\Psi^{(1)} = e^{-\lambda S(\mathbf{r},t)} \Psi,$$

where $e^{-\lambda S}$ is a unitary operator to be defined later, while λ is chosen to be $-1/2\ mc^2$.

$\Psi^{(1)}$ satisfies the equation

$$i\hbar \frac{\partial \Psi^{(1)}}{\partial t} = H^{(1)} \Psi^{(1)},$$

where

$$H^{(1)} = i\hbar \left(\frac{\partial e^{-\lambda S}}{\partial t}\right) e^{\lambda S} + e^{-\lambda S} H e^{\lambda S}. \tag{2}$$

Expanding these terms in powers of λ, one gets

$$\left(\frac{\partial e^{-\lambda S}}{\partial t}\right) e^{\lambda S} = -\lambda \frac{\partial S}{\partial t} + \frac{\lambda^2}{2!}\left[S, \frac{\partial S}{\partial t}\right] - \frac{\lambda^3}{3!}\left[S, \left[S, \frac{\partial S}{\partial t}\right]\right] + \ldots$$

and (3)

$$e^{-\lambda S} H e^{\lambda S} = H - \lambda [S, H] + \frac{\lambda^2}{2!}[S, [S, H]] - \frac{\lambda^3}{3!}[S, [S, [S, H]]] + \ldots$$

Let the odd part of the Hamiltonian in the n-th step be $O^{(n)}$, then the operator S will be defined in the $(n+1)$-st step as

$$S^{(n+1)} = \gamma^0 O^{(n)}.$$

The result of this special form of $S^{(n)}$ and the above value of λ is that at every step we get a new Hamiltonian which contains lowest order odd terms proportional successively to at least one order higher power in λ. Thus the odd terms can be eliminated from the Hamiltonian up to any desired order in λ which is just the non-relativistic approximation. The odd part of the zero order Hamiltonian (1) is

$$O^{(0)} = c\gamma^0 \boldsymbol{\gamma} \mathbf{P}$$

and, thus, the operator for the first transformation is

$$S^{(1)} = \gamma^0 O^{(0)} = c \boldsymbol{\gamma} \mathbf{P}.$$

With the help of equations (2) and (3), in the first step we obtain the wave function and Hamiltonian of the form

$$\Psi^{(1)} = e^{-\lambda S^{(1)}} \Psi = e^{\frac{1}{2mc} \gamma \mathbf{P}} \Psi,$$

$$H^{(1)} = \gamma^0 m c^2 + e\Phi + \frac{1}{2m}\gamma^0 \mathbf{P}^2 - \frac{e\hbar}{2mc}\gamma^0 \Sigma \mathbf{B} +$$

$$+ \frac{e\hbar}{8m^2 c^2}\Sigma(\mathbf{P} \times \mathbf{E} - \mathbf{E} \times \mathbf{P}) - \frac{e\hbar^2}{8m^2 c^2} \operatorname{div} \mathbf{E} + \tag{4}$$

$$+ \frac{ie\hbar}{2mc}\boldsymbol{\gamma}\mathbf{E} - \frac{1}{6m^2 c}\gamma^0 (\boldsymbol{\gamma}\mathbf{P})^3,$$

where $\mathbf{E} = -\nabla \Phi - \frac{1}{c}\frac{\partial \mathbf{A}}{\partial t}$ and $\mathbf{B} = \mathrm{rot}\,\mathbf{A}$ are the electric and magnetic field strengths, respectively. Selecting the odd terms from $H^{(1)}$ we get the second transformation function

$$S^{(2)} = \gamma^0 O^{(1)} = \frac{i e \hbar}{2m} \gamma^0 \boldsymbol{\gamma} \mathbf{E} - \frac{1}{6m^2 c} (\boldsymbol{\gamma} \mathbf{P})^3 .$$

Let us introduce the wave function

$$\Psi^{(2)} = e^{-\lambda S^{(2)}} \Psi^{(1)},$$

which is related to the original one by

$$\Psi^{(2)} = \left[1 + \frac{1}{2mc} \boldsymbol{\gamma} \mathbf{P} + \frac{i e \hbar}{4m^2 c^3} \gamma^0 \boldsymbol{\gamma} \mathbf{E} - \frac{1}{8m^2 c^2} (\mathbf{P}^2 + i \Sigma (\mathbf{P} \times \mathbf{P}))\right] \Psi . \quad (5)$$

The corresponding Hamiltonian $H^{(2)}$ has the form

$$H^{(2)} = \gamma^0 m c^2 + \frac{1}{2m} \gamma^0 \mathbf{P}^2 + e \Phi - \frac{e \hbar}{2mc} \Sigma \mathbf{B} +$$

$$+ \frac{e \hbar}{8m^2 c^2} \Sigma (\mathbf{P} \times \mathbf{E} - \mathbf{E} \times \mathbf{P}) - \frac{e \hbar}{8m^2 c^2} \mathrm{div}\ \mathbf{E} . \quad (6)$$

This Hamiltonian necessarily does not contain any odd term. Such an even operator has the property that if the wave function is given at $t = 0$ as

$$\Psi = (\varphi_1, \varphi_2, 0, 0) \equiv (\varphi, 0) \quad (7)$$

the lower components remain constantly zero. Thus $H^{(2)}$ acts upon the two component spinor essentially and, therefore, it can be rewritten as

$$H^{(2)} = m c^2 + \frac{1}{2m} \mathbf{P}^2 + e \Phi - \frac{e \hbar}{2mc} \boldsymbol{\sigma} \mathbf{B} +$$

$$+ \frac{e \hbar}{8m^2 c^2} \boldsymbol{\sigma} (\mathbf{P} \times \mathbf{E} - \mathbf{E} \times \mathbf{P}) - \frac{e \hbar^2}{8m^2 c^2} \mathrm{div}\ \mathbf{E} + O\left(\frac{1}{m^3}\right). \quad (8)$$

Let us proceed now to derive the expressions for the charge and current density. The Dirac charge and current densities are

$$\varrho = e \Psi^+ \Psi \qquad \mathbf{j} = c e \Psi^+ \gamma^0 \boldsymbol{\gamma} \Psi . \quad (9)$$

We therefore need Ψ expressed through $\Psi^{(2)}$. It can be verified that the inverse of equation (5) is:

$$\Psi = \left[1 - \frac{1}{2mc}\gamma\,\mathbf{P} - \frac{i\,e\,\hbar}{4m^2c^3}\gamma^0\gamma\,\mathbf{E} - \frac{1}{8m^2c^2}\left(P^2 + i\,\Sigma\,(\mathbf{P}\times\mathbf{P})\right)\right]\Psi^{(2)}. \quad (10)$$

The charge and current densities are obtained by substituting equation (10) into (9). Remembering the form of $\Psi^{(2)}$ as given by equation (7) it is easily seen that the expression $\Psi^{(2)+}\,O\,\Psi^{(2)}$ vanishes where O is an arbitrary odd operator.

Proceeding in this way we obtain for the charge density in terms of the two component spinor φ

$$\varrho = e\,\varphi^+\varphi + \frac{e\,\hbar^2}{8m^2c^2}\Delta\,(\varphi^+\varphi) - \frac{e\,\hbar}{4m^2c^2}\ \mathrm{div}\left[\varphi^+\left(\overleftrightarrow{} - \frac{e}{c}\ \overleftrightarrow{\mathbf{A}}\right)\times\sigma\,\varphi\right] + O\left(\frac{1}{m^3}\right). \quad (11)$$

The value for the charge density has been obtained by L. D. LANDAU [4] in a slightly different form and was also obtained in a different manner by A. ZAWADOWSKI [5] and W. HANUS [8].

For the current density we get, similarly,

$$j = \frac{e}{m}\varphi^+\overleftrightarrow{\mathbf{P}}\,\varphi + \frac{e\,\hbar}{2m}\ \mathrm{rot}\ (\varphi^+\sigma\,\varphi) + \frac{e^2\,\hbar}{2m^2c^2}\varphi^+(\mathbf{E}\times\sigma)\,\varphi + O\left(\frac{1}{m^3}\right). \quad (12)$$

It can be easily seen that ϱ and $\mathbf{j}$ are, of necessity, real quantities.

With the aid of the Schrödinger equation corresponding to the Hamiltonian (8) the following identity can be easily verified

$$\frac{\partial}{\partial t}\frac{e\,\hbar}{4m^2c^2}\left[\varphi^+\left(\overleftrightarrow{\mathbf{p}} - \frac{e}{c}\ \overleftrightarrow{\mathbf{A}}\right)\times\sigma\,\varphi\right] = \frac{e^2\,\hbar}{4m^2c^2}\varphi^+(\mathbf{E}\times\sigma)\,\varphi\,.$$

By writing $\frac{\partial}{\partial t}\frac{e\,\hbar}{4m^2c^2}\left[\varphi^+\left(\overleftrightarrow{\mathbf{p}} - \frac{e}{c}\ \overleftrightarrow{\mathbf{A}}\right)\times\sigma\,\varphi\right]$ and $\frac{e^2\,\hbar}{4m^2c^2}\varphi^+(\mathbf{E}\times\sigma)\,\varphi$ for the last term in equation (12) we obtain:

$$\mathbf{j} = \frac{e}{m}\varphi^+\overleftrightarrow{\mathbf{P}}\varphi + \frac{e\,\hbar}{2m}\ \mathrm{rot}\ (\varphi^+\sigma\,\varphi) + \frac{e\,\hbar}{4m^2c^2}\varphi^+(\mathbf{E}\times\sigma)\,\varphi + \\ + \frac{\partial}{\partial t}\frac{e\,\hbar}{4m^2c^2}\left[\varphi^+\left(\overleftrightarrow{p} - \frac{e}{c}\ \overleftrightarrow{\mathbf{A}}\right)\times\sigma\,\varphi\right]. \quad (13)$$

The reason for performing this transformation will be discussed later.

The classical current

For the interpretation of the results obtained let us consider a particle with charge e, mass m, angular momentum $\mathbf{s}$ and magnetic moment $\mathbf{m}$, where $\mathbf{s}$ and $\mathbf{m}$ are connected by

$$\mathbf{m} = \varkappa \mathbf{s} \quad \text{where} \quad \varkappa = \frac{e}{mc} .$$

We shall assume that $\mathbf{m}$ is of order of magnitude $\frac{e\hbar}{2mc}$. It must be emphasized that $\mathbf{m}$ and $\mathbf{s}$ are considered to be given a priori. Thus it is not assumed that they arise from any motion. Their ratio could have been prescribed arbitrarily.

This particle interacts with the electromagnetic field through its charge on the one hand, through its magnetic moment and angular momentum on the other hand.

The interaction energy of the magnetic moment with the field is $-\mathbf{m}\,\mathbf{B}$. When the particle moves with velocity $\mathbf{v}$ the magnetic field strength arising in its rest system is

$$\mathbf{B}' \approx \mathbf{B} - \frac{1}{c} \mathbf{v} \times \mathbf{E} .$$

Thus, the interaction energy of the magnetic moment with the electromagnetic field is given by

$$E = -\mathbf{m}\,\mathbf{B} + \frac{1}{c} \mathbf{m}\,(\mathbf{v} \times \mathbf{E}) . \tag{14}$$

(14) can be interpreted alternatively as follows. When a magnetic moment moves there appears and additional electric moment of the form

$$\pi \approx \frac{1}{c} \mathbf{v} \times \mathbf{m} \tag{15}$$

interacting with the electric field. Now the interaction energy is

$$E = -\mathbf{m}\mathbf{B} - \frac{1}{c} \mathbf{E}\,(\mathbf{v} \times \mathbf{m}) ,$$

which is identical with (14).

In addition to electromagnetic interaction an interaction occurs as a result of the Thomas precession. Let the particle move in a system of reference S_1 at time t with velocity $\mathbf{v}$ and at time $t + \Delta t$ with velocity $\mathbf{v} + \Delta \mathbf{v}$. Let S_2 and S_3 be the rest systems of the particle at times t and $t + \Delta t$. Even if the

Lorentz transformations from the system S_1 to S_2 and similarly from S_2 to S_3 do not contain any rotation the transformation from S_1 to S_3 generally does. Thus the angular momentum of the particle must rotate by a certain angle while it moves from the system S_1 to S_3. The angular velocity of this precession has been given by THOMAS as (see e.g. [6])

$$\boldsymbol{\omega}_0 \approx \frac{1}{2c^2}\,\mathbf{v} \times \frac{d\,\mathbf{v}}{d\,t} \approx \frac{e}{2m\,c^2}\,\mathbf{v} \times \mathbf{E}\,.$$

The energy due to $\boldsymbol{\omega}_0$ can be written as

$$E = -\,\mathbf{s}\,\boldsymbol{\omega}_0 = -\,\frac{1}{2c}\,\mathbf{m}\,(\mathbf{v} \times \mathbf{E})\,. \tag{16}$$

(16) is of a form similar to the second term in (14) but is of quite a different origin.

Before writing the action principle we must deal with with the kinetic energy corresponding to the angular momentum **s**. Since **s** and **m** are given a priori, we cannot find a kinetic energy function. Following J. FRENKEL [7] we give only its variation as

$$\delta^* T \equiv \mathbf{s}\,\delta\,\boldsymbol{\omega} = \frac{1}{\varkappa}\,\mathbf{m}\,\delta\,\boldsymbol{\omega}\,, \tag{17}$$

where $\delta\boldsymbol{\omega}$ is the variation of the angular velocity and the asterisk means that there exists no function T with the total differential (17).

The variation of the action integral for the particle and the electromagnetic field can be written as

$$\delta S = \int (\delta\,L + \delta^*\,L_f^{(1)})\,d^3\,\mathbf{r}\,dt\,,$$

where

$$L = L_f^{(2)} + L_f^{(3)} + L_i^{(1)} + L_i^{(2)} + L_i^{(3)}$$

with

$$L_f^{(2)} = -\,\frac{1}{\gamma}\,m\,c^2\,\delta\,(\mathbf{r} - \mathbf{r}_0)\,,\quad \gamma \equiv \left(1 - \frac{v^2}{c^2}\right)^{-\frac{1}{2}},$$

$$L_f^{(3)} = \frac{1}{8\pi}\,(\mathbf{E}^2 - \mathbf{B}^2)\,,$$

$$L_i^{(1)} = \left(\frac{e}{c}\,\mathbf{A}\,\mathbf{v} - e\,\Phi\right)\delta\,(\mathbf{r} - \mathbf{r}_0)\,,$$

$$L_i^{(2)} = \left(\mathbf{m}\,\mathbf{B} - \frac{1}{c}\,\mathbf{m}\,(\mathbf{v} \times \mathbf{E})\right)\delta\,(\mathbf{r} - \mathbf{r}_0)\,,$$

$$L_i^{(3)} = \frac{1}{2c}\,\mathbf{m}\,(\mathbf{v}\times\mathbf{E})\,\delta\,(\mathbf{r}-\mathbf{r}_0),$$

$$\delta^* L_f^{(1)} = \frac{1}{\varkappa}\,\mathbf{m}\,\delta\,\boldsymbol{\omega}\,\delta\,(\mathbf{r}-\mathbf{r}_0)\,.$$

$r_0(t)$ represents the position of the particle. $L_f^{(2)}$ and $L_f^{(3)}$ are the Lagrangeans of the particle and the free electromagnetic field, respectively. $L_i^{(1)}$ and $L_i^{(2)}$ desribe the interaction of the magnetic moment with the field. $L_i^{(3)}$ is the energy term arising from the Thomas precession.

Since $\mathbf{m}$ is a vector of constant absolute value, its variation is $\delta\mathbf{m} = \delta\boldsymbol{\varphi}\times\mathbf{m}$ where $\delta\boldsymbol{\varphi}$ is the angular vector of the rotation.

Performing the variation and assuming that all quantities vanish at the limit of integration, one finds that

$$\begin{aligned}
\delta S = \int d^3\mathbf{r}\,dt\Bigg\{ & \delta\Phi\left[\frac{1}{4\pi}\,\mathrm{div}\;\mathbf{E} - e\,\delta\,(\mathbf{r}-\mathbf{r}_0) + \frac{1}{c}\,\mathrm{div}\,[\mathbf{v}\times\mathbf{m}\,\delta\,(\mathbf{r}-\mathbf{r}_0)] - \right. \\
& \left. - \frac{1}{2c}\,\mathrm{div}\,[\mathbf{v}\times\mathbf{m}\,\delta\,(\mathbf{r}-\mathbf{r}_0)]\right] + \\
& + \delta\mathbf{A}\left[\frac{1}{4\pi c}\,\frac{\partial\mathbf{E}}{\partial t} - \frac{1}{4\pi}\,\mathrm{rot}\;\mathbf{B} + \frac{e}{c}\,\mathbf{v}\,\delta\,(\mathbf{r}-\mathbf{r}_0) + \mathrm{rot}\,[\mathbf{m}\,\delta\,(\mathbf{r}-\mathbf{r}_0)]\right. + \\
& \left. + \frac{1}{c^2}\,\frac{\partial}{\partial t}\,[\mathbf{v}\times\mathbf{m}\,\delta\,(\mathbf{r}-\mathbf{r}_0)] - \frac{1}{2c^2}\,\frac{\partial}{\partial t}\,[\mathbf{v}\times\mathbf{m}\,\delta\,(\mathbf{r}-\mathbf{r}_0)]\right] + \\
& + \delta\mathbf{r}_0(t)\left[\frac{e}{c}\,\nabla\,(\mathbf{A}\,\mathbf{v}) - e\,\nabla\Phi + \nabla\left(\mathbf{m}\left(\mathbf{B} - \frac{1}{c}\,\mathbf{v}\times\mathbf{E}\right)\right) + \nabla\left(\mathbf{m}\,\frac{1}{2c}\,\mathbf{v}\times\mathbf{E}\right)\right]\delta(\mathbf{r}-\mathbf{r}_0) + \\
& + \delta\mathbf{v}\left[\mathbf{m}\,\gamma\,\mathbf{v} + \frac{e}{c}\,\mathbf{A} - \frac{1}{c}\,\mathbf{E}\times\mathbf{m} + \frac{1}{2c}\,\mathbf{E}\times\mathbf{m}\right]\delta\,(\mathbf{r}-\mathbf{r}_0) + \\
& + \delta\boldsymbol{\varphi}\left[\mathbf{m}\times\left(\mathbf{B} - \frac{1}{c}\,\mathbf{v}\times\mathbf{E}\right) + \frac{1}{2c}\,\mathbf{m}\times(\mathbf{v}\times\mathbf{E})\right]\delta\,(\mathbf{r}-\mathbf{r}_0) + \\
& + \delta\boldsymbol{\omega}\,\frac{1}{\varkappa}\,\mathbf{m}\,\delta\,(\mathbf{r}-\mathbf{r}_0)\Bigg\}. \qquad (18)
\end{aligned}$$

It is to be noted that we have intentionally separated terms arising from the second part of $L_i^{(2)}$ and $L_i^{(3)}$.

From (18) it is easy to get the canonical momentum conjugated to $\mathbf{r}$ as

$$\mathbf{p} = \frac{\partial}{\partial\mathbf{v}}\int L\,d^3\mathbf{r} = \mathbf{m}\,\gamma\,\mathbf{v} + \frac{e}{c}\,\mathbf{A} - \frac{1}{2c}\,\mathbf{E}\times\mathbf{m}\,.$$

Thus, the momentum of the particle can be expressed as

$$m\gamma\mathbf{v} = \mathbf{p} - \frac{e}{c}\mathbf{A} + \frac{1}{2c}\mathbf{E} \times \mathbf{m}\,. \tag{19}$$

Arguments of **A** and **E** must be taken at the position of the particle. Equation (18) gives the two Maxwell equations containing the effective charge and current density.

Substituting (19) into (18) we find

$$\varrho = \varrho_e + \varrho_\pi + \varrho_T = e\,\delta(\mathbf{r} - \mathbf{r}_0) - \frac{1}{2mc}\,\mathrm{div}\left(\left(\mathbf{p} - \frac{e}{c}\mathbf{A}\right) \times \mathbf{m}\,\delta(\mathbf{r} - \mathbf{r}_0)\right),$$

$$\mathbf{j} = \mathbf{j}_e + \mathbf{j}_m + \mathbf{j}_\pi + \mathbf{j}_T = \frac{e}{m}\left(\mathbf{p} - \frac{e}{c}\mathbf{A}\right)\delta(\mathbf{r} - \mathbf{r}_0) + c\ \mathrm{rot}\,(\mathbf{m}\,\delta(\mathbf{r} - \mathbf{r}_0)) +$$

$$+ \frac{1}{2mc}\frac{\partial}{\partial t}\left(\left(\mathbf{p} - \frac{e}{c}\mathbf{A}\right) \times \mathbf{m}\,\delta(\mathbf{r} - \mathbf{r}_0)\right),$$

where

$$\varrho_e = e\,\delta(\mathbf{r} - \mathbf{r}_0)$$

$$\varrho_\pi = -\frac{1}{mc}\,\mathrm{div}\left(\left(\mathbf{p} - \frac{e}{c}\mathbf{A}\right) \times \mathbf{m}\,\delta(\mathbf{r} - \mathbf{r}_0)\right),$$

$$\varrho_T = \frac{1}{2mc}\,\mathrm{div}\left(\left(\mathbf{p} - \frac{e}{c}\mathbf{A}\right) \times \mathbf{m}\,\delta(r - r_0)\right),$$

$$\mathbf{j}_e = \frac{e}{m}\left(\mathbf{p} - \frac{e}{c}\mathbf{A}\right)\delta(\mathbf{r} - \mathbf{r}_0)$$

$$\mathbf{j}_m = c\ \mathrm{rot}\ (\mathbf{m}\,\delta(\mathbf{r} - \mathbf{r}_0))$$

$$\mathbf{j}_\pi = \frac{1}{mc}\frac{\partial}{\partial t}\left(\left(\mathbf{p} - \frac{e}{c}\mathbf{A}\right) \times \mathbf{m}\,\delta(\mathbf{r} - \mathbf{r}_0)\right)$$

$$\mathbf{j}_T = -\frac{1}{2mc}\frac{\partial}{\partial t}\left(\left(\mathbf{p} - \frac{e}{c}\mathbf{A}\right) \times \mathbf{m}\,\delta(\mathbf{r} - \mathbf{r}_0)\right). \tag{20}$$

It is to be noted that equation (18) also contains the equations of motion for the particle, but they are not required here.

It is possible to interpret the classical charge and current densities (eq. (20)) as follows:

a) ϱ_e is, obviously, the static charge density and

$$\mathbf{j}_e = e\,\mathbf{v}\,\delta(\mathbf{r} - \mathbf{r}_0) = \left[\frac{e}{m}\left(\mathbf{p} - \frac{e}{c}\mathbf{A}\right) + \frac{e}{2mc}\mathbf{E} \times \mathbf{m}\right]\delta(\mathbf{r} - \mathbf{r}_0)$$

is the convection current expressed in terms of the canonical momentum **p**.

b) c rot $(\mathbf{m}\,\delta\,(\mathbf{r}-\mathbf{r}_0))$ is the effective current due to magnetic moment $\mathbf{m}$.

c) According to equation (15) the moving magnetic moment corresponds to an additional electrical moment of the form

$$\boldsymbol{\pi} = \frac{1}{mc}\left(\mathbf{p} - \frac{e}{c}\mathbf{A}\right) \times \mathbf{m}\,\delta\,(\mathbf{r} - \mathbf{r}_0)\,.$$

It is known from electrodynamics that this is equivalent to a charge distribution $\varrho_\pi = -\operatorname{div}\boldsymbol{\pi}$. The variation of the polarization in time gives a contribution

$$\mathbf{j}_\pi = \frac{\partial \boldsymbol{\pi}}{\partial t}$$

to the effective current.

d) It has been shown in equations (18) and (20) that terms of the same type arise as a result of the THOMAS precession: i.e.

$$\varrho_T = -\frac{1}{2}\varrho_\pi = \frac{1}{2mc}\operatorname{div}\left[\left(\mathbf{p} - \frac{e}{c}\mathbf{A}\right) \times \mathbf{m}\,\delta\,(\mathbf{r} - \mathbf{r}_0)\right],$$

$$\mathbf{j}_T = -\frac{1}{2}\mathbf{j}_\pi = -\frac{1}{2mc}\frac{\partial}{\partial t}\left[\left(\mathbf{p} - \frac{e}{c}\mathbf{A}\right) \times \mathbf{m}\,\delta\,(\mathbf{r} - \mathbf{r}_0)\right].$$

The total contributions from the THOMAS effective charge and polarization charge and, similarly, from the THOMAS effective current and polarization current are

$$\varrho_\pi + \varrho_T = \frac{1}{2}\varrho_\pi = -\frac{1}{2mc}\operatorname{div}\left[\left(p - \frac{e}{c}A\right) \times \mathbf{m}\,\delta\,(r - r_0)\right],$$

$$\mathbf{j}_\pi + \mathbf{j}_T = \frac{1}{2}\mathbf{j}_\pi = \frac{1}{2mc}\frac{\partial}{\partial t}\left[\left(\mathbf{p} - \frac{e}{c}\mathbf{A}\right) \times \mathbf{m}\,\delta\,(\mathbf{r} - \mathbf{r}_0)\right],$$

respectively.

It is seen that as a result of the THOMAS precession only half the polarization charge and current is effective. Thus, all terms of the classical charge and current have been interpreted.

Interpretation of the quantum mechanical charge and current

The correspondence with the quantum mechanical expressions given in equations (11) and (12) can be stated by taking into account the relations

$$\mathbf{m} \to \frac{e\hbar}{2mc}\boldsymbol{\sigma}, \qquad \mathbf{p} \to \overleftrightarrow{\mathbf{p}} = \frac{\hbar}{i}\overleftrightarrow{\nabla}.$$

It is now obvious why the term $\frac{e^2\hbar}{2m^2c^2}\varphi^+(\mathbf{E}\times\boldsymbol{\sigma})\varphi$ was divided into two parts in equation (13). The term $\frac{\partial}{\partial t}\frac{e\hbar}{4m^2c^2}\varphi^+(\tilde{\mathbf{P}}\times\boldsymbol{\sigma})\varphi$ is the polarization current while $\frac{e^2\hbar}{4m^2c^2}\varphi^+(\mathbf{E}\times\boldsymbol{\sigma})\varphi$ belongs to the expression of the velocity.

The term in the charge density which still has to be interpreted is

$$\varrho_D = \frac{e\hbar^2}{8m^2c^2}\Delta(\varphi^+\varphi). \tag{21}$$

FOLDY has shown that in the FOLDY—WOUTHUYSEN transformation the electron interacts with the field non-locally. In the present approximation this fact is manifested by the contribution of the above term. The interaction of the charge (21) with the electromagnetic field corresponds to the non-local type Darwin term in the Hamiltonian in the static case, since

$$\int\varrho_D\Phi\,d^3\mathbf{r} = -\frac{e\hbar^2}{8m^2c^2}\int\varphi^+\ \mathrm{div}\ \mathbf{E}\,\varphi\,d^3\mathbf{r}\,.$$

Thus, we have succeeded in giving the interpretation of the terms of the charge and current density in the above approximation. The characteristic feature of further approximations is, in addition to the classical terms, the appearance of higher and higher derivatives of the field strengths which corresponds to the non-local interaction of the particle with the electromagnetic field.

Finally, it is to be noted that the procedure can be extended to arbitrary values of spin and also to anomalous magnetic moments.

Acknowledgement

The author wishes to express his gratitude to Professor L. JÁNOSSY for useful comments.

REFERENCES

1. A. I. AKHIEZER and V. B. BERESTETSKY, Quantum Electrodynamics Consultants Bureau Inc., New York, p. 130.
2. L. L. FOLDY and S. A. WOUTHUYSEN, Phys. Rev., **78**, 29, 1950; and D. R. BATES: Quantum Theory, Vol. III.
3. N. N. BOGOLIUBOV and D. V. SHIRKOV, Introduction to the Theory of Quantized Fields, Interscience Publishers Ltd., London, 1959, p. 64.
4. Collected Papers of L. D. LANDAU, Pergamon Press, 1965, p. 155.

5. Private communication.
6. J. D. JACKSON, Classical Electrodynamics, John Wiley and Sons Inc., New York, London, 1962.
7. Я. И. Френкель: Собрание избранных трудов. Том I. стр. 351.
8. W. HANUS, Acta Phys. Polonica, **26**, 1181, 1964; ibid **29**, 463, 1966.

НЕРЕЛЯТИВИСТСКОЕ ПРИБЛИЖЕНИЕ ТОКА ДИРАКА

М. ГУСАР

Р е з ю м е

Применяя преобразование Фолди—Вотхойзена к уравнению Дирака выводятся нерелятивистские выражения плотности заряда и тока с точностью до второго порядка в $\frac{p}{mc}$. Члены полученные сверх нерелятивистской плотности заряда и тока Паули интерпретируются следующим образом. Движущийся магнитный диполь соответствует электрическому, взаимодействующему с электрическим полем как поляризационный заряд $\varrho_\pi = -\operatorname{div}\pi$. Соответствующий этому поляризационному заряду ток появляется в обычной форме $\frac{\partial\pi}{\partial t}$. Прецессия Томаса даёт вклад в плотность заряда и тока $\varrho_T = \frac{1}{2}\operatorname{div}\pi$ и $j_T = -\frac{1}{2}\frac{\partial\pi}{\partial t}$ соответственно, и следовательно эффективной является только половина поляризационных заряда и тока. В токе появляется член типа $E \times \sigma$ поскольку соотношение между механическим и каноническим импульсом в нашем случае не просто $m\gamma v = p - \frac{e}{c}A$. Появляется ешё член типа Дарвина в плотности заряда, который не интерпретировать классически.

Acta Physica Academiae Scientiarum Hungaricae, Tomus 23 (2), pp. 237—245 (1967)

COMMUNICATIONES BREVES

DIE FLUORESZENZ VON 4,4'-BIS-TRIAZINILAMINOSTILBEN-2,2'-DISULFONSÄUREDERIVATEN

Von

A. SZÉKELY

FORSCHUNGSINSTITUT FÜR DIE TEXTILINDUSTRIE, BUDAPEST

(Eingegangen 12. V. 1966)

Die Derivate 4,4'-bis-Triazinilaminostilben-2,2'-Disulfonsäure (im weiteren Triazinilflavonsäuren) sind die Wirkstoffe der in der Textil-, Papier- und Waschmittelindustrie am häufigsten gebrauchten optischen Aufheller.

Ihre Wirkung üben sie vor allem dann aus, wenn sie auf ein Substrat (z. B. Papier) aufgetragen werden [1]. Das Substrat beeinflusst die Form und die Wellenzahl des Maximums nach den Literaturangaben [2] und eigenen Prüfungen nicht oder kaum.

Einige Literaturangaben [3, 4, 5] beweisen, dass der wichtigste jener Faktoren, die die Fluoreszenzfarbe der Aufheller, d. h. die Verteilung der Emission im Spektrum beeinflussen, von der Konzentration der Aufheller abhängig ist. Die Publikationen befassen sich aber mit dem Zusammenhang zwischen den Emissionsspektren am Substrat und in wässrigen Lösungen nicht.

Experimenteller Teil

Zur eingehenderen Klärung der letztgenannten Frage wurden einig. Fluoreszenzmessungen an Aufhellern auf Basis der obengenannten Verbindungen und an ihren Wirkstoffen ausgeführt.

Die Messungen wurden an Aufhellern „Optinol BA" und „Optinol BVS" (Egyesült Vegyiművek, Ungarn) und an deren Wirkstoffen auf Chromatogrammpapier und in wässriger Lösung vorgenommen. Das Chromatogrammpapier hatte bei der gegebenen Belichtung keine eigene Emission, diente nur als Substrat. Die beiden genannten Aufheller enthalten ausser Kochsalz nur die im Triazin-Ring substituierte Triazinilflavonsäure als Wirksubstanz. Das Emissionsspektrum der auf Chromatogrammpapier aufgetragenen Wirkstoffe zeigte praktisch keine Abweichung von der dieselbe Wirkstoffkonzentration aufweisenden Handelsware. Die Gegenwart von Salz hatte also keinen Einfluss auf das Emissionsspektrum.

Der Wirkstoff des Aufhellers Optinol BA zeigte sich im Chromatogramm in Butilazetat-Piridin-Wasser als eine einheitliche Verbindung; im Chromatogramm von Optinol BVS wurden ausser dem Hauptfleck noch zwei blasse Flecke festgestellt die aber gleichfalls von Derivaten der Triazinilflavonsäure herrühren. Das Emissionsspektrum der chemisch nahestehenden Verbindungen — auch dasjenige jener Verbindungen, die sich im Chromatogramm von der Hauptsubstanz eventuell nicht loslösen —, weicht von dem der Wirksubstanz kaum ab, ihre (noch nicht geklärte) Gegenwart oder ihr Fehlen kann also die hier mitgeteilten Ergebnisse nicht wesentlich beeinflussen.

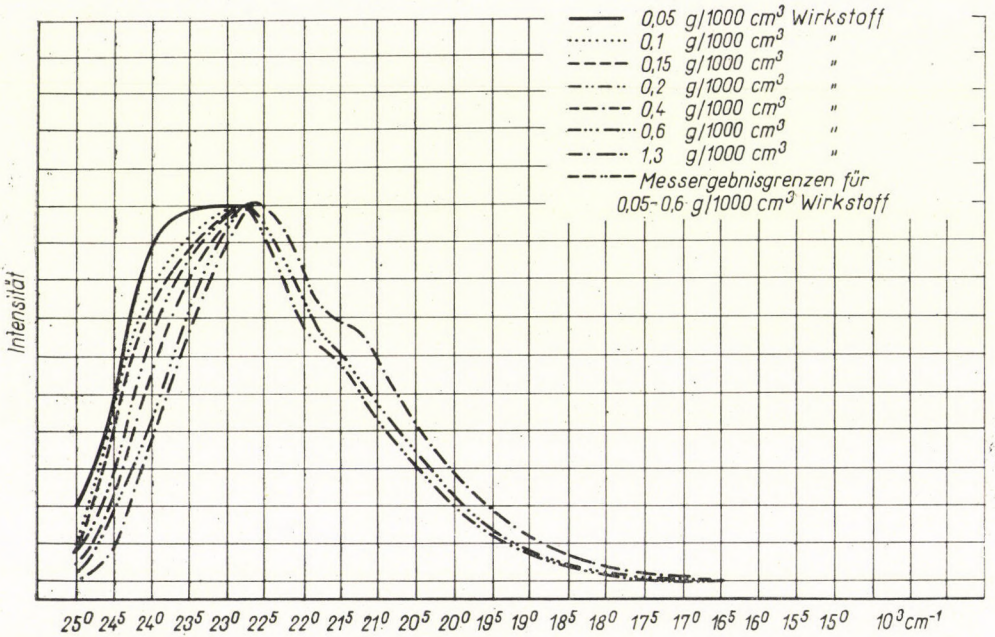

Abb. 1. Emissionsspektrum von Optinol BA auf Chromatogrammpapier

Das System auf dem Chromatogrammpapier verhält sich gemäss dem Gesetz von KUBELKA und MUNK [6] bzw. dessen auf die Fluoreszenz angewandte Variation [7]. Über die Berechnung der Sekundärabsorption und der Sekundärfluoreszenz in Lösungen finden sich Angaben in den Publikationen von BUDÓ und Mitarbeiter [8, 9].

Die bei Belichtung mit nm 365 gewonnenen Emissionsspektren von mit Optinol BA imprägnierten Substraten (7 Konzentrationsvarianten) sind aus Abb. 1, die entsprechenden Emissionsspektren der mit Optinol BVS imprägnierten Substrate aus Abb. 2 ersichtlich. Die entsprechenden Spektren der wässrigen Lösungen enthalten die Abbildungen 3 und 4. Die Normierung auf gleiche Intensität erfolgte bei nm 440 ($22{,}8 \cdot 10^3$ cm $^{-1}$) für Optinol BA und nm 435 ($23{,}0 \cdot 10^3$ cm $^{-1}$) für Optinol BVS.

Aus den ersten zwei Abbildungen geht hervor, dass die Kurven der sechs niedrigeren Konzentrationen im Bereich der kleineren Wellenzahlen ($>$ 22,8, bzw. 23,0 $\cdot$ 10^3 $\cdot$ cm^{-1}) — abgesehen von Streuungen ($\pm$ 5% Intensität und $\pm$ 1 nm) — keine Abweichungen aufweisen, wogegen der Ablauf der Spektren der höchsten Konzentrationen merklich abweichend ist. Bei den grösseren Wellenzahlen ($>$ 22,8, bzw. 23,0 $\cdot$ 10^3 cm^{-1}) ist eine klare konzentrationsabhängige Verschiebung des Spektrums zu beobachten.

Ein Vergleich der beiden Spektren-Serien liess erkennen, dass die beiden nur in ihren Substituenten abweichenden Verbindungen voneinander abwei-

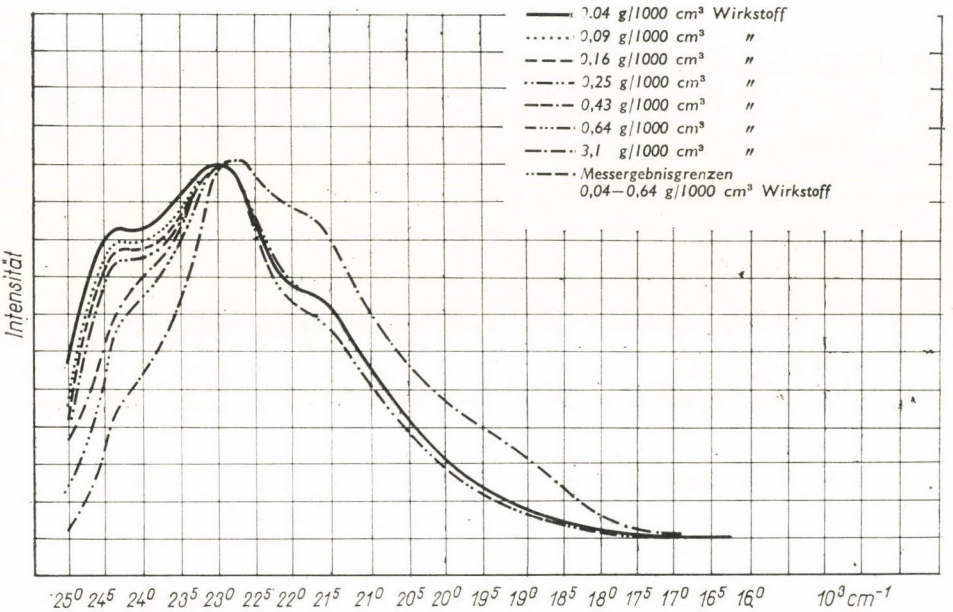

Abb. 2. Emissionsspektren von Optinol BVS auf Chromatogrammpapier

chende Emissionsspektren liefern, was übrigens für ähnliche Verbindungen auch aus der Literatur [2] bekannt ist.

Die Rotverschiebung der wässrigen Lösungen mit steigender Konzentration ist mehr oder weniger gleichmässig (Abb. 3 und 4).

In Abb. 5 wurden — um die Übersichtlichkeit nicht noch weiter zu erschweren —, von den Kurven in Abb. 1 nur drei aufgetragen (0,05, 0,15 und 1,3 g/1000 cm^3 Wirksubstanz), wobei der Versuch unternommen wurde, sie so in Gaussche Kurven[10] zu zerlegen, dass die Wellenzahl der Maxima für die drei Konzentrationen gleich bleibe. Das gelang auch bei zwei Teilbanden (bezeichnet mit II und III); bei den kürzestwelligen Teilbanden (I) zeigten sich kleinere Deformationen. Bei den längstwelligen Teilbanden (IV) wich die Wellenzahl des Maximums der einen Kurve von derjenigen der anderen ab,

und überdies war die Deformation so gross, dass von Gausschen Kurven keine Rede mehr sein konnte.

Abb. 6 veranschaulicht die Emissionskurven von Optinol BVS, ähnlich wie die für Optinol BA in Abb. 5 (Konzentrationen: 0,04, 0,16 und 3,1 g/1000 cm³ Wirksubstanz). Für die Teilbanden gelten im grossen und ganzen die selben Feststellungen wie im obigen Fall.

Aus dem Vergleich von Abb. 5 und 6 ergibt sich, dass die Kurven einen ähnlichen Verlauf haben, dass dagegen die Wellenzahlen der Maxima der

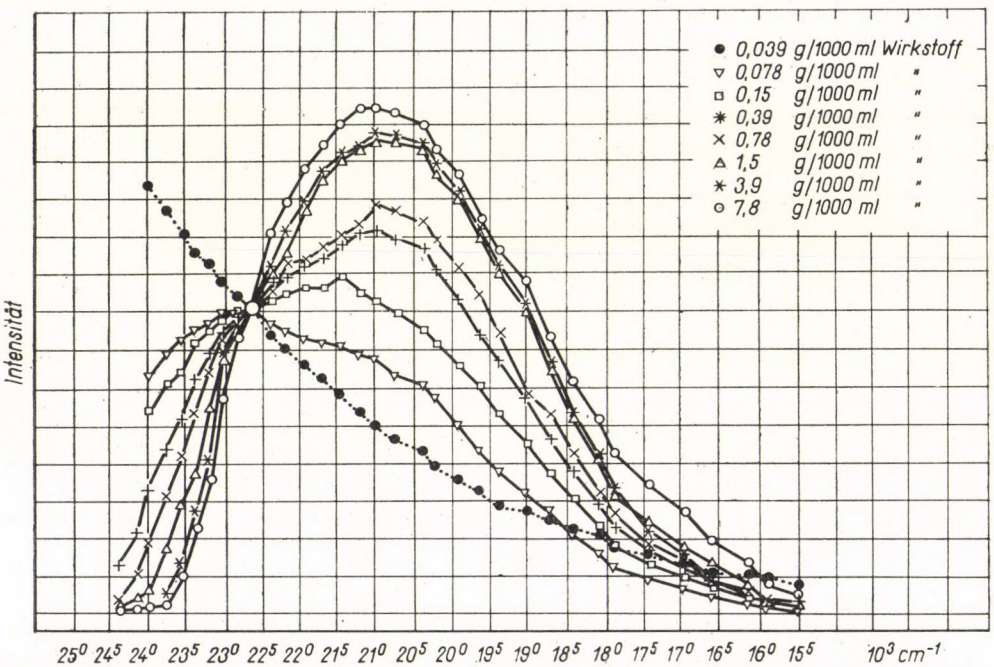

Abb. 3. Emissionsspektrum von Optinol BA in wässriger Lösung

entsprechenden Teilbanden voneinander abweichen. Die grösste Distanz wurde zwischen den Teilbandenmaxima I. ermittelt, die weiteren Teilbandenmaxima näherten sich mit steigender Ordnungszahl. (Ähnliche Zusammenhänge wurden bei Vergleich weiterer Triazinilflavonsäuren gefunden.)

Das Verhältnis der Intensität der Teilbanden ändert sich mit der Konzentration. Mit steigender Konzentration kann festgestellt werden, dass

$$\frac{J_{II,1}}{J_{I,1}} \leq \frac{J_{II,2}}{J_{I,2}} \qquad \frac{J_{III,1}}{J_{II,1}} \leq \frac{J_{III,2}}{J_{II,2}}$$

$$\frac{J_{II,2}}{\varphi_{I,2}} \leq \frac{J_{II,3}}{J_{I,3}} \qquad \frac{J_{III,2}}{J_{II,2}} \leq \frac{J_{III,3}}{J_{II,3}},$$

wobei J die relative Intensität der Teilbanden bei Maximum,
die römischen Zahlen im Index die in den Abbildungen bezeichneten Teilbanden,
die arabischen Zahlen hingegen die Konzentration in der Reihenfolge ihrer Zunahme bedeuten.

An den Abbildungen ist es zwar nicht zu erkennen, aus dem Vergleich der nicht normierten Werte der Spektra hingegen (und noch mehr aus vorangegangenen Messungen [3]) kann festgestellt werden, dass die Intensität der

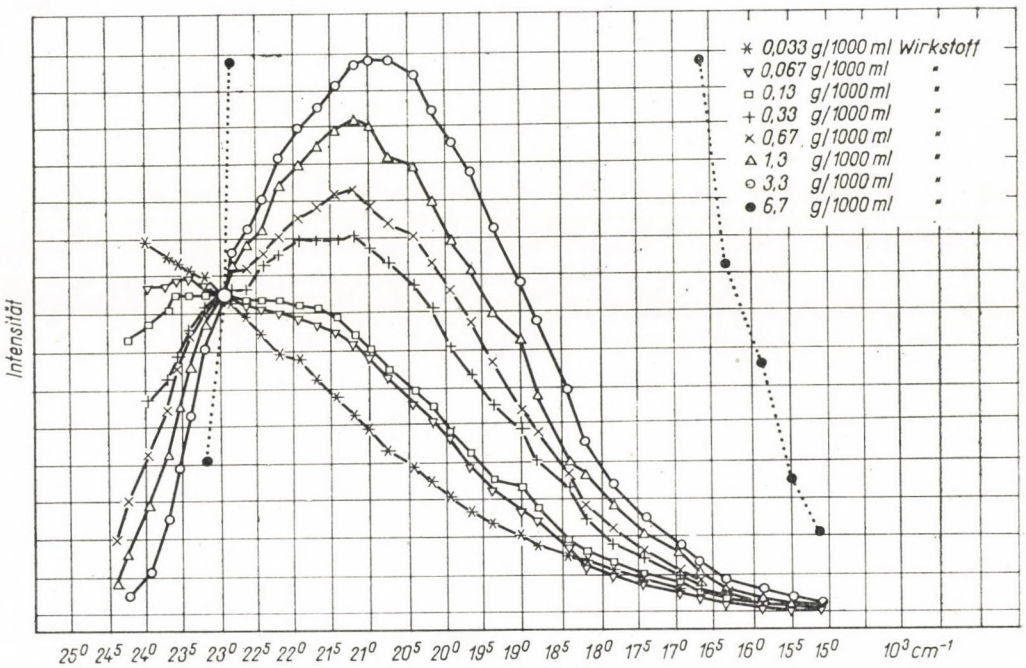

Abb. 4. Emissionsspektrum von Optinol BVS in wässriger Lösung

Teilbanden in absoluter Hinsicht mit steigender Konzentration anfangs zunimmt, dann wieder abnimmt. Von den Brutto-Intensitäten der Fluoreszenz ist diese Erscheinung längst bekannt[11]; für beide Formen der Erscheinungen liefern die Gleichungen von KUBELKA—MUNK [6] die Erklärung.

Die Abb. 7 und 8 zeigen die Spektren der entsprechenden Lösungen, u. zw., ähnlich wie in den Abb. 5. und 6, in Teilbanden zerlegt. Die Konzentrationen wurden so gewählt, dass die auf die Volumeinheit entfallenden Wirkstoffmengen Molekülzahlen nahe bei jenen der in den Abbildungen 5 bzw. 6 veranschaulichten lagen.

Die so dargestellten Spektren konnten derart in Gaussche Kurven aufgelöst werden, dass die Wellenzahlen ihrer Maxima im grössten Teil der

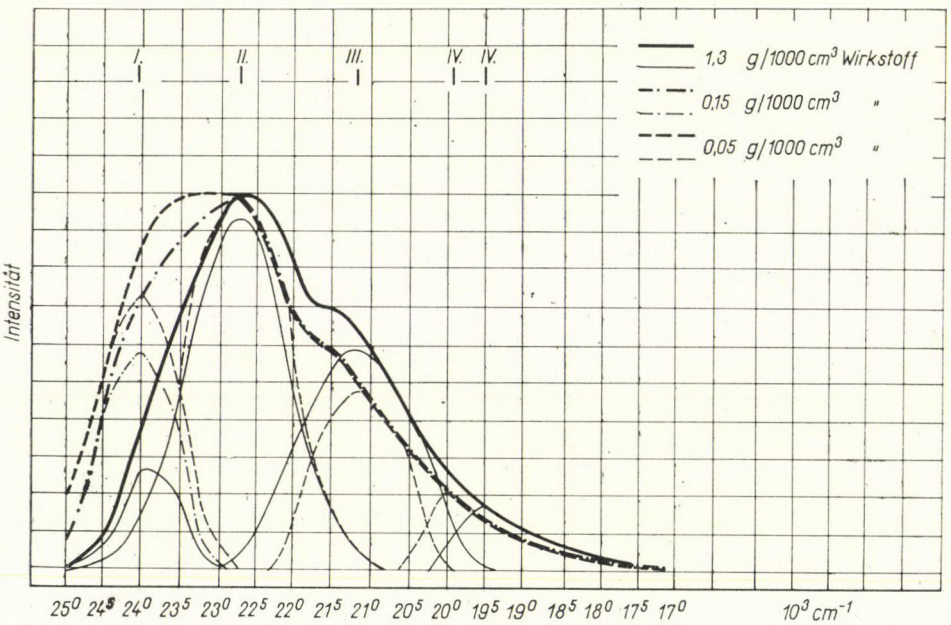

Abb. 5. Emissionsspektren von Optinol BA auf Chromatogrammpapier (in Teilbanden zerlegt)

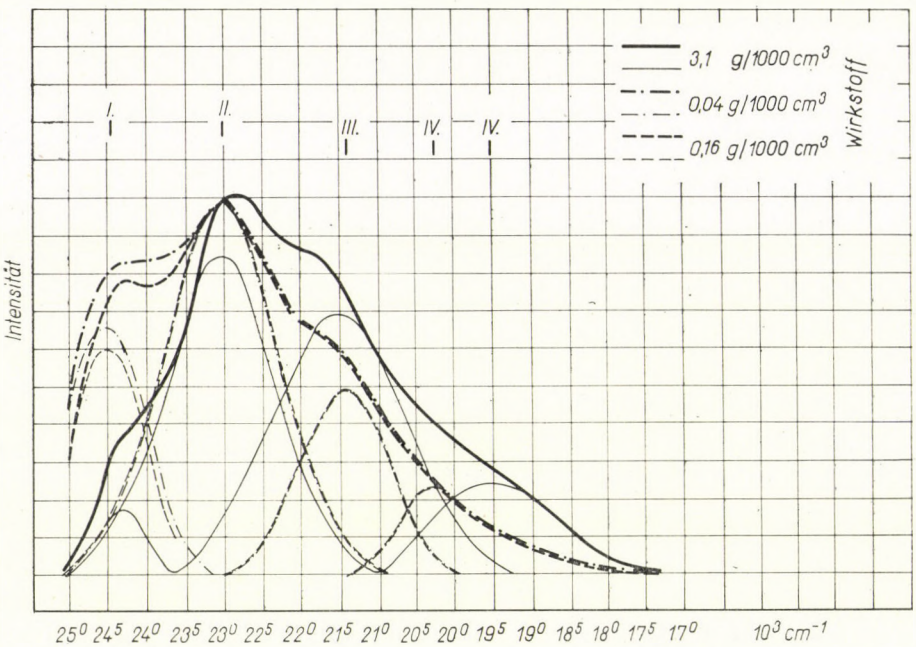

Abb. 6. Emissionspektren von Optinol BVS auf Chromatogrammpapier (in Teilbanden zerlegt)

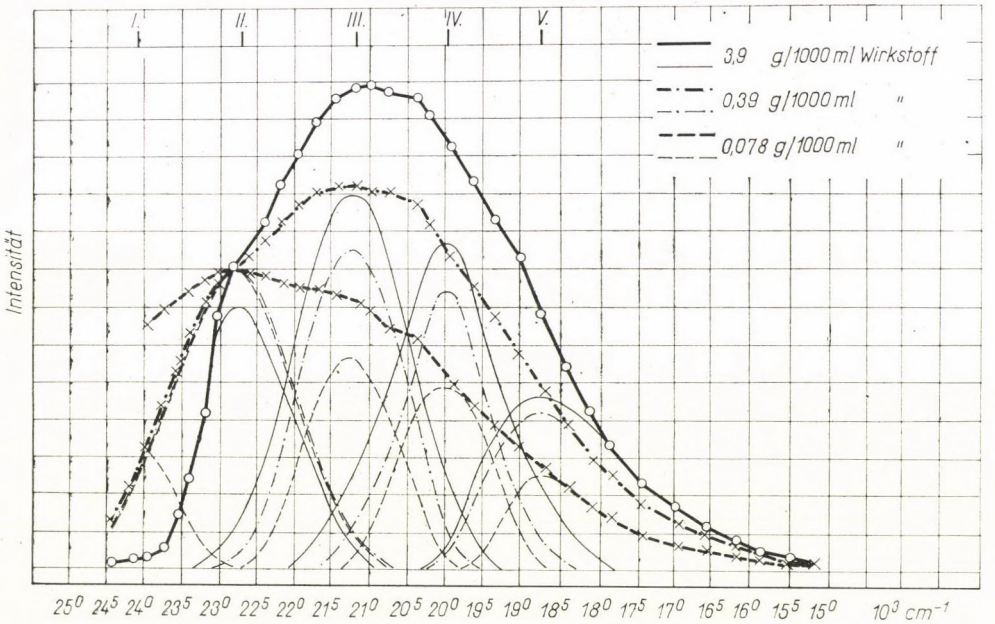

Abb. 7. Emissionsspektren von Optinol BA in wässriger Lösung (in Teilbanden zerlegt)

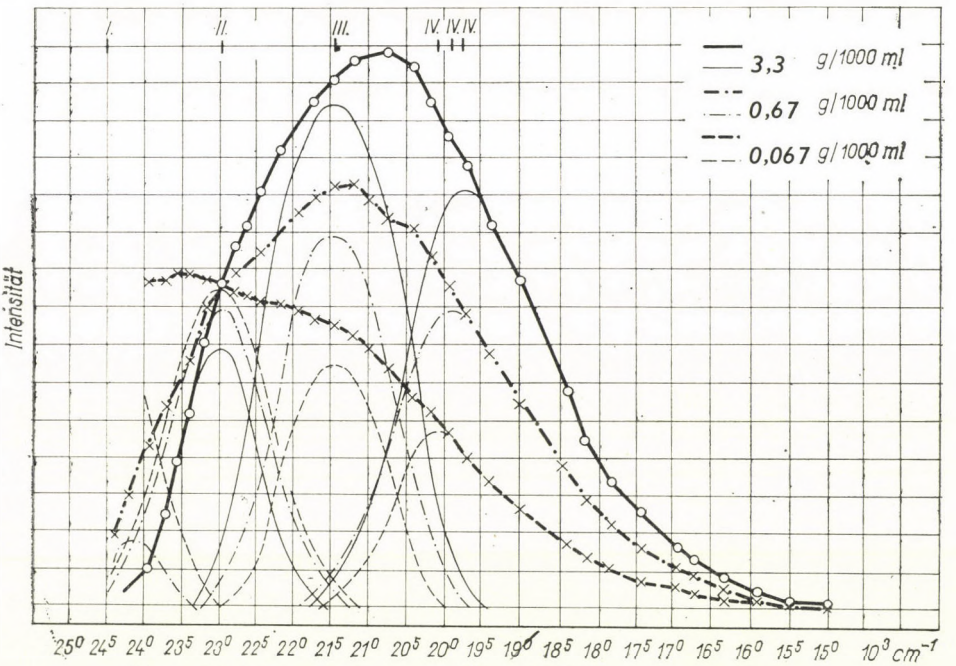

Abb. 8. Emissionsspektren von Optinol BVS in wässriger Lösung (in Teilbanden zerlegt)

Fälle mit jenen der am Substrat gemessenen Spektren übereinstimmte. Bei Optinol BA musste eine Teilbande V aufgenommen werden, die Teilbanden I fehlten in einigen Fällen ganz. Die Deformationen der Teilbanden I und IV (bei Optinol BA von Teilbanden V) waren von der gleichen Art wie diejenigen der Teilbanden von den Aufhellern am Substrat. Ebenso zeigte die mit steigender Konzentration eintretende Verschiebung der Intensitätsverhältnisse der Teilbanden die gleiche Tendenz. In den Intensitätsverhältnissen der Teilbanden der einander entsprechenden Konzentrationen am Substrat und in der Lösung konnten dagegen wesentliche Unterschiede festgestellt werden.

Interpretation der beobachteten Erscheinungen

1. Die von UV-Strahlen ausgelösten Spektren der auf Substrat und in wässriger Lösung geprüften Triazinilfalvonsäure-Derivate konnten (abgesehen von den in den Punkten 2. und 3. erwähnten Einschränkungen) derart in Gaussche Kurven zerlegt werden, dass sich die Wellenzahlen der Teilbanden-Maxima für dieselbe Verbindung im Bereich der gemessenen Konzentrationen nicht änderten.

2. Die deformation der Teilbanden I in den Abbildungen 5—8 können der Sekundärabsorption zugeschrieben werden, die sich mit zunehmender Konzentration immer stärker bemerkbar macht. (Die Triazinilflavonsäuren absorbieren bekanntlich bis zu Wellenlängen von 410—420 nm.)

3. Die Teilbanden IV der Abbildungen 5,6 und 8 bzw. der Teilbanden V in Abb. 7 können nicht mehr als Gaussche Kurven angesehen werden, auch die Wellenzahlen ihrer Maxima stimmen bei den einzelnen Konzentrationen nicht ganz überein. Dagegen verlaufen sie ähnlich wie andere Emissionskurven ähnlichen Charakters [13].

4. Vorausgesetzt, dass der Grund für die mit zunehmender Konzentration eintretenden Rotverschiebung wie in vielen analogen Fällen auch hier in der Assoziation der Wirkstoffmoleküle zu suchen ist und dass die aufgenommenen Teilbanden den einzelnen Assoziationsgraden zugeordnet werden können, kann festgestellt werden, dass bei gegebenen Verbindungen die wässrige Lösung die Assoziation weit mehr fördert als das Substrat.

Dies zeigen auch die folgenden zahlenmässigen Zusammenhänge:

Die Verhältnisse der niedrigsten zu den höchsten Konzentrationen in den Abb. 5—8 sind etwa gleich gross (das 30- bis 70-fache). Das Intensitätsverhältnis der Teilbanden I, II und III verschiebt sich dagegen bei den Lösungen weit stärker, als bei den auf das Substrat aufgetragenen Wirkstoffen.

Für Optinol BA ist

$$\frac{a J_{I,L,1}}{J_{I\,L,2}} : \frac{a J_{II,L,1}}{J_{II,L,2}} : \frac{a J_{III,L,1}}{J_{III,L,2}} = \infty : 1 : 0{,}50$$

$$\frac{bJ_{I,S,3}}{J_{I,S,4}} : \frac{bJ_{II,S,3}}{J_{II,S,4}} : \frac{bJ_{III,S,3}}{J_{III,S,4}} = 2{,}7 : 1 : 0{,}77$$

Im Falle Optinol BVS ist

$$\frac{cJ_{I,L,5}}{J_{I,L,6}} : \frac{cJ_{II,L,5}}{J_{II,L,6}} : \frac{cJ_{III,L,5}}{J_{III,L,6}} = \infty : 1 : 0{,}40$$

$$\frac{dJ_{I,S,7}}{J_{I,S,8}} : \frac{dJ_{II,S,7}}{J_{II,S,8}} : \frac{dJ_{III,S,7}}{J_{III,S,8}} = 3{,}1 : 1 : 0{,}60$$

wo J die Intensität der Teilbanden-Maxima bedeutet, während im Index
L die Lösung,
S den Aufheller am Substrat
die römischen Zahlen die Reihenzahlen der Teilbanden bezeichnen,
1 = 3,9 g/cm³ Wirkstoff,
2 = 0,078 g/cm³ Wirkstoff,
3 = 1,3 g/cm³ Wirkstoff,
4 = 0,05 g/cm³ Wirkstoff,
5 = 3,3 g/cm³ Wirkstoff,
6 = 0,067 g/cm³ Wirkstoff,
7 = 3,1 g/cm³ Wirkstoff,
8 = 0,04 g/cm³ Wirkstoff;
a, b, c und d bedeuten schliesslich Konstanten.

Die Arbeit wurde zum Teil im Forschungsinstitut für die Textilindustrie (TKI), zum Teil im Zentralforschungsinstitut für Physik (KFKI), im Institut für Technische Physik (MFI) und bei der Firma Egyesült Vegyiművek (EV) ausgeführt. Den Leitern der genannten Institute und der Firma sei hier für die Arbeitsmöglichkeit verbindlicher Dank ausgesprochen. Im weiteren sei Dank gesagt Herrn A. Merényi (EV) für die Muster am Substrat und für wertvolle Informationen, Frau L. Nagy (TKI) für die präzise Herstellung und Messung der Lösungen, Herrn Dr. J. Szőke für die Zusammenstellung einer Messanordnung, Herrn J. Schanda und Frl. E. Barta für die Korrektionsmessungen und Herrn Ö. Lendvay (MFI) für wertvolle Ratschläge.

LITERATUR

1. A. Kling-J. Kurz, Melliand, **41**, 339, 1960.
2. M. Pestemer, A. Berger and A. Wagner, SVF, **19**, 420, 1964.
3. I. Rusznák and A. Székely, Melliand, **42**, 923, 1961.
4. J. Lanter, SVF, **19**, 469, 1964.
5. A. Merényi, Kolor. Ért., **7**, 286, 1965.
6. P. Kubelka u. N. Munk, Z. Techn. Physik **12**, 593, 1931.

7. T. H. MORTON, J. Soc. Dyers Colour., **79**, 238, 1963.
8. Á. BUDÓ, R. DOMBI and R. HORVAI, Acta Phys. et Chem. Univ. Szeg. **3**, 1957.
9. Á. BUDÓ und J. KETSKEMÉTY, Acta Phys. Hung., **7**, 207, 1957.
10. GY. SZIGETI, Mitteilungen der math. und naturwiss. Abt. der Ung. Akad. d. Wissenschaften (Vorträge zum Anlass des 125-jährigen Jubiläums.) Akad. Kiadó. 1951.
11. S. MILLSON, Amer. Dyest. Rep., **37**, 423, 1948.
12. R. E. KIRK und D. F. OTHMER, Encyclopedia of Chemical Technology, John Wiley and Sons Inc. New York, 1964. 2. Aufl. Bd 3. p. 737.
13. E. LENDVAY, Acta Phys. Hung., **14**, 187, 1962.

Acta Physica Academiae Scientiarum Hungaricae, Tomus 23 (2), pp. 247—250 (1967)

SUR LA SOLUTION DE L'ÉQUATION DE BOLTZMANN RELATIVISTE SANS COLLISIONS EN PRÉSENCE DE CERTAINS CHAMPS EXTÉRIEURS

I. ABONYI

INSTITUT DE PHYSIQUE THÉORIQUE DE L'UNIVERSITÉ ROLAND EÖTVÖS, BUDAPEST

(Reçu le 17 V. 1966)

Considérons un système de particules identiques douées de masse au repos m_0. Ce système soit soumis à une force extérieure dont le quadrivecteur force se dérive d'un potentiel scalaire $\Phi(x)$:

$$F_i = -\partial_i \Phi\,, \tag{1}$$

où ∂_i représente le quadrivecteur gradient par rapport aux variables de posir tion de l'espace-temps. (Dans ce qui suit, la sommation est sous-entendue su- les indices répétés de 1 à 4, et $x_4 = \text{ict.}$)

Nous nous intéresserons au problème de l'intégration de l'équation de Boltzmann relativiste pour le cas où l'interaction mutuelle des particules peut être négligée (par exemple à cause de la densité très faible). Cela veut dire que le système sera décrit par l'équation

$$(p_i \partial_i + m_0 F_i \nabla_i) f(x, p) = 0\,, \tag{2}$$

où $f = f(x, p)$ est la fonction de distribution qui dépend de quadrivecteurs position x_r et impulsion p_r, et le symbôle ∇_i signifie le quadrivecteur gradient dans l'espace des p_r. [1]

Il est bien connu (cf. par exemple [2]) que pour les particules libres, on déduit la forme fonctionnelle de la solution de l'équation (2) à partir d'un »théorème H« en faisant l'usage des invariants simples de collision. Nous accepterons pour notre cas aussi que le nombre des particules et le quadrivecteur de l'impulsion sont conservés, c'est-à-dire nous allons construire la solution de (2) sous la forme

$$f(x, p) = \exp\left\{\alpha(x) + \beta_r(x) p_r\right\}, \tag{3}$$

où les fonctions $\alpha(x)$ et $\beta_r(x)$ jouent le rôle des multiplicateurs de Lagrange correspondant aux quantités conservées et $\beta_r \beta_r < 0$ pour assurer la convergence des intégrales qui donnent les moyennes. Ici

$$\beta_r = (k\,T)^{-1}\,u_r\,,$$

où u_r est le quadrivecteur vitesse hydrodynamique, T la température absolue, k la constante de Boltzmann.

La substitution de (3) dans (2) nous donne

$$p_r\,\partial_r\,\alpha\,(x) + p_r\,p_s\,\partial_r\,\beta_s\,(x) + m_0\,F_r\,\beta_r\,(x) = 0\,. \tag{4}$$

Si l'on exclut la rotation du système comme corps rigide, rotation qui pent être cachée dans les paramètres β_r, il ne faut retenir des solutions de

$$\partial_r\,\beta_s\,(x) + \partial_s\,\beta_r\,(x) = 0 \tag{5}$$

que les quatre β_r indépendants du quadrivecteur position.

Ce qui reste de l'équation (4) peut être traité en multipliant par $f(x, p)$ et en intégrant sur l'espace des impulsions. Ainsi on obtiendra l'équation

$$\int p_r\,f\,d\,\omega\cdot\partial_r\,\alpha\,(x) - m_0\,(\partial_r\,\Phi)\,\beta_r\int f\,d\,\omega = 0\,, \tag{6}$$

où $d\,\omega$ est l'élément invariant de volume dans l'espace des impulsions [2].

Étant donné que par définition

$$m_0\,u_r\,(x) = \frac{\int p_r\,f\,d\,\omega}{\int f\,d\,\omega} \tag{7}$$

on a tout de suite

$$\alpha\,(x) = (k\,T)^{-1}\,\Phi\,(x) \tag{8}$$

à une constante additive près.

Finalement la fonction de distribution prend la forme

$$f(x, p) = \exp\frac{1}{k\,T}\{\,p_r\,u_r + \Phi\,(x)\,\} \tag{9}$$

à un facteur de normalisation près.

Dans un repère spécial où le système est au repos macroscopiquement, l'exponentielle se réduira à

$$\exp\left\{-\frac{1}{k\,T}\,(E + \Phi)\right\}, \tag{10}$$

où E est l'énergie totale de la particule. Dans ce repère, les modifications relativistes (sauf celle de la masse au repos) viennent de la forme invariante de l'élément de volume $d\,\omega$.

Malheureusement, la généralisation de la solution maxwellienne ne se laisse pas réaliser quand le système est soumis à un champ électromagnétique, où le quadrivecteur force pondéromotrice est

$$F_i = \frac{e}{m_0 c} F_{ik} p_k \text{ avec } F_{ik} = \partial_k A_i - \partial_i A_k . \tag{11}$$

Ici $A_i(x)$ représente le quadrivecteur potentiel. En effet, la condition d'existence d'une solution de la forme (3) de l'équation de Boltzmann

$$\left(p_s \partial_s + \frac{e}{c} F_{ik} p_k \nabla_i\right) f(x, p) = 0 \tag{12}$$

s'écrit

$$p_s \partial_s \alpha(x) + p_r p_s \partial_s \beta_r(x) + \frac{e}{c} F_{ik} p_k \beta_i(x) = 0 . \tag{13}$$

Si l'on veut exclure la rotation rigide du système, on doit poser (5) et ne retenir que des β_i indépendants du quadrivecteur position. Ainsi l'on a

$$p_s \left\{\partial_s \alpha(x) + \frac{e}{c} F_{is}(x) \beta_i\right\} = 0 . \tag{14}$$

Donc, afin que cette équation puisse être satisfaite pour n'importe quelle valeur de p_r, il faut que selon l'équation

$$\partial_s \alpha(x) = -\frac{e}{c} F_{is}(x) \beta_i \tag{15}$$

l'expression $F_{is}(x)\,\beta_i$ soit un quadrivecteur gradient complet. Cela veut dire que le tenseur

$$G_{rs} = (\partial_r \partial_s - \partial_s \partial_r)\,\alpha(x) = \frac{e}{c} \beta_i \left(\partial_s F_{ir}(x) - \partial_r F_{is}(x)\right)$$

doit disparaître pour n'importe quelle paire d'indices r,s. Cette relation peut être aisément mise sous la forme:

$$\beta_i \partial_i F_{rs}(x) = 0 . \tag{16}$$

A cause de (16), *une solution de la forme* (3) *de l'équation de Boltzmann relativiste* (2) *ne peut exister que pour les champs* $F_{is}(x)$ *qui sont constant sur les lignes d'univers.*

Étant donné que β_r est parallèle à u_r, dans un repère où le système est macroscopiquement au repos, (15) a la forme

$$\partial_s \alpha(x) = - F_{4s} \beta_4$$

ou autrement dit, F_{rs} ne peut être qu'un champ tel, dont les composantes magnétiques s'annulent.

BIBLIOGRAPHIE

1. I. Abonyi, Cahier de Physique, N^{os} 171—172, 461, 1964.
2. W. Israel, Journal of Mathematical Physics, **4**, 1163, 1963.

RECENSIO

Collected Scientific Papers by Wolfgang Pauli

Interscience Publishers, John Wiley and Sons, Inc., New York—London—Sidney, 1964. Vol. I. XXVII + 1133, Vol. II. XIII + 1408.

In erster Linie die Physiker und auch die auf den Grenzgebienten der Physik arbeitenden Wissenschaftler haben die Herausgabe der gesammelten wissenschaftlichen Arbeiten von WOLFGANG PAULI, eines des grössten Physikers unseres Zeitalters, mit Freude und Genugtuung vernommen. Dieses monumentale Werk ist unter der Redaktion von R. KRONIG und V. F. WEISSKOPF erschienen und umfasst zwei Bände, der erste mit dem Untertitel »Books and Contributions to Books«, der zweite mit dem Untertitel »Journal Articles, Conference Reports and Contributions to Discussions«.

PAULIS Arbeiten sind in der Physik grundlegend, daher allgemein bekannt, in der Literatur der Physik ständig zitiert und oftmals gewürdigt worden. Wir möchten hier deshalb nur auf zwei seiner bekanntesten zusammenfassenden Arbeiten kurz zu sprechen kommen, die auch heute noch als die unübertroffenen Standardwerke auf ihrem Gebiete gelten, obwohl ihr Erscheinen 45, bzw. 33 Jahren zurückliegt.

Die erste ist die »Relativitätstheorie«, die PAULI im Alter von 21 Jahren geschrieben hat und die er in der Enzyklopädie der Mathematischen Wissenschaften in 1921 veröffentlichte. Den grossen Erfolg dieser berühmten Arbeit beweist, dass diese mit unverändertem Text nur mit einer im Verhältnis zur ganzen kleinen Ergänzung »Supplementary Notes by the Author« im Jahre 1958 in englisch erschienen ist. Auch diese Ergänzung ist in den vorliegenden gesammelten Werken von PAULI enthalten.

EINSTEIN hat diese Arbeit in den Naturwissenschaften **10**, 184, 1922 mit folgenden Worten gewürdigt, die auch im Vorwort der Collected Papers wiedergegeben sind:

»Wer dieses reife und gross angelegte Werk studiert, möchte nicht glauben, dass der Verfasser ein Mann von einundzwanzig Jahren ist. Man weiss nicht, was man am meisten bewundern soll, das psychologische Verständnis für Ideeentwicklung, die Sicherheit der mathematischen Deduktion, den tiefen physikalischen Blick, das Vermögen übersichtlicher systematischer Darstellung, die Literaturkenntnis, die sachliche Vollständigkeit, die Sicherheit der Kritik.«

Die zweite Arbeit, die ich hier kurz erwähnen möchte, ist PAULIS Handbuch-Beitrag »Die allgemeinen Prinzipien der Wellenmechanik« in GEIGER—SCHEELS Handbuch der Physik Bd. XXIV/1, der in 1933 erschien und in der neuen Auflage des Handbuches (herausgegeben von FLÜGGE) in 1958 mit nur wenigen Änderungen und Ergänzungen neu gedruckt wurde. Allein hieraus ist das Genie PAULIS ersichtlich, der es vermochte ein Gebiet der Physik, das erst in 1926 entstand und sich in starker Entwicklung befand, kaum nach dessen Entstehen in einer Weise darzustellen, die es nach einem Vierteljahrhundert als ein immer noch aktuelles Meisterwerk kennzeichnet.

Die Arbeiten PAULIS, die in den beiden Bänden zusammengestellt sind, scheinen vollständig zu sein. Den Herausgebern gebührt Dank und Anerkennung. Möge dieses Werk, das eine erstaunliche Quelle schöpferischen Geistes darstellt, auch in der jungen heranwachsenden Generation von Physikern eine je grössere Verbreitung finden.

P. GOMBÁS

Printed in Hungary

A kiadásért felel Akadémiai Kiadó igazgatója — Műszaki szerkesztő: Farkas Sándor

A kézirat nyomdába érkezett: 1967. II. 3. — Terjedelem: 10,25 (A/5) ív, 17 ábra

67. 63436 Akadémiai Nyomda, Budapest — Felelős vezető: Bernát György

Reviews of the Hungarian Academy of Sciences are obtainable at the following addresses:

ALBANIA
Ndermarja Shtetnore e Botimeve
Tirana

AUSTRALIA
A. KEESING
Box 4886, GPO
Sydney

AUSTRIA
Globus Buchvertrieb
Salzgries 16
Wien I

BELGIUM
Office International de Librairie
30, Avenue Marnix
Bruxelles 5
Du Monde Entier
5, Place St. Jean
Bruxelles

BULGARIA
Raznoiznos
1, Tzar Assen
Sofia

CANADA
Pannonia Books
2, Spadina Road
Toronto 4, Ont.

CHINA
Waiwen Shudian
Peking
P. O. B. 88

CZECHOSLOVAKIA
Artia
Ve Smečkách 30
Praha 2
Poštova Novinova Služba
Dovoz Tisku
Vinohradska 46
Praha 2
Madarská Kultura
Václavské nám. 2
Praha I
Poštova Novinova Služba
Dovoz Tlace
Leningradska 14
Bratislava

DENMARK
Ejnar Munksgaard
Nörregade 6
Copenhagen

FINLAND
Akateeminen Kirjkauppa
Keskuskatu 2
Helsinki

FRANCE
Office International de Docuemntation et Librairie
48, rue Gay Lussac
Paris 5

GERMAN DEMOCRATIC REPUBLIC
Deutscher Buch-Export und Import
Leninstraße 16
Leipzig 701
Zeitungsvertriebsamt
Clara Zetkin Straße 62
Berlin N. W.

GERMAN FEDERAL REPUBLIC
Kunst und Wissen
Erich Bieber
Postfach 46
7 Stuttgart S.

GREAT BRITAIN
Collet's Holdings Ltd.
Dennington Estate
London Rd.
Wellingborough. Northamps.
Robert Maxwell and Co. Ltd.
Waynflete Bldg. The Plain
Oxford

HOLLAND
Swetz and Zeitlinger
Keizersgracht 471—487
Amsterdam C
Martinus Nijhof
Lange Voorhout 9
The Hague

INDIA
Current Technical Literature
Co Private Ltd.
India House OPP
GPO Post Box 1374
Bombay I

ITALY
Santo Vanasia
Via M. Macchi 71
Milano
Libreria Commissionaria Sansoni
Via La Marmora 45
Firenze

JAPAN
Nauka Ltd.
92. Ikebukur O-Higashi 1-chome
Toshima-ku
Tokyo
Maruzen and Co. Ltd.
P. O. Box 605
Tokyo-Central
Far Eastern Booksellers
Kanda P. O. Box 72
Tokyo

KOREA
Chulpanmul
Phenjan

NORWAY
Johan Grundt Tanum
Karl Johansgatan 43
Oslo

POLAND
RUCH
ul. Wronia 23
Warszawa

ROUMANIA
Cartimex
Str. Aristide Briand 14—18
Bucureşti

SOVIET UNION
Mezhdunarodnaia Kniga
Moscow G—200

SWEDEN
Almquist and Wiksell
Gamla Brogatan 26
Stockholm

USA
Stechert Hafner Inc.
31, East 10th Street
New York, N. Y. 10003
Walter J. Johnson
111, Fifth Avenue
New York, N. Y. 10003

VIETNAM
Xunhasaba
19, Tran Quoc Toan
Hanoi

YUGOSLAVIA
Forum
Vojvode Mišića broj 1
Novi Sad
Jugoslovenska Knjiga
Terazije 27
Beograd

The *Acta Physica* publish papers on physics, in English, German, French and Russian.
The *Acta Physica* appear in parts of varying size, making up volumes.
Manuscripts should be addressed to:

Acta Physica, Budapest 502, P. O. B. 24.

Correspondence with the editors and publishers should be sent to the same address.
The rate of subscription to the *Acta Physica* is 165 forints a volume. Orders may be placed with "Kultúra" Foreign Trade Company for Books and Newspapers (Budapest I., Fő u. 32. Account No. 43-790-057-181) or with representatives abroad.

Les *Acta Physica* paraissent en français, allemand, anglais et russe et publient des travaux du domaine de la physique.
Les *Acta Physica* sont publiés sous forme de fascicules qui seront réunis en volumes.
On est prié d'envoyer les manuscrits destinés à la rédaction à l'adresse suivante:

Acta Physica, Budapest 502, P. O. B. 24.

Toute correspondance doit être envoyée à cette même adresse.
Le prix de l'abonnement est de 165 forints par volume.
On peut s'abonner à l'Entreprise du Commerce Extérieur de Livres et Journaux «Kultúra» (Budapest I., Fő u. 32. — Compte-courant No. 43-790-057-181) ou à l'étranger chez tous les représentants ou dépositaires.

«*Acta Physica*» публикуют трактаты из области физических наук на русском, немецком, английском и французском языках.
«*Acta Physica*» выходят отдельными выпусками разного объема. Несколько выпусков составляют один том.
Предназначенные для публикации рукописи следует направлять по адресу:

Acta Physica, Budapest 502, P. O. B. 24.

По этому же адресу направлять всякую корреспонденцию для редакции и администрации.
Подписная цена «*Acta Physica*» — 165 форинтов за том. Заказы принимает предприятие по внешней торговле книг и газет «*Kultúra*» (Budapest I., Fő u. 32. Текущий счет: № 43-790-057-181) или его заграничные представительства и уполномоченные.

44,— Ft

INDEX

A. Szalay and *A. Kovách:* Fission Product Precipitation from the Atmosphere in Debrecen, Hungary, between 1963 and 1965. — *А. Салаи* и *А. Ковач:* Осаждение продуктов деления из атмосферы в г. Дебрецен, Венгрия, в 1963– 1965 гг. 137

G. Knapecz: General Relativistic Theory of Lagrangian Functions I. — *Г. Кнапец:* Общее релятивистская теория лагранжианов. I. 145

Л. Пал: Влияние флуктуации внутреннего магнитного поля на еффект Мэссбауэра. *L. Pál:* The Effect of the Fluctuation of the Internal Magnetic Field on the Mössbauer Pattern. 161

I. Abonyi: The Crocco—Vázsonyi Equation in Relativistic Hydrodynamics of Ideal Fluids. — *И. Абони:* Уравнение Крокко—Важони в релятивистской гидродинамике идеальной жидкости 185

M. Z. v. Krzywoblocki: Gravitational Waves. — *М. З. Крзывоблоцки:* Гравитационные волны. 193

G. Knapecz: Symmetry Theory of the Equations of Motion I. — *Г. Кнапец:* Теория уравнений движения на основе симметрии пространства. I. 203

M. L. Császár und *E. Koczkás:* Das Elektronenbandenspektrum des CsD-Moleküls im sichtbaren Spektralgebiet. — *М. Л. Часар* и *Э. Коцкаш:* Спектр электронной связи молекулы CsD в видимой области 211

M. Huszár: Non-relativistic Approximation of the Dirac Current. — *М. Гусар:* Нерелятивистское приближение тока Дирака 225

COMMUNICATIONES BREVES

A. Székely: Die Fluoreszenz von 4,4'-bis-Triazinilaminostilben-2,2'-Disulfonsäurederivaten 237

I. Abonyi: Sur la solution de l'équation de Boltzmann relativiste sans collisions en présence de certains champs extérieurs 247

RECENSIO

P. Gombás: Wolfgang Pauli: Collected Scientific Papers 251

Acta Phys. Hung. Tom. XXIII. Fasc. 2. Budapest, 6. VI. 1967. Index: 26.022

ACTA PHYSICA

ACADEMIAE SCIENTIARUM HUNGARICAE

TOMUS XXIII FASCICULUS 3

AKADÉMIAI KIADÓ, BUDAPEST
1967

ACTA PHYS. HUNG.

ACTA PHYSICA

A MAGYAR TUDOMÁNYOS AKADÉMIA FIZIKAI KÖZLEMÉNYEI

SZERKESZTŐSÉG ÉS KIADÓHIVATAL: BUDAPEST V., ALKOTMÁNY UTCA 21.

Az *Acta Physica* német, angol, francia és orosz nyelven közöl értekezéseket a fizika tárgyköréből.

Az *Acta Physica* változó terjedelmű füzetekben jelenik meg: több füzet alkot egy kötetet.

A közlésre szánt kéziratok a következő címre küldendők:

Acta Physica, Budapest 502, P. O. B. 24.

Ugyanerre a címre küldendő minden szerkesztőségi és kiadóhivatali levelezés.

Az *Acta Physica* előfizetési ára kötetenként belföldre 120 forint, külföldre 165 forint. Megrendelhető a belföld számára az Akadémiai Kiadónál (Budapest V., Alkotmány utca 21. Bankszámla 05-915-111-46), a külföld számára pedig a „Kultúra" Könyv- és Hírlap Külkereskedelmi Vállalatnál (Budapest I., Fő u. 32. Bankszámla 43-790-057-181 sz.), vagy annak külföldi képviseleteinél és bizományosainál.

Die *Acta Physica* veröffentlichen Abhandlungen aus dem Bereich der Physik in deutscher, englischer, französischer und russischer Sprache.

Die *Acta Physica* erscheinen in Heften wechselnden Umfanges. Mehrere Hefte bilden einen Band.

Die zur Veröffentlichung bestimmten Manuskripte sind an folgende Adresse zu richten:

Acta Physica, Budapest 502, P. O. B. 24.

An die gleiche Anschrift ist auch jede für die Redaktion und den Verlag bestimmte Korrespondenz zu senden.

Abonnementspreis pro Band: 165 Forint. Bestellbar bei dem Buch- und Zeitungs-Aussenhandels-Unternehmen »Kultúra« (Budapest I., Fő u. 32. Bankkonto Nr. 43-790-057-181) oder bei seinen Auslandsvertretungen und Kommissionären.

Acta Physica Academiae Scientiarum Hungaricae, Tomus 23 (3), pp. 253—258 (1967)

QUADRATIC INTERACTIONS IN QUANTUM FIELD THEORY*

By

L. F. LANDOVITZ

BELFER GRADUATE SCHOOL OF SCIENCE, YESHIVA UNIVERSITY, NEW YORK, NEW YORK 10033, USA

(Presented by A. Kónya. — Received 5. VII. 1966)

The effects of a quadratic interaction term in a quantum field theory are studied. It is found that the exact and bare Hilbert spaces are orthogonal. Thus, if such terms occur in a theory, they must be treated exactly prior using the Dyson expansion to calculate the effects of residual interactions.

I

In a recent paper, A. FRENKEL [1] considered the problem of a fermion or boson quantum field interacting with itself via a quadratic interaction, viz.

$$H = H_0 + H_1 ,$$

$$H_0 = \int : \Psi^+ [\vec{\alpha} \cdot \vec{p} + \beta m] \Psi : d^3 x ,$$

$$H_1 = + m_1 \int : \overline{\Psi} \Psi : d^3 x ,$$

$$\left\{ \Psi (\vec{x}, t), \Psi^+ (\vec{x}', t) \right\} = \delta (\vec{x} - \vec{x}') ,$$

$$\left\{ \Psi (\vec{x}, t), \Psi (\vec{x}', t) \right\} = \left\{ \Psi^+ (\vec{x}, t), \Psi (\vec{x}', t) \right\} = 0 .$$

(We shall only consider the fermion case: the boson case can be treated in a similar manner.) He concluded that the renormalized wave-function was zero and, thus, interpreted this to mean that the particles corresponding to the field Ψ have no asymptotic states. In a certain sense, which we shall shortly specify, this conclusion is correct. However, the interpretation of the meaning of this result is incorrect.

If we do not separate the Hamiltonian H into two parts H_0 and H_1, it is clear we can exactly diagonalize it and

$$H = \sum_p [n_{ps}^{(+)} + n_{ps}^{(-)}] E_p ,$$

where $n_{ps}^{(\pm)}$ is the (diagonal) number operator for particles (antiparticles) of momentum $\vec{p}$ and helicity s, and

* Supported in part by the National Science Foundation.

$$E_p = \sqrt{\vec{p}^2 + (m + m_1)^2} \ .$$

If we insist on treating H_1 as a perturbation, then, in terms of the eigenstates of H_0, the exact eigenstates of H have interesting, though familiar properties. We shall treat the problem from this latter point of view. We shall see that the representations of the fields for the two problems, H_0 and H, lead to inequivalent representations.

Further, as can be seen, the spectra of H and H_0 are not the same; but, if the U matrix were unitary, the spectra would have to be the same.

II

In the representation in which H_0 is diagonal,

$$H_0 = \sum_{\vec{p}} (a^{\pm}_{\vec{p}s}\, a_{\vec{p}s} + b^{\pm}_{\vec{p}s}\, b_{\vec{p}s})\, \epsilon(p)\,,$$

$$\{a_{\vec{p}s}, a^{\pm}_{\vec{p}'s'}\} = \delta_{\vec{p}'\vec{p}}\, \delta_{ss'} = \{b_{\vec{p}s}, b^{\pm}_{\vec{p}'s'}\}\,,$$

$$\{a_{\vec{p}s}, b_{\vec{p}'s'}\} = \{a_{\vec{p}s}, b^{\pm}_{\vec{p}'s'}\} = 0$$

and

$$H_1 = +\, m_1 \sum_{\vec{p}} \left\{ \frac{m}{\epsilon} [a^{\pm}_{\vec{p}s}\, a_{\vec{p}s} + b^{\pm}_{\vec{p}s}\, b_{\vec{p}s}] + s\, \frac{|\vec{p}|}{\epsilon} [a^{\pm}_{\vec{p}s}\, b^{+}_{-\vec{p}-s} + b_{-\vec{p}-s}\, a_{\vec{p}s})] \right\}.$$

We can write

$$H = \sum_{\vec{p}s} \mathscr{H}(\vec{p}s)\,,$$

where

$$\mathscr{H}(\vec{p}s) = \epsilon(p)\, [a^{\pm}_{\vec{p}s}\, a_{\vec{p}s} + b^{+}_{-\vec{p}-s}\, b_{-\vec{p}-s}] + \frac{m_1\, m}{\epsilon} [a^{\pm}_{\vec{p}s}\, a_{\vec{p}s} + b^{+}_{-\vec{p}-s}\, b_{-\vec{p}-s}] +$$

$$+\, m_1\, s\, \frac{|\vec{p}|}{\epsilon} [a^{\pm}_{\vec{p}s}\, b^{+}_{-\vec{p}-s} + b_{-\vec{p}-s}\, a_{\vec{p}s}]\,.$$

We now seek a unitary transformation U such that

$$U^{+} H\, U = \sum_{\vec{p}s} E(p) [a^{\pm}_{\vec{p}s}\, a_{\vec{p}s} + b^{\pm}_{\vec{p}s}\, b_{\vec{p}s}] + \text{ const.}$$

If we set

$$U = \prod_{\vec{p}s} U_{\vec{p}s}$$

and

$$U_{\vec{p}s} = e^{\alpha_{\vec{p}s} [a^{\dagger}_{\vec{p}s} b^{\pm}_{-\vec{p}-s} - b_{-\vec{p}-s}\, a_{\vec{p}s}]},$$

then

$$\tan 2\alpha_{\vec{p}s} = s\frac{|\vec{p}|\, m_1}{\epsilon^2 + m\, m_1} = s\ \tan 2\alpha_{\vec{p}}\,,$$

$$U^+ a_{\vec{p}s} U = a_{\vec{p}s}\ \cos\ \alpha_{\vec{p}s} + b^+_{-\vec{p}-s}\ \sin\ \alpha_{\vec{p}s}\,,$$

$$U^+ b_{\vec{p}s} U = b_{\vec{p}s}\ \cos\ \alpha_{-\vec{p}-s} - a^+_{-\vec{p}-s}\ \sin\ \alpha_{-\vec{p}-s}\,.$$

The physical vacuum is the lowest eigenstate of H: thus, in terms of the bare vacuum, the physical vacuum is

$$|\,\mathbf{0}\rangle = U\,|\,0\rangle = \prod_{\vec{p}} U_{ps}\,|\,0\rangle = \prod_{\vec{p}s}(\cos\ \alpha_{\vec{p}s} + a^+_{\vec{p}s}\, b^+_{-\vec{p}-s}\ \sin\ \alpha_{\vec{p}s})\,|\,0\rangle\,.$$

Hence, the physical vacuum contains correlated pairs. Next let us consider the overlap of the bare and physical vacua:

$$\langle\mathbf{0}\,|\,0\rangle = \prod_{\vec{p}}\ \cos\ \alpha_{\vec{p}s} = \prod_{\vec{p}s}\ \cos^2\ \alpha_{\vec{p}}$$

$$\langle\mathbf{0}\,|\,0\rangle = e^{\sum\limits_{\vec{p}}\log\ \cos^2\ \alpha_{\vec{p}}} = e^{\frac{1}{(2\pi)^3}\int d^3p\ \log\ \cos^2\ \alpha_{\vec{p}}} \equiv e^R\,,$$

$$R = \frac{1}{(2\pi)^3}\int d^3p\ \log\ \cos^2\ \alpha_p = \frac{4\pi}{(2\pi)^3}\int_0^\infty p^2\,dp\ \log\ \cos^2\ \alpha_p\,,$$

$$\cos^2\ \alpha_p = \frac{1+\ \cos\ 2\alpha_p}{2} = \frac{1}{2}\left[1 + \frac{\epsilon + \dfrac{m\, m_1}{\epsilon}}{E}\right].$$

Let us divide the integral into two parts: one from 0 to K and then another from K to ∞

$$R = \frac{1}{4\pi^2}\int_0^K p^2\,dp\ \log\ \cos^2\ \alpha_p + \int_K^\infty p^2\,dp\ \log\ \cos^2\ \alpha_p$$

and choose K such that $K \gg m,\, m_1$. For $p \geq K$,

$$\cos^2\ \alpha_p \cong \frac{1}{2}\left[1 + \frac{p\left(1 + \dfrac{1}{2}\dfrac{m^2}{p^2}\right) + \dfrac{m\, m_1}{p}}{p\left(1 + \dfrac{1}{2}\dfrac{(m+m_1)^2}{p^2}\right)}\right] \cong$$

$$\cong \frac{1}{2}\left[1 + \frac{1 + \frac{1}{2}\frac{m^2}{p^2} + \frac{m\,m_1}{p^2}}{1 + \frac{1}{2}\frac{(m+m_1)^2}{p^2}}\right] \cong$$

$$\cong \frac{1}{2}\left[1 + 1 + \frac{1}{2}\frac{m^2}{p^2} + \frac{m\,m_1}{p^2} - \frac{1}{2}\frac{(m+m_1)^2}{p^2}\right] \cong 1 - \frac{1}{4}\frac{m_1^2}{p^2},$$

$$\log \cos^2 \alpha_p \approx -\frac{1}{4}\frac{m_1^2}{p^2}.$$

If we let

$$\frac{1}{2\pi^2}\int_0^K p^2\,dp \log \cos^2 \alpha_p = R_K,$$

then

$$R = R_K - \frac{1}{4}\int_K^\infty \frac{m_1^2}{p^2}\,p^2\,dp = R_K + \frac{1}{4}m_1^2 K - \infty.$$

Thus,

$$\langle \mathbf{0} \mid 0 \rangle = 0$$

and the physical vacuum state is orthogonal to the bare vacuum—in fact, the two Hilbert spaces for any finite number of particles are orthogonal [2]. Thus, the particles do indeed disappear from the Hilbert space of bare states but this does not make them disappear from the theory: it means that there has been a misidentification of asymptotic states. The Dyson expansion has broken down. The similarity of the form of the transformation from bare particles to dressed particles to that of BOGOLIUBOV [3] is noteworthy: the dressed particles are just the Bogoliubov quasi-particles.

III

We can now consider a slightly generalized model which has many of the same properties.

$$H_0 = \int \Psi_1^+ [\vec{\alpha}\cdot\vec{p} + \beta\, m_1]\, \Psi_1\, d^3x + \int \Psi_2^+ [\vec{\alpha}\cdot\vec{p} + \beta\, m_2]\, \Psi_2\, d^3x,$$

$$H_1 = m \int : \overline{\Psi}_1 \Psi_2 + \overline{\Psi}_2 \Psi_1 : d^3x.$$

If we consider the wave function renormalization à la FRENKEL

$$u_{R1}(p) = \left\{1 + \frac{m}{i\gamma\cdot p + m_2} + m^2 \frac{1}{i\gamma\cdot p + m_1}\frac{1}{i\gamma\cdot p + m_2} + \right.$$

$$\left. + m^3 \frac{1}{i\gamma\cdot p + m_2}\frac{1}{i\gamma\cdot p + m_1}\frac{1}{i\gamma\cdot p + m_2} + \ldots\right\} u_1(p) =$$

$$= \left\{1 + m^2 \frac{1}{(i\gamma\cdot p + m_1)(i\gamma\cdot p + m_2)} + m^4 \frac{1}{[(i\gamma\cdot p + m_1)(i\gamma\cdot p + m_2)]^2} + \right.$$

$$\left. + \ldots \right\} u_1(p) + \frac{m}{i\gamma\cdot p + m_2} \left\{1 + m^2 \frac{1}{(i\gamma\cdot p + m_1)(i\gamma\cdot p + m_2)} + \right.$$

$$\left. + m^4 \frac{1}{[(i\gamma\cdot p + m_1)(i\gamma\cdot p + m_2)]^2} + \ldots \right\} u_1(p) =$$

$$= + \frac{1}{1 - \dfrac{-m^2}{(i\gamma\cdot p + m_1)(i\gamma\cdot p + m_2)}} u_1(p) +$$

$$+ \frac{m}{i\gamma\cdot p + m_2} \frac{1}{1 - \dfrac{m^2}{(i\gamma\cdot p + m_1)(i\gamma\cdot p + m_2)}} u_1(p) =$$

$$= \frac{1}{(i\gamma\cdot p + m_1)(i\gamma\cdot p + m_2) - m^2} [(i\gamma\cdot p + m_1)(i\gamma\cdot p + m_2)] +$$

$$+ \frac{m}{i\gamma\cdot p + m_2} \frac{1}{(i\gamma\cdot p + m_1)(i\gamma\cdot p + m_2) - m^2} (i\gamma\cdot p + m_1)(i\gamma\cdot p + m_2) u_1(p) =$$

$$= \left[1 + \frac{m}{i\gamma\cdot p + m_2}\right] \frac{1}{(i\gamma\cdot p + m_1)(i\gamma\cdot p + m_2) - m^2} (i\gamma\cdot p + m_1)$$

$$(i\gamma\cdot p + m_2) u_1(p) = 0$$

and we can see that $u_{R2}(p) = 0$ as well. Again, this is clearly a result of a misidentification of asymptotic fields of precisely the same kind. The true asymptotic fields are linear combinations

Ψ_1 and Ψ_2

$$U^+ \Psi_1 U = \Psi_1 \cos \alpha + \Psi_2 \sin \alpha,$$

$$U^+ \Psi_2 U = \Psi_2 \cos \alpha - \Psi_1 \sin \alpha,$$

$$\tan 2\alpha = \frac{2m}{m_2 - m_1}$$

and

$$U^+ H U = \int \Psi_1^+ [\vec{\alpha}\cdot\vec{p} + \beta\mu_1] \Psi_1 \, d^3x + \int \Psi_2^+ [\vec{\alpha}\cdot\vec{p} + \beta\mu_2] \Psi_2 \, d^3x,$$

$$\mu_1 = \frac{1}{2}(m_1 + m_2) + \frac{1}{2}\sqrt{(m_1 - m_2)^2 + 4m^2},$$

$$\mu_2 = \frac{1}{2}(m_1 + m_2) + \frac{1}{2}\sqrt{(m_1 - m_2)^2 + 4m^2}.$$

Once again if we were to use creation and annihilation operators for the "bare" particles, the Hilbert spaces for H and H_0 would become disjoint. Such an interaction must be eliminated *before* perturbation theory is applied to the rest of the Hamiltonian [4].

REFERENCES

1. A. FRENKEL, Acta Phys. Acad. Sci. Hung., **20**, 167, 1966.
2. It is amusing to note that for one dimension, this phenomenon does not occur whereas for two and higher dimensions it does. Thus, one dimensional models do not have some essential characteristics of more realistic models.
3. N. N. BOGOLIUBOV, Soviet Physics J. E. T. P., **7**, 41, 1958.
4. Such interactions have been utilized in various guises at times in elementary particle theory. Cf. e. g. M. BAKER and S. L. GLASHOW, Nuovo Cimento, **25**, 857, 1962.

КВАДРАТИЧНОЕ ВЗАИМОДЕЙСТВИЕ В КВАНТОВОЙ ТЕОРИИ ПОЛЯ

ЛЕОН Ф. ЛАНДОВИЦ

Р е з ю м е

Изучаются эффекты, обусловленные членом квадратичного взаимодействия в квантовой теории поля. Найдено, что точное и голое Гильбертово пространства ортогональны. Итак, в случае появления таких членов в теории они должны рассматриваться точно, применяя прежде всего формулу Дайсона для определения эффектов остаточных взаимодействий.

Acta Physica Academiae Scientiarum Hungaricae, Tomus 23 (3), pp. 259—276 (1967)

PROBLEMATICS ON THE APPLICATION OF DELAYED COINCIDENCE DEVICES

By

N. A. Eissa* and Gy. Máté

NUCLEAR RESEARCH INSTITUTE OF THE HUNGARIAN ACADEMY OF SCIENCES, DEBRECEN

(Presented by A. Szalay. — Received 13. IX. 1966)

Coincidence circuits have a wide application in nuclear research. This paper deals with their most important features and experiments that can be carried out with these circuits. In this way we shall be concerned with such coincidence circuit parameters as the setting of the delay and of the resolving time. Problems appearing during the application of the normal and sum coincidence are presented. Finally, a description is given of the application of the coincidence circuits for particle identification, for pile up elimination, and for measuring low-energy gamma rays.

I. Introduction

Coincidence circuits are now widely applied in modern nuclear physics. Generally, they are used to show the simultaneity of two or more events, and for measuring very short time intervals. It is generally desirable to improve the technical parameters of coincidence circuits of which the most important is the resolving time. Not only the designer but also the physicist should be thoroughly conversant with the properties of coincidence circuits so that the optimum parameters can be chosen and the circuit used more flexibly.

II. General problems related to coincidence circuits

In all coincidence arrangements, pulses are applied at different inputs and a signal will appear at the circuit output if there is simultaneity of the input pulses. The resolving time of the circuit depends strongly on the width of the input pulses. If the input pulses are of square wave form an output pulse will appear during complete and partial covering of the input pulses. More accurately, if the input pulses are of equal time of duration T, then during a time $2T$, pulses will appear at the output of the circuit. This means that the smaller the pulse width, the better the resolving time of the coincidence circuit. In practice the inpuit pulses are produced by nuclear particle detectors. These detector pulses are generally shaped in such a way that they can provide good resolving power from the point of view of spectroscopic analysis but are

* On leave from Al-Azhar University, Cairo, UAR.

not suitable for triggering coincidence inputs as they are too wide and of variable amplitude.

A typical shape of a detector pulse is shown in Fig. 1. The relatively wide detector pulses can be used to trigger a fast coincidence circuit if we choose that part of the pulse which accurately represents the time of occurrence of the two events as, for example, the starting of the pulse. A very short and well defined pulse shape can be produced which is suitable for triggering the fast coincidence circuit. It is possible to shape the starting point of the pulse so that the resulting pulse width varies from 10^{-7} to 10^{-9} sec. Coincidence circuits

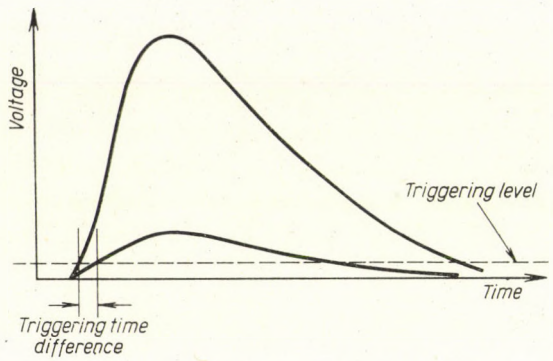

Fig. 1. Typical detector pulse shape. The larger pulse triggers the coincidence circuit earlie than the smaller one although both pulses start simultaneously

having a resolving time of the order of 10^{-12} can be produced [1] but, unfortunately, it is impossible to make use of such a speed even with the fastest detectors. The fastest detectors are scintillation counters for which the time resolution is limited by the time uncertainty of the appearance of the pulses at the photomultiplier anode. This is termed "Jitter" and its order of magnitude is about 10^{-9} sec, or more.

The speed of the coincidence circuit is also limited by the fact that every particle produces pulses having a finite rise time and having different amplitudes. This will give rise to the following problem: In any coincidence circuit an amplitude threshold exists and the input pulses should be higher than this threshold in order to trigger the coincidence circuit. If we want to measure coincidence between large and small pulses, then the large pulses trigger the coincidence circuit earlier than do the small pulses even though both signals are starting simultaneously (see Fig. 1). This difficulty can be partly solved if the triggering level is decreased, but decreasing the threshold is limited by the detector noise. The effect of this phenomenon is always observed at the low energy parts of any spectrum and will be discussed later.

Sometimes it is required in many coincidence measurements to change the resolving time, and this can be done in the following way. The output

signal from the coincidence circuit is integrated and the suitable pulse is chosen by an integral discriminator [2]. Smaller resolving time will be obtained at a higher bias voltage of the discriminator because the output pulse from the coincidence circuit is higher if the two input pulses cover each other completely, and after integration the pulse will reach or exceed the high discrimination level. At low discrimination level the resolving time is larger because in such cases partial covering of the two input pulses will be sufficient to trigger the discriminator. In this way the resolving time is changed by controlling the discrimination level.

The resolving time of the coincidence circuit is measured in the following way: At first, only one detector is used and the same pulses are applied to the coincidence unit which is set at a certain resolving time. In this way it is certain that to every pulse there corresponds another simultaneous pulse of the same amplitude. Then, one of the pulses is delayed to different known values and the coincidence counting rate is measured in each case. The resulting rate distribution is termed a "prompt-prompt" curve. A series of such curves is obtained by changing the resolving time, and then measuring the counting rate as a function of delay (Fig. 2a). The definition of the resolving time is: the half width at half the maximum counting rate. The prompt-prompt definition means that the two input pulses are completely the same, i.e there is no time uncertainty between the two pulses, and the finite but equal threshold at the coincidence input causes no difficulty because in this case coincidences are always between signals of the same amplitude. If the above-mentioned curves are drawn in other cases where the pulses are produced by two independent detectors which are detecting really coincident particles (such as the annihilation radiation), then these curves are termed prompt coincidence curves (Figs 2a and 2c). The resolving time in this latter case is worse than in the earlier one because the effect of the jitter appears here and there is also the effect of coincidence between large and small amplitude pulses.

1. *Basic units of a delayed coincidence circuit*

The general problems mentioned above are usually solved in practice by building a coincidence assembly which consists mainly of the following units (see Fig. 3):

a) Pulse shaper: This produces a uniform short signal from the leading edge of the detector pulses. This unit is generally a vacuum tube or a semiconductor (tunnel diode) univibrator. The threshold of the coincidence circuit is equal to the triggering level of this shaper.

b) Delay unit: This is used for measuring the coincidence curves: for delayed coincidence measurements a delay unit must be inserted in both channels. One of these delay units has a fixed value while the other is variable,

and its value is double that of the fixed one in order that one of pulses can be lagging or leading the other. The actual value of the delay must be higher than the value of the worst adjustable resolving time. It is possible to place the delay unit either after or before the pulse shaper. When it is placed after the

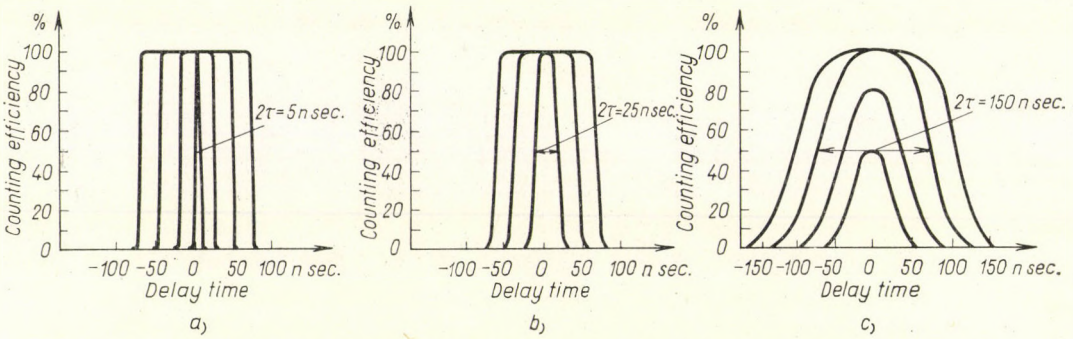

Fig. 2. Characteristic coincidence curves of coincidence circuit: (a) prompt-prompt coincidence curves; (b) prompt coincidence curve, both detectors detect a narrow energy band (differential mode of setting); (c) prompt coincidence curves, both detectors detect the whole energy spectrum (integral mode of setting)

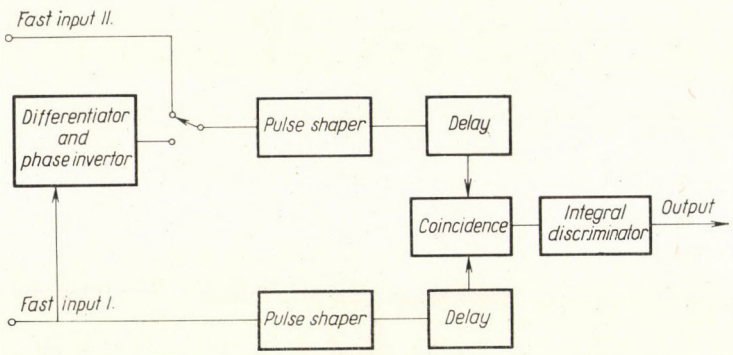

Fig. 3. Block diagram of the basic units of a delayed coincidence circuit. The differentiator and phase invertor unit is used when the circuit is applied for pulse shape discrimination as will be shown later

pulse shaper the delay unit should contain a further shaper to compensate for the pulse distortion caused by the delay unit.

c) Coincidence unit: Different types of circuits exist the most common feature of which is that the output pulse width or pulse height (after integration) depends on the common time interval of the two input pulses.

d) Integral discriminator: Its setting determines the resolving time of the coincidence circuit as mentioned above.

2. *Factors, causing distortion of the coincidence curves*

a) If the measured prompt-prompt coincidence curve is not symmetrical this means that the instrument installation is not correct, as for example, if in the basic coincidence circuit the triggering pulses are not identical and not symmetrical. Another reason for distortion is that the threshold in the two channels of the coincidence circuit are not the same.

b) If the measured integral coincidence curve (Fig. 2c) is distorted, but the prompt-prompt curve is good, then this does not mean a fault, because the curve shape depends on the intensity distribution of the coincidence curve

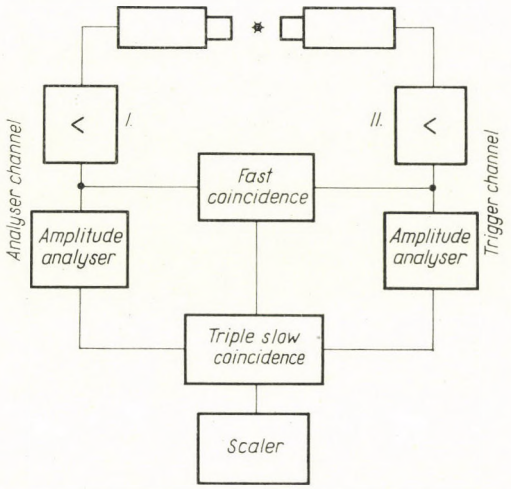

Fig. 4. Block diagram of a slow-fast coincidence system

actually measured. For correct installation only the trumpet curve (to be discussed later) must be used.

3. *Slow-fast system*

A system is termed slow-fast if the coincidence pulses are the same as those which were formed for the energy measurements. It is termed fast-slow, if the fast pulses are separately formed for triggering the fast coincidence unit.

Usually in coincidence measurements it is necessary to know not only the existence of coincidence but also between which energies this coincidence occurs. To fulfil this requirement the construction of the slow-fast coincidence system was necessary. Its block diagram is shown in Fig. 4.

The principle of this system is that two coincidence circuits are used, a fast unit and a slow unit. The fast unit independently of the particle energy determines the existence of coincidence, while the slow unit gives information

about which energies were coincident in the fast unit. The fast unit emits a pulse to the slow unit if two pulses arrive within its resolving time i. e. if the coincidence condition is fulfilled. At the same time the amplitude analysers are also sending pulses to the slow unit and, similarly, will indicate the fulfilment of the amplitude condition.

The number of chance coincidences in slow-fast coincidence is determined experimentally by applying in any branch a delay a few times greater than the resolving time of the fast coincidence (about 5 τ). The chance coincidences in double coincidence can be calculated from the equation: $N_{ch} = 2\tau N_1 N_2$ where τ is the resolving time of the fast unit, N_1 and N_2 are the counting rates at the output of channels I and II. This equation is correct if N_1 and N_2 are smaller than $1/\tau_s$, where τ_s is the resolving time of the slow coincidence unit. In practice this condition is always fulfilled.

In n-fold coincidence the equation is

$$N_{ch} = n\ ^{n-1} N_1 N_2 \ldots N_n.$$

4. *Characteristic curves of the coincidence circuit and choice of the optimum parameters*

The most general question is whether coincidence exists or not. In practice this question is solved by setting both amplitude analysers integrally at low level, then it is ascertained whether triple coincidence exists or not at the slow unit. In other words, in this case each channel allows the whole spectrum independent on between which energies in this coincidence. To determine the energy distribution of the spectrum the following procedure is carried out. Analyser II (sometimes called "trigger channel") is set at a definite energy line of the measured spectrum (i.e. differentially), while by means of analyser I (sometimes called "analyser channel") the whole spectrum is scanned to establish which energies are coincident with the energy defined by analyser II. As an example, consider the case of Co^{60}, where there is coincidence between the 1330 and the 1170 keV lines. Analyser II is set to detect only the 1330 keV line, while analyser I is scanning the whole spectrum, and the triple coincidence unit counts any radiation which is coincident with the 1330 keV line. In such a way the measured coincidence spectrum includes only the energies originating from the 1170 keV line as can be seen from Fig. 5.

During coincidence measurement the question arises: What is the optimum value for resolving time and delay to be chosen during the measurements? The delay setting can be determined from the coincidence curves in Fig. 2 for each mode of measurement. The optimum value is that corresponding to the centre of the coincidence curve where the counting efficiency is maximum. Concerning the resolving time, the aim is to decrease the chance coincidence

rate as low as possible which necessitates a shorter resolving time without counting losses.

As already mentioned, the resolving time is limited by the jitter of the pulses and by their amplitude variation. The first problem can be partially solved by using a faster detector. About the second problem, it has already been mentioned (Fig. 1) that it is impossible to eliminate this phenomenon completely so its effect must be taken into consideration. Its effect can clearly be seen from the difference between the curves in Figs. 2b and 2c where, at the diffe-

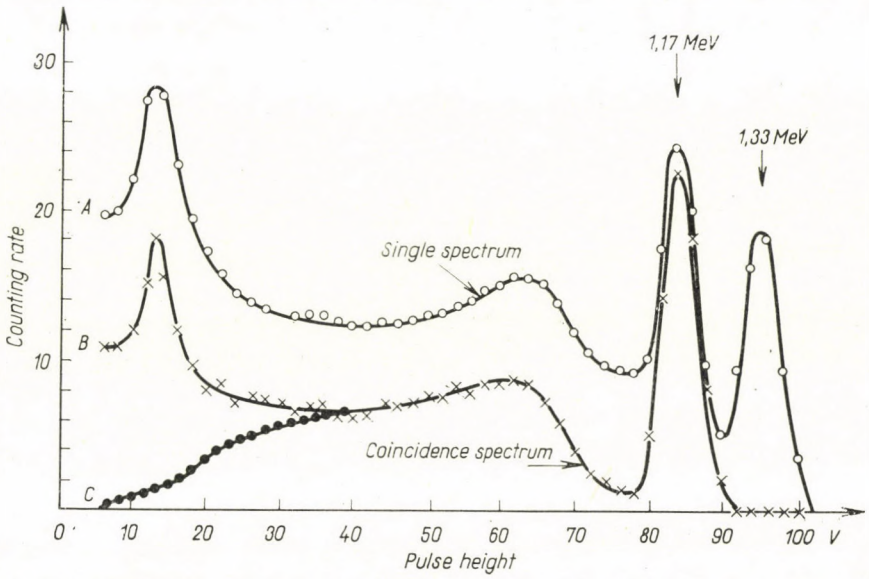

Fig. 5. Co^{60} scintillation spectrum: (a) single spectrum; (b) coincident spectrum with the 1330 keV line at correct setting of the resolving time; (c) distorted coincidence spectrum due to wrong setting of the resolving time

rential setting (2b) of the analysers much better resolving time can be achieved than at the integral setting (Fig. 2c). In the differential mode, coincidences were between a pulse of certain height and another pulse of the same height. This is not always the case because, in general, pulses of different amplitudes trigger the coincidence circuit resulting in a shift of the coincidence curve which can be compensated by the proper setting of the delay lines.

The situation is completely different for the integral mode, where coincidence is sometimes between equal amplitude pulses and at other times between different amplitude pulses. This effect will appear as time fluctuation in the triggering of the coincidence circuit resulting in a broadening of the coincidence curve.

This phenomenon will be clearer after the following example. Adjust the 1330 keV line of Co^{60} at 90 volts pulse height — with small channel width — in

the amplitude analyser of the trigger channel, while the other amplitude analyser — with small channel width — is set at different values of pulse heights between 0 and 80 volts, and in each setting coincidence curves are measured. From the series of coincidence curves, plot the relation between the delay corresponding to the centre of each coincidence curve and the pulse height of the amplitude analyser. A curve similar to that in Fig. 6 is obtained

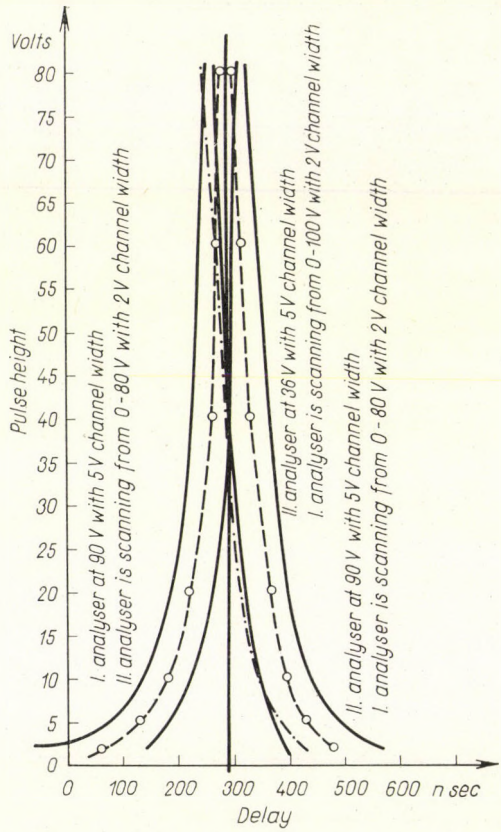

Fig. 6. The shift of the centres of the coincidence curve as a function of the pulse height, "trumpet curves"

where 2τ is drawn at each delay value. The series of these points will form a band whose width shows a variation of 2τ with pulse height. From these curves the optimum parameters can be chosen for any actual measurement. The centers of the coincidence curves coincide at high energies, but at low energies they are shifted. If the role of the trigger and analyser channels are exchanged, then a similar curve with reversed curvature will be obtained. The axis of symmetry represents those cases where the two analysers are set at the same pulse height. The optimum delay for any setting of the amplitude analyser

can be calculated from these two curves. For example, the dashed curve represents the case when analyser II is set at 36 volts while analyser I is scanning the range between 0 and 100 volts. The magnitude of the shift is determined according to the rule that the curve must cross the symmetry axis at the point where the bias of the two analysers is the same.

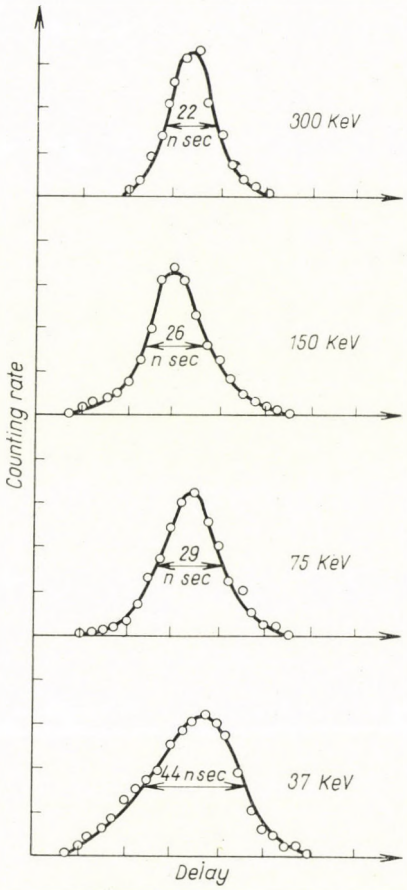

Fig. 7. The effect of energy on the resolving time. The 1330 keV line of Co^{60} was set at 90 volts in the trigger channel. In the other channel the mentioned energy values were set at 20 volts by changing the high tension of its photomultiplier

We shall call this curve "trumpet curve" because of its shape. A given coincidence circuit is better if its curves are less ramified and if at the same time its resolving time is small. The above-mentioned phenomena are effective in those cases when it is desired to measure with much better resolving time than the rise time of the detector pulses, for example, better than 10^{-7} sec in case of NaI(Tl) scintillation detectors. From the trumpet curves the following conclusions can be deduced.

a) The width of the band (2τ) is increased by decreasing the pulse height. This effect is due partly to:

i) Instrumental effect: The large pulses cross the threshold level more steeply than do the smaller pulses and this will cause uncertainty in the triggering.

ii) At smaller energies, the rise time of the pulses fluctuates strictly statistically.

For example, if we decrease the energy of one of the coinciding pulses from 300 to 30 keV, but the pulse height increases to have the same amplitude, then the hand width will increase by a factor of two as shown in Fig. 7.

b) If it is desired to measure so that both channels of the slow-fast system should detect the whole spectrum integrally, then the resolving time of the circuit is limited, and at an energy below a certain value the coincidence spectrum will be cut off. For example, choosing 2τ equal 160 nsec 50% of the coincidence spectrum at 15 volts will be lost (at 15 volts the time difference between the centres of the bands equals 160 nsec). In Fig. 5 curve c shows how the coincidence curve is distorted when too good resolving time is set.

c) The situation is much better if the measurements are carried out in the differential mode because the required delay can always be adjusted. In this case it is possible to achieve 10 times better resolving time which in practice depends on the value of the jitter.

d) An intermediate mode is that when one of the channels is differentially set at a certain energy, while the other is set integrally. Such is the case if one of the analysers is a multichannel analyser, and the other is detecting a certain energy. In this mode the resolving time is improved by a factor of two relative to the pure integral model. According to the earlier example, if a value of 2τ equal 80 μsec is applied, then the coincidence spectrum at 15 volts will have 50% counting losses (there will also be the same order of losses at 90 volts).

The above-mentioned phenomenon can cause distortion of the coincidence spectrum not only at the low energy part but also at the high energy part depending on how the delay line is set.

e) The correct values of the delay time and resolving time, are easily chosen according to the measuring mode. (i) Integral-integral mode: the delay value is set at the value corresponding to the axis of the trumpet curves. The resolving time is determined according to which part of the energy spectrum is involved. (ii) Differential-differential mode: the correct value of the delay is the actual centre of the working band at the given energy. The value of the resolving time is the band width itself (66% efficiency). (iii) Differential-integral mode: the delay is set at the middle of the range between the axis of the trumpet curve and the centre of the working band at the value corresponding to the given energy. The resolving time value is equal to the time

difference between the value corresponding to the axis of the trumpet curve and the centre of the working band at the given energy.

The shape of the trumpet curve is asymmetric if the rise times of the pulses from the two detectors differ. For example, one detector is NaI(Tl) and the other is an organic scintillator ($\beta-\gamma$ coincidence). The trumpet curve will also be asymmetric if the triggering levels of the coincidence circuit are not identical.

III. Field of applications of coincidence circuits and their properties

In the following section we shall speak about a few problems which, according to our experience can be solved by means of coincidence circuits:

1. *Normal coincidence experience*

In practice, the normal coincidence technique is widely used. The block diagram of the circuit is shown in Fig. 4. We have already spoken about its working mechanism, and we shall now show how to solve some interesting problems.

In the case of unknown nuclear processes, it is advisable to start the coincidence measurements by setting the trigger channel integrally at a very low discrimination voltage in order to detect all the existing energies. Then with the analyser channel we scan the whole spectrum getting the coincidence spectrum which contains all coincident energies, but we cannot determine which lines are coincident with each other. To determine this, a second series of measurements should be carried out in which the trigger channel must be set differentially at every single peak in the measured coincidence spectrum, and with the analyser channel we can look for the coincident lines.

In both measurements, it is reasonable to choose a narrow channel width (in the analyser channel) or to use a multichannel analyser in order to secure good resolving power. In the second series of measurements, it is reasonable to choose a large channel width such that the measured line should lie within this width in order to get as high a counting rate as possible. One must be careful to ensure that other lines do not lie within this channel width otherwise false results would be obtained.

This method is in general use but has the disadvantage that it is not easy to detect lines of very low intensity in the presence of other intense lines (the trigger channel may miss this peak if it was not originally visible in the first coincidence series). To overcome this problem the following method can be used. The trigger channel, as in the first series, is set integrally but at the highest energy, while the analyser channel is scanning the whole spectrum

differentially. Then, with the trigger channel we proceed from the high energy downwards in small steps resulting in a series of coincidence spectrum curves. In these series new lines will continually appear as the trigger channel reaches those lines in coincidence with its setting. A nice application of this method can be found in the literature [3]. This method also has a disadvantage in that it always needs a lot of measurements some of which are sometimes redundant.

2. *Sum coincidence experience*

Since 1958 an investigation method termed the "sum coincidence technique" has been used in gamma ray spectroscopy. The most important property of this method is that only the full energy peaks will appear on the measured coincidence spectrum i.e. the Compton part of the spectrum which is always disturbing, completely disappears. Further, the resolution of the spectral lines is much improved. We shall not speak of this method here in detail since it has been described by HOOGENBOOM [4], but we shall mention some of the results obtained during the application of this method, especially because some investigators are not well-acquainted with it.

The original HOOGENBOOM sum coincidence circuit was a slow coincidence system (10^{-6} sec). In the present case we were applying a slow-fast sum coincidence which provides better resolving time (10^{-8} sec). In the case of the slow technique the sum peak constantly appears (when the two gammas are absorbed in the analyser crystal). In the slow-fast technique this sum peak does not appear because each of the gammas must be absorbed in one crystal in order to operate the fast coincidence unit. This is not a shortcoming but, on the contrary, provides a good method for detecting a cascade of low-energy gammas plus a high energy gamma (whose energy is approximately equal to the sum of the two energies).

The most important condition is that both detectors should produce signals of the same amplitude if the detected energies are the same, i.e. the gain in both channels should be the same. To fulfil this condition, stable multipliers and high voltage power supplies should be used. The best method for setting the same pulse height in both channels is to choose a pronounced intense line from the single spectrum (because the summing peak intensity is generally weak and its position is shifted as a result of overloading or non-linear reasons [5], and to set it at a previously chosen level of the sum channel. The setting is carried out by changing the multiplier high tension. We can decide whether the peak is lying in the chosen level or not by setting the amplitude analyser 2 volts lower, then higher than the chosen level, and in both cases we ought to get the same counting rate since in this case we are measuring two symmetrical points on the gaussian distribution. If the peak itself is slightly shifted then this will result in a large difference in the counting rate

at these two points. Generally, this counting rate difference is so high that it is sufficient to use a rate meter for the adjustment.

The measured spectrum must be installed independently in both channels, which can be achieved by switching off the photomultiplier's high tension of either channel and adjusting the other, but this can cause a change in the gain of that photomultiplier. So, it is better to remove the unrequired pulses by shielding the scintillation head against the radiations from the source, or by blocking the pulses themselves to prevent them from reaching the sum circuit.

The following errors may occur during measurements and always give misleading results. If the amplitude analyser is not set at exactly the middle of the sum peak, then the peaks in the sum coincidence spectrum will be shifted i.e. the energy position will be incorrect. Also, if we set at a sum peak of low energy then spurious peaks will appear as a result of high-energy cascade transitions. A method for the determination of these peaks can be found in references [6] and [7].

For angular correlation measurements these disadvantages are not disturbing. So, in this field the sum coincidence techniques can be particularly useful.

Chance coincidences cannot be calculated in the sum coincidence measurements because we do not know the number of counts N_1 and N_2. This can only be measured if a certain delay is introduced into that part of the circuit which is shown in the block diagram (Fig. 8). That is, we must take into consideration that if we delay one pulse with respect to the other, then the pulse height will change at the output of the sum circuit.

The optimum values of resolving time and delay are determined in a similar way to normal coincidence, only here the sum channel plays the role of the trigger channel.

The sum coincidence technique has been generally used until now for the detection of two transitions cascades. It is worth showing here the sum coincidence spectrum for three transition cascades. An example of the sum coincidence spectrum for two and three transitions cascades is shown in Fig. 9. Pm^{144} decays by electron capture to Nd^{144} levels which are de-excited by emission of three gamma rays cascades of energies 695, 615 and 470 keV. In the case of two gammas cascade, two peaks corresponding to the two gammas appear. In the case of triple cascade transitions six peaks (forming two symmetrical groups) appear. The mechanism of formation of these six peaks is that one gamma energy is absorbed in one crystal, while the other two gamma energies are absorbed simultaneously in the second crystal. So, the lower energy group corresponds to the absorption of each of the three single gammas, while the higher energy group corresponds to the absorption of the other two gammas.

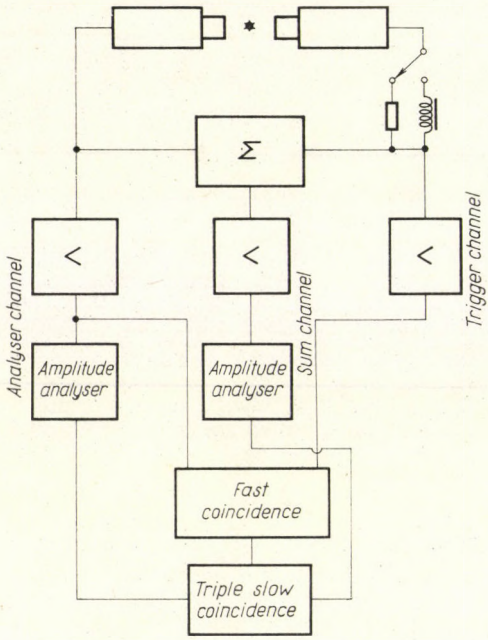

Fig. 8. Block diagram of the sum coincidence technique

3. *Application of coincidence circuits for pulse shape discrimination*

A) Identification of charged particles:

It has been well known that the properties of a scintillator are such that its decay times depend on the type of particle absorbed. In the case of CsI(Tl) crystals the decay time of heavy particles (alphas) is shorter than that of lighter particles (electrons). This will influence the rise time of the pulses at the integrating circuit of the anode of the photomultiplier. The rise time can be measured in the following way [8], (see Fig. 10). The pulses are differentiated by RC circuit and the time difference between the leading edge of the original pulse and the zero crossing point of the differentiated pulse is measured. The crossing point for the shorter rise time is earlier than that for the longer rise time (the position of the crossing point is independent of the amplitude of the original pulse). This time difference is easily measured by a coincidence circuit. The trailing edge of the original pulse triggers one of the channels, while the crossing point of the differentiated pulse (at first, the differentiated pulse is inverted and only the positive part is used) triggers the second coincidence channel. The differentiator and phase invertor unit in Fig. 3 is used for this purpose. By changing the delay we shall obtain few coincidence

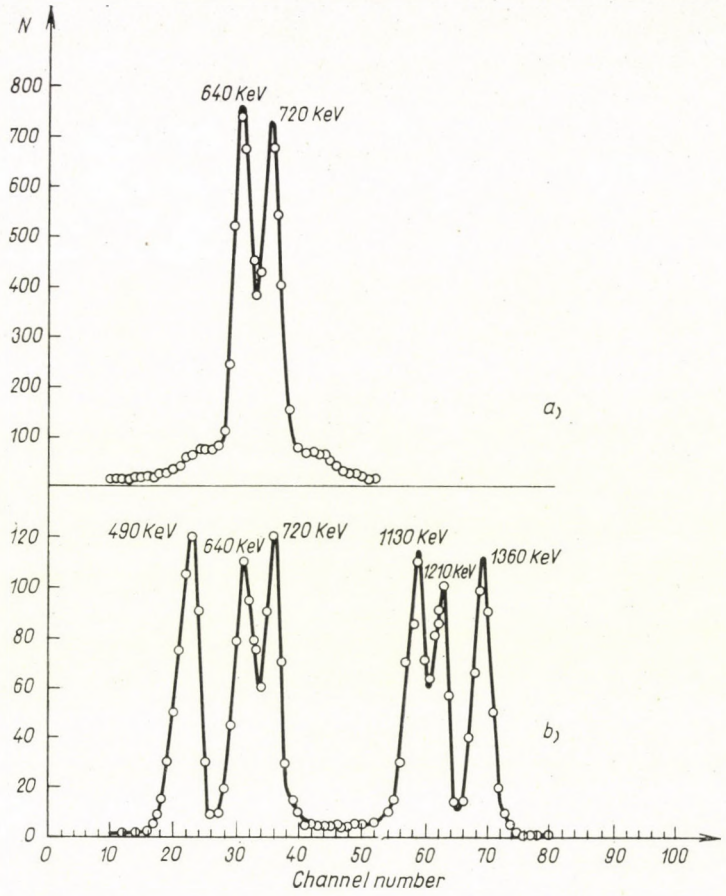

Fig. 9. Pm^{144} sum coincidence spectrum: (a) two gammas cascade spectrum, the amplitude analyser in the sum channel was set at 1360 keV; (b) a three gammas cascade spectrum, the amplitude analyser in the sum channel was set at 1850 volts

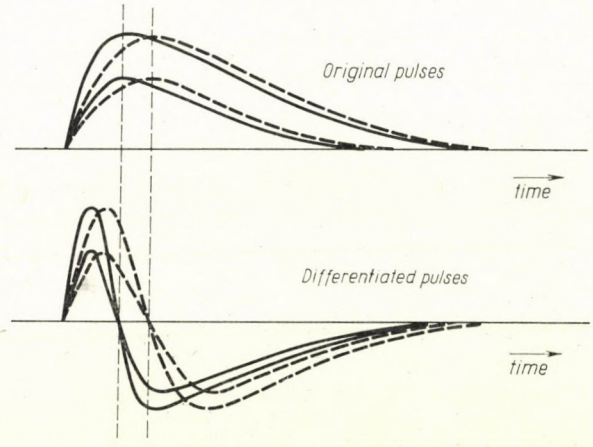

Fig. 10. Detector pulse shape: (a) original shape; (b) differentiated shape. The differentiated pulses cross the base line earlier when their rise time is shorter

curves each of which will correspond to a certain type of particle as shown in Fig. 11.

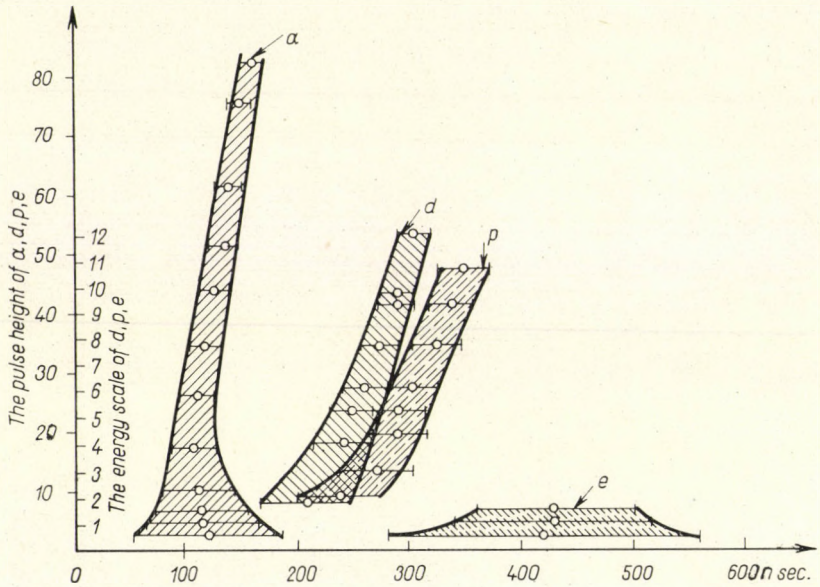

Fig. 11. The separation of different types of particles by a pulse shape discriminator as a function of energy

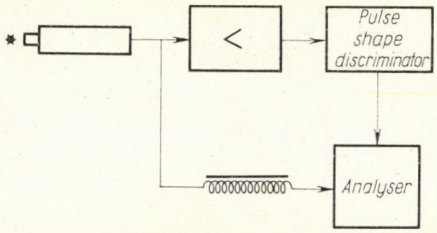

Fig. 12. Pulse shape discriminator arrangement

The resolving time for a pulse shape discriminator is practically independent of the pulse amplitude because in this case large pulses are always coincident with large ones, and small pulses with small ones. So, the resolving time is much better, and is determined by the uncertainty in the shape of the pulses. This fluctuation in the shape depends on the number of emitted photons from the scintillator so, that at higher energies the resolving time is better than at lower energies. In Fig. 11 the separation of different particles as a function of energy is clear. The band widths are equal to 2τ of the corresponding coincidence curve.

The pulse shape discriminator is used for gating the measuring assembly, to record only the pulses of the required shape. The block diagram for any pulse shape measurements is shown in Fig. 12.

B) The elimination of pile up pulses:

In nuclear spectroscopic measurements, it sometimes happens that it is desired to measure a weak high-energy line in the presence of an intense lower-energy line. In such a situation the intense low-energy pulses are superposed giving spurious pulses which have spectral distribution in the higher energy range. These pile-up pulses can be rejected by means of the above-mentioned pulse shape discriminator method [9]. The result of the summing of two pulses is generally a distorted pulse whose rise time is never shorter than the original pulses. If we are choosing the good pulses by means of the pulse shape discrimi-

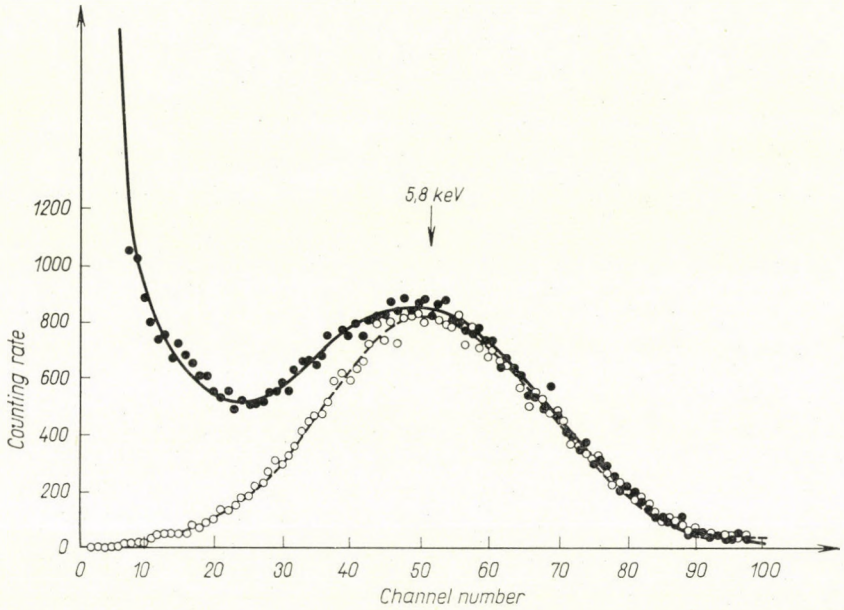

Fig. 13. X-ray spectrum of Fe^{55} measured with pulse shape discriminator (broken line), and without pulse shape discriminator (continuous line)

nator, then the apparatus rejects the superposed pulses. Similar to chance coincidence, it can also happen that two pulses come within the resolving time of the coincidence circuit and will produce a spurious pulse. These pulses can be measured by carefully inserting a certain delay, because here the sum of the two pulses will always result in a longer, and never shorter, rise time than the original pulse.

Generally, the superposed pulses have a distribution of pulse heights reachings double the energy of the intense gamma transition. The probability of triple superposition is always very small.

C) Measurement of low energies:

The pulse shape discriminator can be used for the elimination of dark current pulses, and in such a way that it is easy to measure very low energies. If the shape of the scintillation pulse differs from that of the dark current, then on the basis of the above-mentioned pulse shape discrimination, it is possible to distinguish between both types. Generally, scintillators have relatively longer decay, as NaI(Tl), CsI(Tl) and the new calcium iodide crystals, and the pulse rise time is much longer than the rise of the dark current which is generally produced by one electron from the photo-cathode. A typical example is shown in Fig. 13, where the x-rays of Fe^{55} (5,8 keV) are measured with, and without, the use of a pulse shape discriminator.

Acknowledgement

We wish to thank Professor A. SZALAY, Director of the Nuclear Research Institute of the Hungarian Academy of Sciences for the excellent working conditions and for the hospitality extended to one of the authors (N. A. E.) at the Institute.

REFERENCES

1. W. MEILING, T. SCHINTLMEISTER and F. STARY, Nucl. Instr. and Meth., **21**, 275, 1963.
2. Advances in Electronics and Electron Physics, 8, 255, 1956.
3. E. BOSCHITZ, Zeitschrift für Physik, **154**, 90, 1959.
4. A. M. HOOGENBOOM, Nucl. Instr. and Meth., **3**, 57, 1958.
5. H. G. DEVARE and P. N. TANDOR, Nucl. Instr. and Meth., **22**, 253, 1963.
6. GY. MÁTHÉ, D. BERÉNYI and T. SCHARBERT, Nucl. Instr. and Meth., **26**, 141, 1964.
7. S. O. SCHRIBER and B. G. HOGG, Nucl. Instr. and Meth., **26**, 141, 1964.
8. GY. MÁTHÉ and B. SCHLENK, Nucl. Instr. and Meth., **27**, 10, 1964.
9. GY. MÁTHÉ, Nucl. Instr. and Methods., **23**, 261, 1963.

ПРОБЛЕМАТИКИ ПРИМЕНЕНИЯ ПРИЕМОВ ЗАПАЗДЫВАЮЩЕГО СОВПАДЕНИЯ

Н. А. ЭИССА и ДЬ. МАТЕЙ

Резюме

Сети совпадения широко применяются в исследовании ядер. В данной работе суммируются как их наиболее важные свойства, так и эксперименты, проведенные данными приемами. Таким образом, мы можем рассматривать параметры сетей совпадения как скелет для времен запаздывания и распадения. Представляются проблемы, возникающие при применении нормальной и суммарной совпадений. Наконец, дается описание применения четей совпадений для отождествления частиц, ликвидаций накопления и измерения гамма-лучей низких энергий.

Acta Physica Academiae Scientiarum Hungaricae, Tomus 23 (3), pp. 277—285 (1967)

SYSTEMATICS OF SOME NUCLEAR PROPERTIES OF THE ODD MASS NUCLEI IN THE REGION NEAR THE MASS NUMBER 190

By

Z. MELIGY

EIN SHAMS UNIVERSITY, FACULTY OF SCIENCE, CAIRO, UAR

and

N. A. EISSA

AL-AZHAR UNIVERSITY, FACULTY OF ENGINEERING, CAIRO, UAR

(Presented by A. Szalay. — Received 4. X. 1966)

The systematics of the shell and unified nuclear models have been investigated for the nuclei of Lu, Ta, Re, Ir and Au, which represent the transition region from the spherical nuclei. It was apparent from the comparison of the experimental and theoretical ratios of the first and second excited collective levels, from the quadruple and magnetic moments that the unified model is the most coherent one in this range too, as results from the present analysis. For the Au^{195} nucleus it was possible to assign the spin $5/2^+$ and $7/2^+$ for the levels at 251 and 515 keV from the comparison with other nuclei.

The moment of inertia derived from the experimental results and from the hydrodynamic approximation for the above-mentioned nuclei was compared with Migdal curves for the moment of inertia based on the superfluid model. The results confirm the superfluid description of nuclear matter.

I. Introduction

Considerable data are available on the decay schemes and level systematics of nuclei whose low-lying excitation spectra can be explained by either the single particle or collective models. Much less data are available for the nuclei in the so-called transition regions, i. e. those nuclei of mass 140—152 and 180—200. In the nuclei where the number of neutrons changed from 88 to 90 ($A \sim 150$) a sudden variation of the properties was observed. The energy of the first excited collective level change suddenly as well as the coulomb excitation cross-section. This discontinuity indicates the passage from the exactly spherical form ($Z \sim 50$, $N \sim 82$) to the ellipsoidal form. It is interesting to know whether the inverse transition exists when the region of magic numbers $Z \simeq 82$, $N \simeq 126$ is approached.

We have been investigating the decay schemes of the iridium [1] isotopes $_{77}Ir^{191}$ and Ir^{193}, and it is the purpose of this paper to investigate some of the nuclear properties of these nuclei together with some other odd nuclei. The chosen nuclei were:

$_{71}Lu^{175}$, Lu^{177}, $_{73}Ta^{181}$, $_{75}Re^{183}$, Re^{187}, $_{79}Au^{195}$, Au^{197} and Au^{199}.

The low-energy levels in these nuclei are quite well established and the decay schemes for these nuclei have been taken from the Nuclear Data Sheets [2]. It can be seen that these nuclei represent the passage from the ellipsoidal form to the nearly spherical form.

II. Nuclear properties

The investigated nuclear properties are the following:

1. *Particle levels*

According to experimental results, the deformation of the nuclei exhibits an axial symmetry, and NILSSON [3] has calculated the energy states of the single particles in a spheroidal potential as a function of the deformation δ defined by the intrinsic quadruple moment Q_0. The relation [3] between δ and Q_0 is:

$$Q_0 = 0.8.Z.R^2.\delta\left(1+\frac{2}{3}\delta\right). \tag{1}$$

Q_0 is determined from the Coulomb excitation cross-section.

2. *Collective levels*

In the case of deformed nuclei the values of the energies of a rotation family based on a single particle ground level of a total angular momentum I, are given by [3]:

$$E_I = \frac{h^2}{2_J}\left[I(I+1)+a(-1)^{I+\frac{1}{2}}\left(I+\frac{1}{2}\right)\right], \tag{2}$$

where J is the moment of inertia of the nuclear mass, its value lying between that for a rotating rigid body and the hydrodynamic estimate of BOHR and MOTTELSON [4]. The decoupling factor a vanishes if $K \neq \frac{1}{2}$.

For rotational spectra given by the above formula the ratio of the energies of the second and first excited states depends only on the ground state spin I_0, and for odd A nuclei is given by:

$$\frac{E_2}{E_1} = \frac{2I_0+3}{I_0+1} = \begin{cases} 2{,}4 & \text{for } I_0 = \frac{3}{2} \\ 2{,}29 & \text{for } I_0 = \frac{5}{2} \\ 2{,}22 & \text{for } I_0 = \frac{7}{2} \end{cases} \tag{3}$$

3. *Magnetic moments*

The magnetic moment for a nucleon moving in a spherical potential field [5] is given by:

$$\mu = j\left[G_1 \pm \frac{I}{2I+I}(G_s - G_l)\right], \tag{4}$$

where G_s and G_l are the gyromagnetic ratios for the intrinsic and orbital motions, respectively of the nucleon.

In the case of deformed nuclei the coupling of the nuclear surface with the nucleon motion contributes to the magnetic moment, which is given by the following relation [5] for $I = \Omega_P = K \neq \frac{1}{2}$

$$\mu = \frac{I}{I+1}[G_\Omega I + G_R], \tag{5}$$

where G_R is the gyromagnetic ratio associated with the rotational motion of uniformly charged nuclear matter; its value approximately equals $\frac{Z}{A}$. G_Ω is associated with the intrinsic motion of nucleons.

4. *Quadruple moments*

A non-coupled proton with the total angular momentum j moving in a spherical potential field gives rise to a quadruple moment

$$Q = \frac{2j+1}{2(j+1)} \cdot \langle r^2 \rangle . \tag{6}$$

The average value for r^2 of the proton orbit is $\frac{3}{5} R_0^2$, where $R_0 = 1 \cdot 2 \cdot A^{1/3} \cdot 10^{-13}$ cm.

In the case of deformed nuclei the collective behaviour of the nucleons results in quadruple moments $Q_{\text{coll.}}$ much larger than those associated with the single particle $Q_{\text{s.p.}}$ The observed quadruple moment $Q_{\text{obs.}}$ is of the form

$$Q_{\text{obs.}} = Q_{\text{coll.}} + Q_{\text{s.p.}} \tag{7}$$

$Q_{\text{obs.}}$ is determined by atomic spectroscopy.

The relation between $Q_{\text{obs.}}$ and Q_0 (given by equation 1) depends on the nuclear coupling scheme. For strongly deformed nuclei (strong coupling) this ratio is given by:

$$Q_{\substack{\text{strong}\\\text{coupling}}} = \frac{Q_{\text{obs.}}}{Q_0} = \frac{I}{I+1} \cdot \frac{2I-1}{2I+3}. \tag{8}$$

5. *Moments of inertia*

The moment of inertia of the deformed nucleus J_{exp} can be determined from equation (2). In the hydrodynamic approximation, the moment of inertia is considered to be that of an incompressible fluid and is given by [4]

$$J = \frac{2}{5} M A R_0^2 \left(\frac{\Delta R^2}{R_0}\right), \tag{9}$$

where ΔR represents the difference between the major and minor semi-axes of the spheroid. M denotes the nucleon mass and A is the nuclear mass.

In the above relation the quantity $J_0 = \frac{2}{5} MAR_0^2$ is the moment of inertia of a spherical rigid body in the hydrodynamic approximation.

$$J_{hydro.} = J_0 \delta^2, \tag{10}$$

where

$$\delta = \frac{\Delta R}{R}.$$

The most consistent theory ot the moment of inertia is based on the superfluid model (6,7). In this model the existence of coupled pairs of nucleons and the appropriate energy gap Δ in the level scheme of the nuclei is taken into account. The moment of inertia can be expressed in terms of this energy gap and the matrix elements of the interaction of the pairs of the nucleons.

MIGDAL [8] has well calculated the moment of inertia for an oscillation potential and rectangular potential, as a function of a parameter X_n which is given by:

$$x_n = 27 \left[\frac{\delta}{\left(1 + \frac{1}{3}\delta\right) \Delta_n A^{\frac{1}{3}}}\right] \left(\frac{N}{A}\right)^{\frac{1}{3}} \frac{M}{M_{\text{eff.}}}, \tag{11}$$

where $\frac{M}{M_{\text{eff}}}$ is the ratio between the nucleon mass and its effective mass. In MIGDAL's calculations, this ratio is taken as unity. Δ_n is the energy gap parameter of neutrons which is determined from the nuclear masses according to the following formula:

$$\Delta_n = \frac{1}{2}\left[E_0(N+1) - 2E_0(N) + E_0(N-1)\right], \tag{12}$$

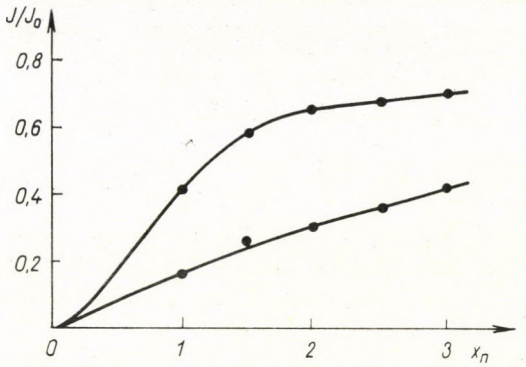

Fig. 1. Theoretical curves of the moment of inertia for oscillator potential (upper) and rectangular potential (lower)

where $E_0(N+1)$, $E_0(N)$ and $E_0(N-1)$ are the binding energies of the nuclei having $(N+1)$, (N) and $(N-1)$ neutrons, respectively. MIGDAL's results are shown in Fig. 1.

III. Results and discussion

1. *Rotational levels over ground levels with* $K \neq \frac{1}{2}$

The energies of the first and second excited rotational levels over the ground state particle level are calculated according to relation (2), and their ratio from relation (3). The results are given in Table (1) and are shown in Fig. 2. It can be seen that a deviation exists only for the iridium and gold nuclei which have small deformations.

Table 1

Isotopes	Ground state spin I_0	E_1 keV	E_2 keV	$(E_2/E_1)_{exp.}$	$(E_2/E_1)_{theor}$	$\frac{(E_2/E_1)_{exp}}{(E_2/E_1)_{theor}}$	$\hbar^2/2J$ keV	$J_{exp.}$ 10^{48} gm cm^2
$_{71}Lu^{175}$	7/2+	113	251	2,22	2,22	1,0	12,5	23,0
Lu^{177}	7/2+	118	251	2,12	2,22	0,96	13,1	23,8
$_{73}Ta^{181}$	7/2+	136	301	2,21	2,22	1,0	15,1	20,7
$_{75}Re^{183}$	5/2+	114	260	2,28	2,29	1,0	16,3	19,2
Re^{185}	5/2+	125	286	2,29	2,29	1,0	17,9	17,5
Re^{187}	5/2+	134	301	2,23	2,29	0,98	19,2	16,3
$_{77}Ir^{191}$	3/2+	129	352	2,70	2,24	1,20	23,8	12,0
Ir^{193}	3/2+	139	362	2,60	2,24	1,16	27,7	11,3
$_{79}Au^{195}$	3/2+	261	525	2,11	2,24	0,94	52,2	6,0
Au^{197}	3/2+	277	546	1,97	2,24	0,68	55,6	5,6
Au^{199}	3/2+	271	515	1,90	2,24	0,85	54,2	5,8

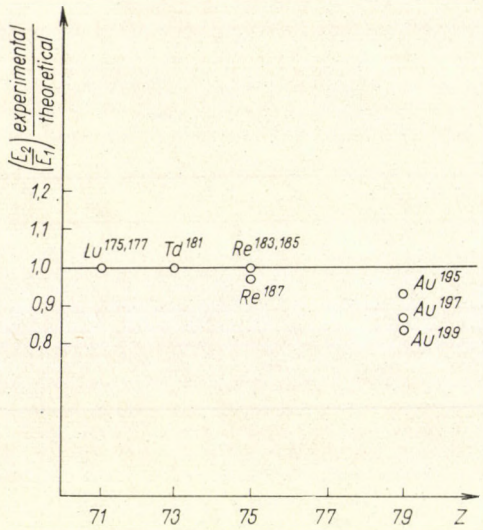

Fig. 2. The experimental to theoretical ratios of the first and second excited collective levels for the shown isotopes

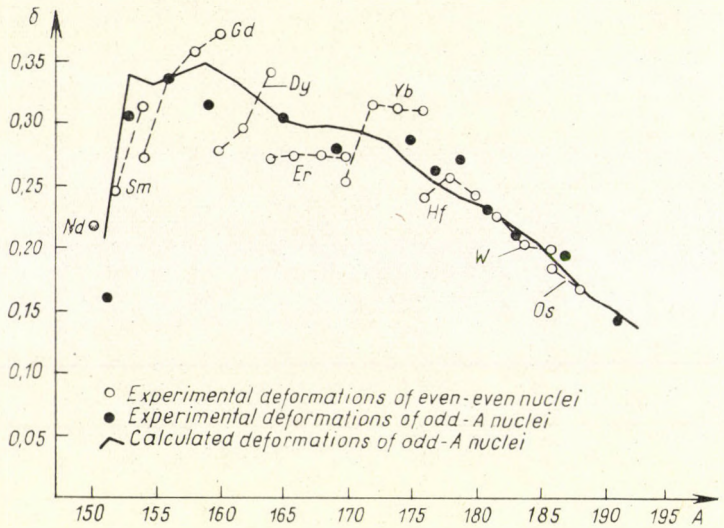

Fig. 3. Variation of deformation with atomic mass

It is worth mentioning here that for Au^{195} the spins of $\frac{5^+}{2}$ and $\frac{7^+}{2}$ can be assigned to the levels at 251 and 515 keV, respectively, as they can be considered as the first and second rotational excited levels above the ground level of spin $\frac{3^+}{2}$ on the basis of comparison with other nuclei.

2. *Moments of inertia*

$J_{exp.}$ was calculated from relation (2), and I_0 was calculated from relation (9), from which $I_{hydro.}$ was deduced according to Fig. 3., due to MOTTELSON [9]. The neutron energy gap Δ_n was calculated from LEVY's tables of atomic masses [10].

Then the corresponding X_n was calculated from relation (11). The results are given in Table (2) and shown in Fig. 4.

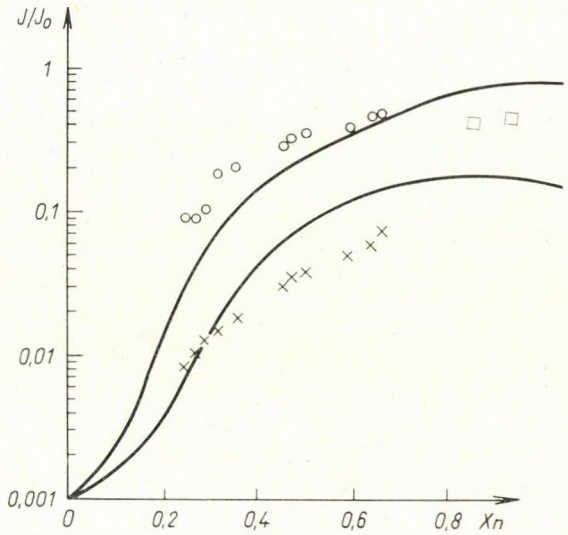

Fig. 4. The calculated values of moment of inertia on MIGDAL curves. × denotes $J_{hydro.}/J_0$, ○ denotes $J_{exp.}/J_0$, and □ is for Gd^{154} and Nd^{150} from MIGDAL's paper [8]

It can be seen that the hydrodynamic approximation results in the lowest values for the moment of inertia, MIGDAL had calculated the moment of inertia for strongly deformed nuclei in the rare earth region on the basis of the superfluid model for two single cases of the potential. The experimental values of (J/J_0) exp for these strongly deformed nuclei lie between the curves of these potentials. The nuclei in the present investigation have small deformation. The experimental values of (J/J_0) exp lie close to the oscillator potential curve. According to relation (11) as δ increases, X_n also increases, and the experimental points approach the oscillator potential curve, and for larger deformations the experimental values lie between the two curves.

The disagreement with MIGDAL theory is not large, and it is probable that a closer correlation with the experimental data could be reached either by a small variation of the parameters in relation (11), or by taking into account a more realistic potential than the oscillator or rectangular potentials. The disagreement could also be due to errors in the experimental parameters.

Table 2

Isotope	δ	Δ_n	x_n	J_0 10^{48} gm cm²	$J_{hydro.}$ 10^{48} gm cm²	$J_{exp.}$ 10^{48} gm cm²	$\frac{J_{hydro}}{J_0}$	$\frac{J_{exp.}}{J_0}$
$_{71}Lu^{175}$	0,26	1,435	0,66	53,2	3,66	25	0,069	0,47
Lu^{177}	0,24	1,435	0,64	53,4	3,13	23,8	0,058	0,44
$_{73}Ta^{181}$	0,22	1,434	0,59	56,0	2,71	20,7	0,048	0,37
$_{75}Re^{183}$	0,19	1,434	0,50	56,5	2,04	19,2	0,036	0,34
Re^{185}	0,18	1,434	0,475	57,6	1,87	17,5	0,033	0,305
Re^{187}	0,17	1,434	0,460	58,8	1,70	16,3	0,029	0,28
$_{77}Ir^{191}$	0,13	1,436	0,36	60,8	1,026	12,0	0,017	0,20
Ir^{193}	0,12	1,436	0,32	62,0	0,893	11,3	0,014	0,18
$_{79}Au^{195}$	0,11	1,434	0,29	63,1	0,77	6,0	0,012	0,10
Au^{197}	0,10	1,435	0,27	64,0	0,64	5,6	0,010	0,087
Au^{199}	0,09	1,436	0,25	65,2	0,53	5,8	0,008	0,089

3. *Quadruple and magnetic moments*

The experimental values for the nuclei for which μ and Q was measured, are given in Table 3 together with the theoretical values calculated according to the shell model and the unified model. From the Table it can be seen that there is no distinction between the accordance of the experimentally measured values and those resulting from the shell or unified models. However, from a comparison of $\mu_{measured}$ and $\mu_{Nilsson}$ and $Q_{strong\ coupling}$ and $Q_{measured}$ it can be seen that the unified model is more coherent for these experimental data.

Table 3

Isotope	I	$\mu_{measured}$	μ_{shell}	$\mu_{Nilsson}$	Q_0 10^{-24} cm²	Q_{shell}	$Q_{measured}$	$Q_{strong\ coupling}$
$_{73}Ta^{181}$	7/2	2,1	1,72	1,50	6,91	0,20	2,70	3,2
$_{75}Re^{185}$	5/2	3,14	4,80	3,50	6,30	0,18	2,80	2,2
$_{77}Ir^{191}$	3/2	0,16	0,12	0,02	3,16	0,14	1,50	0,5
$_{77}Ir^{193}$	3/2	0,16	0,12	0,02	3,22	0,14	1,50	0,5
$_{79}Au^{197}$	3/2	0,14	0,12	0,03	5,60	0,14	0,56	0,4

REFERENCES

1. Z. PLAJNER and N. A. EISSA, Czech. J. Phys., 13, 23, 1963.
2. Nuclear Data Sheets, Published by USA Atomic Energy Comission, 1958, 1962.
3. S. NILSSON, Dan. Mat. Fys. Medd., 29, No. 16, 1955.
4. A. BOHR and B. MOTTELSON, Mat. Fys. Medd. Dan. Vid. selsk., 10, No. 1, 1955.
5. M. MAYER and I. JENSEN, Elementary theory of nuclear shell theory, Wiley and Sons, 1955.
6. B. BARDEEN, L. COOPER and I. SCHRIEFFER, Phys. Rev., **108**, 1175, 1957.

7. B. Bogolyubov, JETF, **3**, 58, 1958.
8. A. Migdal, Nucl. Phys., **13**, 673, 1959.
9. B. Mottelson and S. Nilsson, Phys. Rev., **99**, 1615, 1955.
10. J. Riddell, A table of Levy's empirical atomic masses, AECL No. 339.

СИСТЕМАТИЧНОСТЬ НЕКОТОРЫХ СВОЙСТВ НЕЧЕТНЫХ ЯДЕР В ОБЛАСТИ, БЛИЗКИЙ К МАССОВОМУ ЧИСЛУ 190

З. МЕЛИГИ и Н. А. ЭЙССА

Резюме

Систематичность оболочечной и объединенной ядерных моделей предлагалась для ядер Lu, Ta, Re, Ir и Au, которые представляют собой переходную область из сферических ядер. Из сравнения экспериментальных и теоретических отношений первично и вторично возбужденных коллективных уровней, из квадрупольных и магнитных моментов выходит, что объединенная модель является наиболее когерентной и в этом отношении, как результат данного анализа. Из сравнения с другими ядрами для ядра Au—199 можно было определить спин $5/2^+$ и $7/2^+$.

Определенный из экспериментальных данных и из гидродинамического приближения момент инерции для вышеупомянутых ядер сравнивался с кривыми Мигдала для момента инерции, основанного на сверхтекучей модели. Результаты подтверждают сверхтекучее описание ядерной материи.

Acta Physica Academiae Scientiarum Hungaricae, Tomus 23 (3), pp. 287—290 (1967)

ON THE EXCHANGE ENERGY IN A SCF METHOD USING NON-ORTHOGONAL BASIS FUNCTIONS

By

GY. BÜTI

RESEARCH GROUP FOR THEORETICAL PHYSICS OF THE HUNGARIAN ACADEMY OF SCIENCES, BUDAPEST

(Presented by A. Kónya. — Received 20. X. 1966)

A method is developed for the calculation of exchange energy in a simple SCF method or atomic one-electron eigenfunctions using non-orthogonal basis functions.

Following some earlier works [1] — [7] a simple SCF method of calculating atomic one-electron eigenfunctions was given in a recent paper [8] by GOMBÁS. The main features of this method are as follows.

1. A non-orthogonal set of Slater-type basis functions is used in an analytic variational procedure.

2. The Pauli-principle is taken into account with a pseudopotential.

3. The exchange and correlation energy is calculated with a pseudopotential of SLATER [9] and GOMBÁS [10] in a semiempirical way.

We notice that recently extensive energy band calculations in solids are done in similar ways.

The aim of the present paper is to show that within a reasonable approximation it is possible to calculate the exchange energy in the usual way using the non-orthogonal set of basis functions.

The Hamiltonian of our SCF method for the shell with angular momentum quantum number l is

$$H_l = -\frac{h^2}{8\pi^2 m}\frac{d^2}{dr^2} + \frac{h^2}{8\pi^2 m}\cdot\frac{l(l+1)}{r^2} - \\ -\frac{e^2 Z}{r} - eV_{\mathrm{Cb}} - eV_{\mathrm{Co}} - eV_{\mathrm{G}} - eV_{\mathrm{ex}}, \tag{1}$$

where V_{Cb} is the SCF Coulomb potential including interaction within the shell, V_{Co}, V_{G} and V_{ex} are local pseudopotentials arising from the Coulomb correlation, the Pauli principle and the antisymmetry of the wave function.

Now instead of the semiempirical expression for the exchange energy expression $eV_{\mathrm{ex}}\varphi_{nlm}$ let us take the nonlocal exchange operator originating from the Fock equations

$$A\varphi_{nlm}(\xi) = \sum_{n'l'm'}{}' \int \frac{\varphi_{n'l'm'}(\xi')\,\varphi_{nlm}(\xi')\,\varphi_{n'l'm'}(\xi)}{|r - r'|}\, d\xi' , \tag{2}$$

where $\varphi_{n'l'm'}(\xi)$ are orthogonal spin-orbitals, the summation is over all quantum numbers except ***nlm***, and integration also includes a summation over spin coordinates. However, it is not justified to use expression (2) in our SCF procedure because we choose a non-orthogonal set of basis functions of the form $f_{nl} = Ar^x e^{-\lambda r}$ for the variational trial function. Therefore we are looking for an operator A' such that

$$(\varphi_{nl}, A\varphi_{nl}) = (f_{nl}, A' f_{nl}) , \tag{3}$$

for in this case we can determine the expectation value of the exchange energy with A' and the non-orthogonal set of basis functions in the usual way and therefore the variational procedure can be carried through in the usual way.

The orthogonalized system of basis functions of the method is

$$\varphi_{nl} = c_{nl}\Big[f_{nl} - \sum_{n'=l+1}^{n-1} (\varphi_{n'l}, f_{nl})\,\varphi_{n'l}\Big] ,$$

where

$$c_{nl} = \Big[1 - \sum_{n'=l+1}^{n-1} |(\varphi_{n\,l}, f_{nl})|^2\Big]^{-1/2} .$$

Because of the linearity of A we can write

$$\begin{aligned}(\varphi_{nl}, A\varphi_{nl}) = |c_{nl}|^2 \Big[(f_{nl}, Af_{nl}) + \sum_{m=l+1}^{n-1} \sum_{k=l+1}^{n-1} (\varphi_{ml}, f_{nl}) \times \\ \times (\varphi_{kl}, f_{nl})\,(\varphi_{ml}, A\varphi_{kl}) - \sum_{m=l+1}^{n-1} (\varphi_{ml}, f_{nl})\,(\varphi_{ml}, Af_{nl}) - \\ - \sum_{m=l+1}^{n-1} (\varphi_{ml}, f_{nl})\,(f_{nl}, A\varphi_{ml})\Big] .\end{aligned} \tag{5}$$

Introducing the following notation

$$\begin{aligned}(\varphi_{ml}, f_{nl}) &= s_{lnm} , \\ (\varphi_{ml}, A\varphi_{nl}) &= a_{lmn} , \\ (\varphi_{ml}, Af_{nl}) &= a'_{lnm} ,\end{aligned} \tag{6}$$

and taking into account the hermiticity of A we can write

$$(f_{nl}, A' f_{nl}) = (\varphi_{nl}, A\,\varphi_{nl})$$

$$= |c_{nl}|^2 \left[(f_{nl}, A f_{nl}) + \sum_{m=l+1}^{n-1} \sum_{k=l+1}^{n-1} s_{lnm}\, s_{lnk}\, a_{lmk} - \right. \tag{7}$$

$$\left. - 2 \sum_{m=l+1}^{n-1} s_{lnm}\, a'_{lnm}\right].$$

Since the overlap-integrals in (7) are small, as can be seen from (6) (note that the summation is over overlap-integrals of orthogonal and non-orthogonal basis functions *differing in principal quantum number)*, expression (7) is within a reasonable approximation

$$(f_{nl}, A' f_{nl}) \cong (f_{nl}, A f_{nl}) \tag{8}$$

since $|c_{nl}|^2 = 1$ within the same approximation.

Thus the conclusion is that the exchange can be built in our simple variational procedure by using the exchange operator constructed by the *orthogonalized* one-electron eigenfunctions.

Note that equation (8) is exact within the framework of a procedure introduced by FÉNYES, SZÉPFALUSY, KLEINMAN and PHILLIPS, etc. [11]—[19]. It can be very easily seen that the functions f_{nl} satisfy the equations

$$(H_l^H + A)\, f_{nl} + \int_0^\infty \Phi_{nl}(r, r')\, f_{nl}(r')\, dr' = \varepsilon_{nl} f_{nl}\,,$$

where H_l^H is the Hartree operator and A is handled in this case in just the same way. In the simple SCF method discussed in [8] the operator

$$\int_0^\infty dr'\, \Phi_{nl}(r, r') = \int_0^\infty dr' \sum_{n'=l+1}^{n-1} (\varepsilon_{nl} - \varepsilon_{n'l})\, \varphi_{n'l}(r)\, \varphi^*_{n'l}(r')$$

is approximated with the local potential V_G in (1), (for a discussion see especially[19]) and the error in (8) originates therein.

The author is indebted to Prof. P. GOMBÁS for his interest in this work

REFERENCES

1. P. GOMBÁS and K. LADÁNYI, Acta Phys. Hung., **5,** 313, 1955.
2. P. GOMBÁS and K. LADÁNYI, Acta Phys. Hung., **7,** 255, 1957.
3. P. GOMBÁS and K. LADÁNYI, Acta Phys. Hung., **7,** 263, 1957.
4. P. GOMBÁS and K. LADÁNYI, Acta Phys. Hung., **8,** 301, 1958.
5. P. GOMBÁS and K. LADÁNYI, Z. Physik, **158,** 261, 1960.
6. P. GOMBÁS and T. SZONDY, Acta Phys. Hung., **14,** 335, 1962.
7. P. GOMBÁS and T. SZONDY, Acta Phys. Hung., **17,** 371, 1964.

8. P. Gombás, Theoret. Chim. Acta, **5,** 112, 1966.
9. J. C. Slater, Phys. Rev., **81,** 385, 1951.
10. P. Gombás, Fortschritte der Physik, **13,** 137, 1965.
11. I. Fényes, Csillagászati Lapok, Budapest, **6,** 49, 1943.
12. I. Fényes, Múzeumi Füzetek, Kolozsvár, **3,** 14, 1945.
13. P. Szépfalusy, Acta Phys. Hung., **5,** 323, 1955.
14. E. Antončik, Czechoslov. J. Physics, **4,** 439, 1954.
15. L. Kleinman and J. C. Phillips, Phys. Rev., **116,** 880, 1959.
16. L. Kleinman and J. C. Phillips, Phys. Rev., **117,** 460, 1960.
17. L. Kleinman and J. C. Phillips, Phys. Rev., **118,** 1153, 1960.
18. J. C. Phillips and L. Kleinman, Phys. Rev., **116,** 287, 1959.
19. P. Gombás and D. Kisdi, Theoret. Chim. Acta, **5,** 127, 1966.

ОБ ОБМЕННОЙ ЭНЕРГИИ В МЕТОДЕ САМОСОГЛАСОВАННОГО ПОЛЯ, ИСПОЛЬЗУЮЩЕМ НЕОРТОГОНАЛЬНЫЕ БАСИСНЫЕ ФУНКЦИИ

ДЬ. БЫТИ

Дается метод определения обменной энергии в методе самосогласованного поля с использованием неортогональных базисных функций.

Acta Physica Academiae Scientiarum Hungaricae, Tomus 23 (3), pp. 291—309 (1967)

THE LORENTZ PRINCIPLE AND THE GENERAL THEORY OF RELATIVITY V

By

L. JÁNOSSY and P. KIRÁLY

CENTRAL RESEARCH INSTITUTE OF PHYSICS, BUDAPEST

(Received: 26. I. 1967)

The transformation is given explicitly with the help of which it is possible to obtain a straight system of reference from an arbitrary curvilinear representation. Applying the transformation to a representation in an inhomogeneous region it leads to a *nearly straiggt* system of reference. Making use of the nearly straight representations the explicit form of the Lorentz transformations in inhomogeneous regions is obtained.

Introduction

§ 1. In a number of previous publications [1]—[4] one of the authors (L. J.) has shown how the Lorentz principle (see e.g. Part II) can be extended so as to cover problems of general relativity. The principle can be expressed as follows. If $\mathfrak{Q}$ is a real physical system, then

$$\mathfrak{Q}^* = M_{\mathfrak{p}}(\mathfrak{Q}) \tag{1}$$

is a possible system, where $M_{\mathfrak{p}}$ stands for a Lorentz transformation with parameters $\mathfrak{p}$.

To the principle thus expressed a dynamical principle has to be added to the effect that a system $\mathfrak{Q}$ if adiabatically interfered with changes into a Lorentz deformed system $\mathfrak{Q}^*$.

In the absence of gravitational fields the first part of the principle expressed by (1) can be taken to be strictly valid (at least for the phenomena we know at present) — the dynamical part must be taken to be valid only in a good approximation; the dynamical principle contains a certain amount of uncertainty, as it is not possible to determine precisely the limits inside which interferences can be regarded to be adiabatic. In the presence of gravitational fields the difficulties are further enhanced; even the first part of the Lorentz principle can only be expressed in an approximate manner, valid for small systems only. The formulation of the second part leads to additional difficulties — it is even more difficult in the latter case to give criteria for interferences to be adiabatic. Both difficulties can be overcome if we limit ourselves to actually observed phenomena. However, it seems

necessary to define the Lorentz transformations in a little more detail than we have done it so far.

§ 2. We denote (as in our previous work) the physical quantities themselves by gothic symbols. These quantities can be described by measures if we choose a particular representation. Thus in place of (1) we can also write

$$Q^* = M_{\mathfrak{p}}(Q), \tag{2}$$

where

$$Q = K(\mathfrak{Q}),\ Q^* = K(\mathfrak{Q}^*),\ \mathbf{p} = K(\mathfrak{p});$$

thus Q, Q^* and $\mathbf{p}$ are the representations of $\mathfrak{Q}$, $\mathfrak{Q}^*$, $\mathfrak{p}$ relative to a system of reference K.

The Lorentz transformation $M_{\mathfrak{p}}$ appears in any representation K in the form of a coordinate transformation, although $M_{\mathfrak{p}}$ is not a coordinate transformation but describes a deformation of a physical system $\mathfrak{Q}$ into another physical system $\mathfrak{Q}^*$. Indeed, if $\mathfrak{Q}$ consists of points $\mathfrak{P}_1, \mathfrak{P}_2, \ldots, \mathfrak{P}_N$ then $\mathfrak{Q}^*$ must be taken to consist of corresponding points $\mathfrak{P}_1^*, \mathfrak{P}_2^*, \ldots, \mathfrak{P}_N^*$. Thus the operation $M_{\mathfrak{p}}$ like a coordinate transformation gives to the coordinate measures — of a set of points — a new set of coordinate measures.

In a representation K the orbits of the points $\mathfrak{P}_k$ can be described by four coordinates

$$\mathbf{x}_k(p) = \mathbf{r}_k(p), t(p) \qquad k = 1, 2, \ldots, n$$

where p is the independent parameter with the help of which we can obtain the four-points giving the orbit of $\mathfrak{P}_k$. The four-coordinates of $\mathfrak{P}_k^*$ are some functions of the $\mathbf{x}_k(p)$, thus we may write

$$\mathbf{x}_k^*(p) = \boldsymbol{\lambda}(\mathbf{x}_k(p)) \qquad k = 1, 2, \ldots, N \tag{3}$$

where $\boldsymbol{\lambda}$ is the four-function describing the change $\mathfrak{Q} \to \mathfrak{Q}^*$ in the representation K.

The relation (3) represents the deformation $\mathfrak{Q} \to \mathfrak{Q}^*$ relative to a system of reference K. We may express the relation (3) also with respect to a new system of reference K'. The coordinate measures $\mathbf{x}$ may be taken to change into measures

$$\mathbf{x}' = \mathbf{f}(\mathbf{x}), \tag{4}$$

when changing the representation K into K' where we suppose $\mathbf{f}$ to be a reversible four-function, thus with (4) we have also

$$\mathbf{x} = \mathbf{f}^{-1}(\mathbf{x}').$$

With the help of (4) and (5) we find that the transformation (3) can be expressed in the representation K' as

$$\mathbf{x}'^{*}_{k}(p) = \boldsymbol{\lambda}'\left(\mathbf{x}'_{k}(p)\right), \tag{6a}$$

where

$$\boldsymbol{\lambda}' = \mathbf{f}\,\boldsymbol{\lambda}\,\mathbf{f}^{-1}. \tag{6b}$$

$\boldsymbol{\lambda}'$ is thus the function which is obtained if one applies on to the variables in order the functions $\mathbf{f}^{-1}$, $\boldsymbol{\lambda}$ and $\mathbf{f}$.

We may denote the four-function giving rise to a particular Lorentz transformation by $\boldsymbol{\lambda}_{\mathbf{p}}$ where $\mathbf{p}$ stands for the parameters of the transformation. The Lorentz transformations must be necessarily associative, i.e. together with the successive Lorentz transformations $\boldsymbol{\lambda}_{\mathbf{p}_1}, \boldsymbol{\lambda}_{\mathbf{p}_2}, \ldots, \boldsymbol{\lambda}_{\mathbf{p}_n}$ also

$$\boldsymbol{\lambda}_{\mathbf{p}} = \boldsymbol{\lambda}_{\mathbf{p}_n}\boldsymbol{\lambda}_{\mathbf{p}_{n-1}}\ldots\boldsymbol{\lambda}_{\mathbf{p}_1} \tag{7}$$

is a Lorentz transformation and we may put brackets into the right hand expression in an arbitrary way without changing $\boldsymbol{\lambda}_{\mathbf{p}}$. The relation (7) if fulfilled in one representation K is also fulfilled in any other representation K'. Indeed, with the help of (6) we find from (7)

$$\boldsymbol{\lambda}_{\mathbf{p}} = \boldsymbol{\lambda}'_{\mathbf{p}_n}\boldsymbol{\lambda}_{\mathbf{p}_{n-1}}\ldots\boldsymbol{\lambda}'_{\mathbf{p}} \tag{8a}$$

with

$$\boldsymbol{\lambda}_{\mathbf{p}} = \mathbf{f}\,\boldsymbol{\lambda}_{\mathbf{p}}\,\mathbf{f}^{-1}, \qquad \boldsymbol{\lambda}'_{\mathbf{p}_i} = \mathbf{f}\,\boldsymbol{\lambda}_{\mathbf{p}_i}\mathbf{f}^{-1} \qquad (i = 1, 2, \ldots, n). \tag{8b}$$

§ 3. The functions $\boldsymbol{\lambda}_{\mathbf{p}}$ must be restricted suitably if we want relation (1) to stand.

A neccessary condition for the form of the $\boldsymbol{\lambda}$-s can be obtained from the requirement that light waves propagated inside a system Ω should be transformed into corresponding ones propagated inside Ω^*.

The orbit of a beam of light obeys the relation

$$\dot{\mathbf{x}}(p)\,\mathbf{g}(\mathbf{x}(p))\,\dot{\mathbf{x}}(p) = 0. \tag{9}$$

The corresponding relation for the beam moving inside Ω^* can thus be written

$$\dot{\mathbf{x}}^{*}(p)\,\mathbf{g}(\mathbf{x}^{*}(p))\,\dot{\mathbf{x}}^{*}(p) = 0. \tag{10}$$

Comparing (9) and (10) we find

$$\tilde{\mathbf{M}}(\mathbf{x})\,\mathbf{g}(\mathbf{x}^{*})\,\mathbf{M}(\mathbf{x}) = \mathbf{g}(\mathbf{x}), \tag{11a}$$

with

$$\mathbf{M} = \frac{\partial\,\boldsymbol{\lambda}(\mathbf{x})}{\partial\,\mathbf{x}} \qquad \text{or} \qquad M_{\nu\mu} = \frac{\partial\lambda_{\nu}(\mathbf{x})}{\partial x_{\mu}}. \tag{11b}$$

As we have pointed out previously (11a) and (11b) give ten equations for the four unknown functions $\lambda_\nu(\mathbf{x})$ and therefore the system (11) is in general overdetermined. The system (11) admits solutions if there exist representations K_0 such that

$$K_0(\mathfrak{g}) = \mathbf{g}_0 = \text{independent of the coordinates.} \tag{12}$$

If a representation K_0 satisfying (12) exists, we can take the region $\mathfrak{R}$ in which (12) is valid to be a homogeneous region, i.e. a region in which light is propagated homogeneously. A representation K with

$$\mathbf{g}(\mathbf{x}) = K(\mathfrak{g}), \tag{13}$$

in which $\mathbf{g}(\mathbf{x})$ depends on $\mathbf{x}$ can be taken to be a *curved* representation of the homogeneous region $\mathfrak{R}$. The representation K_0 obeying (12) may be denoted a *straight* representation of $\mathfrak{R}$. If, however, in a region $\mathfrak{R}$ there exists no straight representation K_0, then the region is really inhomogeneous and in such a region the system (11) admits of no solution. In a really inhomogeneous region one can construct approximate solutions of (11); we shall discuss the latter in more detail.

§ 4. Consider the vicinity of a fixed four-point $\mathfrak{x}$. The points $\mathfrak{P}_k$ of a system $\mathfrak{Q}$ should all move in the vicinity of $\mathfrak{x}$ and thus their four-coordinates in a representation K can be written

where
$$\left.\begin{aligned} \mathbf{x}_k(p) &= \mathbf{x} + \xi_k(p), && \text{(a)} \\ \xi_k(p) &= \varrho_k(p), \tau(p), && \text{(b)} \end{aligned}\right\} \tag{14}$$

and

$$\mathbf{x} = K(\mathfrak{x})$$

is the four-coordinate of the point $\mathfrak{x}$. A transformation $\boldsymbol{\lambda}$ changes the point $\mathfrak{x}$ into a point $\mathfrak{x}^*$ with coordinates

$$\mathbf{x}^* = \boldsymbol{\lambda}(\mathbf{x}) = \mathbf{x} + \mu. \tag{15}$$

Thus the transformation shifts the centre of $\mathfrak{Q}$ by a four-vector μ. The deformed system $\mathfrak{Q}^*$ consists of points $\mathfrak{P}_k^*$ all in the vicinity of $\mathbf{x}^*$ and we may write

$$\mathbf{x}_k^*(p) = \mathbf{x}^* + \xi_k^*(p). \tag{16}$$

Separating the four-dimensional shift from the homogeneous part of the transformation, we may write

$$\boldsymbol{\lambda}_\mathbf{p}(\mathbf{x} + \xi) = \mu + \boldsymbol{\Lambda}_\mathbf{p}(\xi), \tag{17a}$$

and thus the homogeneous part of the transformation can be written

$$\xi^* = \Lambda_p(\xi) \qquad \text{with} \qquad \Lambda_p(0) = 0. \tag{17b}$$

Denoting

$$\frac{\partial \Lambda_p(\xi)}{\partial \xi} = \mathbf{M}(\xi), \tag{17c}$$

the condition (11a) may also be written

$$\tilde{\mathbf{M}}(\xi)\, g(x + \mu + \xi^*)\, \mathbf{M}(\xi) = g(x + \xi). \tag{18}$$

The relation (18) being identical with (11) does not admit exact solutions apart from exceptional cases. However, we can take as approximate solutions of (18) a four-function $\Lambda_p(\xi)$ which for a fixed value of μ satisfy (18) in a good approximation in a small vicinity of x. As was shown in Part IV we can construct e.g. functions $\Lambda_p(\xi)$ which satisfy (18) and its first derivative into ξ for $\xi = 0$ and we may take such functions $\Lambda_p(\xi)$ as approximate solutions.

The above requirement does not, however, define the approximate solutions with a sufficient accuracy. Indeed, the conditions

$$\frac{\partial^k}{\partial \xi^k}(\tilde{\mathbf{M}}\, g^*\, \mathbf{M} - g) = 0 \qquad \text{for} \qquad \xi = 0,\ k = 0, 1, \tag{19a}$$

where we have written short

$$\mathbf{M}(\xi) = \mathbf{M},\ g(x + \xi) = g \qquad \text{and} \qquad g(x + \mu + \xi^*) = g^* \tag{19b}$$

define together with (13) only the coefficients in the development of $\lambda_p(x + \xi)$ up to the second order terms. The higher order terms remain arbitrary when we take (19a, b) as the definition of the Lorentz transformation — the latter terms may, however, affect the function $\lambda_p(x + \xi)$ to an appreciable extent.

§ 5. So as to restrict the ambiguity in the definition (19) one might require the higher order terms to be "small". However, the latter requirement has no definite meaning, as it is not independent of the choice of representation. Indeed, if we have a representation in which the higher order terms are small (or for that matter even zero) then in another representation which is obtained by a strongly non-linear coordinate transformation, the higher order terms may become very large.

In the case of a homogeneous region we can extend the definition by requiring that the coefficient of the higher order terms should be zero in a *straight* representation. The latter definition brings us back to the definition of the Lorentz transformation as given in Part I.

The extension of the above definition to inhomogeneous regions can be formulated by requiring that in an *almost straight* representation the terms of the higher order coefficients should be *small*. The latter definition was given in Part IV in a qualitative manner and the physical implications of such a definition were discussed there. In this article we try to formulate the concepts used in Part IV in a more quantitative manner.

The almost straight representation

§ 6. In a homogeneous region $\mathfrak{R}$ in the vicinity of a fixed point $\mathfrak{x}$ where we have

$$K(\mathfrak{g}) = \mathbf{g}(\mathbf{x} + \xi), \quad K(\mathfrak{x}) = \mathbf{x},$$

there exists a coordinate transformation

$$\xi' = \mathbf{F}(\xi), \quad \mathbf{F}(0) = 0,$$

such that

$$\widetilde{\mathbf{M}}(\xi)\, \mathbf{g}_0\, \mathbf{M}(\xi) = \mathbf{g}(\mathbf{x} + \xi), \tag{20}$$

where $\mathbf{g}_0$ is an arbitrary propagation tensor. We may assume for the sake of simplicity

$$\mathbf{g}_0 = \mathbf{g}(\mathbf{x}), \tag{20a}$$

i.e. we may suppose that the transformation does not change the value of $\mathbf{g}$ in the point $\mathbf{x}$.

Expanding the various quantities into powers of ξ we may write remembering also (20a)

$$\mathbf{F}(\xi) = \xi + \frac{1}{2}\overset{(3)}{\mathbf{F}}\xi^2 + \frac{1}{6}\overset{(4)}{\mathbf{F}}\xi^3 + \ldots \tag{21}$$

where $\overset{(k)}{\mathbf{F}}$ is a k-dimensional matrix and we write short

$$\left[\overset{(k+1)}{\mathbf{F}}\,\xi^k\right]_\nu = \sum_{\mu_1 \ldots \mu_k} \overset{(k+1)}{\mathbf{F}}_{\nu\mu_1\mu_2\ldots\mu_k}\, \xi_{\mu_1}\, \xi_{\mu_2} \ldots \xi_{\mu_k}\,. \tag{21a}$$

Similarly we have

$$\mathbf{M}(\xi) = 1 + \overset{(3)}{\mathbf{F}}\,\xi + \frac{1}{2}\overset{(4)}{\mathbf{F}}\,\xi^2 + \ldots. \tag{21b}$$

Furthermore we may write also

$$\widetilde{\mathbf{M}}\,(\xi) = \mathbf{1} + \xi\,\overset{\widetilde{(3)}}{\mathbf{F}} + \frac{1}{2}\xi^2\,\overset{\widetilde{(4)}}{\mathbf{F}} + \ldots, \tag{21c}$$

where the transposition sign on a matrix with several suffices is meant to signify a cylic permutation of the suffices. Thus

$$\overset{(\widetilde{k})}{\mathbf{F}} = (1, 2, \ldots, k)\overset{(k)}{\mathbf{F}} = c_k \overset{(k)}{\mathbf{F}}, * \tag{21d}$$

where

$$c_k = (1, 2, \ldots, k)$$

i.e. c_k is the operator giving rise to a cyclic permutation shifting the suffices by one step to the right. Analogously c_k^l will denote the operator shifting the suffices by l steps to the right.

Similarly we may develop $\mathbf{g}$ as follows:

$$\mathbf{g}(\mathbf{x} + \xi) = \mathbf{g}_0 + \overset{(3)}{\mathbf{g}}\,\xi + \frac{1}{2}\overset{(4)}{\mathbf{g}}\,\xi^2 + \ldots . \tag{21e}$$

Using the series (21b)—(21e) we may develop both sides of (20) into a power series and comparing the coefficients we obtain a recursion for the $\overset{(k)}{\mathbf{F}}$ ($k = 3,4, \ldots$). Indeed, we find

$$\widetilde{\mathbf{M}}(\xi)\,\mathbf{g}_0\,\mathbf{M}(\xi) = \sum_k \left(\sum_{l=0}^{k} \frac{c_{k+2}^l}{l!(k-l)!} \overset{(l\widetilde{+}2)}{\mathbf{F}}\,\mathbf{g}_0\,\overset{(k-l+2)}{\mathbf{F}} \right) \xi^k . \tag{22a}$$

The coefficients of ξ^k ($k = 1,2, \ldots$) appearing inside the brackets on the right hand side of (22a) are not necessarily symmetric in the last k suffices. However, we may replace these coefficients by symmetric expressions.

*Concerning permutation operators the following conventions will be used:

1) A permutation operator P applied to an arbitrary matrix $\mathbf{A}$ gives rise to a new matrix $P\mathbf{A}$ with elements

$$[P\mathbf{A}]_{\nu_1, \nu_2, \ldots, \nu_n} = A_{P[\nu_1, \nu_2, \ldots, \nu_n]} ,$$

where $P[\nu_1, \nu_2, \ldots \nu_n]$ is a permutation of $\nu_1, \nu_2, \ldots \nu_n$.

The successive application of two permutation operators P_1, P_2 gives in accordance with the previous definition a matrix $P_2P_1\mathbf{A}$ with elements

$$[P_2\,P_1\,\mathbf{A}]_{\nu_1, \nu_2, \ldots, \nu_n} = [P_1\,\mathbf{A}]_{P_2[\nu_1, \nu_2, \ldots, \nu_n]} = A_{P_1P_2[\nu_1, \nu_2, \ldots, \nu_n]},$$

thus the indices are permuted firstly by P_2 and then by P_1, i.e. in an order reversed to that of the operators.

2) We use for permutation operators the cyclic notation, e.g.

$$[(1, 3, 2)\,\mathbf{A}]_{\nu_1, \nu_2, \ldots, \nu_n} = A_{\nu_2, \nu_3, \nu_1, \nu_4, \ldots, \nu_n}.$$

Thus the primitive cyclic permutation of k indices applied in (21d) has the effect

$$[c_k \overset{(k)}{\mathbf{F}}]_{\nu_1, \nu_2, \ldots, \nu_k} = \overset{(k)}{\mathbf{F}}_{\nu_k, \nu_1, \nu_2, \ldots, \nu_{k-1}} .$$

$$\frac{1}{k!}\overset{(k+2)}{\Theta} = \frac{1}{k!}\sum_{P}''\left(\sum_{l=0}^{k}\frac{c_{k+2}^{l}}{l!\,(k-l)!}\overset{(\widetilde{l+2})}{\mathbf{F}}\,\mathbf{g}_0\,\overset{(k-l+2)}{\mathbf{F}}\right), \tag{22b}$$

without changing the numerical value of the right hand expression; $\sum_{P}''$ is supposed to be the summation over the $k!$ permutations of the suffices $3, 4, \ldots, k+2$. (The two dashes on the summation sign indicate that the first two suffices are not to be permuted.) Thus we have also

$$\widetilde{\mathbf{M}}(\xi)\,\mathbf{g}_0\,\mathbf{M}(\xi) = \sum_{k}\frac{1}{k!}\overset{(k+2)}{\Theta}\,\xi^{k}. \tag{23}$$

So as to obtain an explicit recursion from (22a) we remember the symmetry properties of the $\overset{(k+2)}{\mathbf{F}}$, i.e. remember that it follows from (21a), (21b) that the $\overset{(k+2)}{\mathbf{F}}$ have the symmetries

$$(2, l)\,\overset{(k+2)}{\mathbf{F}} = \overset{(k+2)}{\mathbf{F}} \quad \text{for} \quad \left.\begin{matrix} l = 3, 4, \ldots, k+2 \\ k = 1, 2, \ldots\ . \end{matrix}\right\}. \tag{24}$$

Also the $\overset{(k+2)}{\mathbf{g}}$ obey symmetries. We find from the definitions

$$(1, 2)\,\overset{(k+2)}{\mathbf{g}} = (3, l)\,\overset{(k+2)}{\mathbf{g}} = \overset{(k+2)}{\mathbf{g}} \quad l = 4, 5, \ldots, k+2\,. \tag{25}$$

From (24) and (25) it follows that

$$c_{k+2}^{k}\left(\overset{(\widetilde{k+2})}{\mathbf{F}}\,\mathbf{g}_0\right) + \mathbf{g}_0\,\overset{(k+2)}{\mathbf{F}} = (\mathbf{1} + c_3^{-1})\,(\mathbf{g}_0\,\overset{(k+2)}{\mathbf{F}}) \tag{26}$$

where $c_3 = (1, 2, 3)$ is the operator signifying the cyclic permutation of the first three suffices of the matrix upon which it is applied and c_3^{-1} denotes its inverse.

Splitting off $\overset{(k+2)}{\Theta}$ the terms with $l = 0$ and $l = k$ we may also write, remembering the symmetry properties of the matrices involved and that according to (21) $\overset{(2)}{\mathbf{F}} = 1$

$$\overset{(k+2)}{\Theta} = (\mathbf{1} + c_3^{-1})\,(\mathbf{g}_0\,\overset{(k+2)}{\mathbf{F}}) + \overset{(k+2)}{\mathbf{\Phi}} \tag{22c}$$

with

$$\overset{(k+2)}{\mathbf{\Phi}} = \sum_{P}''\left(\sum_{l=1}^{k-1}\frac{c_{k+2}^{l}}{l!\,(k-l)!}\overset{(\widetilde{l+2})}{\mathbf{F}}\,\mathbf{g}_0\,\overset{(k-l+2)}{\mathbf{F}}\right). \tag{22d}$$

Introducing (22a) — (22c) into (20) and comparing the coefficients on both

sides we find thus with the help of (26)

$$(\mathbf{1}+c_3^{-1})(\mathbf{g}_0 \overset{(k+2)}{\mathbf{F}}) = \overset{(k+2)}{\mathbf{g}} - \overset{(k+2)}{\mathbf{\Phi}} . \tag{27}$$

So as to determine $\overset{(k+2)}{\mathbf{F}}$ from (27) we denote

$$\mathbf{x}_l = c_3^{-l}(\mathbf{g}_0 \overset{(k+2)}{\mathbf{F}}), \quad y_l = c_3^{-l}(\overset{(k+2}{\mathbf{g}} - \overset{(k+2)}{\mathbf{\Phi}}),$$

where c_3^{-l} is the operator signifying the application of c_3^{-1} l-times. We have thus e.g. $c_3^{-3} = \mathbf{1}$. Applying c_3^{-1} successively upon (27) we obtain thus the following set of equations

$$\begin{aligned} \mathbf{x}_0 + \mathbf{x}_1 &= y_0 \\ \mathbf{x}_1 + \mathbf{x}_2 &= y_1 \\ \mathbf{x}_0 + \mathbf{x}_2 &= y_2 \end{aligned} \tag{28}$$

and therefore

$$\mathbf{x}_0 = \frac{1}{2}(y_0 - y_1 + y_2) = \frac{1}{2}(c.p.)_{-3} y_0 ,$$

and

$$\overset{(k+2)}{\mathbf{F}} = \frac{1}{2} g_0^{-1}\big((c.p.)_{-3}(\overset{(k+2)}{\mathbf{g}} - \overset{(k+2)}{\mathbf{\Phi}}) \quad k = 1, 2, 3, \ldots, \tag{29}$$

where we use the symbol $(c.p.)_{-3}$ for summing over the cyclic permutations of the first suffices with alternating signs. Thus we have

$$(c.p.)_{-3}\,\mathbf{A} = (\mathbf{1} - c_3^{-1} + c_3^{-2})\,\mathbf{A}.$$

§ 7. The $\overset{(k+2)}{\mathbf{F}}$ as expressed by (29) satisfy the relation (27) and as it can be seen easily also the symmetry relation (24) for $l = 3$. Thus we find from (29) the identity

$$\overset{(k+2)}{\mathbf{F}} = (2, 3) \overset{(k+2}{\mathbf{F}} \quad k = 1, 2, 3, \ldots . \tag{29a}$$

However, (29) gives only a necessary condition for the values of the $\overset{(k+2)}{\mathbf{F}}$ if $k > 1$. Indeed, the expression (29) for $\overset{(k+2)}{\mathbf{F}}$ may or may not satisfy (24) for $l > 3$. If (29) does not satisfy some of the latter conditions, then we arrive at a contradiction and the system (20) admits of no solution.

Thus whether or not the symmetry conditions

$$(2, l) \overset{(k+2)}{\mathbf{F}} = \overset{(k+2)}{\mathbf{F}} \qquad \begin{aligned} l &= 4, 5, \ldots, k+2 \\ k &= 2, 3, \ldots \end{aligned} \tag{30}$$

are fulfilled depends on the properties of the matrices $\overset{(k+2)}{\mathbf{g}}$; the values (29) for the $\overset{(k+2)}{\mathbf{F}}$ put into (21b) give then and only then a transformation matrix $\mathbf{M}(\xi)$ fulfilling (20) provided they satisfy the conditions (30), i.e. if we have

$$(\mathbf{1} - (2, l))\,((c.\,p.)_{-3}(\overset{(k+2)}{\mathbf{g}} - \overset{(k+2)}{\mathbf{\Phi}})) = 0 \tag{31}$$

$$\text{for } l = 4, 5, \ldots, k+2 \qquad k = 2, 3, \ldots .$$

§ 8. Considering $k = 1$ we find from (29) remembering that in accord with (22d) $\overset{(3)}{\mathbf{\Phi}} = 0$

$$\overset{(3)}{\mathbf{F}} = \frac{1}{2}\,\mathbf{g}_0^{-1}\,((c.\,p.)_{-3}\,\overset{(3)}{\mathbf{g}}). \tag{32}$$

Thus the $\overset{(3)}{\mathbf{F}}$ are identical with the Christoffel brackets. The $\overset{(3)}{\mathbf{F}}$ thus obtained possess the proper symmetry properties.

For $k = 2$ we find from (22d)

$$\overset{(4)}{\mathbf{\Phi}} = \sum_P{}'' c_4\,(\overset{\sim}{\overset{(3)}{\mathbf{F}}}\,\mathbf{g}_0\,\overset{(3)}{\mathbf{F}}).$$

Since $\sum_P{}''$ can be replaced by $1 + (3, 4)$, taking into consideration the symmetries of the matrix under the sum we find also

$$\overset{(4)}{\mathbf{\Phi}} = ((2, 4) + (2, 3))\,(\overset{\sim}{\overset{(3)}{\mathbf{F}}}\,\mathbf{g}_0\,\overset{(3)}{\mathbf{F}}) \tag{33}$$

and

$$\overset{(4)}{\mathbf{F}} = \frac{1}{2}\,\mathbf{g}_0^{-1}\,(c.\,p.)_{-3}\,(\overset{(4)}{\mathbf{g}} - \overset{(4)}{\mathbf{\Phi}}). \tag{34}$$

The above expression is symmetric in the second and third suffices but not neccessarily in the second and fourth, respectively in the third and fourth suffices. Thus (34) gives only then the second order coefficient of the development of $\mathbf{F}(\mathbf{x})$ provided

$$(\mathbf{1} - (2, 4))\,((c.\,p.)_{-3}(\overset{(4)}{\mathbf{g}} - \overset{(4)}{\mathbf{\Phi}})) = 0. \tag{35}$$

Considering the symmetry properties of the matrices involved (35) can also be written

$$(c.\,p.)_4\,(\overset{(4)}{\mathbf{g}} - \overset{(4)}{\mathbf{\Phi}}) = 0 \tag{36}$$

with

$$(c.\,p.)_4 = 1 - c_4^{-1} + c_4^{-2} - c_4^{-3} = 1 - c_4 + c_4^2 - c_4^3.$$

The left hand expression is representing the Riemann—Christoffel tensor; more precisely writing

$$\overset{(4)}{\mathbf{R}}_1 = (1-(2,4))(c.p.)_{-3}(\overset{(4)}{\mathbf{g}} - \overset{(4)}{\mathbf{\Phi}}) = (c.p.)_4(\overset{(4)}{\mathbf{g}} - \overset{(4)}{\mathbf{\Phi}}) \tag{36a}$$

one finds that

$$\overset{(4)}{\mathbf{R}} = -\frac{1}{2}(2,3)\overset{(4)}{\mathbf{R}}_1$$

gives the Riemann—Christoffel tensor in the usual definition. (The explicit expression for $\overset{(4)}{\mathbf{\Phi}}$ is given by (32) and (33)).

Thus (34) has then and only then the correct symmetry properties if

$$\overset{(4)}{\mathbf{R}}_1 = 0. \tag{37}$$

For $k = 3$ we find an expression for $\overset{(5)}{\mathbf{F}}$; the latter has proper symmetry properties provided apart from (37) we have also

$$\overset{(5)}{\mathbf{R}}_1 = 0\,, \qquad \overset{(5)}{\mathbf{R}}_2 = 0\,,$$

where

$$\overset{(5)}{\mathbf{R}}_l = (1-(2,l))\,(c.p.)_{-3}\,(\overset{(5)}{\mathbf{g}} - \overset{(5)}{\mathbf{\Phi}})\,, \qquad l = 4,5$$

and similarly we find that (20) possesses solutions then and only then if

$$\left.\begin{aligned} &\overset{(k+2)}{\mathbf{R}}_l = 0 \qquad k = 2,3,4,\ldots \\ &\qquad\qquad\quad l = 1,2,\ldots,k-1. \end{aligned}\right\} \tag{38}$$

If the conditions (38) are satisfied then the transformation function $\mathbf{F}(\xi)$ can be obtained from (21), (22d) and (29).

§ 9. With the help of (38) we can thus find out whether or not a representation

$$K(\mathfrak{g}) = \mathbf{g}(\mathbf{x}+\xi) \tag{39}$$

of the propagation tensor represents a homogeneous region in terms of curvilinear coordinates or whether the region in which (39) is valid is truly inhomogeneous.

In the case where not all the relations (38) hold, the matrices $\overset{(k+2)}{\mathbf{F}}$ obtained from the recursion defined by (22d) and (29) do not possess the required symmetry properties. We may introduce symmetrized matrices

$$\frac{1}{(k+1)!}\sum_P{}' \overset{(k+2)}{\mathbf{F}} = \overset{(k+2)}{\mathscr{F}} \tag{40}$$

where Σ' stands for summation over the permutation of the last $k+1$ suffices. If the $\overset{P}{\mathbf{F}}_{(k+2)}$ as obtained from (29) are already symmetric in the last $k+1$ suffices, then we have

$$\overset{(k+2)}{\mathbf{F}} = \overset{(k+2)}{\mathscr{F}}. \tag{41}$$

From (40) and (41) it follows that

$$\overset{(3)}{\mathscr{F}} = \overset{(3)}{\mathbf{F}}, \tag{41a}$$

therefore the coefficients $\overset{(k+2)}{\mathbf{F}}$ and $\overset{(k+2)}{\mathscr{F}}$ differ only for $k > 1$. If, however, the $\overset{(k+2)}{\mathbf{F}}$ have not the suitable symmetries, then they differ from the $\overset{(k+2)}{\mathscr{F}}$.

We may define a function $\mathbf{F}(\xi)$ putting

$$\mathbf{F}(\xi) = \xi + \frac{1}{2}\overset{(3)}{\mathscr{F}}\xi^2 + \dots \tag{42}$$

however, one finds independently of whether or not (41) holds that

$$\overset{(k+1)}{\mathbf{F}}\,\xi^k = \overset{(k+1)}{\mathscr{F}}\,\xi^k,$$

since the summation which is involved in forming the above products eliminates the non symmetric parts of $\overset{(k+1)}{\mathbf{F}}$ as can be seen with the help of (21a). Thus (42) defines the same function as (21) together with (29) does. However, the function $\mathbf{F}(\xi)$ thus defined is then and only then a solution of (20), if (41) is satisfied. If (41) is not satisfied, then $\mathbf{F}(\xi)$ given by (42) can be taken to be an *approximate* solution of (20), and the representation K' obtained from K by putting

$$\xi' = \mathbf{F}(\xi) \tag{43}$$

can be taken to be an *almost straight* representation.

§. 10. So as to see the properties of the almost straight representation thus obtained we may determine the representation

$$K'(\mathfrak{g}) = \mathbf{g}_0(\mathbf{x}' + \xi')$$

of $\mathfrak{g}$ in the almost straight system of reference K'.

We start thus from the relation

$$\widetilde{\mathbf{M}}(\xi)\,\mathbf{g}_0(\mathbf{x}' + \xi')\,\mathbf{M}(\xi) = \mathbf{g}(\mathbf{x} + \xi) \tag{44}$$

and take $\mathbf{M}(\xi)$ to be the transformation matrix associated with the approximate transformation (43); thus (44) permits to determine the propagation matrix $\mathbf{g}_0$ in the representation where its elements are *almost constant.*

Supposing

$$\left.\begin{aligned} \xi' = \mathbf{F}(\xi) &= \xi + \frac{1}{2!}\overset{(3)}{\mathbf{F}}\xi^2 + \frac{1}{3!}\overset{(4)}{\mathscr{F}}\xi^3 + \dots && \text{(a)} \\ \mathbf{M}(\xi) &= \mathbf{1} + \overset{(3)}{\mathbf{F}}\xi + \frac{1}{2!}\overset{(4)}{\mathscr{F}}\xi^2 + \dots && \text{(b)} \\ \mathbf{g}_0(\mathbf{x}' + \xi') &= \overset{(2)}{\mathbf{g}_0} + \overset{(3)}{\mathbf{g}_0}\xi' + \frac{1}{2!}\overset{(4)}{\mathbf{g}_0}\xi'^2 + \dots && \text{(c)} \\ \mathbf{g}(\mathbf{x} + \xi) &= \mathbf{g}_0 + \overset{(3)}{\mathbf{g}}\xi + \frac{1}{2!}\overset{(4)}{\mathbf{g}}\xi^2 + \dots && \text{(d)} \end{aligned}\right\} \tag{45}$$

we may insert (45) into (44) and compare coefficients of the developments on both sides. We find from the comparison of the constant and the first order terms using the definition of $\overset{(3)}{\mathbf{F}}$

$$\overset{(2)}{\mathbf{g}_0} = \mathbf{g}_0\,, \qquad \overset{(3)}{\mathbf{g}_0} = 0\,. \tag{46a}$$

Making use of (46a) the comparison of the second order terms gives

$$\xi^2\overset{\widetilde{(4)}}{\mathscr{F}}\mathbf{g}_0 + \mathbf{g}_0\overset{(4)}{\mathscr{F}}\xi^2 + \overset{(4)}{\mathbf{g}_0}\xi^2 = \overset{(4)}{g}\,\xi^2 - 2\,(\xi\,\overset{\widetilde{(3)}}{\mathbf{F}}\,\mathbf{g}_0\,\overset{(3)}{\mathbf{F}}\,\xi),$$

thus using (33) one obtains

$$\overset{(4)}{\mathbf{g}_0} + (1 + c_3^{-1})\,(\mathbf{g}_0\overset{(4)}{\mathscr{F}}) = \overset{(4)}{\mathbf{g}} - \overset{(4)}{\mathbf{\Phi}}.$$

Since from the definition of $\overset{(4)}{\mathbf{F}}$ it follows that

$$(1 + c_3^{-1})\,(\mathbf{g}_0\overset{(4)}{\mathbf{F}}) = \overset{(4)}{\mathbf{g}} - \overset{(4)}{\mathbf{\Phi}},$$

we find

$$\overset{(4)}{\mathbf{g}_0} = -\,(1 + c_3^{-1})\,(\mathbf{g}_0(\overset{(4)}{\mathscr{F}} - \overset{(4)}{\mathbf{F}})). \tag{46b}$$

But we find from (40)

$$\overset{(4)}{\mathscr{F}} - \overset{(4)}{\mathbf{F}} = -\frac{1}{3}\big((1 - (2,4)) + (1 - (3,4))\big)\overset{(4)}{\mathbf{F}};$$

remembering that

$$(2,3)\,(\mathbf{1}-(2,4))\,(2,3)=(\mathbf{1}-(3,4))$$

we have further making use also of (36a)

$$\mathbf{g}_0\,(\overset{(4)}{\mathscr{F}}-\overset{(4)}{\mathbf{F}})=-\frac{1}{3}(\mathbf{1}+(2,3))\,(\mathbf{1}-(2,4))\,(\mathbf{g}_0\overset{(4)}{\mathbf{F}})=-\frac{1}{6}(\mathbf{1}+(2,3))\overset{(4)}{\mathbf{R}}_1. \tag{46c}$$

Introducing (46c) into (46b) we have

$$\overset{(4)}{\mathbf{g}}_0=\frac{1}{6}\,(1+c_3^{-1})\,(\mathbf{1}+(2,3))\overset{(4)}{\mathbf{R}}_1. \tag{46d}$$

From the definition (36a) we find easily the symmetry properties of $\overset{(4)}{\mathbf{R}}_1$; one finds thus

$$(1,4)\,(2,3)\equiv(1,2)\,(3,4)\equiv-(1,3)\equiv-(2,4)\equiv\mathbf{1}\quad\text{mod}\quad\overset{(4)}{\mathbf{R}}_1,$$

where the $\equiv$ sign signifies that the operators applied to $\overset{(4)}{\mathbf{R}}_1$ give the same result. Making use of the above symmetries, we find that (46d) can be simplified; one finds as the result of a short calculation

$$\overset{(4)}{\mathbf{g}}_0=\frac{1}{6}(\mathbf{1}+(1,2))\overset{(4)}{\mathbf{R}}_1. \tag{46e}$$

We see thus that the transformation (43) leads to a representation of $\mathfrak{g}$ in which the first derivatives of $\overset{(3)}{\mathbf{g}}$ are equal to zero for $\xi=\xi'=0$ and the second derivatives $\overset{(4)}{\mathbf{g}}$ are of the order of the components of the Riemann—Christoffel tensor $\overset{(4)}{\mathbf{R}}$. The latter representation (as long as we concern ourselves with derivatives up to the second order only) can thus be regarded indeed as a nearly straight representation.

As it was pointed out before at least some of the second derivatives $\overset{(4)}{\mathbf{g}}$ must be as great as of the order of the components of $\overset{(4)}{\mathbf{R}}$, since $\overset{(4)}{\mathbf{R}}$ is obtained as a linear combination of the components of $\overset{(4)}{\mathbf{g}}$. Thus there cannot exist a representation in which $\overset{(3)}{\mathbf{g}}=0$, and the components of $\overset{(4)}{\mathbf{g}}$ are essentially smaller than the values given in (46d).

The transformation (43) is so defined that the coefficients $\overset{(k)}{\mathscr{F}}$ of the expansion terms of $\mathbf{F}(\xi)$ should be functions of the derivatives of $\mathbf{g}$ only;

and the transformation should lead to a straight representation K' if the region considered is a homogeneous one. The coefficients $\overset{(k+2)}{\mathcal{F}}$ of such a transformation are defined by (29) and (40). It can be seen easily that further transformations satisfying the above conditions can be constructed. Indeed, we may put

$$\overset{(\bar{k})}{\mathcal{F}} = \overset{(k)}{\mathcal{F}} + \overset{(k)}{\mathbf{L}},$$

where the elements of $\overset{(k)}{\mathbf{L}}$ are of the order of those of $\overset{(k)}{\mathbf{R}_l}$ and the former vanish with the latter. Thus the functions

$$\xi'' = \bar{\mathbf{F}}(\xi) = \sum_k \overset{(\overline{k+1})}{\mathcal{F}}\, \xi_k \tag{47}$$

can also be used to obtain a coordinate transformation which leads to a nearly straight representation just as the functions $\mathbf{F}(\xi)$ do.

In particular we may suppose that

$$\overset{(4)}{\mathbf{L}} = (\overset{(8)}{\mathbf{\Lambda}}\, \overset{(4)}{\mathbf{R}_1})^{(4)}, \tag{48}$$

where $\overset{(8)}{\mathbf{\Lambda}}$ is an eight-dimensional matrix and (48) stands short for

$$\overset{(4)}{\mathbf{L}}_{\nu\mu\varkappa\lambda} = \sum_{\nu'\mu'\varkappa'\lambda'} \overset{(8)}{\Lambda}_{\nu\mu\varkappa\lambda\nu'\mu'\varkappa'\lambda'}\, \overset{(4)}{\mathbf{R}}_{\nu'\mu'\varkappa'\lambda'}.$$

The components of $\overset{(8)}{\mathbf{\Lambda}}$ can be taken to be symmetric in the suffices $\mu\, \varkappa\, \lambda$, further they may be taken to have symmetries in the last suffices $\nu'\mu'\varkappa'\lambda'$ similar to the symmetries of the components of $\overset{(4)}{\mathbf{R}_1}$; in this manner the $\overset{(8)}{\mathbf{\Lambda}}$ can have $80 = 20 \times 1600$ independent components. The orders of the components of $\overset{(8)}{\mathbf{\Lambda}}$ should be taken such that the components of the $\overset{(4)}{\mathbf{L}}$ obtain orders of magnitude not exceeding those of the $\overset{(4)}{\mathbf{R}_1}$.

Using the transformation (47) in place of (43) we obtain a representation $\mathbf{g}_0$ of $\mathfrak{g}$ the second derivatives of which are given by

$$\overset{(4)}{\mathbf{g}_0} = \frac{1}{6}(\mathbf{1} + (1, 2))(\overset{(4)}{\mathbf{R}_1} + \overset{(4)}{\mathbf{L}}).$$

The representations thus obtained can also be taken to be almost straight. The various possible choices of $\overset{(8)}{\mathbf{\Lambda}}$ define the nearly straight representations in the second order approximation for which the value of $\mathbf{g}_0$ at $\xi = 0$ is fixed.

Submitting a nearly straight representation to a linear transformation we obtain another nearly straight representation, where $\mathfrak{g}$ is represented in the centre $\mathfrak{x}$ of the region by some matrix

$$\mathbf{g}_0' = \tilde{\mathbf{M}}^{-1}\,\mathbf{g}_0\,\mathbf{M}^{-1}.$$

In the latter representation the Riemann—Christoffel tensor $\overset{(4)}{\mathfrak{R}}_1$ is represented by a four-dimensional matrix $\overset{(4)}{\mathbf{R}}_1'$ and it is seen that the second derivatives $\overset{(4)}{\mathbf{g}}_0'$ of $\mathbf{g}_0'$ will be of the order of the components of $\overset{(4)}{\mathbf{R}}_1'$ if the components of $\overset{(4)}{\mathbf{g}}_0$ were of the order of $\overset{(4)}{\mathbf{R}}_1$. Thus a nearly straight representation subjected to a linear transformation can still be considered as a nearly straight representation.

Summarizing the considerations of the last paragraph we can thus construct transformations

$$\bar{\bar{\mathbf{F}}}(\xi) = \mathbf{M}\,\bar{\mathbf{F}}(\xi) = \mathbf{M}\,(\mathbf{F}(\xi) + \mathbf{L}(\xi))\,,$$

which lead from an arbitrary representation of a region to a nearly straight representation. The matrices $\mathbf{M}$ have constant elements, the expansions of the functions $\mathbf{L}(\xi)$ start with the second order terms and the coefficients $\overset{(k)}{\mathbf{L}}$ of this expansion must not exceed the order of magnitude of the corresponding elements of the matrices $\overset{(k)}{\mathfrak{K}}_l$.

The generalized Lorentz transformation

§ 11. Generalizing the considerations given above, we can now give explicit expressions for the transformations which we can consider as Lorentz transformations in an inhomogeneous region.

We denote thus a Lorentz transformation a transformation which associates to a four point $\mathbf{x} + \xi$ another point $\mathbf{x}^* + \xi^*$ with

$$\mathbf{x}^* = \mathbf{x} + \mu \qquad \xi^* = \Lambda_p\,(\xi), \tag{50}$$

where

$$\Lambda_p\,(0) = 0$$

such that the relation

$$\mathbf{M}_p\,(\xi)\,\mathbf{g}^*\,(\mathbf{x} + \xi)\,\mathbf{M}_p\,(\xi) = \mathbf{g}(\mathbf{x} + \xi)\,, \tag{51}$$

with

$$\mathbf{g}^*\,(\mathbf{x} + \xi) = \mathbf{g}(\mathbf{x}^* + \xi^*)$$

is satisfied in as good an approximation as it is possible. Considering (51) for $\xi = 0$ we find for

$$\mathbf{M}_p = \mathbf{M}_p(0)$$

the following explicit expressions:

$$\mathbf{M}_p = \alpha^{*-1} \Lambda_p \alpha , \tag{52}$$

where Λ_p is the matrix representing an ordinary Lorentz transformation in an orthogonal representation, i.e. Λ_p is a solution of the relation

$$\tilde{\Lambda}_p \Gamma \Lambda_p = \Gamma$$

(see for notations e.g. Part I), α and α^* are matrices satisfying

$$\tilde{\alpha} \Gamma \alpha = \mathbf{g}(\mathbf{x}) = \overset{(2)}{\mathbf{g}}, \qquad \alpha^* \Gamma \alpha^* = \mathbf{g}(\mathbf{x} + \mu) = \overset{(2)}{\mathbf{g}}{}^* .$$

Writing in particular

$$\mathbf{g} = \begin{pmatrix} \mathbf{G} & \mathbf{V} \\ \mathbf{V} & -C^2 \end{pmatrix} \tag{53}$$

we may put

$$\alpha = \begin{pmatrix} \mathbf{a} & 0 \\ \mathbf{b} & \gamma \end{pmatrix} \tag{54}$$

with

$$\mathbf{a} = \mathbf{G}^{1/2} \left(\mathbf{1} + \frac{\mathbf{v} \circ \mathbf{V}}{C(c + C)} \right) ,$$
$$\mathbf{b} = -\mathbf{V}/c\,C , \tag{54a}$$
$$\gamma = C/c ,$$

and a similar expression can be obtained for α^*. We may thus represent the $\mathbf{M}_p$ in terms of elements $\mathbf{G}$, $\mathbf{V}$, $-C^2$ of $\mathbf{g}$ together with those of $\mathbf{G}^*$, $\mathbf{V}^*$, $-C^{*2}$ of $\mathbf{g}^*$ and the parameter $\mathbf{p}$ is that of an ordinary Lorentz transformation Λ_p.

We may thus put

$$\Lambda_p(\xi) = \mathbf{M}_p \mathbf{F}(\xi)$$

and developing in powers of ξ we may write

$$\mathbf{F}(\xi) = \xi + \frac{1}{2} \overset{(3)}{\mathbf{F}} \xi^2 + \dots . \tag{55}$$

From the relations (51) we can obtain a recursion for the coefficients $\overset{(k)}{\mathbf{F}}$. The latter recursion has the same form as that obtained in § 6. The relation (29) can be taken to express the coefficients of the expression (55) if the definition (22d) of the $\overset{(k+2)}{\Phi}$ is generalized so as to read

$$\overset{(k+2)}{\Phi} = \sum_P{}'' \sum_{l+m+n=k} \frac{c^l_{k+2}}{l!\, m!\, n!} \overset{(\widetilde{l+2})}{\mathbf{F}} \overset{(\widetilde{m+2})}{\mathbf{g}^*} \overset{(n+2)}{\mathbf{F}} . \tag{56}$$

The transformations (50) thus defined satisfy (51) exactly if the latter relations admit of solutions at all. In particular if $\mathbf{x}$ and $\mathbf{x}^*$ both lie in a homogeneous region then such solutions exist and are represented by (55).

In the cases where (51) does not admit of exact solutions then (55) gives an approximate solution of (51) such that the difference of the two sides of (51) when expanded in powers of ξ contains coefficients of the orders of the matrices $\overset{(k+2)}{\mathbf{R}_l}$ and $\overset{(k+2)}{\mathbf{R}^*_l}$.

The coefficients of the expansion (55) are also of the order of these matrices if we use a representation which is almost straight both in the vicinities of $\mathbf{x}$ and of $\mathbf{x}^*$.

In this sense we can say that the coefficients of the higher order terms of $\mathbf{F}(\xi)$ are small if we use an almost straight representation.

In a strongly curved representation the coefficients of the expansion (55) may be large. These large coefficients arise from the curved representation just in the same manner as the Lorentz transformations in a homogeneous region deviate strongly from the linear form and contain large higher order terms if we write them down in curvilinear coordinates.

We note further that the transformation (55) may also be extended and replaced by

$$\overline{\mathbf{F}}(\xi) = \mathbf{F}(\xi) + \mathbf{L}(\xi),$$

where $\mathbf{L}(\xi)$ is a function the coefficients of which are of the order of the elements of the $\overset{(k+2)}{\mathbf{R}_l}$ and the $\overset{(k+2)}{\mathbf{R}^*_l}$ and $\mathbf{L}(\xi)$ is so constructed that it vanishes if the $\overset{(k+2)}{\mathbf{R}_l}$ and the $\overset{(k+2)}{\mathbf{R}^*_l}$ vanish.

The $\mathbf{L}(\xi)$ give the explicit expression for the undeterminacy of the Lorentz transformations the physical aspects of which were discussed in our former publications.

REFERENCES

1. L. JÁNOSSY, Acta Phys. Hung., **21,** 1, 1966.
2. L. JÁNOSSY, Acta Phys. Hung., **21,** 17, 1966.
3. L. JÁNOSSY, Acta Phys. Hung., **21,** 329, 1966.
4. L. JÁNOSSY, Acta Phys. Hung., **23,** 53, 1967.

ПРИНЦИП ЛОРЕНЦА И ОБЩАЯ ТЕОРИЯ ОТНОСИТЕЛЬНОСТИ

Часть V

Л. ЯНОШИ и П. КИРАЙ

Даётся явный вид преобразования, с помощью которого можно получить в однородной области прямолинейную систему отсчёта из произвольного криволинейного представления. Применение этого преобразования к представлению в неоднородной области приводит к *почти прямолинейной* системе отсчёта. Пользуяси почти прямолинейными представлениями мы получим явный вид преобразований Лоренца в неоднородных областях.

Acta Physica Academiae Scientiarum Hungaricae, Tomus 23 (3), pp. 311—313 (1967)

COMMUNICATIONES BREVES

ETUDE DE FORMALISME POUR METHODES DE PERTURBATIONS

J. RAVATIN et G. MESNARD
FACULTÉ DES SCIENCES, LYON, FRANCE

(Reçu le 19. X. 1966)

Dans une précédente publication nous avons défini certains opérateurs agissant sur des tableaux triangulaires de fonctions d'onde [1] renfermant le potentiel d'information d'un système physique.

Ces générateurs étaient de la forme $\Gamma_{A,\lambda}\, A$ appartenant à un espace hermitien $\mathscr{H}$ et λ au corps des complexes $\mathscr{C}$.

Nous nous proposons, en utilisant l'équation de Schrödinger associée, d'établir une autre équation permettant de traiter directement les problèmes de perturbation.

Au générateur $\Gamma_{A,\lambda}$ faisons correspondre, l'élément $\Omega_{A,\lambda} = A\Omega_{1,0} + \lambda\Omega_{0,1}$ que nous appellerons également générateur.

Nous avons:

$$\Omega_{A,\lambda} + \Omega_{A',\lambda'} = \Omega_{A+A',\lambda+\lambda'},$$

$$\mu\Omega_{A,\lambda} = \Omega_{\mu A,\mu\lambda} \qquad (\mu \in \mathscr{C}).$$

Les $\Omega_{1,0}$ et $\Omega_{0,1}$ forment ainsi la base d'un espace vectoriel de dimension 2, U; l'élément neutre pour l'addition est $\Omega_{0,0}$.

Si A appartient à $\mathscr{H}$, $\Omega_{A,\lambda}$ appartient à $(\mathscr{H} \times \mathscr{C}) \times U$. $\mathscr{H}$ et U et sont 2 espaces vectoriels construits sur le même corps; ainsi leur produit est un espace vectoriel. La multiplication définie sur les Γ ne correspond pas à une loi interne pour les Ω.

Faisons le produit $U \times U = U^2$.

La base du nouvel espace vectoriel est $\Omega_{1,0}^2$; $\Omega_{1,0}\,\Omega_{0,1}$ $\Omega_{0,1}\,\Omega_{1,0}$; $\Omega_{0,1}^2$. Nous identifions $\Omega_{0,1}\,\Omega_{1,0}$ avec $\Omega_{0,0}$; d'après la correspondance avec les Γ c'est le vecteur nul.

Considérons les 3 vecteurs non nuls. Soit un espace vectoriel V et $L(V)$ l'ensemble des applications linéaires de V dans V. Celles-ci constituent également un espace vectoriel auquel on donne une structure d'algèbre A par une loi multiplicative [2].

Considérons maintenant l'ensemble des applications linéaires de A dans A, $L(A) = A_s$ ce nouvel ensemble possède une structure d'algèbre appelée par CRAWFORD "super algèbre" [3] et [4].

Soit Φ un élément de A; Φ est sensé définir un état en Mécanique Quantique. L'opérateur d'état va jouer le rôle du vecteur d'état dans la représentation habituelle.

Considérons le super opérateur hamiltonien k du système et l'observable s, définis dans A_s. Il leur correspond dans A les opérateurs K et S; leurs générateurs associés sont:

$$\Omega_{s,1}\,; \qquad \Omega_{S,1},$$
$$\Omega_{k,1}\,; \qquad \Omega_{K,1}.$$

De l'équation

$$i\hbar \frac{ds}{dt} = i\hbar \frac{\partial s}{\partial t} + [s, k]$$

et de la relation: $[\Omega_{A,1},\ \Omega_{B,1}] = [A, B]\,\Omega_{1,0}^2 + (A - B)\Omega_{1,0}\Omega_{0,1}$ où A et $B \in A$ ou A_s, on tire la relation

$$i\hbar\,\Omega \frac{ds}{dr},\ 1\Omega_{1,0} = i\hbar\,\Omega \frac{\partial s}{\partial r},\ {}_1\Omega_{1,0} + [\Omega_{s,1}\,,\,\Omega_{k,1}] - (s - k)\,\Omega_{1,0}\,\Omega_{0,1}$$

et à l'équation $i\hbar \dfrac{\partial \Phi}{\partial t} = k\Phi$ on fait correspondre l'équation:

$$i\hbar \frac{\partial \Phi}{\partial t}\,\Omega_{1,0}^2 = [\Omega_{K,1}\,,\,\Omega_{\Phi,1}] - (K - \Phi)\,\Omega_{1,0}\,\Omega_{0,1}.$$

Telle est l'écriture de l'équation de Schrödinger en utilisant les 2 formalismes, opérateur d'état et générateur.

Si U est l'opérateur statistique de Von Neumann [3] ($U \in A$) alors $U = \Phi^2$ et:

$$i\hbar \frac{\partial u}{\partial t}\,\Omega_{1,0}^2 = [\Omega_{u,1}\,,\,\Omega_{\Phi,1}] - (U - \Phi)\,\Omega_{1,0}\,\Omega_{0,1}.$$

Nous voyons, grâce à ce formalisme, apparaître la différence de deux opérateurs d'état; ceci est intéressant pour une méthode de perturbation. En particulier on peut s'arranger pour que $K - \Phi = W$, où W est la partie diagonale de l'opérateur "level-shift" de Watson [5].

De même, le commutateur, dans cette même équation, peut conduire à des écritures entrant dans le cadre de l'algèbre de Lie, en particulier pour les développements du genre de ceux de Primas [3].

Ces techniques offrent l'avantage de fournir une approximation toujours unitaire à tous les ordres.

BIBLIOGRAPHIE

1. J. RAVATIN et G. MESNARD, Il Nuovo Cimento, série X, **32,** 1015, 1964; Il Nuovo Cimento (sous presse).
2. N. BOURBAKI, VII- livre II- Algèbre — Chapître 3, 1044 Algèbre multilinéaire.
3. J. A. CRAWFORD, Il Nuovo Cimento, **10**, 698, 1958; A. MECKLER, Il Nuovo Cimento, Suppl. 12. p. 1, 1959; M. ROSENBLUM, Duke Math. J., **23,** 263, 1956; G. LUMER et M. ROSENBLUM, Proc. Am. Math. Soc., **10,** 32, 1959; J. SCHWINGER, Proc. Nat. Acad. Sci., **46,** 257, 570, 1960; H. PRIMAS, Helv. Phys. Acta, **34,** 331, 1961.
4. B. ANWELL et H. PRIMAS, Molecular Physics, **6,** 225, 1963;
   P. R. HOLMES, Finite dimensional vector spaces (Van Nostrand) 2ème édition, 1958.
   J. DIXMIER, Algèbres d'opérateurs dans l'espace hilbertien Ed. Gauthier—Villars—Paris, 1957.
5. K. M. WATSON, Phys. Rev., **89**, 575, 1963.

Acta Physica Academiae Scientiarum Hungaricae, Tomus 23 (3), pp. 315—316 (1967)

HIGHER DIMENSIONAL SPACES AND SYMMETRIES ARISING ON GRAVITATIONAL FIELDS

By

M. SÜVEGES

RESEARCH GROUP FOR THEORETICAL PHYSICS OF THE HUNGARIAN ACADEMY OF SCIENCES, BUDAPEST

(Received 4. XI. 1966)

It has been shown [1] that the linear pseudo-groups defined by Levi-Civita transport (LCt) are physical invariance groups in gravitational fields, supposed to be Riemannian manifolds M_n. Various consequences of this have been discussed [1, 2, 8] and we now show how these symmetries give rise to higher dimensional spaces and symmetries on an ordinary M_n. The point is that the tangent space $T_x(M_n)$ at x is not simply a Euclidean space E_n in the ordinary sense but each $T_x(M_n)$ is provided with a superstructure defined by the holonomy group (hg) [2, 3] $\Psi_x(M_n)$ at x. The curvature tensor and its covariant derivatives which vanish in E_n, just determine this superstructure since their $\overset{\varkappa}{\lambda}$-domains [4] span [2, 4] the Lie-algebra of the restricted hg $\Psi_x^0(M_n)$ defined by the nullhomotopic class [3] of the loop space at x.

Now the group manifold M_r of the r-parameter group $\Psi_x^0(M_n)$ is a metric space with $g_{ab} = c^n_{am}c^m_{bn}$ (Latin and Greek indices run from 1 to r and from 1 to n) where c^n_{am} are the structure constants of $\Psi_x^0(M_n)$. Thus, we have an r-dimensional metric space M_r at each $x \in M_n$ [7] and the real problem is to determine the groups induced on these spaces by LCt in M_n. This has been done in [10] by applying the theorem of [1] to two distinct parallel vector fields along the same curve τ and we here summarize the results and work out some consequences. The transformations are defined by a formal (non-integrable) parallel transport, defined with an induced hybrid connection Γ' [4], and they have the properties: If e^a_x are coordinates (infinitesimal transformations of $\Psi_x^0(M_n)$ in the tangent space $T_x(M_r)$, with metric g_{ab}, of M_r at the identity, the transformations are of the form $e^a_y = a^a_b(\tau_y\tau_x)e^b_x$ with a^a_b invertible and e^a_x arbitrary for any curve τ connecting x and $y \in M_n$. They define linear pseudo-groups [5] and leave invariant the quadratic form $g_{ab}\, e^a e^b$ of M_r(in terms of [8] these are just isometric mappings of holonomy fibres over different points into each other). Also, g_{ab} of M_r is a covariant constant [4] of the induced connection Γ'.

With these results we can now discuss the dimensions and signatures involved. The metric tensor $g_{\alpha\beta}$ of M_n is covariant constant, therefore if it has signature (t, s), $t + s = n$, then $\Psi_x^0(M_n)$ is a subgroup of the compact or non-

compact rotation group $SO_{t,s}(n; R)$ and manifolds can be classified according to these subgroups. If this subgroup $\Psi_x^0(M_n)$ has r parameters then we have M_r arising on M_n at each x and its signature (v, w), $v + w = r$, can be determined from the structure constants of $\Psi_x^0(M_n)$. The classification is then according to the dimension of M_r and its signature. The group $\Psi_x^{0\prime}(M_r)$ induced on $T_x(M_r)$ by $\Psi_x^0(M_n)$ is, of course, a subgroup of $SO_{v,w}(r, R)$ since g_{ab} of M_r is a covariant constant of Γ'. Moreover its Lie-algebra is spanned by the $\overset{c}{b}$-domain of c_{ba}^c [4].

For the special case of Einstein manifolds the signature is (3, 1), therefore $\Psi_x^0(M_n)$ is a subgroup of the restricted Lorentz group $L_+^\uparrow$ and manifolds can be classified in the usual way (for references see [6]). For a nonvacuum Einstein manifold $\Psi_x^0(M_n)$ has six parameters [6]. Therefore $T_x(M_r)$ is six dimensional and its signature is easily determined to be (3, 3). Consequently, the group induced by $\Psi_x^0(M_n)$ is a subgroup of $SO_{3,3}(6, R)$ acting on $T_x(M_6)$. If the linear unimodular subgroup of $GL(4; R)$ is realized by LCt then so is the full $SO_{3,3}(6; R)$ since these groups are locally isomorphic [9]. In summary we have the following groups and spaces on a non-vacuum Einstein manifold: $\Psi_x^0(M_n)$ $(L_+^\uparrow)$ acting on $T_x(M_4)$ (sign (3, 1)), $\Psi_x^{0\prime}(M_6)$ (subgroup of $SO_{3,3}(6; R)$) acting on $T_x(M_6)$ sign (3,3)) for any $x \in M_4$, linear pseudogroups mapping $T_x(M_4)$ into $T_y(M_4)$ and linear pseudogroups mapping $T_x(M_6)$ into $T_y(M_6)$. $T_y(M_4)$ and $T_x(M_6)$ are, of course, linearly independent at each $x \in M_4$ and $T_x(M_6)$ vanishes in a flat space.

It must be noted that these are local considerations reflected in the fact that only the identity component $\Psi_x^0(M_n)$ of the hg has been considered.

REFERENCES

1. M. SÜVEGES, Acta Phys. Hung., **20,** 41, 1966.
2. M. SÜVEGES, Acta Phys. Hung., **20,** 51, 1966; Phys. Letters **20,** 265, 1966.
3. A. LICHNEROWICZ, Theorie globale des connexions et des groupes d'holonomie (Edizioni Cremonese, Roma, 1962).
4. J. A. SCHOUTON, Ricci-Calculus, Chapt. VII. (Springer-Verlag, Berlin—Göttingen—Heidelberg, 1954).
5. O. VEBLEN and J. H. C. WHITEHEAD, The foundations of differential geometry (The University Press, Cambridge, 1953).
6. W. BEIGELBÖCK, Z. Physik **179,** 148, 1964.
7. Isospace has been located in the group manifold of the hg by R. P. TREAT, Phys. Rev. Letters **12,** 407, 1964.
8. M. SÜVEGES, Acta Phys. Hung. **20,** 273, 1966.
9. E. CARTAN, Ann. Sci. l'Ecole Norm. Sup. **31,** 263, 1914.
10. M. SÜVEGES, to be published.

Acta Physica Academiae Scientiarum Hungaricae, Tomus 23 (3), pp. 317—320 (1967)

A SEMIEMPIRICAL METHOD FOR THE CALCULATION OF THE EXCITED STATES OF MOLECULES

By

J. LADIK

CENTRAL RESEARCH INSTITUTE FOR CHEMISTRY OF THE HUNGARIAN ACADEMY OF SCIENCES, BUDAPEST

(Received 19. I. 1967)

Introduction

In the usual approach we calculate the excited states of molecules with the aid of the unoccupied states obtained by the solution of the appropriate matrix eigenvalue problem. This has been done in the most non-empirical calculations and always in the case of the different semiempirical calculations (for instance HÜCKEL or P—P—P LCAO MO calculations). In all these cases the excitation energies have been determined as the difference of the total energy of the ground state and that of the excited state. The total energy of the excited state has been calculated in all these methods also with the aid of the eigenvalues and eigenvectors obtained for the ground state.

The purpose of the present paper is to point out that it is more correct to use a completely different solution for each excited state, than for the ground state and at the same time to propose a new method for the calculation of the excitation energies of molecules. This method will take into account that the ground state is usually a *closed shell system*, while the excited states are *open shell systems*. Therefore the method essentially consists of the combination of the closed and open shell SCF LCAO MO methods. In the present paper it will be formulated in a semiempirical form for π electron systems and in a subsequent one we shall give a non-empirical formulation.

Method

Let us suppose that we have solved the eigenvalue problem of the matrix $\mathbf{F}^{(\mathrm{SCF})}$, which has the elements in the PARISER—PARR—POPLE approximation [1, 2]

$$F_{t,t}^{(\mathrm{SCF})} = -I_t + \frac{1}{2} P_{t,t}^{(\mathrm{SCF})} (I_t - E_t) + \sum_{s \neq t}^{n} (P_{s,s}^{(\mathrm{SCF})} - z_s) \gamma_{t,s}, \tag{1}$$

$$F_{t,s}^{(\mathrm{SCF})} = \beta_{t,s} - \frac{1}{2} P_{t,s}^{(\mathrm{SCF})} \gamma_{t,s}. \tag{2}$$

Here I_t and E_t stand for the ionization potential and electronaffinity respectively, of the tth atom in its appropriate valence state, z_s is the number of π electrons contributed by the sth atom and the $\beta_{t,s} = <\varphi_t |\mathrm{H}^{\mathrm{core}}| \varphi_s>$ the resonance integral the method takes into account only between nearest neighbours and treats as empirical parameter. The Coulomb integrals $\gamma_{t,s} = <\varphi_t\varphi_s \left|\frac{1}{r_{12}}\right| \varphi_t\varphi_s>_{1,2}$ are usually approximated in the P—P—P method in such a way [1, 2, 3], which gives for them a value which is only about 2/3 of the theoretical value. The bond orders $P_{t,s}^{(\mathrm{SCF})}$ are defined as

$$P_{t,s}^{(\mathrm{SCF})} = \sum_{j=1}^{n} C_{t,j}^{(\mathrm{SCF})} C_{s,j}^{(\mathrm{SCF})} K_j, \tag{3}$$

where K_j denotes the number of electrons in the jth MO. Thus in a ground state with closed shell we have $K_j = 2$ for the first n_f MO-s (n_f denotes the number of filled orbitals) and $K_j = 0$ for the virtual MO-s.

Having the SCF eigenvalues and eigenvectors we can calculate the total energy of the molecule in its ground state with the aid of the expression

$$E_{\mathrm{total}}^{(\mathrm{grounds.})} = \frac{1}{2} \sum_{i=1}^{n} K_i (H_i + \varepsilon_i) = \frac{1}{2} \Big[\sum_t P_{t,t} \Big(- I_t - \sum_{s \neq t} z_s \gamma_{t,s}\Big) + \\ + \sum_{t,s \neq t} P_{t,s} \beta_{t,s} + \sum_{i=1}^{n} K_i \varepsilon_i \Big], \tag{4}$$

where $H_i = <\psi_i| H^{\mathrm{core}} |\psi_i>$ (H^{core} is the core Hamiltonian and ψ_i stands for the ith MO), ε_i is the ith eigenvalue. All other quantities have been defined previously.

On the other hand we can calculate an arbitrary excited state using a semiempirical version of the different orbitals for different spins method proposed by DEWAR [4]. According to this method we have to determine simultaneously the SCF eigenvalues and eigenvectors of the matrices $\mathbf{F}^{\alpha}$ and $\mathbf{F}^{\beta}$ which have the elements

$$F_{t,t}^{\alpha} = - I_t + P_{t,t}^{\beta} (I_t - E_t) + \sum_{s \neq t}^{n} (P_{s,s}^{\alpha} + P_{s,s}^{\beta} - z_s) \gamma_{t,s}, \tag{5}$$

$$F_{t,s}^{\alpha} = \beta_{t,s} - P_{t,s}^{\alpha} \gamma_{t,s} \tag{6}$$

and

$$F_{t,t}^{\beta} = - I_t + P_{t,t}^{\alpha} (I_t - E_t) + \sum_{s \neq t}^{n} (P_{s,s}^{\beta} + P_{s,s}^{\alpha} - z_s) \gamma_{t,s}, \tag{7}$$

$$F_{t,s}^{\beta} = \beta_{t,s} - P_{t,s}^{\beta} \gamma_{t,s}, \tag{8}$$

respectively. The elements of the charge-bond order matrices $\mathbf{P}^{\alpha}$ and $\mathbf{P}^{\beta}$ are defined as

$$P^{\alpha}_{t,s} - \sum_{j=1}^{n} K^{\alpha}_{j} C^{\alpha}_{t,j} C^{\alpha}_{s,j} \tag{9}$$

and

$$P^{\beta}_{t,s} = \sum_{j=1}^{n} K^{\beta}_{j} C^{\beta}_{t,j} C^{\beta}_{s,j}, \tag{10}$$

respectively, where K_j and K_j are now either 1 or 0. All the other quantities occurring in equations (5) and (6) were defined previously in connection with the simple P—P—P method.

It is clear that to begin the calculation we need a starting $\mathbf{P}^{\alpha(0)}$ and $\mathbf{P}^{\beta(0)}$ matrix. If we are interested in a given excited state, we can use the SCF eigenvectors of the previous closed shell P—P—P calculation of the molecule to form the elements of the starting $\mathbf{P}^{\alpha(0)}$ and $\mathbf{P}^{\beta(0)}$ matrices with the aid of expressions (9) and (10). In this way we can perform the starting charge-bond order matrices for any excited state with any multiplicity.*

Having obtained the C^{α}_{j} and C^{β}_{j} SCF eigenvectors and the ε^{α}_{j} and ε^{β}_{j} SCF eigenvalues belonging to the excited state under consideration, we can calculate the total energy of the excited state with the aid of the expression

$$\begin{aligned} E^{(\text{exc. s.})}_{\text{total}} &= E^{\alpha}_{\text{total}} + E^{\beta}_{\text{total}} = \frac{1}{2} \sum_{\delta=\alpha,\beta} \sum_{j=1}^{n} K^{\delta}_{j} (H^{\delta}_{j} + \varepsilon^{\delta}_{j}) = \\ &= \frac{1}{2} \sum_{\delta=\alpha,\beta} \sum_{j=1}^{n} K^{\delta}_{j} \Big[\sum_{t=1}^{n} C^{\delta 2}_{j,t} \Big(- I_t - \sum_{s \neq t}^{n} z_s \gamma_{t,s} \Big) + \\ &\quad + \sum_{t,s \neq t} C^{\delta}_{j,t} C^{\delta}_{j,s} \beta_{t,s} + \varepsilon^{\delta}_{j} \Big]. \end{aligned} \tag{11}$$

Finally combining (4) and (11) we obtain for the excitation energy

$$\Delta E = |E^{(\text{gr.})}_{\text{total}} - E^{(\text{exc.})}_{\text{total}}|. \tag{12}$$

* For instance, if we have an eight centre system with 10 π electrons, in the ground state the first five MO-s (if we number them according to increasing energies) are doubly filled with electrons. If we want to calculate for instance the triplet state arising from the promotion of one electron from the 4th MO to the 6th, we can construct the elements of our starting charge and bond order matrices $\mathbf{P}^{\alpha(0)}$ and $\mathbf{Pr}^{\alpha(0)}$ as follows:

$$P^{\alpha(0)}_{t,s} = \sum_{j=1}^{6} C_{t,j} C_{s,j}, \; P^{\beta(0)}_{t,s} = \sum_{j=1}^{3} C_{t.j} C_{s,j} + C_{t,5} C_{s,5}.$$

In a similar way for the singlet excited state arising from the $4 \to 6$ transition, we obtain

$$P^{\alpha(0)}_{t,s} = \sum_{j=1}^{5} C_{t,j} C_{s,j}, \; P^{\beta(0)}_{t,s} = \sum_{j=1}^{3} C_{t,j} C_{s,j} + C_{t,5} C_{s,5} + C_{t,6} C_{s,6}.$$

Concluding remarks

In connection with the proposed method the difficulty should be mentioned that it is not sure that starting with matrices $\mathbf{P}^{\alpha(0)}$ and $\mathbf{P}^{\beta(0)}$, constructed with the aid of the ground state solution, it will be possible to obtain always a different solution for each excited state. According to the results of preliminary calculations, however, it seems so that the method works quite well for the first triplet excited state [5]. It can be hoped that on the basis of further numerical calculations it will be possible to decide, in which cases the suggested procedure can be applied with success.

Another disadvantage of the method is that we need a completely different solution for each excited state. According to our experiences with the semiempirical different orbitals for different spins method in the case of the ground state of radicals, the SCF procedure converges in 10—40 iteration steps [6]. This means that with the aid of an IBM 7090 computer we can obtain a solution for a given excited state of a system with 10 centres within less than a minute.

Finally it should be pointed out that the many electron wave function obtained by DEWAR's method is not an eigenfunction of the square of the total spin operator S^2. Therefore it would be necessary to project out of it with the aid of the appropriate projection operator that component which corresponds to the multiplicity of the excited state under consideration. Since, however, the method is a semiempirical one (we treat the $\beta_{t,s}$ integrals as empirical parameters and the method of approximation of the integrals $\gamma_{t,s}$ is also only empirically justified), it seems to be not very important to carry out the projection procedure. Of course in a non-empirical version of the proposed method this cannot be avoided.

Acknowledgement

The author should like to express his gratitude to Academician G. SCHAY for calling his attention to the problem and to Professor P.—O. LÖWDIN for his critical remarks and stimulating discussions.

REFERENCES

1. R. PARISER and R. G. PARR, J. Chem. Phys., **21**, 466, 1953; **21**, 761, 1953.
2. J. A. POPLE, Trans. Far. Soc., **49**, 1375, 1953.
3. N. MATAGA and K. NISHIMOTO, Z. Physik. Chemie, **13**, 140, 1957.
4. M. J. S. DEWAR, Rev. Mod. Phys., **35**, 586, 1963.
5. J. AVERY, personal communication.
6. J. LADIK, G. BICZÓ, B. MOHOS, F. TÜDŐS and J. RÉDLY, Proceedings Conference on Some Aspects of Physical Chemistry, Budapest, 1966, Vol. III, p. 427.

RECENSIONES

I. E. FARQUHAR: Ergodic Theory in Statistical Mechanics

Interscience Publishers, London—New York—Sidney — 1964

This is a book written for "us, physicists" on that part of ergodic theory which we have to know better than "they, mathematicians". We must acknowledge at once that the author fulfils this attractive claim with great mastery.

The book starts with a discussion of the aims of ergodic theory and its position within the body of statistical mechanics. In the part devoted to classical statistical mechanics one chapter describes purely mathematical results (theorems of BIRKHOFF, LEWIS, VON NEUMANN and HOPF), the presentation containing just as many mathematical details as are necessary to understand clearly the assumptions and results: then a separate chapter deals with the application of these mathematical theorems to physical situations. This is followed by a review of ergodic theories lying somewhat aside from the main current of the theory: those of KHINCHIN, UHLHORN and the classical theory of ALBERTONI, BOCCHIERI and LOINGER. The last part devoted to quantal ergodic theories, starts with a critical exposition of von NEUMANN's theory, containing the author's own results; finally the several recent approches to quantum ergodic theory are described.

An attractive feature of the presentation is that it points out similarities and analogies between apparently quite different theorems, finding classical counterparts of quantum statements, and vice versa. The book offers an excellent opportunity to acquire a working knowledge about the evergrowing literature of ergodic theory, and provides a great aid in distinguishing physical ideas against the background of sophisticated mathematics. However, the presentation is perhaps somewhat more eclectic than is usual in the case of a monograph, and this is undoubtedly due to the sceptical position taken by the author against the achievements of ergodic theory (as expressed in the concluding remarks); that is, the author does not consider any one of the existing theories worthy to have the presentation of the others grouped around it. This is, of course, a matter of personal taste; let it be mentioned only that we regard the use of VAN HOVE's diagonal singularity condition for an ergodicity criterion (as done by PROSPERI and by GOLDEN and LONGUET-HIGGINS) as a point of paramount importance, which permits ergodic theory to be looked upon much more optimistically than the author does. Perhaps the most physical statement of KHINCHIN "statistical concepts describe those properties of a dynamical system that are independent of the initial conditions" (quoted on p. 63) would have also merited the position of an organizing principle in writing the monograph. Nevertheless, FARQUHAR's book is highly recommended to anyone interested in the fundamental problems of statistical mechanics.

T. GESZTI

The Structure and Evolution of Galaxies

Proceedings of the 13th Solvay Conference on Physics, September 1964. Interscience Publishers, London 1965, 174 pages.

AMBARTSUMIAN's epoch-making ideas on the instability of the nuclei of galaxies were the beginnings of a new cosmogony, which now constitutes the most interesting part of astronomy. Development in this field is very rapid. Since the 1964 Solvay Conference several symposia have been held on the same topic — the latest was at Biurakan in May, 1966 —

and, therefore, some results presented in this book are already out of date. But the vivid discussions, which followed every report, make the reading of the book profitable even now.

The introductory report was presented by AMBARTSUMIAN on the nuclei of galaxies and their activity. This was followed by OORT's lecture on the structure and evolution of galaxies. The young Dutch astronomer, L. WOLTJER, discussed the problem of galactic magnetic fields. After SPITZER's and SALPETER's reports on the formation and evolution of stars, MINKOWSKI and HOYLE gave two lectures on supernovae and supernovae remnants. The final topic was that of extragalactic radiosources, with reports by BOLTON, MARTIN SCHMIDT and the BURBIDGES. The concluding general discussion was introduced by OPPENHEIMER. He enumerated those astronomical problems dealt with at the conference, which are not well understood by physicists.

The book can be recommended not only to astronomers, but also to all physicists interested in problems of very large energy sources.

L. DETRE

The Solar Wind

Edited by Robert J. Mackin, Jr. and Marcia Neugebauer, published by Pergamon Press' Oxford—London—Edinburgh—New York—Paris—Frankfurt 1966, 420 pages, £ 5 net

The book contains the proceedings of a conference held at the California Institute of Technology Pasadena, on April 1—4, 1964 and sponsored by the Jet Propulsion Laboratory. The topic of the book, is the supersonic plasma which originates in the solar corona and blows out through the interplanetary space creating remarkable effects in the neighbourhood of the Earth and at even greater distances from the Sun. The historical and philosophical perspective of the theme is provided by S. CHAPMAN's illuminating Foreword. The experimental data collected in Session I contain the most complete presentation of the interplanetary data gathered by the Mariner—2 Venus spacecraft, together with early data from the IMP—1 satellite giving the first clear picture of the turbulent region created in the Earth's magnetosphere by the solar wind. Session II deals with theories of the interplanetary plasma and fields, and of energetic particles. Excellent contributions to Session III are F. L. SCARF's lecture on the origin of the solar wind and H. E. PETSCHEK's original suggestion of a wave-propagation mechanism for the development of solar flares. Geophysicists will be mostly interested in Session IV about the interaction of the solar wind and the magnetosphere. The IMP—1 (Explorer 18) data are presented by E. F. LYON (Mass. Inst. of Technology), and N. F. NESS (Goddard Space Flight Center). Papers of the last Session discuss the interaction of the solar wind with comets and with the Moon. N. F. NESS reported remarkable observations that indicated the existence, on the dark side of the Moon, of a long, field-free tail which may be called a magnetic corpuscular eclipse region, bordered by an irregular magnetic field.

The participants of the Conference represented the fields of theoretical and experimental interplanetary physics, plasma physics, aerodynamics, radio astronomy and astrophysics. From the exchange of views between scientists with such different backgrounds always arise significant physical insights, and this was the most impressive result of the Conference.

L. DETRE

D. PINES and PH. NOZIÈRES: Theory of Quantum Liquids, 1: Normal Fermi Liquids

Benjamin Inc., New York, 1966

The book represents the first volume of a two volume work devoted to an important and developing branch of physics. The first volume contains the theory of normal Fermi liquids i.e. liquid He^3 and conduction electrons in metals which are not superconducting, while in the second one the authors will be concerned with superfluid Bose systems and superconductors.

"Normal Fermi Liquids' is an outstanding contribution to the subject providing a unified yet simple account of the field. The authors have avoided the use of sophisticated

mathematical techniques putting the emphasis on a detailed analysis and discussion of the physical ideas involved. Thus, their monograph can be approached easily and is also useful for experimentalists and non-specialist theoreticians. Moreover, the book is intended for graduate students attending a course in quantum statistical mechanics, or low temperature theory.

"Normal' Fermi Liquids' consists of five chapters.

In Ch. 1 after introducing the important physical concept of a quasiparticle, the authors present the semiphenomenological Landau theory for neutral Fermi liquids. With its help a number of macroscopic properties of the system are described in subsequent sections: equilibrium properties, transport properties and response to long wavelength external perturbations. Finally, the theory is applied to liquid He^3.

Ch. 2 is devoted to the general theory of the response of a many-particle system to weakly coupled macroscopic and microscopic external probes. The theory is applied to the example of the density correlations in a neutral Fermi liquid. The formal description of response and correlation in multi-particle systems at finite temperature is also given.

Chapters 3 and 4 are concerned with charged Fermi liquids which differ considerably from the neutral ones owing to the long range of the Coulomb interaction. Ch. 3 is the analogue of Ch. 1 in that it contains the generalization of the Landau theory to include the new physical features caused by the Coulomb interaction. The notions of screening and plasma oscillation are introduced and dealt with in detail.

Ch. 4, the analogue of Ch. 2, is devoted to response and correlations in homogeneous electron systems. First the formal properties of dielectric response functions are established, and the theory is then applied to various problems of physical interest such as the scattering of fast electrons by an electron system, quantum plasma coupled to a longitudinal phonon field, calculation of the net effective electron-electron interaction in the electron-phonon system and coupling between the electron liquid and the transverse electromagnetic field.

A survey of the microscopic theories of the electron liquid is given in Ch. 5. The chapter begins with the formulation of the Hartree-Fock approximation. The random phase approximation and its application to the model problem of the high density electron gas are then discussed in detail. The equation of motion method is introduced and used to establish the generalized random phase approximation and, finally, approximations for metallic densities are considered.

The Appendix contains an introduction to second quantization and every chapter is completed with problems and a list of references.

This excellent book, published by Benjamin Inc. with a high standard of printing will certainly become one of the most widely used texts in the field of quantum liquids.

P. SZÉPFALUSY

M. A. PRESTON: **Physics of the Nucleus**

Addison-Wesley Publishing Company, Inc., pp. X + 361, Reading, Massachusetts, Palo Alto, London, 1962. Preis: 15.00 $.

Dies Buch gibt weder eine rein experimentelle noch eine rein theoretische Behandlung der Kerne, sondern vereinigt beide Behandlungsweisen in einer sehr zufriedenstellenden Weise. Der mathematische Apparat wird auf das möglichste Minimum reduziert. Der Autor entwickelt die Grundgedanken und danach die Theorie der Kernmodelle, deduziert daraus wie sich der Kern gegenüber verschiedenen Experimenten verhält und vergleicht schliesslich dieses Verhalten der Kerne mit dem empirischen Befund.

Der Inhalt zergliedert sich in die folgenden Teile: I. Grundlegende Eigenschaften der Atomkerne, II. Kernmodelle, III. Elektromagnetische Eigenschaften der Kerne, IV. Radioaktivität, V. Kernreaktionen.

Sowohl den Studierenden als dem auf diesem Gebiet arbeitenden Fachmann wird dieses Buch ein sehr willkommenes Hilfsmittel bieten.

P. GOMBÁS

O. S. BERYLAND, R. I. GAVRILOVA and A. P. PRUDNIKOV:

Tables of Integral Error Functions and Hermite Polynomials

(19th volume of the Mathematical Tables Series), translated from the original in Russian by P. Basu, pp. VI + 163, Pergamon Press, Oxford, London, New York, Paris, 1962. Price: £ 5.

In a short introduction the authors summarize the fundamental properties of the tabulated functions, the method of calculation, the special features of the tables, the arrangement of the tables and rules for using them. In the further part of the book the integral error function and the Hermite polynominals are tabulated with an accuracy of six figures.

P. GOMBÁS

J. M. ZIMAN: **Principles of the Theory of Solids**

Cambridge University Press, Cambridge, 1964. pp. XVI + 360, Price: 45 s.

The author gives an outline of the principles of the solid state without going into details. In the Preface the author says: "This book aims to present as simply as possible, the elements of the theory of the physics of perfect crystalline solids. It is a book full of ideas, not facts. It is an exposition of principles, not a description of the phenomena."

The book is divided into the following chapters: 1. Periodic Structure, 2. Lattice Waves, 3. Electron States, 4. Static Properties of Solids, 5. Electron-Electron Interaction, 6. Dynamics of Electrons, 7. Transport Properties, 8. Optical Properties, 9. The Fermi Surface, 10. Magnetism, 11. Superconductivity.

The book can be recommended to everybody who is interested in the theory of solids.

P. GOMBÁS

H. S. GREEN and C. A. HURST: **Order Disorder Phenomena**

Monographs in Statistical Physics Vol. 5, Editor: I. Prigogine, pp. 10 + 363, Interscience Publishers John Wiley and Sons, London—New York—Sidney, 1964.

This book presents a treatment of the statistical mechanics of phase transitions. Special attention has been paid to the Ising model of two-dimensional lattices which is treated on the basis of the Pfaffian technique.

The book is divided into the following chapters: 1. Introduction, 2. Applications (Theory of Ferromagnetism, Antiferromagnetism, Binary Alloys, Lattice Models of Fluids and Solids, Association Problems), 3. Rectangular Ising Lattice, 4. General theory, 5. Some Special Lattices, 6. Alternative Methods (Method of Onsager, Combinatorial Solution of the Two-Dimensional Ising Problem), 7. Outstanding Problems (Lattice with Crossed Bonds; Second Neighbour Interactions and the Three-Dimensional Model, Lattice in a Magnetic Field,) 8. 8. Mathematical Appendices.

Obviously, the book must have been limited in size and therefore, regrettably enough, the authors could not include some important problems in this wide field of study. Nevertheless, the book covers tightly connected topics and is concise in itself. The exposition is clear and easy to follow. I am sure those who read the book will be grateful to the authors for this excellent work.

P. GOMBÁS

P. B. JONES: **The Optical Model in Nuclear and Particle Physics**

Interscience Publishers, New York, London, pp. VIII + 118, 1963.

This is the 14th volume of the Interscience Tracts on Physics and Astronomy edited by R. E. MARSHAK. The author meant this small book as an introduction to the principles of the optical model of the nucleus. The book contains a short account of the giant resonances, the

theory of FESHBACH, PORTER and WEISSKOPF, and the measurement of nuclear size. Further the author discusses derivations of the model based on expansions of the scattering amplitude in powers of the strength of the nucleon-nucleon potential and on the dispersion formalisms for nuclear and potential scattering. The last chapter deals with the model at intermediate and high nucleon energies and the determination of nuclear structure.

Though the style of the book is necessarily rather condensed, nevertheless the exposition is always clear. The book is recommended for those who want to get an insight into this field in a short time.

P. GOMBÁS

MUKUL R. KUNDU: **Solar Radio Astronomy**

Interscience Publishers, New York, 1965, XI + 660 pages, $ 19.75

In 1942 HEY discovered solar radio emission at metre wavelengths associated with sunspots. In the same year SOUTHWORTH, Jr., detected the thermal microwave radiation from the Sun. At present we are at the beginning of the third sunspot cycle during which solar radio waves have been recorded and studied. The author of this monumental book brings a complete synoptic picture of the nature of solar radio emission obtained with moderate angular resolution over the now accessible spectrum. In the near future earth-based solar observations will be supplemented by observations from space-craft from which the Sun can be observed over most of the electromagnetic spectrum.

After introductory chapters on the optical features of the active sun, on propagation and generation of radio waves in the solar atmospehere and on techniques of solar radio observations, two chapters deal with the quiet sun radiation and the slowly varying component. Nine chapters deal with bursts and their connections with X-ray emission, geomagnetic storms, and solar cosmic rays. The author concludes his book with chapters on the outer corona and on radar observations of the Sun. A bibliography of over 500 papers itself renders the book indispensable.

This book will remain the leading work in its field for many years to come, and it can be recommended not only to solar radio astronomers, but also to physicists and geophysicists interested in radiophysics of magneto-ionic media, in the acceleration of electrons and ions to cosmic ray energies by the Sun, in solar-terrestrial relationships, and in space science and technology.

JÚLIA BALÁZS

E. Fenyves and **O. Haiman**

The Physical Principles of Nuclear Radiation Measurements

In English · Approx. 900 pages · 370 figures, 29 tables · 17 × 24cm · Cloth

The introductory part of the book contains a short history of nuclear radiation detection apparatus and methods, and a brief summary of the new trends expectable in this field. The special part details the interactions of nuclear radiation and matter, and radiation penetration through absorbers. The underlying physical principles of particle counters and particle track detectors, their construction and utilization in some of their typical applications are then described. One appendix treats the role played by particle counters and particle track detectors in the discovery of new elementary particles, another one outlines the statistical methods of evaluation of counting results. A survey on electronic ancillary apparatus complements the book.

Akadémiai Kiadó

Publishing House of the Hungarian Academy of Sciences
Budapest 502. P.O.B. 24

Printed in Hungary

A kiadásért felel az Akadémiai Kiadó igazgatója — Műszaki szerkesztő: Farkas Sándor

A kézirat a nyomdába érkezett: 1967. V. 18. — Terjedelem: 6,75 (A/5) ív, 17 ábra

67.63882 Akadémiai Nyomda, Budapest — Felelős vezető: Bernát György

The *Acta Physica* publish papers on physics, in English, German, French and Russian.
The *Acta Physica* appear in parts of varying size, making up volumes.
Manuscripts should be addressed to:

Acta Physica, Budapest 502, P. O. B. 24.

Correspondence with the editors and publishers should be sent to the same address.
The rate of subscription to the *Acta Physica* is 165 forints a volume. Orders may be placed with "Kultúra" Foreign Trade Company for Books and Newspapers (Budapest I., Fő u. 32. Account No. 43-790-057-181) or with representatives abroad.

Les *Acta Physica* paraissent en français, allemand, anglais et russe et publient des travaux du domaine de la physique.
Les *Acta Physica* sont publiés sous forme de fascicules qui seront réunis en volumes.
On est prié d'envoyer les manuscrits destinés à la rédaction à l'adresse suivante:

Acta Physica, Budapest 502, P. O. B. 24.

Toute correspondance doit être envoyée à cette même adresse.
Le prix de l'abonnement est de 165 forints par volume.
On peut s'abonner à l'Entreprise du Commerce Extérieur de Livres et Journaux «Kultúra» (Budapest I., Fő u. 32. — Compte-courant No. 43-790-057-181) ou à l'étranger chez tous les représentants ou dépositaires.

«*Acta Physica*» публикуют трактаты из области физических наук на русском, немецком, английском и французском языках.
«*Acta Physica*» выходят отдельными выпусками разного объема. Несколько выпусков составляют один том.
Предназначенные для публикации рукописи следует направлять по адресу:

Acta Physica, Budapest 502, P. O. B. 24.

По этому же адресу направлять всякую корреспонденцию для редакции и администрации.
Подписная цена «*Acta Physica*» — 165 форинтов за том. Заказы принимает предприятие по внешней торговле книг и газет «*Kultúra*» (Budapest I., Fő u. 32. Текущий счет: № 43-790-057-181) или его заграничные представительства и уполномоченные.

29,— Ft

INDEX

L. F. Landovitz: Quadratic Interaction in Quantum Field Theory. — *Л. Ф. Ландовиц:* Квадратичное взаимодействие в квантовой теории поля. 253

N. A. Eissa and *Gy. Máté:* Problematics on the Application of Delayed Coincidence Devices. — *Н. А. Эисса* и *Дь. Матей:* Проблематики применения запаздывающего совпадения. 259

Z. Meligy and *N. A. Eissa:* Systematics of Some Properties of the Odd Mass Nuclei in the Region Near the Mass Number 190. — *З. Мелиги* и *Н. А. Эйсса:* Систематичность некоторых свойств нечетных ядер в области, близкий к массовому числу 190. 277

Gy. Büti: On the Exchange Energy in a SCF Method Using Nonorthogonal Basis Functions. — *Дь. Быти:* Об обменной энергии в методе самосогласованного поля, использующем неортогональные басисные функции 287

L. Jánossy and *P. Király:* The Lorentz Principle and the General Theory of Relativity. Part. V. — *Л. Яноши:* Принцип Лоренца и общая теория относительности. Часть V 291

COMMUNICATIONES BREVES

J. Ravatin and *G. Mesnard:* Etude de formalisme pour méthodes de perturbations. 311

M. Süveges: Higher Dimensional Spaces and Symmetries Arising on Gravitational Fields. 315

J. Ladik: A Semiempirical Method for the Calculation of the Excited States of Molecules. 317

RECENSIONES

T. Geszti: I. E. Farquhar, Ergodic Theory in Statistical Mechanics. 321

L. Detre: The Structure and Evolution of Galaxies 321

L. Detre: R. J. Mackin,—M. Neugebauer, The Solar Wind. 322

P. Szépfalusy: D. Pines—Ph. Nozières, Theory of Quantum Liquids. 322

P. Gombás: M. A. Preston, Physics of the Nucleus. 323

O. S. Beryland—R. I. Gavrilova—A. P. Prudnikov, Tables of Integral Error Functions and Hermite Polynomials. 324

J. M. Ziman, Principles of the Theory of Solids. 324

H. S. Green—C. A. Hurst, Order Disorder Phenomena. 324

P. B. Jones: The Optical Model 324

J. Balázs: Mukul R. Kundu, Solar Radio Astronomy. 325

ACTA PHYSICA

ACADEMIAE SCIENTIARUM HUNGARICAE

TOMUS XXIII FASCICULUS 4

AKADÉMIAI KIADÓ, BUDAPEST
1967

ACTA PHYS. HUNG.

ACTA PHYSICA

A MAGYAR TUDOMÁNYOS AKADÉMIA FIZIKAI KÖZLEMÉNYEI

SZERKESZTŐSÉG ÉS KIADÓHIVATAL: BUDAPEST V., ALKOTMÁNY UTCA 21.

Az *Acta Physica* német, angol, francia és orosz nyelven közöl értekezéseket a fizika tárgyköréből.

Az *Acta Physica* változó terjedelmű füzetekben jelenik meg: több füzet alkot egy kötetet.

A közlésre szánt kéziratok a következő címre küldendők:

Acta Physica, Budapest 502, P. O. B. 24.

Ugyanerre a címre küldendő minden szerkesztőségi és kiadóhivatali levelezés.

Az *Acta Physica* előfizetési ára kötetenként belföldre 120 forint, külföldre 165 forint. Megrendelhető a belföld számára az Akadémiai Kiadónál (Budapest V., Alkotmány utca 21. Bankszámla 05-915-111-46), a külföld számára pedig a „Kultúra" Könyv- és Hírlap Külkereskedelmi Vállalatnál (Budapest I., Fő u. 32. Bankszámla 43-790-057-181 sz.), vagy annak külföldi képviseleteinél és bizományosainál.

Die *Acta Physica* veröffentlichen Abhandlungen aus dem Bereiche der Physik in deutscher, englischer, französischer und russischer Sprache.

Die *Acta Physica* erscheinen in Heften wechselnden Umfanges. Mehrere Hefte bilden einen Band.

Die zur Veröffentlichung bestimmten Manuskripte sind an folgende Adresse zu richten:

Acta Physica, Budapest 502, P. O. B. 24.

An die gleiche Anschrift ist auch jede für die Redaktion und den Verlag bestimmte Korrespondenz zu senden.

Abonnementspreis pro Band: 165 Forint. Bestellbar bei dem Buch- und Zeitungs-Aussenhandels-Unternehmen »Kultúra« (Budapest I., Fő u. 32. Bankkonto Nr. 43-790-057-181) oder bei seinen Auslandsvertretungen und Kommissionären.

Acta Physica Academiae Scientiarum Hungaricae, Tomus 23 (4), pp. 327—340, (1967)

THERMAL NEUTRON FLUX DISTRIBUTION AND FLUX TRAP EFFECT IN THE ACTIVE CORE OF THE UA—RR—I REACTOR

By

E. A. SAAD

UAR ATOMIC ENERGY ESTABLISHMENT, CAIRO, UAR

N. A. EISSA

AL-AZHAR UNIVERSITY, CAIRO, UAR

I. BARTCHOUK

THE UKRAINIAN ACADEMY OF SCIENCE, KIEV, USSR

O. H. EL-MOFTY

UAR ATOMIC ENERGY ESTABLISHMENT, CAIRO, UAR

and

A. F. EL-BIDEWY

EIN SHAMS UNIVERSITY, CAIRO, UAR

(Presented by A. Szalay. — Received 13. IX. 1966)

The thermal neutron flux distribution at various points of the active core and irradiation channels of the UAR water-water reactor, was measured by the neutron activation method of copper and gold foils. An increase in the thermal neutron flux in the active core is achieved by creating a water cavity of 7 cm^2 section. The thermal neutron flux in the cavity is increased 2.3 and 2.6 times compared with that in the active core and the irradiation channels, respectively.

1. Introduction

The knowledge of actual neutron flux distribution at various points of the active core and reactor channels is strictly indispensable for defining optimal conditions for sample irradiation by reactor neutrons and for calculating the U^{235} burn up. In many cases it is often desirable to irradiate samples in the reactor by high thermal neutron fluxes. Maximum neutron fluxes in the reactor depend on its power and the volume of active core.

As a rule, the sample irradiation channels in research reactors are beyond the core at a distance from its boundary where the thermal neutron flux created by the reflector is maximum. In water-water research reactors of the MTR and WWR-M type [9, 10, 11], the use of a beryllium reflector enables maximum thermal neutron fluxes in the reflector to be obtained 30% higher than the maximum thermal neutron fluxes in the core.

Another possibilty for increasing the thermal flux in a reactor is the creation of a cavity inside the core filled with the moderating material. Since the cavity is surrounded on all sides by fissile material and the thermal neutron life-time in the cavity is longer than that in the core, consequently, the thermal neutron flux inside the cavity is higher than that in the core. In works [9, 10]

it is shown that in this way the thermal neutron flux in the cavity of the WWR-M type reactor is increased by 3—4 times compared with that in the core. The value of the increase in the thermal neutron flux depends on the size of the cavity and the character of the moderator in it. A great deal of research has been devoted to a study of optimal cavities in the WWR-S type reactors. Results have been given of theoretical and experimental investigations on the dependence of the increase in the maximum thermal neutron flux for a cylindrical cavity at the reactor core axis, on its diameter and the material of the moderator in it [12]. Here, the location of the EK-10 fuel assemblies in the core was the same as in the WWR-S reactors, a square lattice with parameter 17.7 mm. The cavities were filled with ordinary water, heavy water, beryllium, and graphite, and were studied. From this work it follows that the maximum increase in the thermal neutron flux (3.8 times higher than the flux with no cavity) is obtained when the cavity has a diameter of 12 cm and ordinary water is used as a moderator. Another work [13] also describes the use of EK-10 fuel elements, but with a triangular lattice. Cavities filled with ordinary water were created along the core axis. The core had the form of a regular hexagon. Cavities of different dimensions for the pitches of the triangular lattices $a = 15$ mm and $a = 19$ mm have been studied. As the authors reported, all the measurements were normalized to an identical total number of fissions in the core, though the core volumes were different. The maximum flux in cavity with such normalization has been found to be $D = 8.7$ cm at the cavity diameter for $a = 19$ mm and $D = 9.6$ cm for $a = 15$ mm at the diameter.

To obtain the increase in the thermal neutron flux in the UA-RR-1 reactor, a water cavity of square section $a = 7$ cm was made by extracting one fuel assembly. To determine the increase in the thermal neutron flux, measurements of flux distribution in the core and cavity were performed.

The measurements show that the maximum thermal neutron flux in the middle horizontal plane of the reactor at the cavity axis is 2.3 greater than the thermal flux at the same point in an unperturbated reactor, and 2.6 as high as that in the irradiation channels.

Since the cavities studied in [12] and [13] are ideal both in form and position in the core and cannot be realized in our reactor core owing to its constructional characteristics, it is a matter of interest to study the possibility of obtaining a cavity of optimal dimensions or to evaluate its differences from the optimal one.

2. Some data on the UA—RR—1 reactor and the active core

The UA-RR-1 reactor at the U.A.R. atomic energy establishment is a WWR-S type reactor. The construction and main characteristics of the

WWR-S reactor have been given in a number of papers [1, 3, 4]. Its thermal power is 2 MW, the neutron flux in the centre of the active core is about $2 \cdot 10^{13}$ n/cm^2·sec at 2 MW. The core is constructed to have 51 sections of fuel elements. Each section containes 15—16 fuel elements (EK-10 type) made of 10% enriched U^{235}. Ordinary water serves as a moderator, coolant, and reflector. The reactor was loaded in 1961 and has been in operation since

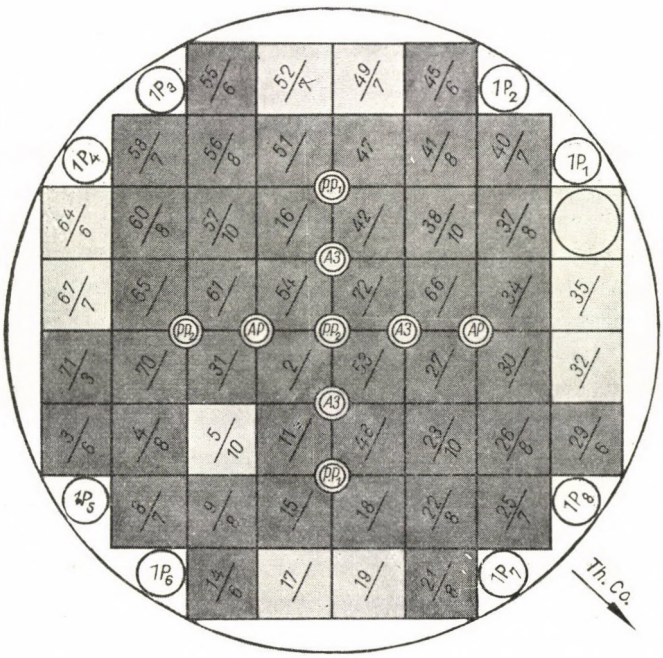

Fig. 1a. Horizontal cross-section of active core

then. By the present time the energy generated amounts to 296 MW days. Fig. 1a shows the active core configuration.

A technological section having fuel elements is shown in Fig. 2. At present, the active core contains 42 fuel sections with fuel elements. In order to obtain an increased thermal neutron flux for sample irradiation one of the sections was replaced by a displacer [5]. Samples are usually irradiated inside special channels filled with water and located at the corners of the active area ($1P_1$, $1P_2$ $1P_3$, $1P_4$, $1P_5$, $1P_6$, $1P_7$, $1P_8$, Fig. 1a) and displacers put in the cells with no fuel elements present. Next to the $1P_1$ channel, there is a dry channel Pd for short-time irradiation. This channel goes through the whole reactor and is connected with a transport tube leading to the first hot cell. There are nine horizontal channels radially approaching the active core centre.

The graphite thermal column on one side of the active core is intended to obtain pure thermal neutrons. Safety and control rods are in the active core centre.

3. Method of measurements

The measurements of thermal neutron flux distribution in the core were performed using the activation of copper foils. Copper foils were used as neutron indicators for the following reasons:

There are no difficulties in the preparation of copper foils. The half life of Cu^{64} is rather long (T 1/2 = 12.8 hr) which is very useful to facilitate the measurements. The copper activation cross-section (4.3 $\pm$ 0.2 barn) has almost no resonances below 200 eV and is close to the 1/V dependence over a wide range of neutron energies.

The copper foils 0.2 mm thick, 3 mm diameter were stamped using a special press. The foils were weighed within an accuracy of $\pm 0.5\%$. The average weight of a foil is 3.2 mg. Variations in weights of the individual foils were taken into consideration.

To put foils between the fuel elements in the core, the copper foils were incorporated in holders made of plexiglass. The holders provide an easy method of mounting and extracting foils and permit convenient loading and unloading. Plexiglass also has nearly the same moderating properties as water. Therefore, a fair amount of plexiglass in the active core does not cause any perturbation in neutron flux or in reactivity. Apart from this, plexiglass is not subject to neutron activation.

The copper foils were arranged in the holders so as to obtain the thermal neutron flux distribution in the middle horizontal plane of the active core. Another layer of foils covered with 0.6 mm cadmium cladding was arranged at a distance of 2.5 cm up and down the middle plane. This layer was used to determine the activity caused by neutrons having energies up to 0.4 eV which is the cut-off energy of cadmium.

After irradiation the holders were extracted from the core and the foils were arranged in special storage cells designed to prevent misplacement when measuring the activity.

The foils' activity was measured by an end window G. M. counter. The window is about 5 mg/cm^2 thickness. The dead time of the counter was determined by an experimental method using two sources, and its stability was checked using a standard source Sr^{90}. To check up the indicator purity a decay curve for one of the irradiated foils was built during the process of measurement. The obtained half life coincided with the tabulated data. All foils activity was reduced to one and the same time (time of shutdown), corrections for foil weight deviations and for counter dead-time were introduced.

To obtain the thermal neutron flux in the measured points a relation between the thermal neutron flux in the irradiation channels and the corresponding thermal activity of copper foils was determined.

The thermal neutron flux in the UA-RR-1 reactor channels was measured using the activation method of gold foils. The activation cross-section of Au 197 is 98.8 barns and its half life is 2.7 days. Both bare and cadmium covered gold foils were prepared by the same method as the copper foils, and they were arranged in the same holders in positions corresponding to the middle horizontal plane of the active core. Irradiation of gold foils was carried out for one hour at a reactor power of 2 kW. The gold foil activity was measured using the $\beta-\gamma$ coincidence method described in [8]. After applying all corrections, as for example, the screening effect of cadmium on neutrons of energy higher than 0.4 eV and the screening effect of gold and cadmium on the resonance of 5 eV of gold, the thermal neutron flux in the irradiation channels was calculated at 2 MW.

4. Thermal neutron flux distribution

In order to obtain a full picture of the thermal flux distribution in the active core, the foil holders were loaded along two core diagonals *AB* and *CD* and along the sample irradiation channels axis (Fig. 1b). The numbers in Fig. 1b are the serial numbers of the holders.

To obtain the thermal neutron flux distribution in the vertical direction, along the fuel length and beyond the active core, and also in the cavity, holders 10, 17, 4 and 5 were made longer and were filled along their total length with both bare and cadmium covered foils.

Results and discussion

Results of measurements given in Fig. 3 show the thermal neutron flux distribution in the middle horizontal plane of the active core. The points measured along the diagonal *AB* crossing a water cavity are drawn in a continous curve (holders from 2 to 13, Fig. 1b) and those measured along the diagonal *CD* are drawn in a dotted curve (holders from 14 to 25, Fig. 1b). The thermal neutron flux distribution along the diagonal *CD* represents, as expected, a bell shaped curve. The curve shows a central depression which is due to the neutron absorption caused by control rods. This effect is also noticed in the curve representing the diagonal *CD*. At both ends of the curve the thermal neutron flux increases again. These points correspond to the thermal flux in the irradiation channels near each end in which the thermal flux increases due to the neutron reflection in water. The thermal neutron flux

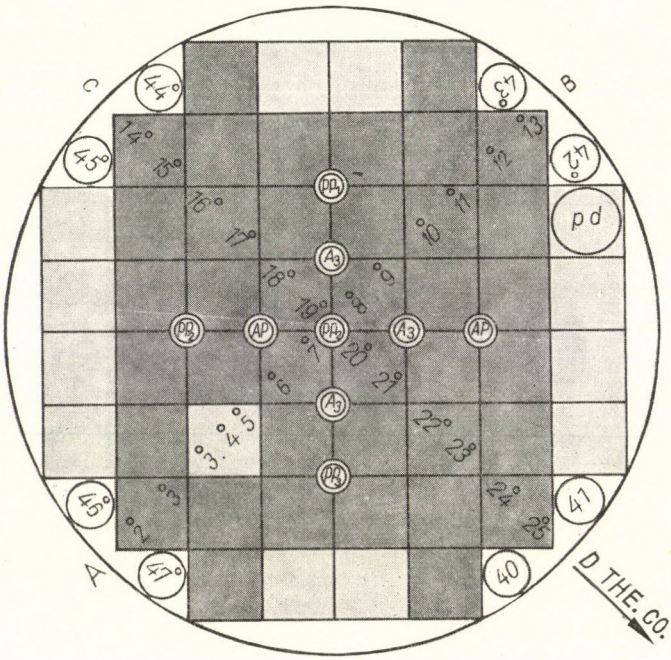

Fig. 1b. Arrangement of holders in the active core and channels

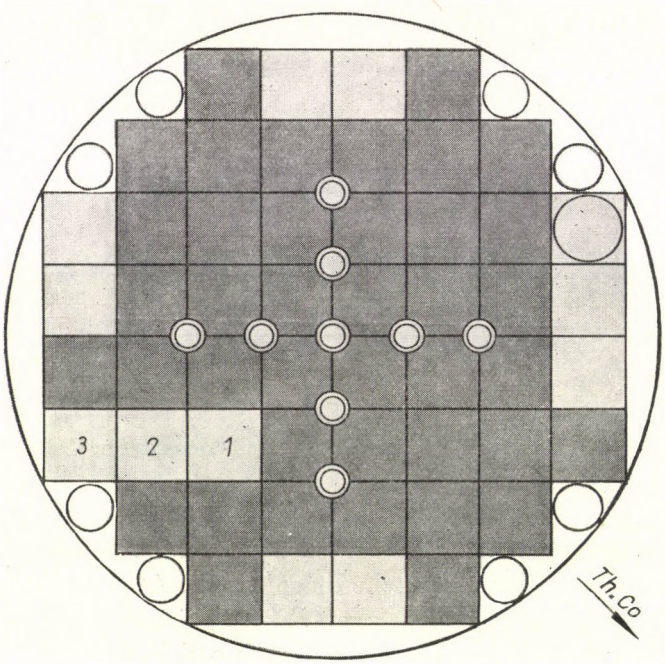

Fig. 1c. Different configurations of cavity in the core

distribution along the diagonal AB shows a major difference from that along the diagonal CD. At the points of the water cavity the thermal neutron flux is higher than in the core. In the cavity centre the thermal neutron flux is 2.4 times as high as that in the reactor centre and about 2.6 times the neutron flux in the sample channels.

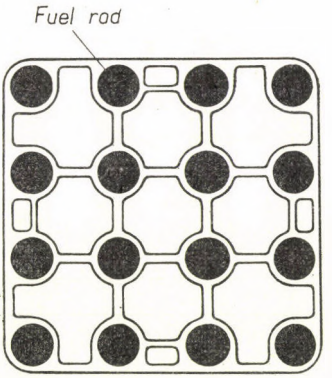

Fig. 2. Horizontal view of a fuel section filled with fuel rods

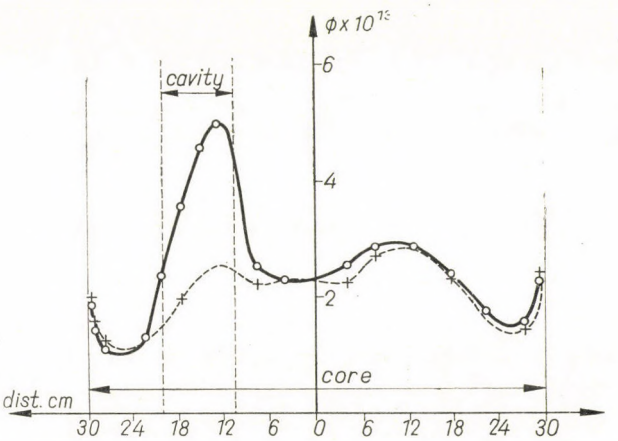

Fig. 3. Thermal neutron flux distribution in the centre of active core

Fig. 4a shows the thermal neutron flux distribution in the vertical direction for the holders 10 and 17 (Fig. 1b). These holders lie at the same distance from the control rods. The two curves have an identical character. They are distorted cosine curves with maxima shifted towards the lower ends. The shift of maxima down from the core middle plane is due to the effect of the control rods. The peaks' rise at the ends of the curves is due to the neutron reflection in water. This effect is well shown in the upper parts of the curves. The dashed curve in Fig. 4a shows a theoretical distribution of thermal flux

for an ideal core. This distribution was based on the three group theory calculations of thermal flux distribution [6]. The theoretical curve was normalized to give the same area of that part covered by the length of the active core. The observed difference in the reflector region can be explained as being due

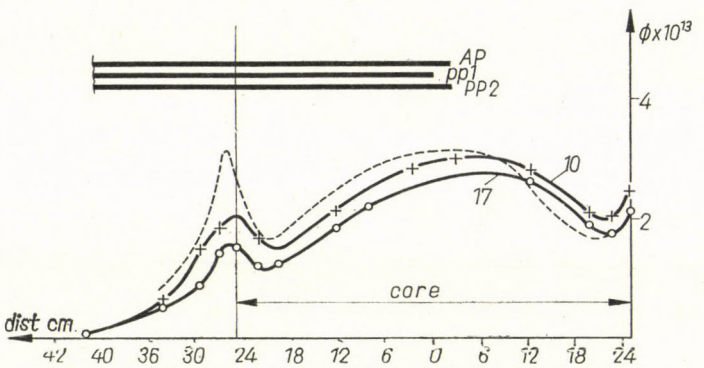

Fig. 4a. Vertical distribution of thermal flux in the active core

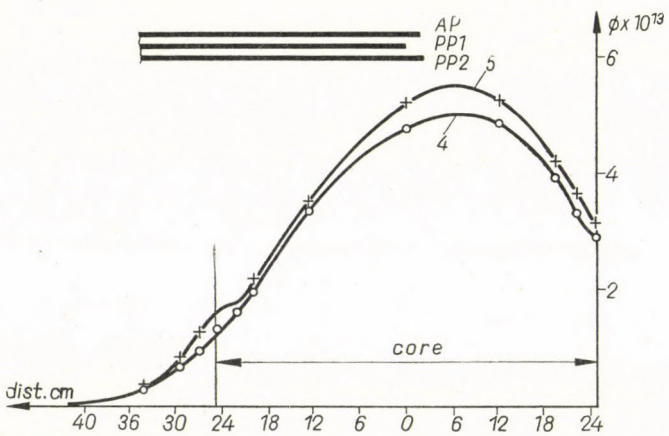

Fig. 4b. Vertical distribution of thermal flux in the cavity

to the excess of structural materials and supports in this region which were not taken into consideration in the theoretical calculations of the ideal core. The deviation of the experimental curve from the theoretical one in the central part is due to the effect of control rods which appear mainly as a depression in the upper part of the curve making the observed shift of maximum below the centre of the active core.

Fig. 4b shows the vertical distribution in the water cavity for holders 4 and 5 (Fig. 1b). The curve for holder 4 does not exhibit the reflector effect

and in the curve of holder 5, the effect is not clearly revealed. This is because of the absence of fuel elements in this position.

The flux distribution in one of the irradiation channels ($1P_7$) is shown in Fig. 5.

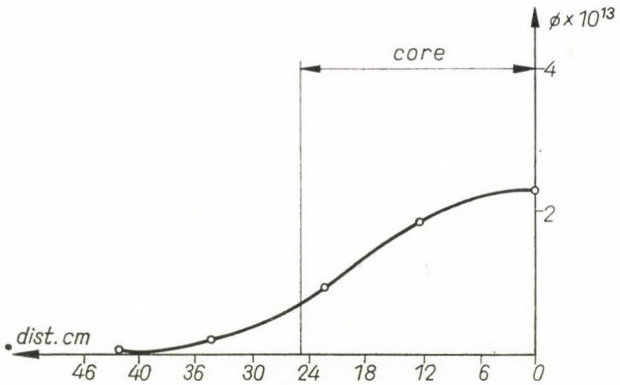

Fig. 5. Thermal flux distribution in the reactor channels

5. Thermal neutron flux trap effect

The construction of the UA-RR-1 reactor core (Fig. 1a) is such that inside it the following restrictions limit the creation of water cavities similar to those investigated previously.

1 — The assemblies are of square section having a dimension 60×60 mm, so the cavity can be only of a square or rectangular shape made by extracting one or more (2 or 3) fuel assemblies.

2 — Since the regulating and safety rods are located in the core centre between the fuel sections, the creation of a cavity on the core axis or in places adjacent to control rods is rejected for practical reasons. Such cavities can only be located in some definite places of the core off the centre and away from the regulating and safety rods.

It has been mentioned that works [12, 13] deal with a theoretical and experimental study of cavities created along the core axis. For such cases, theoretical calculations are much simplified, since the problem is reduced to one dimension. For a cavity at an off centre position, the calculations are complex in practice because of the Laplacian complication in the equations of neutron diffusion that are usually employed for this purpose, so that the problem becomes multidimensional.

In view of this we shall represent here the experimental study of increase in the thermal neutron flux at different real configurations of cavities. The

measurements of thermal neutron flux distribution have been made for five cases (Fig. 1c).

Experiment № 1, when all fuel sections are present.

Experiment № 2, when fuel section № 1 is extracted, 2 and 3 are present.

Experiment № 3, when fuel section 1 and 2 are extracted, and 3 is present.

Experiment № 4, when fuel sections 1, 2 and 3 are extracted.

Experiment № 5, when fuel section № 2 is extracted, 1 and 3 are present.

The extracted assemblies were not completely withdrawn from the reactor but were placed in other positions in the core at the corner opposite to the thermal column, i.e. the volume of the active core remains unchanged in all experiments.

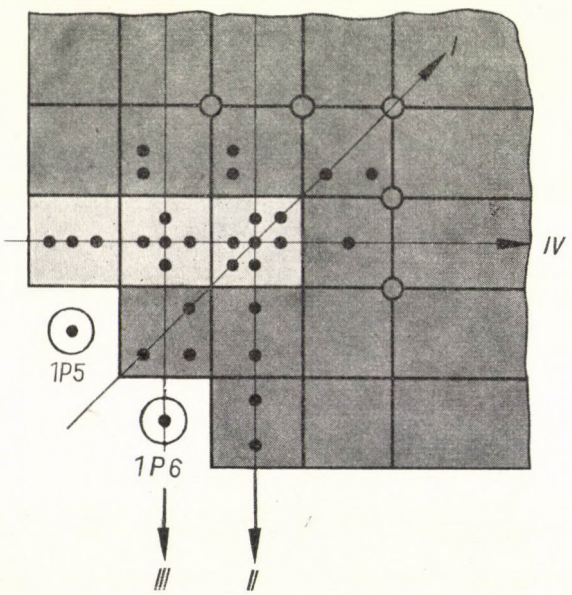

Fig. 6. Arrangement of holders in cavities

It was noticed that with such replacement of the fuel sections the neutron fluxes are not changed in the channels $1P_1$, $1P_2$, $1P_7$ and $1P_8$. Accordingly, the copper foils irradiated in these channels were used as monitors. The normalization of fluxes in all experiments was made with respect to these foils. Since the volume of the core in all experiments is unchanged, such a normalization refers to both neutron flux and reactor power.

In place of the fuel assemblies extracted from the core, assemblies with no fuel but having the holders with indicators were inserted.

Fig. 6 shows the positions of indicators. These positions are sufficient to build the curves of thermal neutron flux distribution in directions I—IV for all experiments and for their comparison.

Results and discussion

Figs. 7—10 represent the curves of thermal neutron flux distribution in all four directions for all experiments normalized to the same reactor power.

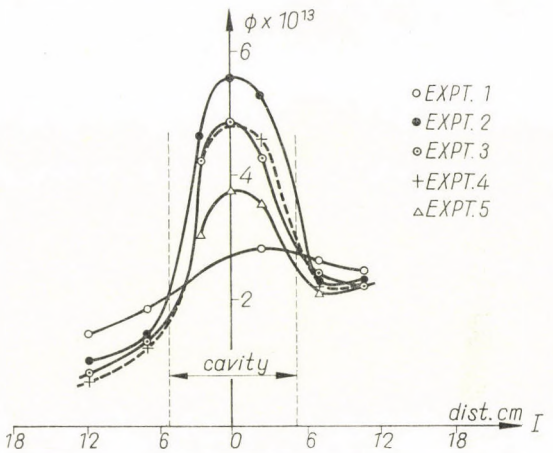

Fig. 7. Thermal neutron flux distribution for different configurations of cavity in direction I

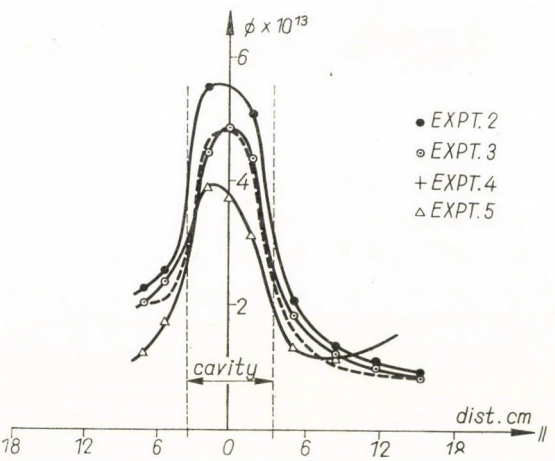

Fig. 8. Thermal neutron flux distribution for different configurations of cavity in direction II

The zero point of the curves corresponds to the centre of the first cavity except in Fig. 9 where the zero corresponds to the centre of the second section removed.

Fig. 7 represents the thermal neutron flux distribution in direction I for all configurations. From the curves it is seen that the maximum flux in this direction is obtained when only one fuel section is removed (cavity № 1), where there is no great difference between cavities 2 and 3.

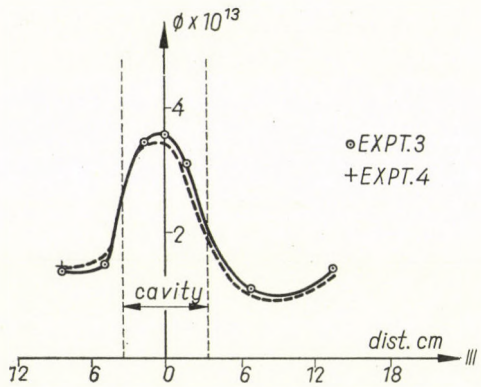

Fig. 9. Thermal neutron flux distribution for different configurations of cavity in direction III

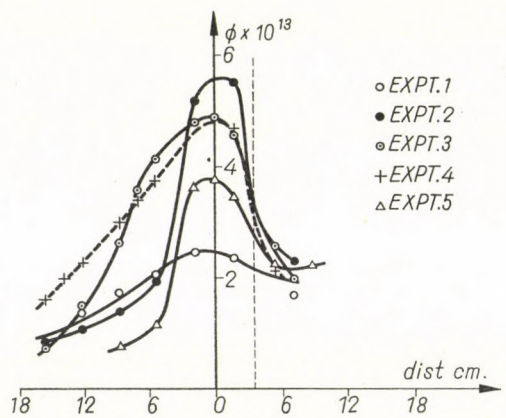

Fig. 10. Thermal neutron flux distribution for different configurations of cavity in direction IV

The same applies to direction II which is shown in Fig. 8. Fig. 9 represents the thermal neutron flux distribution in direction III for cavities 2 and 3 only, since the other configurations cannot be represented in this direction. Fig. 10 represents the effect of cavity on the thermal neutron flux in direction IV as a function of distance along the axis.

All these curves show a negligible difference in increase in the neutron flux with the cavities formed by extracting 2 and 3 fuel assemblies, but the maximum thermal flux is obtained when only one fuel section (cavity № 1)

is removed. So, such a cavity is suitable and gives the maximum peak in the UR-RR-1 reactor.

The discrepancy between our data and data [12] is due to the fact that the cavity created in [12] is an ideal one both in form and in position. The difference between our data and data [13] may be explained as follows: The curves obtained in [13] at various dimensions of cavity were normalized to the same number of fissions in cores of different volumes.

6. Conclusion

From the data obtained it follows that for practical use to reach an increase in thermal neutron flux in the active core of the UR-RR-1 reactor (WWR-S type) the use of a water cavity created by extracting one fuel section is the most preferable, i.e. the creation of a cavity having the dimensions 7×7 cms. Under these conditions the increase in the thermal neutron flux is 2.3 as high as the thermal flux at the same point without perturbation, and about 2.6 times the flux in the irradiation channels.

REFERENCES

1. N. A. Lazukov, I. E. Chelnokov and V. P. Ivanov, Atomic Energy **5**, 1, 44, 1958 (USSR).
2. L. David, International Current Conference on the Physics and Technique of Research Reactors, Report Progha 1963.
3. V. V. Gonchorov, Geneva Conference, 1958, Report.
4. V. V. Gonchorov, Geneva Conference, 1964, Report.
5. H. Hulubei, I. Purica, I. Rosescu and M. Sabau, The Soviet Journal of Atomic Energy, **12**, 1963.
6. M. I. Michaiel and A. A. Lukyanov, Report U.A.R. Cairo, UAR, AEE, 9, 1965.
7. J. V. Gordeev, D. A. Kardashov and A. V. Malyshev, Nuclear-Physical Constants, Moscow, 1963.
8. I. Hamouda, E. Eisa and M. Elshishini, Report U.A.R. Cairo, UAR, AEE, 11, 1963.
9. D. M. Kaminkev, K. A. Konoplev, U. V. Patrov and R. G. Pikulik, IDEA Symposium on Exponential and Critical Experiments 1964, Report Sm-42/84.
10. M. Y. Pasechnik, I. F. Bartchouk and V. P. Vertebay, Third United Nations International Conference on the Peaceful Uses of Atomic Energy, 1964, Report A (Conf. 28) P/325, Ukrani, USSR.
11. D. M. Kaminkev and K. A. Konoplev, third United Nations International Conference on the Peaceful Uses of Atomic Energy. 1964, Report A (Conf. 28) P/325, USSR.
12. H. Hulubei, L. Parica, T. Rosescu and M. Sabau, The Soviet Journal of Atomic Energy, **12**, N6, 562, 1963.
13. F. Szabó, Third United Nations International Conference on the Peaceful Uses of Atomic Energy 1964 Report A (Conf. 28) P/650 Hungary.

РАСПРЕДЕЛЕНИЕ ПОТОКА ТЕПЛОВЫХ НЕЙТРОНОВ И ЭФФЕКТ ЛОВУШКИ ПОТОКА В АКТИВНОЙ ЗОНЕ РЕАКТОРА UA—RR—I

Е. А. САД, Н. А. ЭЙССА, И. БАРЧУК, О. Г. ЭЛ-МОФТИ и А. Ф. ЭЛ-БАЙДВИ

Р е з ю м е

Распределение потока тепловых нейтронов в разных точках активной зоны и канала облучения водно-водяного реактора UAR измерялось нейтронно-активационным методом при помощи латунной и золотой фольги. В активной зоне достигалось заметное увеличение потока тепловых нейтронов созданием водной полости поперечного сечения в 7 см². Поток тепловых нейтронов в полости увеличился в 2,3 и 2,6 раза по сравнению со значением в активной зоне и в канале облучения соответственно.

Acta Physica Academiae Scientiarum Hungaricae, Tomus 23 (4), pp. 341—347, (1967)

MEASUREMENT OF THE LIFETIME OF ATOMIC EXCITED LEVELS BY TIME ANALYSER*

By

J. BAKOS and J. SZIGETI

CENTRAL RESEARCH INSTITUTE OF PHYSICS, BUDAPEST

(Presented by L. Jánossy. — Received 20. IX. 1966)

The lifetimes of atomic excited states in different noble gases have been measured by the method of time analysis. Some of the lifetime values are those of the initial levels of laser transitions (ArII), the others are those of the final levels of different gas lasers (Ne). The principle of the measuring apparatus is considered and effects disturbing the measurement are discussed.

In the search for newer laser material the most important characteristics which are needed are the lifetime values of the initial and terminal levels of the planned laser transition. For the measurement of the lifetime in gases there is the very efficient coincidence method of HERON—MCWHIRTER and RHODERICK [5], and the modified form of this method was used by BENNETT [8] in the measurement of the different neon levels planned as the initial level of the He—Ne laser. Independently of that work, lifetime measuring apparatus based on exactly the same principle as that of BENNETT was built by us and used for the determination of the lifetimes of the levels in various noble gases namely He, Ne, Ar, Ar^+ atoms. Recently, PENDLETON and HUGHES and KLOSE [2, 10] have published data about He and Ne lifetime values measured by the same method.

1. The measuring apparatus

Fig. 1 shows the block diagram of the measuring apparatus. The atoms are excited in the glass tube (3) by the collimated electron beam originating from the gun (A). The energy of the exciting electrons varies from 20 to 130 V. The continuous flow of the electrons is periodically interrupted by applying negative voltage pulses from the inverter (2) to the control grid (B) of the tube. The light of the excited atoms which propagates perpendicularly to the electron beam is collimated to the entrance slit of the grating monochromator (5) by the lens (4). The monochromator selects the light of the proper wavelength that belongs to the transition starting from the level the lifetime

* Lecture presented at II. Ogolnopolska Konferencja Radiospektroskopia i Elektronika Kwantowa in Posnan, 1966.

of which is to be measured. The photomultiplier (6) responds to the arrival of light quanta by voltage pulses which are amplified by the amplifier (7) and fed to the input 1. of the time to height converter (8). The pulse generator (1) simultaneously drives the inverter of the control grid of the light tube and the first grid of the converter tube in the time to the height converter.

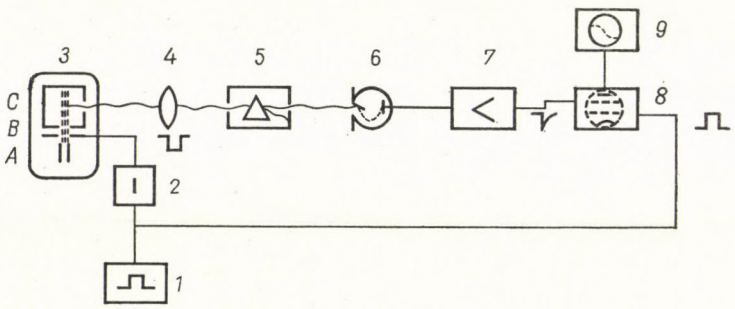

Fig. 1

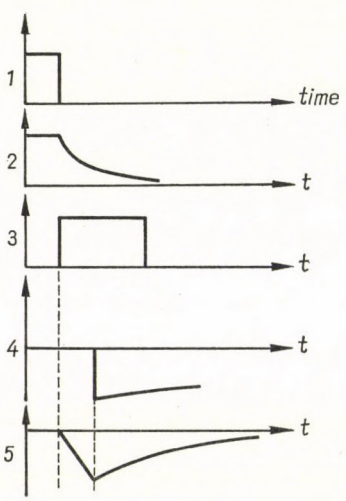

Fig. 2

The converter tube is "off" except for the time interval corresponding to the width of the driving pulse. The current flowing through the converter tube in the "on" state is arrested by the pulse of the multiplier. Thus, the charge on the plate of the converter tube is proportional to the time difference between the leading edge of the starting pulse and the stopping pulse of the photomultiplier. The time sequence of the pulses can be seen clearly in Fig. 2. The amplitudes of the pulses from the plate of the converter tube are analyzed by a 128-channel pulse-height analyzer. The probability of the appearance

of light quanta depends exponentially on time and therefore the content (N) of the channels varies with the channel number (n) in the following manner

$$N = N_0 \exp\left(-\frac{n}{\tau}\right).$$

One channel corresponds to one nanosecond, τ is the mean lifetime of the level measured in nanosecond units. Owing to the background (B) caused by the dark current of the photomultiplier and the scattered light, the content of the channels varies as

$$N = N_0 \exp\left(-\frac{n}{\tau}\right) + B.$$

Table 1

The lifetimes of He states

	Singlet			Triplet		
	S	*P*	*D*	*S*	*P*	*D*
7						143 ± 41 [3]
6						
5	144 ± 3 [2] 133 ± 8.5 [3]		*57 ± 2 (40)* [1] 79 ± 6 [2] 43.5 ± 15 [3]	113 ± 4 [2] 100 ± 10 [3]	235 ± 2 [2] 222 ± 14.8 [3]	52.6 ± 14 [3]
4	*90 ± 7* [1] 97 ± 2 [2] 87 ± 7.5 [3]		*41.6 ± 1.3* [1] 35 ± 4 [4] 47 ± 5 [2] 33.3 ± 5.5 [3]	*67 ± 1.4* [1] 68 ± 1 [2] 67.5 ± 1 [5] 64.6 ± 4.17 [3] 59 ± 6 [4] 77.5 ± 4 [6]	165 ± 1 [2] 153 ± 2 [5] 143 ± 14.3 [3]	*93 ± 6* [1] 120 ± 20 [4] 37 ± 6 [2]
3	54.2 ± 3 [3]		18 ± 5 [4] 16 ± 2 [2] 16.1 ± 3.9 [3]	40.8 ± 0.8 [3]	*112 ± 6* [1] 100 ± 8 [7] 91 ± 8 [4] 115 ± 2 [2] 115 ± 5 [5] 100 ± 5 [3]	25 ± 5 [4] 15 ± 2 [2] 10 ± 5 [5] 14.3 ± 3.3 [3]
2					90.5 ± 9.8 [3]	

Table 2

The lifetimes

Outer electron	$3P$			
Core (j)	$^2P_{1/2}$			
j'	1/2		3/2	
J	0	1	1	2
[13]	51		118	110
	46			
[12]	39			85
[14]	15 ± 1.0	19 ± 2		19 ± 1
[10]	14.7 ± 0.6	16.3 ± 0.6	18.0 ± 0.9	22 ± 1
Our results	13.26 ± 0.48	45 ± 3	26.2 ± 2.6	30.1 ± 1.8
	(41)	(21)	(12)	(40)
	14.8 ± 0.15		36.9 ± 4	28.1 ± 1
	(7.6)		(47)	(17)
	P_1	P_2	P_5	P_4

The results of the measurements, i.e. the contents of the channels are fed subsequently to an electronic computer. The values of the parameters N_0, τ and B are calculated by the maximum likelihood method. The response of the apparatus to the sudden drop in light intensity is also taken into account by measuring the time response and folding it with the probability of the appearance of light quanta.

The response of the apparatus was determined by measuring the decay curve of the 3^1P state of He at low gas pressure ($2\,\mu$), the lifetime of which is theoretically known to be short (1.7 nsec). The measured mean decay time used in the above-mentioned convolution integral was 4.7 nsec.

2. Effects disturbing the measurement

Disturbing effects are the imprisonment of resonance radiation, the excitation transfer in atom-atom collision and cascade transitions from overlying levels.

The imprisonment of resonance radiation usually causes the lifetime of the resonance levels to be longer than the true one quenching the transition to the ground level and hindering the measurement of the true lifetime of

of Ne states

$3P$					
$^2P_{3/2}$					
1/2		3/2		5/2	
0	1	1	2	2	3
			115	109	
			90	115	200
			29 ± 12		
23 ± 2		20.3 ± 0.6	22 ± 1	24.3 ± 0.8	22.5 ± 0.9
37 ± 2.7			26.3 ± 1.0	34.9 ± 2.64	19.5 ± 1.6
(40)			(42)	(42)	(19.5)
28.2 ± 0.85				28.4 ± 1.28	
(7.6)			22 ± 0.6	(7.6)	
33.2 ± 1			(7.6)	32.2 ± 1.7	
(17.5)				(47)	
P_3	P_{10}	P_7	P_6	P_8	P_9

resonance levels at higher pressures of the gas. Therefore, efforts are made to decrease the pressure as low as possible. Another way to minimize this effect is to reduce the diameter of the excitation chamber (C) and of the tube.

The rate of atom-atom collision also depends strongly on gas pressure. The consequence of the excitation transfer is the measurement of a lifetime value, which depends on the lifetimes of the two coupled levels and the cross-section of the collision.

Cascade effects must be taken into account in the evaluation of data by taking the transition probabilities and the excitation cross-sections of the levels from other measurements, or by theoretical considerations.

Pressure is usually reduced at the expense of the light intensity of the tube. Moreover, since the spectrum is rather rich in lines, the width of the monochromator slit must be narrowed to separate the lines from one another. Therefore the exciting current density must be as high as possible.

In view of the facts mentioned above, the tube was constructed so that the current density was 60 mA/cm^2 in the collimated electron beam with cross-sectional diameter 0.8 mm. Thus, the measurement is possible in as rich a spectrum as that of argon and in most cases the lines are separated from one another. To minimize the imprisonment, the chamber diameter was chosen to be 1 cm.

3. The results of the measurements

At first we measured the lifetimes of the helium levels mainly for checking the measuring set. The results agree well with the theoretical and experimental lifetime values reported in the literature. In this part of the measurements the results were calculated by the least square method (Table 1). Our results are underlined in Table 1. The differences in the lifetime values of the levels 5^1D, 4^3D can be explained as due to disturbing effects [1].

Table 2 shows the results of the lifetime measurements of the levels of Ne atoms. The results of other authors are listed in the upper part of the rectangles. The results of our measurement are collected in the lower part of the rectangles. The RACAH's notations of the levels are given at the top of the Table. The PASHEN's notations are at the bottom of the Table. Beside each of our results the pressure values are indicated in brackets. The measured levels are the terminal levels of the He—Ne red and infrared laser transitions. The disagreement with OSHEROVICH's and GRIFFITH's data can be explained by the high gas pressure used in their measurements [16].

The measured lifetime values of ionized argon atoms can be seen in Table 3. Here MOORE's notation has been for identification of the levels. The states marked by asterisks are the initial level of the argon blue laser. In the measurements, the pressure of the gas was very low, therefore the disturbing effects were negligible. The errors of measurements are less than 2% [15].

Table 3

The lifetimes of Ar^+ states

State	Wavelength Å	Gas Pressure (μ)	Lifetime $\tau \pm \Delta\tau$ (nsec)	Ref. [11]	Remarks
$4p^2P^0_{3/2}$*	4764.89	1.4	8.5 ± 0.14	9.4 ± 0.5	
	4545.08	1.4	8.4 ± 0.13		
$4p^2D^0_{3/2}$*	4965.12	1.4	9.9 ± 0.16	9.8 ± 0.2	
$4p^4P^0_{3/2}$	4735.93	2.4	9.6 ± 0.11		Measured together with the 4726.91 Å
$4p^2P^0_{1/2}$*	4657.94	1.4	8.0 ± 0.13	8.7 ± 0.3	$(4s^2P_{3/2} - 4p^2D^\circ_{3/2})$ line
$4p^2S^0_{1/2}$*	4579.39	2.4	8.7 ± 0.15	8.8 ± 0.3	Measured together with the 4589.93 Å
$4p^4D^0_{1/2}$*	4879.90	1.4	10.3 ± 0.20		$(4s'^2D_{3/2} - 4p'^2F^\circ_{5/2})$ line
$4p^4D^0_{5/2}$					
$4p^4P^0_{5/2}$	4806.07	2.0	10.3 ± 0.19		
$4p'^2F^0_{7/2}$	4609.6	2.0	9.0 ± 0.16		
$4p^4D^0_{7/2}$	4348.11	3.0	9.9 ± 0.17		

REFERENCES

1. J. Bakos and J. Szigeti, Acta Phys. Hung., **21**, 149, 1966.
2. W. R. Pendleton, Jr. and R. H. Hughes, Phys. Rev., **138**, A, 1683, 1965.
3. P. J. Kindlmann and W. R. Bennett, Bull. Am. Phys. Soc., **8**, 87, 1963.
4. R. G. Fowler, T. M. Holzberlein, C. H. Jacobson and S. J. B. Corrigan, Proc. Phys. Soc., **84**, 539, 1964.
5. S. Heron, R. W. P. McWhirter and E. H. Rhoderick, Proc. Phys. Soc., **A 234**, 565, 195.
6. R. G. Bennett and F. W. Dalby, Journ. Chem. Phys., **31**, 434, 1959.
7. А. Л. Ошерович, И. Т. Савич, Опт. и Спектр., **4**, 715, 1958.
8. W. R. Bennett, Adv. in Quant. Electronics, Edited by J. R. Singer, p. 28, New York—London, 1961.
9. R. Ladenburg, Rev. Mod. Phys., **5**, 243, 1933.
10. J. Z. Klose, Phys. Rev., **141**, 181, 1966.
11. W. R. Bennett, P. J. Kindlmann, G. N. Mercer and J. Sunderland, Appl. Phys. Let., **5**, 158, 1964.
12. J. H. E. Griffiths, Proc. Roy. Soc., **143**, 588, 1933.
13. А. Л. Ошерович, Т. М. Петелин, Докл. Акад. Наук СССР, **129**, 544, 1959.
14. W. R. Bennett, P. J. Kindlmann and G. N. Mercer, Appl. Opt. Suppl., **2**, 34, 1965.
15. J. Bakos, J. Szigeti and L. Varga, Phys. Let., **20**, 503, 1966.
16. Й. Бакош, Й. Сигети и Л. Варга, Опт. и Спектр. **23**, 478, 1967.

ОПРЕДЕЛЕНИЕ ВРЕМЕНИ ЖИЗНИ АТОМНЫХ ВОЗБУЖДЕННЫХ УРОВНЕЙ ВРЕМЕННЫМ АНАЛИЗАТОРОМ

Й. БАКОШ и Я. СИГЕТИ

Резюме

Методом временного анализа измерялось время жизни атомных возбужденных состояний в разных благородных газах. Некоторые значения времени жизни с начальными уровнями лазерных переходов (Ar II), другие — с конечными уровнями разных газовых лазеров (Ne). Рассматриваются принципы измерительной аппаратуры, дискутируются эффекты, возмущающие измерения.

Acta Physica Academiae Scientiarum Hungaricae, Tomus 23 (4), pp. 349—361, (1967)

DETERMINATION OF THE COUNTING EFFICIENCY IN CASES OF RADIATION MEASUREMENT OF THE WIDESPREAD SOLID ALPHA SOURCES

By

Á. TÓTH

MÉV HEALTH SERVICE, PÉCS

(Presented by L. Pál. — Received 20. IX. 1966)

The dependence of alpha counting efficiency on energy, source thickness and instrument constant are described in a more comprehensive manner than in former publications. The efficiency value calculated theoretically is also supported by experiment.

1. Introduction

The determination of the total Q activity of extended, solid alpha sources is a problem occurring frequently in many fields of science (e.g. experimental nuclear physics, geology, geophysics, radiation protection, environmental dosimetry, etc.). Difficulties arise in measurement practice owing to the lack of a standard of identical parameters (e.g. radiation energy, source thickness) with the samples of unknown alpha activity to be measured; either no standard source is available or the parameters of the available source differ from those of the samples to be measured rendering a conversion unavoidable. This is why it is important to know the dependence of alpha-counting efficiency on energy (or range), source thickness and instrument constant. An illustrative example will be given to show the substantial dependence of efficiency on energy and source thickness. These problems will be dealt with here from a theoretical point of view, providing a more comprehensive picture than do earlier publications, and the calculated efficiency value will be supported experimentally.

2. Definition of the total efficiency of alpha-counting

The total alpha-counting efficiency may be written in the form:

$$\eta_t = \frac{n_é}{Q} = \frac{n}{Q} \cdot G = \eta \cdot G, \tag{1}$$

where n is the counting rate in [cpm] observable with a given instrument under specified conditions (i.e., $G \approx 1$; value of the just detectable alpha

energy $E_{\min}$, or range $R_{\min}$; thickness of absorbent between radiation source and detector; source thickness and alpha energy, or range); Q = total activity of sample in 4π solid angle, in [dpm]; $G = \dfrac{\Omega}{2\pi}$ = solid angle factor; η = "partial" counting efficiency, when $G = 1$. Otherwise, any counting rate for solid angles $G < 1$ measurable by the instrument is: $n_{\acute{e}} = G \cdot n$ [cpm].

For simplicity the increase of total efficiency due to alpha-particle backscatter from the tray supporting the specimen will be neglected below. (This backscatter should be not more than 5% in the worst case.) This neglect is absolutely justified when the radiation of a not too thin alpha-source with a low atomic number produced on an unpolished surface is registered [1].

Total alpha-counting efficiency may also be written in the form

$$\eta_t = \frac{G}{Q} \int_{\acute{e}=R_{\min}}^{R} \left(\frac{dn}{dR}\right) dR = \frac{G}{Q} \int_{E_{\min}}^{E_0} \left(\frac{dn}{dE}\right) dE \left[\frac{\text{cpm}}{\text{dpm}}\right], \tag{2}$$

where R is the range of the alpha-particle in question in air [cm], and $d = R_{\min}$ the alpha-particle range [air cm] just detectable with the given measuring apparatus. E_0 is the initial energy of alpha-particles, whereas $E_{\min}$ is the energy corresponding to $R_{\min}$.

3. Concept and importance of the universal figure of merit, the just detectable range d of alpha-radiation measuring instruments

To be able to detect an alpha particle with a given measuring instrument, alpha particles arriving at the sensitive surface (or in the volume) of the instrument should have a certain energy $E_{\min}$ greater than zero. In detectors operating on the ionization principle it is a certain minimum ion number, whereas in the case of scintillating instruments a certain minimum scintillating photon number that corresponds to $E_{\min}$ required to put the registering instrument into action.

It seems to be expedient to substitute for ion or photon number "units" the range in air $d = R_{\min}$ corresponding to the given required alpha energy of value $E_{\min}$ to determine the figure of merit of the measuring instrument, since this will make it possible to include distances in the following efficiency expressions (see Table 1) in identical dimensions in [air cm], referring to normal conditions. d clearly represents a fictitious, not a real, distance.

The value of d depends on several factors [2]: 1) on the geometrical factor G; 2) on the pressure and temperature of the air (therefore its value should always be reduced to normal conditions); 3) on collection and, in the case of multipliers, on accelerating voltage; 4) on the sensitivity and stability of the electronic unit (amplifier-forming-recording circuit).

It should be emphasized that the value of d does not depend on the alpha energy E_0 [3]. This is a most important fact leading to the universality of d: having determined d for actual measuring conditions (see the possibilities for determining d hereafter), with the help of formulae as shown in Table 1, the partial alpha-counting efficiency will be known for any alpha energy of value E_0 and source thickness under otherwise unchanged conditions.

For alpha detectors operating with ZnS(Ag) the efficiency of detection will increase [4] with the increased length of the path travelled by the alpha particles in the ZnS(Ag) medium, and with the proximity of the ZnS(Ag) grains to one another. This involves the requirement that the ZnS(Ag) layer should be thick enough to absorb the total energy of alpha particles of the highest energy to be measured; it is also desirable that alpha particles should make impact on the phosphorus with the greatest possible energy.

It is clear that the ZnS(Ag) layer must not be so thick as to absorb its own scintillating light to any considerable extent. Natural alpha-radiating sources of the highest energy completely lose their energy in a 25 mg/cm^2 thick ZnS(Ag) layer, a thickness of which the self-scintillation light absorption is unimportant.

4. Data, designations and assumptions required for the calculation of alpha-counting efficiency

Designations

τ	thickness of alpha source [air cm];
R	range of given alpha particles in [air cm];
$(\tau \ll R)$	thickness of self-absorptionless alpha source [air cm];
$(\emptyset < \tau < R)$	thickness of "thick", i.e. self-absorbing alpha source [air cm];
$(\tau = R)$	thickness of "infinitely thick" alpha source [air cm];
$(\tau > R)$	thickness of alpha source exceeding the "infinitely thick" source thickness [air cm].

Remark: The last two designations are used to calculate the total emission of alpha sources. When speaking of the effective alpha source thickness from which alpha particles are instrumentally just detectable, the appropriate designations are: $\tau = [R - d - a]$, or $\tau > [R - d - a]$. The effective source thickness is thus smaller than total source thickness.

a thickness of the absorbent between the active surface of the source and the sensitive surface [air cm];

d range just detectable with the detector [air cm];

Δl branching fraction (see explanation below).

Assumptions

a) the geometrical factor is $G \approx 1$;
b) the so-called "edge effect" is insignificant;
c) the range-straggling [6, 7] is negligible;
d) the detecting surface is disk-shaped, the detecting volume has cylindrical geometry (e.g. in case of a gas-flow proportional circulating gas counter, where $a \approx \emptyset$);
e) not more than one alpha particle will be emitted per disintegration (thus $\Delta l \leqslant 1$);
f) the alpha radiation source of a completely even and plain surface is mono-energetic and activity distribution along source thickness and source surface is homogeneous;
g) thickness a of the absorbent between source and detector surface does not depend on the angle between the path direction of the alpha particle and the normal of the source surface;
h) the detector absorbs the total energy of arriving alpha particles;
i) alpha-counting efficiency is independent of position on the detecting surface;
j) stability in time of the alpha-counting efficiency and of the background is convenient [5].

5. Calculation of the alpha-counting efficiency

A given edge-effectless alpha source of thickness τ [air cm], density ϱ [g/cm^3], surface A [cm^2], having a homogeneous activity distribution along its thickness emits in air under normal conditions (15 °C, 760 mmHg) a number N of alpha particles of range R [cm] per gram and minute in solid angle 4π (see Fig. 1, which, though referring to a special case, shows conditions and designations). Values of stopping powers: for the material of the alpha-source: $s = \frac{R_f}{R} = \frac{sR}{R}$ for the material between source and detector surface of thickness a [air cm]: $s_1 = \frac{R_a}{R} = \frac{s_1 \cdot R}{R}$. Total ranges in the material of the source: $R_f = sR$ [cm]; in the absorbent: $R_a = s_1 \cdot R$ [cm]. The just detectable range should be d [air cm].

In a conveniently chosen coordinate system it is not difficult to prove by plotting the volume element and the number of alpha-particles derived from this volume element propagating in an appropriate solid angle element, and finally integrating over the appropriate limits that the value of the counting rate n_τ [cpm] as indicated by the detector for an alpha-source of

thickness ($\emptyset < \tau < R$) [2, 6, 7, 8] will be:

$$n_\tau = \frac{NA\varrho s\tau}{4}\left[\frac{2(R-d-a)-\tau}{(R-d}\right][\text{cpm}]. \tag{3}$$

The counting rate for the source ($\tau \geqslant [R-d-a]$) of infinite thickness will be:

$$n_R = \frac{NA\varrho s}{4}\left[\frac{(R-d-a)^2}{(R-d)}\right][\text{cpm}]. \tag{4}$$

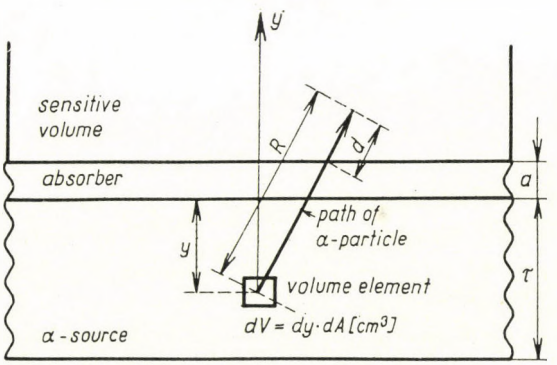

Fig. 1

Since total activity of the source with a thickness ($\emptyset < \tau < R$) is in solid angle 4π:

$$Q_\tau = NA\varrho s\tau \quad [\text{dpm}], \tag{5}$$

(Q_τ obviously depending neither on d, nor on a) the partial counting efficiency for an alpha source of thickness ($\emptyset < \tau < R$) on the basis of equations (3) and (5) will be:

$$\eta = \frac{n_\tau}{Q_\tau} = \frac{1}{4}\left[\frac{2(R-d-a)-\tau}{(R-d)}\right]\left[\frac{\text{cpm}}{\text{dpm}}\right]. \tag{6}$$

Since the total activity of the infinitely thick (i.e. sR air cm thick) alpha source in 4π solid angle is:

$$Q_R = NA\varrho SR\ [\text{dpm}], \tag{7}$$

therefore on the basis of equations (4) and (7) thus the partial counting efficiency for a source of infinite thickness ($\tau = R$) will be:

$$\eta = \frac{n_R}{Q_R} = \frac{1}{4}\cdot\frac{(R-d-a)^2}{R(R-d)}\left[\frac{\text{cpm}}{\text{dpm}}\right]. \tag{8}$$

Remark: For the time being the solid angle factor is assumed to be

$$G = \frac{\Omega}{2\pi} = 1.0.$$

Calculation of average alpha-counting efficiency when several types of alpha-radiating elements are present in the alpha source

When the number of the alpha-active elements in the source is $j > 1$, and their Δl branching (or activity) fractions are known, where

$$j = \left(\frac{\text{alpha activity of the given daughter element}}{\text{alpha activity of the parent element}} \right),$$

equations (3), (4), (6) and (8) may also be applied. In such cases the value η_f will be calculated separately for each alpha-emitting element, each value being weighted according to Δl activity fractions, and averaged. Thus the average, partial alpha-counting efficiency is [2, 7]:

$$\bar{\eta}_j = \frac{\sum_{j=1}^{j} \Delta l \cdot \eta_j}{\sum_{j=1}^{j} \Delta l} = \frac{1}{j} \sum_{j=1}^{j} \Delta l \cdot \eta_j . \tag{9}$$

It should be noted [7] that for most of the more important alpha-emitters of the U, AcU and Th series $\Delta l = 1$. Therefore, in these cases $\sum_{j=1}^{j} \Delta l = j$, while for ThC: $\Delta l = 0.35$ and for ThC': $\Delta l = 0.65$.

6. Comparative survey of alpha-counting efficiency expressions applied to measuring conditions (see paragraph 4) as dealt with in this paper

The survey of and orientation among the various cases is facilitated by Table 1 based on equations (6), (8) and (9), from which all cases may be deduced. When several genetically connected alpha-emitting elements forming a radio-active series are present in an alpha source, the average efficiency will be obtained by applying the operations as indicated in equation (9), to any equation satisfying the actual conditions selected from among those shown in Table 1. E.g.: for the case $R > \tau > \phi$; $a > \phi$ and $d > \phi$ [see equation (6)], when $\Delta l = 1$, average counting efficiency will be:

$$\bar{\eta} = \frac{1}{2j} \cdot \sum_{j=1}^{j} \Delta l \cdot \left| \frac{R_j - d - a - \frac{\tau}{2}}{R_j - d} \right|,$$

where R_j: range in air of the jth element of the radio-active decay series, in [cm].

Table 1

The dependence of partial alpha-counting efficiency η on thickness and range for various values of absorbent thickness a and just detectable range d, in case of mono-energetic, homogeneous alpha-sources (Range straggling, "edge-effect" and backscattering from radiation source support are neglected)

Thickness of alpha source	Alpha counting efficiency η [cpm/dpm]*			
	$a > 0,\quad d > 0$	$a = 0,\ d > 0$	$a > 0,\ d = 0$	$a = 0,\ d = 0$
	not ideal detector		ideal detector	
Infinitely thin ($\tau \ll R$)	$\frac{1}{2} \cdot \frac{R-d-a}{R-d}$	$\approx \frac{1}{2}\frac{R-d}{R}$	$\frac{1}{2}\frac{R-a}{R}$	$\frac{1}{2}$
$R > \tau > 0$	$\frac{1}{2} \cdot \frac{R-d-a-\left(\frac{\tau}{2}\right)}{R-d}$ (see equation (6))	$\frac{1}{2}\left[1-\frac{\tau}{2(R-d)}\right]$	$\frac{1}{2}\left[\frac{R-a-\left(\frac{\tau}{2}\right)}{R}\right]$	$\frac{1}{2}\left[1-\frac{\tau}{2R}\right]$**
Infinitely thick ($\tau = R$)	$\frac{1}{4} \cdot \frac{(R-d-a)^2}{R\cdot(R-d)}$ (see equation (8))	$\frac{1}{4} \cdot \frac{R-d}{R}$	$\frac{1}{4}\left[\frac{R-a}{R}\right]^2$	$\frac{1}{4}$
($\tau > R$)	$\frac{1}{4} \cdot \frac{(R-d-a)^2}{\tau\cdot(R-d)}$	$\frac{1}{4} \cdot \frac{R-d}{\tau}$	$\frac{1}{4}\frac{(R-a)^2}{\tau\cdot R}$	$\frac{1}{4}\frac{R}{\tau}$

Remarks to Table 1

* (observed counting rate [cpm]/total alpha-decay rate of source in solid angle 4π, [dpm]), when $G = 1$;

** In this case $(\tau/2R)$ is the fraction of the alpha-particles absorbed by the source, i.e. self-absorption. Therefore, condition $\tau < (0.02R)$ must be satisfied to reach less than 1% self-absorption.

7. Possibilities for practical determination of factors required for the calculation of alpha-counting efficiency (including some of the author's own measurement results)

It is clear from Table 1 that counting efficiency η can only be calculated when the following are known;

a) the air-equivalent source thickness τ [air cm],
b) the absorbent thickness a [air cm],
c) just or minimum-detectable range d [air cm],
d) the range R of the alpha-particle (or ranges) of the alpha-particles having a branching fraction Δl [air cm],
e) in the case of decay series their j, and Δl values.

All these will be investigated more closely below.

a) *Determination of thickness τ of the alpha-emitting source in [air cm].*

It is known [2], that the air-equivalent source thickness is

$$\tau = \frac{G_F}{s \cdot \varrho} \qquad [\text{air cm}], \tag{10}$$

where G_F is the surface density of the alpha-source in [g/cm^2]. G_F may easily be determined by weight and surface measurements, while the product of $(s \cdot \varrho)$ can be calculated from the Bragg—Kleeman approximate equation [9], yielding

$$s \cdot \varrho \approx 3{,}2 \cdot 10^{-4} \cdot W^{1/2}, \tag{11}$$

where W is the average atomic weight, derived on the "atomic fraction" basis. However, the use of equation (11) will lead to results 5% to 30% lower than the real values [9]. When substituting $Z^{2/3}$, (Z being the atomic number), for $W^{1/2}$ into equation (11), the error will decrease to 5% or less for elements belonging to the upper part of the periodic system, while it will exceed 5% for light elements.

Should the element composition of the sample or the appropriate W be unknown, the goal may nevertheless be reached by an absorption measurement [8], or by adding a material of known atomic weight [10] to the sample; $(s \cdot \varrho)$ will, thus be eliminated.

Whether sample thickness may be neglected ($\tau \approx \emptyset$) or not, should be decided by weight or alpha-spectrum-measurement.

τ may also be determined if both an extremely thin sample and also a sample of finite τ thickness [1, 12] of the given alpha-emitting source are available.

b) *Determination of thickness of the absorbent between alpha-source and detector* is no particular problem, as the absorbent will be air, or probably aluminium. By measuring the surface density of aluminium, the appropriate air-equivalent thickness can easily be calculated knowing that [11] 1 cm air $\approx$ 1.5 mg Al/cm^2. (However, for the experimental conditions of [1]: 1.63 mg Al/cm^2 $\approx$ 1 cm air).

c) *Experimental determination of the just (or minimum) detectable range d*

Absorbing foils consisting of a known element (e.g. Al) increasing in thickness are placed on a mono-energetic, infinite thin alpha-source (e.g. Po^{210}) to establish the dependence of the counting rate (or efficiency) n_a on thickness a of the absorbent for the given measuring conditions (discrimination level, amplification, voltages, geometry, etc.). There should be no holes in the Al foil; the foil must also absorb alpha-particles emanating incidentally from the edge of the alpha-source. At a certain adjustment of the utilized portable transistorized scintillation alpha-counting instrument [18], with

electromechanical and rate-meter registration, the following curve was obtained when placing Al absorbent foils on infinitely thin Po^{210} (Fig. 2).
n_a is the backgroundless counting rate observed for Al absorbent of thickness a. Thus, the section of the extension of the straight line and axis a, i.e. $(R - d)$,

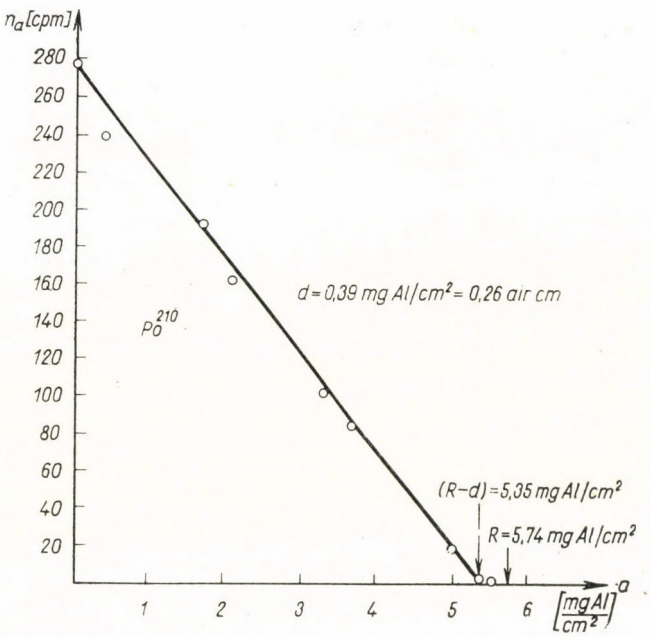

Fig. 2

is 5.35 mg Al/cm². Since the range of Po^{210} particles of 5.3 MeV energy and a range of $R = 3.83$ [air cm] in Al is

$$R_{Al} = \left(\frac{R}{s_L}\right) = \left(\frac{3.83}{1800}\right) = 2.125 \quad 10^{-3} \text{ cm},$$

i. e.:

$$R_{Al} = 5.74 \left[\frac{\text{mg Al}}{\text{cm}^2}\right];$$

thus $$d = (5.74 - 5.35) = 0.39 \text{ mg Al/cm}^2 = \frac{0.39}{1.5} = 0.26 \text{ [air cm]}.$$

s_L is the relative linear *stopping power* mentioned in connection with the deduction of equations (3)—(8); its value was taken from [13].

(A similar result with deviations of only a few per cent was obtained for d when the Al absorption curve was derived from infinitely thin alpha-sources composed of (U^{238} + U^{234}).) In the above case it is not necessary to know the absolute Q activity of the alpha-source. Yet when Q is known and the efficiency $\eta = \frac{n_a}{Q}$ is plotted against a, the tangent of the slope angle of the obtained straight line will be the converse of $(R - d)$; d can also be derived in this way.

The value of d may be regarded as being essentially an integral discriminating level. In this context it is worth mentioning that great care should be taken in the correct adjustment of the energy threshold E_{min} of the given apparatus, since for infinitely thick ($\tau = R$) alpha-sources the average radiation energy E_m [15] represents only 27.4% of E_0. When $E_0 = 5$ MeV, $E_m = 1.4$ MeV, being approx. 0.73 [air cm]. Therefore d must be considerably smaller than 0.73 air cm (background problems increase!). When measuring thin sources (e.g. $\frac{\tau}{R}$ being 0.1 and, thus, $E_m = 0.73 \cdot E_0$) this adjustment is not too critical.

d) and e) The ranges of alpha-emitting sources being sufficiently different, the range(s) in air R of alpha particles emitted from a source of unknown material composition can be determined by measuring the absorption in Al or in air [1, 12], or by changing the pressure [14]. If, on the other hand, the energies of alpha-active compounds of absolutely unknown composition do not differ to a sufficient degree, the ionization or semi-conductor alpha spectrum of a very thin sample of the compound must be investigated. Every single energy (including R_j-s) and even branching fractions (peak area proportions) Δl may be derived from the analysis of the alpha spectrum. Of course the value of j will similarly be known. Now equation (9) may be applied to any of the cases to calculate $\overline{\eta}$.

No particular difficulty should arise (this is, as a matter of fact, a very common case in practice) when the element or elements composing the samples are known; and when the measurement of many of these samples is routine work.

8. Example to illustrate the dependence of efficiency on energy and source thickness for identical a, d and G

Under identical conditions of measurement ($G = 1$, $a = 0.2$ [air cm], $d = 0.3$ [air cm]) comparison is made between efficiency values obtained from a single alpha emitter of great energy (RaC', in this case $R = 6.87$ [air cm]), in a thin ($\tau = 0.5$ [air cm]) sample on the one hand, and on the other, between the values of another single alpha emitter of low energy (U^{238}) in an infinitely

thick ($\tau = R = 2.69$ [air cm] $= 2.69 \times 0.32 \times 20.4$ [mg/cm^2] $= 17.6$ [mg/cm^2]) sample:

In this way either $\eta(\tau = 0.5;\ R = 6.87) = 0.462$;
or $\eta(\tau = R = 2.69) = 0.187$.

The latter efficiency is 2.5 times lower than for the great energy alpha emitter in a thin sample!

Thus, experimental conditions must be carefully watched, as the dependence of efficiency on energy and source thickness is extremely great.

9. Experimental check of calculated efficiencies

We had at our disposal a source ($U^{238} + U^{234}$) of $G_F = 0.0975$ [mg/cm^2] surface density which, therefore, could be considered as infinitely thin, with known $Q = 778$ dpm/4π of absolute activity and 25 mm active surface diameter. It was established by spectrum analysis [16] that no alpha-emitter is to be found in the source other than those mentioned, and that these are in radio-active equilibrium. Thus $\Delta l = 1$ and $j = 2$. Air-equivalent source thickness corresponding to the above surface density (taking $Z^{2/3}$ instead of $W^{1/2}$; see equations (10) and (11)) is:

$$\tau = \frac{G_F}{0{,}32 \cdot Z^{2/3}} = \frac{9{,}75 \cdot 10^{-2}}{0{,}32 \cdot 20{,}4} = 0{,}015 \quad [\text{air cm}] \approx \emptyset$$

which is negligibly small (representing only about 0.5% of the range in air).

As regards our equipment and normal conditions: $d = 0.3$ [air cm]; $a = 0.2$ [air cm]. Thus the operations as equation (9) are to be applied to case ($\tau = \emptyset$ or $\tau \ll R$; $d > \emptyset$ and $a > \emptyset$) of Table 1. For this case the so-called average "partial" efficiency when $G = \dfrac{\Omega}{2\pi} = 1$ is:

$$\bar{\eta} = \frac{1}{2j} \sum_{j=1}^{j=2} \frac{R_j - d - a}{R_j - d} = \frac{1}{4}\left[\frac{R_1 - d - a}{R_1 - d} + \frac{R_2 - d - a}{R_2 - d}\right]. \qquad (12)$$

Since $R_1 = 2.685$ [air cm] and $R_2 = 3.260$ [air cm], therefore,

$$\bar{\eta} = \frac{1}{4}(0.916 + 0.932) = 0.462\,.$$

As, in fact, $G < 1.0$, total average alpha-counting efficiency on the basis of equation (1) gives:

$$\bar{\eta}_t = 0.462 \times 0.935 = 0.433\,.$$

The value of the solid angle corresponding to actual conditions was taken from a curve constructed following the data of the Table of [17].

The total counting efficiency actually measured for the same source with the same instrument under identical conditions amounted to $\eta_t = 0.440$. The difference is unimportant: $100 \frac{0.007}{0.44} = 1.6\%$. With the aid of foreign made U^{233} and U^{235} standards (diameter also = 25 mm, but $a = 0.17$ [air cm]) the total alpha-counting efficiency was 0.45. One of the equations has thus been supported experimentally by results within acceptable error limits. Even a greater deviation would be tolerable, as the surface of the alpha-source was only half (diameter = 25 mm) the sensitive surface (diameter = 50 mm) of the detector. In turn it was established by moving a not infinitely thin ($U^{238} + U^{234}$) source of 5 mm diameter horizontally under the sensitive surface that the efficiency is substantially independent of the place along the horizontal surface of a circle of 40 mm diameter drawn around the axis of the detector. This being the case, the agreement between calculated and measured efficiency is justified. It may be assumed that the other equations of Table 1 will also lead to adequate results. On this assumption, when measuring the counting rate $n_{\dot{e}}$ [cpm] of a sample of known material, but unknown activity Q [dpm], with a knowledge of η_t under the given conditions, the total alpha-activity sought for will be, on the basis of equation (1):

$$Q_x = \frac{n_{\dot{e}}}{\eta_t} \text{ [dpm]}.$$

REFERENCES

1. M. L. CURTIS, et al., Nucleonics **13,** № 5, 38, 1955.
2. N. B. KEEVIL and W. E. GRASHAM, Canad. Journ. Res., **21,** Sec. A, No. 3. 21, 1943.
3. F. N. BYRNE, The Sci. Proc. Royal Dublin Society, Ser. A., No. 14, **1,** 343, 1963.
4. J. P. ANTHONY, CEA-760, 1958.
5. TÓTH ÁRPÁD, Magyar Fizikai Folyóirat XIII., 2. füzet, 129, 1965.
6. R. D. EVANS, Phys. Rev., **45,** 29, 1934.
7. G. D. FINNEY and R. D. EVANS, Phys. Rev., **48,** 503, 1935.
8. V. I. BARANOV, et al., "Laboratornüje rabotü i zadacsi po radiometrii", Atomizdat, Moszkva, 1964, 144—150.
9. R. D. CHERRY, *in:* "The Natural Radiation Environment" (eds., J. A. S. Adams and W. M. Lowder), Rice University, Semicentennial Publications (1964), 407—424.
10. J. KOLHÖRSTER, Strahlentherapie, **94,** 602, 1954.
11. W. A. ARON, et al., AECU-663, 1949.
12. E. BLEULER and G. J. GOLDSCHMIDT, "Experimental Nucleonics", Rinehart Comp., Inc., New York, 275, 1959.
13. W. J. PRICE, "Nuclear Radiation Detection", McGraw Hill, Book Comp., Inc., New York, 1958; p. 21. (Russian translation).
14. P. HUBER and F. WIDDER, Helv. Phys. Acta, **33,** 567, 1960.
15. I. CHUDACEK, Czechoslov. Journ. Phys. **8,** 396, 1958.
16. NAGY LÁSZLÓ, NAGY TIBOR, KFKI, Budapest (personal communication, 1966).
17. UCRL-12 004, 32—34, 1964.
18. Á. TÓTH, II. Symposium on Health Physics, Pécs, Hungary, Sept. 26—30, 1966, Vol. II, pp. 75—79.

ОПРЕДЕЛЕНИЕ ЭФФЕКТИВНОСТИ СЧЁТА ДЛЯ СЛУЧАЯ НЕТОЧЕЧНЫХ ТВЁРДЫХ α-ИЗЛУЧАЮЩИХ ИСТОЧНИКОВ

А. ТОТ

Р е з ю м е

Сообщение знакомит с зависимостью эффективности счёта α-частиц от энергии, — толщины излучающего источника, — и также от констант прибора.

Эти вопросы рассматриваются с охватом ранних сообщений. Теоретически расчитанное значение эффективности подтверждается опытными данными.

Acta Physica Academiae Scientiarum Hungaricae, Tomus 23 (4), pp. 363—372, (1967)

ON THE EFFECT OF A HIGH MAGNETIC FIELD ON RECOMBINATION THROUGH CENTRES*

By

G. PATAKI and F. BELEZNAY

RESEARCH INSTITUTE FOR TECHNICAL PHYSICS OF THE HUNGARIAN ACADEMY OF SCIENCES, BUDAPEST

(Presented by G. Szigeti. — Received 25. X. 1966)

In the present paper the effect of a high magnetic field on recombination is discussed for three different recombination models: (i) simple Shockley—Read centres; (ii) S—R centres plus traps for holes and (iii) recombination centres with two charge conditions. It is shown that in all three models the lifetimes may vary markedly (by an order of magnitude) if the Fermi level, with increasing magnetic field, goes through any energy level relevant in the recombination. The numerical calculations refer to n-type InSb and $T = 130$ °K, assuming, because of lack of proper experimental data, recombination centres with hypothetical parameters.

Introduction

In recent years interest in the behaviour of semiconductors in high magnetic fields has increased markedly. The quantized motion of electrons in the conduction band, the appearence of the Landau levels, leads to various interesting effects. Among these are the oscillating character of galvanomagnetic, thermomagnetic effects and the magneto-optical phenomena. In $A^{III}B^{V}$ semiconducting compounds the quantization of conducting electrons, because of their small effective masses, may be achieved much more easily than in the classical semiconductors.

In the present paper the recombination is investigated in high magnetic fields. In the case of radiative recombination, it has been shown by the authors [1] that the matrix element of the electron transition between the conduction band and an acceptor state does not depend on the magnetic field in the first approximation if the "deformation" of acceptor states is neglected. On the contrary, KHOVARSKY and CHAYKOVSKY [2] have found that for radiationless recombination the lifetime may increase in high magnetic fields. In spite of their results, it will be assumed in the present paper that the capture constants are independent of the magnetic field and only the effect of the change in the density of states on recombination will be considered.

Three recombination models are studied: (i) simple Shockley—Read centre; (ii) S — R centre plus traps for holes and (iii) recombination centre with

* Part of this work was presented at a Conference on the "Physics of Semiconducting Compounds" Swansea, Sep. 1966.

two charge conditions. It is shown, for all cases treated, that one may obtain a field-dependent lifetime if the Fermi level goes through any energy level relevant in the recombination, with increasing magnetic field. Thus, with the aid of the magnetic field a "mapping" of a part of the forbidden gap may be achieved without changing the temperature. Owing to the lack of proper experimental data, the numerical calculations were carried out with hypothetical but realistic parameters for n-type InSb.

1. Lifetimes for the recombination models considered

Relatively few experimental data are available on recombination mechanisms in $A^{III}B^{V}$ compounds. It is known, however, that at reduced temperatures the recombination centres play an important role in the determination of lifetime. Thus, WERTHEIM [3], ZITTER et al. [4]. LAFF and FAN [5], GULYAEVA et al. [6] have shown that simple $S - R$ centre and multi-electron centres should be taken into account. Recently, HAGEBBER and FAN [7] supposed the existence of traps with excited states in GaSb. On the basis of the experimental evidence it seems to be useful to consider the models enumerated in the Introduction. For the sake of completeness, the differential equation system of recombination for multi-electron centre plus traps for holes will be given. Omitting the simple but tedious calculations, only the final expressions for lifetimes are reported here. Let N_r be the concentration of recombination centres with possible charge conditions s $(0, 1 \ldots M)$ and n_s that in the state "s" (in equilibrium n_{s0}). The concentration of traps is N_t. The filled and empty traps are denoted by $n_t(n_{t0})$ and $p_t(p_{t0})$, resp. The differential equation of recombination for the cases considered can easily be obtained on the basis of a previous paper by one of the authors [8], if the excited states are neglected and the term responsible for hole capture by the traps is taken into account.*

$$\frac{dn}{dt} = -\sum_{s=1}^{M} U_s^{s-1}(n),$$

$$\frac{dn_s}{dt} = U_s^{s-1}(n) + U_s^{s+1}(p) - U_{s+1}^{s}(n) - U_{s-1}^{s}(p), \tag{1}$$

$$\frac{dp}{dt} = -\sum_{s=0}^{M-1} U_s^{s+1}(p) - U_t(p),$$

* Evidently, similar equations can also be obtained for electron traps and for traps with excited states.

where the net capture rates are given by

$$\begin{aligned} U_s^{s-1}(n) &= c_n(s-1 \to s)[nn_{s-1} - n_0 \Gamma_s^{s-1} n_s], \\ U_s^{s+1}(p) &= c_p(s+1 \to s)[pn_{s+1} - p_0 \Gamma_s^{s+1} n_s], \\ U_t(p) &= c_{tp}[pn_t - p_0 \Gamma_t p_t]. \end{aligned} \tag{2}$$

Here $c_n(s-1 \to s)$ and $c_p(s+1 \to s)$ are the electron and hole capture parameters of the transitions $(s-1 \to s)$ and $(s+1 \to s)$ while c_{tp} is the capture parameter of the traps. $\Gamma_i^j \equiv n_{jo}/n_{io}$; $\Gamma_t \equiv \dfrac{n_{t0}}{p_{t0}}$; $n(n_0)$ and $p(p_0)$ are the electron and hole concentrations, resp. Further equations can be obtained, using the condition of electrical neutrality and the normalisation for the possible states of the centres:

$$n + \sum_{s=0}^{M} s n_s + n_t + N_a = p + N_d, \tag{3}$$

$$\begin{aligned} \sum_{s=0}^{M} n_s &= N_r, \\ n_t + p_t &= N_t. \end{aligned} \tag{4}$$

Fully ionized donors and acceptors and neutral empty recombination centres and traps have been assumed.

(i) Simple S—R model

If the trace and the determinant of the differential equation system for this case are denoted by $T(A_r)$ and $D(A_r)$, respectively, then, assuming the two lifetimes τ_r and τ_t to be well separated ($\tau_r \gg \tau_t$) one obtains (see e.g. [9]):

$$\tau_r \approx \frac{T(Ar)}{D(A_r)}; \qquad \tau_t \approx \frac{1}{T(A_r)}$$

and $T(A)_r$ and $D(A)_r$ are given by

$$\begin{aligned} T(A_r) &= c_{rn} N_r \left(\frac{n_0}{n_{r0}} + \frac{p_{r0}}{N_r} \right) + c_{rp} N_r \left(\frac{p_0}{p_{r0}} + \frac{n_{r0}}{N_r} \right) \\ D(A_r) &= c_{rn} c_{rp} N_r \left(n_0 + p_0 + \frac{n_{r0} p_{r0}}{N_r} \right). \end{aligned} \tag{5}$$

For our purposes, it was more suitable in Eqs. (5) to introduce the concentrations n_{ro} and p_{ro} instead of the usual parameters of the $S—R$ model (n_1, p_1).

*(ii) Recombination centres plus traps for holes**

The steady state lifetime of this model has been given by WERTHEIM [10]. Both the steady state and transient lifetimes have been studied by LŐRINCZY et al. [11], where the model was applied for the kinetics of surface recombination. If the differential equation system (1) is linearized for the given case ($s[0, 1]$) and traps for holes, the lifetimes are easily obtained as the roots of the equation of third degres: $b_3\tau^3 + b_2\tau^2 + b_1\tau + b_0 = 0$, where the coefficients are given by

$$b_0 = -1\,; \qquad b_1 = A_t + T(A_r) + c_{tp}\, n_{t0}\,;$$

$$b_2 = -\left[A_t\, T(A_r) + A_p\, c_{tp}\, n_{t0} + D(A_r) + c_{rn}\, p_{r0}\, c_{tp}\, n_{t0} + A_n\, c_{tp}\, n_{t0}\right];$$

$$b_3 = +\left[c_{tp}\, n_{t0}\, c_{rn}\, p_{r0}\, A_p + A_t\, D(A_r)\right].$$

Here $T(A_r)$ and $D(A_r)$ are given by Eq. (5) while the other notations are the same as in [11] with the difference that here the quantities n_{ro}, p_{ro}, etc. are introduced, i.e.:

$$A_n = c_{rn}\, N_r \frac{n_0}{n_{r0}}\,; \qquad A_p = c_{rp}\, N_r \frac{p_0}{p_{r0}}\,; \qquad A_t = c_{tp}\, N_t \frac{p_0}{p_{t0}}\,.$$

The lifetimes τ_r and τ_t are given by $\tau_r \approx -\dfrac{b_2}{b_3}$ and $\tau_t \approx -\dfrac{b_1}{b_2}$ with a similar approximation as previously.

(iii) Centres with two charge conditions

This model was examined in detail for InSb in [5]. For the sake of a better comparison we shall use the same notations as those in the paper cited. Only the steady state lifetimes of electrons and holes (τ_n, τ_p) will be given. Here, the traps will be omitted. The centres may have the charge conditions $s[0, 1,2]$. If in Eq. (1) the notations are altered as follows:

$$c_n(0 \to 1) \equiv r_{c1}\,; \qquad c_p(1 \to 0) \equiv r_{v1}\,;$$

$$c_n(1 \to 2) \equiv r_{c2}\,; \qquad c_p(2 \to 1) \equiv r_{v2}\,;$$

* *Note added in proof:* In a recent paper by HOLLIS et al. [15] it was shown that at reduced temperatures both the lifetime and Hall data may be quantitatively explained using two sets of simple S—R centres. There is no difficulty in extending the present calculations for this model.

and the following abbreviations are used:

$$A_1 = \frac{(1-F_1)(1-F_2^2)}{[1-F_2(1-F_1)]^2}; \qquad A_2 = \frac{F_1(1-F_2)(2-F_1)}{[1-F_2(1-F_1)]^2};$$

$$B_i = 1 + \frac{r_{ci}}{r_{vi}} \frac{n_0}{p_0} \frac{1-F_i}{F_i},$$

where

$$F_1 = \frac{n_{10}}{n_{00}+n_{10}}; \qquad F_2 = \frac{n_{20}}{n_{10}+n_{20}},$$

then the the ratio of the lifetimes is

$$\frac{\tau_p}{\tau_n} = \left\{1 + \frac{N_r}{p_0}\left[\frac{r_{c1}}{r_{v1}} \frac{A_1}{B_1}(1-F_1) + \frac{r_{c2}}{r_{v2}} \frac{A_2}{B_2}(1-F_2)\right]\right\} \times$$

$$\times \left\{1 + \frac{N_r}{p_0}\left[\frac{A_1}{B_1} F_1 + \frac{A_2}{B_2} F_2\right]\right\}^{-1}$$

and τ_n is given by

$$\tau_n = \left[N_r\left(1 + \frac{n_0}{p_0} \frac{\tau_p}{\tau_n}\right)\right]^{-1}\left[\frac{r_{c1}}{B_1}(1-F_1) + \right.$$

$$\left. + \frac{r_{c2}}{B_2} F_1\right]^{-1}\left[\frac{1-F_2(1-F_1)}{1-F_2}\right].$$

This expression for τ_n is slightly different from that of paper [5]. There, the term $\frac{r_{c2}}{B_2}$ is multiplied by $(1-F_1)$ instead of F_1. In our case, however, $r_{c1}(1-F_1)$ and $r_{c2}F_1$ are proportional to $r_{c1}n_{00}$ and $r_{c2}n_{10}$, respectively, as one might expect.

2. Determination of the Fermi level and the filling of the centres

The expressions for the lifetimes have been given in the previous Section. To use these formulae, both the capture parameters and the filling of the centres are needed. In the absence of a magnetic field the following expressions

can be used:

$$n_0 = N_c \cdot \exp\left(-\frac{E_c - F_0}{kT}\right); \qquad n_{t0} = \frac{N_t}{1 + \exp\left(\frac{E_t - F_0}{kT}\right)},$$

$$\frac{n_{s0}}{N_r} = \frac{g_s \exp\left(\frac{sF_0 - E_s}{kT}\right)}{\sum_s g_s \exp\left(\frac{sF_0 - E_s}{kT}\right)}, \tag{9}$$

where F_0 is the Fermi level, and g_s is the degeneracy of the level E_s. (It is assumed that $g_0 = 1$, $g_1 = 2$.) Inserting these expressions into the equation of electrical neutrality, the Fermi level and, thus also, the concentrations n_{s0}, n_{r0}, etc. can be determined. In a magnetic field the statistics of the electrons in the conduction band changes markedly. For a nondegenerate band, taking all Landau levels into account ($n = 0, 1, \ldots$) ANSELM has given a closed formula to determine the electron concentration [12]:

$$n_0 = \frac{N_c}{z} \exp\left(-\frac{E_c - F_0(H)}{kT}\right), \tag{10}$$

where $z = \frac{shx}{x}$ and $x = \frac{\hbar\,\omega_c}{2kT}$. Here ω_c is the cyclotron frequency of the conduction electrons with effective masses m_n. A similar formula is valid also for holes, but for the materials in question m_p is much larger than m_n.Thus, for the magnetic fields used their effect on the holes may be neglected. The magnetic field may also change the states of the deep levels, but in this paper this effect will be neglected. (A more detailed discussion is given in Sec. 4.) Using Eq. (10) the magnetic field dependence of the Fermi level can be determined from the condition of electrical neutrality:

$$\frac{N_c}{z} \exp\left(-\frac{E_c - F_0(H)}{kT}\right) + \\ + \sum_s s n_{s0}(H) + n_{t0}(H) + N_a = p_0(H) + N_d. \tag{11}$$

Knowing $F_0(H)$ the concentrations $n_0(H)$, $n_{s0}(H)$, etc. can also be determined.

3. Results of the calculations

The calculations were carried out for n-type InSb. To obtain a significant effect for p-type material either extremely high magnetic fields or very low temperatures are needed, but in this last case the Fermi level is too far from

any recombination centre which may be expected in InSb. From the equation (10) it can be seen that assuming a fixed value for n_0, the Fermi level will be shifted towards the conduction band if a magnetic field is applied. One may expect a magnetic field-dependent lifetime if the Fermi level, with increasing field, goes through the energy level of any centre taking part in the recombination process. So, taking into account the previous remarks,

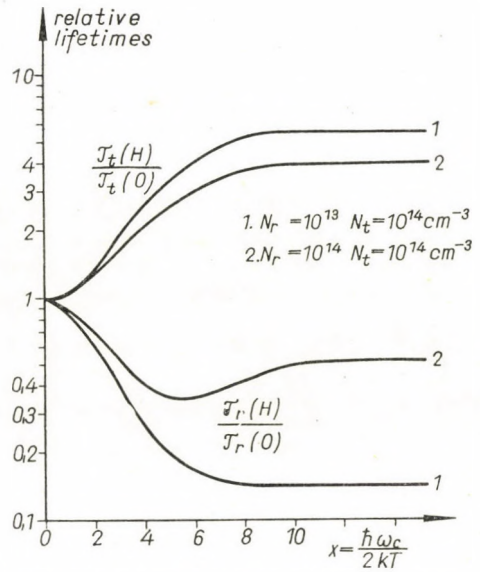

Fig. 1a. Magnetic field dependence of relative lifetimes for model (ii).

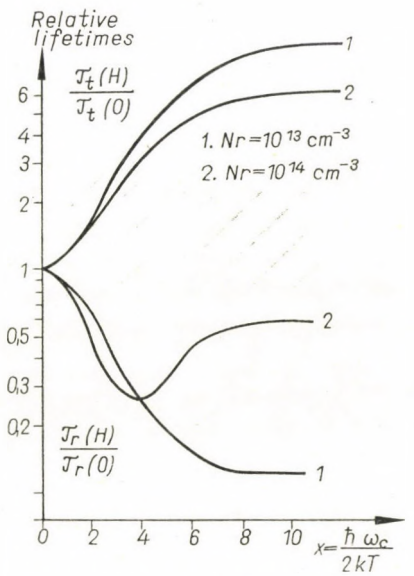

Fig. 1b. Magnetic field dependence of relative lifetimes for model (i).

the centre should be situated above the Fermi level at $H = 0$. The calculations were carried out for $T = 90$ °K and for $T = 130$ °K but here only the results for $T = 90$ °K are given because, if the lifetimes are plotted as a function of the dimensionless parameter $x = \dfrac{\hbar \omega_c}{2kT}$ one obtains similar curves for both temperatures. ($\hbar \omega_c = 1{,}16 \cdot 10^{-8} \left(\dfrac{m_0}{m_n}\right) H$ [eV] if H is expressed in oersteds).

In Fig. 1a the magnetic field dependence of relative lifetimes $\dfrac{\tau_r(H)}{\tau_r(0)}$ and $\dfrac{\tau_t(H)}{\tau_t(0)}$ is shown according to model (ii) where both recombination centres and traps are present. In Fig. 1b the curves refer to the results of calculations for model (i), using the same parameters as previously and omitting the traps ($E_r = 0.022$ eV; $N_r = 10^{13}$, 10^{14} cm^{-3}; $c_{rn} = c_{rp}$; $n_0 = 6.01 \times 10^{13}$ cm^{-3}). It can be seen that if $N_r < n_0$ both relative lifetimes are monotonic functions

of the field, while for $N_r > n_0$, τ_r passes through a minimum. This difference also appears in the behaviour of the Fermi level at these concentrations of recombination centres as can be seen in Fig. 2, where the function $F_0(H)$ is plotted. If $N_r < n_0$ the Fermi level rises above E_c while if $N_r > n_0$ it goes through E_r but remains below the bottom of the conduction band.

The magnetic field dependence of τ_p for centres with two charge conditions (model (iii)) is given in Fig. 3. Donor type centres were assumed (n_{00} has two positive charges).

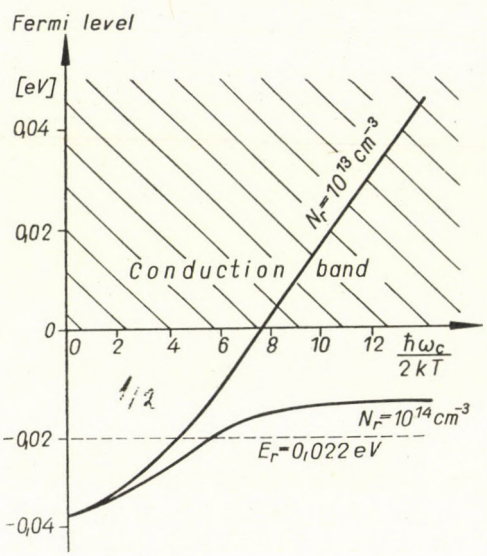

Fig. 2 Variation of the Fermi level in a magnetic field for model (i).

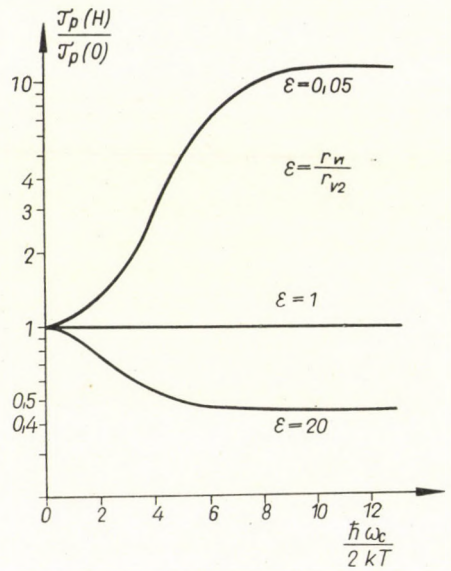

Fig. 3. Magnetic field dependence of relative hele-lifetime for model (iii).

For $E_1 = 0.12$ eV and $E_2 = 0.03$ eV (energies are measured from the conduction band); at a given value of N_r, the ratio of the capture parameters $\frac{r_{v1}}{r_{v2}}$ was varied. From the curves of Fig. 3 it can be seen that the field dependence is very sensitive to the value of $\frac{r_{v1}}{r_{v2}}$.

4. Discussion of the results and conclusions

In the previous calculations the "deformation" of localized states in a magnetic field, the magnetic field dependence of capture parameters and the quantization of holes have been neglected.

The increase of the ionization energies of donor atoms in a magnetic field, as was shown by YAFET and KEYES [13, 14] may lead to the "freezing

out" of the electrons from the conduction band and thus n_0 may depend directly on the magnetic field. It is not difficult to see, however, that at the temperatures considered the donor atoms will be still fully ionized in spite of increased ionization energies.

The correctness of the field-independent capture parameters should be examined for each model separately. It was shown in [1] to be correct for radiative recombination while for radiationless recombination with electron-phonon interaction, this assumption is incorrect [2]. Calculations for Auger-type recombination are in progress.

The deformation of lower lying states may lead to essential changes in the capture cross-sections and ionization energies. This effect depends on the parameter $\hbar\,\omega_c/E_r$ which has a small value for moderate fields. In our case the quantity $\hbar\,\omega_c/E_r$ is not small. In spite of this, it seems interesting to consider the effect of high magnetic fields on the recombination caused by the change in the density of states, only, because it will take place whether the capture parameters depend on the field explicitly or not. As for the quantization of holes, at $H = 100\ kG$ and $T = 90\ ^\circ\mathrm{K}$ $\dfrac{\hbar\,\omega_{cp}}{kT} \approx 1$ while for electrons $\dfrac{\hbar\,\omega_c}{kT} \approx 14$. Thus, the changes in the statistics of the holes may be neglected [see Eq. (10)].

Spin splitting may also be neglected as it is connected with the free electron mass $m_0 \gg m_n$.

The previous calculations have shown that the lifetimes may vary by an order of magnitude if the conditions are chosen properly. The same shift of the Fermi level towards the conduction band can also be achieved by reducing the temperature. The two cases, however, may differ from each other markedly. For example for model (ii) the lifetime *increases* with decreasing temperature, which shows an activation energy characteristic for *traps* [11]. On the contrary, if a magnetic field is applied the lifetime *decreases* and the energy level of the *recombination centre* can be determined.

The magnetic field dependence of lifetime τ_p is very sensitive to the ratio r_{v1}/r_{v2} (Fig. 3). If r_{v1}/r_{v2} is greater or less than unity the lifetime τ_p decreases or increases, respectively. In case of $r_{v1}/r_{v2} = 1$, it does not show any magnetic field dependence. It should be remarked, however, that the case $r_{v1}/r_{v2} < 1$ is very unlikely as the transition $(s = 2 \to s = 1)$ has a probability less than that of $(s = 1 \to s = 0)$ because of the Coulomb field of the centre.

As for the experimental check of the present calculations, the PME effect seems to be too complex to determine the lifetimes because the effect of a high magnetic field on the transport phenomena must also be taken into account. Only direct methods seem to be suitable. The photoconductivity decay method for InSb was used in [3]. From the experimental point of view

GaAs seems to be preferable because of the usual degeneracy of conduction electrons in InSb.

In the present paper we have dealt with bulk recombination only, but similar calculations may be carried out for surface recombination and $g - r$ noise. In case of $g - r$ noise the filling of the centres will affect not only through the lifetimes but also through other quantities, similarly to the transient photoconductivity decay where besides the lifetime the amplitude will obviously depend on the concentration of empty centres as well.

Finally, the following conclusions may be drawn:

1) *For all three models* the lifetimes depend strongly on the magnetic field if the Fermi level is driven through an energy level, relevant in the recombination.

2) With the aid of the magnetic field a "mapping" of a part of the forbidden band is possible, without changing the temperature.

3) The magnetic field dependence of the lifetimes can be used to determine the parameters of the centres, e.g. concentrations and capture constants.

REFERENCES

1. F. Beleznay and G. Pataki, phys. stat. sol., **8,** 805, 1965.
2. В. А. Коварский и И. А. Чайковский, ФТТ, **7,** 2505, 1965.
3. G. K. Wertheim, Phys. Rev., **104,** 662, 1956.
4. R. N. Zitter, A. F. Strauss and A. E. Attard, Phys. Rev., **115,** 266, 1959.
5. R. A. Laff and H. Y. Fan, Phys. Rev., **121,** 53, 1962.
6. А. С. Гулаева, М. И. Иглицын и Л. В. Петрова, ФТТ, **6,** 1552, 1964.
7. M. A. Habegger and H. Y. Fan, Phys. Rev., **138,** A598, 1965.
8. G. Pataki, Int. Conf. Semiconductor Physics, Paris, Dunod, Paris, 1964, p. 823.
9. G. Pataki, Acta Phys. Hung., **13,** 119, 1961.
10. G. K. Wertheim, Phys. Rev., **109,** 1086, 1958.
11. A. Lőrinczy, G. Pataki and G. Pásztor. Acta Phys. Hung., **21,** 107, 1966.
12. А. И. Ансельм и Б. М. Аскеров, ФТТ, **2,** 2821, 1960.
13. Y. Yafet, R. W. Keyes and E. N. Adams, J. Phys. Chem. Solids, **1,** 137, 1956.
14. R. W. Keyes and R. J. Sladek, J. Phys. Chem. Solids, **1,** 143, 1956.
15. J. E. L. Hollis, S. C. Choo and E. L. Heasell, J. Appl. Phys., **38,** 1626, 1967.

О ВЛИЯНИИ СИЛЬНЫХ МАГНИТНЫХ ПОЛЕЙ НА РЕКОМБИНАЦИЮ ПРОИСХОДЯЩУЮ ЧЕРЕЗ РЕКОМБИНАЦИОННЫЕ ЦЕНТРЫ

Г. ПАТАКИ и Ф. БЕЛЕЗНАИ

Резюме

В настоящей статье рассмотрено влияние сильных магнитных полей в случае трёх разных рекомбинационных моделей; (i) Шокли—Рид центры; (ii) Ш—Р центры плюс ловушки для дырок и (iii) двукратно заряжённые центры. Показано, что во всех перечисленных случаях времена жизни могут значительно (на порядок) изменяться, если уровень ферми — с увеличением магнитного поля — переходит через какой либо энергетический уровень играющий роль в процессе рекомбинации. Численные результаты относятся к InSb n-типа и $T = 130\,°K$, предполагая — за недостатком пригодных экспериментальных данных — рекомбинационные центры с гипотетическими параметрами.

Acta Physica Academiae Scientiarum Hungaricae, Tomus 23 (4), pp. 373—379, (1967)

EXPERIMENTAL INVESTIGATION OF THE SPATIAL COHERENCE OF A He—Ne LASER

By

L. CSILLAG, M. JÁNOSSY and K. KÁNTOR

CENTRAL RESEARCH INSTITUTE OF PHYSICS, BUDAPEST

(Presented by L. Jánossy — Received 25. X. 1966)

Measurements have been carried out on the spatial coherence of a He—Ne laser with the help of a Mach—Zehnder interferometer. The results obtained from the measurements verify the complete spatial coherence expected from theory for single mode operation of a laser.

1. Introduction

The multiple slit diffraction experiments performed with the first He—Ne laser showed qualitatively that light radiated by a gas laser is spatially coherent over the whole cross-section of the laser beam [1]. In connection with this, the question arises how spatial coherence is actually generated in a laser. The first fairly obvious assumption was that spatial coherence of laser radiation is created by the process of stimulated emission in the laser cavity [2].

Later on, further considerations gave a quite different explanation of the phenomenon. It has been shown by several authors [3, 4] that when monochromatic light is reflected continuously to and fro between the mirrors of the laser resonator, a steady state will be attained gradually in the resonator as a result of the process of diffraction of light on the mirrors. For this reason only certain wave forms, otherwise called modes, will remain in the laser cavity, the frequency, the phase and amplitude distribution of which over the mirrors is determined by the geometry of the laser resonator. It has been assumed, here, that light is monochromatic. Thus, no problem of coherence arises as monochromatic light is necessarily completely coherent. However, it was shown by WOLF [5] that quasi-monochromatic light which is initially only partially space coherent or even incoherent will become completely coherent in a similar way after a sufficient number of passes through the laser resonator even though the resonator is passive in the sense that no light is generated within it.

According to this consideration spatial coherence is created by diffraction of light waves on the laser mirrors in such a way that the waves with inappropriate phases are gradually suppressed at the successive passes through the resonator. The only role which stimulated emission plays in this connection

is that it compensates in a coherent manner for losses of light in the resonator. The spatial coherence will be complete if a single mode survives and the effect of spontaneous emission is negligible. In that case spatial coherence of laser radiation can be considered as ideal.

2. Measurements on spatial coherence

Quantitative measurements on spatial coherence of a gas laser have been performed by BERTOLOTTI, DAINO and SETTE on a He—Ne laser with the help of a double slit [6]. According to the results obtained the degree of coherence decreases considerably with increasing separation of the apertures. As it turned out later on the reason for this was the multi-mode operation of the laser. In a further experiment performed by the same authors the case of single mode operation was also investigated and the degree of coherence was found to be almost unity [7]. The report contains, however, no further details.

We have carried out investigations on spatial coherence with the help of a Mach—Zehnder interferometer which appeared to be more suitable than the double slit arrangement generally used because it allows for measurements of higher accuracy. Our first experiment [8] was carried out on a He—Ne laser operating in the infrared at the wavelength $\lambda = 1.15\ \mu$. The measurements performed in three different transverse modes (TEM_{00}, TEM_{10}, TEM_{30}) showed a high degree of coherence over the whole cross-section of the laser beam. The degree of coherence obtained deviated in general, however, by a few per cent from ideal coherence ($|\gamma_{12}|$ was 0.94—0.97).

We therefore repeated our measurements under more favourable experimental conditions with a laser operating now in the visible part of the spectrum at the wavelength $\lambda = 0.6328\ \mu$ [9]. The results of the second measurement quantitatively verify the theoretical results showing complete spatial coherence in the case of single mode operation of the laser.

3. The principle of measurement

The degree of coherence $|\gamma_{12}|$ between two points P_1 and P_2 of the electromagnetic field can be determined from the following relation [10]

$$|\gamma_{12}| = \frac{I_{\max} - I_{\min}}{I_{\max} + I_{\min}} \frac{I_1 + I_2}{2\sqrt{I_1 I_2}}, \tag{1}$$

where I_1 and I_2 are the intensities of the beams emerging from P_1 and P_2. The first factor is the visibility of the interference pattern produced by the

two beams. I_{max} and I_{min} denote the maximum and minimum intensity, respectively.

Fig. 1 shows the Mach—Zehnder interferometer with which the two points P_1 and P_2 can easily be located anywhere on the cross-section of the laser beam. The beam entering the interferometer is split into two parts which finally interfere at the point of observation M. As can be seen from the

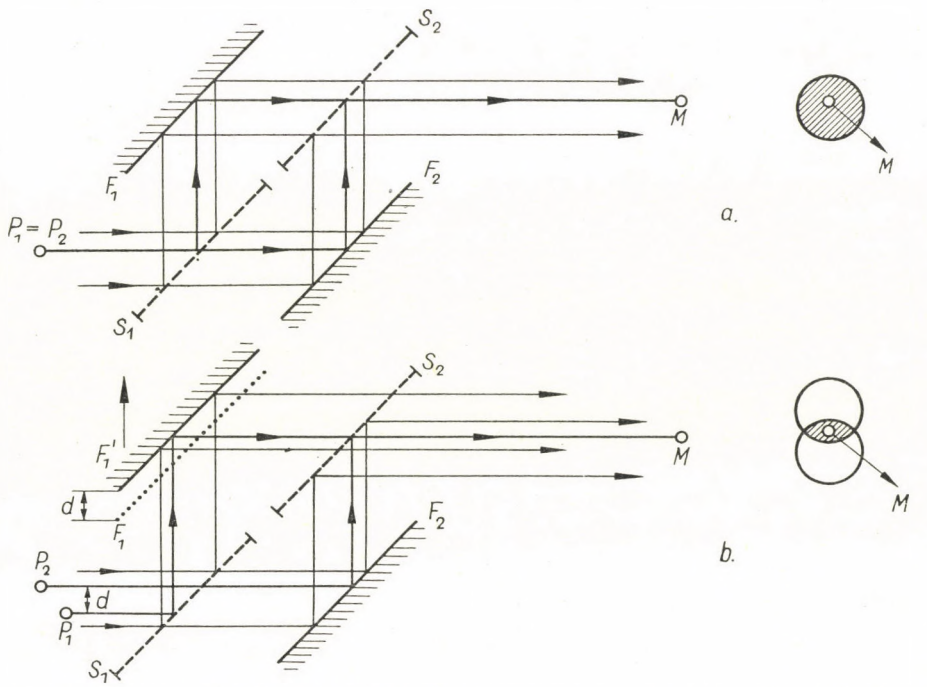

Fig. 1. Interference in the Mach—Zehnder interferometer, cases a) and b). F_1 and F_2 denote full mirrors, S_1 and S_2 semi-transparent mirrors, M point of observation (left). The shaded part on the cross-section of the two beams shows where interference arises (right)

Figure in case a) when the mirrors F_1 and F_2 are placed symmetrically, the two points P_1 and P_2 are identical, which means, that the beam emerging from the point $P_1 = P_2$ of the cross-section interferes with itself at point M. Whereas, when the mirror F_1 is displaced by the distance d into position F_1' the two points lie in different places of the laser beam, and the projection of their distance on the cross-section of the beam is also d. In the latter case the interference arising at point M is produced by two beams emerging from different points. Thus, by measuring the intensities I_{max} and I_{min} of the interference pattern and I_1, I_2 of the interfering beams, the degree of coherence $|\gamma_{12}|$ between two points P_1 and P_2 lying at a distance d from each other on the cross-section of the laser beam can be determined. The point P_2

may be chosen by moving the detector along the cross-section of the laser beam. P_1 is given by the position of mirror F_1.

If the laser resonator consists of spherical mirrors the wave fronts of the light radiated by the laser will also be spherical. Because of this, by changing the position of the mirror F_1 (i.e. by changing the distance d of the two points), the path difference of the interfering beams changes by differing amounts over the whole field where interference arises (Fig. 2). Accordingly, the spacing of the interference fringes will be wider or narrower, and in this way the value of the visibility obtained in the measurement will appreciably depend on the size of the aperture of the detector. This difficulty can be over-

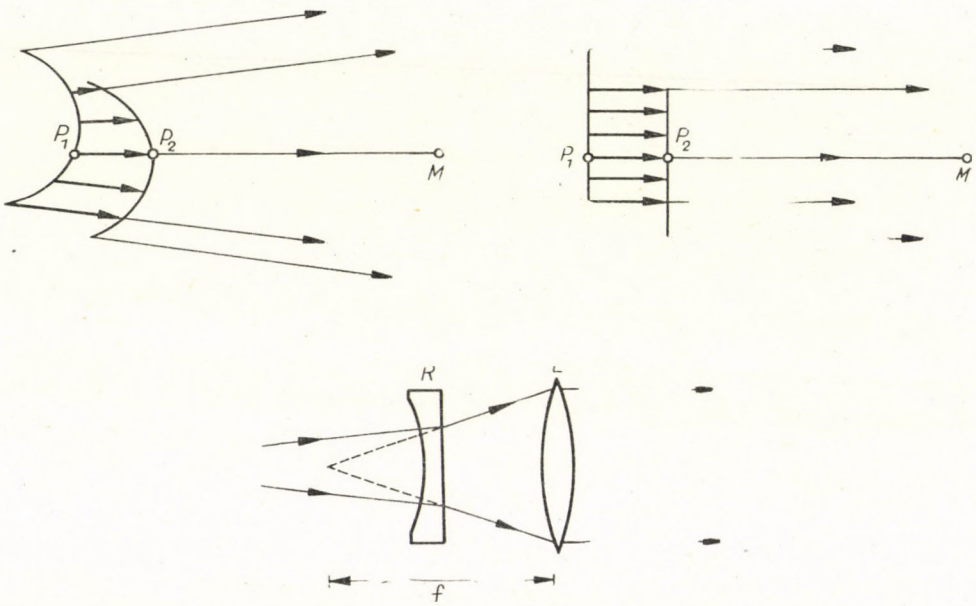

Fig. 2. The path difference between the interfering beams. Top left: spherical waves. Top right: plane waves. Bottom: Plane waves can be produced with the help of a lens L. R denotes the laser mirror through which the divergent beam is emerging

come by placing a lens in the path of the laser beam in such a way that the focus of the inserted lens falls into the virtual focus of the divergent beam. The waves thus become practically plane waves and in this way the path difference of the interfering beam will be the same at every point of the interference field. The interference pattern now consists of only a single wide interference fringe which is dark or bright according to the path difference of the beams. By slightly changing the path difference both the intensity maxima $I_{\max}$ and minima $I_{\min}$ of the interference pattern can be determined.

4. The measuring arrangement

Fig. 3 shows the measuring arrangement. The d.c. laser operated at the wave length $\lambda = 0.6328\mu$. The resonator consisted of two dielectrical mirrors with a curvature of $r = 75$ cm, which were fixed with four invar rods at a distance of 50 cm from one another. The length of the laser tube was 30 cm, and its inner diameter was 2 mm. By a suitable adjustment of the

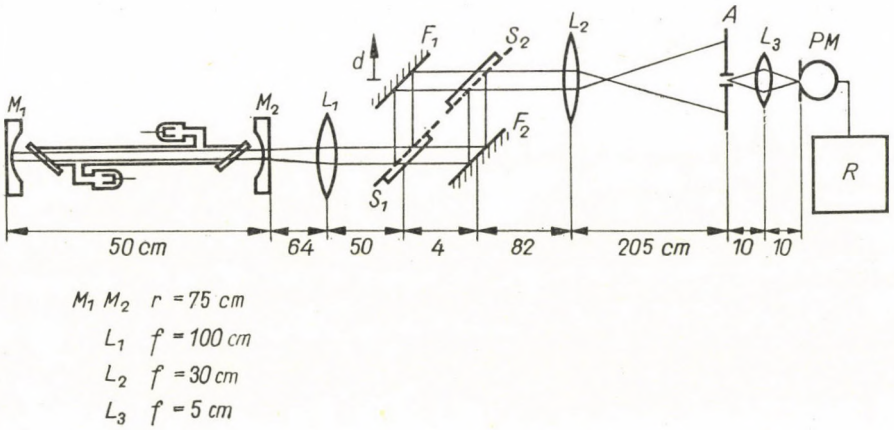

Fig. 3. Block diagram of the measuring arrangement. M_1, M_2 laser mirrors, L_1 lens for producing a plane wave front; F_1, F_2 full mirrors, S_1, S_2 semi-transparent mirrors of Mach—Zehnder interferometer, L_2 lens for enlarging the laser beam, A aperture, L_3 lens to focus aperture on photomultiplier cathode, PM photomultiplier, R registering galvanometer

mirrors and using an appropriate current density in the discharge tube, it was possible to select the desired modes. The Mach—Zehnder interferometer was mounted on a Hilger N200 interferometer. To overcome effects arising from the finite size of the aperture of the detector the laser beam leaving the interferometer was enlarged with the aid of a lens of $f = 30$ cm focal distance. Thus, the diameter of 0.4 mm of the aperture of the detecting photomultiplier (EMI 6256B) was equal to about 1/40th of the diameter of the laser beam. The visibility of the interference pattern was determined from the registration of four or five intensity maxima and minima obtained through the mirror F_1 being slowly moved by a motor for a distance of about 3 μ.

5. Discussion of the results

From the results of the measurements we determined $|\gamma_{12}|$ according to relation (1). In Fig. 4 we have plotted the values of $|\gamma_{12}|$ obtained from the measurements and the intensity distribution I of the corresponding modes

indicating the position of the points P_2, fixed in the origin of the coordinate system, and P_1 lying at a distance d from P_2. It can be seen from the Figure that the degree of coherence obtained in the mode TEM_{00} is practically 1 and is 0.98 in the mode TEM_{10}. The results of the measurements thus verify the ideal spatial coherence expected from theory for single mode operation.

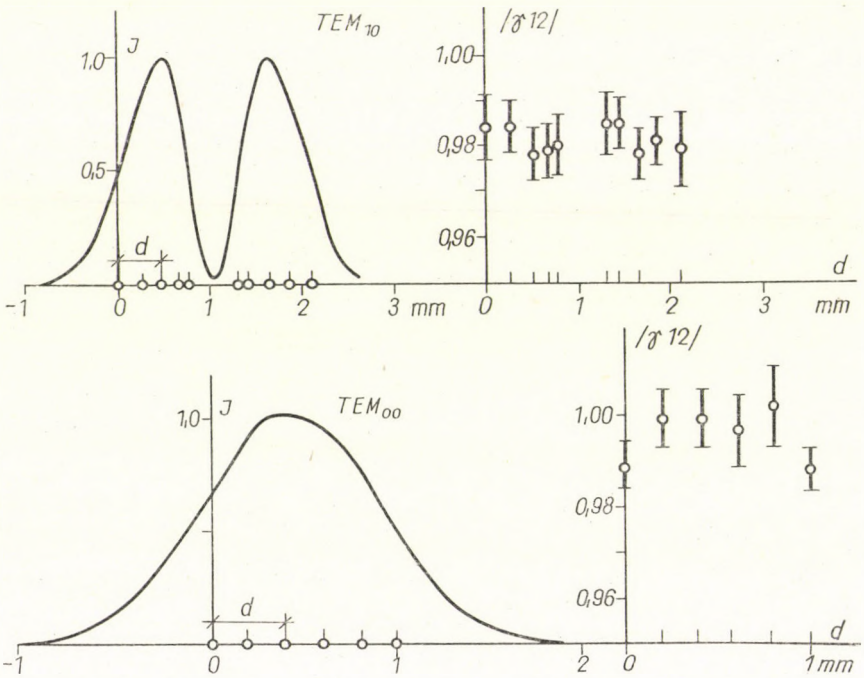

Fig. 4. The degree of coherence $|\gamma_{12}|$ obtained at various distances d between two points on the cross-section of the laser beam (right) and the intensity distribution I of the modes (left)

The deviation of 2% from ideal coherence in the mode TEM_{10} may be attributed to the effect of some other weakly excited transverse modes and the same effect may also have been responsible for the deviation observed in our previous measurement [8].

The decrease of spatial coherence when several transverse modes are excited simultaneously may be explained in the following way: because the frequencies of the individual transverse modes differ in general from one another, the intensity of the observed interference pattern will be the sum of the intensities of the single interference patterns produced by the various modes. As the modes have different phases and different intensity distributions compared with one another the single interference patterns do not completely overlap each other. Thus the visibility of the resulting interference pattern

will be lower than that of the single interference patterns. Since the degree of coherence is related to the visibility of the interference fringes, a decrease in the visibility also gives a decrease in the degree of coherence.

REFERENCES

1. D. R. Herriott, J. Opt. Soc. Amer., **52,** 31, 1962.
2. J. C. Vienot, Rev. Opt., **40,** 9, 1961.
3. A. G. Fox and T. Li, BSTJ, **40,** 453, 1961.
4. G. D. Boyd and J. P. Gordon, BSTJ, **40,** 489, 1961.
5. E. Wolf, Phys. Letters, **3,** 166, 1963.
6. M. Bertolotti, B. Daino and D. Sette, Il Nuovo Cim., **33,** 1705, 1964.
7. M. Bertolotti, B. Daino, F. Gori and D. Sette, Il Nuovo Cim., **38,** 1505, 1965.
8. M. Jánossy, L. Csillag and K. Kántor, Phys. Letters, **18,** 124, 1965.
9. L. Csillag, M. Jánossy and K. Kántor, Phys. Letters, **20,** 636, 1966.
10. M. Born and E. Wolf, Principles of Optics, Pergamon Press, London, 1959. p. 503.

ЭКСПЕРИМЕНТАЛЬНОЕ ИССЛЕДОВАНИЕ ПРОСТРАНСТВЕННОЙ КОГЕРЕНТНОСТИ ЛАЗЕРА He—Ne

Л. ЧИЛЛАГ, М. ЯНОШИ и К. КАНТОР

Р е з ю м е

Проводились измерения в связи с пространственной когерентностью Лазера He—Ne при помощи интерферометра Маха—Цандера. Полученные из измерений результаты подтверждают совершенную пространственную когерентность, следующую из теории в случае простых операций Лазера.

Acta Physica Academiae Scientiarum Hungaricae, Tomus 23 (4), pp. 381—392, (1967)

ИСПОЛЬЗОВАНИЕ (β^+ $\gamma^\pm$) СОВПАДЕНИЙ ПРИ ИССЛЕДОВАНИИ ПОЗИТРОННОГО РАСПАДА ЯДЕР

Э. ВАТАИ

ИНСТИТУТ ЯДЕРНЫХ ИССЛЕДОВАНИЙ ВАН, ДЕБРЕЦЕН

(Пердставлено Ш. Салаи — Поступило 9. XI. 1966)

Проведен подробный анализ возможностей применения метода (β^+ $\gamma^\pm$) совпадений для определения эффективности регистрации ($S_{\beta+}$) детекторов позитронов и посредством этого для определения активностей препаратов, испускающих позитроны. Такой анализ необходим, т. к. аннигиляционные кванты возникают в определенном объеме, и для случая нельзя применить формулы для точечного источника. Указываются возможные пути учета или уменьшения влияния объемного распределения аннигиляции:

1) Численное интегрирование;

2) Увеличение расстояния между источником и детектором аннигиляционных квантов. Применение β абсорбента, и также использование эффективности регистрации $S_{\beta+}$ близко 100%.

Правильный выбор условий измерения дают возможность уменьшить влияние объемного распределения мест аннигиляций на точность определения эффективности регистрации позитронов ($S_{\beta+}$) до 10^{-3} и меньше.

1. Введение

То свойство позитронов, что они, соединяясь с электронами детектора, или замедляющей среды, за время порядка 10^{-9} сек испускаются в виде двух фотонов (однофотонным излучением можно пренебречь) возможно использовать для определения эффективности регистрации детекторов позитронного излучения. Эффективностью регистрации или счета называем отношение регистрированных и возникающихся частиц, в то же время эффективностью называем отношение чисел регистрированных и попадающихся в детектор частиц. Использование метода совпадений даёт возможность избегать коррекции, учитывающие специфические свойства источника и детектора, и таким образом получить более точные результаты.

Однако применение метода совпадений ($\beta^+\gamma^+$) затруднено, потому что даже в случае точечного источника позитронов позитроны аннигилируются в конечном объёме, линейные размеры которого в воздухе при 1 атм. составляют несколько метров, в твёрдом теле несколько мм в зависимости от энергии. Таким образом источник аннигиляционных квантов в зависимости от условий эксперимента может иметь значительный объём. Этим объясняется, что в настоящее время имеются только две попытки использования этого метода. А. Уилямсом [1] был использован протечный пропорцио-

нальный счётчик небольшого размера, где позитроны аннигилировались в основном в стенке счётчика. Зависимость вероятности детектирования аннигиляционных квантов от места аннигиляции учитывалась путём измерения зависимости счёта совпадений от расстояния детектора от источника и производилась экстраполяция на бесконечное расстояние. В измерениях, проведенных ранее автором [2], уменьшение объёма аннигиляции позитронов произведен в дополнительном измерении, в котором имелся абсорбент вокруг источника. Несмотря на то, что некоторые свойства метода рассмотрены в [3], более полный анализ возможностей и условий применения метода до настоящего времени не имеется.

2. Метод (β^+ γ^+) совпадений и условия его применимости

Общеизвестный метод совпадений [4], в случае точечного источника для схемы распада, показанного на рис. 1а., может быть характеризован следующими выражениями:

$$N_\gamma = DS_\gamma\,; \quad N_{\beta-} = DS_\beta\,; \quad N_{\beta\gamma} = DS_\gamma S_\beta\,. \tag{1}$$

Эти экспериментальные данные дают возможность определить активность (D) и эффективность детектирования гамма (S_γ) и бета (S_β) детекторов:

$$D = \frac{N_\gamma N_\beta}{N_{\gamma\beta}}\,; \quad S_\gamma = \frac{N_{\beta\gamma}}{N_\beta}\,; \quad S_\beta = \frac{N_{\beta\gamma}}{N_\gamma}\,. \tag{2}$$

Коррекции, необходимые из-за абсорбции γ квантов в β детекторе, также коррекции в случае более сложной схемы распада, даны в работе Кэмпиона [5].

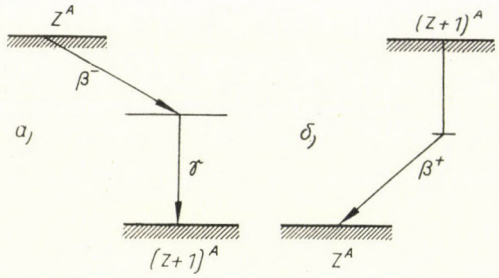

Рис. 1. Простейшие схемы а) β^- и б) β^+ распада, дающие возможность применить метод совпадений

В случае протяжённого источника, также для случая перехода в основное состояние путём эмиссии позитронов (рис. 1. б), подобные формулы могут быть написаны только для данной точки «источника» из-за зависимости

эффективностей от места возникновения кванта, и необходимо интегрировать по объёму для получения полного числа импульсов.

$$N_{\gamma\pm} = \int_V n(x,y,z)\, S_{\gamma\pm}(x,y,z)\, dv\,.$$

$$N_{\beta^+} = \int_V n(x,y,z)\, S_{\beta^+}(x,y,y)\, dv\,, \tag{3}$$

$$N_{\beta^+\gamma\pm} = \int_V n(x,y,z)\, S_{\beta^+}(x,y,z)\, S_{\gamma\pm}(x,y,z)\, dv\,,$$

где $n\ (x,\ y,\ z)$ — плотность аннигиляции, причём

$$\int_V n(x,y,z)\, dv = DP_{\beta^+}.$$

P_{β^+} — вероятность распада ядра путем эмиссии позитрона.

Как ниже покажем, между местом аннигиляции и фактом регистрации позитрона в детекторе, основанном на поглощении энергии, может быть установлено однозначное соответствие. Счетчиком позитронов будут зарегистрированы только те частицы, потеря энергии которых в чувствительном объеме счетчика больше некоторого порогового $E_{\text{пор}}$. Предполагая, что источник находится в положении 2π или 4π у детектора, тогда не дают счёт те позитроны, для которых $E_{\beta^+} < E_{\text{пор}}$ (аннигилируются вблизи источника), и релятивистские позитроны, с малой удельной ионизацией (аннигилируются далеко от источника). Этот означает, что $S_{\beta^+}(x,\ y,\ z) = 0$ вблизи источника и делеко от него, а в некотором промежутке $S_{\beta^+}(x,\ y,\ z) = 1$. То есть умножение на $S_{\beta^+}(x,\ y,\ z)$ под знаком интеграла может быть заменено изменением объёма интегрирования $V \to V_1$, если удовлетворены следующие соотношения:

$$S_{\beta^+}(x,y,z) = 0\,, \quad \text{если} \quad (x,y,z) \notin v_1\,,$$

$$S_{\beta^+}(x,y,z) = 1\,, \quad \text{если} \quad (x,y,z) \in v_1\,.$$

Таким образом уравнения (3) будут иметь следующий вид:

$$N^{\gamma\pm} = \int_V n(x,y,z)\, S_{\gamma^+}(x,y,z)\, dv,$$

$$N_{\beta^+} = \int_{V_1} n(x,y,z)\, dv, \tag{4}$$

$$N_{\beta^+\gamma\pm} = \int_{V_1} {}_n(x,y,z)\, S_{\gamma^+}(x,x,z)\, dv.$$

В этом общем случае уравнения типа (2) могут быть рассчитаны только путём численного интегрирования.

Однако можно показать, что условия измерений могут быть выбраны таким образом, чтобы погрешность, внесенная зависимостью эффективности γ^+ детектора от места аннигиляции, была маленькой или легко поддающейся подсчёту. Эти условия следующие (см. рис. 2.).

1. а) Нерегистрированные позитроны должны поглощаться в объёме V_2, линейные размеры которого намного меньше расстояния γ^+ детектора от источника. Это условие может быть удовлетворено. В случае 4π детекторов необходимо выбрать чувствительный объём и $E_{\text{пор}}$ таким образом,

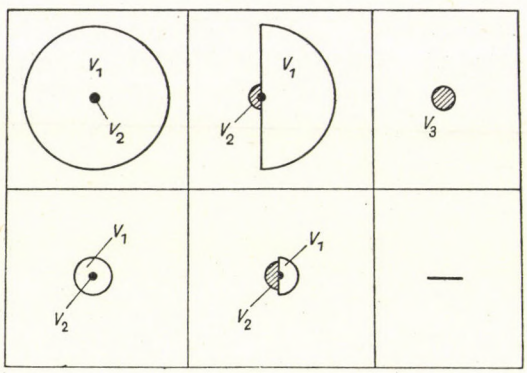

Рис. 2. Место аннигиляции нерегистрированных (штрихованная часть) и регистрированных позитронов (нештрихованная часть) в случае однородного поглощения в счетчике. $V = V_1 + V_2$

чтобы детектировались и релятивистские электроны, и в этом случае позитроны малой энергии ($E_{\beta^+} < E_{\text{пор}}$) аннигилируют вблизи источника. В случае 2π детекторов, кроме выполнения вышеуказанных требований, необходимо поместить β-поглотитель на противоположной с чувствительным объемом сторону источника, в котором на несколько мм-ов пути позитроны затормозятся. Применить данный метод в случае, когда β детектор удалён от источника, нельзя.

Учитывая это, $N_{\gamma\mp}$ принимает следующий вид:

$$N_{\gamma\pm} = \int_1 n(x,y,z)\, S_{\gamma\pm}(x,y,z)\, dv + \int_2 n(x,y,z)\, S_{\gamma\pm}(x,y,z)\, dv\,.$$

Разлагая второй член в ряд Тэйлора с остаточным членом первой степени и учитывая (4) получаем:

$$N_{\gamma\pm} = N_{\beta^+\gamma\pm} + \int_{V_2} n(x,y,z)\left[S_{\gamma\pm}(0,0,0) + x\frac{\partial}{\partial x} S_{\gamma\pm}(\Theta x, \Theta y, \Theta z) + \right.$$
$$\left. + y\frac{\partial}{\partial y} S_{\gamma\pm}(\Theta x, \Theta y, \Lambda z) + z\frac{\partial}{\partial z} S_{\gamma\pm}(\Theta x, \Theta y, \Theta z)\right] dv\,. \tag{5}$$

Выделяя первый член из интеграла и преобразуя выражение:

$$N_{\gamma^\pm} - N_{\beta^+\gamma^\pm} = S_{\gamma^\pm}(0,0,0)\int_{v_2} n(x,y,z)\,dv + R_1\,, \tag{6}$$

где $0 \leqslant \theta \leqslant 1$

$\int_{1_2} n(x,y,z)\,dv$ — число нерегистрированных позитронов

R_1 — поправочный член.

б) Проведем дополнительное измерение, в котором для всех позитронов выполняется условие, заданное в а), но объем может быть различным (V_3). Это может быть достигнуто путем приложения β поглотителей к источнику также со стороны (сторон) чувствительного объема. Разумеется, при этом не происходит регистрация позитронов. Число импульсов в этом случае:

$$N_{\gamma^\pm}^{\text{погл}} = \int_{v_2} n^{\text{погл}}(x,y,y)\,S_{\gamma^\pm}(x,y,z)\,a^{\text{погл}}(x,y,z)\,dv\,,$$

где $a^{\text{погл}}(x, y, z)$ — дополнительное поглощение в β поглотителе.

Разлагая и это в ряд Тэйлора, получаем выражение, аналогичное с (6).

$$N_{\gamma^+}^{\text{погл}} = {}_{\gamma^\pm}(0,0,0)\,a^{\text{погл}}(0,0,0)\int_{v_3} n^{\text{погл}}(x,y,z)\,dv + R_2\,, \tag{7}$$

где $\int_{v_3} n^{\text{погл}}(x, y, z)dv$ — полное число позитронов.

Вычитая соответствующие остаточные члены с обоих сторон уравнений (6) и (7), также разделяя уравнение (6) с уравнением (7) получаем вероятность того, что позитрон не будет зарегистрирован в β детекторе:

$$1 - S_{\beta^+} = a^{\text{погл}}\,\frac{N_{\gamma^\pm} - N_{\beta^+\gamma^\pm} - R_1}{N_{\gamma^\pm}^{\text{погл}} - R_2}\,. \tag{8}$$

При выводе этой формулы не делали никаких приближений. Для вычисления R_1 и R_2 можно делать приближения, но с этим вопросом займёмся только при рассмотрении возможной точности метода. При правильном выборе условий эксперимента в нулевом приближении можно с ними пренебречь.

2) В случае применения более плотного детектора (сцинтилляционного и полупроводникого счётчика, или пропорционального счетчика малого размера) условия эксперимента могут быть выбраны таким образом, чтобы уже при условиях счета позитронов все позитроны поглотились в объеме, линейные размеры которого намного меньше расстояния $\gamma^\pm$ детектора от источника.

В этом случае $N_{\gamma\pm}^{\text{погл}}$ может быть заменена на $N_{\gamma\mp}$.

$$N_{\gamma\pm} = S_{\gamma\pm}(0,0,0)\int_{v} n(x,y,z)\,dv + R_2^1 . \tag{9}$$

Преобразуется и уравнения (8):

$$1 - S_{\beta^+} = \frac{N_{\gamma\pm} - N_{\beta^+\gamma\pm} - R_1}{N_{\gamma\pm} - R_2^1} . \tag{10}$$

Легко видеть, что если R_1 и R_2^1 в (10) пренебрежимо малы, тогда (10) переходит в третье уравнение (2), действительное в случае совпадений с точечным источником.

Знание S_{β^+} дает возможность определить активность препарата в отношении испускания позитрона [третья формула (1)], и если определим другим путем активность в отношении захвата электронов из атомной оболочки, можно определить и полную активность и отношение ε/β^+.

Если распад происходит на возбужденный уровень, дополнительное измерение $(\beta^+\gamma)$ совпадений, и знание S_{β^+} дает возможность определить отношение ε/β^+ (см. например [1, 2]). В этом случае соответствующие формулы будут:

$$N_\gamma = DS_\gamma ; \qquad N_{\beta\gamma} = DP_{\beta^+} S_{\beta^+} S_\gamma ; \qquad P_{\beta^+} = \frac{1}{S_{\beta^+}} \frac{N_{\beta^+\gamma}}{N_\gamma} ,$$

где P_{β^+} — вероятность перехода на данный уровень путем испускания позитрона на один распада.

Замечание: Так как позитронный распад всегда сопровождён захватом электронов атомной оболочки, из данных измерений $(\beta^+\gamma)$ или $(\beta^+\gamma^\pm)$ совпадений отдельно не могут быть рассчитаны данные, получаемые из измерений $(\beta^-\gamma)$ совпадений.

3. Точность метода $(\beta^+\gamma^\pm)$ совпадений

Точность метода определяется величиной остаточных членов R_1 и R_2 или возможностью их точного расчёта. Величина R_1 дана выражением (5)

$$R_1 = \int_{v_2} n(x,y,z)\left(x\frac{\partial}{\partial x} + y\frac{\partial}{\partial y} + z\frac{\partial}{\partial z}\right) S_{\gamma\pm}(\theta x, \theta y, \theta z)\,dv.$$

Для оценки максимальной величины интеграла в место остаточного члена ряда Тэйлора запишем дифференциал эффективности регистрации

$dS_{\gamma\mp}$. Учитывая также приближённое равенство $S_{\gamma\mp} = \Omega\varepsilon$, где Ω — телесный угол, ζ — эффективность, остаточный член принимает следующий вид:

$$R_1 = \int_{v_2} n\,\Omega\,\varepsilon\,\frac{d\Omega}{\Omega}\,dv + \int_{v_2} n\,\Omega\,\varepsilon\,\frac{d\varepsilon}{\varepsilon}\,dv. \tag{11}$$

(Для краткости описания переменные опущены.)

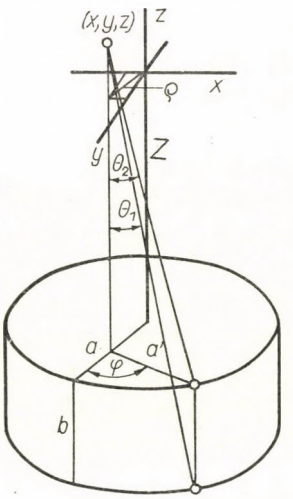

Рис. 3. Объяснение обозначений, встречающихся при определения гамма-эффективности для протяжённого источника

Дальнейшее приближение на основе формулы телесного угла по работе [6] даёт:

$$\frac{d\Omega}{\Omega} \sim \frac{3}{2}\,\frac{\varrho^2}{Z^2} \cdot \text{если}\ \frac{\varrho}{a}\ u\ \frac{a}{Z} \ll 1. \tag{12}$$

Так же по результатам, описанным в Приложении:

$$\frac{d\varepsilon}{\varepsilon} \simeq \frac{\varrho^2}{a^2} + 2\,\frac{z}{Z}. \tag{13}$$

Обозначения даны на рис. 3. Производя эти замены в (11) получаем:

$$R_1 \lesssim \left(\frac{3}{2Z^2} + \frac{1}{a^2}\right)\int_{v_2} n\,\Omega\,\varepsilon\,\varrho^2\,dv + \frac{2}{Z}\int_{v_2} n\,\Omega\varepsilon\,z\,dz. \tag{14}$$

Первый интеграл является достаточно малым, т. к. пропорционален с $(\varrho/Z)^2$. Покажем, что второй интеграл имеет такой же порядок малости. Для этой цели запишем приближенное равенство

$$\Omega\varepsilon \simeq (\Omega\varepsilon)_0\left(1 + \frac{d\Omega}{\Omega} + \frac{d\varepsilon}{\varepsilon} + \frac{d\varepsilon}{\varepsilon}\right)$$

во второй интеграл. Учитывая (12) и (13) и пренебрегая с членами третьего порядка малости и выше, получаем:

$$\frac{2}{Z}\int\limits_{v_2} n(\Omega\varepsilon)_0\, z\, dv + \frac{4}{Z^2}\int\limits_{v_2} n(\Omega\varepsilon)_0 z^2\, dv\,.$$

Легко показать, что в случае однородного абсорбента первый интеграл равен нулю. Объем v_2 является симметричным относительно плоскости $z = 0$, а подинтегральная функция нечетная т. к. функция распределения плотности аннигиляции симметричная, z асимметричная, а $\Omega\varepsilon)_0$ постоянная функция.

Учитывая, что $\varrho \sim$ и $\varrho \leqslant \varrho_{\max}$ (14) может быть переписано в следующую форму:

$$R_1 \lesssim \left(\frac{11}{2z^2} + \frac{1}{a^2}\right)\varrho^2_{\max}\int\limits_{v_2} n\, S^0_{\gamma\pm}\, dv\,.$$

Величина интеграла дает приближенное число аннигиляционных квантов, которые возникались в соответствующем объеме и были зарегистрированы $\gamma^{\pm}$ детектором.

По этому для остаточных членов действительны следующие ограничения:

$$\begin{aligned} R_1 &< \left(\frac{11}{2Z^2} + \frac{1}{a^2}\right)(\varrho^{v_2}_{\max})^2 (N_{\gamma\pm} - N_{\beta^+\gamma\pm}),\\ R_2 &< \left(\frac{11}{2Z^2} + \frac{1}{a^2}\right)(\varrho^{v_3}_{\max})^2 N^{\text{погл}}_{\gamma^\pm}, \qquad (16)\\ R'_2 &< \left(\frac{11}{2Z^2} + \frac{1}{a^2}\right)(\varrho^{\max}_{v})^2 N_{\gamma\pm}. \end{aligned}$$

Верхняя приставка у $\varrho_{\max}$ означает объем, в котором максимум должен быть взят. После этого выражения (8) и (10) могут быть написаны:

$$\begin{aligned} 1 - S_{\beta^+} &= a^{\text{погл}}\frac{(N_{\gamma\pm} - N^{\beta^+\gamma^\pm})(1 - r_1)}{N^{\text{погл}}_{\gamma^\pm}(1 - r)} =\\ &= a^{\text{погл}}\frac{\Phi_{\gamma\pm} - N_{\beta^+\gamma^\pm}}{N^{\text{погл}}_{\gamma^\pm}}(1 - r_1 + r_2 - r_1 r_2 + r_2^2 \ldots), \end{aligned} \qquad (17a)$$

$$\begin{aligned} 1 - S_{\beta^+} &= \frac{(N_{\gamma\pm} - N_{\beta^+\gamma\pm})(1 - r_1)}{N_{\gamma\pm}(1 - r'_2)} =\\ &= \frac{N_{\gamma\pm} - N_{\beta^+\gamma^\pm}}{N_{\gamma\pm}}(1 - r_1 + r'_2 - r_1 r'_2 + r'^2_2 \ldots), \end{aligned} \qquad (17б)$$

где

$$r_1 = \frac{R_1}{N_{\gamma^\pm} - N_{\beta^+\gamma^\pm}} < \left(\frac{11}{2Z_2} + \frac{1}{a^2}\right)(\varrho_{\max}^{\nu_2})^2,$$

$$r_2 = \frac{R_2}{N_{\gamma^\pm}^{\text{погл}}} < \left(\frac{11}{2Z^2} + \frac{1}{a^2}\right)(\varrho_{\max}^{\nu_3})^2,$$

$$r_2' = \frac{R_2'}{N_{\gamma^\pm}} < \left(\frac{11}{2Z^2} + \frac{1}{a^2}\right)(\varrho_{\max}^{\nu})^2.$$

Учитывая эти результаты, метод ($\beta^+\gamma^\pm$) совпадений может быть применен при следующих условиях:

1) В сущности при любых заданных параметрах эксперимента остаточные члены r_1, r_2 и r_2' могут быть рассчитаны с необходимой точностью. Современные счётно-решающие машины позволяют провести такие расчёты.

2) Условия эксперимента могут быть выбраны таким образом, чтобы остаточные члены были бы пренебрежимы при необходимой точности. Для примера оценим величину остаточных членов в случае 4π сцинтилляционного детектора позитронов. В этом случае максимальный пробег является достаточно малым, что даёт возможность применить второй метод (ур. 17б). Принимая $\varrho_{\max}^{\nu} = 5$ мм, $a = 25$ мм и $Z = 250$ мм, также учитывая, что пробег нерегистрированных позитронов намного меньше регистрированных ($\varrho_{\max}^{\nu_1} \ll \varrho_{\max}^{\nu}$), в первом приближении остаточные члены дают 5%-ную коррекцию в определении ($1 - S_{\beta^+}$). Однако ошибка определения S_{β^+} будет намного меньше, если используем большие значения S_{β^+}. Например при $S_{\beta^+} \sim 90\%$, и при указанных выше условиях пренебрежение с остаточными членами может внести систематическую ошибку меньше 0,5%, а при $S_{\beta^+} \sim 99\%$ меньше 0,05%.

В то же время полученные выше результаты показывают, что при применении метода необходимо появить некоторую осторожность, и пренебрегать с остаточными членами разрешается только при хорошей геометрии и высокой эффективности регистрации позитронов.

Автор считает своим приятным долгом выразить благодарность академику Ш. Салаи, директору Института, за обеспечение хороших рабочих условий и д-ру Д. Берени за полезные дискуссии.

ЛИТЕРАТУРА

1. A. Williams, Nucl. Phys., **52**, 324, 1964.
2. E. Vatai, Acta Phys. Hung., **20**, 217, 1966.
3. E. Vatai, Term. tud. doktori disszertáció, Kossuth L. Tudományegyetem, Debrecen, 1965.
4. S. De Benedetti and R. W. Findley, Encyclopedia of Physics, Edited by S. Flügge, Vol. 45. Nuclear Instrumentation I., pp. 255. Springer-Verlag, 1958.
5. P. J. Campion, Int. Journ. App. Rad. Isotopes, **4**, 232, 1959.

6. Приборы для регистрации ядерных излучений. Ред. А. Снелл. Перевод с англ. АТОМИЗДАТ, Москва, 1965, стр. 350.
7. A. L. Stanford and W. K Rivers, Rev. Sci. Instr., **29**, 406, 1958.

Приложение

Оценка $d\varepsilon/\varepsilon$

Целесообразным является применение аналитического выражения ε-а, которого можем получить из формулы, опубликованной Стендфордом и Риверсом в [7], заменой $h \to Z$ и $a \to a' = \varrho\cos\varphi + \sqrt{a^2 - \varrho^2 \sin^2\varphi}$. Обозначения см. на рис. 3.

Таким образом эффективность при данных z и ϱ даётся выражением:

$$\varepsilon = \int_0^{2\pi} (I_1 + I_2)\, d\varphi\,,$$

где

$$I_1 = \int_0^{\theta_1} \left\{1 - \exp\left[-\frac{\mu(E)\, b}{\cos\theta}\right]\right\} \sin\theta\, d\,\theta = \int_0^{\theta} i_1(\theta)\, d\,\theta,$$

$$I_2 = \int_{\theta_1}^{\theta_2} \left\{1 - \exp\left[\frac{\mu(E)\,(Z+z)}{\cos\theta} - \frac{\mu(E)\,(\varrho\cos\varphi + \sqrt{a^2 - \varrho^2\sin^2\varphi}}{\sin\theta}\right]\right\},$$

$$\sin\theta\, d\,\theta = \int_{\theta_2}^{\theta_1} i_2(\theta)\, d\,\theta$$

и

$$\theta_1 = \operatorname{arctg}\frac{a'}{b+Z}\,; \qquad \theta_2 = \operatorname{arctg}\frac{a'}{Z}\,.$$

Ищем производную, учитывая зависимость пределов интегрирования от ϱ и z.

$$\frac{\delta\varepsilon}{\delta\varrho} = \int_0^{2\pi} \left(\frac{\delta I_1}{\delta\varrho} + \frac{\delta I_2}{\delta\varrho}\right) d\varphi,$$

$$\frac{\delta I_1}{\delta\varrho} = \frac{\delta\theta_1}{\delta\varrho}\, i_1(\theta_1) + \int_0^{\theta_1} \frac{\delta\, i_1(\theta)}{\delta\varrho}\, d\theta,$$

$$\frac{\delta I_2}{\delta\varrho} = \frac{\delta\theta_2}{\delta\varrho}\, i_2(\theta_2) - \frac{\delta\theta_1}{\delta\varrho}\, i_2(\theta_1) + \int_{\theta_1}^{\theta_2} \frac{\delta\, i_2(\theta_2)}{\delta\varrho}\, d\delta\,.$$

Учитывая непрерывность функции поглощения $i_1(\Theta) = i_2(\Theta_1)$, также его исчезание на краях кристалла $i_2(\Theta_2) = 0$ и независимость $i_1(\Theta)$ от ϱ и z, то есть $\partial i_1(\Theta)/\partial\varrho = 0$, получаем следующее выражение:

$$\frac{\delta\varepsilon}{\delta\varrho} = \int_0^{2\pi} d\varphi \int_{\theta^1}^{\theta_2} \frac{\delta i_1(\theta)}{\delta\varrho}\, d\theta = \int_{\theta_1}^{2\pi} d\varphi \int_0^{\theta_2} \mu(E)\, \frac{\varrho \sin^2\varphi}{\sqrt{a^2 - \varrho^2 \sin^2\varphi}}\Bigg) \cdot$$

$$\cdot \exp\left[\frac{\mu(E)\,(Z+z)}{\cos\theta} - \frac{\mu(E)\,(\varrho\cos\varphi + \sqrt{a^2 - \varrho^2\sin\varphi}}{\sin\theta} \right] d\theta \cdot$$

Экспонент показывает, какая часть гамма излучения проходит через кристалл при $\Theta_1 < \Theta < \Theta_2$. Так как это всегда $\lesssim 1$, интеграл увеличивается при замене экспонента на единицу.

$$\frac{\delta\varepsilon}{\delta\varrho} \lesssim \int_0^{2\pi} \mu(E) \left(\cos\varphi - \frac{\varrho \sin\varphi}{\sqrt{a^2 - \delta^2 \sin^2\varphi}} \right) (\theta_2 - \theta_1)\, d\varphi\,.$$

При $\varrho \ll a$ и $a,\ b \ll z$ можем применить следующие приближения: $\Theta_1 \sim \dfrac{a}{b+Z}$. $\Theta_2 \sim \dfrac{a}{z}$ Учитывая разложения только до квадратичного члена по ϱ/a и a/z получаем:

$$\left|\frac{\delta\varepsilon}{\delta\varrho}\right| \lesssim \pi\,\mu(E)\,\frac{\varrho b}{Z(b+Z)}\,.$$

Аналогично:

$$\left|\frac{\delta\varepsilon}{\delta z}\right| \lesssim 2\pi\,\mu(E)\,\frac{ba^2}{Z(b+Z)^2}\,,$$

$$\varepsilon \sim \pi\,\mu(E)\,\frac{ba^2}{(b+Z)^2}\,.$$

В последнем случае учитывали разложение показательной функции до первого неисчезающего члена, и что в нашем случае $\mathrm{I}_2 \ll \mathrm{I}_1$.

Наконец

$$\frac{d\varepsilon}{\varepsilon} \lesssim \frac{1}{\varepsilon}\left(\left|\frac{\partial\varepsilon}{\partial\varrho}\right| \varrho + \left|\frac{\partial\varepsilon}{\partial z}\right| z \right) \lesssim \frac{\varrho^2}{a^2} + 2\,\frac{z}{Z}\,.$$

ON THE USE OF THE ($\beta^+ \gamma^{\pm}$) COINCIDENCE METHOD IN INVESTIGATIONS ON POSITRON EMITTING NUCLIDES

E. VATAI

Abstract

A detailed analysis of possibilities of the ($\beta^+ \gamma^{\pm}$) coincidence method for determination of positron detector counting efficiency ($S_{\beta+}$), and accordingly possibilities for positron activity determinations of sources are given. Such analysis is necessary, because the annihilation quanta are emitted from a finite volume, and the equations for a point source in this case are not valid. The following ways to account or reduce the effect of the annihilation spatial distribution are possible:

1) Numerical integration;

2) Increasing the distance between the source and detector of annihilation quanta. The use of beta absorbent and high value of counting efficiency ($S_{\beta+} \sim 100\%$).

The use of proper measurement parameters make possible to reduce the effect of spatial distribution of annihilation on the accuracy of counting efficiency ($S_{\beta+}$) determination to 10^{-3} or less.

Acta Physica Academiae Scientiarum Hungaricae, Tomus 23 (4), pp. 393—405, (1967)

EFFECT OF DISLOCATIONS ON GALVANOMAGNETIC PROPERTIES OF *n*-TYPE Ge

By

B. PŐDÖR

RESEARCH INSTITUTE FOR TECHNICAL PHYSICS OF THE HUNGARIAN ACADEMY OF SCIENCES, BUDAPEST

(Presented by G. Szigeti. — Received 20. XII. 1966)

In this paper the influence of dislocations on the carrier concentration and mobility in *n*-type germanium single crystals is examined both experimentally and theoretically. Conductivity and Hall effect was measured on plastically bent crystals over the temperature range 80—300 °K. From the experimental results a dislocation acceptor level, 0.33 eV below the conduction band edge is deduced. The electrostatic interaction energy of the captured electrons along the dislocation line and its dependence on the occupation rate of these acceptor centres is discussed. A theoretical formula for the scattering effect of charged dislocations is deduced. The experimental values of electron mobility measured perpendicularly to the dislocations are in reasonable agreement with the predictions of this formula.

1. Introduction

The dislocations generated by plastic deformation exert a strong influence on the electrical properties of semiconductor single crystals. There are broken bonds in diamond type semiconductor single crystals along the edge dislocation lines. Three of the valence electrons of the atoms situated on the dislocation line are paired, the fourth is unpaired. These dangling bonds may capture electrons from the conduction band, and they behave as acceptor centres. This effect is particularly important in *n*-type semiconductors. Moreover, the dislocations scatter the conduction electrons, thus their mobility is reduced.

In *n*-type semiconductors the mutual electrostatic interaction energy of the captured electrons along the dislocation line influences strongly the occupation statistics of these acceptor sites as pointed out by W. T. READ [1]. The distance between the broken bonds as well as between the acceptor centres along the dislocation line is considerably smaller than the mean distance between the dislocation lines. A mutual interaction exists between the electrons captured along the dislocation line. Moreover, they interact with the positive space charge formed around the negatively charged dislocation line. The electrons are captured by dislocations from the conduction band until the increase in electrostatic interaction energy of the electron prevents it.

The conduction electrons are scattered by the potential field of the negatively charged dislocation line and that of the surrounding screening positive space charge, and their mobility will be reduced.

The validity of READ's model was proved to some extent by the Hall effect and by the conductivity measurements on plastically bent n-type germanium, respectively [3], [4], [5]. This also applies to the Hall effect and magnetoresistivity measurements on n-type silicon single crystals deformed by plastic compression [6]. Different values of energy levels of these acceptors have been published by various authors: -0.2 eV [3], -0.18eV [4], -0.50 eV [5]. Fitting the theoretical curves based on READ's model to the experimental points, a dislocation density was considered, many times greater than that calculated from the bending radius. According to the majority of recent measurements the energy level associated with the dislocations in n-type germanium lies closer to the middle of the energy gap than stated in earlier works [8].

The effect of edge dislocations on the electron concentration and mobility in high purity n-type germanium has been examined in the present work. The energy level of acceptor centres associated with the dislocations and the interaction energy of electrons captured along the dislocation line has been determined. According to Hall constant versus temperature measurements the acceptor level associated with the dislocations lies about in the middle of the forbidden band. The experimental values of the electron mobility measured perpendicularly to the dislocations are in reasonable agreement with those calculated from the analysis of the scattering processes on charged dislocations.

2. Experimental techniques

High-purity Sb doped n-type germanium single crystals grown in our laboratory by the horizontal zone levelling method in direction [111] were used. Room temperature resistivity determined by the four-point probe technique was 25 Ω cm, donor concentration determined by low temperature Hall measurements was 6.5×10^{13} cm^{-3}. The initial dislocation density determined by the counting of etch pits on as-grown crystals was about $3-5\times$ $\times10^{3}$cm^{-3}.

Dislocations were generated by plastic bending. A structure of parallel dislocations can be generated in this way. Equation $N_{\mathrm{disl}} = (\mathrm{rb})^{-1}$ shows the dislocation density in terms of the bending radius and Burgers vector. Samples with dimensions of $14\times4.5\times1.2$ mm were cut from the crystal, the face with dimensions of 14×1.2 mm was perpendicular to the [112] axis. The longest edge formed an angle of 45° to the direction [111]. The bending axis was parallel to direction [112], the slip plane was the plane [111], and the Burgers vector was parallel to the direction [110] and perpendicular to the bending axis, i.e. to the direction of the dislocations. Samples were bent in graphite shapes of given curvature in a purified H_2 stream at 730 °C. The nominal

radii of curvature of the graphite shapes were 25, 50 and 150 mm, respectively, the nominal dislocation densities were 10^7, 5×10^6, and 1.6×10^6 cm^{-2}, respectively. Samples were plated with tin before deformation to prevent contamination during high temperature treatment [7]. This tin layer was removed by etching in hydrochloric acid after the deformation or heat treatment.

Samples were ground to 0.5 mm thickness after deformation. Potential probes, Sb doped gold leads, two on each side, were attached by thermocompression to the side planes of the samples. Current leads were soldered to the ends of the samples. Conductivity and Hall effect were measured by the d.c. compensation method between 80 and 300 °K. The magnetic field was 3300 Gauss, the current was perpendicular to the bending axis (direction of dislocations), and the magnetic field was perpendicular to both.

3. Experimental results

Typical results of our galvanomagnetic measurements on an as-grown, a heat-treated and a deformed sample are plotted in Figs 1, 2 and 3. According to these results acceptor centres were not produced merely by heat treatment. Tin plating prevented the contamination of the samples during the heat treatment. In bent crystals the electron concentration decreased as shown by

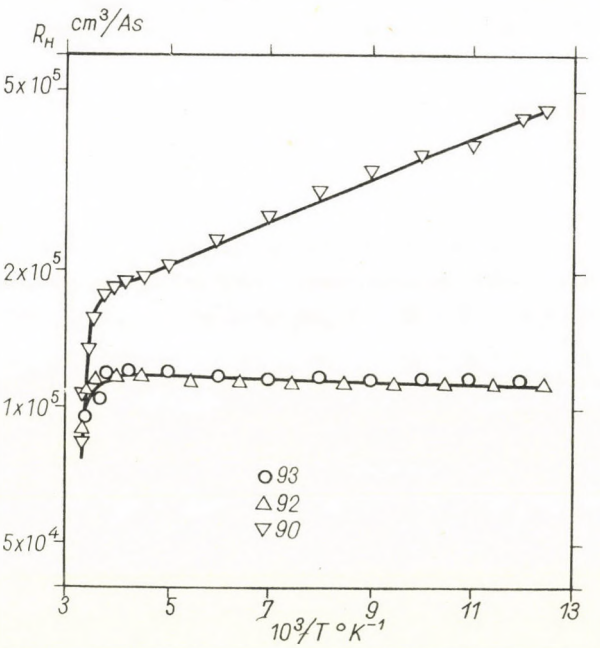

Fig. 1. Hall effect vs reciprocal temperature in deformed and undeformed samples. 93 — original, 92 — heat treated, 90 — bent sample, $N_{disl} = 10^7$ cm^{-2}

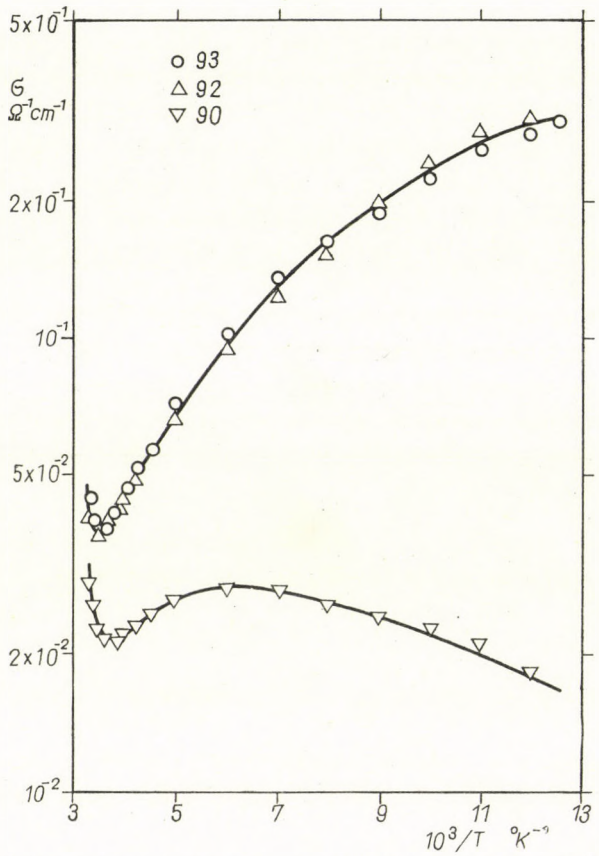

Fig. 2. Conductivity vs reciprocal temperature in deformed and undeformed samples. 93 — original, 92 — heat treated, 90 — bent sample, $N_{\text{disl}} = 10^7\ \text{cm}^{-2}$

Hall coefficient values of unbent and bent crystals. Edge dislocations generated by plastic deformation introduced acceptor energy levels in the forbidden energy gap. The occupation probability of these acceptor levels increases with decreasing temperature as seen in Fig. 1. Because of the scattering effect of dislocations the decrease of conductivity is greater than that of the carrier concentration. The mobility of electrons perpendicular to the dislocations is strongly reduced as shown in Fig. 3.

4. Interpretation of the experimental results

4.1. The change of the carrier concentration

In agreement with other publications [3], [4], [5], the results of our measurements show that in *n*-type germanium single crystals acceptor centres are introduced by plastic deformation. The occupation probability of these acceptors is a function of the temperature as shown in Fig. 1.

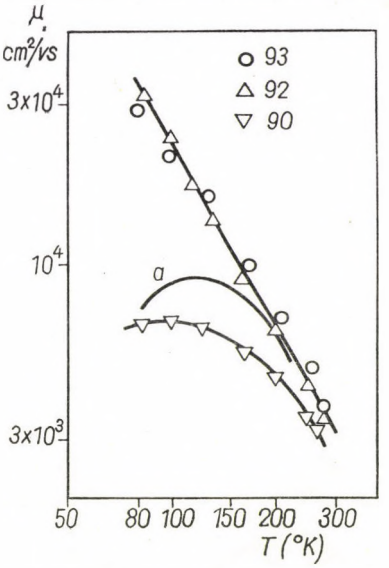

Fig. 3. Mobility vs temperature in deformed and undeformed samples. 93 — original, 92 — heat treated, 90 — bent sample, $N_{disl} = 10^7$ cm^{-3}. *a* — computed curve for the bent sample, based on eq. (11)

According to READ's model the occupation probability of these acceptor sites is controlled by the electrostatic interaction energy of the electrons along the dislocation line, and by the energy level of these acceptor centres. The total energy of electrons captured on the dislocation line is the sum of the acceptor energy and of the interaction energy.

These acceptor centres are occupied at absolute zero temperature provided the total energy of a single captured electron does not exceed the energy level of the shallow donor states below the conduction band. With rising temperature an increasing number of captured electrons leaves the dislocation states, and enters the conduction band, and the occupation probablility of these acceptor sites decreases.

This process might be described by the statistical methods used in semiconductors. The energy of the captured electron consists of two parts, one of which is the function of the occupation probability. The following model is essentially identical with the model called "Fermi statistics" in [1].

Supposing there are shallow donor and deep acceptor levels in the forbidden band with densities N_d and N_a respectively, we have to consider the temperature range high enough to completely ionize the shallow donor levels. Further, if it is not high enough to create a significant number of holes in the valence band, then the Fermi level is far from the lower edge of the conduction band, and Maxwell—Boltzmann statistics can be applied to the description of the electrons in the conduction band and the contribution of holes can be

neglected. The Fermi level may lie close to the deep acceptor levels, and for describing their occupation probability, Fermi—Dirac statistics are to be used.

Electrons lost by the donors enter either the conduction band or the deep acceptor states, and

$$N_d = n + n_a, \tag{1}$$

where n is the concentration of the electrons in the conduction band, n_a is the concentration of the electrons captured on the acceptor levels. Denoting

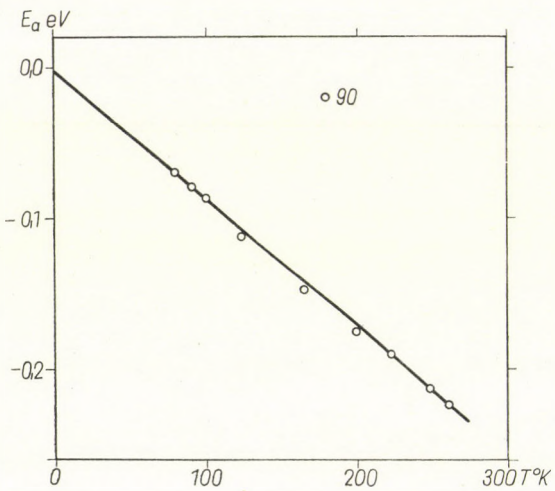

Fig. 4. Total energy of captured electrons on the dislocation vs temperature. 90 — bent sample, $N_{\text{disl}} = 10^7\ \text{cm}^{-2}$

the density of states at the lower edge of the conduction band by N_c, we obtain

$$n = N_c \exp \frac{E_F}{kT}\,. \tag{2}$$

The positive direction of energy points from the valence band to the conduction band, and the lower edge of the conduction band is the zero level. Denoting the total energy of the electrons captured at the acceptor sites by E_a, then

$$n_a = \frac{N_a}{1 + 1/2 \exp \dfrac{E_a - E_F}{kT}} \tag{3}$$

is obtained.

The 1/2 factor in the denominator accounts for the degeneration according to the spins [10]. From (1), (2) and (3).

$$n\frac{N_a - N_d + n}{N_d - n} = \frac{N_c}{2}\exp\frac{E_a}{kT}\,. \tag{4}$$

Expression (4) was used to interpret the experimental results. Equating N_d with the donor concentration measured on the undeformed samples, and determining N_a from the dislocation density calculated from the bending radius and from the distance between the broken bonds along the dislocation line, we obtain

$$N_a = \frac{N_{\text{disl}}}{c} = \frac{1}{c\,b\,r}\,.$$

Carrier concentration has been determined from the Hall coefficient, measured on bent samples.

The density of states at the lower edge of the conduction band with $m_{\text{eff}} = 0.39$ m is, according to [10],

$$N_c = 2\left(\frac{2\pi\, m_{\text{eff}}\, kT}{h^2}\right)^{3/2}.$$

The total energy of the captured electrons, E_a, was determined by this procedure in several samples at several temperature values. A typical set of values is shown in Fig. 4. The $E_a(T)$ curves in all samples considered are very close to one another. The temperature dependence of the total energy, E_a, is nearly linear in the temperature range 80—270 °K. Extrapolating this straight line to $T = 0$ °K the energy axis is intersected at about $E = 0$ eV energy at the lower edge of the conduction band. The temperature dependence of the total energy of captured electrons can be approximated as

$$E_a = -8{,}6\cdot 10^{-4}\,T$$

(E_a in eV and T in °K). The value of this constant is in good agreement with the value of -8.0×10^{-4} eV/°K deduced from a slightly different model [11]. But it differs significantly from the value of -4×10^{-4} eV/°K, describing the temperature dependence of the forbidden band in germanium. The fact that the extrapolated values of E_a at absolute zero temperature are nearly equal to zero justifies the validity of the basic assumptions of the model.

Plotting E_a versus the occupation probability of the acceptor sites, f, and extrapolating it to the value of $f = 0$, the energy of the acceptor levels

and the electrostatic interaction energy can be separated, since the electrostatic energy becomes zero when $f = 0$. The occupation probability, f, can be deduced from the following expression

$$f = \frac{Nd - n}{N_a} = \frac{c}{N_{\text{disl}}} (Nd - n) .$$

A typical set of values of E_a versus f is plotted in Fig. 5. The points lie along a straight line in a good approximation. The energy of the acceptor levels is

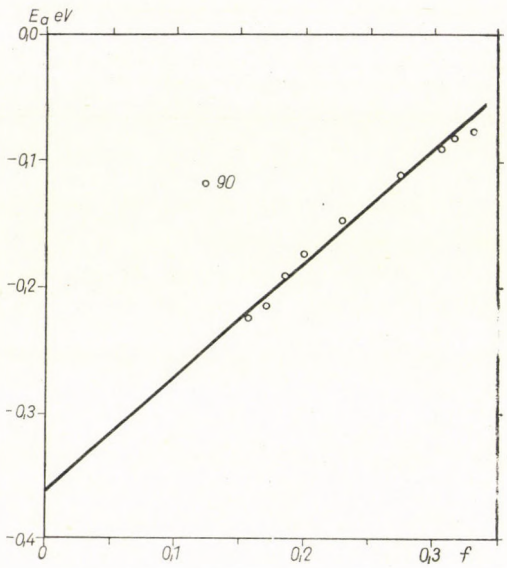

Fig. 5. Total energy of captured electrons on the dislocation vs occupation probability. ○ 90 — bent sample, $N_{\text{disl}} = 10^7$ cm^{-2}

given by the intersection of this straight line with the energy axis, and the electrostatic interaction energy is given by the slope of this straight line multiplied by f. The slopes of the different curves plotted for the different samples are nearly equal, and the average value is

$$C = \frac{E_{\text{el}}}{f} = (1{,}53 \pm 0{,}5)\,\text{eV} .$$

The value of the constant of the interaction energy can be interpreted using the following simple model. The screened potential of the charged dislocation can be deduced from the Poisson equation as follows (c.f. [12]),

$$U(r) = -\frac{ef}{2\pi\, ec} K_0\left(\frac{r}{\lambda_D}\right) , \tag{5}$$

where ε is the dielectric constant, $K_0(x)$ is the zero-order Bessel function of the second kind, c is the distance between the acceptor centres along the dislocation line, r is the distance measured from the dislocation line, and λ_D is the Debye length

$$\lambda_D = \left(\frac{\varepsilon kT}{e^2 n} \right)^{1/2}. \tag{6}$$

The electrostatic energy of a captured electron in this potential field is

$$E_{\mathrm{el}} = \frac{e^2 f}{2\pi \varepsilon c} K_0 \left(\frac{d}{\lambda_D} \right),$$

where d is a distance of the order of the lattice constant, characterizing the localization of the captured electrons in the dislocation.

We obtain $\lambda_D = 6 \times 10^{-5}$ cm from equation (6), with the following typical values for the parameters: $\varepsilon/\varepsilon_0 = 16$, $T = 100$ °K, $n = 2 \times 10^{13}$ cm^{-3}, if $d = 6 \times 10^{-8}$ cm, which is nearly equal to the lattice constant, then $d/\lambda_D = 10^{-3}$. From the series expansion valid for small values of the argument of $K_0(x)$ we have

$$K_0(10^{-3}) \cong -0{,}577 - \ln \frac{10^{-3}}{2} \cong 7.$$

Then we obtain from (5) with the value of $c = 4 \times 10^{-8}$ cm

$$C = \frac{E_{\mathrm{el}}}{f} = 3{,}1 \text{ eV}.$$

This value is of the same order of magnitude as the corresponding experimental result. This agreement between the experimental and theoretical values is not strongly influenced by the exact localization of the captured electron because of the properties of the logarithmic function. We obtain the energy of the acceptor level, E_{a0}, extrapolating the E_a values to $f = 0$. The mean value of this energy level is

$$E_{a0} = -(0{,}33 \pm 0{,}07) \text{ eV}.$$

This value of the energy level lies between the values published by other authors obtained by Hall measurements on bent crystals (c.f. -0.2 eV [3], -0.18 eV [4], -0.5 eV [5]), and is very near to the value of -0.28 eV obtained from the data of [11], extrapolating to $f = 0$. It is interesting to note that in works [3] and [4] it was necessary in the analyses based on READ's model to use 3—8 times greater dislocation densities than those calculated from the

bending radius. Measurements of the lifetime of non-equilibrium minority carriers in plastically deformed germanium resulted in an energy level about in the middle of the forbidden band [13], and later —0.4 eV [8]. The result of the measurement of the spectral response of photoconductivity in plastically deformed germanium at about 80 °K was —0.45 eV [9].

From recent measurements we concluded that the energy level of dislocations lies closer to the middle of the conduction band than determined in [3], [4] and [5] based on READ's analysis.

5. Interpretation of the experimental results

4.2. Effect of dislocations on electron mobility

Electron mobility perpendicular to the dislocations is strongly reduced below room temperature as shown in Fig. 3. The decrease in mobility is slightly higher than that appearing in [3], [4], [14].

The decrease of electron mobility can be interpreted on the basis of the scattering effect of the potential field around the charged dislocations. Scattering effect reduces the mean free path of the electrons perpendicular to the dislocations, but has a negligible effect on the mean free path of electrons parallel to the dislocations. Another mechanism appears to play a role, too, as stated in [2]. According to this work, the macroscopic mobility of electrons can be reduced because of the curved path of electrons avoiding the space charge cylinders around the charged dislocations.

The scattering effect of the potential field of the dislocations has been treated theoretically [18]. The scattering cross-section as well as the relaxation time can be determined, with a knowledge of the scattering potential. Relaxation time can be expressed by the scattering cross-section, according to [15], in the case of cylindrical symmetry as follows

$$\tau_{\text{dis}}^{-1} = N_{\text{dis}} v_{\perp} \int_0^{2\pi} (1 - \cos\vartheta) |A(\vartheta)|^2 d\vartheta, \tag{7}$$

where $|A(\vartheta)|$ is the absolute value of the scattering amplitude, the square of which is equal to the scattering cross-section, $v_{\perp}$ is the component of electrons velocity perpendicular to the dislocations, and N_{dis} is the dislocation density. The scattering amplitude can be determined using the Born approximation. Treating the cylindrical symmetric case similarly to the spherical one (c.f. [16]), the scattering amplitude is obtained from the following expression

$$|A(\vartheta)| = \frac{me\sqrt{2\pi}}{\hbar^2\sqrt{k_{\perp}}} \int_0^{\infty} U(r) I_0\left(2k_{\perp} r \sin\frac{\vartheta}{2}\right) r\, dr, \tag{8}$$

where m is the effective mass of electrons, $k_\perp$ is the component of the electron wave number vector perpendicular to the dislocations, and $I_0(x)$ is the zero order Bessel function of the first kind. Substituting the potential (5) into expression (8), and integrating it, the scattering amplitude

$$|A(\vartheta)| = \frac{me^2 f \sqrt{2\pi}}{2\pi \varepsilon a \hbar^2 \sqrt{k_\perp}} \cdot \frac{1}{\lambda_D^{-2} + 4k_\perp^2 \sin^2 \frac{\vartheta}{2}}$$

is obtained. Substituting this expression for the scattering amplitude into (7), and integrating it, the following result is obtained:

$$\tau_{\text{disl}} = \frac{8\varepsilon^2 a^2 m^2 \left(\frac{\hbar^2}{4m^2 \tau_D^2} + v_\perp^2 \right)^{3/2}}{N_{\text{disl}} e^4 f^2 \lambda_D} . \tag{9}$$

The electron mobility can be obtained by solving the Boltzmann transport equation. According to the usual method the electron mobility in an arbitrary direction is

$$\mu = \frac{e}{kT} \cdot \frac{\int \tau v^2 x f_0 d^3 \vec{v}}{\int f_0 d^2 \vec{v}} , \tag{10}$$

where v_x is the x component of electron velocity vector, f_0, is the classical distribution function of electrons ($f_0 \sim \exp - E/kT$). Substituting expression (9) for the relaxation time into (10), and performing the integration approximately (in the temperature range considered the neglect of the first term in the brackets in (9) does not cause serious errors), and for the electron mobility perpendicular to the dislocations we obtain

$$\mu_{\text{disl}} = \frac{30 \sqrt{2\pi}\, \varepsilon^2 a^2 (kT)^{3/2}}{N_{\text{disl}} e^3 f^2 \lambda_D m^{1/2}} . \tag{11}$$

This expression was used for the interpretation of the mobility measurements. Equation (11) is slightly different from the corresponding expression given in [16], based on a potential function, different from (5). Equation (11) indicates a stronger scattering than the corresponding expression in [16] with corresponding screening. The mobility given by (11) is smaller by an order of magnitude than the expression given in [8], standing for the scattering effect of the mechanical deformation field around the dislocation line. Since the reciprocal values of the relaxation times resulting from different physical mechanisms are additive, the scattering caused by the charge of dislocations in n-type semiconductors gives the dominant effect below room temperature.

The mobility measured on deformed samples is the resultant of the scattering of electrons by acoustic phonons and by charged dislocations. The resulting mobility in usual approximation is

$$\mu_{\text{def}}^{-1} = \mu_{\text{disl}}^{-1} + \mu_{\text{lattice}}^{-1}. \tag{12}$$

The lattice mobility, μ_{lattice}, caused by the scattering of electrons by acoustic phonons has been determined using the deformation potential theory [10]. In n-type germanium this is equal to the mobility measured on relatively pure samples, below room temperature. In our case it is equal to the mobility measured on undeformed samples.

The mobility in deformed crystals was determined from the expressions (11) and (12). The dislocation density, N_{disl}, was calculated from the bending radius, and the Debye length was calculated from carrier concentrations measured on bent crystals. The following values of the parameters were used: $\varepsilon/\varepsilon_0 = 16$, $m/m_{\text{electron}} = 0.3$, $c = 3.5 \times 10^{-8}$ cm. The calculated curve for one typical sample is plotted in Fig. 3 together with the measured values. The difference between the calculated and measured values is less than a factor of 2, therefore this agreement can be regarded as reasonable.

I wish to express my acknowledgement to Dr. Z. Bodó for valuable discussions, and to Mr. T. Németh for having prepared the germanium crystals and for his assistance in the course of the chemical work.

REFERENCES

1. W. T. Read, Phil. Mag., **45**, 775, 1954.
2. W. T. Read, Phil. Mag., **46**, 111, 1955.
3. G. L. Pearson, W. T. Read and F. J. Morin, Phys. Rev., **93**, 666, 1954.
4. R. A. Logan, G. L. Pearson and D. A. Kleinmann, J. Appl. Phys., **30**, 885, 1959.
5. R. M. Broudy, Advances in Physics, **12**, 135, 1963.
6. K. Kamada, J. Phys. Soc. Jap., **15**, 998, 1960.
7. Т. Р. Фигиельски, А. Д. Беляев, ФТТ, **6**, 2146, 1964.
8. M Jastrzebska and T. Figielski, phys. stat. sol., **7**, K101, 1964.
9. Z. Golacki, T. Figielski and M. Jastrzebska, phys. stat. sol., **11**, K35, 1965.
10. S. R. Smith, Semiconductors, Cambridge University Press, 1965.
11. Ю. В. Гуляеч, ФТТ, **3**, 1094, 1961
12. В. Л. Бонч-Бруевич, В. Б. Гласко, ФТТ, **3**, 36, 1961.
13. G. K. Wertheim and G. L. Pearson, Phys. Rev., **107**, 694, 1957.
14. Л. И. Колесник, ФТТ, **6**, 1253, 1964.
15. В. Л. Бонч-Бруевич, ФТТ, **3**, 47, 1961.
16. Е. М. Кузнецова, ФТТ, **3**, 1987, 1961.
17. D. L. Dexter and F. Seitz, Phys. Rev., **86**, 964 1952.
18. B. Pődör, phys stat. sol., **16**, K167, 1966.

ВЛИЯНИЕ ДИСЛОКАЦИЙ НА ПЛОТНОСТЬ И ПОДВИЖНОСТЬ НОСИТЕЛЕЙ ТОКА ГЕРМАНИЯ *n*-ТИПА

Б. ПЭДЭР

Р е з ю м е

В этой работе экспериментально и теоретически рассмотрено влияние дислокаций на плотность и подвижность носителей тока в монокристаллах германия n-типа. Электропроводность и эффект Холла были измерены в области температур от 80 до 300 °К на пластично изогнутых кристаллах. Из экспериментальных результатов получено положение акцепторных уровней, связанных с дислокациями, на расстоянии 0,33 эв от дна зоны проводимости. Рассмотрен вопрос об электростатической энергии взаимодействия электронов на дислокации и вопрос о зависимости этой энергии от степени заполнения вышеупомянутых акцепторных уровней. Теоретически получено выражение для описания рассеивающего действия заряженных дислокаций. Экспериментальные значения подвижности электронов, измеренные перпендикулярно на дислокации, удовлетворительно согласуются с предсказанными этой формулой значениями.

Acta Physica Academiae Scientiarum Hungaricae, Tomus 23 (4), pp. 407—414, (1967)

INVESTIGATION OF THE SIGNAL SHAPE GIVEN BY $n-p$ AND $p-n$ TYPE SEMICONDUCTOR DETECTORS WITH PULSE SHAPE DISCRIMINATION

By

GY. MÁTHÉ

NUCLEAR RESEARCH INSTITUTE OF THE HUNGARIAN ACADEMY OF SCIENCES, DEBRECEN

(Presented by A. Szalay — Received 20. XII. 1966)

The pulse shapes of $n - p$ and $p - n$ show a wide variation if the range of the detected particle exceeds the width of the depletion layer. Thus, long-range particles can be eliminated from the spectrum with a pulse shape discriminator. Owing to local defects some detectors supply pulses of less than the usual height, which results in the appearance of a "tail" in the spectrum. These pulses can be eliminated from the spectrum with pulse shape discrimination.

Introduction

A general trend in modern nuclear particle detection is to obtain maximum information from the signals given by the detectors. Thus, the number of detected particles can be determined from the number of counts and the energy of the particles from the pulse height. With scintillation detectors and ionization chambers the detected particles can be identified by the rise-time of the pulses [1—4]. This concept of the possibility of obtaining information about the nature of the particle was also raised when semiconductor detectors first appeared. Based on theoretical considerations, several authors calculated the rise-time of pulses to be expected with different kinds of detectors [5—8]. Others determined experimentally the slope of the pulses as a function of the voltage applied on the detector [8—10]. In the case of lithium ion-drift detectors, C. A. J. AMMERELAN et al. [11] and J. C. LEGG [12] succeeded in discriminating particles above the energy of 8 MeV by the aid of pulse shape discriminators. It has been shown by several authors that in the case of particles with a range longer than the depletion layer width of the detector the rise-time of pulses obtained from the detectors became considerably longer than the rise-time of pulses obtained when the particle remained within the depletion layer [13, 14]. This phenomenon was later used by J. O. FUNSTEN [15] to eliminate particles passing through the detector from the energy spectrum.

In the course of our measurements we investigated by the aid of a base-line cross-over type of pulse shape discriminator the properties of pulse shapes given by $p - n$ and $n - p$ type detectors of different resistances. As a result of the experiments we found, in agreement with the literature [11, 12], that

at lower energies it was not possible to discriminate the particles owing to the considerable fluctuation shown in pulse shape. We assume the fluctuation in the rise-time of pulses to be the result of noises of various origin. Pulses passed through amplifiers of limited band-width are probably not suitable for the precise measurement of pulse rise-time.

Even under these restricted conditions the pulse shape discriminator proved to be useful for the detection of pulses given out by particles with a range even slightly longer than the depletion layer width, and for eliminating them from the measured spectrum, if necessary. Another possibility was given as well, namely, that with some detectors where presumably there was a discontinuity in the material which caused the appearance of tails on the low-energy side of peaks, such pulses could be eliminated by their rise-time, which differed from the usual rise-time.

Experimental conditions

In our investigations we attempted to discriminate alpha particles and protons. The alpha particles were obtained from a Th(C + C') source and the required energy was reached by air damping. Protons were produced by the reaction $^{10}B(d, p)^{11}B$ induced by deuterons obtained from the 700 kV cascade generator of the Institute, and the required energy was reached by damping with Al foils.

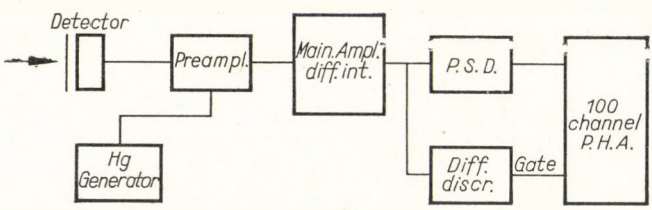

Fig. 1. The schematic block diagram of the measuring apparatus. The amplified signals of the detector are converted by the PSD zero cross-over type pulse shape discriminator to pulses proportional in height to the rise-time of pulses. The "time spectrum" is measured by a 100 channel amplitude analyser. The analyser is gated by a differential discriminator permitting the analysis of a narrow energy interval only

The measurements were carried out on three different detectors. One of them was an *n*-type detector with 200 mm^2 surface and 800 Ohm.cm resistance, the second one with 16 mm^2 surface and 2000 Ohm.cm resistance was a detector with a surface blocking layer prepared from *n*-type base material and the third was a detector with a diffusion blocking layer, with a 7 mm^2 surface and 10 000 Ohm.cm resistance prepared from *p*-type base material. The schematic block diagram of the measuring apparatus can be seen in Fig. 1.

The pre-amplifier was constructed on the basis of principles worked out by R. L. CHASE et al. [16]. In the measurements where the rise-time of pulses given by the detector was studied, the charge-sensitive feed-back and boot-strapping were disconnected from the pre-amplifier, because this decreased the band-width of the system and caused it to depend on the voltage applied on the detector. In the above conditions pulses with a rise-time of 0.1 μsec passed through the pre-amplifier without distortion.

The main amplifier is supplied with a single integrating and differentiating circuit usual for semiconductor detectors. Without integration and differentiation it transmits pulses with a rise-time of 0.2 μsec without distortion. When measuring rise-time we took great care not to change the parameters of the amplifier within a set of measurements because variation of the amplifier gain might lead to a slight variation of the amplifier band-width, and this would falsify the results of the measurement.

The noise of the electronic system was 10 keV. Measuring the alpha spectrum of the Th(C + C') preparate we obtained a resolving power of 40 keV with the 200 mm^2 $p - n$ detector, 20 keV with that of 16 mm^2 and 20 keV with the 7 mm^2 $n - p$ detector.

For pulse shape discrimination the base-line-cross-over system was applied, and this proved to be successful in the case of scintillation counters [17]. By its aid even 1 nsec differences in the rise-time could be detected. The system converts the differences in the rise-time to pulse-height variations with a time-to-amplitude converter circuit. Thus, the amplitude spectrum appearing at the output is the "time-spectrum" of the rise-time of pulses given by the detector.

The amplified signals of the detector are sent beside the pulse shape discriminator to a differential discriminator and its signals are used to gate the multi-channel analyser measuring the time spectrum. In this way we could always select a narrow band from the relatively wide energy spectrum set by the absorbents. Thus, the energy dependence could not influence the results of measurements.

As has already been mentioned in the Introduction and as will be seen later, particle identification is restricted by the fluctuation shown in rise-time, because the fluctuation considerably widens the peaks of the time spectrum, so that the peaks belonging to different particles become undistinguishable. The question might be raised whether the widening of peaks is, perhaps, the consequence of the selective properties of the pulse shape discriminator. To answer this question we produced signals similar to the signal of the semiconductor detectors with a Hg relay, and investigated their rise-time for different signal to noise ratios. The measurements proved that the broadening was caused mainly by the noise of the detector and the amplifier.

In order to obtain quantitative data at the evaluation of time spectra

on the differences shown in the rise-time, the signals of the calibrating pulse generator were integrated in a different degree. Thus, data can be given on the length of time corresponding to a channel on the time spectra. These values are given in nsec in each Figure.

Experimental results

Before investigating the rise-time of pulses it is absolutely essential to determine at a given voltage on the detector the maximum energy where the proton still remains within the sensitive volume of the detector. For this

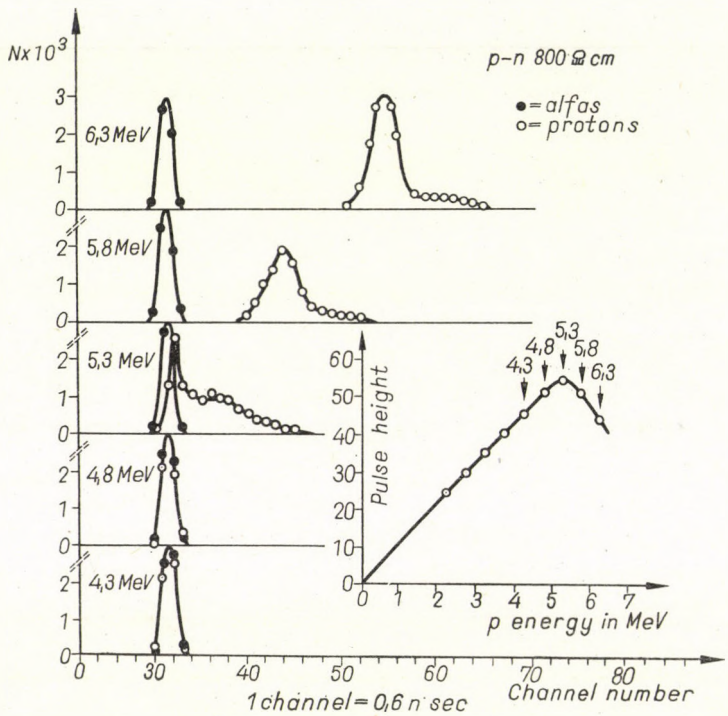

Fig. 2. The time spectrum of $p-n$ 800 Ohm · cm detector for alpha particles and protons

purpose the pulse-height distribution was taken in dependence on the energy. At the energy where there is a deviation from the straight line obtained, the range of the particle is equal to the width of the depletion layer. At energies above this a decrease in the pulse amplitude follows and a slow component due to the diffusion of charge carriers [13] in the rise-time of the pulses.

Results obtained with the 800 Ohm.cm p — n detectors can be seen in Fig. 2 and those obtained with the 10 000 Ohm.cm n — p detectors in Fig. 3. The inset shows the energy-pulse height dependence for protons at a given

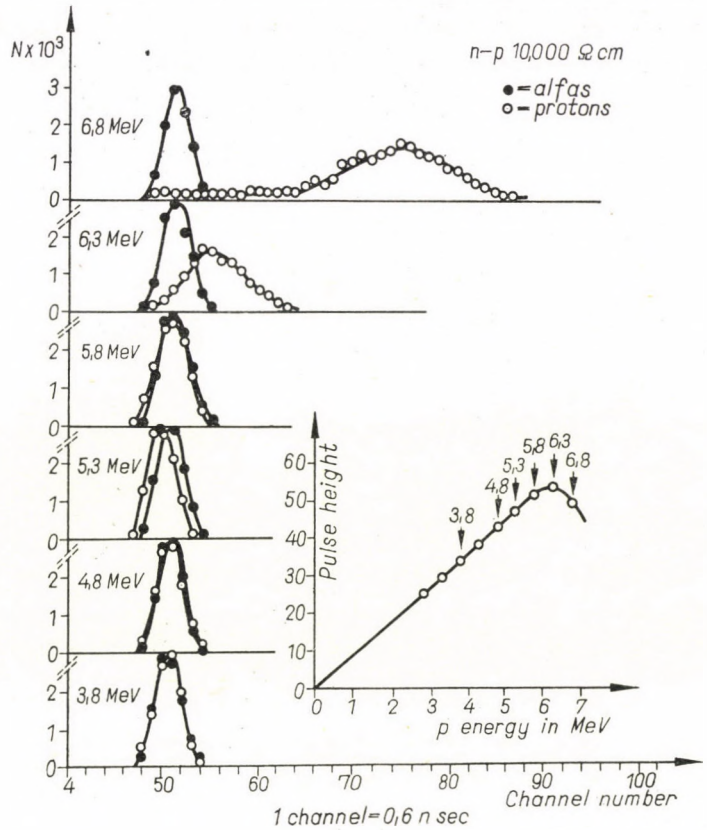

Fig. 3. The time spectrum of $n-p$ 10 000 Ohm · cm detector for alpha particles and protons

detector voltage. The results of the 2000 Ohm.cm detector are essentially identical with those shown in Fig. 2 and, therefore, they are not presented separately.

With *$p-n$ detectors* in the case of energies where the proton remains within the depletion layer there is not even the slightest difference between the rise-time of pulses given by alpha-particles and by protons. At the energy where the length of the proton trace reaches and exceeds the width of the detector, pulses of longer rise-time appear very sensitively. From the shape of the proton time spectrum it follows also that at this critical energy some particles remain wholly within the depletion layer, while the range of others is already longer. This may be due to two causes, either the energy band chosen is too wide, therefore there are particles with shorter and longer ranges as well, or the width of the depletion layer is not homogeneous enough. In any case, it can be seen that the applied pulse shape discrimination offers a sensitive method to study the width of the depletion layer.

At higher energies where the range of protons exceeds the width of the depletion layer the rise-time of the pulses becomes longer and longer. On the other hand, the rise-time of pulses given by alpha particles maintains a constant value independent of their energy.

The fluctuation shown in the rise-time, i.e. the width of the peaks, is considerably greater than the pulses having a diffusion origin.

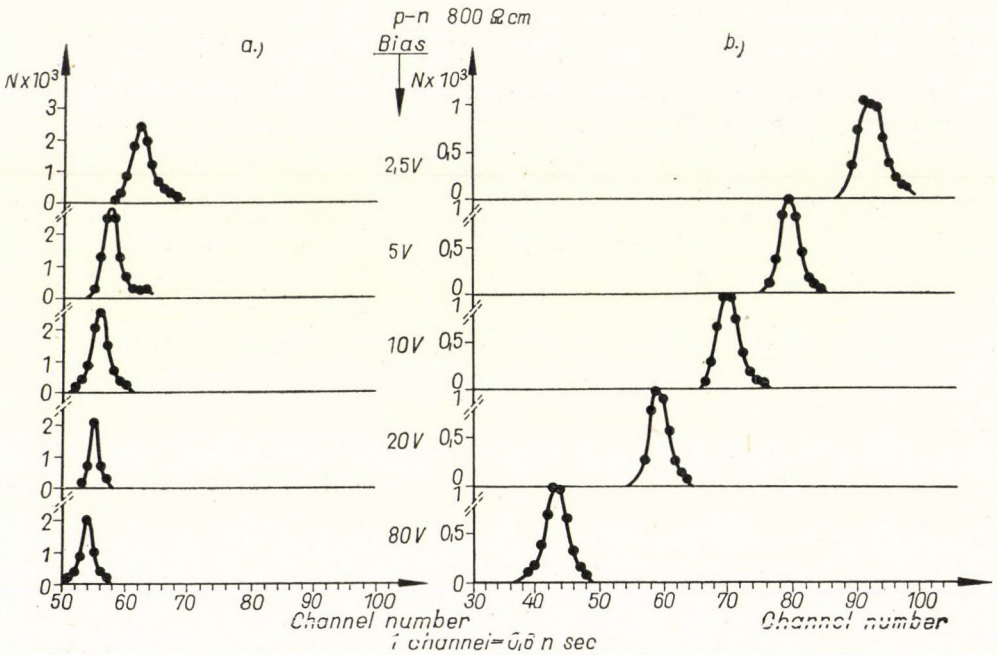

Fig. 4. The time spectra of the signals given by the $p-n$ 800 Ohm · cm detector at different voltages on the detector, a) without charge sensitive feed-back, b) with charge sensitive feed-back. The ~6 MeV alpha particles of Th(C + C') were detected

With n — p *detectors* the results obtained were similar to the former case, the only difference being that, in agreement with theoretical calculations [5, 6], here the protons could be separated from alpha particles even if the proton remained inside the sensitive volume and its range approached the width of the depletion layer. Unfortunately, the difference in the rise-time is so small at the given energy and the fluctuation in the rise-time is so great that this is not applicable for particle separation. The behaviour of the detector was investigated at lower energies and according to expectations its separation properties became worse. Because of its limited working data the detector could not be used at higher energies to observe the separation of the alpha peak from the proton peak.

The rise-time of pulses given by alpha particles is independent of the energy of the particles, as with $p - n$ detectors. This fact makes it possible to select, with the aid of a differential discriminator, those particles from the spectra measured by semiconductor detectors, which remain inside the depletion layer. However, it must be noted that the variation of the detector voltage changes the rise-time of signals given by particles remaining inside the deple-

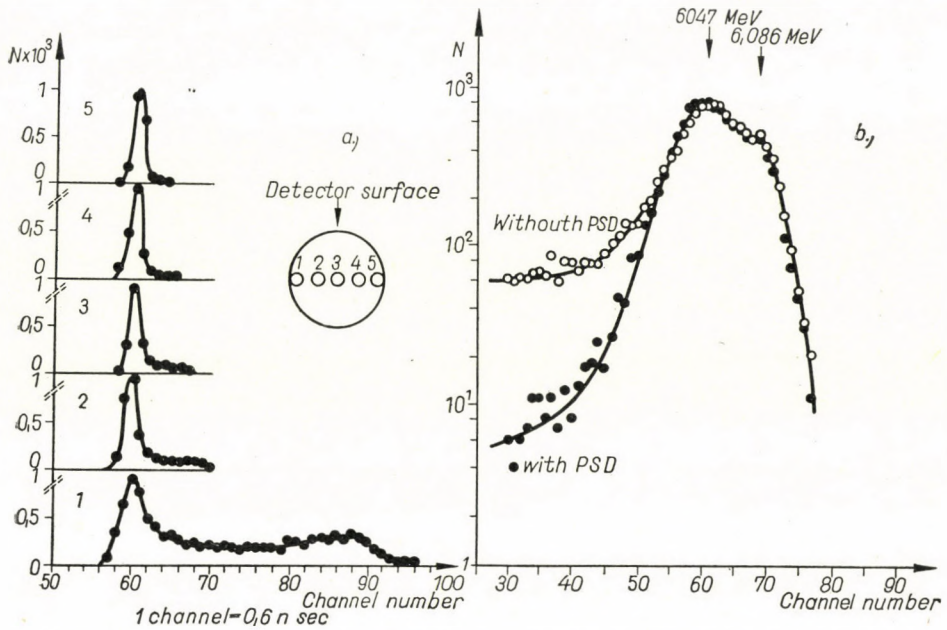

Fig. 5. a) The time spectrum of the pulses of a $p-n$ detector. The surface of the detector was irradiated with a collimated alpha beam at different places. b) The amplitude spectrum of the same detector with PSD without and with gating. The whole surface of the detector was irradiated with alpha particles of Th(C + C') (Only the energies 6.047 and 6.086 MeV can be seen expanded)

tion layer. The change is particularly strong in the case of charge sensitive feed-back. This does not affect the separation of long range particles, since in real measurements the voltage on the detector must be kept constant.

The effect of the voltage of the detector on the rise-time of pulses measured with a pre-amplifier both with and without charge sensitive feed-back is shown in Fig. 4. The curves were obtained with 6 MeV alpha particles and with an 800 Ohm.cm $p - n$ detector.

In the case of some semiconductor detectors the appearance of a tail was observed in the amplitude spectra on the low energy side of the peaks. This is due presumably to some irregularity in the material of the detector. From the study of the signals of the detector it was found that the rise-time

of pulses forming the tail was longer than the normal rise-time. Thus, it was possible to eliminate the undesirable tail from the spectrum.

Fig. 5a shows the pulses of different rise-time obtained from the detector when its different parts were irradiated with a collimated beam. The time spectra show clearly that on the left side of the detector and on the parts marked 1, 2 and 3 pulses with long rise-times appear.

Selecting only the "good" pulses causes a considerable improvement in the time spectrum. Fig. 5b shows the alpha spectrum of the Th(C + C') preparate both with and without pulse shape discrimination.

The author expresses his gratitude to Prof. A. SZALAY, Director of the Institute for enabling the work to be carried out, to Mr. B. SCHLENK for operating the cascade, and to Professor FLEROV, Director of the Joint Institute for Nuclear Research, Dubna, for providing the detectors.

REFERENCES

1. F. S. EBY and W. K. JENTSCHKE, Phys. Rev., **96,** 911, 1954.
2. HERTZ, Lehrbuch der Kernphysik, BD I. 586. B. G. Teubner Verlagsgesellschaft, Leipzig.
3. R. B. OWEN, IRE Trans. Nucl. Sci., NS-9, 285, 1962.
4. B. SOUČEK and R. L. CHASE, Brookhaven National Laboratory, BNL 10653, 1966
5. P. A. TOVE and K. FALK, Nucl. Instr. and Meth., **12,** 278, 1961.
6. P. A. TOVE and K. FALK, Nucl. Instr. and Meth., **29,** 66, 1964.
7. A. ALBERIGI QUORONTA, M. MERTINI, G. OTTOVIANI and G. ZANORINI, Nucl. Instr. and Meth., **29,** 173, 1964.
8. O. MEYER and H. J. LANGMANN, Nucl. Instr. and Meth., **34,** 77, 1965.
9. H. M. MANN, J. W. HASLETT and G. P. LIETZ, IRE Trans. Nucl. Sci., NS-8 1 51, 1961
10. C. T. TAYMO and J. W. MAYER, IRE Trans. Nucl. Sci., NS-8, 157, 1961.
11. C. A. J. AMMERELAN, R. F. RUMPHORT and L. A. CH. KOERTS, Nucl. Instr. and Meth., **22,** 189, 1963.
12. J. C. LEGG, Nucl. Instr. and Meth., **36,** 343, 1965.
13. G. AMSEL, P. BARUCH and O. SMULKOWSKI, IRE Trans. Nucl. Sci., NS-8 21, 1961.
14. J. W. MAYER, Proc. of the Ashewille Conference, Nat. Acad. Sci.-Nat. Res. Coun. Pub. No. 871 (1960. Sept) 1.
15. H. O. FUNSTEN, IRE Trans. Nucl. Sci., NS-9, 190, 1962.
16. R. L. CHASE, W. A. HIGINLOTHAM and G. L. MILLER, IRE Trans. Nuc l. Sci., NS-8, 147 Fig. 1, 1961.
17. R. FÜLLE, GY. MÁTHÉ and D. NETZBAND, Nucl. Instr. and Meth., **36,** 250, 1965.

ИССЛЕДОВАНИЕ ФОРМЫ СИГНАЛА ПОЛУПРОВОДНИКОВЫХ ДЕТЕКТОРОВ ТИПА $n - p$ И $p - n$ ДИСКРИМИНАТОРОМ ИМПУЛЬСНЫХ ФОРМ

ДЬ. МАТЭ

Р е з ю м е

Форма сигналов детекторов типа $n - p$ и $p - n$ показывает заметное изменение, если пробег регистрированной частицы превышает толщину слоя пространственного заряда. Таким образом, дискриминатором импульсных форм сигналы частиц, обладающие большим пробегом, могут удаляться из спектра. Некоторые детекторы из-за местных дефектов дают сигналы меньшие нормальных, что приведет к появлении «хвоста» в спектре. Эти «хвосты» могут быть отфильтрованы дискриминацией импульсных форм.

Acta Physica Academiae Scientiarum Hungaricae, Tomus 23 (4), pp. 415—424, (1967)

ON THE OPTICAL PROPERTIES OF VANADIUM PENTOXIDE SINGLE CRYSTALS

By

I. HEVESI

INSTITUTE OF EXPERIMENTAL PHYSICS, JÓZSEF ATTILA UNIVERSITY, SZEGED

(Presented by A. Budó. — Received 2. II. 1967)

Optical absorption coefficients of V_2O_5 single crystals in the region of the intrinsic absorption edge have been calculated for different temperatures. Measurements at temperatures above room temperature show a shift of the absorption curves towards longer wavelengths with increasing temperature. From the analysis of the curves, the intrinsic absorption edge was found to have an exponential dependence corresponding to direct forbidden transitions, whereas its long wave tail seems to follow URBACH's rule. Measurements with light polarized parallel to the *a* and the *c* axis respectively lead to two distinct absorption curves, with two intersections in the wavelength range investigated.

Introduction

The investigations described in two publications [1—2] dealing with our work on optical absorption of V_2O_5 single crystals differ from those published by previous investigators [3—5] mainly in two points. First, our absorption measurements were made with polarized light, taking into consideration the orientation of polarization to the crystallographic axes. This enabled us to study the optically anisotropic behaviour of V_2O_5. Further, by using thin crystal plates and extending our measurements over a greater temperature range, we were able to study and analyse the absorption in the region of the intrinsic edge. This made it possible to calculate the band gap and to determine its dependence on temperature.

Recently N. KENNY, C. R. KANNEWURF and D. H. WHITMORE [6] have given an account of their researches on V_2O_5, made at room temperature, contemporaneously with our work. For the wavelength range of our investigations ($470m\mu - 820m\mu$), their results are similar to ours. Deviations are not significant, considering the differences in the methods of calculation and the different ways of preparing the samples.

The importance of researches on the optical behaviour of V_2O_5 single crystals, particularly in the region of the intrinsic edge, is accentuated by the fact that the use of thermal methods for investigations on V_2O_5 in the intrinsic region is impeded by the relatively great band gap width and low melting point. It is to be expected from the present investigations and further pro-

jected work to obtain a deeper insight into the band structure of V_2O_5 and to contribute thereby to the understanding of its semiconductor properties.

In the present paper we wish to present some further results of our work connected with our investigations briefly described in the short note [2].

1. Experimental equipment and method

The equipment used for measuring transmission at room temperature, method of measurement and preparation of samples have been described in [1]. The most important change introduced for our present measurements

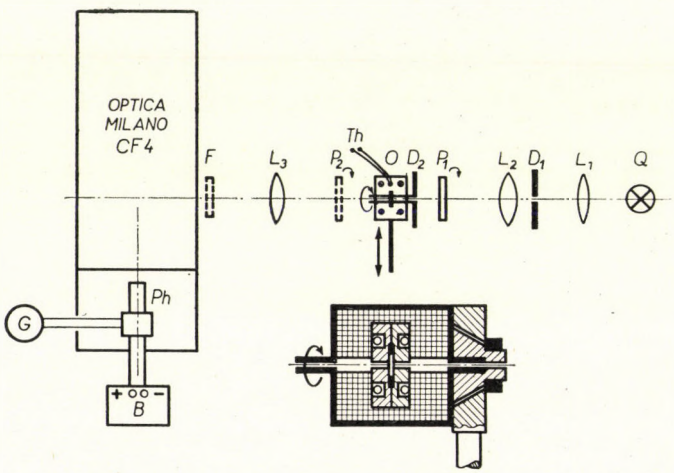

Fig. 1a. Diagram of the optical arrangement. Q: light source; L_1, L_2, L_3: lenses; P_1, P_2: polaroid filters; D_1, D_2: diaphragms; O: furnace; Th: thermocouple; B: power supply; G: galvanometer; Ph: photomultiplier; F: glass filter. *Fig. 1b.* Section of the electric furnace

was to use an electric furnace for heating the sample holder to render possible transmission measurements to be made at temperatures as high as 400 °C. A diagram of the equipment is given in Fig. 1a. The polaroid filter P_2 (represented by a broken line) has been used to adjust the extinction position of the crystals, the filter F eliminating ultra-violet radiation for measurements at wavelengths $\lambda > 600$ mμ (see [1]). The samples of different thickness were fixed in a special sample holder which could be withdrawn from the interior of the electric furnace O (see Fig. 1b). The furnace could be rotated round the beam of light as axis, and removed from the path of the light on a sliding support. Good thermal insulation and elimination of undesirable air currents on both sides of the sample holder were secured by the construction of the furnace device. A copper-constantan thermocouple was used to measure the temperature.

To determine the absorption coefficients, transmission was measured with plates of different thicknesses at various temperatures, with linearly

polarized light perpendicularly incident to the (010) crystal plate, the direction of vibration relative to the *c* axis being: 1) parallel to the *c* axis (designed as || polarization), 2) parallel to the *a* axis, i.e. normally to the *c* axis (⊥ polarization).

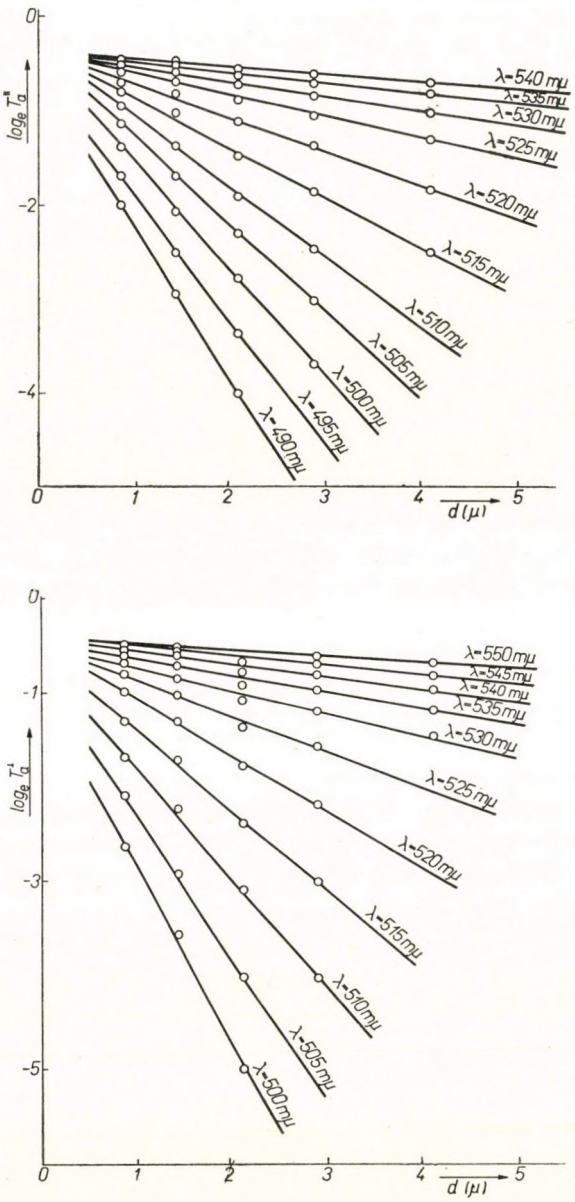

Fig. 2a. Dependence of transmission on the thickness of the sample for || polarization at different wavelengths. *2b.* Dependence of transmission on the thickness of the sample for ⊥ polarization at different wavelengths

As described in [2], absorption coefficients in the region of the intrinsic edge have been calculated on the basis of the following formula for the average transmission:

$$T_a = T_0 \exp(-Kd) . \tag{1}$$

The thickness d has been determined on the basis of the interference structure of $T(\lambda)$ curves obtained with plates of some μ thickness (see [1]). As average values T_a of the transmission we used the mean of the envelopes of transmission maxima and minima. The use of (1) for our calculations proved to be justified by Figs. 2a and 2b, in which $\ln T_a$ versus d curves at room temperature are plotted for $\parallel$ and $\perp$ polarizations, respectively. Absorption coefficients $K^{\parallel}$ and $K^{\perp}$ for both polarizations, determined at different temperatures, were calculated from the slopes of the straight lines obtained for every 5th μ wavelength in the spectral range investigated.

2. Results

Figs. 3 and 4 present typical results of measurements concerning the dependence of transmission $T(\lambda)$ on the thickness of the sample and tempera-

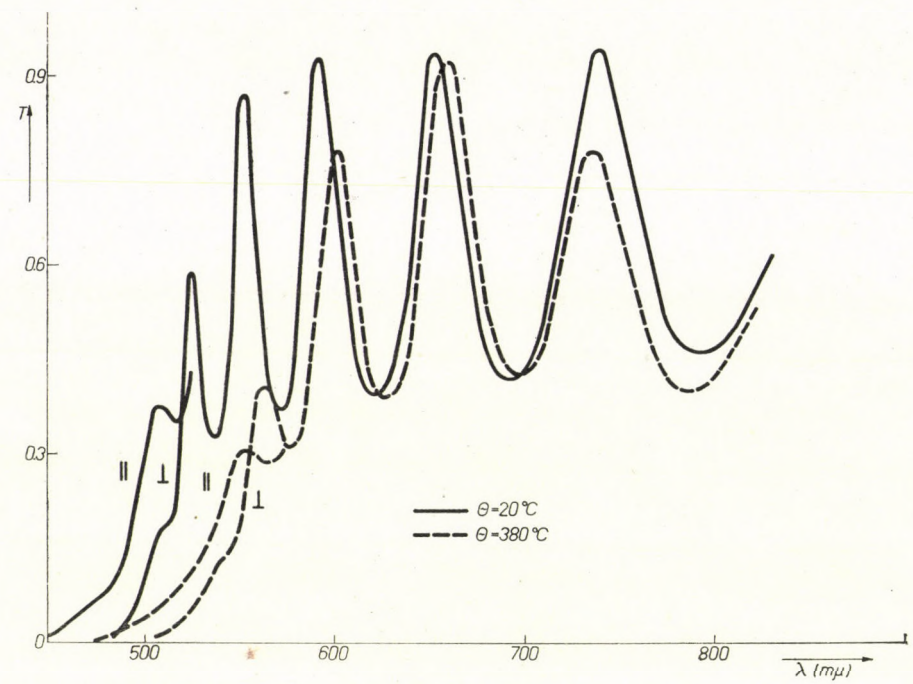

Fig. 3. Transmission curves of a V_2O_5 single crystal plate of thickness $d = 0.82\ \mu$, measured at $\Theta = 20$ °C and $\Theta = 380$ °C, for $\parallel$ and $\perp$ polarization

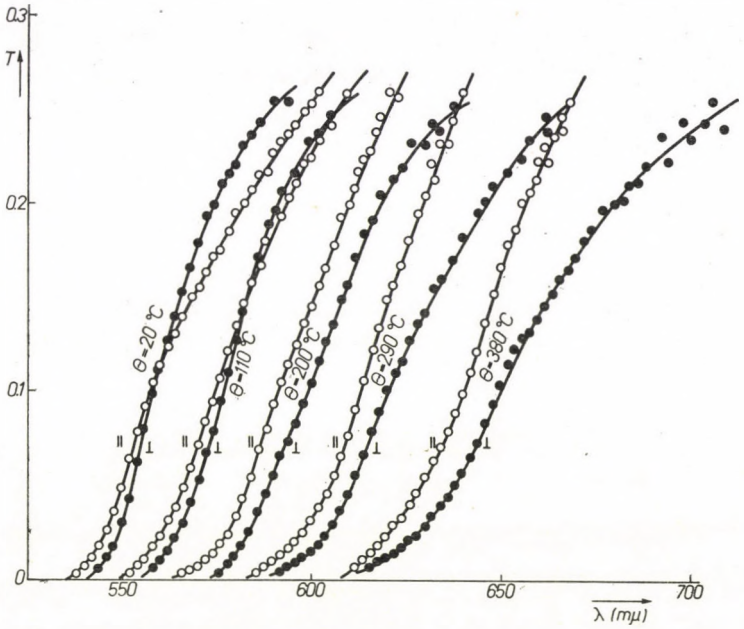

Fig. 4. Transmission curves of a V_2O_5 single crystal plate of thickness $d = 65\ \mu$, measured at five different temperatures for || and ⊥ polarization

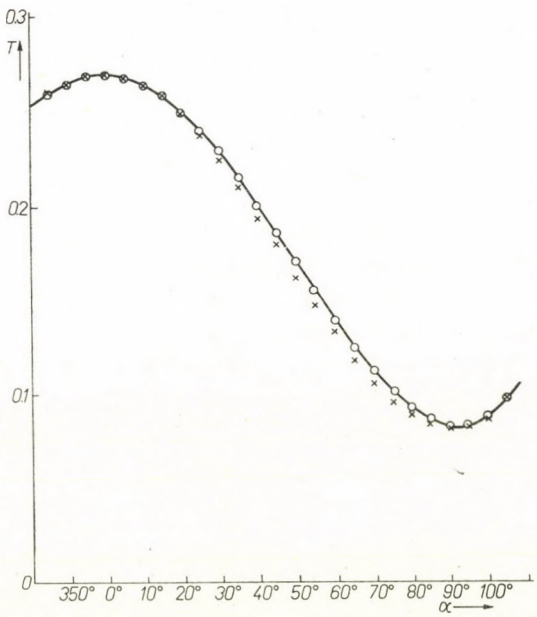

Fig. 5. Changes in transmission with different angles between the plane of vibration of the polarized light and the c crystal axis, measured in a V_2O_5 single crystal plate of thickness $d = 0.82\ \mu$ at $\lambda = 500$ mμ

ture, obtained with a thinner ($d = 0.82\mu$) and a thicker ($d = 65\mu$) V_2O_5 single crystal plate at various temperatures with || and $\perp$ polarization. Fig. 3 shows the transmission curves of the thinner sample for $\perp$ polarization, measured from 480mμ to 820mμ wavelength at room temperature (solid line), and at 380 °C (broken line). To avoid confusion, for || polarization only the starting sections of the transmission curves obtained at the same tempe-

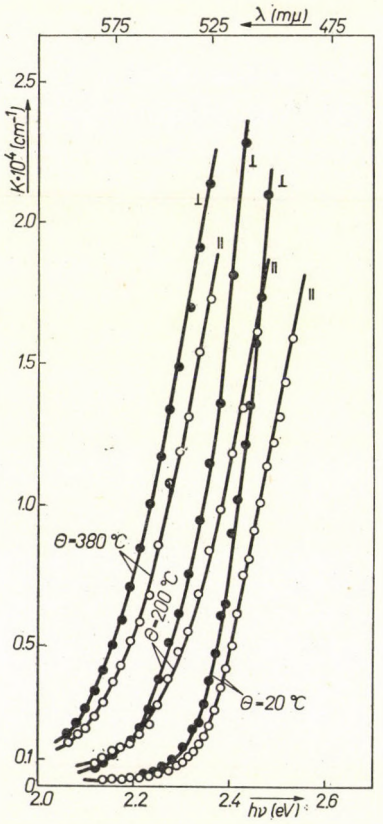

Fig. 6. Absorption curves in the region of the intrinsic absorption edge for || and $\perp$ polarization at three temperatures

ratures are shown in this Figure. Fig. 4, containing results obtained with the thicker plate, gives the ascending sections of transmission curves measured at five different temperatures for || polarization (open circles) and $\perp$ polarization (filled circles), respectively. It can be seen from the Figure that the transmission curves show a considerable shift towards greater wavelengths with increasing temperature.

Fig. 5 shows the transmission of the thinner plate ($d = 0.82\,\mu$) as a function of the angle α between the c crystal axis and the plane of vibration of the

linearly polarized light beam perpendicularly incident on the surface of the crystal. Transmission curves for $\lambda = 500$ mμ were measured at intervals of five degrees, $\alpha = 0°$ corresponding to || polarization, and $\alpha = 90°$ to $\perp$ polarization respectively. The transmission T_α for an angle α can be expressed in

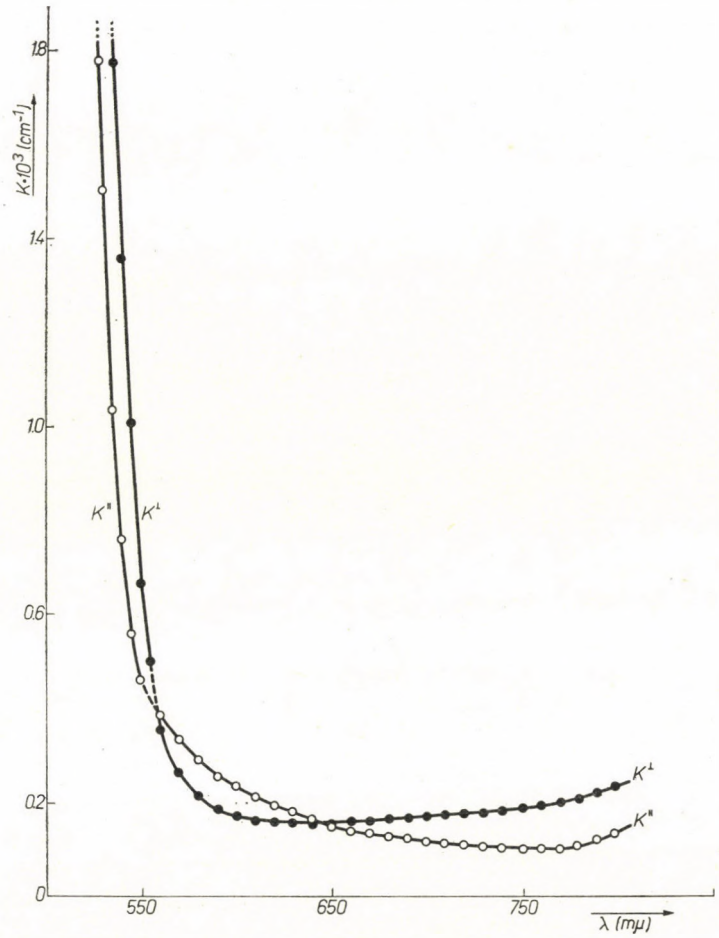

Fig. 7. Absorption curves for || and $\perp$ polarization, calculated with different methods for the region of the intrinsic absorption edge and for greater wavelengths

terms of the transmission $T^{||}$ and $T^{\perp}$ (corresponding to $\alpha = 0°$ and $\alpha = 90°$, respectively) with the formula $T_a = T^{\perp} + (T^{||} - T^{\perp}) \cos^2 \alpha$. The values calculated with this formula (marked by crosses in the Figure) fit well to the measured values. In our measurements, the above relation between T_a, $T^{||}$ and $T^{\perp}$ was found to be valid in the whole spectral range investigated and for the temperatures considered.

Absorption curves are presented in Figs. 6 and 7. In Fig. 6 absorption coefficients in the region of the intrinsic absorption edge are plotted for || and ⊥ polarization and three temperatures, showing the shift of the absorption edge towards lower photon energies with increasing temperatures. Fig. 7 shows absorption curves $K^{||}(\lambda)$ and $K^{\perp}(\lambda)$, calculated with the method given in [1] for $\lambda > 560\text{m}\mu$ and with the method described in the present paper for $\lambda < 560\text{m}\mu$. The curves plotted for both regions fit well in the connected ranges (given with broken lines), and the curves calculated with both methods

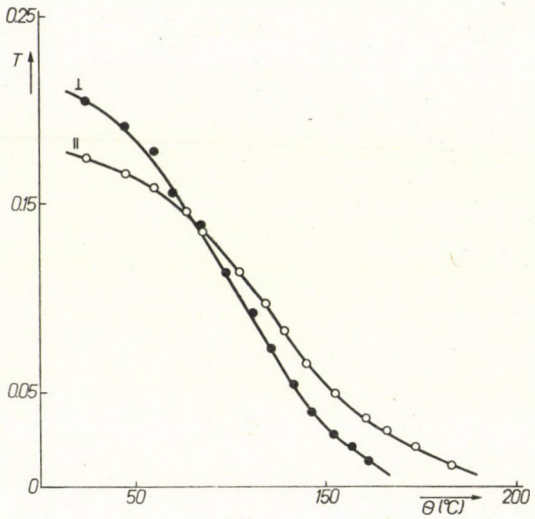

Fig. 8. Temperature dependence of transmission in a V_2O_5 single crystal plate of thickness $d = 65\ \mu$, measured at $\lambda = 575\ \text{m}\mu$ for || and ⊥ polarization

show an intersection of $K^{||}$ and $K^{\perp}$ at the same wavelength ($\lambda \sim 555\text{m}\mu$). It can be seen that $K^{\perp}$ is less than $K^{||}$ from $\sim 555\text{m}\mu$ to $\sim 650\text{m}\mu$, where the curves have another intersection. With the known values of the refractive indices and absorption coefficients for || and ⊥ polarization, it is to be expected on the basis of (1) that for thicker samples and in the spectral range where $K^{\perp} < K^{||}$ there will be a wavelength range for which $T^{\perp} > T^{||}$. This is confirmed by an inspection of Fig. 4, where for $575\text{m}\mu$ $T^{\perp} > T^{||}$ at room temperature, while $T^{\perp} < T^{||}$ at 110 °C and 200 °C. The dependence of $T^{||}$ and $T^{\perp}$ on temperature Θ (°C) is shown in intervals of 10 °C in Fig. 8 for $\lambda = 575\ \text{m}\mu$. The anisotropic behaviour of V_2O_5 is not restricted to the range of the intrinsic absorption edge, as can be seen from Fig. 7.

It is to be noticed that in the $K^{||}$ and $K^{\perp}$ curves for room temperature published by N. KENNY, C. R. KANNEWURF and D. H. WHITMORE [6] no intersection can be seen in the spectral range $480\text{m}\mu$—$850\text{m}\mu$; only one is to be found at about $1220\text{m}\mu$.

3. Discussion

The analysis of the curves measured in the region of the intrinsic absorption edge and presented in Fig. 6 has been given in the short note [2]. It was found that the absorption coefficients in the long wave-tail of the absorption edge follow URBACH's rule $K = K_0 \exp\left(\beta \frac{h\nu}{kT}\right)$ [7], i.e. the absorption shows an exponential dependence on both photon energy and temperature, whereas the short wavelength range of the absorption spectrum fits well to the exponential law $Kh\nu \propto (h\nu - E_g)^{3/2}$ describing forbidden direct band-to-band transitions [8]. The dependence of the band gap width E_g on temperature was found to obey the relation $E_g = E_{g0} + aT$, where $a = -6.1 \times 10^{-4}$ eV/degree, $E_{g0} = 2.49$ eV, and $a = -7.3 \times 10^{-4}$ eV/degree, $E_{g0} = 2.54$ eV for $\parallel$ and $\perp$ polarization, respectively.

The exponential energy dependence of the intrinsic absorption edge, found also in several other materials (see e.g. [9]), can be attributed to energy states tailing off into the forbidden gap [10—11]. These states, generally ascribed to the presence of lattice disorders of different kinds, would allow transitions at photon energies which are less than those corresponding to direct band transitions. It seems probable that nonstoichiometric defects, present in V_2O_5 single crystals [6], have a role in producing such energy states in the band gap. Attempts at a theoretical interpretation (see e.g. [10—11]) of the exponential dependence of the intrinsic absorption edge (generally referred to as URBACH's rule) have not led to unambiguous results so far. More theoretical and experimental researches will be needed to throw further light on the mechanism of the band-to-band transition in V_2O_5 single crystals.

The theoretical interpretation of the existence of different absorption edges for $\parallel$ and $\perp$ polarization, respectively, appearing similarly in other materials (see e.g. [9, 12—13]), is also a problem to be solved. According to DRESSELHAUS [14], a theoretical analysis of the fundamental absorption in anisotropic crystals shows that, for indirect transitions, the shape of the absorption edges would be the same both for allowed and forbidden transitions. For direct transitions, however, the frequency dependence of absorption should be different in both cases. Thus, the shift of the absorption edge could be accounted for by a change in the shape of the edge. DEXTER [10] suggested that polarization dependence could be explained by a difference in the matrix elements for $\parallel$ and $\perp$ transitions. These models, however, do not seem to be confirmed by the absorption curves for $\parallel$ and $\perp$ polarization found in our investigation.

Absorption in the longer wavelength range beyond the intrinsic absorption edge has been dealt with in the paper of N. KENNY, C. R. KANNEWURF

and D. H. WHITMORE [6] who extended their investigations to wavelengths of 7.5μ.

For diffuse reflection spectra of V_2O_5 see [15].

Acknowledgement

The author wishes to thank to Professor A. BUDÓ, Director of the Institute of Experimental Physics, József Attila University, Szeged, for his continued interest and to Professor Z. BODÓ, Budapest, for valuable comments during the work.

REFERENCES

1. I. HEVESI, Acta Phys. Hung., **23**, 75, 1967.
2. Z. BODÓ and I. HEVESI, phys. stat. sol., **20**, K45, 1967.
3. А. Н. Арсеньева и Б. В. Курчатов, ЖЭТФ, **4**, 576, 1934.
4. J. BOROS, Z. Phys., **126**, 721, 1949.
5. T. KAWAGUCHI, XVIII Congress of Pure and Applied Chemistry, Montreal, 1961.
6. N. KENNY, C. R. KANNEWURF and D. H. WHITMORE, J. Phys. Chem. Solids, **27**, 1237, 1966.
7. F. URBACH, Phys. Rev., **92**, 1324, 1953.
8. J. BARDEEN, F. J. BLATT and L. H. HALL, Photoconductivity Conference, Atlantic City, 1954, p. 146. John Wiley, New York, 1956.
9. D. DUTTON, Phys. Rev., **112**, 785, 1958.
10. D. L. DEXTER, Suppl. Nuovo Cimento, **7**, 245, 1958.
11. D. REDFIELD, Phys. Rev., **130**, 916, 1963.
12. H. GOBRECHT and A. BARTSCHAT, Z. Phys., **136**, 224, 1953.
13. J. J. LOFERSKI, Phys. Rev., **93**, 707, 1954.
14. G. DRESSELHAUS, Phys. Rev., **105**, 135, 1957.
15. I. HEVESI, Acta Phys. et Chem. Szeged, **13**, 39, 1967.

ОПТИЧЕСКИЕ СВОЙСТВА МОНОКРИСТАЛЛОВ ПЯТИОКИСИ ВАНАДИЯ

И. ХЕВЕШИ

Резюме

Вычислялись коэффициенты поглощения монокристаллов пятиокиси ванадия в области края основной полосы поглощения. Получено, что кривые поглощения смещаются в длинноволновую сторону с ростом температуры. Анализ показывает, что в коротковолновой области край основной полосы поглощения следует по степенному закону для прямых запрещенных переходов, а в длинноволновой области край основной полосы поглощения следует по правилам Урбахта. Используя линейно поляризованный свет параллельно кристаллическим осям *a* и *c*, получаются две кривые края основной полосы поглощения.

Acta Physica Academiae Scientiarum Hungaricae, Tomus 23 (4), pp. 425—441, (1967)

INVESTIGATIONS WITH MODIFIED UNIVERSAL POTENTIAL FIELDS

By

A. JUCYS, I. I. GLEMBOCKYS

INSTITUTE OF PHYSICS AND MATHEMATICS OF THE ACADEMY OF SCIENCES OF THE LITHUANIAN SSR, VILNIUS, USSR

and

R. GÁSPÁR

INSTITUTE OF THEORETICAL PHYSICS, KOSSUTH LAJOS UNIVERSITY, DEBRECEN, 10 and RESEARCH GROUP FOR THEORETICAL PHYSICS OF THE HUNGARIAN ACADEMY OF SCIENCES, BUDAPEST

(Presented by A. Kónya. — Received 1. IV. 1967)

Calculations have been made with various forms of the universal potential field for the ground state of the atom Fe and that of the ions Fe^+, Fe^{3+}, Fe^{5+} and for the $1s^2\ 2s^2\ 2p^6\ 3s^2\ 3p^6\ 3d^{10}\ 4f$ excited state of the Cu atom.

In a series of investigations one of the authors [1] calculated atomic one-electron eigenvalues and wave functions for the elements of the IB and VI groups of the periodic table. The one-electron Schrödinger-equation was solved with a potential field, which is a generalization of the self-consistent field. The exchange potential was taken into account in its statistical approximate form $\varkappa\varrho^{1/3}$, where ϱ is the charge density and $\varkappa = (3/\pi)^{1/3}\, e^2$ is a constant. The potential field has an analytical form and can be transformed to any value of the atomic number Z by a simple scale transformation. In this sense the potential field is called universal. In its original form the universal potential field was given for neutral atoms and the aim of the present paper is to investigate the possibility of the generalization of including ions.

The universal potential field of a neutral atom has been given in [1] as

$$V = \frac{Z_p\, e}{r} + \frac{\varkappa}{e}\varrho^{1/3} = \frac{Ze}{r}\ \frac{e^{-\lambda_0 x}}{1 + A_0 x} + \frac{c'}{e}\ \frac{e^{-ax}}{1 + Ax}, \tag{1}$$

where

$$c' = \varkappa Z^{2/3}\, c \tag{2}$$

and

$$\lambda_0 = 0{,}1837, \qquad A = 1{,}05, \qquad c = 3{,}1\, a_0^{-1}, \qquad \alpha' = 0{,}04$$

$$A = 9 \quad \text{and} \quad \mu = \frac{0{,}885341}{Z^{1/3}}\, a_0 \tag{3}$$

are constants and

$$x = r/\mu \tag{4}$$

is a scaled variable. r is the distance of the electron from the nucleus. Z_p, the effective atomic number and ϱ the density are given by the relation (1). Z is the atomic number, e the elementary charge and a_0 is the radius of Bohr's smallest atomic orbital in the H-atom. A simplified Fermi—Amaldi type correction [2] was used to obtain the potential field of the ion from that of the neutral atom. The potential energy of an ion with $N - a$ electrons is given:

$$V\mu^2 = V_x = \frac{\mu\alpha I}{x} + \frac{Z - \alpha I}{2Z}\left(\frac{\gamma}{2x}\frac{e^{-\lambda_0 x}}{1 + A_0 x} + \xi\frac{e^{-\alpha' x}}{1 + Ax}\right), x \leq x_0 \tag{5a}$$

$$V\mu^2 = V_x = \frac{\mu I}{x}, \qquad x > x_0 \tag{5b}$$

where x_0 is the value of x, when the values of (5a) and (5b) are equal and $I = a + 1$

$$\gamma = 2Z\,\mu\,a_0^{-1} \quad \text{and} \quad \xi = 2\varkappa\, c\, 0{,}885341^2\, e^{-2}. \tag{6}$$

Using the potentials (1) or (5) the following one-electron Schrödinger equation was solved

$$\frac{d^2 f}{dx^2} + \left[2V_x - \frac{l(l+1)}{x^2} - \varepsilon\right] f = 0 \tag{7}$$

with the boundary conditions

$$\begin{aligned} &f(0) = 0, \\ &f^{(l-1)}(0) = 0, \\ &f^{(l)}(0) = \text{const.}, \\ &\lim_{r\to\infty} f(r) = 0. \end{aligned} \tag{8}$$

The eigenvalue parameter is given by

$$\varepsilon = 2E\,\mu^2\, e^{-2}\, a_0^{-1} \tag{9}$$

and E is the one-electron energy parameter of the nontransformed Schrödinger equation.

The potential field (5) has been used for various values of the parameter α (See the Tables). For the value $\alpha = 0$ (5) gives a modified form of (1) which has been used earlier [3]. For $\alpha = 1$ we get the Fermi—Amaldi type

modification of (1) and for intermediate values allowance is made for a semi-empirical adjustment of the potential.

Calculations have been made for the ground states of the ions Fe, Fe^{+}, Fe^{3+} and Fe^{5+} and for the $1s^2\,2s^2\,2p^6\,3s^2\,3p^6\,3s^{10}\,4f$ excited configuration of the Cu atom. In the Tables 1—13 we have displayed the values of the wave functions calculated by this method and by the "self-consistent field" method, where it was available. In Tables 14, 15 and 16 we give the one-electron energy eigenvalues for the above mentioned ionic and atomic configurations.

The calculations were performed on the BESZM-2M computer of the Lithuanian Academy of Sciences the use of which is gratefully acknowledged. For the numerical integration of the differential equation (7) the extrapolation formula

$$\delta^2 f_i = (\Delta x)^2 \left(f_i'' + \frac{1}{12}\,\delta^2 f_i'' \right) \tag{10}$$

was used. The starting interval at the integration had the value 0.006 and the integration net was constructed by doubling the interval after each 20 steps.

REFERENCES

1. See e.g. R. GÁSPÁR, Acta Phys. Hung., **3**, 263, 1954.
2. See e.g. P. GOMBÁS, Die statistische Theorie des Atoms und ihre Anwendungen, Springer-Verlag, Wien, 1949; p. 65.
3. R. GÁSPÁR and K. MOLNÁR-IVANECSKÓ, Acta Phys. Hung., **6**, 105, 1956.
4. R. E. WATSON, Iron series Hartree-Fock calculations, 1959.

Table 1

One-electron eigenfunction f_{1S} in the ground state configuration of the Fe atom determined by the modified universal potential fields and the self consistent field

a) solution of the Hartree—Fock equation;

b) solution of the equation

$$\left[\frac{d^2}{dx^2} + \frac{\gamma}{x}\,\frac{e^{-\lambda_0 x}}{1+A_0 x} + \xi\,\frac{e^{-\alpha x}}{1+A_x} - \frac{l(l+1)}{x^2} - \varepsilon\right] P = 0\,;$$

c) solutions of the equation

$$\left[\frac{d^2}{dx^2} + 2V - \frac{l(l+1)}{x^2} - \varepsilon\right] P = 0$$

with

$$2V = \frac{2\mu\alpha I}{x} + \frac{Z-\alpha I}{Z}\left(\frac{\gamma}{x}\,\frac{e^{-\lambda_0 x}}{1+A_0 x} + \xi\,\frac{e^{-\alpha x}}{1+Ax}\right), \qquad x \leq x_0$$

$$2V = \frac{2\mu I}{x}, \qquad x > x_0$$

where $\alpha = 1$, $\alpha = 0$ and $\alpha = 0.5$;

x	a	b	$c(\alpha = 1)$	$c(\alpha = 0)$	$c(\alpha = 0.5)$
0.00	0.000	0.000	0.000	0.000	0.000
0.03	1.797	1.860	1.861	1.860	1.861
0.06	2.874	2.949	2.950	2.949	2.949
0.09	3.449	3.506	3.508	3.506	3.507
0.12	3.682	3.708	3.709	3.708	3.709
0.18	3.545	3.504	3.505	3.504	3.505
0.24	3.041	2.950	2.950	2.950	2.950
0.30	2.451	2.333	2.332	2.333	2.333
0.36	1.900	1.775	1.773	1.775	1.774
0.48	1.064	0.956	0.954	0.956	0.955
0.60	0.564	0.486	0.484	0.486	0.485
0.72	0.289	0.238	0.237	0.238	0.238
0.84	0.145	0.114	0.114	0.114	0.114
1.08	0.036	0.025	0.025	0.025	0.025
1.32	0.009	0.005	0.005	0.005	0.005
1.56	0.002	0.001	0.001	0.001	0.001
1.80	0.001				

Table 2

One-electron eigenfunctions f_{2S} in the ground state configuration of the Fe atoms determined by the modified universal potential fields and the self-consistent field. For the meaning of the various quantities see the heading of Table 1

x	a	b	$c(\alpha = 1)$	$c(\alpha = 0)$	$c(\alpha = 0.5)$
0.00	0.000	0.000	0.000	0.000	0.000
0.03	0.541	0.556	0.561	0.556	0.559
0.06	0.849	0.862	0.869	0.862	0.866
0.09	0.980	0.981	0.989	0.981	0.985
0.12	0.982	0.965	0.972	0.965	0.969
0.18	0.731	0.675	0.679	0.675	0.677
0.24	0.304	0.216	0.215	0.216	0.215
0.30	−0.176	−0.284	−0.290	−0.284	−0.287
0.36	−0.638	−0.753	−0.763	−0.753	−0.758
0.48	−1.380	−1.476	−1.491	−1.476	−1.484
0.60	−1.327	−1.882	−1.897	−1.882	−1.890
0.72	−2.016	−2.026	−2.037	−2.026	−2.031
0.84	−2.018	−1.988	−1.993	−1.988	−1.991
1.08	−1.715	−1.639	−1.633	−1.639	−1.636
1.32	−1.287	−1.201	−1.189	−1.201	−1.195
1.56	−0.898	−0.824	−0.809	−0.824	−0.816
1.80	−0.598	−0.541	−0.527	−0.541	−0.534
2.28	−0,245	−0.216	−0.207	−0.216	−0.211
2.76	−0.096	−0.081	−0.076	−0.081	−0.079
3.24	−0.033	−0.030	−0.027	−0.030	−0.028
3.72	−0.016	−0.010	−0.009	−0.010	−0.010
4.68	−0.003	−0.001	−0.001	−0.001	−0.001
5.64	−0.001				

Table 3

One-electron eigenfunction f_{2p} in the ground state configuration of the Fe atom determined by the modified universal potential field and the self consistent field. For the meaning of the various quantities see the heading of Table 1

x	a	b	$c(\alpha = 1)$	$c(\alpha = 0)$	$c(\alpha = 0.5)$
0.00	0.000	0.000	0.000	0.000	0.000
0.03	0.035	0.039	0.039	0.039	0.039
0.06	0.125	0.138	0.140	0.138	0.139
0.09	0.252	0.277	0.281	0.277	0.279
0.12	0.402	0.440	0.446	0.440	0.443
0.18	0.732	0.792	0.802	0.792	0.797
0.24	1.057	1.129	1.143	1.129	1.136
0.30	1.345	1.420	1.437	1.420	1.428
0.36	1.582	1.651	1.670	1.651	1.661
0.48	1.389	1.923	1.950	1.933	1.941
0.60	2.001	2.009	2.022	2.009	2.016
0.72	1.971	1.944	1.950	1.944	1.947
0.84	1.847	1.792	1.792	1.792	1.792
1.08	1.473	1.389	1.378	1.389	1.384
1.32	1.082	0.997	0.981	0.997	0.989
1.56	0.754	0.683	0.665	0.683	0.674
1.80	0.507	0.453	0.437	0.453	0.445
2.28	0.215	0.188	0.177	0.188	0.183
2.76	0.089	0.075	0.068	0.075	0.071
3.24	0.038	0.029	0.026	0.029	0.027
3.72	0.017	0.011	0.009	0.011	0.010
4.68	0.003	0.001	0.001	0.001	0.001
5.64					
6.60					
7.56					

Table 4

One-electron eigenfunction f_{3S} in the ground state configuration of the Fe atom determined by the modified universal potential field and the self-consistent field. For the meaning of the various quantities see the heading of Table 1

x	a	b	$c(\alpha = 1)$	$c(\alpha = 0)$	$c(\alpha = 0.5)$
0.00	0.000	0.000	0.000	0.000	0.000
0.03	0.199	0.203	0.213	0.203	0.208
0.06	0.310	0.314	0.330	0.314	0.322
0.09	0.356	0.356	0.373	0.356	0.365
0.12	0.353	0.347	0.363	0.347	0.355
0.18	0.253	0.233	0.243	0.233	0.238
0.24	0.089	0.056	0.057	0.056	0.057
0.30	−0.093	−0.132	−0.141	−0.132	−0.137
0.36	−0.263	−0.304	−0.321	−0.304	−0.313
0.48	−0.518	−0.545	−0.573	−0.545	−0.559
0.60	−0.633	−0.633	−0.661	−0.633	−0.648
0.72	−0.619	−0.592	−0.612	−0.592	−0.603
0.84	−0.509	−0.458	−0.466	−0.458	−0.463
1.08	−0.124	−0.053	−0.032	−0.053	−0.043
1.32	0.313	0.377	0.422	0.377	0.400
1.56	0.688	0.735	0.792	0.735	0.764
1.80	0.960	0.988	1.047	0.988	1.018
2.28	1.204	1.208	1.247	1.208	1.229
2.76	1.183	1.171	1.178	1.171	1.176
3.24	1.040	1.014	0.993	1.014	1.004
3.72	0.861	0.823	0.783	0.823	0.803
4.68	0.534	0.485	0.434	0.485	0.459
5.64	0.304	0.263	0.200	0.263	0.241
6.60	0.163	0.137	0.106	0.137	0.120
7.56	0.083	0.069	0.050	0.069	0.059
9.48	0.019	0.017	0.010	0.017	0.013
11.40	0.004	0.004	0.002	0.004	0.003
13.32	0.001	0.001		0.001	0.001
15,24					

Table 5

One-electron eigenfunction f_{3p} in the ground state configuration of the Fe atom determined by the modified universal potential fields and the self-consistent field. For the meaning of the various quantities see the heading of Table 1

x	a	b	$c(\alpha = 1)$	$c(\alpha = 0)$	$c(\alpha = 0.5)$
0.00	0.000	0.000	0.000	0.000	0.000
0.03	0.012	0.014	0.015	0.014	0.014
0.06	0.044	0.048	0.052	0.048	0.050
0.09	0.089	0.097	0.104	0,097	0.101
0.12	0.142	0.153	0.165	0.153	0.159
0.18	0.257	0.273	0.294	0.273	0.284
0.24	0.367	0.385	0.413	0.385	0.399
0.30	0.459	0.474	0.508	0.474	0.492
0.36	0.528	0.537	0.575	0.537	0.557
0.48	0.587	0.580	0.617	0.580	0.599
0.60	0.554	0.528	0.555	0.528	0.542
0.72	0.450	0.407	0.419	0.407	0.414
0.84	0.299	0.244	0.239	0.244	0.242
1.08	−0.062	−0.128	−0.166	−0.128	−0.147
1.32	−0.417	−0.477	−0.540	−0.477	−0.509
1.56	−0.710	−0.755	−0.830	−0.755	−0.793
1.80	−0.923	−0.951	−1.027	−0.951	−0.991
2.28	−1.131	−1.131	−1.184	−1.131	−1.159
2.76	−1.134	−1.116	−1.133	−1.116	−1.126
3.24	−1.030	−1.001	−0.986	−1.002	−0.995
3.72	−0.885	−0.851	−0.809	−0.851	−0.831
4.68	−0.594	−0.558	−0.493	−0.558	−0.525
5.64	−0.372	−0.341	−0.278	−0.341	−0.308
6,60	−0.223	−0.201	−0.150	−0.201	−0.173
7.56	−0.129	−0.115	−0.079	−0.115	−0.095
9,48	−0.040	−0.037	−0.021	−0.037	−0.028
11.40	−0.011	−0.011	−0.005	−0.012	−0.008
13.32	−0.003	−0.003	−0.001	−0.004	−0.002
15.24		−0.001		−0.001	

Table 6

One-electron eigenfunction f_{3d} in the ground state configuration of the Fe atom determined by the modified universal potential fields and the self-consistent field. For the meaning of the various quantities see the heading of Table 1

x	a	b	$c(\alpha = 1)$	$c(\alpha = 0)$	$c(\alpha = 0.5)$
0.00	0.000	0.000	0.000	0.000	0.000
0.03	0.000	0.000	0.000	0.000	0.000
0.06	0.001	0.001	0.001	0.001	0.001
0.09	0.002	0.002	0.003	0.002	0.002
0.12	0.004	0.004	0.006	0.004	0.005
0.18	0.011	0.013	0.017	0.013	0.015
0.24	0.024	0.027	0.036	0.027	0.032
0.30	0.041	0.046	0.061	0.046	0.054
0.36	0.063	0.070	0.092	0.069	0.082
0.48	0.119	0.128	0.168	0.127	0.150
0.60	0.187	0.197	0.258	0.196	0.230
0.72	0.260	0.271	0.353	0.269	0.316
0.84	0.336	0.346	0.448	0.343	0.402
1.08	0.478	0.487	0.625	0.484	0.563
1.32	0.600	0.609	0.770	0.605	0.698
1.56	0.694	0.705	0.877	0.700	0.802
1.80	0.763	0.776	0.949	0.772	0.876
2.28	0.836	0.856	1.006	0.851	0.946
2.76	0.846	0.873	0.980	0.868	0.942
3.24	0.819	0.850	0.909	0.845	0.894
3.72	0.774	0.805	0.815	0.800	0.822
4.68	0.666	0.686	0.616	0.683	0.658
5.64	0.567	0.563	0.444	0.562	0.504
6.60	0.482	0.455	0.311	0.455	0.377
7.56	0.410	0.363	0.214	0.366	0.278
9.48	0.298	0.230	0.098	0.237	0.148
11.40	0.217	0.145	0.044	0.157	0.077
13.32	0.157	0.091	0.019	0.105	0.040
15.24	0.112	0.058	0.008	0.071	0.020
19.08	0.053	0.023	0.002	0.033	0.005
22.92	0.023	0.009		0.015	0.001
26.76	0.009	0.004		0.007	
30.60	0.003	0.002		0.003	

Table 7

One-electron eigenfunction f_{3s} in the ground state configuration of the Fe atom determined by the modified universal potential fields and the self-consistent field. For the meaning of the various quantities see the heading of Table 1

x	a	$c(\alpha = 1)$	$c(\alpha = 0)$	$c(\alpha = 0.5)$
0.00	0.000	0.000	0.000	0.000
0.03	0.199	0.223	0.203	0.213
0.06	0.311	0.344	0.314	0.330
0.09	0.357	0.389	0.355	0.373
0.12	0.353	0.379	0.346	0.363
0.18	0.253	0.253	0.232	0.243
0.24	0.089	0.058	0.056	0.057
0.30	−0.093	−0.150	−0.132	−0.141
0.36	−0.263	−0.338	−0.303	−0.321
0.48	−0.519	−0.598	−0.544	−0.573
0.60	−0.634	−0.687	−0.633	−0.661
0.72	−0.620	−0.630	−0.591	−0.612
0.84	−0.510	−0.472	−0.458	−0.466
1.08	−0.125	−0.010	−0.053	−0.032
1.32	0.313	0.466	0.377	0.422
1.56	0.690	0.847	0.734	0.792
1.80	0.962	1.101	0.987	1.047
2.28	1.206	1.278	1.207	1.247
2.76	1.183	1.179	1.170	1.178
3.24	1.039	0.968	1.014	0.994
3.72	0.860	0.743	0.823	0.783
4.68	0.532	0.387	0.486	0.434
5.64	0.303	0.184	0.266	0.220
6.60	0.162	0.083	0.142	0.106
7.56	0.082	0.036	0.074	0.050
9.48	0.019	0.006	0.020	0.010
11.40	0.004	0.001	0.005	0.002
13.32	0.001		0.001	
15.24				

Table 8

One-electron eigenfunction f_{3p} in the ground state configuration of the Fe atom determined by the modified universal potential fields and the self-consistent field. For the meaning of the various quantities see the heading of Table 1

x	a	$c(\alpha = 1)$	$c(\alpha = 0)$	$c(\alpha = 0.5)$
0.00	0.000	0.000	0.000	0.000
0.03	0.012	0.016	0.014	0.015
0.06	0.045	0.055	0.048	0.052
0.09	0.090	0.111	0.097	0.104
0.12	0.143	0.176	0.153	0.165
0.18	0.259	0.312	0.272	0.294
0.24	0.369	0.438	0.383	0.413
0.30	0.461	0.539	0.473	0.508
0.36	0.529	0.608	0.535	0.575
0.48	0.589	0.648	0.578	0.617
0.60	0.556	0.577	0.526	0.555
0.72	0.452	0.427	0.406	0.419
0.84	0.301	0.231	0.243	0.239
1.08	−0.062	−0.205	−0.127	−0.166
1.32	−0.419	−0.599	−0.475	−0.540
1.56	−0.712	−0.898	−0.752	−0.830
1.80	−0.926	−1.093	−0.948	−1.027
2.28	−1.135	−1.224	−1.127	−1.184
2.76	−1.136	−1.139	−1.113	−1.133
3.24	−1.030	−0.961	−0.999	−0.986
3.72	−0.883	−0.764	−0.850	−0.809
4.68	−0.590	−0.435	−0.560	−0.439
5.64	−0.368	−0.228	−0.347	−0.278
6.60	−0.220	−0.114	−0.210	−0.150
7.56	−0.127	−0.055	−0.126	−0.079
9.48	−0.039	−0.012	−0.044	−0.021
11.40	−0.011	−0.003	−0.015	−0.005
13.32	−0.003		−0.005	−0.001
15.24	−0.001		−0.002	

Table 9

One-electron eigenfunction f_{3S} in the ground state configuration of the Fe atom determined by the modified universal potential fields and the self-consistent field. For the meaning of the various quantities see the heading of Table 1

x	a	$c(\alpha = 1)$	$c(\alpha = 0)$	$c(\alpha = 0.5)$
0.00	0.000	0.000	0.000	0.000
0.03	0.202	0.239	0.190	0.222
0.06	0.316	0.370	0.293	0.344
0.09	0.363	0.418	0.332	0.389
0.12	0.360	0.406	0.324	0.379
0.18	0.259	0.269	0.217	0.252
0.24	0.091	0.058	0.053	0.058
0.30	−0.095	−0.166	−0.123	−0.150
0.36	−0.269	−0.368	−0.283	−0.338
0.48	−0.529	−0.644	−0.509	−0.598
0.60	−0.644	−0.731	−0.592	−0.686
0.72	−0.629	−0.658	−0.554	−0.630
0.84	−0.515	−0.476	−0.430	−0.472
1.08	−0.124	0.038	−0.053	−0.010
1.32	0.317	0.552	0.348	0.466
1.56	0.697	0.947	0.683	0.846
1.80	0.974	1.195	0.922	1.100
2.28	1.227	1.322	1.140	1.277
2.76	1.205	1.164	1.125	1.178
3.24	1.050	0.910	1.005	0.968
3.72	0.854	0.663	0.857	0.743
4.68	0.499	0.309	0.573	0.389
5.64	0.262	0.130	0.336	0.187
6.60	0.127	0.052	0.210	0.086
7.56	0.059	0.020	0.120	0.039
9.48	0.011	0.003	0.036	0.007
11.40	0.002		0.010	0.001
13.32			0.003	
15.24			0.001	

Table 10

One-electron eigenfunction f_{3p} in the ground state configuration of the Fe^{+3} atom determined by the modified universal potential fields and the self-consistent field. For the meaning of the various quantities see the heading of Table 1

x	a	$c(\alpha = 1)$	$c(\alpha = 0)$	$c(\alpha = 0.5)$
0.00	0.000	0.000	0.000	0.000
0.03	0.013	0.017	0.012	0.016
0.06	0.046	0.061	0.043	0.055
0.09	0.092	0.123	0.086	0.111
0.12	0.147	0.194	0.136	0.175
0.18	0.265	0.345	0.242	0.312
0.24	0.377	0.483	0.341	0.438
0.30	0.471	0.592	0.420	0.538
0.36	0.541	0.665	0.476	0.607
0.48	0.601	0.700	0.515	0.647
0.60	0.567	0.611	0.469	0.576
0.72	0.461	0.434	0.363	0.427
0.84	0.307	0.207	0.220	0.231
1.08	−0.064	−0.284	−0.108	−0.205
1.32	−0.430	−0.711	−0.417	−0.598
1.56	−0.732	−1.019	−0.666	−0.897
1.80	−0.951	−1.202	−0.844	−1.091
2.28	−1.157	−1.276	−1.019	−1.222
2.76	−1.148	−1.124	−1.032	−1.138
3.24	−1.030	−0.896	−0.965	−0.960
3.72	−0.872	−0.671	−0.871	−0.764
4.68	−0.568	−0.336	−0.665	−0.436
5.64	−0.343	−0.153	−0.475	−0.232
6.60	−0.198	−0.066	−0.325	−0.119
7.56	−0.109	−0.028	−0.214	−0.060
9.48	−0.030	−0.004	−0.087	−0.014
11.40	−0.008	−0.001	−0.033	−0.003
13.32	−0.002		−0.012	
15.24			−0.004	

Table 11

One-electron eigenfunction f_{3S} in the ground state configuration of the Fe^{+5} atom determined by the modified universal potential fields and the self-consistent field. For the meaning of the various quantities see the heading of Table 1

x	a	$c(\alpha = 1)$	$c(\alpha = 0)$	$c(\alpha = 0.5)$	$c(\alpha = 0.2)$
0.00	0.000	0.000	0.000	0.000	0.000
0.03	0.208	0.254	0.165	0.229	0.192
0.06	0.326	0.393	0.255	0.354	0.297
0.09	0.374	0.444	0.288	0.400	0.336
0.12	0.371	0.431	0.281	0.389	0.328
0.18	0.266	0.283	0.189	0.259	0.219
0.24	0.093	0.057	0.046	0.057	0.052
0.30	−0.098	−0.182	−0.106	−0.156	−0.127
0.36	−0.278	−0.396	−0.245	−0.350	−0.290
0.48	−0.545	−0.685	−0.442	−0.616	−0.516
0.60	−0.663	−0.768	−0.516	−0.703	−0.597
0.72	−0.646	−0.679	−0.486	−0.639	−0.554
0.84	−0.528	−0.474	−0.382	−0.471	−0.423
1.08	−0.124	0.089	−0.062	0.013	−0.034
1.32	0.333	0.634	0.283	0.504	0.375
1.56	0.724	1.038	0.578	0.889	0.711
1.80	1.007	1.274	0.799	1.139	0.947
2.28	1.255	1.348	1.042	1.292	1.152
2.76	1.215	1.135	1.105	1.168	1.135
3.24	1.041	0.847	1.052	0.941	1.020
3.72	0.830	0.587	0.935	0.712	0.863
4.68	0.464	0.247	0.649	0.370	0.550
5.64	0.232	0.093	0.403	0.177	0.317
6.60	0.107	0.033	0.233	0.080	0.171
7.56	0.047	0.011	0.128	0.035	0.088
9.48	0.007	0.001	0.035	0.006	0.021
11.40	0.001		0.009	0.001	0.005
13.32			0.002		0.001
15.24					

Table 12

One-electron eigenfunction f_{3p} in the ground state configuration of the Fe^{+5} atom determined by the modified universal potential fields and the self-consistent field. For the meaning of the various quantities see the heading of Table 1

x	a	$c(\alpha = 1)$	$c(\alpha = 0)$	$c(\alpha = 0.5)$	$c(\alpha = 0.2)$
0.00	0.000	0.000	0.000	0.000	0.000
0.03	0.013	0.019	0.010	0.016	0.013
0.06	0.048	0.067	0.036	0.058	0.045
0.09	0.096	0.134	0.073	0.116	0.090
0.12	0.153	0.211	0.115	0.183	0.143
0.18	0.277	0.374	0.205	0.325	0.254
0.24	0.393	0.523	0.289	0.455	0.357
0.30	0.491	0.639	0.356	0.558	0.440
0.36	0.563	0.714	0.404	0.628	0.497
0.48	0.625	0.743	0.439	0.666	0.534
0.60	0.589	0.634	0.403	0.587	0.482
0.72	0.478	0.431	0.317	0.426	0.366
0.84	0.316	0.176	0.198	0.217	0.211
1.08	−0.073	−0.363	−0.074	−0.240	−0.138
1.32	−0.456	−0.815	−0.336	−0.646	−0.461
1.56	−0.769	−1.123	−0.553	−0.947	−0.715
1.80	−0.994	−1.288	−0.718	−1.135	−0.893
2.28	−1.195	−1.300	−0.920	−1.239	−1.059
2.76	−1.167	−1.090	−1.005	−1.127	−1.066
3.24	−1.028	−0.824	−1.003	−0.931	−0.996
3.72	−0.852	−0.584	−0.943	−0.729	−0.886
4.68	−0.525	−0.259	−0.738	−0.412	−0.682
5.64	−0.295	−0.104	−0.519	−0.217	−0.410
6.60	−0.155	−0.039	−0.340	−0.109	−0.250
7.56	−0.078	−0.014	−0.212	−0.053	−0.146
9.48	−0.017	−0.002	−0.074	−0.011	−0.045
11.40	−0.003		−0.023	−0.002	−0.013
13.32	−0.001		−0.007		−0.003
15.24			−0.002		

Table 13

One-electron eigenfunctions f_{4f} in the excited state $1s^2\,2s^2\,2p^6\,3s^2\,3p^6\,3d^{10}\,4f$ of the Cu atom determined by the modified universal potential fields and the self-consistent field. For the meaning of the various quantities see the heading of Table 1

x	a	$c(\alpha = 1)$	$c(\alpha = 0)$
0.00	0.000	0.000	0.000
0.24	0.000	0.000	0.000
0.48	0.000	0.000	0.000
0.72	0.000	0.000	0.000
1.08	0.000	0.000	0.000
1.32	0.000	0.001	0.000
1.56	0.000	0.001	0.000
1.80	0.000	0.002	0.000
2.28	0.000	0.003	0.000
2.76	0.000	0.005	0.000
3.24	0.000	0.007	0.000
3.72	0.000	0.009	0.001
4.68	0.001	0.015	0.001
5.64	0.001	0.022	0.002
6.60	0.002	0.030	0.002
7.56	0.003	0.040	0.003
9.48	0.006	0.063	0.007
11.40	0.011	0.089	0.012
13.32	0.018	0.118	0.019
15.24	0.027	0.148	0.028
19.08	0.051	0.207	0.051
22.92	0.080	0.257	0.081
26.76	0.111	0.292	0.113
30.60	0.147	0.311	0.147
38.28	0.207	0.308	0.207
45.96	0.247	0.269	0.247
53.32	0.264	0.215	0.264
61.32	0.259	0.162	0.259
76.69	0.209	0.081	0.209
92.04	0.143	0.036	0.144
107.40	0.087	0.015	0.088
122.76	0.051	0.006	0.050
153.48	0.014	0.001	0.013
184.20	0.003		0.003
214.92	0.001		0.001

Table 14

One-electron eigenvalues in the atomic unit of the Fe atom in the ground state determined by the modified universal potential fields and the self-consistent field. For the meaning of the various quantities see the heading of Table 1

	1s	2s	2p	3s	3p	3d
a	261.1	31.58	27.07	3.810	2.411	0.2273 Fe $d^8\,^3F$
b	259.2	29.19	25.24	3.406	2.239	0.3046
$c(\alpha = 1)$	262.3	31.25	27.44	4.500	3.312	1.250
$c(\alpha = 0)$	259.2	29.19	25.24	3.406	2.239	0.3063
$c(\alpha = 0.5)$	260.8	30.22	26.34	3.950	2.770	0.7595

Table 15

One-electron eigenvalues in the atomic unit of the Fe^+ ion in the ground state determined by the modified universal potential fields and the self-consistent field. For the meaning of the various quantities see the heading of Table 1

	1s	2s	2p	3s	3p	3d
a	261.4	31.98	27.46	4.231	2.828	0.6937 Fe^+ $d^7\,^4F$
$c(\alpha = 1)$	265.3	33.32	29.64	5.623	4.426	2.303
$c(\alpha = 0)$	259.2	29.19	25.24	3.408	2.243	0.3714
$c(\alpha = 0.5)$	262.3	31.25	27.44	4.500	3.312	1.250

Table 16

One-electron eigenvalues in the atomic unit of the Fe^{3+} and Fe^{5+} ions in the ground state and the Cu atom in the excited state $1s^2\,2s^2\,2p^2\,3s^2\,3p^6\,3d^{10}\,4f$ determined by the modified universal potential fields and the self-consistent field. For the meaning of the various quantities see the heading of Table 1

	Fe^{+3}		Fe^{+5}		Cu
	3s	3p	3s	3p	4f
a	5.529	4.092 Fe^{+3} $d^5\,^6S$	7.199	5.718 Fe^{+5} $d^3\,^4F$	0.06250
$c(\alpha = 1)$	7.943	6.758	10.35	9.204	0.04678
$c(\alpha = 0)$	3.624	2.536	4.756	3.715	0.03126
$c(\alpha = 0.5)$	5.625	4.429	6.805	5.618	
$c(\alpha = 0.2)$			5.267	4.154	

ИССЛЕДОВАНИЯ МОДИФИЦИРОВАННЫМИ УНИВЕРСАЛЬНЫМИ ПОТЕНЦИАЛЬНЫМИ ПОЛЯМИ

А. ЮЦИС, И. И. ГЛЕМБОЦКИС и Р. ГАШПАР

Р е з ю м е

Вычисления проводились с помощью разных видов универсального потенциального поля для основных состояний атома Fe, для ионов Fe^+, Fe^{3+}, Fe^{5+}, а также и для возбужденного состояния $1s^2\,2s^2\,2p^6\,3s^2\,3p^6\,3d^{10}\,4f$ атома Cu.

Acta Physica Academiae Scientiarum Hungaricae, Tomus 23 (4), pp. 443—448, (167)

ZUR PRÜFUNG DER PSEUDOPOTENTIALMETHODE AM WASSERSTOFFATOM

Von

P. GOMBÁS und O. KUNVÁRI

FORSCHUNGSGRUPPE FÜR THEORETISCHE PHYSIK, UNGARISCHE AKADEMIE DER WISSENSCHAFTEN. BUDAPEST

(Eingegangen: 3. IV. 1967)

Es werden mit den verschiedenen Besetzungsverbotpotentialen sowohl mit den statistischen als mit den wellenmechanischen einige Zustände des Wasserstoffatoms berechneund die Resultate mit einander verglichen. Hierbei zeigt sich, dass nicht nur das wellenmechanische Besetzungsverbotpotential, sondern auch die statistischen zu sehr guten Resultaten führen, obwohl bei den letzteren ein Versagen zu erwarten wäre, da ja das Wasserstoffatom für diese das extremste Beispiel darstellt.

Zur näherungsweisen Ersetzung des Paulischen Besetzungsverbotes vollbesetzter Elektronenzustände wurden verschiedene Pseudopotentiale hergeleitet und zwar sowohl statistische als wellenmechanische.[1] Um ein konkretes Beispiel vor Augen zu haben, wollen wir ein Atom mit einem Valenzelektron, also z.B. ein Alkaliatom, zugrunde legen, wo das Valenzelektron infolge des Paulischen Besetzungsverbotes in die von den Rumpfelektronen vollbesetzten Quantenzustände nicht hinabfallen kann. Dies lässt sich näherungsweise durch Pseudopotentiale, die sogenannten Besetzungsverbotpotentiale beschreiben. Diese sind Abstossungspotentiale, durch die das Hinabstürzen des Valenzelektrons in die tieferen Rumpfelektronenzustände verhindert wird.

In chronologischer Reihenfolge wurden zuerst die statistischen Besetzungsverbotpotentiale hergeleitet, von denen zwei verschiedenen Formen bekannt sind. Uns interessiert im folgenden das mit G_l bezeichnete Besetzungsverbotpotential, das auf ein Elektron im Zustand mit der Nebenquantenzahl l wirkt und folgende Gestalt hat[2]

$$G_l = -\frac{\pi^2 e a_0}{8(2l+1)^2}(D_l^2 + 2D_l P_l) - \frac{1}{8} e a_0 \frac{1}{r^2}. \qquad (1)$$

D_l bedeutet die radiale Dichte der Rumpfelektronen mit der Nebenquantenzahl l, P_l die im wellenmechanischen Sinne gedeutete radiale Dichte des Valenzelektrons im betreffenden Zustand mit der Nebenquantenzahl l, und r die

[1] Man vgl. hierzu P. GOMBÁS, Pseudopotentiale, Springer, Wien, New-York, 1967; im folgenden als I. zitiert.

[2] Man vgl. hierzu I, S. 70 ff.

Entfernung vom Kern; e ist die positive Elementarladung und a_0 der erste Bohrsche Wasserstoffradius.

Die wellenmechanische Form für das Besetzungsverbotpotential (genauer Besetzungsverbotoperator) ist ein nicht-lokales Pseudopotential, das folgende Gestalt hat[3]

$$-\frac{1}{e}\Phi_{nl}(r, r') = -\frac{1}{e}\sum_{n'=l+1}^{n-1}(\varepsilon - \varepsilon_{n'l})\,\varphi_{n'l}(r)\,\varphi^*_{n'l}(r'). \tag{2}$$

Hierbei wird vorausgesetzt, dass sich das Valenzelektron im Quantenzustand (n, l) befindet, dessen Energie wir kurz mit ε bezeichneten. $\varepsilon_{n'l}$ und $\varphi_{n'l}$ bedeuten die Energien und die radialen Eigenfunktionen der Rumpfelektronenzustände $(n'l)$.

Durch Heranziehen eines dieser Besetzungsverbotpotentiale wird der Orthogonalisierung der Eigenfunktion des Valenzelektrons im Zustand (n, l) auf die Eigenfunktionen der energetisch tiefer liegenden Rumpfelektronenzustände mit derselben Nebenquantenzahl l Rechnung getragen, man kann also so vorgehen, als ob die Rumpfelektronen gar nicht existierten und für das Valenzelektron den energetisch absolut tiefsten Zustand in dem mit einem der Pseudopotentiale erweiterten elektrostatischen Potential, dem sogenannten modifizierten Potentialfeld, bestimmen.

Anstatt der Lösung der Schrödingergleichung für das modifizierte Potentialfeld, ist es bei der hier angestrebten Genauigkeit zweckmässiger von dem Ausdruck der Energie für das Valenzelektron auszugehen und die Eigenfunktion und den Energieeigenwert des Valenzelektrons aus dem Minimumsprinzip der Energie zu bestimmen.

Für die Energie ε des Valenzelektrons in einem Zustand mit der Nebenquantenzahl l ergibt sich mit der auf 1 normierten Eigenfunktion des Valenzelektrons im Falle des Pseudopotentials G_l

$$\varepsilon = \frac{1}{2}e^2 a_0 \int_0^\infty f'^2\,dr + \frac{1}{2}e^2 a_0\, l(l+1)\int_0^\infty \frac{1}{r^2}f^2\,dr - e\int_0^\infty (V + G_l)f^2\,dr, \tag{3}$$

wo f' die Ableitung von f nach r bezeichnet und V das elektrostatische Potential des Atomrumpfes ist.

[3] Man vgl. hierzu I, S. 107 ff.

Für den Fall, dass man das wellenmechanische nichtlokale Pseudopotential $-\frac{1}{e}\Phi_{nl}$ zugrunde legt, ergibt[4] sich für die Energie des Valenzelektrons

$$\varepsilon = \int f^*(r)\, H_l f(r)\, dr + \\ + \frac{1}{1 - \sum_{n'=l+1}^{n-1} |(\varphi_{n'l}, f)|^2} \left[\sum_{n'=l+1}^{n-1} |(\varphi_{n'l}, f)|^2 \int f^*(r)\, H_l f(r)\, dr - \right. \\ \left. - \sum_{n'=l+1}^{n-1} \varepsilon_{n'l} |(\varphi_{n'l}, f)|^2 \right], \tag{4}$$

wo der erweiterte Hamilton Operator H_l folgende Bedeutung hat

$$H_l = -\frac{1}{2} e^2 a_0 \frac{d^2}{dr^2} - \frac{1}{2} e^2 a_0 \frac{l(l+1)}{r^2} - eV \tag{5}$$

und $(\varphi_{n'l}, f)$ wie üblich das Überlappungsintegral bezeichnet, also

$$(\varphi_{n'l}, f) = \int_0^\infty \varphi^*_{n'l} f\, dr \tag{6}$$

ist.

Man kann nun in erster Näherung für f den einfachen Ansatz machen

$$f = A r^\varkappa e^{-\lambda r}, \tag{7}$$

wo A eine Normierungskonstante bedeutet und $\varkappa$ sowie λ Variationsparameter bezeichnen, die aus der Minimumsforderung der Energie zu bestimmen sind.

Mit diesem Ansatz wird die Energie schon gut approximiert. Für die Eigenfunktion erhält man jedoch nur für das äusserste sogenannte Hauptmaximum eine gute Näherung, im Inneren des Atoms kann jedoch f^2 nur einen Mittelwert des Verlaufes des exakten radialen Eigenfunktionsquadrates geben. Eine auch im Inneren des Atoms sehr gute Approximation für die Eigenfunktion ergibt sich, wenn man die Eigenfunktion (7) auf die Eigenfunktionen der Rumpfelektronenzustände mit gleicher Nebenquantenzahl orthogonalisiert.

Zur Prüfung der Pseudopotentiale wollen wir das hier skizzierte Verfahren in erster Näherung auf das Wasserstoffatom anwenden, das allerdings im Falle der statistischen Pseudopotentiale das extremste Beispiel darstellt; für dieses Atom wäre ein Versagen dieser Potentiale zu erwarten.[5]

[4] P. GOMBÁS, I, S. 120.

[5] Berechnungen dieser Art für das Wasserstoffatom mit einem Pseudopotential G_l, das sich von (2) nur in Glieder, die von höherer Ordnung klein sind, unterscheidet, wurden schon früher von ANTONČIK (Czechosl. Journ. Phys. 7, 118, 1957) durchgeführt.

Mit dem Pseudopotential G_l gestalten sich die Termberechnungen des Wasserstoffatoms sehr einfach. Natürlich sind hier nur die angeregten Terme von Interesse, denn für die bei vorgegebener Nebenquantenzahl jeweils tiefsten Terme, d.h. $1s$-, $2p$-, $3d$-, ... Zustände ist $G_l \equiv 0$ und das Verfahren führt in diesen Fällen bei dem Ansatz (7) der Eigenfunktion zu den exakten Energien und Eigenfunktionen. Es kommen also nur die angeregten Zustände in Frage, bei deren Berechnung man so zu verfahren hat, dass man annimmt, dass die tiefer liegenden Zustände mit derselben Nebenquantenzahl, wie der zu berechnende, voll besetzt sind. Man wird also z.B. bei der Berechnung des $3s$-Zustandes des H-Atoms das Pseudopotential so wählen, als ob die Zustände $1s$ und $2s$ voll (d.h. mit je zwei Elektronen) besetzt wären.

Auf diese Weise haben wir mit dem statistischen Pseudopotential G_l die Energieniveaus $2s$-, $3s$-, $4s$- und $3p$- des H-Atoms und mit dem wellenmechanischen Pseudopotential $-\frac{1}{e}\Phi_{nl}$ die Energieniveaus $2s$-, $3s$- und $3p$- des H-Atoms bestimmt. Die Resultate sind für die Variationsparameter der Funktion (7) in der Tabelle 1 und für die Energieeigenwerte in Tabelle 2 zusammengestellt. Zum Vergleich sind in der Tabelle 2 auch die empirischen Energien angegeben.[6]

Tabelle I

Die Werte der Variationsparameter $\varkappa$ und λ; die Werte für λ in $1/a_0$-Einheiten

	Mit G_l berechnet		Mit Φ_{nl} berechnet	
	$\varkappa$	λ	$\varkappa$	λ
$2s$	2	0,374	2,8	0,565
$3s$	3	$0{,}225_5$	3,8	0,341
$4s$	4	0,159	—	—
$3p$	3	$0{,}268_5$	3,8	0,355

Tabelle II

Die Energien einiger Wasserstoffzustände mit G_l und Φ_{nl} berechnet und die empirischen Energien; alle Energien in e^2/a_0-Einheiten

	ε mit G_l berechnet	ε mit Φ_{nl} berechnet	ε empirisch
$2s$	$-0{,}1254$	$-0{,}1249$	$-0{,}12500$
$3s$	$-0{,}0534$	$-0{,}0562$	$-0{,}05555..$
$4s$	$-0{,}0292$	—	$-0{,}03125$
$3p$	$-0{,}0581$	$-0{,}0555_5$	$-0{,}05555..$

[6] Bei der Berechnung des $3p$-Zustandes mit dem G_l-Potential haben wir zunächst — um dem exakten Verlauf der Eigenfunktion für kleine r-Werte Rechnung zu tragen — $\varkappa = 2$ gesetzt, womit man $\varepsilon = -0{,}0560\ e^2/a_0$ erhält.

Aus einem Vergleich der in der Tabelle 2 angegebenen Energien mit den empirischen Werten ist zu sehen, dass die Energien, die man mit dem Pseudopotential G_l erhält, die empirischen fast ebensogut approximieren wie die Energien, die sich mit dem wellenmechanischen Pseudopotential $-\frac{1}{e}\Phi_{nl}$ ergeben. Dies zeigt, dass in diesem Fall das sehr einfache statistische Pseudopotential G_l für das genauere, bedeutend kompliziertere wellenmechanische Pseudopotential einen sehr guten Ersatz darstellt. Dies ist für den Fall des Wasserstoffatoms sehr überraschend, da sich in diesem Fall für die tieferen Energiezustände das Besetzungsverbot immer nur auf wenige Zustände bezieht, deren statistische Behandlungsweise, die dem Pseudopotential zugrunde liegt, nicht begründet werden kann.

Man kann nun noch weitergehen, indem man die so berechneten Eigenfunktionen nach dem Schmidtschen Verfahren orthogonalisiert.[7] Wenn man die orthonormierten Eigenfunktionen mit φ_{nl} bezeichnet, so hat man

$$\varphi_{nl} = C_{nl}\left[f_n - \sum_{n'=l+1}^{n-1} (\varphi_{n'l}, f_n)\,\varphi_{n'l}\right], \tag{8}$$

wo C_{nl} den Normierungsfaktor

$$C_{nl} = \frac{1}{\left[1 - \sum_{n'=l+1}^{n-1} |(\varphi_{n'l}, f_n)|\right]^{1/2}} \tag{9}$$

und $(\varphi_{n'l}, f_n)$ wieder das Überlappungsintegral bezeichnet, also

$$(\varphi_{n'l}, f_n) = \int_0^\infty \varphi^*_{n'l}, f_n\, dr \tag{10}$$

ist.[8]

Auf diese Weise haben wir die Eigenfunktion des $2s$- und $3s$-Zustandes in erster Näherung berechnet. Es ergibt sich mit den auf Grund des Pseudopotentials $-\frac{1}{e}\Phi_{nl}$ bestimmten Eigenfunktionen eine praktisch vollkommene Übereinstimmung mit den exakten Eigenfunktionen. Mit den auf Grund des Pseudopotentials G_l bestimmten Eigenfunktionen ist die Übereinstimmung in dieser ersten Näherung insbesondere in den äusseren Gebieten des Atoms bedeutend schlechter.

Die Durchführung des grössten Teiles der numerischen Rechnungen verdanken wir Frl. Zs. Ozoróczy.

[7] Man vgl. hierzu I, S. 103 ff.

[8] Statt f haben wir hier f_n geschrieben, um anzudeuten, dass sich diese Eigenfunktion auf den Zustand mit der Hauptquantenzahl n bezieht.

ОБ ИСПЫТАНИИ МЕТОДА ПСЕВДОПОТЕНЦИАЛОВ В СЛУЧАЕ АТОМА ВОДОРОДА

П. ГОМБАШ и О. КУНВАРИ

Р е з ю м е

Различными потенциалами запрета заполнения, как статистическим, так и волново-механическим, вычисляются некоторые состояния атома водорода. Результаты вычислений сопоставляются. Из сопоставления вытекает, что наряду с волново-механическим потенциалом запрета заполнения и статистический ведет к очень хорошим результатам, хотя у последнего можно было бы ожидать отказа от службы, так как атом водорода для этого представляет экстренный пример.

Acta Physica Academiae Scientiarum Hungaricae, Tomus 23 (4), pp. 449—452, (1967)

COMMUNICATIONES BREVES
EFFECT OF CONCENTRATION ON FLUORESCENCE SPECTRUM OF EOSIN

By

S. S. RATHI and M. K. MACHWE

DEPARTMENT OF PHYSICS AND ASTROPHYSICS, UNIVERSITY OF DELHI, DELHI-7, INDIA

(Received 12. I. 1967)

Introduction

FRANK and VAVILOV [1], by assuming the configuration quenching to be superimposed on collision quenching, were able to explain the experimental results for the fluorescence yield in the presence of a foreign quencher. This theory has also been used to explain the concentration quenching of fluorescence. But in many instances the experimental results for self-quenching show a deviation from the above theory. In order to explain the observed self-quenching, F. PERRIN [2], put forward the following relation:

$$Q = Q_0 \cdot e^{-kc},$$

where Q_0 and Q are the yields of fluorescence in the unextinguished and extinguished states respectively, c is the concentration of the fluorescent substance and k is a constant which determines the quenching probability of an excited molecule by an unexcited molecule of the same kind.

Eosin in solution can exist as neutral molecules, monoanions, dianions and dimers, and in a given solution the proportion of each variety will depend upon the concentration of the dye. Hence, a change in the nature of the fluorescence spectrum with concentration is expected. The present investigation was undertaken to study the fluorescence spectrum for higher concentrations of Eosin and also to check the validity of PERRIN's formula under these conditions.

Experimental

The experimental arrangement used for fluorescence intensity measurements is the same as that employed in our earlier investigation [3]. The fluorescent and transmitted intensities are measured by the null method, using photoelectric cells. The fluorescence of Eosin blue in Glycerine-Water mixture (50—50% by volume) excited by the mercury wave-length $\lambda = 5460$ Å is recorded by a Hilger's constant deviation spectrograph and the fluorescence spectrum intensities obtained using a recording microphotometer.

Results and discussion

Fig. 1 shows the spectrum of Eosin fluorescence for concentrations $1 : 7.5 \times 10^{-6}$ g/c.c., $2 : 2.5 \times 10^{-5}$ g/c.c. and $3 : 7.5 \times 10^{-5}$ g/c.c. It can be seen that there is a marked difference between the fluorescence spectra for concentrations 1 and 3. It appears that the spectrum intensity curve 3 results from super-imposition of two intensity curves, one having its maxim-

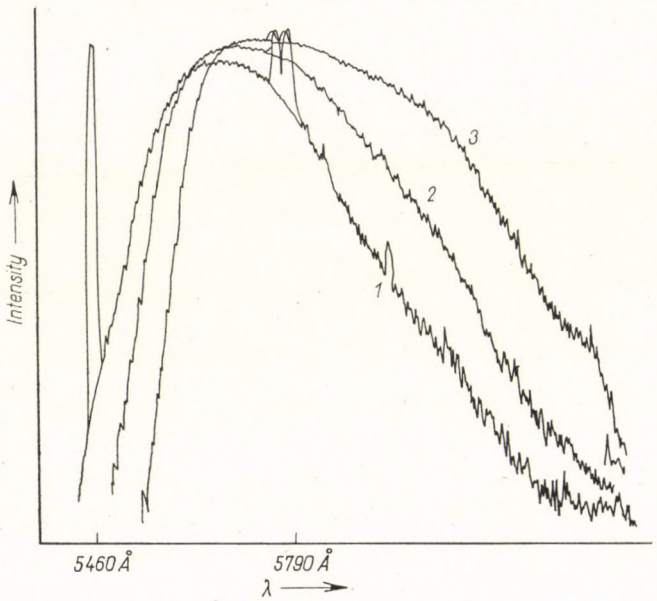

Fig. 1. Microphotometer record of the fluorescence spectrum of Eosin for concentrations 1: 7.5×10^{-6} g/c.c., 2: 2.5×10^{-5} g/c.c. and 3: 7.5×10^{-5} g/c.c.

um at $\lambda \sim 5680$ Å in the same region as curve 1 and the other having its maximum at $\lambda \sim 6030$ Å on the longer wave-length side.

PARKER [4] has observed a single maximum in the fluorescence spectrum of Eosin in glycerine at $\lambda \sim 5650$ Å. But he has reported two peaks in the delayed fluorescence of Eosin, one at $\lambda \sim 5650$ Å due to fluorescence and the other at $\lambda \sim 6890$ Å due to phosphorescence. The peak at $\lambda \sim 5680$ Å in the present investigation corresponds to PARKER's peak due to fluorescence. As the intensity of the peak at $\lambda \sim 6030$ Å in the spectral intensity curve 3 is comparable to that of the peak at $\lambda \sim 5680$ Å and also, as the former does not lie in the region of PARKER's second peak, the possibility of this peak at $\lambda \sim 6030$ Å being interpreted as due to phosphorescence is ruled out. The peak at $\lambda \sim 5680$ Å obtained with lower concentrations may be due to Eosin dianions as Eosin is known to exist in doubly ionised form in very dilute

solution. But at higher concentrations there may be more monoanions and dimers. These may be responsible for the peak at $\lambda \sim 6030$ Å which appears only at higher concentrations. The view is supported by the fact that the intensity of this peak increases with increasing concentration. PARKER's failure to observe the peak at $\lambda \sim 6030$ Å may be due to the fact that the concentrations used by him were not high enough.

Eosin in dilute solution ionises as 2 Na^+ ions and the rest carrying two negative charges, the addition of NaOH should, therefore, give rise to a

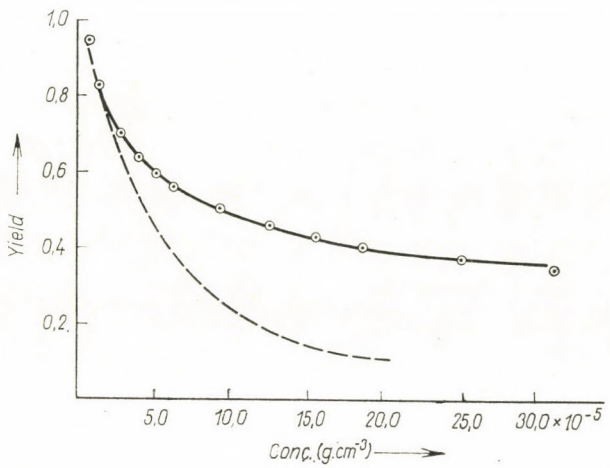

Fig. 2. Dependence of the relative fluorescence yield of Eosin on its concentration in a glycerine-water mixture (50—50% volume). ——— Experimental curve; - - - - calculated from PERRIN's formula

change in the nature of the fluorescence spectrum. However, we have observed no change in the spectral nature of the fluorescence of Eosin on adding NaOH to it. This rules out the possibility of the peak at $\lambda \sim 6030$ Å being interpreted as due to monoanions. So the peak at $\lambda \sim 6030$ Å which appears in higher concentrations of Eosin must be due to fluorescent Eosin dimers.

Fig. 2 shows the variation of the fluorescence yield with the concentration of Eosin in solution. No set of parameters has been found to exist which would make the experimental data agree with PERRIN's formula over the entire range of concentration employed. The yield decay appears to follow PERRIN's formula in the concentration range 6.0×10^{-6} g/c.c. to 3.0×10^{-5} g/c.c. beyond which the yield decay is much less than would be expected from this formula. This can be explained by the fluorescent dimer formation. As both the monomers and dimers fluoresce, with the dimer formation the effective

concentration will be lower than the actual concentration in PERRIN's formula. And hence, the fluorescence yield decays less rapidly than is required by PERRIN's formula.

Acknowledgement

The authors are grateful to Dr. K. GOPALAKRISHNAN and SHRI JUGAL KISHORE for their help during the course of this work. One of us, S. S. RATHI, acknowledges with thanks the receipt of a C.S.I.R. fellowship.

REFERENCES

1. I. M. FRANK and S. I. VAVILOV, Z. f. Physik, **69**, 100, 1931.
2. F. PERRIN, Ann. de Physique, **17**, 283, 1932.
3. J. KISHORE, et al., Ind. J. Phys., **8**, 415, 1962.
4. C. A. PARKER and C. G. HATCHARD, Trans. Faraday Soc., **57**, 1894, 1961.

Acta Physica Academiae Scientiarum Hungaricae, Tomus 23 (4), pp. 453—455, (1967)

RELATIVISTIC TRION MODEL FOR HADRONS

By

K. LADÁNYI

RESEARCH GROUP FOR THEORETICAL PHYSICS, HUNGARIAN ACADEMY OF SCIENCES, BUDAPEST

(Received 11. V. 1967)

This note contains some remarks about an SO_6 model of strong interactions. An appropriate description of the SO_6 model is provided by the trion theory of BACRY, NUYTS and VAN HOVE [1, 2]. In this model the fundamental field is a (6×4)-component trion spinor $t_m(x\alpha)$, where $\alpha(\alpha = 1 \ldots 4)$ and $m(m = 1 \ldots 6)$ indicate the Dirac spinor and SO_6-spin indices, respectively. According to HEISENBERG's suggestions [3, 4] it will be assumed that the field operator $t_m(x\,\alpha)$ satisfies a nonlinear spinor equation. In a previous paper [5] we have considered the general symmetry properties characterizing the field equation[1] [2]

$$-i\gamma^\mu \frac{\partial}{\partial x^\mu} t_m + GO^{(3)}_{mm'} O^{(3)}_{nn'} [T\gamma^\mu t_n (\bar{t}_{m'} \gamma_\mu t_{n'}) + \\ + Ti\gamma^5 \gamma^\mu t_n (\bar{t}_{m'} i\gamma^5 \gamma_\mu t_{n'})] = 0\,, \tag{1}$$

where T is Wick's chronological operator and the local interaction term is defined by the usual limiting procedure. The explicit form of the matrix $O^{(3)}$ is

$$O^{(3)} = \begin{pmatrix} 0 & 1 \\ 1 & 0 \end{pmatrix}, \tag{2}$$

where 0 and 1 are three-dimensional null and unit matrices, respectively. By going over to the "variables"

$$X_a(x\,\alpha) = \frac{1}{2}[t_a(x\,\alpha) + t_{3+a}(x\,\alpha)], \\ a = 1, 2, 3 \tag{3}$$
$$X_{3+a}(x\,\alpha) = -\frac{i}{2}[t_a(x\,\alpha) - t_{3+a}(x\,\alpha)],$$

[1] The coupling constant G has the dimension of (length)^2 and $\gamma^5 = \gamma^0\gamma^1\gamma^2\gamma^3$

[2] Summation over repeated indices is understood.

it can be readily verifed that eq. (1) is form-invariant under the transformations of the SO_6 group[3]. In addition, the interaction Lagrangian is characterized by $GL(6, C)^{(+)} \otimes GL(6, C)^{(-)}$ invariance[4] with $GL(6, C)^{(+)}$ and $GL(6, C)^{(-)}$ referring to the positive and negative chiral projections of the field operator t_m, respectively [5].

The dynamical properties of the model may be discussed by using the covariant Fock method [6]. Nonperturbative decompositions of the many-point amplitudes result in appropriate ladderlike approximations. The amplitudes of trion-antitrion pairs, characterized by rest energy $\varkappa$, spin $s(s = 0, 1)$ and representation $R(R = 1, 15, 20'')$ of SO_6 [7], may be considered in a relatively simple way. The coupling of trions to these trion-antitrion pairs are characterized by the coupling constants $g^{(s,R)}(\varkappa^2)$. By requiring the existence of the local nonlinear interaction term of the field equation (1) we obtain the following sum rules

$$S_{\varkappa^2}\left[g^{(1,1)}(\varkappa^2)\right]^2 = \frac{7}{6}\pi^2, \qquad S_{\varkappa^2}\left[g^{(1,15)}(\varkappa^2)\right]^2 = \frac{1}{2}\pi^2,$$
$$S_{\varkappa^2}\left[g^{(1,20'')}(\varkappa^2)\right]^2 = \frac{1}{6}\pi^2, \tag{4}$$

$$S_{\varkappa^2}\left[g^{(0,1)}(\varkappa^2)\right]^2 = \frac{21}{2}\pi^2, \qquad S_{\varkappa^2}\left[g^{(0,15)}(\varkappa^2)\right]^2 = \frac{9}{2}\pi^2,$$
$$S_{\varkappa^2}\left[g^{(0,20'')}(\varkappa^2)\right]^2 = \frac{3}{2}\pi^2, \tag{5}$$

where the symbol $S\varkappa_2$ denotes a complete summation over the subscript $\varkappa^2$ (the summation includes an integration $\int d\varkappa^2$ over the continuous part of its range).

Equation (1) is covariant under the transformations of the γ^5 and SO_6 groups. We may assume, along the lines suggested by HEISENBERG [3, 4], NAMBU and JONA-LASINIO [8], BAKER and GLASHOW [9] and many others, that the breakdown of these symmetries is spontaneous. A generalized ladder approximation may be obtained for the Fock amplitudes corresponding to trion systems. The effective-mass operator and the generalized form factors of trions are defined as the solutions of a variational problem resulting from the requirement of the optimal convergence of higher approximations. Details of these calculations will be given elsewhere [10].

[3] SO_6 is the group of real rotations with determinant one.

[4] The noncompact group $GL(6, C)$ consists of all nonsingular complex linear transformations in 6-dimensional space.

REFERENCES

1. H. Bacry, J. Nuyts and L. Van Hove, Nuovo Cimento, **35,** 510, 1965.
2. L. Van Hove in: Preludes in Theoretical Physics, ed. A. De-Shalit, H. Feshbach and L. Van Hove, Amsterdam, 1965.
3. H. P. Dürr, W. Heisenberg, H. Mitter, S. Schlieder and K. Yamazaki, Zeits. f. Naturforsch., **14a,** 442, 1959 and subsequent papers.
4. W. Heisenberg: Introduction to the Unified Field Theory of Elementary Particles, to be published.
5. K. Ladányi, Nuovo Cimento, **45,** 289, 1966.
6. E. g. P. T. Matthews and A. Salam, Proc. Roy. Soc., A **221,** 128, 1954.
7. I. S. Gerstein and M. L. Whippmann, Phys. Rev., **137,** B 1522, 1965.
8. Y. Nambu and G. Jona-Lasinio, Phys. Rev., **122,** 345, 1961.
9. M. Baker and S. L. Glashow, Phys. Rev., **1928,** 2462, 1962.
10. K. Ladányi, Nuovo Cimento, to be published.

RECENSIONES

Nucleon Structure

Proceedings of the International Conference at the Stanford University, June 24—27, 1963, edited by R. Hofstadter u. L. J. Schiff, p. X + 421, Stanford University Press, Stanford, 1964.

The Conference at Stanford of which the lectures are contained in this book, was devoted mainly to the structure of the proton and the neutron. The invited papers dealt with the theoretical background, nucleon form factors, relativistic deuteron theory, the most recent experimental results on electron and positron scattering, theory of strong interactions, symmetry properties of elementary particles and their interactions, electromagnetic and weak interaction form factors, and anti-nucleon effects. One third of the book deals with contributed papers on a wide variety of theoretical and experimental topics.

Thanks are due to the editors that with the publication of this volume they have made these lectures, delivered by outstanding physicists, available to a large public.

P. GOMBÁS

A. A. SOKOLOV: Elementary Particles

translated from original in Russian by W. E. Jones, p. VI + 75, Pergamon Press, Oxford etc., The Macmillan Company, New York, 1964. Price: 10.— s.

This little book gives an excellent survey of the experimental facts and the theory of elementary particles with a minimum of mathematics. It contains the following chapters: Prediction of the positron by Dirac and its experimental discovery; Nucleons and pions (nuclear field quanta); Beta-disintegration and the discovery of the neutrino; The problem of the non-conservation of the parity; "Abandoned and strange" particles, "resonons".

It is written in a very clear style and can be recommended to all those who want to gain an insight into this very important field of physics without becoming involved in too much mathematics.

P. GOMBÁS

R. BROUT and P. CARRUTHERS: Lectures on the Many-Electron Problem

(10th volume of the Interscience Monographs and Texts in Physics and Astronomy edited by R. E. Marshak) VIII + 204, Interscience Publishers, New York, London, Sydney, 1963.

This book is based on a course given by R. BROUT at Cornell University on the many-body problem which dealt mainly with the following two subjects: the first is an introduction to the linked cluster development of the many-body perturbation theory with a parallel development in classical statistics, quantum adiabatic zero temperature theory, and finally quantum statistics; the second is a development of the many-electron problem from the plasma point of view.

The book is divided into the following chapters: 1. The many-body problem in classical mechanics, 2. Field theoretical methods; linked cluster expansion, 3. Electron correlation; quantum mechanical treatment, 4. Dielectric formulation of the many-body problem, 5. Application to the theory of metals.

The book is written very clearly and can be recommended warmly to all scientists working in this field and also to students who want to become acquainted with this branch of

study. The reader will only regret that the authors, as they say in the Preface, had neither time nor space to write further on some of the more elegant developments of many-body theory or on the beautiful applications that have been found in physical problems.

P. GOMBÁS

P. ROMAN: Advanced Quantum Theory

XIV + 735, Addison—Wesley Publishing Comp. Inc., Reading, Massachusetts, 1965.
Price: 17.50 $

The author explains the purpose of this book in the Preface as follows: "I observed that there is dire need for a text which, although incomplete in many ways, is unified in style and presentation and could lead the student, in a gentle manner, from the realm of basic quantum mechanics (in which he has already acquired a working knowledge) to the peaks of present day research methods and concepts."

I think everybody teaching quantum mechanics would agree with the author, and I think he has filled a real gap in the literature very successfully.

The book deals with the following topics, Part I: 1. The framework of Quantum Theory. 2. Elements of relativistic quantum mechanics. Part II: 3. Potential scattering. 4. General formal theory of collision phenomena. Part III: 5. Symmetry transformations and conservation laws. 6. Some explicit applications of group theoretical methods in quantum theory. Appendices: 1. Linear algebra of Hilbert space, 2. The rudiments of group theory, 3. Some properties of the Dirac equation, 4. On Green's functions.

P. GOMBÁS

H. MUIRHEAD: The Physics of Elementary Particles

XVI + 738, Pergamon Press, Oxford, London, Edinburgh, New York, Paris, Frankfurt, 1965.
Price: £ 7.

This is an excellent book for everybody who wants to get familiar, without too much mathematical formalism, with the theory of elementary particles. It is intended for post-graduate students and for experimentalists working in high energy nuclear physics.

The book deals with the following topics: The discovery and classification of elementary particles, the intrinsic properties of the particles, preliminaries to a quantized field theory, the quantum theory of non-interacting fields, the symmetry properties of free fields, the interaction of fields (wave functions, phase shifts and potentials, the S-matrix, specific forms for the S-matrix, the invariance properties of interacting systems, dispersion relation and related topics), electromagnetic interactions, the weak interactions, strong interactions (resonances and strange particles, reactions).

Although the physics of elementary particles is developing rapidly I am convinced that this book will be a standard work in this field for a long time to come.

P. GOMBÁS

A. A. SOKOLOW, J. M. LOSKUTOW und I. M. TERNOW: Quantenmechanik

(aus dem Russischen übersetzt von Dipl.-Phys. H. Fischer, in deutscher Sprache herausgegeben von G. Heber), Akademie Verlag, Berlin, 1964.

Das Buch gibt eine systematische Darstellung der Quantenmechanik. Es zergliedert sich in drei Kapitel. Das erste befasst sich mit der nicht relativistischen Wellenmechanik, wobei viele Anwendungsmöglichkeiten behandelt werden und zwar nicht nur die Standardfälle sondern auch andere, wie z. B. die Grundlagen der Theorie der Festkörperphysik. Im zweiten Kapitel werden die relativistische Quantenmechanik, die Theorie der Atome mit mehreren Elektronen, sowie die Elemente der Theorie der Moleküle gebracht. Das dritte Kapitel behandelt die Grundzüge der Kernphysik, der zweiten Quantelung und der Elementarteilchentheorie.

Die Grundlage dieses ausgezeichneten Lehrbuches bilden die Vorträge von Professor A. A. SOKOLOW, die er an der Physikalischen Fakultät der Moskauer Staatlichen Lomonossow-

Universität seit 1945 hält. Es enthält eine Reihe von Übungen in Form von sehr gut ausgewählten Aufgaben, die dem Leser eine selbstständige Mitarbeit ermöglichen. Das Buch ist didaktisch vorzüglich aufgebaut, die Darstellungsweise ist sehr leicht verständlich, die Probleme sind bis in die Einzelheiten durchgerechnet. Es wird nicht nur den Studierenden, sondern auch den Hochschullehrern zu ihren Vorlesungen sowie für die Atomphysikern in ihrer Forschungsarbeit ein erstklassiges Hilfsmittel darstellen; es reiht sich in die besten Bücher auf diesem Gebiet ein. Durch die deutsche Auflage wird erfreulicherweise dieses hervorragende Werk einem weiteren grossen Kreis von Physikern zugänglich gemacht.

P. GOMBÁS

A. S. DAVYDOV: **Quantum Mechanics**

(aus dem Russischen übersetzt von D. ter Haar), XIV + 680 S., Pergamon Press, Oxford, London, Edinburg, New York, Paris, Frankfurt, 1965. Price: 90 s.

Dies ist eines der besten Bücher unter der grossen Auswahl von Büchern über Quantenmechanik. Es wird darin ein grosses Gebiet der Quantentheorie in sehr übersichtlicher und gründlicher Weise bearbeitet. Die üblichen Probleme bilden die Grundlage, an die sich viele weitere anschliessen, die in Büchern über Quantenmechanik nur teilweise und selten oder meistens überhaupt nicht vorzufinden sind. Von diesen möchten wir nur die folgenden nennen: die Dichtematrix und ihre Anwendungen, zero-Spin Teilchen in der relativistischen Quantenmechanik, S-matrix Theorie, Neutronenstreuung, Theorie der chemischen Kräfte, Grundlagen der Theorie der Festkörperphysik, zweite Quantelung.

Vom Übersetzer wurden cca 200 Aufgaben hinzugefügt; die sehr gut ausgewählt sind und zum Selbststudium wesentlich beitragen.

Es sei hier auch auf ein kleines Versehen hingewiesen. Auf S. 358 wird behauptet, dass die zur Zeit genauste Lösung der Thomas—Fermischen Gleichung die von BUSH und CALDWELL (1931) sei. Dies ist jedoch nicht der Fall, denn seither existieren wesentlich genauere Lösungen (man vgl. Flügges Handbuch der Physik Bd. 36. S. 126 ff., Springer, Berlin—Göttingen—Heidelberg 1956).

Dieses Buch wird sowohl für den jungen Studierenden als auch für den auf diesem Gebiet arbeitenden Physiker ein äusserst wertvolles Hilfsmittel darstellen.

P. GOMBÁS

T. A. LITTLEFIELD and N. THORLEY: **Atomic and Nuclear Physics**

(An Introduction),
p. VIII + 436, D. Van Nostrand Company Ltd., London, Toronto, New York, Princeton (New Jersey), 1963.

Die Verfasser setzen sich zum Ziel den Leser in die Physik der Atomhülle und des Atomkerns mit möglichst minimalem matematischen Apparat einzuführen. Es gründet sich auf Vorlesungen für Stundenten in den ersten Semestern an der Universität Newcastle. In Anbetracht der ungeheueren Fülle des Stoffes können natürlich in dem sehr eng begrenzten Volumen überall nur die grundlegenden Experimente und die empirischen Feststellungen gebracht werden. Von den theoretischen Grundlagen werden höchstens die elementarsten Begriffe und Zusammenhänge erwähnt, was bei der bewussten Meidung des mathematischen Apparates, auch nicht anders zu erwarten ist. Am Ende von jedem Kapitel befinden sich gut ausgewählte Aufgaben, an Hand deren sich der Studierende in das Gebiet einarbeiten kann. Die Verbreitung des Buches wird sehr stark von den Ansprüchen abhängen, die die verschiedenen Universitäten an ihre Studenten in den ersten Semestern stellen.

P. GOMBÁS

W. A. HARRISON: **Pseudopotentials in the Theory of Metals**

p., XVI + 336 W. A. Benjamin Inc., New York, Amsterdam, 1966. $ 12.00

Dies Buch gibt eine teilweise Übersicht der Pseudopotentialmethode und deren vielseitigen Anwendungen auf dem Gebiete der Theorie der Metalle. Es ist leicht verständlich geschrieben und umfasst eine grosse Fülle von Anwendungen, woraus hervorgeht, dass die Pseudopotentialmethode heute in der Metalltheorie eine der wichtigsten Methoden darstellt.

Ausser diesen Vorzügen weist jedoch dieses Buch einen erheblichen Mangel auf: Nach der Darstellung des Autors scheint die Pseudopotentialmethode mit den wellenmechanischen Besetzungsverbotoperatoren durch PHILLIPS und KLEINMAN (1959) begründet worden zu sein. Dass die Methode mit diesen Operatoren tatsächlich schon bedeutend früher von FÉNYES in 1943 begründet und von SZÉPFALUSY in 1955 von der Wellenmechanik her fast auf dieselbe Weise wie von PHILLIPS und KLEINMAN hergeleitet wurde, scheint dem Verfasser vollkommen unbekannt zu sein.

Ebenso nimmt der Verfasser keinerlei Notiz davon, dass die keinesfalls unwichtigeren statistischen Pseudopotentiale (die später die Veranlassung für FÉNYES und SZÉPFALUSY für die Herleitung der wellenmechanischen Besetzungsverbotoperatoren gegeben haben) von anderen Autoren schon in 1935 entwickelt und seither wesentlich ausgebaut wurden. Auch werden die zahlreichen Anwendungen dieser Pseudopotentiale insbesondere auf Metalle nirgends erwähnt, obwohl die ganze einschlägige Literatur an einer allgemein zugänglichen Stelle und zwar in der neuen Auflage des Handbuches d. Physik Bd. 36/2, S. 168 ff. u. S. 208 ff. (Springer, Berlin, 1956) ausführlich angegeben ist. Mann sollte bei einer zusammenfassenden Darstellung eines Gebietes der Physik mit mehr Objektivität und Sorgfalt vorgehen, denn sonst bekommt der Leser von diesem nur ein sehr einseitiges Bild.

P. GOMBÁS

"KULTURA", Budapest, offers

MATHEMATICAL SETS:

TRUDY SEMINARA PO VEKTORNOMU I TENZORNOMU ANALIZU

Abhandlungen aus dem Seminar für Vektor- und Tensoranalysis.
Mémoires du Séminaire pour l'Analyse vectorielle et tensorielle

Reprint

Vols. 1—13, Moscow—Leningrad 1933—1966 clothbound — US $ 240.—

Vols. 1—4 are published chiefly in Western languages. Vol. 4 contains the proceedings of the 1st International Conference for Tensor Differential Geometry, held in Moscow, 1934. Editors: Professor V. F. Kagan and P. K. Razhevskij

A MAGYAR TUDOMÁNYOS AKADÉMIA III., MATEMATIKAI ÉS FIZIKAI OSZTÁLYÁNAK KÖZLEMÉNYEI

Vols. 1—17, Budapest, 1950—1967 clothbound — US $ 170.—
in original issues — US $ 136.—

Hungarian language publication of the Mathematical and Physical Section of the Hungarian Academy of Sciences.

MATEMATIKAI LAPOK

Partly reprinted

Vols. 1—18, Budapest, 1949/50—1967 clothbound — US $ 196.—
paperbound, resp. in original issues — US $ 160.—

Mathematical quarterly, published by the Bolyai Mathematical Society in Hungarian, with summaries in congress languages, bringing regularly the bibliography of Hungarian mathematical literature. Editor: Professor P. Turán.
In preparation, the complete series available about the end of 1968:

MATEMATIKAI ÉS FIZIKAI LAPOK

Mostly reprinted

Vols. 1—50, Budapest, 1892—1943, all published with General Index

clothbound — US $ 850.—
paperbound, resp. in original issues — US $ 750.—
Prepublication price, valid until June 30, 1968: clothbound — US $ 800.—
paperbound, resp. in original issues — US $ 700.—

Fundamental periodical of Hungarian mathematical and physical researches. Published by the L. Eötvös Mathematical and Physical Association in Hungarian, since 1920 contains also ample summaries in German language. Most of the authors may be ranked amongst the best scientists of that period.

Mathematical editors: G. Rados (1892—1913)
L. Fejér (1914—1932)
B. Kőnig (1933—1943)

INTERNATIONAL MATHEMATICAL JOURNALS FROM HUNGARY:

The Hungarian ACTA — periodicals publish original scientific treatises in English, German, French or Russian, written by outstanding authors from Hungary and other countries.

ACTA MATHEMATICA ACADEMIAE SCIENTIARUM HUNGARICAE

Mostly reprinted

Vols. 1—18, Budapest, 1950—1967, with HUNGARICA ACTA MATHEMATICA

Vol. 1, 1949, and Supplement to vol 5. clothbound US $ 323.—
paperbound, resp. in original issues US $ 285.—

ACTA SCIENTIARUM MATHEMATICARUM (Institutum Bolyaianum Universitatis Szegediensis)

Mostly reprinted

Vols. 1—28, Szeged, 1922—1967 clothbound US $ 464.—
paperbound, resp. in original issues US $ 406.—

PUBLICATIONES MATHEMATICAE (Institutum Mathematicum Universitatis Debreceniensis)

Partly reprinted

Vols. 1—14, Debrecen, 1949—1967 clothbound US $ 210.—
paperbound, resp. in original issues US $ 182.—

ANNALES UNIVERSITATIS SCIENTIARUM BUDAPESTIENSIS DE R. EÖTVÖS NOMINATAE. Sectio Mathematica

Partly reprinted

Vols. 1—9, Budapest, 1958—1966, including memorial vol. 3/4, devoted to L. Fejér — Clothbound US $ 90.—
Paperbound US $ 72.—

STUDIA SCIENTIARUM MATHEMATICARUM HUNGARICA auxilio consilii Instituti Mathematici Academiae Scientiarum Hungaricae

Vols. 1—2, Budapest, 1966—1967 clothbound US $ 28.—
in original issues US $ 24.—

PUBLICATIONS OF THE MATHEMATICAL INSTITUTE OF THE HUNGARIAN ACADEMY OF SCIENCES (A Magyar Tudományos Akadémia Matematikai Kutató Intézetének Közleményei)

Partly reprinted, published mostly in congress languages.

Old Series: Vol. 1—3, Budapest, 1952—1954 all published
New Series: Vols. 1—9, Budapest, 1956—1965 all published
clothbound US $ 134.—
paperbound, resp. in original issues US $ 110.—

Single volumes off all above periodicals may be quoted at request

Subscription price of forthcoming volumes US $ 12.—each

Reviews of the Hungarian Academy of Sciences are obtainable at the following addresses:

ALBANIA

Ndermarja Shtetnore e Botimeve
Tirana

AUSTRALIA

A. Keesing
Box 4886, GPO
Sydney

AUSTRIA

Globus Buchvertrieb
Salzgries 16
Wien I

BELGIUM

Office International de Librairie
30, Avenue Marnix
Bruxelles 5
Du Monde Entier
5, Place St. Jean
Bruxelles

BULGARIA

Raznoiznos
1, Tzar Assen
Sofia

CANADA

Pannonia Books
2, Spadina Road
Toronto 4, Ont.

CHINA

Waiwen Shudian
Peking
P. O. B. Nr. 88

CZECHOSLOVAKIA

Artia
Ve Smečkách 30
Praha 2
Poštova Novinova Služba
Dovoz Tisku
Vinohradská 46
Praha 2
Madarská Kultura
Praha I
Václavské nám. 2
Poštova Novinova Služba
Dovoz Tlace
Leningradska 14
Bratislava

DENMARK

Ejnar Munksgaard
Nörregade 6
Copenhagen

FINLAND

Akateeminen Kirjakauppa
Keskuskatu 2
Helsinki

FRANCE

Office International de Documentation et Librairie
48, rue Gay Lussac
Paris 5

GERMAN DEMOCRATIC REPUBLIC

Deutscher Buch-Export und Import
Leninstraße 16
Leipzig 701
Zeitungsvertriebsamt
Clara Zetkin Straße 62
Berlin N. W.

GERMAN FEDERAL REPUBLIC

Kunst und Wissen
Erich Bieber
Postfach 46
7 Stuttgart S.

GREAT BRITAIN

Collet's Holdings Ltd.
Dennington Estate
London Rd.
Wellingborough, Northamps.
Robert Maxwell and Co. Ltd.
Waynflete Bldg. The Plain
Oxford

HOLLAND

Swetz and Zeitlinger
Keizersgracht 471—487
Amsterdam C.
Martinus Nijhof
Lange Voorhout 9
The Hague

INDIA

Current Technical Literature
Co. Private Ltd.
India House OPP.
GPO Post Box 1374
Bombay I

ITALY

Santo Vanasia
Via M. Macchi 71
Milano
Libreria Commissionaria Sansoni
Via La Marmora 45
Firenze

JAPAN

Nauka Ltd.
92. Ikebukur O-Higashi 1-chome
Toshima-ku
Tokyo
Maruzen and Co. Ltd.
P. O. Box 605
Tokyo-Central
Far Eastern Booksellers
Kanda P. O. Box 72
Tokyo

KOREA

Chulpanmul
Phenjan

NORWAY

Johan Grundt Tanum
Karl Johansgatan 43
Oslo

POLAND

RUCH
ul. Wronia 23
Warszawa

ROUMANIA

Cartimex
Str. Aristide Briand 14—18
Bucureşti

SOVIET UNION

Mezhdunarodnaja Kniga
Moscow G—200

SWEDEN

Almquist and Wiksell
Gamla Brogatan 26
Stockholm

USA

Stechert Hafner Inc.
31, East 10th Street
New York, N. Y. 10003
Walter J. Johnson
111, Fifth Avenue
New York, N. Y. 10003

VIETNAM

Xunhasaba
19, Tran Quoc Toan
Hanoi

YUGOSLAVIA

Forum
Vojvode Mišića broj 1
Novi Sad
Jugoslavenska Knjiga
Terazije 27
Beograd

Printed in Hungary

A kiadásért felel az Akadémiai Kiadó igazgatója. Műszaki szerkesztő: Farkas Sándor

A kézirat a nyomdába érkezett: 1967. IX. 29. — Terjedelem: 12 (A/5) ív. 49 ábra

67.64478 Akadémiai Nyomda, Budapest — Felelős vezető: Bernát György

The *Acta Physica* publish papers on physics, in English, German, French and Russian.

The *Acta Physica* appear in parts of varying size, making up volumes.

Manuscripts should be addressed to:

Acta Physica, Budapest 502, P. O. B. 24.

Correspondence with the editors and publishers should be sent to the same address.

The rate of subscription to the *Acta Physica* is 165 forints a volume. Orders may be placed with "Kultúra" Foreign Trade Company for Books and Newspapers (Budapest I., Fő u. 32. Account No. 43-790-057-181) or with representatives abroad.

Les *Acta Physica* paraissent en français, allemand, anglais et russe et publient des travaux du domaine de la physique.

Les *Acta Physica* sont publiés sous forme de fascicules qui seront réunis en volumes.

On est prié d'envoyer les manuscrits destinés à la rédaction à l'adresse suivante:

Acta Physica, Budapest 502, P. O. B. 24.

Toute correspondance doit être envoyée à cette même adresse.

Le prix de l'abonnement est de 165 forints par volume.

On peut s'abonner à l'Entreprise du Commerce Extérieur de Livres et Journaux «Kultúra» (Budapest I., Fő u. 32. — Compte-courant No. 43-790-057-181) ou à l'étranger chez tous les représentants ou dépositaires.

«*Acta Physica*» публикуют трактаты из области физических наук на русском, немецком, английском и французском языках.

«*Acta Physica*» выходят отдельными выпусками разного объема. Несколько выпусков составляют один том.

Предназначенные для публикации рукописи следует направлять по адресу:

Acta Physica Budapest 502, P. O. B. 24.

По этому же адресу направлять всякую корреспонденцию для редакции и администрации.

Подписная цена «*Acta Physica*» — 165 форинтов за том. Заказы принимает предприятие по внешней торговле книг и газет «*Kultúra*» (Budapest I., Fő u. 32. Текущий счет: № 43-790-057-181) или его заграничные представительства и уполномоченные.

INDEX

E. A. Saad, N. A. Eissa, I. Bartchouk, O. H. El-Mofty and *A. F. El-Bidewy:* Thermal Neutron Flux Distribution and Flux Trap Effect in the Active Core of the UA-RR-I Reactor. — *Е. А. Сад, Н. А. Эйсса, И. Барчук, О. Г. Эл-Мофти и А. Ф. Эл-Байдеви:* Распределение потока тепловых нейтронов и эффект ловушки потока в активной зоне реактора UA—RR—I. 327

J. Bakos and *J. Szigeti:* Measurement of the Lifetime of Atomic Excited Levels by Time Analyser. — *Й. Бакош* и *Я. Сигети:* Определение времени жизни атомных возбужденных уровней временным анализатором 341

Á. Tóth: Determination of the Counting Efficiency in Cases of Radiation Measurement of the Widespread Solid Alpha Sources. — *А. Тот:* Определение эффективности счёта случая неточечных твёрдых α-излучающих источников 349

G. Pataki and *F. Beleznay:* On the Effect of a High Magnetic Field on Recombination Through Centres. — *Г. Патаки* и *Ф. Белезнаи:* О влиянии сильных полей на рекомбинацию, происходящую через рекомбинационные центры 363

L. Csillag, M. Jánossy and *K. Kántor:* Experimental Investigation of the Spatial Coherence of a He—Ne Laser. — *Л. Чиллаг, М. Яноши* и *К. Кантор:* Экспериментальное исследование пространственной когерентности лазера He—Ne. 373

Э. Ватаи: Использование метода ($\beta^{\vdash}\gamma^{\pm}$) совпадений при исследовании позитронного распада ядер. — *E. Vatai:* On the Use of the ($\beta^{+}\gamma^{\pm}$) Coincidence Method in Investigations on Positron Emitting Nuclides 381

B. Pődör: Effect of Dislocations on Galvanomagnetic Properties of *n*-Type Ge. — *Б. Пэдэр:* Влияние дислокаций на плотность и подвижность носителей тока германиа *n*-типа 393

Gy. Máthé: Investigation of the Signal Shape Given by $n - p$ and $p - n$ Type Semiconductor Detectors with Pulse Shape Discrimination. — *Дь. Матэ:* Исследование формы сигнала полупроводниковых детекторов типа *n-p* и *p-n* дискриминатором импульсных форм 407

I. Hevesi: On the Optical Properties of Vanadium Pentoxide Single Crystals. — *И. Хевеши:* Оптические свойства монокристаллов пятиокиси ванадия 415

A. Jucys, I. I. Glembockys and *R. Gáspár:* Investigations with Modified Universal Potential Fields — *А. Юцис, И. И. Глембоцкис* и *Р. Гашпар:* Исследования модифицированными универсальными потенциальными полями 425

P. Gombás und *O. Kunvári:* Zur Prüfung der Pseudopotentialmethode am Wasserstoffatom. — *П. Гомбаш* и *О. Кунвари:* Об испытании метода псевдопотенциалов в случае атома водорода 443

COMMUNICATIONES BREVES

S. S. Rathi and *M. K. Machwe:* Effect of Concentration on Fluorescence Spectrum of Eosin 449

K. Ladányi: Relativistic Trion Model for Hadrons 453

RECENSIONES

P. Gombás: R. Hofstadter—L. J. Schiff, Nucleon Structure 457

A. A. Sokolov, Elementary Particles 457

R. Brout—P. Carruthers, Lectures on the Many-Electron Problem 457

P. Roman, Advanced Quantum Theory 458

H. Muirhead, The Physics of Elementary Particles 458

A. A. Sokolov—J. M. Loskutow—I. M. Ternow, Quantenmechanik 458

A. S. Davydov, Quantum Mechanics 459

T. A. Littlefield—N. Thorley, Atomic and Nuclear Physics 459

W. A. Harrison, Pseudopotentials in the Theory of Metals 459

Acta Phys. Hung. Tom. XXIII. Fasc. 4. Budapest, 30. XII. 1967 Index: 26.022